Development and application of well-defined titanium alkoxide pre-catalysts

Lunn, Matthew D. G.

Award date:
2002

Awarding institution:
University of Bath

Development And Application Of Well-Defined Titanium Alkoxide Pre-Catalysts

Submitted by Matthew D. G. Lunn

for the degree of PhD of the University of Bath

2002

ProQuest LLC
789 East Eisenhower Parkway
P.O. Box 1346
Ann Arbor, MI 48106-1346

For Mum, Dad, Lily and Jessie

Acknowledgements

I would like to thank my supervisor Professor Matthew Davidson for his support, guidance and encouragement, throughout the last three years, which has been invaluable at all stages of my PhD.

The work described in this thesis also owes a great debt to Drs. Richard Price and Andrew Johnson, Rich for his patience and advice during my first year in Bath and Andy for the same qualities over my final two years. Special thanks must also go to Andy for his help during the writing of this thesis both with the content itself and repeated proof reading. Academically, I must also thank Dr. Mary Mahon for much of the crystallography in this thesis along with Drs. Michael Whittlesey, Andrew Weller and Steve Black for help and advice relating to NMR spectroscopy.

During the course of my PhD I have worked closely with my industrial sponsors, Synetix, and many people there have given me a great deal of support and encouragement. Special thanks must go to Drs. Bruno Stengel, Martin Partridge and John Ridland who have always been ready to offer invaluable advice on all aspects of my work both in Bath and during my time at Billingham. In addition special thanks must go to David Jenkins who helped me greatly with the in situ infra red work carried out in Billingham.

I have been lucky during my three years to share a lab with some excellent people who have put up with me with the minimum of exasperation. Rich, Andy, Phil, Marie, Steve, Andreas, Gillian, Tom and Cheryl have all in some way contributed to the work described in this thesis and therefore deserve a lot of thanks.

I would also like to thank all my friends both here in Bath and elsewhere who have helped me through the last three years even when at my most insufferable.

Last but by no means least the biggest thanks must go to my family and in particular my Mum and Dad who have always supported me through everything I have done and without whom none of this would be possible.

Abstract

This thesis details the synthesis and characterisation of titanium alkoxide complexes as potential pre-catalysts for the synthesis of polyurethanes. In addition it also describes initial studies into the reactivity and selectivity of a cross section of these pre-catalysts in polyurethane synthesis by utilising both model and commercially relevant systems. The titanium species described have the general formula $Ti(L)_x(O^iPr)_y$ and are synthesised by the reaction of $Ti(O^iPr)_4$ with a variety of protic chelating species.

Chapter 1 provides an introduction to the field, describing the reactivity of metal alkoxides in general and titanium alkoxides in particular, followed by a brief introduction to polyurethanes themselves. Chapter 2 details the experimental techniques used to synthesise the pre-catalysts while Chapter 3 presents the experimental data for these syntheses. A range of titanium complexes with monoanionic salicylaldimine Schiff base ligands with various steric and electronic properties are described in Chapter 4 including eleven new crystal structures. These complexes show the effect of variation of ligand properties on complex structure and several structural types are observed in the metal complexes. Chapter 5 describes some complexes of polyanionic Schiff bases with titanium including a number of novel complex types and five new crystal structures. Chapter 6 describes the titanium complexes of three families of ligands related to the Schiff bases; hydrazones, azines and oximes, each of these exhibits novel structural types and several of the complexes described have interesting supramolecular chemistry in the solid-state. This chapter includes twelve new crystal structures. Chapter 7 describes a number of miscellaneous titanium alkoxide complexes, including five new crystal structures, and this is followed by Chapter 8 which describes attempts to form activated titanium alkoxide pre-catalysts, which are analogous to those used in polyolefin synthesis with non-coordinating anions and includes the crystal structures of five new complexes. The final chapter describes our studies of polyurethane synthesis using a range of our pre-catalysts. This includes NMR studies of model systems with a range of catalysts to assess the rate of urethane formation. In addition in situ infra red studies are described which detail polyurethane formation from commercial pre-polymer systems using some of our pre-catalysts.

Abbreviations

Ac	Acetyl group
acac	Acetyl acetonate
Ar	A generic aryl group
BArF	$B(C_6F_5)_4^-$ anion
BHET	Bis-hydroxyethyl-terephthalate
Bu	Butyl group
BuLi	Butyl lithium
Cat	Catalyst
C.D.	Compact disc
CHN	Carbon/Hydrogen/Nitrogen (elemental analysis)
cif	Crystallographic information file
COSY	Correlated spectroscopy
Cp	Cyclopentadiene
CSD	Cambridge Structural Database
DBTDL	Di-butyl-tin-di-laurate
DFT	Density functional theory
DMT	Dimethyl terephthalate
e	An electron
e.e.	Enantiomeric excess
Et	Ethyl group
EXAFS	Extended X-ray absorption fine structure
FAB	$B(C_6F_5)_3$ neutral species
Hal	Halogen
H-bond	Hydrogen bond
8-HQ	8-Hydroxyquinoline (and sometimes a titanium complex of this ligand, chapter 9)
ICI	Imperial Chemical Industries
IPA	Isopropyl alcohol
L	A generic ligand
L^{rc}	A generic ligand which has rearranged by ring closure
M	A generic metal

MAO	Methyl aluminoxane
MDI	4,4'-methylene-bis-phenylisocyanate
Me	Methyl group
MHz	Megahertz
MOCVD	Metal organic chemical vapour deposition
Mw	Molecular weight
N/A	Not applicable
nacac	Mono-imine derivatised acetyl acetonate group
NMR	Nuclear magnetic resonance
NOESY	Nuclear Overhauser enhancement spectroscopy
O-N-O	A Schiff base ligand which is dianionic and tridentate (chapter 5)
PET	Polyethylene terephthalate
Ph	Phenyl group
ppm	Parts per million
Pr	Propyl group
R	A generic alkyl group
Sal	Salicylaldimine
TAA	Titanium bis-acetylacetonate bis-isopropoxide
TEHT	Tetra-ethylhexyl-titanate $Ti(OCh(C_2H_5)C_5H_{11})_4$
Tf	Triflate group
thf	Tetrahydrofuran
TiPT	Tetra-isopropyl-titanate $Ti(OC_3H_7)_4$
TMS	Tetra methyl silane
TMSCN	Trimethylsilyl cyanide
TPA	Terephthalic acid
VSEPR	Valence shell electron pair repulsion
VT	Variable temperature
XANES	X-ray absorption near edge structure
xs	Excess

Contents

Chapter 1

Introduction

This thesis is concerned with the derivatives of titanium tetra-isopropoxide (TiPT) with the general formula $Ti_xL_y(O^iPr)_z$ where L is an anionic ligand other than a monodentate alkoxide. Their synthesis and characterisation, both in solution and the solid state, are discussed along with some investigations of their use as pre-catalysts for the synthesis of polyurethanes. This chapter provides a general overview of the topic with more detailed background information given in the relevant discussion chapters. As an introduction to the work described in this thesis the first two sections of this chapter discuss the chemistry of metal alkoxides in general and titanium alkoxides in particular. This is followed by a brief introduction to polyurethanes and a summary of previous work on polyurethane synthesis using titanium alkoxides.

1.1 Homoleptic Metal Alkoxides

Homoleptic metal alkoxides are an important class of metal complexes, which are used widely in current chemical research. The use of these compounds in various roles has been extensively reviewed recently in a number of important papers and books[1].

Metal alkoxides have the basic formula $[M(OR)_x]_n$ and are formed by the replacement of the hydroxyl hydrogen of an alcohol with a metal atom. They are common and generally stable for the majority of the metals, both main group and d-block, with the notable exception of the homoleptic platinum group metal alkoxides (Ru, Rh, Pd, Os, Ir, Pt)[2]. These platinum group alkoxides are thought to be more labile due to β-hydrogen elimination and are generally not isolatable under ambient conditions. Homoleptic alkoxides of metals are synthesised by a number of methods the most important of which are described in the following section.

---

[1] D.C. Bradley, R.C. Mehrotra, I.P. Rothwell and A. Singh, *Alkoxo and Aryloxo Derivatives of Metals*, Academic Press, London, (2001); L.G. Hubert-Pfalzgraf, *Coord. Chem. Rev.*, **180**, 967 (1998), N.Y. Turova, E.P. Turevskaya, M.I. Yanovskaya, V.G. Kessler and D.E. Tcheboukov, *Polyhedron*, **17**, 899 (1998), R.C. Mehrotra and A. Singh, *Prog. Inorg. Chem.*, **46**, 239 (1997), R.C. Mehrotra, S. Sogani and A. Singh, *Chem. Rev.*, **94**, 1643 (1994), R.C. Mehrotra, S. Sogani and A. Singh, *Chem. Soc. Rev.*, **23**, 215 (1994),

[2] R.C. Mehrotra, S.K. Agarwal and Y.P.Singh, *Coord. Chem. Rev.*, **68**, 101(1985)

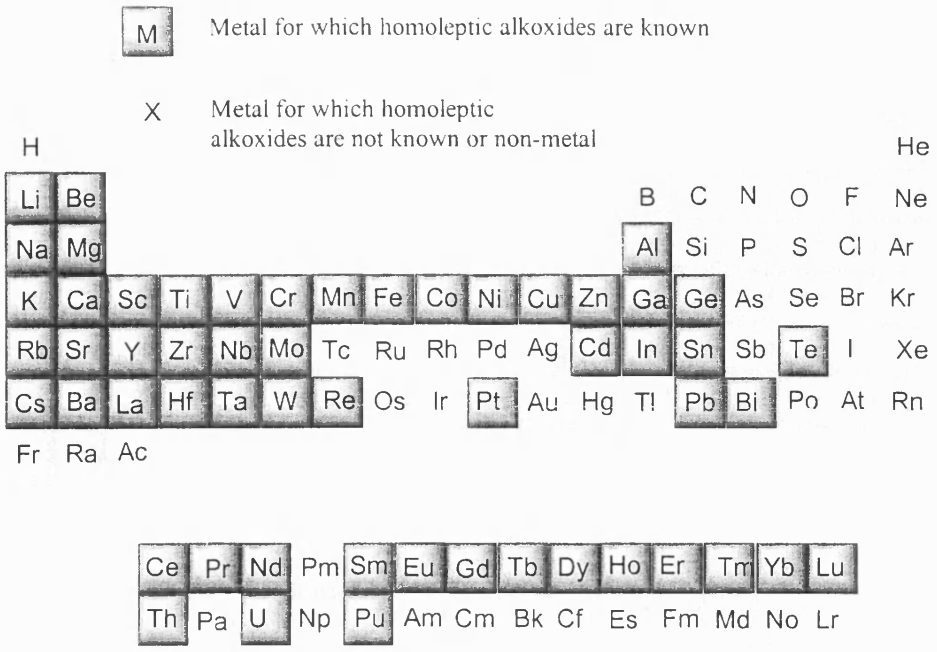

Figure 1.1: Periodic table showing the spread of homometallic homoleptic metal alkoxides across the periodic table

1.1.1 Synthesis

Reaction of metals with alcohols

Metals that have a great degree of electropositive character can react directly with the alcohol of choice to form the homoleptic alkoxide. This reaction proceeds uncatalysed for the group 1 metals and sterically compact alcohols with the evolution of hydrogen gas as a by-product. In addition, use of I_2 or $HgCl_2$ as a catalyst can promote the formation of the homoleptic alkoxides of groups 2 and 3 and the f-block metals using this method

$$M + n\,ROH \longrightarrow M(OR)_n + 0.5n\,H_2(g)\uparrow$$

Figure 1.2: Direct reaction of metal and alcohol

Electrochemical techniques

A wide range of homoleptic metal alkoxides have been synthesised by the anodic dissolution of the required metal in electrolyte containing alcohols[3]. This method, which is particularly useful for the direct synthesis of alkoxides of less electropositive metals, is very promising due to the fact that it is simple, continuous and non-polluting. The following reactions represent the process for a metal, M, in an alcohol, ROH.

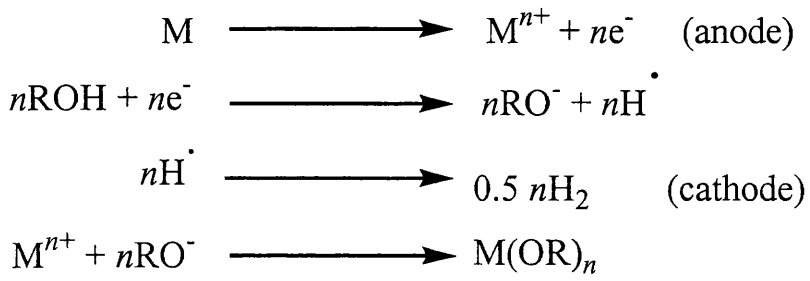

Figure 1.3: Electrochemical reaction of metal and alcohol

Direct reaction of metal halides with alcohols

The most common synthetic route to metal alkoxides is the reaction of the metal halide with the corresponding alcohol to give the required product and HCl.

Figure 1.4: Direct reaction of a metal chloride and an alcohol

This method can be used for most metals although in many cases the product is not the required homoleptic alkoxide and instead a mixed chloro/alkoxide is produced.

Reaction of metal chlorides with alcohols in the presence of a base

As the direct reaction of metal halides and alcohols tends to cause the formation of mixed chloro/alkoxo compounds most homoleptic metal alkoxides are formed by the

[3] V.A. Shreider, E.P. Turevskaya, N.I. Kozlova and N.Ya. Turova, *Inorg. Chim. Acta*, **13**, L73 (1981)

reaction of the metal halide with the alcohol in the presence of a base. The two most common routes are the use of ammonia gas and alkali metal alkoxides.

The ammonia route[4] involves the bubbling of ammonia gas through the reaction mixture in a non-polar solvent. This has the advantage of easy removal of the ammonium chloride by-product by filtration and the unreacted ammonia by evaporation. In addition, it avoids the formation of heterobimetallic alkoxides, which can be formed through the use of alkali metal alkoxides.

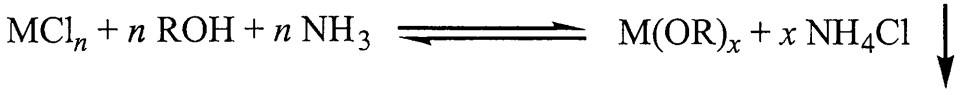

Figure 1.5: Reaction of a metal chloride and an alcohol in the presence of ammonia

The sodium or potassium alkoxide route (transmetallation) is the most versatile route for most p and d block metals, and although there can be problems with formation of heterobimetallic by-products, it is widely used for a number of homoleptic alkoxides.

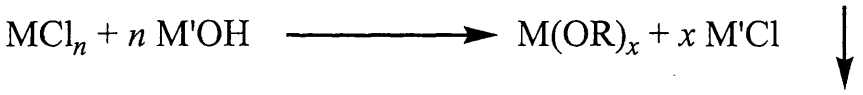

Figure 1.6: Reaction of a metal chloride and alkali metal alkoxide

Other synthetic methods

Other methods for the synthesis of homoleptic alkoxides which will not be discussed further here include preparations from metal hydroxides and oxides, alcohol exchange reactions with metal alkoxides themselves, transesterification reactions and synthesis from metal dialkylamides

[4] R.C. Mehrotra and A. Singh, *Prog. Inorg. Chem.*, **46**, 239 (1997) and references therein

1.1.2 Physical and chemical properties

Physical properties

The physical properties of the metal alkoxides depend on a combination of the nature of the R group on the alkoxide (sterics and electronics) and the metal itself (valency, atomic radius, stereochemistry and coordination number). Despite this wide variety of influences a few effects are noticeable across the range of metal alkoxides. It has previously been noted[1] that metal alkoxides exhibit characteristics usually associated with a degree of covalency in the metal to ligand bonding, which would not be expected on consideration of the high electronegativity of oxygen. The ionic character of the metal-oxygen bonds would be expected to range between 65 and 80% depending on the electropositivity of the metal. However, the majority of metal alkoxides are relatively volatile and soluble in common organic solvents, which could suggest that they have significant covalent character. A number of potential reasons for a possible reduction in ionic character of the ligand-metal bonds have been described and a combination of all of these factors could be the cause of the observed effect. The reasons suggested are the inductive effect of the alkyl group in the alkoxide, the donation of lone pair electrons in p-orbitals on oxygen into d-orbitals on the metal (figure 1.7 below) and the formation of oligomeric clusters through formation of alkoxide bridges between metals.

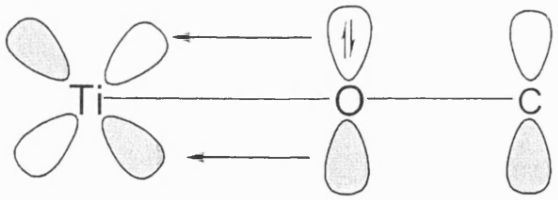

Figure 1.7: π donation from oxygen to vacant d-orbitals on titanium

However, recent research, particularly on early transition metal alkoxides, suggests that very little or no π bonding of the type shown in figure 1.7 occurs, and that the bonding in these compounds is in essence ionic[5]. This research does not give an

[5] T. W. Coffindaffer, B. D. Steffy, I. P. Rothwell, K. Folting. J. C. Huffman and W. E. Streib,. *J. Am. Chem. Soc.*, **111**, 4742 (1989); G. D. Smith, P. E. Fanwick and I. P. Rothwell, *Inorg. Chem.*, **29**, 3221 (1990); W. A. Howard, T. M. Trnka and G. Parkin, *Inorg. Chem.*, **34**, 5900 (1995).

alternate explanation for the seemingly covalent properties of the compounds although the solubility in organic solvents could be due to the lipophillic alkyl shell formed by the alkoxide ligands.

Chemical properties

The chemistry and reactivity of the metal alkoxides is dominated by the nature of the metal-oxygen bond. The polarisation of this bond, with a δ^+ charge on the metal and a δ^- charge on the oxygen, makes the metal susceptible to attack by nucleophiles and the oxygen to attack by electrophiles. This combination of susceptibilities makes the metal alkoxides highly reactive particularly with hydroxylic reagents such as alcohols and phenols, and particularly water[4]. Although the detailed reaction chemistry of the metal alkoxide family of compounds will not be discussed here it is important to note their high reactivity with water, which leads to a need for stringent anhydrous conditions when carrying out reactions involving them if hydrolysis is to be avoided.

1.2 Titanium Alkoxides

1.2.1 Synthesis

Although titanium alkoxides [$Ti(OR)_4$] can be synthesised by electrochemical routes[6] by far the most important route to the simple homoleptic alkoxides is the reaction of the metal chloride with an alcohol. The direct reaction of $TiCl_4$ with alcohols[7] yields mixed chloro/alkoxide compounds with the formula $TiCl_2(OR)_2(ROH)_2$ and to form the homoleptic products the use of a base is required.

$$TiCl_4 + ROH \text{ (excess)} \rightleftharpoons TiCl_2(OR)_2(ROH)_2 + 2HCl \uparrow$$

Figure 1.8: Synthesis of a mixed titanium chloro/alkoxide

The most common base used for these syntheses is ammonia with the homoleptic alkoxide being produced with the by-product NH_4Cl being removed by filtration. This method, which is still the preferred industrial route to simple 'small chain' titanium

[6] *Gerr. Offen. Pat.* 2005835 (1970); *Fr. Pat.* 2091229 (1972).
[7] D.C. Bradley, M.A. Saad and W. Wardlaw, *J. Chem. Soc.*, 2002 (1954); Y.T. Wu, Y.C. Ho, C.C. Lin and H.M. Gau, *Inorg. Chem.*, **35**, 5948 (1996)

alkoxides, was first reported in 1939[8] and titanium alkoxides were the first metal alkoxides to be produced via this method.

$$TiCl_4 + \underset{\text{(excess)}}{4\ ROH} + 4\ NH_3 \longrightarrow Ti(OR)_4 + 4\ NH_4Cl \downarrow$$

Figure 1.9: Synthesis of a titanium alkoxide using ammonia

In addition, to ammonia, homoleptic titanium alkoxides can also be produced using sodium alkoxides as a base with the first reported synthesis being carried out in 1924[9]. Specific titanium alkoxides can also be synthesised by alcohol exchange with another alkoxide[10]. This is particularly true for the synthesis of branched alkoxides from linear ones, as the equilibria for these reactions generally lies in favour of the branched product. The reactions can also be driven by the removal of the more volatile alcohol product by distillation, with the reaction either carried out in neat alcohol or in an inert solvent. If chosen carefully this solvent may reduce the boiling temperature of the volatile product alcohol via azeotropic effects and therefore also reduce the risk of unwanted side reactions.

1.2.2 Bonding

The bond lengths in titanium alkoxides vary with the relationship (μ_3) bridging > (μ_2) bridging > terminal. In addition for terminal alkoxides and particularly aryloxides the shorter bond distances are associated with larger bond angles, which in some cases are close to 180°C. This effect has generally been assumed to be due to donation of lone pair π-electrons from the oxygen atoms to the vacant d-orbitals on titanium, as described in section 1.1.2 (page 6), with amounts of π donation ranging from two to four electrons. In general, larger angles are associated with greater amounts of π donation. Although a number of papers have described this effect in titanium aryloxides little has been described for alkoxides. However, recently, Molina and

[8] J. Nelles, *Brit. Pat.*, 512452 (1939)
[9] F. Bischoff and H. Adkins, *J. Am. Chem. Soc.*, **46**, 256 (1924)
[10] I. Shiiava, W.T. Schwarz Jr. and H.W. Post, *Chem. Rev.*, **61**, 1 (1961); C. Campbell, S.G. Bott, R. Larsen and W.G. van der Sluys, *Inorg. Chem.*, **33**, 4950 (1994)

Sundberg et al.[11] have used computational methods to compare bond angles in a range of $TiX_3(OMe)$ complexes where X is a hydride or halide with corresponding germanium compounds. In the germanium compounds π donation is disfavoured due to the LUMO d-orbitals being too high in energy for interaction in comparison to the titanium compounds where the d-orbitals are at much lower energy. In this work the C-O-M angles for both metals were compared with the titanium species having almost linear bonds while the corresponding germanium species showed bond angles of approximately 120° suggesting a multiple bonding character in the titanium complexes due to π donation, which is absent in the germanium compounds.

This evidence, however, seems to be contradicted by correlation analysis of terminal isopropoxide complexes of titanium found by a search of the Cambridge Structural Database (CSD)[12]. This analysis (figure 1.10 overleaf) seems to show little or no correlation between the bond length to titanium and the bond angle at the alkoxide oxygen atom. If the multiple bonding model described above was correct it would be expected that as the bond angle approached linearity the bond length would decrease due to the increased amount of π donation due to the increased orbital overlap. This leads us to suggest that, at least in the case of titanium isopropoxide complexes, the bonding is essentially ionic in character and that the M-O-C bond angle is a poor indicator of π bonding, a theory which has been put forward by other workers previously for similar systems[5].

[11] J.A. Dobado, J.M. Molina, R. Uggla and M.R. Sundberg, *Inorg. Chem.*, **39**, 2831 (2000)

[12] (a) The CSD system program Conquest (Version 1.4) was used to compile selected structural parameters in target titanium complex, which contain terminally bound isopropoxide units. CSD entries were accepted for analysis if they were classified as error-free, without disorder, and had $R < 0.10$. (b) F. H Allen. and O. Kennard, *Chem. Des. Autom. News*, **8**, 1 (1993). (c) F. H Allen. and O. Kennard, *Chem. Des. Autom. News*, **8**, 31 (1993).

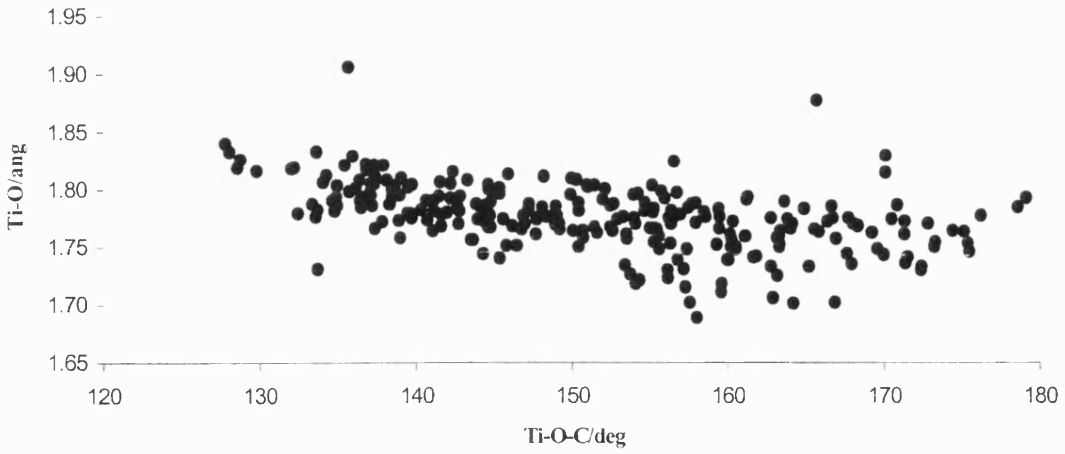

Figure 1.10: Correlation of Ti-O bond length and Ti-O-C bond angle for titanium isopropoxide complexes.

1.2.3 Molecular complexity and structure

Titanium alkoxides tend to associate as the metal atoms attempt to achieve an octahedral geometry through formation of μ_2 and μ_3 alkoxide bridges. The level of association actually achieved by the titanium alkoxide depends greatly on the size and level of branching in the alkyl group of the ligand with the larger and more highly branched groups having lower levels of association than the short chain unbranched compounds.

Ebullioscopy and cryoscopy have suggested molecular complexities for the titanium homoleptic alkoxides[13] in solution of 4 i.e. $[Ti(OMe)_4]_4$, 3 i.e. $[Ti(OEt)_4]_3$, approximately 1.4 (for the isopropoxide) and 1 i.e. $[Ti(O^tBu)_4]$. The molecular complexities have also been studied by EXAFS and XANES[14], which suggest that ethoxide and n-butoxide are trimers while isopropoxide is a monomer. However this final value has more recently been disputed due to use of mass spectrometry[15], which

[13] C.G. Barraclough, R.L. Martin and G. Winter, *J. Chem. Soc.* 758 (1964)
[14] F. Babonneau, S. Doeuff, A. Leaustic, C. Sanchez, C. Cartier and M. Verdaguer, *Inorg. Chem.*, **27**, 3166 (1988)
[15] S.M. Damo, K. Lam, A. Rheingold and M.A Walters, *Inorg. Chem.*, **39**, 1635 (2000)

seems to suggest that the tetra-isopropoxide has a significant amount of dimeric character in the gas phase and therefore should also exist as a dimer in solution.

Crystallographically only three homoleptic titanium alkoxides have been characterised. Titanium ethoxide[16] and methoxide[17] show similar tetrameric structures as shown below for the tetra-methoxide with four μ_2 and two μ_3 bridging alkoxides.

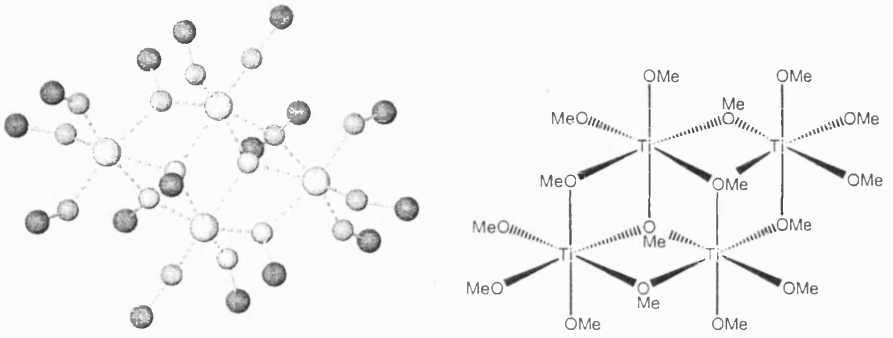

Figure 1.11: Crystal structure of titanium tetra-methoxide[17]

In contrast titanium tetra-neopentoxide[18] has a dimeric structure, shown below, with two μ_2 alkoxide bridges. This structure has been used as vindication of the mass spectroscopy results for titanium tetra-isopropoxide as neopentoxide is considered to be sterically more bulky than isopropoxide and therefore less likely to associate.

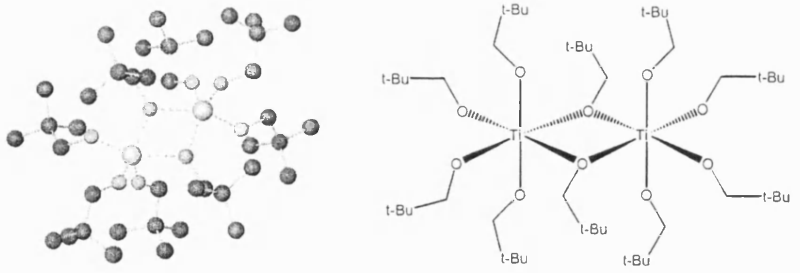

Figure 1.12: Crystal structure of titanium tetra-neopentoxide[18]

[16] J.A. Ibers, *Nature*, **19**, 686 (1963)
[17] D.A. Wright and D.A. Williams, *Acta Cryst. Sect. B*, **24**, 1107 (1968)
[18] T.J. Boyle, T.M. Alam, E.M. Mechenbier, B.L. Scott and J.W. Ziller, *Inorg. Chem.*, **36**, 3293 (1997)

1.2.4 Chemical properties

The reactivity of the homoleptic titanium alkoxides is typical for the metal alkoxides in general and is characterised by reactions with hydroxylic reagents such as water, alcohols[19], carboxylic acids[20], oximes[21] and β-diketones[22]. The reactivity of the alkoxides with a number of these reagents will be discussed in relevant discussion chapters later in this thesis, but it is important to note the huge range of compounds, which have been isolated and characterised, based on the alkoxides and these reagents. The most important of the reactions to always be considered when working with the homoleptic alkoxides however is that with water, which is discussed below.

As mentioned above the titanium alkoxides are typical of all electropositive metal alkoxides in that they react readily with water to form compounds with a combination of alkoxo, oxo and hydroxo groups. The reaction has been postulated[23] to begin through nucleophillic coordination of water followed by hydrolysis and then the formation of titanoxane products as shown in figure 1.13 below.

$$Ti(OR)_4 + H_2O \longrightarrow Ti(OR)_4(OH_2) \longrightarrow Ti(OR)_3(OH) + ROH$$

$$Ti(OR)_3(OH) + Ti(OR)_4 \longrightarrow (RO)_3Ti\text{-}O\text{-}Ti(OR)_3 + ROH$$

Figure 1.13: Reaction of a metal alkoxide and water

This reaction is particularly important as it is a very facile process and therefore, if it is to be avoided, stringently anhydrous conditions must be maintained when using titanium alkoxides.

However, the reaction has been exploited by, among others, Klemperer et al. who have used controlled hydrolysis of homoleptic titanium alkoxides to isolate a number

[19] I.D. Verma and R.C. Mehrotra, *J. Chem. Soc.*, 2966 (1960)
[20] I.D. Verma and R.C. Mehrotra, *J. Prakt. Chem.*, **8**, 235 (1959)
[21] A. Singh, C.K. Sharma, A.K. Rai, V.D. Gupta and R.C. Mehrotra, *J. Chem. Soc. (A)*, 2440 (1971)
[22] A. Yamamoto and S. Kambara, *J. Am. Chem. Soc.*, **79**, 4344 (1957)
[23] D.E. Putzig and T.W. del Pesco, *Kirk Othmer Encyclopedia of Chemical Technology*, **24**, 275 (1997)

of different structural types of titanoxane with from three to eighteen titanium atoms, which they have then used as precursors for the sol-gel process[24].

1.3 Industrial applications of titanium alkoxides[23]

Titanium alkoxides are utilised in a number of ways in industry including as catalysts for organic transformations, for the removal of NO_x in power stations, as precursors in the production of novel materials, as catalysts in bulk chemical processes and as additives in inks, paints and adhesives. The large scope of these processes will not be discussed in detail here but some of the more important roles for these compounds are detailed below with more detailed information on specific processes outlined in later discussion chapters.

1.3.1 Titanium alkoxides as precursors for metal oxide films

Thin films of metal oxides are used widely in the electronics industry and TiO_2 layers are common insulators in electronic devices. By far the most common method of producing the thin uniform layers required for this use is metal oxide chemical vapour deposition (MOCVD)[25], which uses volatile metal precursors. These are subsequently volatilised in a stream of inert gas, prior to decomposition on the desired substrate surface. Titanium alkoxides are ideal for this application as they have the benefit of being relatively volatile metal sources, which also possess multiple oxygen containing ligands. The most commonly used titanium alkoxide for this application is $Ti(O^iPr)_4$[26].

1.3.2 Titanium alkoxides as sol-gel precursors

A second industrial use for titanium alkoxides in the production of materials is in the sol-gel process as precursors to ceramics[27]. As with MOCVD the final product is titania (TiO_2) but unlike MOCVD high temperatures are not required for the initial hydrolysis and the volatility of the alkoxide is relatively unimportant.

---

[24] V.W. Day, T.A. Eberspacher, Y.W. Chen, J.L. Hao and W.G. Klemperer, *Inorg. Chim. Acta*, **229**, 391 (1995); C.F. Campana, Y. Chen, V.W. Day, W.G. Klemperer and R.A. Sparks, *J. Chem. Soc. Dalton Trans.*, 691 (1996)

[25] A.R. Barron, '*CVD of Non-Metals*' (Ed. W.S. Rees Jr.), VCH, Weinheim (1996)

[26] Y.M. Wu, D.C. Bradley and R.M. Nix, *Appl. Surface Sci.*, **64**, 21 (1992) and references therein

[27] C.J. Brinker and G.W. Scherer, '*Sol-Gel Science: The Physics and Chemistry of Sol-Gel Processing*', Academic Press, New York (1990)

The process exploits the high reactivity of the alkoxides with water and involves hydrolysis of the titanium alkoxide, or a derivative, in a controlled fashion in a solvent. This solvent is then removed by evaporation leading to the formation of fine TiO_2 powders, which are then compacted and heated to form a ceramic. Because control of the hydrolysis reaction is essential to allow formation of high quality products, additives such as β-diketonates are often added to the alkoxide to reduce the hydrolysis rate.

The ceramics and glasses formed in the sol-gel process are widely utilised in both the electronic and optical industries where high purity titania products are highly desirable.

1.3.3 Titanium alkoxides as catalysts for organic transformations

Titanium alkoxides, and their derivatives are used in a number of organic transformations as simple catalysts and to allow asymmetric control of enantioselective reactions. A number of transformations will be discussed in relevant discussion chapters later in this thesis when they relate to the work therein. However in the context of this review of important titanium alkoxide chemistry the most famous application, Sharpless epoxidation, for which K.B. Sharpless was awarded the Nobel Prize for chemistry in 2001, will be discussed here.

The most important role of a metal alkoxide derived catalyst in organic synthesis is the asymmetric epoxidation of allylic alcohols, which was first reported by Katsuki and Sharpless in 1980[28]. A review of both the history and methodology of this work was published in 1986 by Sharpless[29] and only a brief resume is given below.

[28] T. Katsuki and K.B. Sharpless, *J. Am. Chem. Soc.*, **102**, 5974 (1980)
[29] K.B. Sharpless, *Chem. Britain.*, (Jan. 1986)

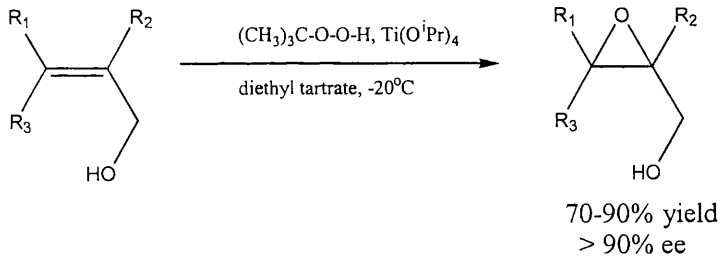

Figure 1.14: Sharpless epoxidation

Sharpless and Katsuki discovered a catalyst consisting of titanium tetra-isopropoxide and (+)-diethyl tartrate was highly efficient for the enantioselective synthesis of epoxides from allylic alcohols using *tert*-butyl peroxide as an oxygenating agent.

The reaction proceeds with enantiomeric excesses of over 90% and has been used in both the synthesis of natural products and drugs[30] and the kinetic resolution of racemic allylic alcohols[31]. Since the initial discovery a large amount of work has been done to perfect the technique, the discussion of which is outside the scope of this thesis.

1.3.4 Titanium alkoxides as catalysts for polymerisation processes

Titanium alkoxides are used widely in industry as catalysts for polymerisation reactions. The most well known role for titanium complexes in polymerisations is as catalysts for processes related to the Ziegler-Natta polymerisation of olefins and although, in the majority of cases, the titanium species involved are metallocenes some alkoxides are also mentioned in the patent literature[32].

A second group of important industrial processes in which titanium alkoxides have an important role is in esterifications. The simple alkoxides are used in the formation of simple esters as catalysts for the reaction between carboxylic acids and alcohols. This role is common, despite the deactivation of the catalyst by hydrolysis caused by the

[30] K.B. Sharpless, C.H. Behrens, T. Katsuki, A.W.M. Lee, V.S. Martin, M. Takatani, S.M. Viti, F.J. Walker and S.S. Woodward, *Pure Appl. Chem.*, **55**, 589 (1983)
[31] V.S. Martin, S.S. Woodward, T. Katsuki, Y. Yamada, M. Ikeda and K.B. Sharpless, *J.Am. Chem. Soc.*, **103**, 6237 (1981)
[32] Examples include; R.C. Job, *PCT Int. Appl.*, WO 2000-US18008 (2001); A. Sato, Y. Fujiwara and A. Imai, *Jpn. Kokai, Tokyo Koho*, JP 11228616 (1999); T. Shiraishi, K. Matsuura and H. Kamiishi, *Eur. Pat. Appl.*, EP 581611 (1994)

water formed during the condensation, and is used in the synthesis of synthetic lubricants among other products[33]. A second related process, in which the homoleptic alkoxides are involved, is industrial synthesis of methyl methacrylate. The synthesis of this important monomer, which is the starting material for the synthesis of poly-methyl methacrylate, is carried out by a transesterification reaction mediated by the titanium alkoxide.

Finally the third and possibly most important esterification reaction catalysed by the titanium alkoxides is the condensation polymerisation of di-carboxylic acids and glycols to form polyesters. Polyesters are an important group of polymers[34], which have a diverse number of applications including as packaging, fibres and magnetic tapes in addition to many others. The most common polyester produced industrially is polyethylene terephthalate (PET), which has numerous uses as both a fibre and an engineering plastic.

High molecular weight polyesters such as PET and equivalents can be synthesised by one of two routes each of which involve the intermediate bis–hydroxyethyl terephthalate (BHET). The first and older route forms BHET through the reaction of dimethyl terephthalate (DMT) and ethylene glycol, which is catalysed by a number of metal ions but principally Zn^{2+} and Mn^{2+}. The more recent route to BHET is by direct esterification of terephthalic acid (TPA) with ethylene glycol, a process for which the best catalysts have been shown to be organotin species, such as dialkyltin oxide, and titanium alkoxides, such as titanium tetra-isopropoxide. The two routes are shown in figure 1.15 overleaf.

[33] T. Keating, *Brit. Pat.*, 1, 374, 263, (1974)
[34] M.P. Stevens, '*Polymer Chemistry An Introduction*', Oxford University Press, Oxford, Ch. 12 (1999); G.W. Parshall and S.D. Ittel, '*Homogeneous Catalysis*', Wiley, New York, Ch.11 (1992)

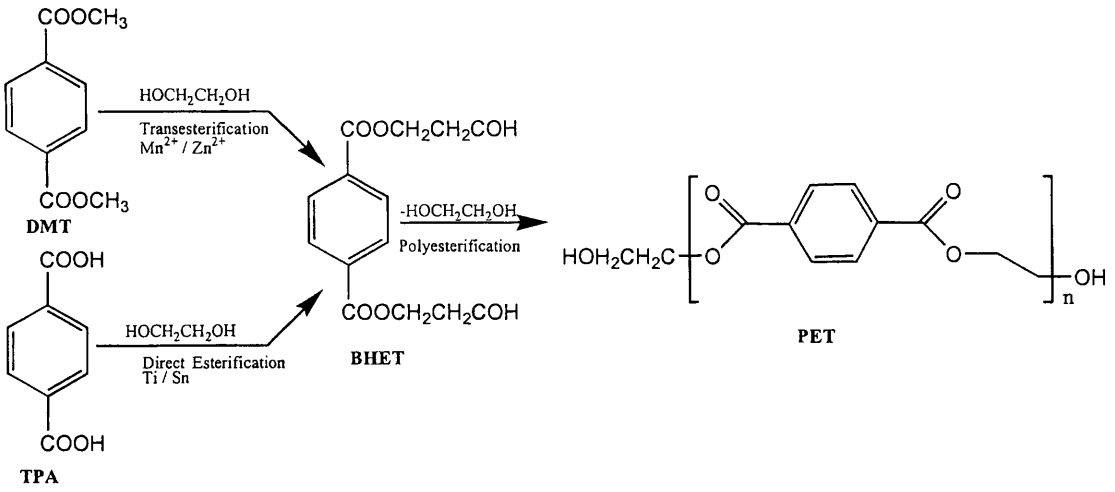

Figure 1.15: Synthesis of polyesters

Titanium tetra-alkoxides have been shown to be excellent catalysts for this reaction, utilising the chemistry that is described in the section on esterification above. Although there is large amount of patent literature on the use of titanium alkoxides in this process, very little can be found in the non-patent literature[35] and the subject is open to much more detailed investigation.

A third industrial polymerisation in which titanium alkoxides and their derivatives look set to have a significant catalytic role is the synthesis of polyurethanes. The investigation of this potential role is the main topic of this thesis and, as background to this, the following section discusses in more detail polyurethanes and the potential for the use of titanium alkoxides in their synthesis.

1.4 Polyurethanes

1.4.1 Uses[36]

Polyurethanes were first synthesised by I.G. Farben in Germany prior to World War II[37] and since that time a large number of companies have been involved in their production. In 1993 the industry used approximately six million tons of starting

[35] L. Nondek and J. Malek, *Makromol. Chem.*, **178**, 2211 (1977); J. Otton and S. Ratton, *J. Polymer Sci. Part A: Polymer Chem.*, **29**, 377 (1991)
[36] H. Ulrich, '*Chemistry and Technology of Isocyanates*', Wiley, Chichester (1996)
[37] O. Bayer, *Angew. Chem.*, **59**, 257 (1947)

materials and currently the main companies involved in their synthesis are Dupont and Huntsman.

There are five main polyurethane products with the most common being flexible foams. These foams are formed by addition of water and surfactants to the reaction mixture. The water reacts with isocyanate in the reaction mixture to form carbon dioxide, which is used as the blowing agent, and ureas, which are used as chain extenders. The foams formed in this way are widely used in the furniture industry as cushioning materials, the automotive industry as both cushioning materials in seating and instrument panels and sound insulation and more recently as the main component in many type of sports shoes including the air-sole in Nike trainers.

The other main uses of polyurethanes are as rigid foams for insulation and as elastomers in coatings, sports apparel, wire coatings and footballs (the football used in the World Cup in the U.S.A. in 1994 was made primarily of polyurethane). Other uses include the adhesive resins used to form preorientated strand board, a replacement for MDF, and biomedical applications such as artificial skin, catheter tubing and wound dressings.

1.4.2 Synthesis

Polyurethanes are a family of polymers formed by the reaction between isocyanates and alcohols to form urethane (carbamate) linkages as shown in figure 1.16 below.

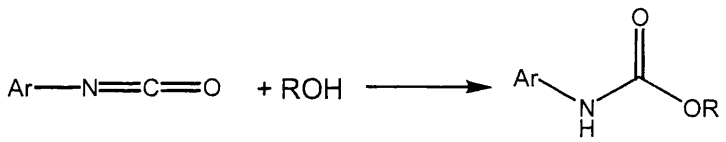

Figure 1.16: Formation of a urethane linkage

In the formation of polymers the reaction is generally between a di-isocyanate, such as 4,4'-methylene-bis-phenylisocyanate (MDI), and a high molecular weight polyether (Mw typically 2000-3000), as shown in figure 1.17 below.

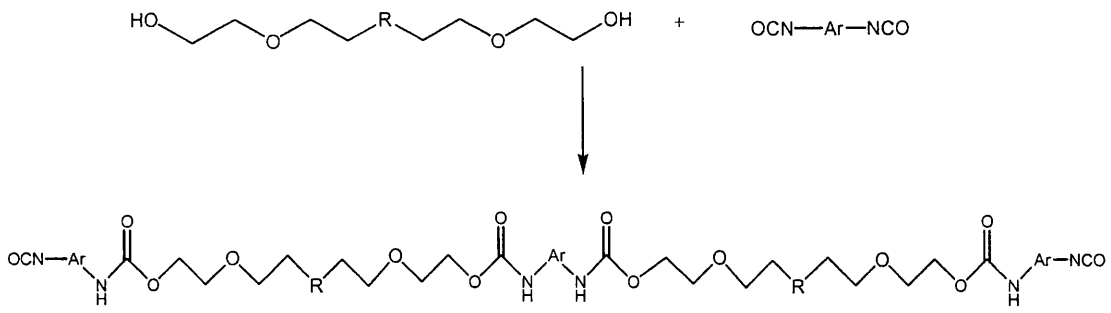

Figure 1.17: Polyurethane formation

The reaction between these two monomers leads to the formation of block co-polymers, which can be further derivatised by introduction of urea or cyclic isocyanurate groups to help control the polymer properties.

The polyurethanation reaction between an aromatic isocyanate and an alcohol occurs readily and, on the laboratory scale, no catalyst is required[38]. Industrially, however, catalysts are used for both acceleration of reaction rate and control of by-product production.

The polyurethanation reaction can lead to many by-products, which can be to a greater or lesser extent undesirable. These various products are shown in figure 1.18 overleaf and the degree to which their formation occurs influences the properties of the final polymer. One of the most important challenges in the synthesis of polyurethanes is control of these products by control of either reaction conditions, the nature and stoichiometry of monomers, presence of additives or the catalyst itself.

[38] T.W. Brocks, C. Bledsoe and J. Rodriguez, *Macromol. Synth. Coll. Vol. 1*, 381 (1977)

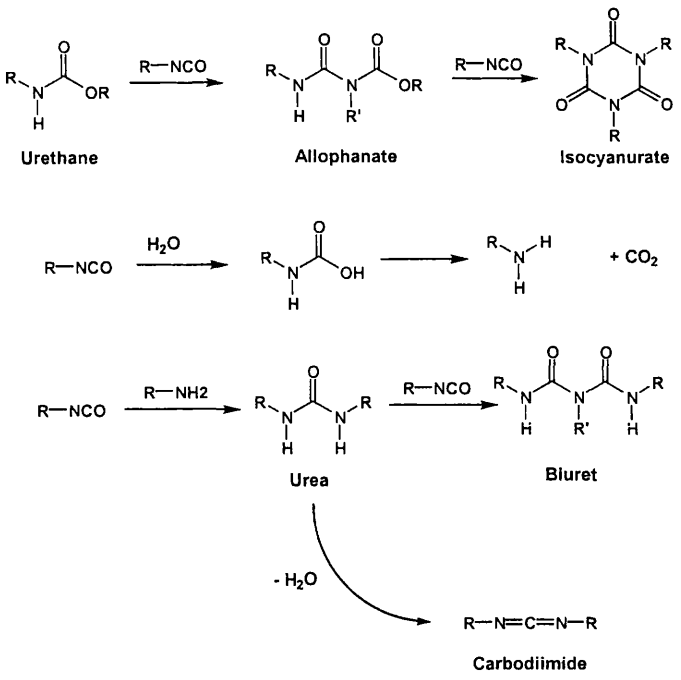

Figure 1.18: By-products in the synthesis of polyurethanes

Currently in industry two main types of catalyst are used either alone or in combination. The first group are the tertiary amines such as those shown in figure 1.19 below.

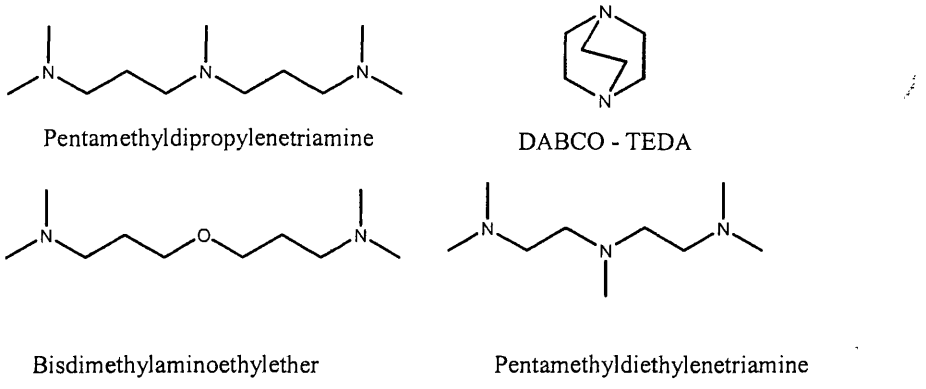

Figure 1.19: Tertiary amine catalysts for synthesis of polyurethanes

These are thought to catalyse the reaction by forming a hydrogen bonded complex with the glycol or polyether causing polarisation of its hydroxyl group and increasing the nucleophillicity of the glycol oxygen, thereby increasing the rate of the reaction[33].

The second group of commonly used catalysts is tin based: for example tin alkyls or di-butyl tin di-laurate. It has been proposed that these catalysts act as shown in figure 1.20 below[39]. Complexation of the isocyanate to the tin species is followed by insertion into the tin alkoxide bond. Addition of an alcohol then leads to formation of an alkoxide, which displaces the coordinated urethane to regenerate the catalyst.

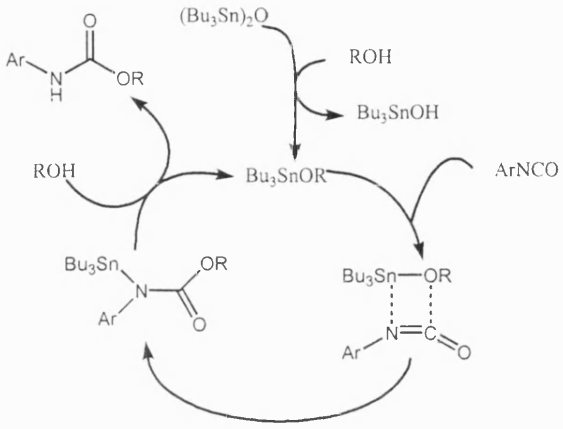

Figure 1.20: Formation of a urethane using a tin catalyst

Often a combination of the tertiary amines and the tin catalysts are used and this combination of their complementary effects leads to increased activity in the reaction.

1.4.3 Titanium alkoxides as catalysts for polyurethane synthesis

There is very little work in the primary literature, which describes the use of titanium alkoxides as polyurethane pre-catalysts. The first mention of reactions between titanium alkoxides and isocyanates was reported by Burger in 1964[40] when he observed by infra red spectroscopy that simple titanium alkoxides form 1:1 or 1:2 adducts with some isocyanates. This work was developed by Meth-Cohn et al.[41] who showed that a wide number of isocyanates react rapidly and exothermically at 0°C with titanium alkoxides to give the expected insertion products.

[39] A.J. Bloodworth and A.G. Davies, *J. Chem. Soc.*, 5238 (1965); R.P. Houghton and A.W. Mulvaney, *J. Organomet. Chem.*, **518**, 21 (1996)
[40] H.Burger, *Monatsh.*, **95**, 671 (1964)
[41] O. Meth-Cohn and D. Thorpe, *J. Chem. Soc. (C)*, 132 (1970)

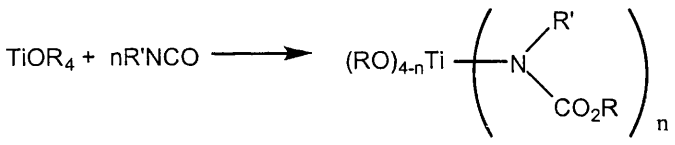

Figure 1.21: Isocyanate insertion into a Ti-O bond

These insertion products will then react with alcohol to give the urethane product.

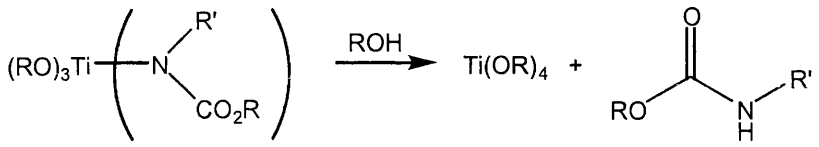

Figure 1.22: Urethane formation

This reactivity was observed for all titanium alkoxides studied, with only the tetra-aryloxides giving particularly slow rates, a factor that was linked to their slow rate of hydrolysis. In addition to this, multiple insertions were observed, giving the isocyanurate ring and, using the correct conditions, a linear nylon type polymer.

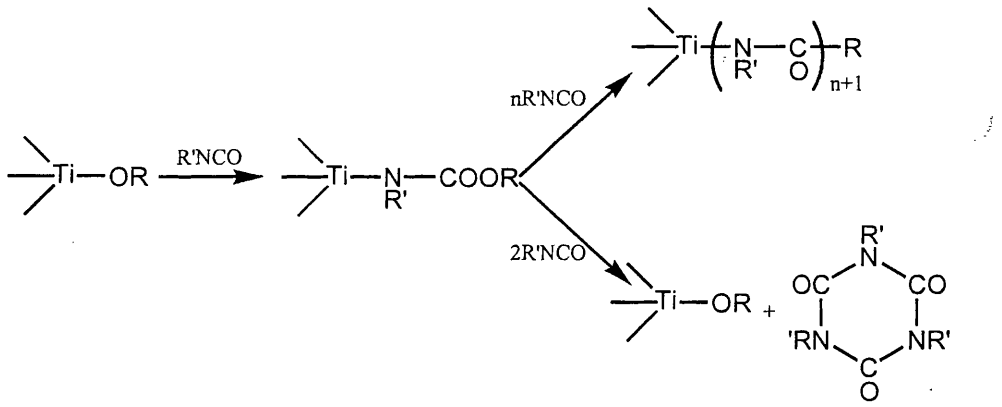

Figure 1.23: Nylon and isocyanurate synthesis

More recently, Errington and co-workers[42] have expanded this work using single crystal X-ray crystallography to structurally characterise the insertion products of the reaction between titanium tetra-isopropoxide and phenyl isocyanate. This work has

[42] S. Wintersgill, R.J. Errington, R.Coxall, M.N.S. Hill and C. Skinner, *unpublished results*

shown that isocyanates insert sequentially with mono-insertion products being formed when reactions are carried out between the alkoxide and one or two equivalents of isocyanate. Further additions of an equivalent of isocyanate to a ratio of four isocyanates per titanium lead to bis-insertion products as shown in figure 1.24 below.

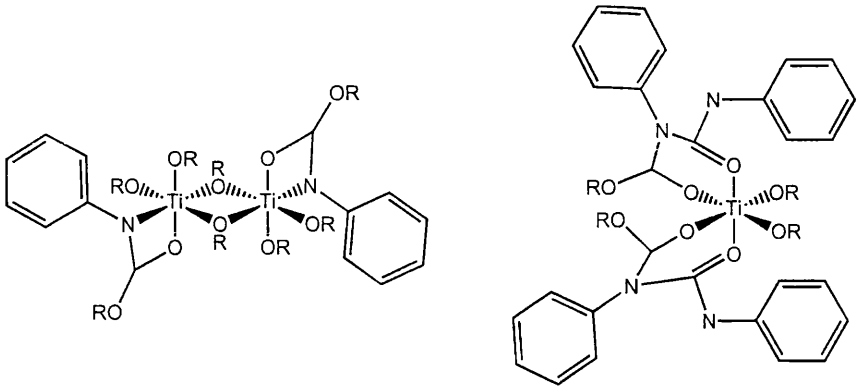

Figure 1.24: Insertion products of titanium isopropoxide and phenyl isocyanate

The work described above for the reactions of isocyanates with titanium alkoxides led us to believe that titanium alkoxide complexes could potentially be a useful class of catalysts for polyurethane synthesis. The current catalysts, which are used for the synthesis of polyurethanes industrially, are often based on toxic tin or mercury species, which are either already subject to environmental legislation, or are likely to be in the future[43]. For this reason there is a drive for the development of novel catalyst systems, which can compete with the current catalysts and if possible give even greater selectivity for the various reaction by-products. We have investigated the use of titanium alkoxide complexes as a new family of non-toxic catalysts, which can perform this role.

The use of homoleptic titanium alkoxides as catalysts for this process has been shown previously in the Davidson group to be unproductive. Although they catalyse the reaction, and it proceeds at a very fast rate, they are highly selective for the synthesis of the cyclic trimer (isocyanurate) shown in figure 1.18 (page 20) which is unfavourable in polyurethane synthesis.

[43] M.A. Champ, *Sci. Total Environ.*, **258**, 21 (2000)

We wished to overcome this problem of selectivity by introducing chelating 'control' ligands into the complex while retaining one or more monodentate alkoxide ligands where polymerisation could take place. It was hoped that by subtle variation of the steric and electronic properties of these 'control' ligands it would be possible to fine-tune the selectivity of the catalyst. Initial work in our group concentrated on the use of a well-defined catalyst species titanium bis-8-hydroxyquinolinate bis-isopropoxide (shown in figure 1.25 below)

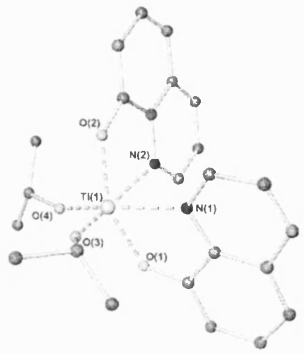

Figure 1.25: 8-Hydroxyquinolinate catalyst

This catalyst was shown to catalyse the urethane formation reaction but only at a much-reduced rate when compared to the homoleptic alkoxide. Because of this drastic lowering of reaction rate and the fact that derivatisation of the 'control' ligand was non-trivial we decided to look at some other, similar, related catalyst families. We wished to base these catalyst families on ligands, which were either commercially available or readily synthesised from simple precursors and also allowed trivial variation of electronic or steric properties. We wished to fulfil these criteria while, where possible, keeping some of the features of the 8-hydroxyquinoline ligand, namely the phenolic group, which should render the control ligands unreactive to isocyanate insertion, and a second nitrogen donor, to allow formation of a stable chelate. The ligands we chose to fulfil these criteria fall in to several categories and some examples are shown in figure 1.26 overleaf.

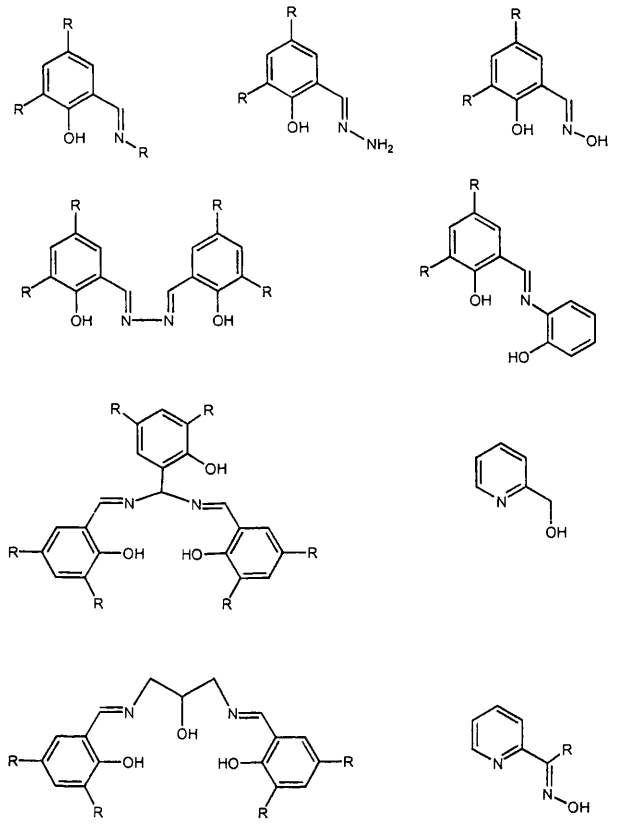

Figure 1.26: Examples of some of the ligand types discussed in this thesis

By far the majority of the ligand families we studied are derivatives of the inexpensive starting material, salicylaldehyde (figure 1.27 overleaf), which is easily derivatised to form a huge range of potential ligands and can be bought with several different R groups on the phenyl ring allowing a huge range of ligands with differing electronic and steric properties and functionalities to be synthesised. In addition the complexes formed between some Schiff bases of salicylaldehyde and $TiCl_4$ have recently been shown to be highly effective catalysts in polyolefin synthesis (see introduction to chapter 4), which may be a good indicator that their alkoxide analogues will be effective as catalysts for our polymerisation reactions.

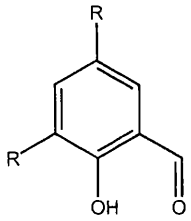

Figure 1.27: Salicylaldehyde, a highly versatile ligand building block

The following two chapters describes the experimental details for the synthesis of a number of the complexes formed between various ligands and TiPT. Chapters 4-8 then discuss the results obtained in these syntheses and describe what structural information we have obtained for our pre-catalysts. This is then followed by the final chapter, which describes our studies into the use of a cross-section of our catalysts in polyurethane synthesis, which is separated into kinetic and selectivity studies.

Chapter 2

General experimental techniques

The following chapter briefly describes the general techniques used during manipulation of the products described in chapters 3-8 of this thesis. The sections describe the inert atmosphere techniques used during the synthesis of the metal complexes and the various methods of analysis, which have been utilised to characterise the products. The chapter does not detail the catalytic screening methodology, which is described in chapter 9 of this thesis.

2.1 Inert atmosphere techniques

Due to the air-sensitive and hygroscopic nature of the complexes studied in this work, it was necessary to employ inert atmosphere techniques in order to facilitate their study. Standard vacuum line techniques (Figure 2.1) were, therefore, used for all synthetic work[1]. Syntheses were performed under an atmosphere of argon from the manifold supply, using pre-dried solvents and, where appropriate, pre-dried starting materials.

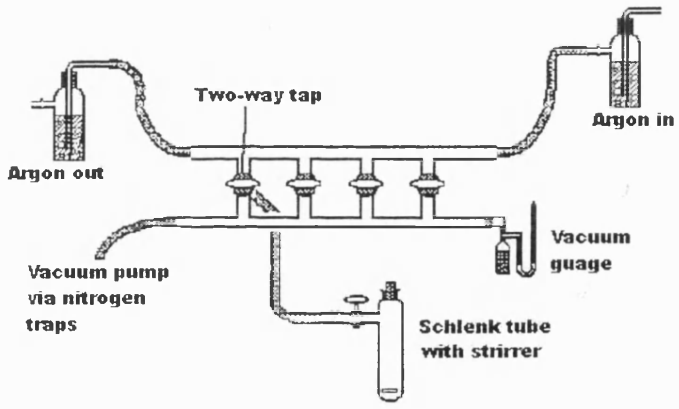

Figure 2.1: Schematic representation of a vacuum line

Reactions were generally carried out in Schlenk tubes (or similar vessels), dried in an oven at 130°C for several hours, evacuated to approximately 10^{-2} Torr three times and flushed with dry argon from the manifold supply. Solids were pre-weighed in a dry, oxygen-free glove box (Figure 2.2) either into an airtight vial (being then introduced under a positive pressure of inert gas) or directly into the Schlenk tube. Air-sensitive and hygroscopic liquid reagents and solvents were introduced via a dry syringe.

[1] R.J. Errington, *'Advanced Practical Inorganic and Metalorganic Chemistry'*, 2nd Edn., Blackie Academic and Professional, London (1997).

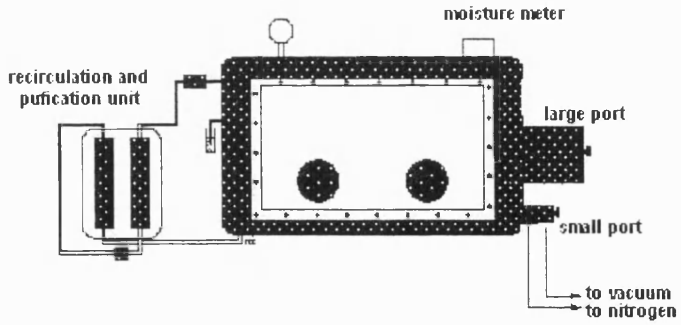

Figure 2.2: Schematic representation of a glove box

Products were isolated in a glove box using filter sticks of varying porosities. The latter were evacuated on a vacuum line and flushed with an inert gas. The separation of desired product and filtrate could then be achieved by inversion of the filtration apparatus, and subsequent separation. Products were dried *in vacuo* before transferral to a glove box for analysis.

Introduction of products to the glove box was through one of its two ports, which must be evacuated and flushed with argon at least three times in order to maintain the inert atmosphere within the box. The moisture and oxygen levels were monitored by meters (moisture levels were maintained between 2 and 4ppm and oxygen levels kept below 10ppm).

Argon in the glove box is constantly recirculated through two purification columns by. Initially, a copper catalyst (BASF Cu catalyst R11) removes oxygen as copper oxide followed by passage through a molecular sieve (BDH 3,16"), which removes moisture.

The purification columns must be occasionally regenerated when they cease to function efficiently, i.e. oxygen and moisture levels become too high. This is achieved by heating the columns to 180 °C. The copper column is treated with a reforming gas (80% N_2, 20% H_2), whilst the molecular sieve is evacuated with a rotary pump - the steam removed being condensed into a cold trap.

2.2 Starting materials and solvents

Starting materials were of the highest quality available. Solvents used (e.g. thf, benzene, hexane, toluene, acetonitrile) were freshly distilled over the appropriate drying agents. Deuterated solvents, used for NMR spectroscopy, were stored over molecular sieves in the glove box or supplied in glass ampoules, which were opened in a glove box as required. They were also, on occasion, distilled over appropriate drying agents (e.g. alkali metal).

Titanium alkoxides were stored in Schlenk tubes under argon and transferred using a dry syringe to the reaction vessel.

2.3 Nuclear magnetic resonance (NMR) spectroscopy

The majority of metal complexes were characterised by both ^{1}H and ^{13}C NMR spectroscopy. The basic spectra were in most cases supplemented by use of proton-proton and proton-carbon correlation experiments, which aided in assignment of the spectra. In addition ^{19}F spectra, variable temperature studies and NOESY experiments were carried out where they were relevant and would aid assignment of structure.

All samples were prepared in a glove box, typically by dissolution of between 1 and 10mg of the sample in a suitable pre-dried deuterated solvent. Suitable protection from air and moisture was provided either by an NMR tube fitted with a Youngs cap or by use of a standard NMR tube fitted with a plastic cap, Teflon tape and plastic film.

Standard ^{1}H NMR spectra were recorded for each of the compounds either on a Varian 400 NMR spectrometer at 400MHz or on a Bruker Avance 300 NMR spectrometer at 300MHz. The ^{13}C spectra were recorded on the same spectrometers at 100 and 75.5 MHz respectively, while the ^{19}F spectra were carried out exclusively on the Varian spectrometer at 376MHz. All chemical shifts are reported relative to TMS; where possible coupling constants have been reported and are quoted in Hz.

2.4 Elemental analysis

Carbon, hydrogen and nitrogen content was determined for nearly all characterised products. These were prepared in the glove box, with the CHN analysis being prepared on between 1 and 2 mg of sample sealed in an aluminium capsule, using an Exeter Analytical Inc. CE-440 Elemental Analyser.

2.5 X-Ray diffraction studies

This technique gives the best, readily available information about solid-state structure. Suitable single crystals (they must be generally no smaller than 0.1 x 0.1 x 0.1 mm^3 and no larger than 0.5 x 0.5 x 0.5 mm^3) were grown in Schlenk tubes under argon atmospheres at various temperatures (-40 to 20 °C).

Due to the air-sensitivity of these crystals they must be carefully treated before undertaking a diffraction study. The method utilised was to coat a suitably sized crystal with perfluorinated ether oil, which is inert to reaction and transparent to the X-rays. A crystal treated in this way may then be mounted onto the goniometer by means of a glass fibre. The oil is frozen by the introduction of cold, nitrogen gas, which also prevents decomposition and fixes the orientation of the crystal.

Collection of data takes place at low temperature (150K in Bath) in order to minimise lattice vibrations and reduce the likelihood of decomposition. Unless otherwise stated, data was collected on a Nonius kappa CCD diffractometer using graphite-monochromated Mo-Kα radiation (λ=0.71074Å).

Chapter 3

Experimental Results

This chapter details the synthesis of all of the titanium complexes discussed in this thesis. The details for each experiment include the relevant, assigned, spectroscopic data where available along with elemental analysis results where obtained. In the cases where single crystal X-ray was possible the relevant parameters are discussed in the following chapters (4-8), together with a summary of the crystallographic data in the appendix and full data including 'cif' files on the accompanying C.D. The experimental details for the metal complexes are separated by chapter, appear in the order in which they appear in the following chapters and are preceded by the ligand syntheses for the compounds in that chapter. Experimental details for the polymerisation studies, which have been conducted, are presented along with the results of these studies in chapter 9.

All metal complex syntheses were carried out under an inert atmosphere utilising the techniques described in chapter 2 with an argon manifold supply. Materials were isolated in a glove box filled with argon. Crystallisation was carried out at room temperature unless otherwise stated. Yields are isolated yields based on titanium. Ligands were synthesised by literature methods, references for which can be found in this chapter.Unless otherwise stated the alkoxide groups in the figures in the following chapter refer to O^iPr groups.

3.1 Experimental data for chapter 4

3.1.1 Ligand synthesis

The following figure shows the ligands, which were synthesised for use in the work described in chapter 4.

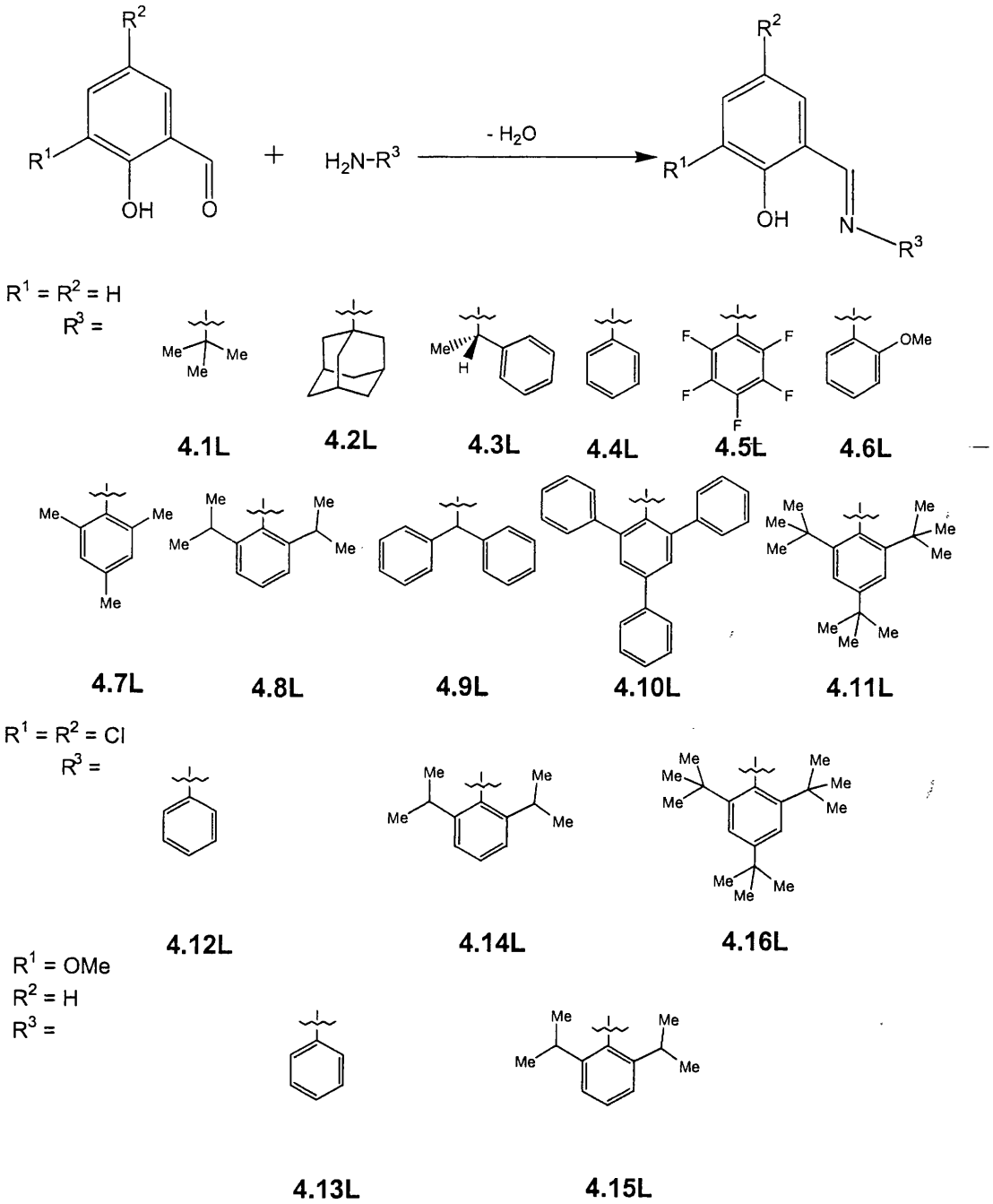

The ligands used in chapter 4

All of the ligands in the figure above were readily prepared by the condensation of the parent salicylaldehyde with commercially available primary amines or aniline derivatives in methanol using standard procedures[1] and isolated as sharp melting white to yellow crystalline solids following recrystallisation in 70-98% yields.

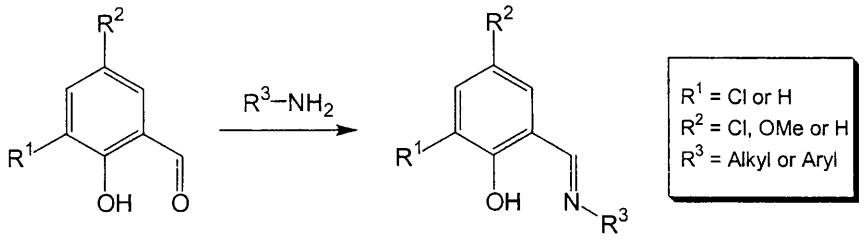

The synthesis of Schiff base ligands

3.1.2 Complex synthesis

Complex 4.1: Complex of *tert*-butyl amine salicylaldimine and TiPT

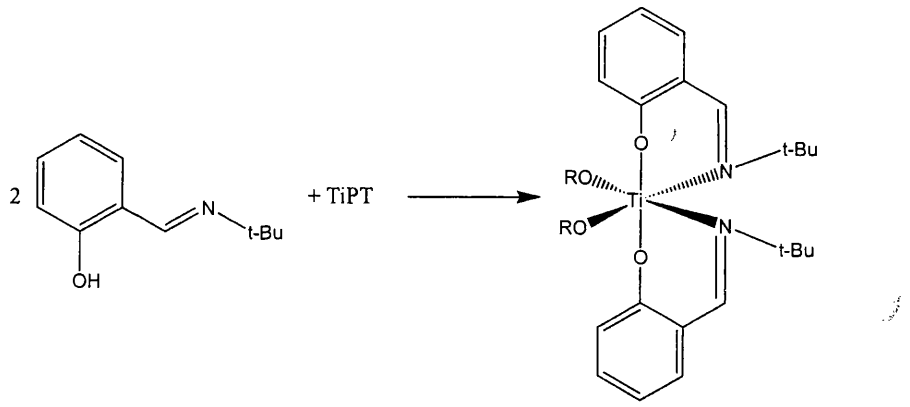

4.1L Complex 4.1

A solution of 0.36g (2 mmol) of ligand 4.1L was prepared in dry toluene (10ml) under an inert atmosphere. To this was added 0.3ml (1mmol) of TiPT to give a yellow solution. This solution was vigorously stirred for two hours at reflux. The solvent was removed *in vacuo* to give a yellow residue. This product was suspended in hexane and toluene added until dissolution occurred on warming. Standing at room temperature yielded a microcrystalline yellow product.

Yield = 0.36g (70.2%)
Melting Point = 77-81°C

[1] C. Wang, S. Fredrich, T.R. Younkin, R.T. Li, R.H. Grubs, D.A. Bansleben and M.W. Day, *Organometallics*, **17**, 3149 (1999) and references therein.

^{1}H NMR Spectrum: 300MHz, solvent $CDCl_3$

δ/ppm	Integral	Multiplicity	Coupling/Hz	Assignment
1.17	12H	broad singlet		Isopropyl C**H**$_3$
1.36	18H	singlet		*t*-Butyl C**H**$_3$
4.62	2H	septet	6.0	Isopropyl C**H**
6.60-6.85	4H	broad multiplet		Aromatic C**H**
7.18-7.26	2H	broad multiplet		Aromatic C**H**
7.27-7.45	2H	broad multiplet		Aromatic C**H**
8.34	2H	singlet		Imine C**H**

$^{13}C\{^{1}H\}$ NMR Spectrum: 75.5MHz, solvent $CDCl_3$

δ/ppm	Assignment
25.8	Isopropyl **C**H$_3$
30.9	t-Butyl **C**H$_3$
61.4	t-Butyl **C**(CH$_3$)
77.6	Isopropyl **C**H
118.5, 119.3, 123.8, 132.5, 133.2	Aromatic
160.0	Aromatic *ipso* to phenol
166.5	Imine **C**H

Elemental Analysis: $C_{28}H_{42}N_2O_4Ti$

	C	H	N
Calculated %	64.9	8.10	5.40
Observed %	65.1	8.17	5.41

Complex 4.2: Complex of adamantyl amine salicylaldimine and TiPT

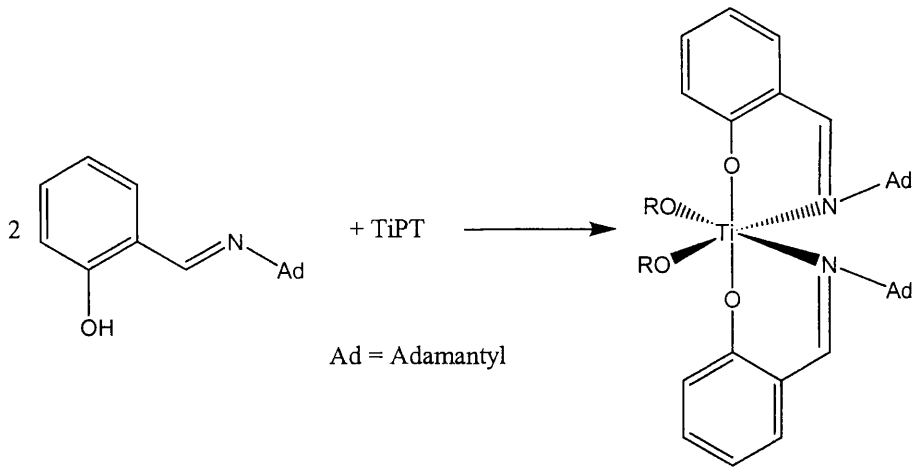

4.2L Complex 4.2

A solution of 0.45g (2 mmol) of ligand 4.2L was prepared in dry toluene (10ml) under an inert atmosphere. To this was added 0.3ml (1mmol) of TiPT to give a yellow solution. This solution was vigorously stirred for two hours at reflux. The solvent was removed *in vacuo* to give a yellow residue. This product was suspended in hexane and toluene added until dissolution occurred on warming. Standing at room temperature yielded a yellow powder.

Yield = 0.38g (57.0%)
Melting Point = 102-104°C

^{1}H NMR Spectrum: 300MHz, solvent $CDCl_3$

δ/ppm	Integral	Multiplicity	Coupling/Hz	Assignment
1.22	12H	broad singlet		Isopropyl C**H**$_3$
1.53-2.09	30H	broad multiplet		Adamantyl C**H** and C**H**$_3$
4.69	2H	broad multiplet		Isopropyl C**H**
6.67-6.82	4H	multiplet		Aromatic C**H**
7.14-7.28	2H	multiplet		Aromatic C**H**
7.32-7.46	2H	multiplet		Aromatic C**H**
8.30	2H	singlet		Imine C**H**

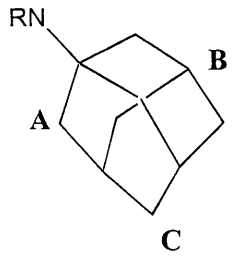

$^{13}C\{^{1}H\}$ NMR Spectrum: 75.5MHz, solvent $CDCl_3$

δ/ppm	**Assignment**
26.0	Isopropyl **C**H_3
30.2	Adamantyl **C**H (**B**)
36.7	Adamantyl **C**H_2 (**C**)
43.3	Adamantyl **C**H_2 (**A**)
78.4	Isopropyl **C**H
117.8, 118.7, 119.4, 131.7, 132.5	Aromatic
160.4	Aromatic *ipso* to phenol
162.9	Imine **C**H

Elemental Analysis: $C_{40}H_{54}N_2O_4Ti$

	C	H	N
Calculated %	71.2	8.01	4.15
Observed %	71.6	8.01	4.09

Complex 4.3: Complex of 1-amino-1-phenyl-ethane salicylaldimine and TiPT

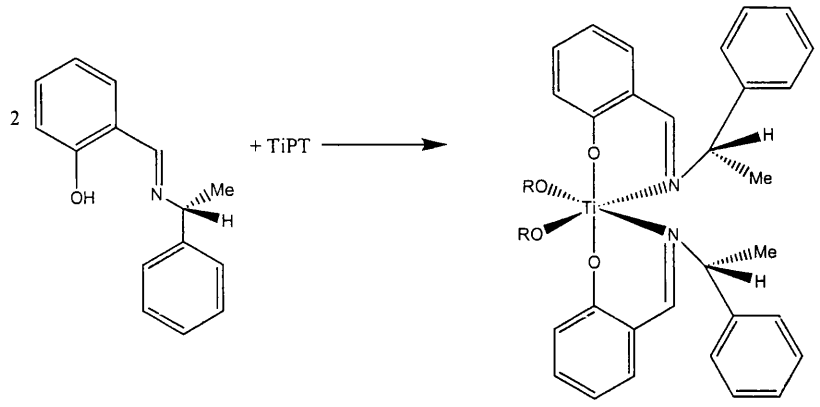

4.3L Complex 4.3

A solution of 0.45g (2 mmol) of ligand 4.3L was prepared in dry toluene (20ml) under an inert atmosphere. To this was added 0.3ml (1mmol) of TiPT to give a yellow solution. This solution was vigorously stirred for two hours at reflux. The solvent was removed *in vacuo* to give a yellow residue. This product was recrystallised from a minimum of toluene to give a microcrystalline yellow product which was washed with hexane.

Yield = 0.44g (71.6%)
Melting Point = 115-117°C

^{1}H NMR Spectrum: 300MHz, solvent $CDCl_3$

δ/ppm	Integral	Multiplicity	Coupling/Hz	Assignment
1.02	12H	singlet		Isopropyl CH_3
1.45	6H	broad singlet		Ligand CH_3
4.67	2H	septet	6.0	Isopropyl CH
5.29	2H	broad multiplet		Ligand CH
6.64	2H	multiplet		Aromatic CH
6.79	2H	multiplet		Aromatic CH
6.97	2H	doublet of doublets	7.5, 1.5	Aromatic CH
7.06-7.15	10H	broad multiplet		Aromatic CH
7.23	2H	multiplet		Aromatic CH

7.88	2H	singlet		Imine C**H**

$^{13}C\{^{1}H\}$ NMR Spectrum: 75.5MHz, solvent $CDCl_3$

δ/ppm	**Assignment**
21.6	Ligand CH_3
25.7	Isopropyl CH_3
62.5	Ligand **C**H
78.6	Isopropyl **C**H
117.5, 119.4, 123.0, 126.9, 127.6, 128.9, 128.9, 134.2, 134.5	Aromatic
163.7	Aromatic *ipso* to phenol
164.7	Imine **C**H

Elemental Analysis: $C_{36}H_{42}N_2O_4Ti$

	C	H	N
Calculated %	70.4	6.84	4.56
Observed %	69.6	6.84	4.42

Complex 4.4: Complex of aniline salicylaldimine and TiPT

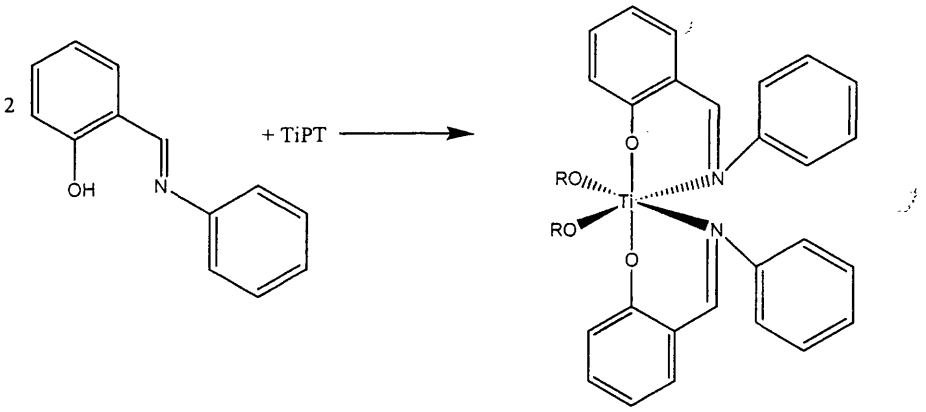

4.4L Complex 4.4

A solution of 0.39g (2 mmol) of ligand 4.4L was prepared in dry toluene (20ml) under an inert atmosphere. To this was added 0.3ml (1mmol) of TiPT to give a yellow solution. This solution was vigorously stirred for two hours at reflux. The solvent was removed *in vacuo* to give a yellow residue. This product was recrystallised from a minimum of toluene to give a crystalline yellow product, which was washed with hexane.

Yield = 0.38g (68.2%)
Melting Point = 87-90°C

^{1}H NMR Spectrum: 300MHz, solvent $CDCl_3$

δ/ppm	**Integral**	**Multiplicity**	**Coupling/Hz**	**Assignment**
1.23	12H	singlet		Isopropyl C**H**$_3$
4.90	2H	septet	6.0	Isopropyl C**H**
6.14	2H	multiplet		Aromatic C**H**
6.49	2H	multiplet		Aromatic C**H**
6.78-7.04	14H	multiplet		Aromatic C**H**
7.87	2H	singlet		Imine C**H**

^{13}C{^{1}H} NMR Spectrum: 75.5MHz, solvent $CDCl_3$

δ/ppm	**Assignment**
26.0	Isopropyl **C**H$_3$
79.1	Isopropyl **C**H
117.8, 119.8, 123.1, 126.2, 128.4, 134.3, 135.3, 154.3	Aromatic
163.7	Aromatic *ipso* to phenol
166.3	Imine **C**H

Elemental Analysis: $C_{32}H_{34}N_2O_4Ti$

	C	H	N
Calculated %	68.8	6.09	5.01
Observed %	68.5	6.13	4.98

Complex 4.5: Complex of penta-fluoroaniline salicylaldimine and TiPT

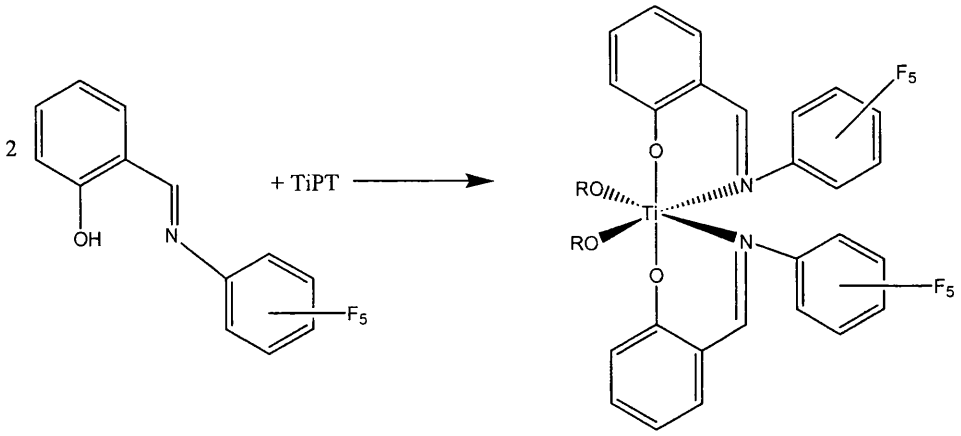

4.5L Complex 4.5

A solution of 0.57g (2 mmol) of ligand 4.5L was prepared in dry toluene (10ml) under an inert atmosphere. To this was added 0.3ml (1mmol) of TiPT to give a yellow solution. This solution was vigorously stirred for two hours at reflux. The solvent was removed *in vacuo* to give a yellow residue. This product was suspended in hexane and toluene added until dissolution occurred on warming. Standing at room temperature yielded a crystalline yellow product, which was washed with hexane.

Yield = 0.60g (80.9%)
Melting Point = 143-147°C

^{1}H NMR Spectrum: 300MHz, solvent $CDCl_3$

δ/ppm	Integral	Multiplicity	Coupling/Hz	Assignment
1.11	12H	singlet		Isopropyl C**H**$_3$
4.77	2H	septet	5.8	Isopropyl C**H**
6.46	2H	multiplet		Aromatic C**H**
6.76	2H	multiplet		Aromatic C**H**
7.20	2H	doublet of doublets	8.0, 1.6	Aromatic C**H**
7.34	2H	multiplet		Aromatic C**H**
8.07	2H	singlet		Imine C**H**

$^{13}C\{^{1}H\}$ NMR Spectrum: 75.5MHz, solvent $CDCl_3$

δ/ppm	Assignment
25.5	Isopropyl **C**H_3
80.7	Isopropyl **C**H
118.0, 118.9, 121.2, 135.0, 136.5, 156.5	Aromatic
164.9	Aromatic *ipso* to phenol
171.8	Imine **C**H

^{19}F NMR Spectrum: 376 MHz, solvent $CDCl_3$

δ/ppm	Multiplicity	Coupling/Hz	Assignment
-148.3	multiplet		Aromatic C**F**
-160.07	triplet	21.0	Aromatic C**F**
-164.4	multiplet		Aromatic C**F**

Elemental Analysis: $C_{32}H_{24}F_{10}N_2O_4Ti$

	C	H	N
Calculated %	52.1	3.28	3.79
Observed %	51.7	3.31	3.78

Complex 4.6: Complex of 2-methoxy aniline salicylaldimine and TiPT

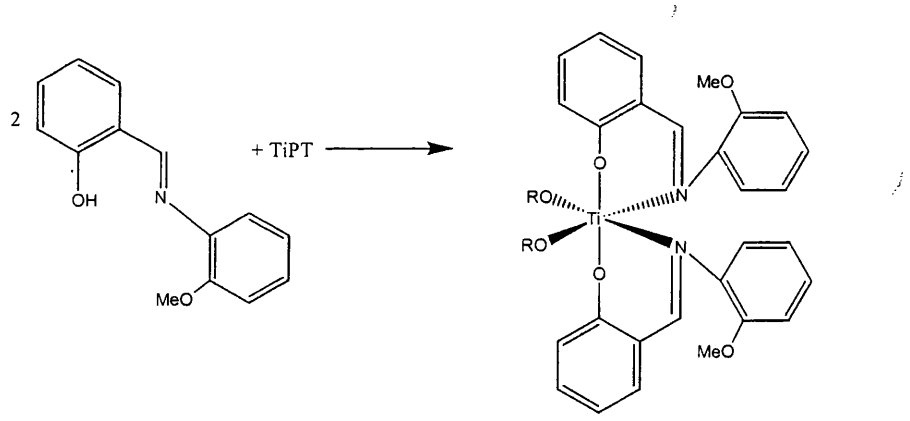

4.6L Complex 4.6

A solution of 0.45g (2 mmol) of ligand 4.6L was prepared in dry toluene (10ml) under an inert atmosphere. To this was added 0.3ml (1mmol) of TiPT to give a yellow solution. This solution was vigorously stirred for two hours at reflux. The solvent was removed *in vacuo* to give a yellow residue. This product was recrystallised from a minimum of toluene to give a microcrystalline yellow product which was washed with hexane.

Yield = 0.46g (74.2%)

Melting Point = 172-175°C

^{1}H NMR Spectrum: 300MHz, solvent $CDCl_3$

δ/ppm	Integral	Multiplicity	Coupling/Hz	Assignment
1.19	12H	singlet		Isopropyl C**H**$_3$
3.38	6H	singlet		O**CH**$_3$
4.88	2H	septet	6.0	Isopropyl C**H**
5.99-6.20	2H	multiplet		Aromatic C**H**
6.20-6.28	2H	multiplet		Aromatic C**H**
6.36-6.47	2H	multiplet		Aromatic C**H**
6.62-6.97	8H	multiplet		Aromatic C**H**
7.43-7.56	2H	multiplet		Aromatic C**H**
7.89	2H	singlet		Imine C**H**

^{13}C{^{1}H} NMR Spectrum: 75.5MHz, solvent $CDCl_3$

δ/ppm	Assignment
26.8	Isopropyl **C**H$_3$
56.0	O**C**H$_3$
79.5	Isopropyl **C**H
111.7, 117.7, 119.8, 120.6, 123.8, 126.9, 127.8, 134.5, 135.2, 143.6, 151.6	Aromatic
163.9	Aromatic *ipso* to phenol
169.7	Imine **C**H

Elemental Analysis: $C_{34}H_{38}N_2O_6Ti$

	C	H	N
Calculated %	66.0	6.15	4.53
Observed %	66.5	6.09	4.45

Complex 4.7: Complex of 2,4,6-tri-methyl aniline salicylaldimine and TiPT

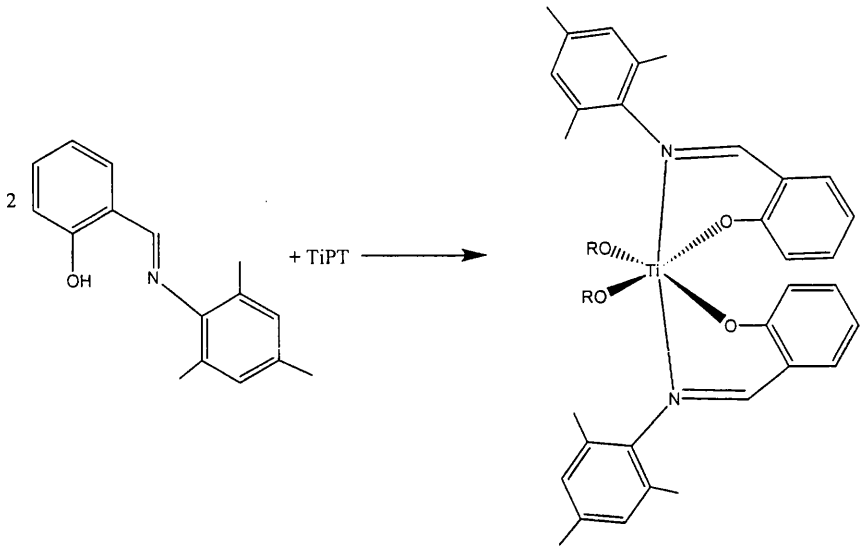

4.7L Complex 4.7

A solution of 0.48g (2 mmol) of ligand 4.7L was prepared in dry toluene (10ml) under an inert atmosphere. To this was added 0.3ml (1mmol) of TiPT to give a yellow solution. This solution was vigorously stirred for two hours at reflux. The solvent was removed *in vacuo* to give a yellow residue. This product was suspended in hexane and toluene added until dissolution occurred on warming. Standing at room temperature yielded a crop of yellow blocks, which were washed with hexane.

Yield = 0.37g (57.8%)
Melting Point = 151-153°C

^{1}H NMR Spectrum: 300MHz, solvent $CDCl_3$

δ/ppm	Integral	Multiplicity	Coupling/Hz	Assignment
0.38	12H	doublet	12.0	Isopropyl C**H**$_3$
2.21	3H	singlet		*para* C**H**$_3$ on mesityl
2.38	6H	singlet		*ortho* C**H**$_3$ on mesityl
3.45	2H	septet	9.0	Isopropyl C**H**
6.52	2H	multiplet		Aromatic C**H**
6.59-6.62	2H	multiplet		Aromatic C**H**
6.83	4H	singlet		Aromatic *meta* C**H** on mesityl
7.08	2H	doublet of doublets	7.8, 1.8	Aromatic C**H**

7.22	2H	multiplet		Aromatic C**H**
7.88	2H	singlet		Imine C**H**

$^{13}C\{^{1}H\}$ NMR Spectrum: 75.5MHz, solvent $CDCl_3$

δ/ppm	**Assignment**
19.8	*ortho* **C**H_3
21.1	*para* **C**H_3
24.9	Isopropyl **C**H_3
77.7	Isopropyl **C**H
115.7, 119.9, 121.7, 129.0, 131.5, 134.6, 135.4, 135.7, 151.7	Aromatic
167.8	Aromatic *ipso* to phenol
169.2	Imine **C**H

Elemental Analysis: $C_{38}H_{46}N_2O_4Ti$

	C	H	N
Calculated %	71.0	7.17	4.36
Observed %	71.3	7.15	4.32

Complex 4.8: Complex of 2,4-di-isopropyl aniline salicylaldimine and TiPT

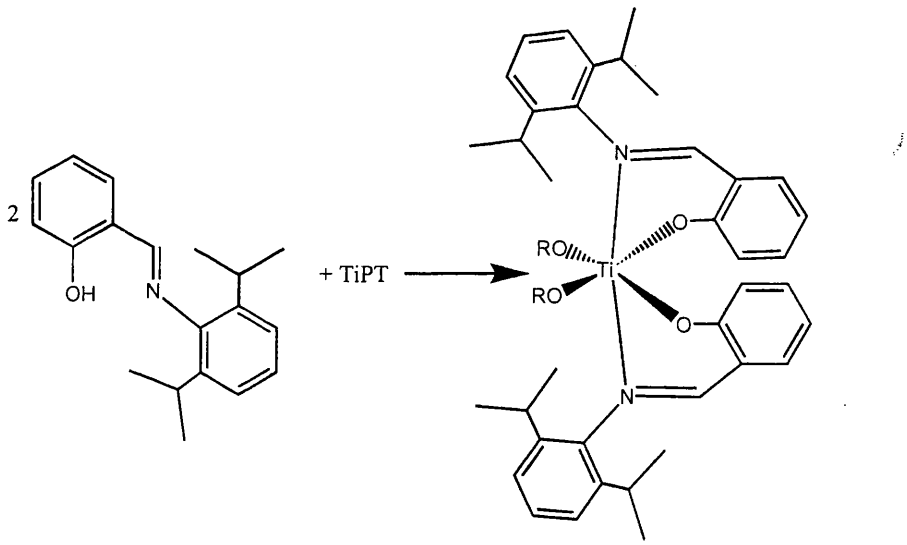

4.8L Complex 4.8

A solution of 0.56g (2 mmol) of ligand 4.8L was prepared in dry toluene (10ml) under an inert atmosphere. To this was added 0.3ml (1mmol) of TiPT to give a yellow solution. This solution was vigorously stirred for two hours at reflux. The solvent was

removed *in vacuo* to give a yellow residue. This product was recrystallised from a minimum of toluene to give a crop of yellow blocks, which were washed with hexane.

Yield = 0.60g (83.3%)
Melting Point = 162-166°C

^{1}H NMR Spectrum: 300MHz, solvent $CDCl_3$

δ/ppm	**Integral**	**Multiplicity**	**Coupling/Hz**	**Assignment**
0.51	12H	broad singlet		Isopropoxide **CH_3**
1.25	24H	broad singlet		Isopropyl aniline **CH_3**
3.77	2H	septet	7.0	Isopropoxide **CH**
3.87	4H	septet	9.2	Isopropyl aniline **CH**
6.62-6.65	4H	multiplet		Aromatic **CH**
7.19-7.27	8H	multiplet		Aromatic **CH**
7.35-7.39	2H	multiplet		Aromatic **CH**
8.05	2H	singlet		Imine **CH**

^{13}C{^{1}H} NMR Spectrum: 75.5MHz, solvent $CDCl_3$

δ/ppm	**Assignment**
25.3	Isopropoxide **CH_3**
27.5	Isopropyl aniline **CH**
27.5	Isopropyl aniline **CH_3**
77.8	Isopropoxide **CH**
115.6, 120.0, 124.2, 124.2, 126.9, 135.0, 136.0, 142.2, 152.2	Aromatic
167.5	Aromatic *ipso* to phenol
169.5	Imine **CH**

Elemental Analysis: $C_{44}H_{58}N_2O_4Ti$

	C	H	N
Calculated %	72.7	8.00	3.86
Observed %	72.3	8.01	3.76

Complex 4.9: Complex of diphenyl-methylamine salicylaldimine and TiPT

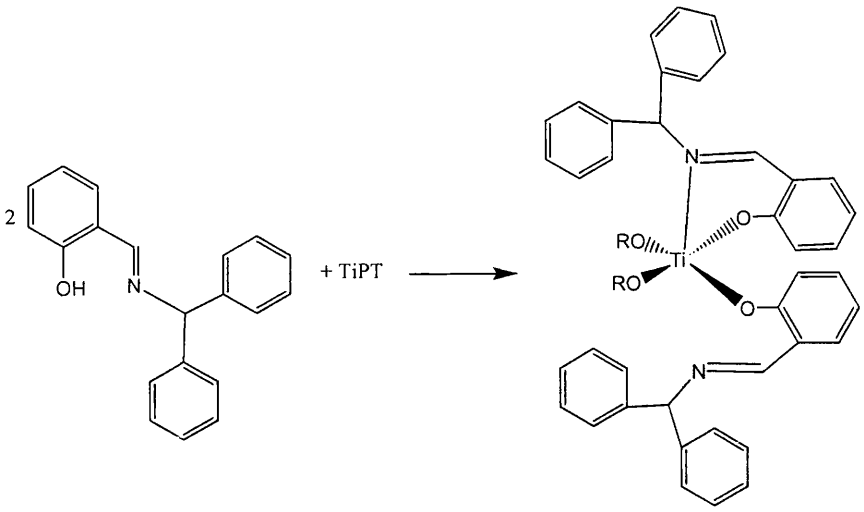

4.9L Complex 4.9

A solution of 0.57g (2 mmol) of ligand 4.9L was prepared in dry toluene (10ml) under an inert atmosphere. To this was added 0.3ml (1mmol) of TiPT to give a yellow solution. This solution was vigorously stirred for two hours at reflux. The solvent was removed *in vacuo* to give a yellow residue. This product was recrystallised from a minimum of toluene to give a crop of yellow blocks, which were washed with hexane.

Yield = 0.49g (66.2%)
Melting Point = 122-124 °C

^{1}H NMR Spectrum: 300MHz, solvent $CDCl_3$

δ/ppm	Integral	Multiplicity	Coupling/Hz	Assignment
0.92	12H	doublet	6.4	Isopropyl C**H**$_3$
4.50	2H	septet	8.9	Isopropyl C**H**
6.44	2H	singlet		C**H**Ph$_2$
6.57-6.60	2H	multiplet		Aromatic C**H**
6.72-6.73	2H	multiplet		Aromatic C**H**
6.82-6.84	4H	multiplet		Aromatic C**H**
7.02-7.27	20H	multiplet		Aromatic C**H**
7.79	2H	singlet		Imine C**H**

$^{13}C\{^{1}H\}$ NMR Spectrum: 75.5MHz, solvent $CDCl_3$

δ/ppm	Assignment
24.3	Isopropyl **C**H_3
70.2	N-**C**HPh_2
77.8	Isopropyl **C**H
115.9, 118.2, 121.3, 125.8, 126.9, 128.1, 133.1, 139.9	Aromatic
162.6	Aromatic *ipso* to phenol
166.3	Imine **C**H

Elemental Analysis: $C_{46}H_{46}N_2O_4Ti$

	C	H	N
Calculated %	74.8	6.23	3.79
Observed %	74.7	6.20	3.78

Complex 4.10: Complex of 2,4,6-triphenylaniline salicylaldimine and TiPT

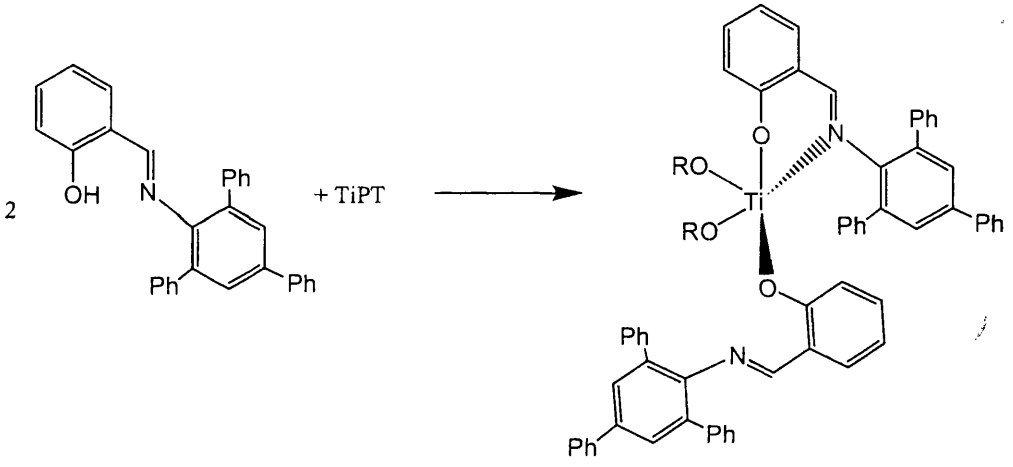

4.10L Complex 4.10

A solution of 0.85g (2 mmol) of ligand 4.10L was prepared in dry toluene (10ml) under an inert atmosphere. To this was added 0.3ml (1mmol) of TiPT to give a yellow solution. This solution was vigorously stirred for two hours at reflux. The solvent was removed *in vacuo* to give a yellow residue. This product was recrystallised from a minimum of toluene to give a crop of yellow blocks, which were washed with hexane.

Yield = 0.59g (58.4%)
Melting Point = 115-119°C

^{1}H NMR Spectrum: 300MHz, solvent $CDCl_3$

δ/ppm	**Integral**	**Multiplicity**	**Coupling/Hz**	**Assignment**
0.70	12H	doublet	6.4	Isopropyl C**H**$_3$
4.14	2H	septet	9.0	Isopropyl C**H**
6.3-7.7	42H	multiplet		Aromatic C**H**
8.29	2H	singlet		Imine C**H**

$^{13}C\{^{1}H\}$ NMR Spectrum: 75.5MHz, solvent $CDCl_3$

δ/ppm	**Assignment**
25.6	Isopropyl **C**H$_3$
80.6	Isopropyl **C**H
119.1, 120.2, 125.7, 127.2, 127.4, 127.5, 127.7, 128.3, 128.5, 129.3, 130.3, 130.5, 135.3, 138.3, 140.1, 150.2 –	Aromatic —
164.3	Aromatic *ipso* to phenol
165.9	Imine **C**H

Elemental Analysis: $C_{68}H_{58}N_2O_4Ti$

	C	H	N
Calculated %	80.5	5.71	2.76
Observed %	80.4	5.73	2.73

Complex 4.11: Complex of 2,4,6-tri-*tert*-butyl-aniline salicylaldimine and TiPT

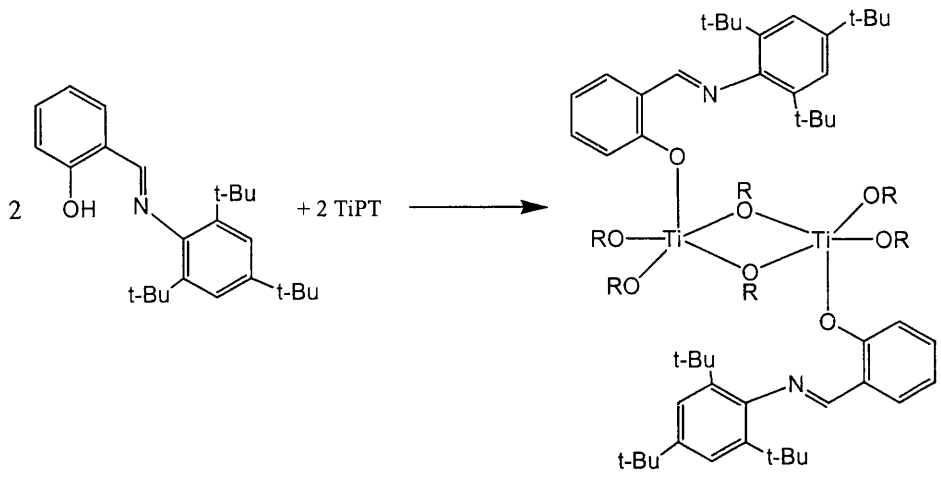

4.11L

Complex 4.11

A solution of 0.37g (1 mmol) of ligand 4.11L was prepared in dry toluene (10ml) under an inert atmosphere. To this was added 0.3ml (1mmol) of TiPT to give a yellow solution. This solution was vigorously stirred for two hours at reflux. The solvent was removed *in vacuo* to give a yellow residue. This product was recrystallised from a minimum of hexane to give a crop of yellow blocks.

Yield = 0.48g (81.7%)
Melting Point = 122-125°C

^{1}H NMR Spectrum: 300MHz, solvent $CDCl_3$

δ/ppm	**Integral**	**Multiplicity**	**Coupling/Hz**	**Assignment**
0.99	36H	doublet	9.0	Isopropyl C**H**$_3$
1.24	18H	singlet		*para t*-Butyl C**H**$_3$
1.27	36H	singlet		*ortho t*-Butyl C**H**$_3$
4.43	6H	septet	6.3	Isopropyl C**H**
6.80-6.94	4H	multiplet		Aromatic C**H**
7.11-7.38	4H	multiplet		Aromatic C**H**
7.96-8.14	4H	multiplet		Aromatic C**H**
8.56	2H	singlet		Imine C**H**

$^{13}C\{^{1}H\}$ NMR Spectrum: 75.5MHz, solvent $CDCl_3$

δ/ppm	**Assignment**
26.6	Isopropyl **C**H_3
31.9	*ortho t*-Butyl **C**H_3
32.5	*para t*-Butyl **C**H_3
35.0	*ortho t*-Butyl **C**$(CH_3)_3$
36.4	*para t*-Butyl **C**$(CH_3)_3$
77.6	Isopropyl **C**H
120.9, 121.9, 122.5, 127.8, 132.6, 138.9, 141.2, 151.9, 158.4	Aromatic
165.1	Aromatic *ipso* to phenol
168.2	Imine **C**H

Elemental Analysis: $C_{68}H_{110}N_2O_8Ti_2$

	C	H	N
Calculated %	69.3	9.34	2.38
Observed %	69.0	9.18	2.39

Complex 4.12: Complex of aniline dichloro-salicylaldimine and TiPT

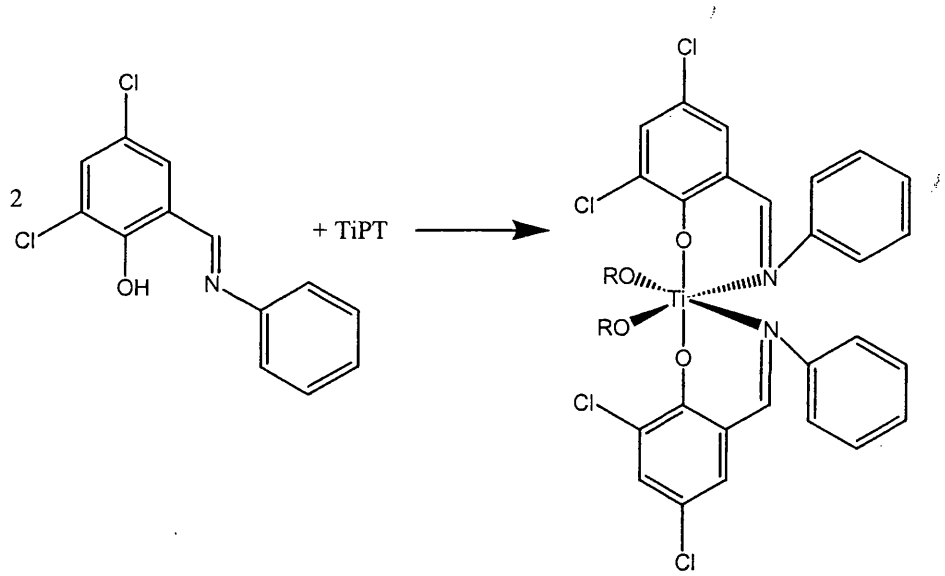

4.12L Complex 4.12

A solution of 0.53g (2 mmol) of ligand 4.12L was prepared in dry toluene (20ml) under an inert atmosphere. To this was added 0.3ml (1mmol) of TiPT to give a yellow solution. This solution was vigorously stirred for two hours at reflux. The solvent was removed *in vacuo* to give a yellow residue. This product was recrystallised from a

minimum of toluene to give a crystalline yellow product, which was washed with hexane.

Yield = 0.42g (60.3%)
Melting Point = 180-183°C

^{1}H NMR Spectrum: 300MHz, solvent $CDCl_3$

δ/ppm	**Integral**	**Multiplicity**	**Coupling/Hz**	**Assignment**
0.82	12H	singlet		Isopropyl C**H**$_3$
4.90	2H	septet	6.0	Isopropyl C**H**
6.75-7.52	14H	multiplet		Aromatic C**H**
7.75	2H	singlet		Imine C**H**

$^{13}C\{^{1}H\}$ NMR Spectrum: 75.5MHz, solvent $CDCl_3$

δ/ppm	**Assignment**
26.0	Isopropyl **C**H$_3$
80.8	Isopropyl **C**H
120.9, 123.4, 125.3, 126.6, 128.7, 131.6, 134.3	Aromatic
164.6	Imine **C**H

Elemental Analysis: $C_{32}H_{30}N_2O_4TiCl_4$

	C	H	N
Calculated %	55.3	4.32	4.03
Observed %	64.5	4.44	4.22

Complex 4.13: Complex of aniline methoxy-salicylaldimine and TiPT

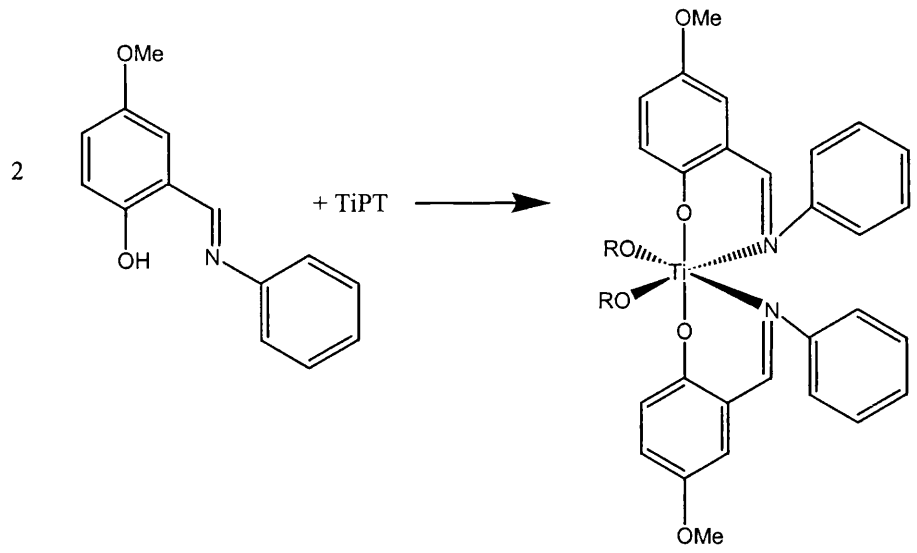

4.13L Complex 4.13

A solution of 0.45g (2 mmol) of ligand 4.13L was prepared in dry toluene (20ml) under an inert atmosphere. To this was added 0.3ml (1mmol) of TiPT to give a yellow solution. This solution was vigorously stirred for two hours at reflux. The solvent was removed *in vacuo* to give a yellow residue. This product was suspended in hexane and toluene added until dissolution occurred on warming. Standing at room temperature yielded a crystalline yellow product, which was washed with hexane.

Yield = 0.38g (61.9%)
Melting Point = 122-126°C

^{1}H NMR Spectrum: 300MHz, solvent $CDCl_3$

δ/ppm	Integral	Multiplicity	Coupling/Hz	Assignment
1.21	12H	broad singlet		Isopropyl C**H**$_3$
3.62	6H	singlet		OC**H**$_3$
4.85	2H	septet	5.8	Isopropyl C**H**
5.85-7.70	16H	multiplet		Aromatic C**H**
7.73	2H	singlet		Imine C**H**

^{13}C{^{1}H} NMR Spectrum: 75.5MHz, solvent $CDCl_3$

δ/ppm	Assignment
26.0	Isopropyl **C**H$_3$

56.4	OCH_3
78.7	Isopropyl **C**H
115.7, 120.2, 122.1, 123.1, 123.6, 125.9, 128.0, 151.3, 154.0	Aromatic
165.5	Imine **C**H

Elemental Analysis: $C_{34}H_{38}N_2O_6Ti$

	C	H	N
Calculated %	66.02	6.19	4.53
Observed %	66.20	6.16	4.40

Complex 4.14: Complex of 2,4-di-isopropyl aniline 2,4-dichloro-salicylaldimine and TiPT

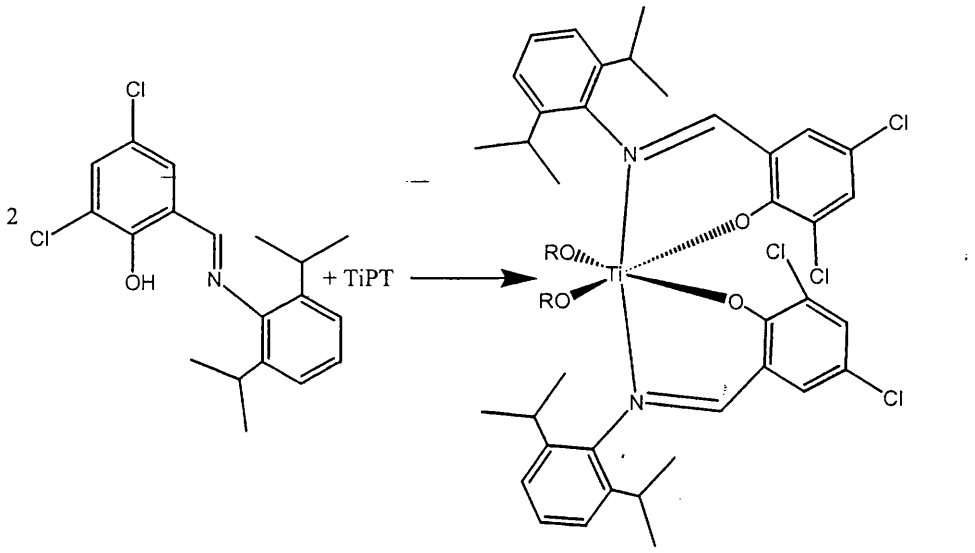

4.14L Complex 4.14

A solution of 0.67g (2 mmol) of ligand 4.14L was prepared in dry toluene (10ml) under an inert atmosphere. To this was added 0.3ml (1mmol) of TiPT to give a yellow solution. This solution was vigorously stirred for two hours at reflux. The solvent was removed *in vacuo* to give a yellow residue. This product was suspended in hexane and toluene added until dissolution occurred on warming. Standing at room temperature yielded a crop of yellow blocks, which were washed with hexane.

Yield = 0.28g (32.4%)
Melting Point = 141-147°C

^{1}H NMR Spectrum: 300MHz, solvent $CDCl_3$

δ/ppm	**Integral**	**Multiplicity**	**Coupling/Hz**	**Assignment**
0.70	12H	broad doublet		Isopropoxide **C**H_3

1.05	24H	broad doublet		Isopropyl aniline C**H**$_3$
3.45	4H	broad septet		Isopropyl aniline C**H**
4.35	2H	broad septet		Isopropoxide C**H**
6.80-7.42	10H	multiplet		Aromatic C**H**
7.95	2H	singlet		Imine C**H**

$^{13}C\{^{1}H\}$ NMR Spectrum: 75.5MHz, solvent $CDCl_3$

δ/ppm	**Assignment**
23.2	Isopropoxide **C**H$_3$
24.7	Isopropyl aniline **C**H
26.4	Isopropyl aniline **C**H$_3$
78.3	Isopropoxide **C**H
120.9, 122.7, 123.7, 125.4, 133.1, 139.8, 149.6	Aromatic
159.3	Imine **C**H

Elemental Analysis: $C_{44}H_{56}N_2O_4Ti$

	C	H	N
Calculated %	61.1	6.30	3.24
Observed %	55.9	5.69	3.02

Complex 4.15: Complex of 2,4-di-isopropyl-aniline 4-methoxysalicylaldimine and TiPT

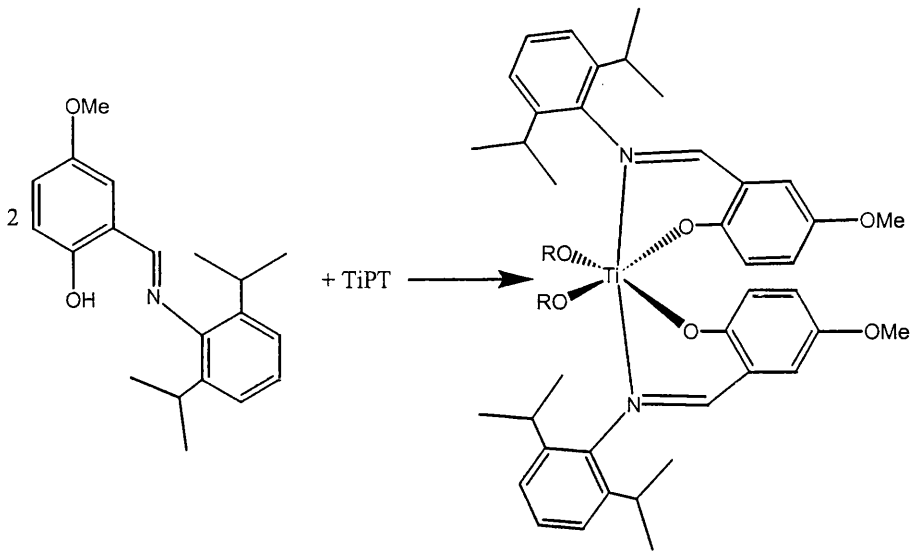

4.15L Complex 4.15

A solution of 0.60g (2 mmol) of ligand 4.15L was prepared in dry toluene (10ml) under an inert atmosphere. To this was added 0.3ml (1mmol) of TiPT to give a yellow solution. This solution was vigorously stirred for two hours at reflux. The solvent was removed *in vacuo* to give a yellow residue. This product was suspended in hexane and toluene added until dissolution occurred on warming. Standing at room temperature yielded a crop of yellow blocks, which were washed with hexane.

Yield = 0.46g (57.8%)
Melting Point = 148-152°C

^{1}H NMR Spectrum: 300MHz, solvent $CDCl_3$

δ/ppm	Integral	Multiplicity	Coupling/Hz	Assignment
0.82	12H	broad doublet		Isopropoxide **CH_3**
1.20	24H	broad doublet		Isopropyl aniline **CH_3**
3.32	6H	singlet		**OCH_3**
3.68	4H	broad septet		Isopropyl aniline **CH**
4.40	2H	broad septet		Isopropoxide **CH**
6.20-7.45	12H	multiplet		Aromatic **CH**
7.95	2H	singlet		Imine **CH**

Elemental Analysis: $C_{46}H_{62}N_2O_6Ti$

	C	H	N
Calculated %	70.2	7.89	3.56
Observed %	70.2	7.84	3.65

Complex 4.16: Complex of 2,4,6-tri-*tert*-butyl-aniline 2,4-dichloro-salicylaldimine and TiPT

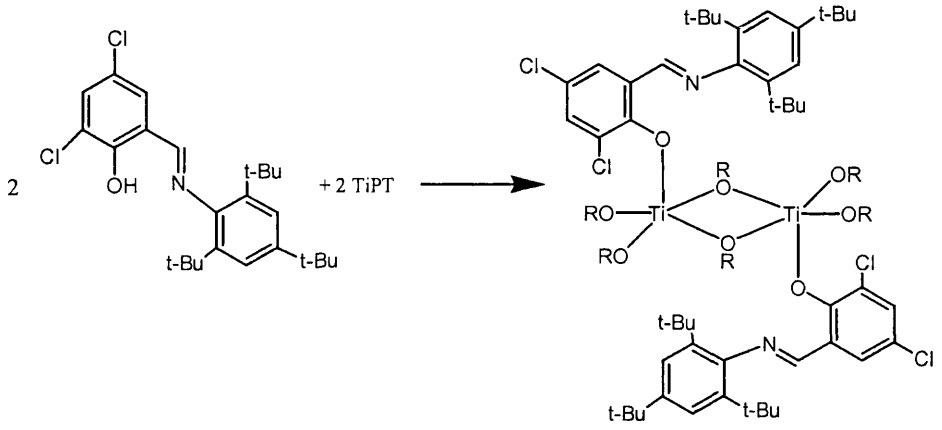

4.16L Complex 4.16

A solution of 0.87g (2 mmol) of ligand 4.16L was prepared in dry toluene (10ml) under an inert atmosphere. To this was added 0.3ml (1mmol) of TiPT to give a yellow solution. This solution was vigorously stirred for two hours at reflux. The solvent was removed *in vacuo* to give a yellow residue. This product was recrystallised from a minimum of hexane to give a crop of yellow blocks.

Yield = 0.18g (23.0%)
Melting Point = 161-166°C

^{1}H NMR Spectrum: 300MHz, solvent $CDCl_3$

δ/ppm	**Integral**	**Multiplicity**	**Coupling/Hz**	**Assignment**
0.82	36H	broad doublet		Isopropyl C**H**$_3$
1.15	54H	broad signal		*t*-Butyl C**H**$_3$
4.45	6H	broad septet		Isopropyl C**H**
7.05-7.90	8H	multiplet		Aromatic C**H**
8.35	2H	singlet		Imine C**H**

Elemental Analysis: $C_{68}H_{106}N_2O_8Ti_2Cl_4$

	C	H	N
Calculated %	65.1	7.61	2.71
Observed %	61.8	7.98	2.23

3.2 Experimental data for chapter 5

3.2.1 Ligand synthesis

The ligands synthesised for use in the reactions in chapter 5 are shown in the figure below.

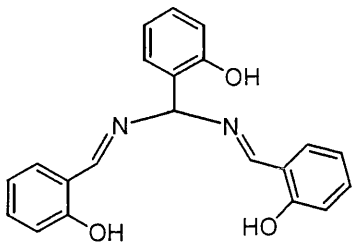

5.1L

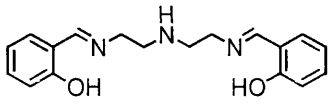

5.2L

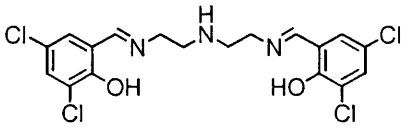

5.3L

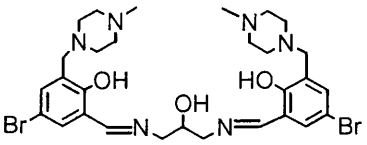

5.4L

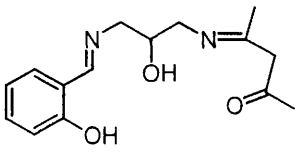

5.5L

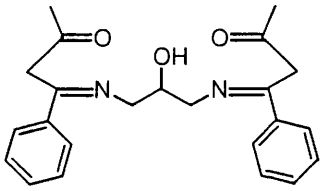

5.6L

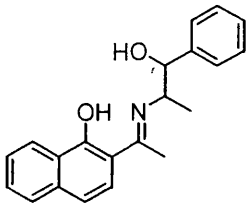

5.7L

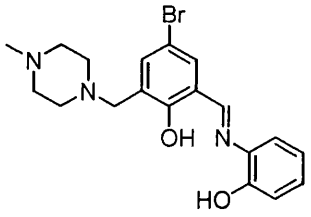

5.8L

Ligands used in chapter 5

Ligand 5.1L was readily synthesised using the method described by Takajo et al.[2]. The recrystallised product was recovered in good yield (~70%) and used without further purification.

Ligands 5.2L and 5.3L were prepared by the method described by Taylor et al. from the relevant salicylaldehyde derivative[3]. The oily products were isolated in a slightly impure state, as described by Taylor, in average yield (~50%).

Ligand 5.4L derived from the reaction of 4-Bromo-2-Formyl-6-(4-methylpiperazin-1-ylmethyl)phenol with 1,3-diamino-propan-2-ol. The parent salicylaldehyde derivative was synthesised according to the procedure described by Fenton et al.[4] and reacted with the diamino alcohol according to the method described by Lacroix et al. to give the hygroscopic product in average yield after purification (~65%)[5].

Ligand 5.5L was synthesised by the method described by Murray et al. with a purified yield of ~60%[6].

Ligand 5.6L was synthesised by a variation of the method described by Murray et al. using two equivalents of the acetylacetonate derivative to give an oily, slightly impure product in poor yield (~35%).

Ligand 5.7L was synthesised using the method described by Braun et al. to give the yellow crystalline product in a yield of ~60%[7].

Ligand 5.8L was synthesised form the starting salicylaldehyde, whose synthesis was described by Fenton et al., by the method described by Alyea et al[8].

---

[2] S. Kambe, T. Takajo, K. Saito, T. Hayashi, A. Sakurai and H. Midorikawa, *Synthesis*, 802 (Dec. 1975)
[3] W.M. Coleman and L.T. Taylor, *Inorg. Chem.*, **10**, 2195 (1971)
[4] J.D. Crane, D.E. Fenton, J.M. Latour and A.J. Smith, *J. Chem. Soc. Dalton Trans.*, 2979 (1991)
[5] F. Averseng, P.G. Lacroix, I. Malfant, N. Perisse, C. Lepitit and K. Nakatani, *Inorg. Chem.*, **40**, 3797 (2001)
[6] P.E. Kruger, B. Moubaraki, K.S. Murray and E.R.T. Tiekink, *J. Chem. Soc. Dalton Trans.*, 2129 (1994)
[7] R. Fleischer, H. Wunderlich and M. Braun, *Eur. J. Org. Chem.*, 1063 (1998)
[8] E.C. Alyea, A. Malek and P.H. Merrell, *Trans. Met. Chem.*, **4**, 172 (1979)

3.2.2 Complex synthesis

Complex 5.1: Complex of a *tris*-phenolic salicylaldimine derived from ammonia with TiPT

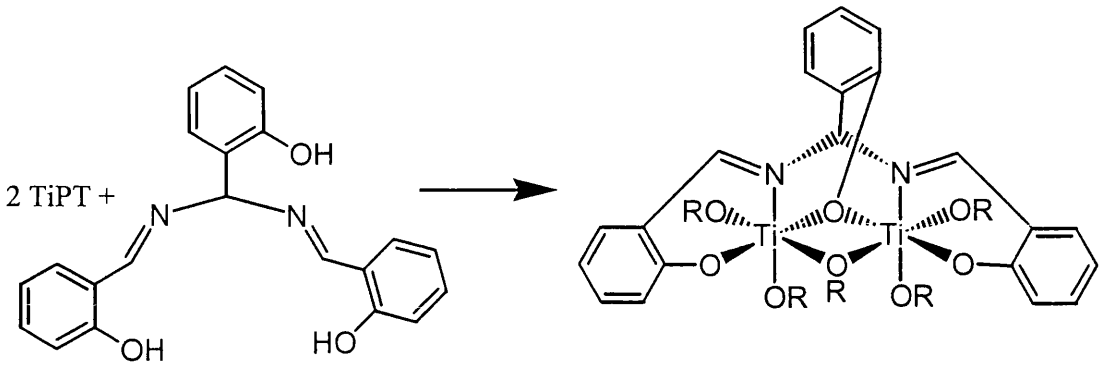

5.1L Complex 5.1

A solution of 0.35g (1 mmol) of ligand 5.1L was prepared in dry toluene (10ml) under an inert atmosphere. To this was added 0.6ml (2mmol) of TiPT to give an orange solution. This solution was vigorously stirred for one hour and heated to reflux. The solvent was removed *in vacuo* to give an orange solid product. This product was recrystallised from a minimum of toluene to give a crop of pale orange blocks.

Yield = 0.37g (50.4%)
Melting Point = 194-197 °C (dec.)

^{1}H NMR Spectrum: 300MHz, solvent $CDCl_3$

δ/ppm	Integral	Multiplicity	Coupling/Hz	Assignment
0.24	6H	doublet	6.1	Isopropyl CH_3 *trans* to nitrogen
0.34	6H	doublet	6.1	Isopropyl CH_3 *trans* to nitrogen
0.97	6H	doublet	6.3	Bridging isopropyl CH_3
1.30	6H	doublet	6.2	Isopropyl CH_3 *trans* to bridging isopropoxide
1.34	6H	doublet	6.1	Isopropyl CH_3 *trans* to bridging isopropoxide

3.37	2H	septet	6.1	Isopropyl C**H** *trans* to nitrogen
4.76	1H	septet	6.3	Bridging isopropyl C**H**
5.18	2H	septet	6.1	Isopropyl C**H** *trans* to isopropoxide
5.27	1H	singlet		N-(PhO)C**H**-N
6.66	4H	doublet	7.6	Aromatic C**H**
6.85	1H	triplet	7.4	Aromatic C**H**
7.02	1H	doublet	8.0	Aromatic C**H**
7.09-7.19	3H	multiplet		Aromatic C**H**
7.23-7.29	3H	multiplet		Aromatic C**H**
8.17	2H	singlet		Imine C**H**

$^{13}C\{^{1}H\}$ NMR Spectrum: 75.5MHz, solvent $CDCl_3$

δ/ppm	**Assignment**
24.3	Bridging isopropyl **C**H_3
25.5, 25.6, 25.8	Isopropyl **C**H_3
73.2	Bridging isopropyl **C**H
77.3	Isopropyl **C**H *trans* to nitrogen
79.2	Isopropyl **C**H *trans* to bridging isopropoxide
102.0	N-(PhO)**C**H-N
115.0, 117.9, 119.1, 120.3, 121.3, 121.7, 125.7, 126.7, 128.6, 129.4, 130.0, 131.3, 134.1, 135.3	Aromatic
162.5	Imine **C**H
164.3, 165.5	Aromatic *ipso* to phenol

Elemental Analysis: $C_{36}H_{50}N_2O_8Ti_2$

	C	H	N
Calculated %	58.9	6.86	3.81
Observed %	58.3	6.84	3.78

Complex 5.2: Complex of diethylene triamine bis-salicylaldimine and TiPT

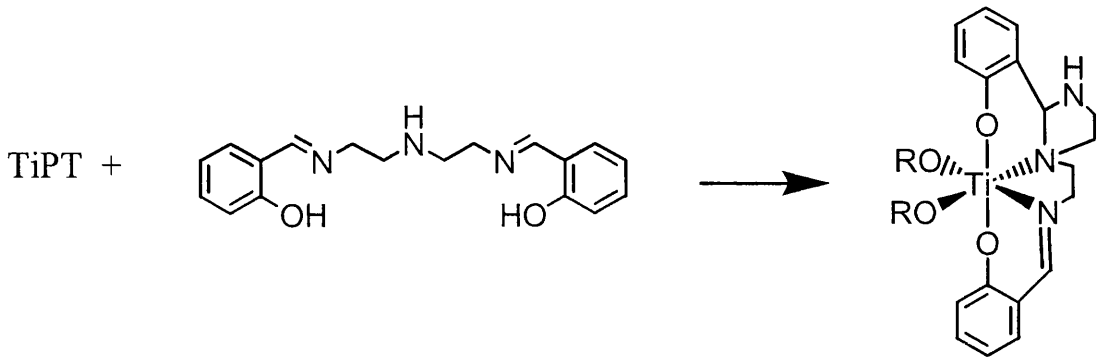

5.2L Complex 5.2

A solution of 0.31g (1 mmol) of the salicylaldimine derivative of di-ethylene triamine, 5.2L, was prepared in dry toluene (10ml) under an inert atmosphere. To this was added 0.3ml (1mmol) of TiPT to give an orange solution. This solution was vigorously stirred for one hour and heated to reflux. The solvent was removed *in vacuo* to give an orange solid product. This product was recrystallised from a minimum of hexane to give a crop of orange needles.

Yield = 0.42g (88.3%)
Melting Point = 165-167 °C (dec.)

^{1}H NMR Spectrum: 300MHz, solvent $CDCl_3$

δ/ppm	Integral	Multiplicity	Coupling/Hz	Assignment
0.91	3H	doublet	6.0	Isopropyl C**H**$_3$
0.95	3H	doublet	6.1	Isopropyl C**H**$_3$
1.23	3H	doublet	6.1	Isopropyl C**H**$_3$
1.37	3H	doublet	6.1	Isopropyl C**H**$_3$
2.52-2.65	2H	multiplet		Methylene C**H**$_2$
3.09-3.61	6H	multiplet		Methylene C**H**$_2$
3.99	1H	doublet	13.4	HRN-(R)C**H**-NR$_2$
4.28	1H	septet	6.1	Isopropyl C**H**
5.00	1H	septet	6.1	Isopropyl C**H**
6.22-6.25	1H	multiplet		Aromatic C**H**

6.50-6.55	1H	multiplet		Aromatic C**H**
6.67-6.73	2H	multiplet		Aromatic C**H**
6.94-7.08	3H	multiplet		Aromatic C**H**
7.27-7.33	1H	multiplet		Aromatic C**H**
7.78	1H	singlet		Imine C**H**

$^{13}C\{^{1}H\}$ NMR Spectrum: 100MHz, solvent $CDCl_3$

δ/ppm	**Assignment**
25.5, 25.6	Isopropyl **C**H_3 *trans* to imine
26.3, 26.5	Isopropyl **C**H_3 *trans* to amine
44.2, 54.8, 56.7, 57.9	Methylene **C**H_2
76.3	Isopropyl **C**H *trans* to amine
78.4	Isopropyl **C**H *trans* to imine
88.8	HRN-(R)**C**H-NR_2
117.4, 118.2, 119.2, 119.3, 122.2, 123.7, 128.6, 129.4, 133.7, 134.9	Aromatic
163.5	Imine **C**H
163.9, 164.2	Aromatic *ipso* to phenol

Elemental Analysis: $C_{24}H_{33}N_3O_4Ti$

	C	H	N
Calculated %	60.3	6.95	8.84
Observed %	60.3	6.84	8.70

Complex 5.3: Complex of diethylene triamine 2,4-dichloro salicylaldimine and TiPT

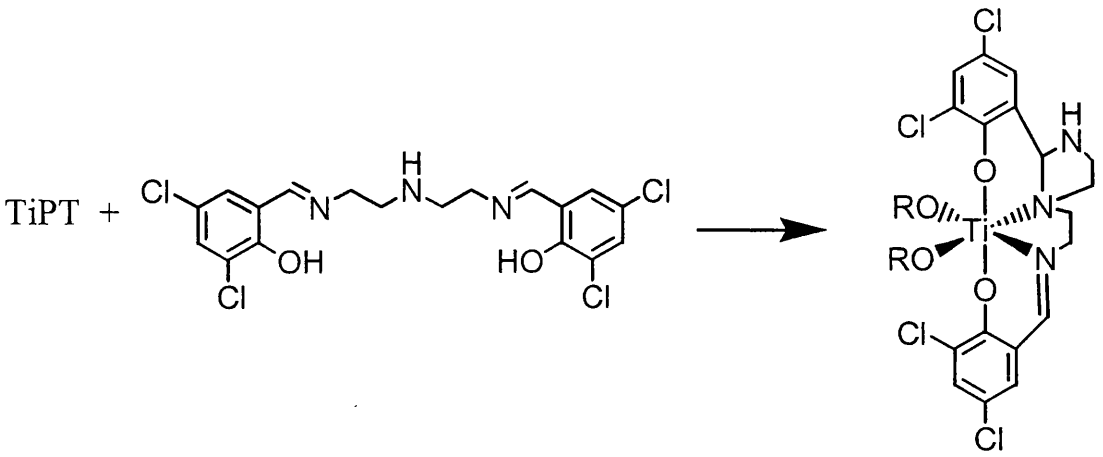

5.3L Complex 5.3

A solution of 0.90g (2 mmol) of 2,4-dichloro salicylaldimine derivative of di-ethylene triamine, 5.3L, was prepared in dry toluene (10ml) under an inert atmosphere. To this was added 0.6ml (2mmol) of TiPT to give a yellow solution. This solution was vigorously stirred for one hour and heated to reflux. The solvent was removed *in vacuo* to give an yellow solid product. This product was recrystallised from a minimum of hexane to give a crop of yellow needles.

Yield = 0.68g (55.5%)
Melting Point = 185-186 °C (dec.)

^{1}H NMR Spectrum: 300MHz, solvent $CDCl_3$

δ/ppm	Integral	Multiplicity	Coupling/Hz	Assignment
0.95	3H	doublet	6.0	Isopropyl C**H**$_3$
0.99	3H	doublet	6.1	Isopropyl C**H**$_3$
1.29	3H	doublet	6.1	Isopropyl C**H**$_3$
1.35	3H	doublet	6.1	Isopropyl C**H**$_3$
2.63-2.69	2H	multiplet		Methylene C**H**$_2$
3.12-3.29	4H	multiplet		Methylene C**H**$_2$
3.46-3.61	2H	multiplet		Methylene C**H**$_2$
3.99	1H	doublet	13.1	HRN-(R)C**H**-NR$_2$

4.38	1H	septet	6.1	Isopropyl C**H**
4.97	1H	septet	6.2	Isopropyl C**H**
6.92	1H	doublet	2.6	Aromatic C**H**
6.98	1H	doublet	2.7	Aromatic C**H**
7.08	1H	doublet	2.6	Aromatic C**H**
7.39	1H	doublet	2.7	Aromatic C**H**
7.79	1H	singlet		Imine C**H**

$^{13}C\{^{1}H\}$ NMR Spectrum: 75.5MHz, solvent $CDCl_3$

δ/ppm	**Assignment**
23.2, 23.4	Isopropyl **C**H_3 *trans* to imine
23.6, 23.9	Isopropyl **C**H_3 *trans* to amine
41.8, 52.6, 54.2, 55.6	Methylene **C**H_2
75.5	Isopropyl **C**H *trans* to amine
80.2	Isopropyl **C**H *trans* to imine
85.3	HRN-(R)**C**H-NR_2
118.5, 119.3, 120.9, 122.1, 122.3, 123.3, 125.6, 128.3, 129.0, 132.0	Aromatic
155.7, 156.2	Aromatic *ipso* to phenol
160.6	Imine **C**H

Elemental Analysis: $C_{24}H_{29}N_3O_4TiCl_4$

	C	H	N
Calculated %	47.1	4.75	6.87
Observed %	46.8	4.71	6.93

Complex 5.4: Complex of 4-bromo 2-formyl 6-(4-methylpiperazin-1-ylmethyl) phenol Schiff base with 1,3-diamino isopropanol with TiPT

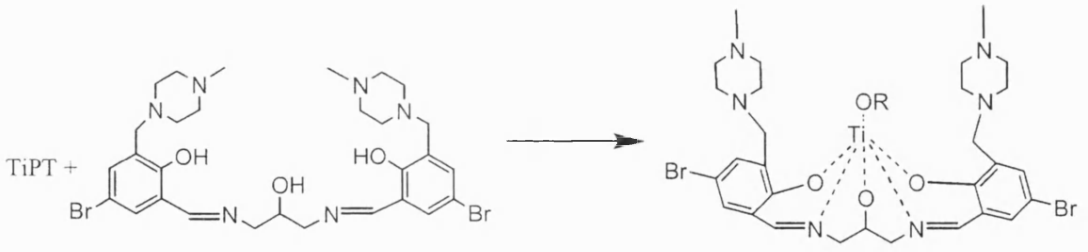

5.4L Complex 5.4

A solution of 0.68g (1 mmol) of ligand 5.4L was prepared in dry toluene (10ml) under an inert atmosphere. To this was added 0.3ml (1mmol) of TiPT to give a red solution. This solution was vigorously stirred for one hour and heated to reflux. The solvent was removed *in vacuo* to give a red solid product. This product was suspended in hexane and toluene added until dissolution occurred on warming. Standing at room temperature yielded a crop of red plates.

Yield = 0.66g (84.4%)
Melting Point = 177-181 °C

^{1}H NMR Spectrum: 300MHz, solvent $CDCl_3$

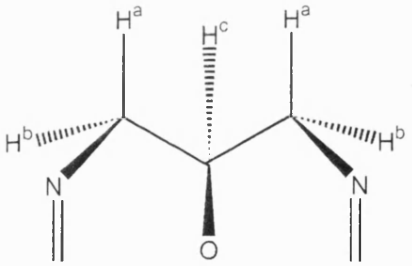

δ/ppm	Integral	Multiplicity	Coupling/Hz	Assignment
1.15	6H	doublet	6.2	Isopropyl C**H**$_3$
2.21	6H	singlet		N-C**H**$_3$
2.34	16H	broad singlet		Piperazine C**H**$_2$ groups
3.09	2H	doublet	14.8	Diastereotopic C**H**$_2$
3.47	2H	doublet	14.8	Diastereotopic C**H**$_2$
3.83	2H	doublet		H^a coupled to H^b only

4.29	2H	multiplet		H^b coupled to H^a and H^c
4.70	1H	multiplet		H^c coupled to H^b only
4.79	1H	broad septet		Isopropyl C**H**
7.11	2H	singlet		Aromatic C**H**
7.46	2H	singlet		Aromatic C**H**
8.06	2H	singlet		Imine C**H**

$^{13}C\{^1H\}$ NMR Spectrum: 75.5MHz, solvent $CDCl_3$

δ/ppm	**Assignment**
26.0	Isopropyl **C**H_3
46.5	N-**C**H_3
53.4	Piperazine **C**H_2 group
55.6	Piperazine **C**H_2 group
55.8	Mannich methylene **C**H_2
67.1	Methylene **C**H_2
75.2	Methylene **C**H_2
79.8	Isopropyl **C**H
109.8	Methine **C**H
123.4, 129.4, 130.1, 132.5, 137.4, 161.1	Aromatic carbon atoms
162.6	Imine **C**H

Elemental Analysis: $C_{32}H_{44}N_6O_4Br_2Ti$

	C	H	N
Calculated %	49.0	5.65	10.71
Observed %	49.3	5.54	10.40

Complex 5.5: Complex of the imine formed from acetylacetone, salicylaldehyde and 1,3-diamino isopropanol with TiPT

5.5L Complex 5.5

A solution of 1.11g (4 mmol) of ligand 5.5L was prepared in dry toluene (10ml) under an inert atmosphere. To this was added 1.2ml (4mmol) of TiPT to give a yellow solution. This solution was vigorously stirred for one hour and heated to reflux. The solvent was removed *in vacuo* to give a yellow solid product. This product was suspended in hexane and toluene added until dissolution occurred on warming. Standing at room temperature yielded a yellow microcrystalline product.

Yield = 1.21g (79.6%)
Melting Point = 163-169°C

^{1}H NMR Spectrum: 300MHz, solvent $CDCl_3$

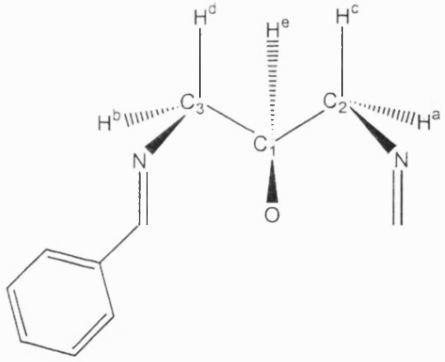

δ/ppm	Integral	Multiplicity	Coupling/Hz	Assignment
1.14	3H	doublet	6.1	Isopropyl C**H**$_3$
1.19	3H	doublet	6.1	Isopropyl C**H**$_3$
1.78	3H	singlet		Nacac C**H**$_3$ next to nitrogen
1.83	3H	singlet		Nacac C**H**$_3$ next to oxygen
3.51	1H	doublet	13.7	H^c coupled to H^a only

3.81	1H	doublet	14.0	H^d coupled to H^b only
3.87	1H	doublet of doublets	5.4, 13.7	H^a coupled to H^e and H^c
4.35	1H	doublet of doublets	5.5, 13.0	H^b coupled to H^d and H^e
4.67	1H	multiplet		H^c coupled to H^a and H^b
4.86	1H	septet	6.2	Isopropyl C**H**
5.09	1H	singlet		Nacac C**H**
6.65-6.71	2H	multiplet		Aromatic C**H**
7.13-7.30	2H	multiplet		Aromatic C**H**
8.19	1H	singlet		Imine C**H**

$^{13}C\{^1H\}$ NMR Spectrum: 75.5MHz, solvent $CDCl_3$

δ/ppm	**Assignment**
21.8, 24.6	Isopropoxide **C**H_3
25.7, 25.8	Nacac **C**H_3
60.7	C_2 (on figure above)
69.1	C_3 (on figure above)
75.4	C_1(on figure above)
79.0	Isopropoxide **C**H
103.7	Nacac **C**H
118.0, 119.4, 132.4, 134.8	Aromatic **C**H
119.4, 163.5	Aromatic **C**
164.2, 174.6	Nacac **C**=N and **C**-O
167.4	Imine **C**H

Elemental Analysis: $C_{21}H_{17}N_2O_4Ti$

	C	H	N
Calculated %	56.9	6.36	7.37
Observed %	56.4	6.28	7.16

Complex 5.6: Complex of the diimine of phenyl acac and 1,3 diamino isopropanol with TiPT

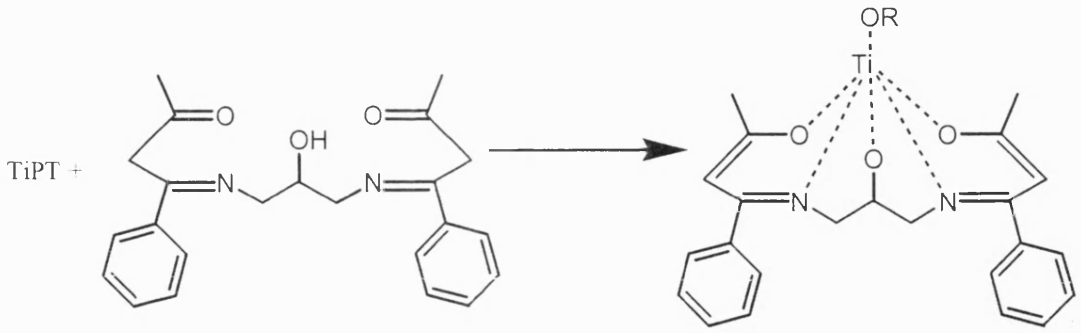

5.6L Complex 5.6

A solution of 0.38g (1 mmol) of ligand 5.6L was prepared in dry toluene (10ml) under an inert atmosphere. To this was added 0.3ml (1mmol) of TiPT to give a pale yellow solution. This solution was vigorously stirred for one hour and heated to reflux. The solvent was removed *in vacuo* to give a yellow solid product. This product was recrystallised from a minimum of hexane to give a crop of pale yellow blocks.

Yield = 0.31g (64.3%)
Melting Point = 158-160°C

^{1}H NMR Spectrum: 300MHz, solvent $CDCl_3$

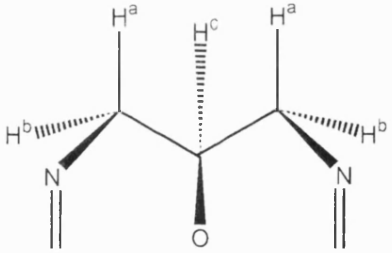

δ/ppm	Integral	Multiplicity	Coupling/Hz	Assignment
1.13	6H	doublet	6.2	Isopropyl C**H**$_3$
1.95	6H	singlet		Nacac C**H**$_3$
3.62	2H	doublet	13.8	H^a coupled to H^b only
4.10	2H	doublet of doublets	5.3, 13.8	H^a coupled to H^b and H^c
4.68	1H	triplet	5.3	H^c coupled to H^b only
4.82	1H	septet	6.2	Isopropyl C**H**

5.86	2H	singlet		Nacac C**H**
7.14-7.22	6H	multiplet		Aromatic C**H**
7.61-7.69	4H	multiplet		Aromatic C**H**

$^{13}C\{^{1}H\}$ NMR Spectrum: 75.5MHz, solvent $CDCl_3$

δ/ppm	**Assignment**
22.2	Nacac **C**H_3
25.9	Isopropyl **C**H_3
63.0, 63.2	Methylene **C**H_2
75.6	Methine **C**H
79.1	Isopropyl **C**H
101.0	Nacac **C**H
127.1, 128.4, 130.0	Aromatic **C**H
138.0	Aromatic **C**
167.9	RR'**C**-N
169.7	RR'**C**-O

Elemental Analysis: $C_{26}H_{30}N_2O_4Ti$

	C	H	N
Calculated %	64.7	6.27	5.81
Observed %	64.5	6.25	5.80

Complex 5.7: Complex of the imine formed from 2-acetyl-1-naphthol and norephedrine with TiPT

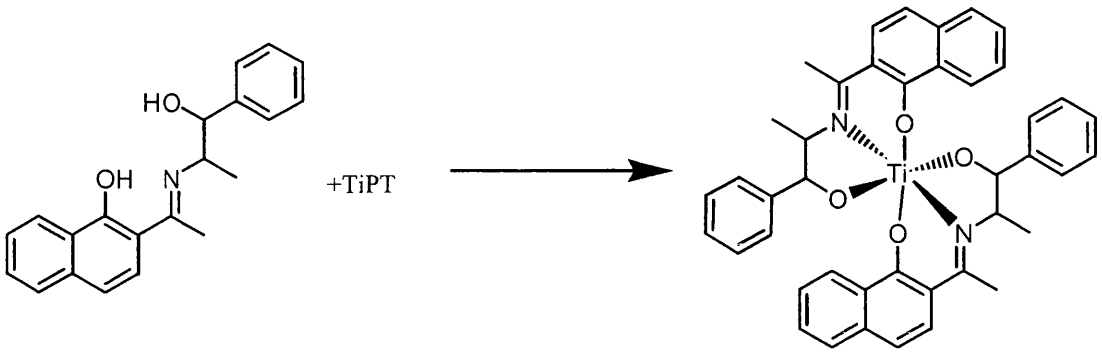

5.7L Complex 5.7

A solution of 0.64g (2 mmol) of ligand 5.7L was prepared in dry toluene (10ml) under an inert atmosphere. To this was added 0.6ml (2mmol) of TiPT to give a green/yellow solution. This solution was vigorously stirred for one hour and heated to reflux. The solvent was removed *in vacuo* to give a pale green solid product. This product was recrystallised from a minimum of hexane at –20°C to give a crop of pale yellow needles.

Yield = 0.14g (38.5% based on ligand)
Melting Point = 35-38°C

^{1}H NMR Spectrum: 400MHz, solvent $CDCl_3$

δ/ppm	Integral	Multiplicity	Coupling/Hz	Assignment
1.47	6H	doublet	6.8	Norephedrine CH_3
2.73	6H	singlet		Acetyl CH_3
4.90	2H	multiplet		Norephedrine CH next to imine
6.25	2H	doublet	4.0	Norephedrine CH next to benzene
6.81-6.87	4H	multiplet		Aromatic CH
7.06-7.09	2H	multiplet		Aromatic CH
7.18-7.22	4H	multiplet		Aromatic CH
7.30-7.34	4H	multiplet		Aromatic CH

7.45-7.49	8H	multiplet		Aromatic C**H**

$^{13}C\{^{1}H\}$ NMR Spectrum: 75.5MHz, solvent $CDCl_3$

δ/ppm	**Assignment**
16.8	Norephedrine **C**H_3
20.1	Acetyl **C**H_3
72.8	Norephedrine **C**H next to imine
86.0	Norephedrine **C**H next to benzene
118.4, 118.8, 125.6, 125.8, 126.8, 127.4, 128.3, 129.1, 129.5, 129.7, 130.5, 137.1, 143.0, 163.1, 170.1	Aromatic and imine carbon signals

Elemental Analysis: $C_{21}H_{17}N_2O_4Ti$

	C	H	N
Calculated %	73.90	5.61	4.10
Observed %	71.0	6.05	3.26

Complex 5.8: Complex of 4-bromo 2-formyl 6-(4-methylpiperazin-1-ylmethyl) phenol Schiff base with 2-amino phenol with TiPT

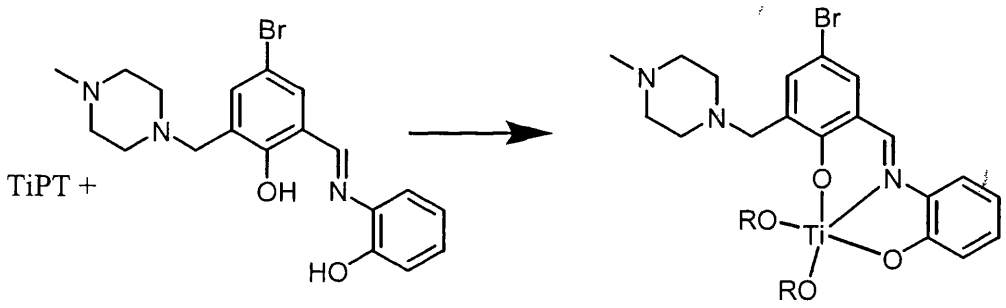

5.8L Complex 5.8

A solution of 0.40g (1 mmol) of ligand 5.8L was prepared in dry toluene (10ml) under an inert atmosphere. To this was added 0.3ml (1mmol) of TiPT to give a deep red solution. This solution was vigorously stirred for one hour and heated to reflux. The solvent was removed *in vacuo* to give a red solid product. This product was suspended in hexane and toluene added until dissolution occurred on warming. Standing at room temperature yielded a crop of deep red blocks.

Yield = 0.27g (47.5%)
Melting Point = 188-190 °C

^{1}H NMR Spectrum: 300MHz, solvent $CDCl_3$

δ/ppm	Integral	Multiplicity	Coupling/Hz	Assignment
1.05	12H	broad doublet		Isopropyl C**H**$_3$
2.21	3H	singlet		N-C**H**$_3$
2.39	8H	broad signal		Piperazine methylene C**H**$_2$ groups
3.45	2H	broad singlet		Methylene C**H**$_2$
4.62	2H	broad signal		Isopropyl C**H**
6.54-6.67	2H	multiplet		Aromatic amino phenol C**H**
6.96-6.99	1H	multiplet		Aromatic amino phenol C**H**
7.20-7.26	2H	multiplet		Aromatic amino phenol C**H** and bromo phenol C**H**
7.50	1H	singlet		Aromatic bromo phenol C**H**
8.45	1H	singlet		Imine C**H**

$^{13}C\{^{1}H\}$ NMR Spectrum: 100MHz, solvent $CDCl_3$

δ/ppm	Assignment
25.8	Isopropyl **C**H$_3$
46.5	N-**C**H$_3$
53.5, 55.6	Piperazine methylene **C**H$_2$
56.0	Methylene **C**H$_2$
80.3	Isopropyl **C**H
110.4, 114.2, 116.8, 118.8, 123.9, 129.9, 130.1, 133.7, 137.4, 137.8, 153.4	Aromatic carbon atoms
161.4	Imine **C**H

Elemental Analysis (Dimer): $C_{50}H_{68}N_6O_8Ti_2Br_2$

	C	H	N
Calculated %	52.9	6.00	7.41
Observed %	52.9	5.98	7.27

3.3 Experimental data for chapter 6

3.3.1 Ligand syntheses

The ligands synthesised for use in the reactions in chapter 6 are shown in the figure below.

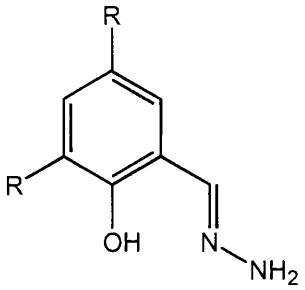

6.1L: R = H
6.2L: R = t-Bu

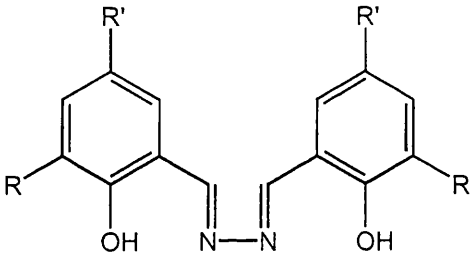

6.3L: R = t-Bu, R' = t-Bu
6.4L: R = OMe, R' = H
6.5L: R = CH_2-(Methylpiperazine), R' = Br

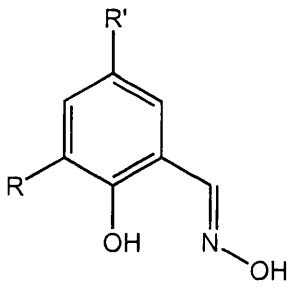

6.6L: R = H, R' = H
6.7L: R = Cl, R' = Cl
6.8L: R = H, R' = NO_2

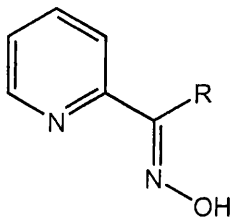

6.9L: R = H
6.11L: R = Ph
6.12L: R = Py

Ligands used in chapter 6

Ligand 6.1L was purchased from Aldrich and used as received.

Ligands 6.2L, 6.3L, 6.4L and 6.5L were synthesised by the methods described by Kaushik et al. and used without further purification[9].

Ligand 6.6L was purchased from Aldrich and purified by recrystallisation from petroleum ether.

Attempts were made to synthesise ligands 6.7L and 6.8L by the resin method described by Ballini et al. but these proved unsuccessful[10]. They were eventually synthesised in poor yield by the method described by Dayagi et al.[11]

Ligands 6.9L, 6.11L and 6.12L were purchased from Aldrich and used as received.

3.3.1 Complex synthesis

Complex 6.1: Complex of salicylaldehyde hydrazone and TiPT

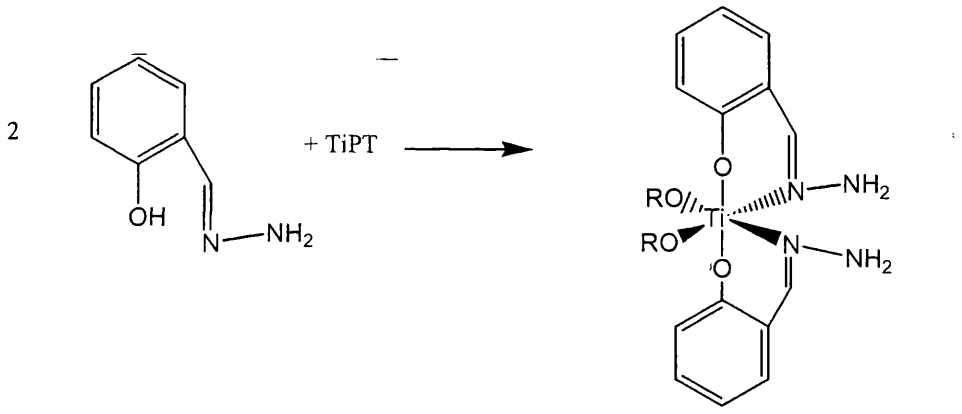

6.1L Complex 6.1

A solution of 0.82g (6 mmol) of salicylaldehyde hydrazone, 6.1L, was prepared in dry toluene (10ml) under an inert atmosphere. To this was added 0.9ml (3mmol) of TiPT to give a bright yellow solution. This solution was vigorously stirred for one hour. The solvent was removed *in vacuo* to give a pale yellow solid product. This product was suspended in hexane and toluene added until dissolution occurred on warming. Standing at room temperature yielded a crop of yellow blocks.

Yield = 1.12g (85.6%)
Melting Point = 140-143 °C

[9] B. Khera, A.K. Sharma and N.K. Kaushik, *Bull. Chem. Soc. Jpn.*, **58**, 793 (1985)
[10] R. Ballini, L. Barboni and P. Filippone, *Chem. Lett.*, 475 (1997)
[11] S. Dayagi and Y. Degani in '*The Chemistry Of The Carbon Nitrogen Double Bond*', Ed. S. Patai, Interscience, New York, 61 (1970)

^{1}H NMR Spectrum: 300MHz, solvent $CDCl_3$

δ/ppm	Integral	Multiplicity	Coupling/Hz	Assignment
1.04	12H	doublet	6.1	Isopropyl C**H**$_3$
4.63	2H	septet	6.2	Isopropyl C**H**
5.57	4H	singlet		Hydrazone N**H**$_2$
6.69	2H	doublet of doublets	4.9, 1.1	Aromatic C**H**
6.78	2H	doublet	8.2	Aromatic C**H**
7.00	2H	doublet	7.7	Aromatic C**H**
7.18	2H	multiplet		Aromatic C**H**
7.62	2H	singlet		Imine C**H**

^{13}C{^{1}H} NMR Spectrum: 75.5MHz, solvent $CDCl_3$

δ/ppm	Assignment
25.6	Isopropyl **C**H$_3$
79.2	Isopropyl **C**H
118.5	Aromatic
118.9	Aromatic
122.0	Aromatic *ipso* to imine
131.3	Aromatic
132.3	Aromatic
146.9	Imine CH
162.4	Aromatic *ipso* to phenol

Elemental Analysis: $C_{20}H_{28}N_4O_4Ti$

	C	H	N
Calculated %	55.1	6.47	12.84
Observed %	54.8	6.40	12.70

Complex 6.2: Complex of 2,4-di-*tert*-butyl-salicylaldehyde hydrazone and TiPT

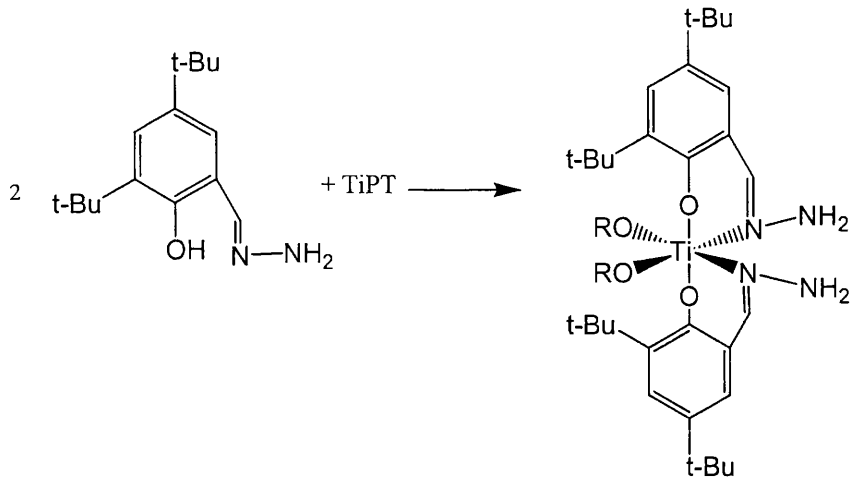

6.2L Complex 6.2

A solution of 0.50g (2 mmol) of 2,4-di-*tert*-butyl-salicylaldehyde hydrazone, 6.2L, was prepared in dry toluene (10ml) under an inert atmosphere. To this was added 0.3ml (1mmol) of TiPT to give a bright orange solution. This solution was vigorously stirred for one hour. The solvent was removed *in vacuo* to give a bright red solid product. This product was recrystallised from a minimum of hexane to give a crop of red blocks.

Yield = 0.39g (59.1%)
Melting Point = 220-224 °C (dec.)

^{1}H NMR Spectrum: 300MHz, solvent $CDCl_3$

δ/ppm	Integral	Multiplicity	Coupling/Hz	Assignment
0.90	12H	two overlayed doublets	5.9	Isopropyl C**H**$_3$
1.22	18H	singlet		*t*-Butyl C**H**$_3$
1.46	18H	singlet		*t*-Butyl C**H**$_3$
4.55	2H	septet	6.1	Isopropyl C**H**
5.48	4H	singlet		Hydrazone N**H**$_2$
6.87	2H	singlet		Aromatic C**H**
7.29	2H	singlet		Aromatic C**H**
7.7	2H	singlet		Imine C**H**

$^{13}C\{^{1}H\}$ NMR Spectrum: 75.5MHz, solvent $CDCl_3$

δ/ppm	Assignment
26.0	Isopropyl **C**H_3
30.2	C(**C**H_3)$_3$
31.9	C(**C**H_3)$_3$
34.5	**C**(CH_3)$_3$
35.6	**C**(CH_3)$_3$
78.6	Isopropyl **C**H
121.2	Aromatic *ipso* to imine
125.9	Aromatic **C**H
127.1	Aromatic **C**H
137.6	Aromatic **C**(*t*-Bu)
139.6	Aromatic **C**(*t*-Bu)
148.7	Imine **C**H
159.7	Aromatic *ipso* to phenol

Elemental Analysis: $C_{36}H_{60}N_4O_4Ti$

	C	H	N
Calculated %	65.5	9.09	8.48
Observed %	66.2	9.35	7.90

Complex 6.3: Complex of 2,4-di-*tert*-butyl-salicylaldehyde azine and TiPT

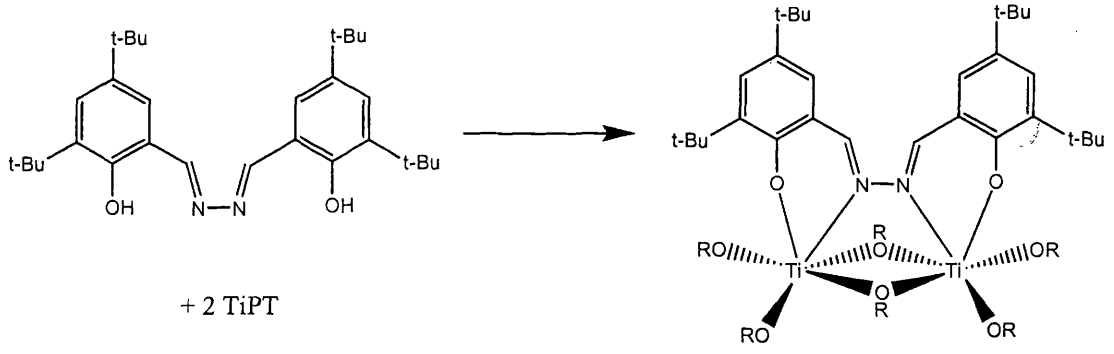

6.3L Complex 6.3

A solution of 0.36g (1 mmol) of 2,4-di-*tert*-butyl-salicylaldehyde azine, 6.3L, was prepared in dry toluene (10ml) under an inert atmosphere. To this was added 0.6ml (2mmol) of TiPT to give a yellow solution. The solution was vigorously stirred for one hour and heated to reflux. Reduction in volume of the toluene resulted in precipitation of a yellow solid. The product was recrystallised from the remaining toluene to give a crop of yellow blocks.

Yield = 0.46g (57.3%)

Melting Point = 243-246 °C

^{1}H NMR Spectrum: 300MHz, solvent $CDCl_3$

δ/ppm	Integral	Multiplicity	Coupling/Hz	Assignment
0.77	12H	broad doublet of doublets		Isopropyl C**H**$_3$
1.02	6H	doublet	6.0	Restricted rotation isopropyl C**H**$_3$
1.20	6H	doublet	6.0	Restricted rotation isopropyl C**H**$_3$
1.21-1.29	30H	multiplet		Isopropyl C**H**$_3$ and *t*-butyl C**H**$_3$
1.46	18H	singlet		*t*-Butyl C**H**$_3$
4.37	2H	septet	6.0	Isopropyl C**H**
4.77	2H	septet	6.0	Restricted rotation isopropyl C**H**
4.88	2H	septet	6.1	Isopropyl C**H**
7.12	2H	singlet		Aromatic C**H**
7.37	2H	singlet		Aromatic C**H**
7.89	2H	singlet		Imine C**H**

^{13}C{^{1}H} NMR Spectrum: 75.5MHz, solvent $CDCl_3$

δ/ppm	Assignment
22.0	Restricted rotation isopropyl **C**H$_3$
22.1	Restricted rotation isopropyl **C**H$_3$
23.8	Isopropyl **C**H$_3$
23.9	Isopropyl **C**H$_3$
27.9	C(**C**H$_3$)$_3$
29.5	C(**C**H$_3$)$_3$
32.1	**C**(CH$_3$)$_3$
33.3	**C**(CH$_3$)$_3$
72.3	Restricted rotation isopropyl **C**H
75.1	Isopropyl **C**H
75.9	Isopropyl **C**H
117.8	Aromatic *ipso* to imine
126.2	Aromatic **C**H

127.0	Aromatic **C**H
135.8	Aromatic **C**(*t*-Bu)
136.4	Aromatic **C**(*t*-Bu)
149.6	Imine **C**H
159.8	Aromatic *ipso* to phenol

Elemental Analysis: $C_{48}H_{84}N_2O_8Ti_2$

	C	H	N
Calculated %	63.2	9.21	3.07
Observed %	63.0	9.14	3.39

Complex 6.4: Complex of *o*-vanillin azine and TiPT

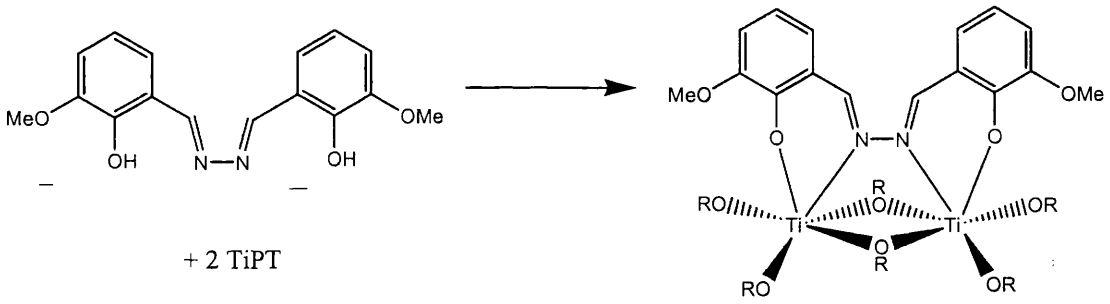

6.4L Complex 6.4

A solution of 0.60g (2mmol) of *o*-vanillin azine, 6.4L, was prepared in dry toluene (10ml) under an inert atmosphere. To this was added 1.2ml (4mmol) of TiPT to give a yellow solution. The solution was vigorously stirred for one hour and heated to reflux. The solvent was removed *in vacuo* to yield a yellow solid. This product was suspended in hexane and toluene added until dissolution occurred on warming. Standing at room temperature yielded a crop of yellow blocks.

Yield = 0.86g (57.4%)
Melting Point = 147-148 °C

^{1}H NMR Spectrum: 300MHz, solvent $CDCl_3$

δ/ppm	**Integral**	**Multiplicity**	**Coupling/Hz**	**Assignment**
0.80	12H	doublet of doublets	5.5	Isopropyl C**H**$_3$
1.12	12H	doublet of doublets	6.5	Isopropyl C**H**3
1.23	6H	doublet	6.0	Restricted rotation isopropyl C**H**$_3$

1.32	6H	doublet	6.0	Restricted rotation isopropyl C**H**$_3$
3.84	6H	singlet		O**CH**$_3$
4.39	2H	septet	6.1	Isopropyl C**H**
4.71	2H	septet	6.2	Isopropyl C**H**
4.95	2H	septet	6.1	Restricted rotation isopropyl C**H**
6.59	2H	multiplet		Aromatic C**H** *para* to phenol
6.85	2H	singlet		Aromatic C**H**
6.92	2H	singlet		Aromatic C**H**
7.87	2H	singlet		Imine C**H**

$^{13}C\{^1H\}$ NMR Spectrum: 75.5MHz, solvent $CDCl_3$

δ/ppm	**Assignment**
25.2	Isopropyl **C**H$_3$
26.1	Isopropyl **C**H$_3$
27.2	Restricted rotation isopropyl **C**H$_3$
27.5	Restricted rotation isopropyl **C**H$_3$
59.4	O**C**H$_3$
76.3	Isopropyl **C**H
79.6	Isopropyl **C**H
80.7	Restricted rotation isopropyl **C**H
118.1	Aromatic **C**H *para* to phenol
120.6	Aromatic **C**H
122.2	Aromatic *ipso* to imine
126.1	Aromatic **C**H
151.5	Aromatic *ipso* to OMe
152.8	Imine **C**H
158.8	Aromatic *ipso* to phenol

Elemental Analysis: $C_{34}H_{56}N_2O_{10}Ti_2$

	C	H	N
Calculated %	54.6	7.45	3.74
Observed %	54.5	7.49	3.69

Complex 6.5: Complex of 4-bromo-2-formyl-6-(4-methylpiperazin-1-ylmethyl) phenol azine and TiPT

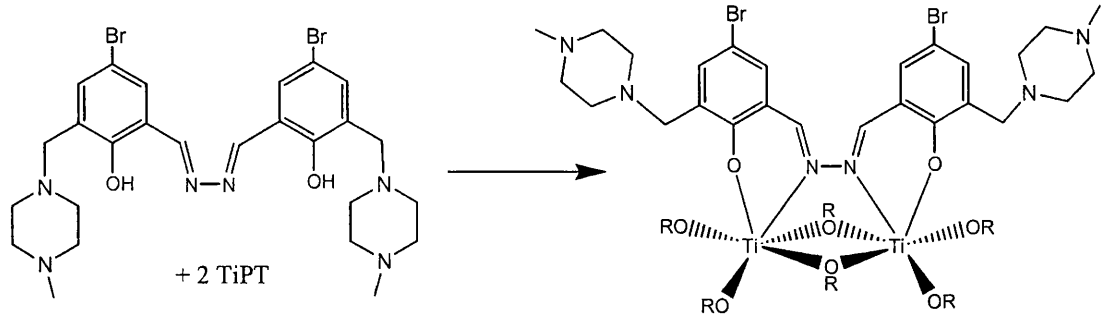

6.5L Complex 6.5

A solution of 0.62g (1mmol) of 4-bromo-2-formyl-6-(4-methylpiperazin-1-ylmethyl)phenol azine, 6.5L, was prepared in dry toluene (10ml) under an inert atmosphere. To this was added 0.6ml (2mmol) of TiPT to give a deep orange solution. The solution was vigorously stirred for one hour and heated to reflux. The solvent was removed *in vacuo* to yield a red/orange solid. This product was suspended in hexane and toluene added until dissolution occurred on warming. Standing at room temperature yielded a crop of red blocks.

Yield = 0.89g (83.2%)
Melting Point = 175-179 °C

^{1}H NMR Spectrum: 300MHz, solvent $CDCl_3$

δ/ppm	Integral	Multiplicity	Coupling/Hz	Assignment
0.80	12H	doublet of doublets	6.3	Isopropyl CH_3
0.99	6H	doublet	6.2	Restricted rotation isopropyl CH_3
1.12	6H	doublet	6.2	Restricted rotation isopropyl CH_3
1.24	12H	doublet of doublets	7.5	Isopropyl CH3
2.24	6H	singlet		NCH_3
2.41	16H	broad multiplet		Piperazine CH_2 groups
3.47-3.68	4H	doublet of doublets	48.3, 14.4	NCH_2Ph
4.34	2H	septet	6.1	Isopropyl CH

4.64	2H	septet	6.3	Restricted rotation isopropyl C**H**
4.89	2H	septet	6.1	Isopropyl C**H**
7.20	2H	singlet		Aromatic C**H**
7.53	2H	singlet		Aromatic C**H**
7.74	2H	singlet		Imine C**H**

$^{13}C\{^{1}H\}$ NMR Spectrum: 75.5MHz, solvent $CDCl_3$

δ/ppm	**Assignment**
22.8	Restricted rotation isopropyl **C**H_3
23.1	Restricted rotation isopropyl **C**H_3
24.6	Isopropyl **C**H_3
24.9	Isopropyl **C**H_3
45.2	N**C**H_3
52.3 and 54.3	Piperazine **C**H_2 groups
55.0	N**C**H_2Ph
73.8	Restricted rotation isopropyl **C**H
77.0	Isopropyl **C**H
78.0	Isopropyl **C**H
106.9	Aromatic **C**Br
119.9	Aromatic *ipso* to imine
129.5	Aromatic **C**CH_2N
131.3	Aromatic **C**H
135.7	Aromatic **C**H
149.0	Imine **C**H
161.5	Aromatic *ipso* to phenol

Elemental Analysis: $C_{44}H_{74}N_6O_8Ti_2Br_2$

	C	H	N
Calculated %	49.4	6.93	7.87
Observed %	47.1	6.47	7.24

Complex 6.6 Complex of salicylaldoxime and TiPT (2Ti:3L)

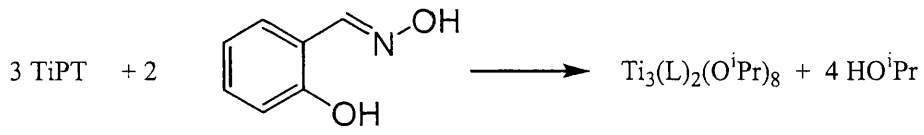

6.6L Complex 6.6

A solution of 1.37g (10mmol) of salicylaldoxime, 6.6L, recrystallised from petroleum ether, was prepared in dry toluene (10ml) under an inert atmosphere. To this was added 4.5ml (15mmol) of TiPT to give an orange solution. This solution was vigorously stirred for one hour and heated to reflux. The solvent was removed *in vacuo* to give an orange solid product. This product was suspended in hexane and toluene added until dissolution occurred on warming. Standing at room temperature yielded a crop of orange blocks.

Yield = 2.12 g (47.8%)
Melting Point = 147-150 °C

^{1}H NMR Spectrum: 400MHz, solvent $CDCl_3$

δ/ppm	Integral	Multiplicity	Coupling/Hz	Assignment
0.71	6H	doublet	5.6	Isopropyl **CH$_3$** (non-trapped)
0.81	6H	doublet	6.0	Isopropyl **CH$_3$** (non-trapped)
1.15	6H	doublet	6.0	Isopropyl **CH$_3$** (trapped)
1.21	6H	doublet	6.4	Isopropyl **CH$_3$** (trapped)
1.23	6H	broad doublet		Isopropyl **CH$_3$** (trapped)
1.24	6H	broad doublet		Isopropyl **CH$_3$** (trapped)
1.29	6H	doublet	6.0	Isopropyl **CH$_3$** (non-trapped)
1.34	6H	doublet	6.4	Isopropyl **CH$_3$** (non-trapped)
4.39	2H	septet	6.4	Isopropyl **CH** (non-trapped)
4.73	2H	septet	6.4	Isopropyl **CH** (trapped)
4.80	2H	septet	6.0	Isopropyl **CH** (trapped)
4.93	2H	septet	6.0	Isopropyl **CH** (non-trapped)

6.68	4H	multiplet		Aromatic C**H**
7.09	2H	doublet		Aromatic C**H**
7.18	2H	doublet		Aromatic C**H**
7.96	2H	singlet		Imine C**H**

$^{13}C\{^{1}H\}$ NMR Spectrum: 100MHz, solvent $CDCl_3$

δ/ppm	**Assignment**
24.6, 24.9, 25.7, 25.7, 26.0, 26.0, 26.6, 26.7	Isopropyl **C**H_3
75.6, 77.6, 78.7, 79.1	Isopropyl **C**H
114.3	Aromatic *ipso* to imine
118.3, 120.7, 130.8, 132.1	Aromatic **C**H
151.2	Imine **C**H
162.6	Aromatic *ipso* to phenol

Elemental Analysis: $C_{38}H_{66}N_2O_{12}Ti_3$

	C	H	N
Calculated %	51.5	7.50	3.16
Observed %	50.6	7.27	2.91

Complex 6.7: Complex of 2,4-dichloro salicylaldoxime and TiPT (2Ti:3L)

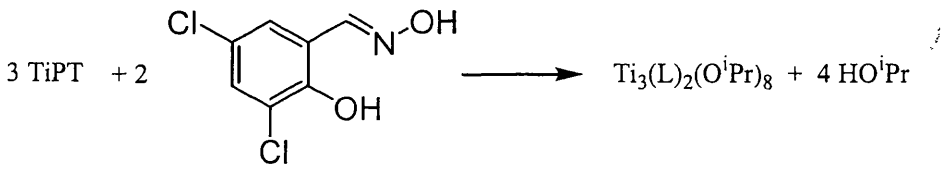

6.7L Complex 6.7

A solution of 0.41g (2 mmol) of 2,4-dichloro salicylaldoxime, 6.7L, was prepared in dry toluene (10ml) under an inert atmosphere. To this was added 0.9ml (3mmol) of TiPT to give an orange solution. This solution was vigorously stirred for one hour and heated to reflux. The solvent was removed *in vacuo* to give an orange solid product. This product was suspended in hexane and toluene added until dissolution occurred on warming. Standing at room temperature yielded a crop of orange blocks.

Yield = 0.84g (84.0%)
Melting Point = 136-139°C

^{1}H NMR Spectrum: 300MHz, solvent $CDCl_3$

δ/ppm	Integral	Multiplicity	Coupling/Hz	Assignment
0.73	6H	doublet	6.1	Isopropyl **C**H$_3$ (non-trapped)
0.84	6H	doublet	6.1	Isopropyl **C**H$_3$ (non-trapped)
1.10	6H	doublet	6.2	Isopropyl **C**H$_3$ (trapped)
1.20	6H	doublet	6.1	Isopropyl **C**H$_3$ (trapped)
1.23	6H	doublet	6.4	Isopropyl **C**H$_3$ (trapped)
1.24	6H	doublet	6.1	Isopropyl **C**H$_3$ (trapped)
1.31	6H	doublet	6.1	Isopropyl **C**H$_3$ (non-trapped)
1.35	6H	doublet	6.1	Isopropyl **C**H$_3$ (non-trapped)
4.39	2H	septet	6.1	Isopropyl **C**H (non-trapped)
4.66-4.83	4H	multiplet		Isopropyl **C**H (trapped)
4.94	2H	septet	6.1	Isopropyl **C**H (non-trapped)
6.97	2H	doublet	2.6	Aromatic **C**H
7.30	2H	doublet	2.5	Aromatic **C**H
7.88	2H	singlet		Imine **C**H

^{13}C{^{1}H} NMR Spectrum: 75.5MHz, solvent $CDCl_3$

δ/ppm	Assignment
23.0, 23.4, 24.2, 24.2, 24.6, 24.9, 25.3, 25.5	Isopropyl **C**H$_3$
74.7, 78.1, 78.4, 79.0	Isopropyl **C**H
120.6, 120.7, 123.0	Aromatic
127.2, 130.5	Aromatic **C**H
149.1	Imine **C**H
155.8	Aromatic *ipso* to phenol

Elemental Analysis: $C_{38}H_{62}N_2O_{12}Ti_3Cl_4$

	C	H	N
Calculated %	44.6	6.10	2.73
Observed %	43.4	5.96	2.59

Complex 6.8: Complex of 4-nitro salicylaldoxime and TiPT (2Ti:3L)

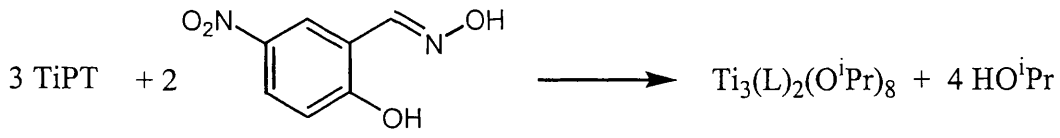

6.8L Complex 6.8

A solution of 0.36g (2 mmol) of 4-nitro salicylaldoxime, 6.8L, was prepared in dry toluene (10ml) under an inert atmosphere. To this was added 0.9ml (3mmol) of TiPT to give a yellow solution. This solution was vigorously stirred for one hour and heated to reflux. The solvent was removed *in vacuo* to give an orange solid product. This product was suspended in hexane and toluene added until dissolution occurred on warming. Standing at room temperature yielded a crop of yellow blocks.

Yield = 0.63g (64.5%)
Melting Point = 211-214 °C (dec.)

^{1}H NMR Spectrum: 300MHz, solvent $CDCl_3$

δ/ppm	Integral	Multiplicity	Coupling/Hz	Assignment
0.71	6H	doublet	6.1	Isopropyl C**H**$_3$ (non-trapped)
0.87	6H	doublet	6.1	Isopropyl C**H**$_3$ (non-trapped)
1.11	6H	doublet	6.2	Isopropyl C**H**$_3$ (trapped)
1.21-1.26	18H	multiplet		Isopropyl C**H**$_3$ (trapped)
1.32	6H	doublet	6.1	Isopropyl C**H**$_3$ (non-trapped)
1.36	6H	doublet	6.1	Isopropyl C**H**$_3$ (non-trapped)
4.42	2H	septet	6.1	Isopropyl C**H** (non-trapped)
4.70	2H	septet	6.2	Isopropyl C**H** (trapped)
4.77	2H	septet	6.2	Isopropyl C**H** (trapped)
4.95	2H	septet	6.1	Isopropyl C**H** (non-trapped)
6.74	2H	doublet	9.9	Aromatic C**H** *ortho* to phenoxide
8.01	2H	singlet		Imine C**H**

8.08	2H	singlet		Aromatic C**H** *meta* to phenoxide
8.11	2H	doublet		Aromatic C**H** *meta* to phenoxide

$^{13}C\{^{1}H\}$ NMR Spectrum: 75.5MHz, solvent $CDCl_3$

δ/ppm	**Assignment**
24.5, 24.9, 25.6, 25.6, 25.8, 25.8, 26.6, 26.7	Isopropyl **C**H_3
76.1, 80.0, 80.3, 80.6	Isopropyl **C**H
119.7	Aromatic
120.0	Aromatic **C**H
127.7	Aromatic
128.3	Aromatic **C**H
139.1	Aromatic *ipso* to nitro
150.6	Imine **C**H
168.5	Aromatic *ipso* to phenol

Elemental Analysis: $C_{38}H_{64}N_4O_{20}Ti_3$

	C	H	N
Calculated %	46.7	6.61	5.74
Observed %	47.2	6.54	5.66

Complex 6.9: Complex of *syn*-pyridine-2-aldoxime and TiPT

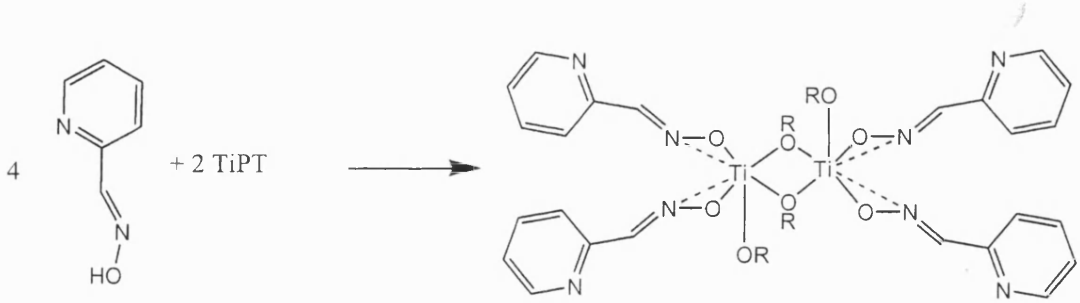

6.9L Complex 6.9

A solution of 1.22g (10 mmol) of *syn*-pyridine-2-aldoxime, 6.9L, was prepared in dry acetonitrile (10ml) under an inert atmosphere. To this was added 1.5ml (5mmol) of TiPT to give a bright orange suspension. This suspension was vigorously stirred at reflux for one hour to give a yellow solution. On cooling this solution yielded a crop of colourless blocks.

Yield = 0.90g (23.4%)
Melting Point = 132-135°C

^{1}H NMR Spectrum: 400MHz, solvent $CDCl_3$

δ/ppm	**Integral**	**Multiplicity**	**Coupling/Hz**	**Assignment**
1.17	12H	broad singlet		Isopropyl C**H**$_3$
4.52	2H	broad singlet		Isopropyl C**H**
7.21	2H	singlet		Aromatic C**H**
7.63-7.83	2H	multiplet		Aromatic C**H**
8.30-8.53	2H	multiplet		Aromatic and Imine C**H**

$^{13}C\{^{1}H\}$ NMR Spectrum: 75.5MHz, solvent $CDCl_3$

δ/ppm	**Assignment**
25.9	Isopropyl **C**H$_3$
77.6	Isopropyl **C**H
121.4, 122.1, 124.2, 136.9	Aromatic (one missing)
149.8	Imine **C**H

Elemental Analysis: $C_{36}H_{48}N_8O_8Ti_2$

	C	H	N
Calculated %	53.0	5.93	13.72
Observed %	52.2	5.90	13.60

Complex 6.10: Hydrolysis of the complex of *syn*-pyridine-2-aldoxime and TiPT

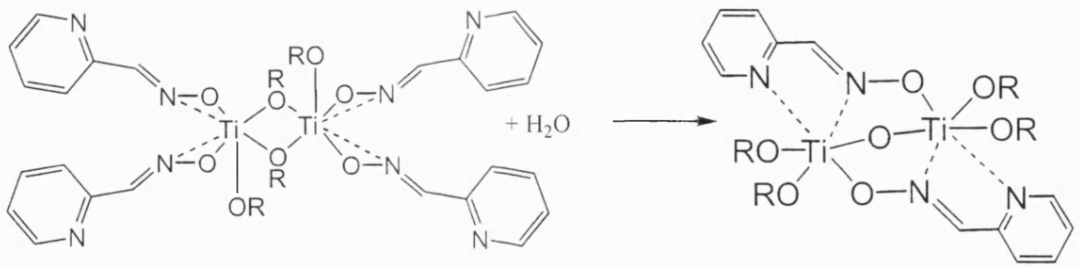

Complex 6.9 Complex 6.10

After synthesis and recovery by filtration of the titanate of *syn*-pyridine-2-aldoxime and TiPT the filtrate was left to stand in an argon atmosphere for 24 hours. Over this time the solution yielded a crop of large clear crystals.

Yield = 0.32g (10.9%)
Melting Point = 181-183°C

^{1}H NMR Spectrum: 400MHz, solvent $CDCl_3$

δ/ppm	Integral	Multiplicity	Coupling/Hz	Assignment
0.85	6H	doublet	6.0	Isopropyl C**H**$_3$
0.94	6H	doublet	6.2	Isopropyl C**H**$_3$
1.28	6H	doublet	6.0	Isopropyl C**H**$_3$
1.33	6H	doublet	6.0	Isopropyl C**H**$_3$
4.49	2H	septet	6.0	Isopropyl C**H**
4.99	2H	septet	5.8	Isopropyl C**H**
7.14	2H	multiplet		Aromatic C**H**
7.22	2H	multiplet		Aromatic C**H**
7.54	2H	singlet		Imine C**H**
7.73	2H	multiplet		Aromatic C**H**
8.81	2H	multiplet		Aromatic C**H**

Complex 6.11: Hydrolysis product of the complex of phenyl-2-pyridyl-ketoxime and TiPT

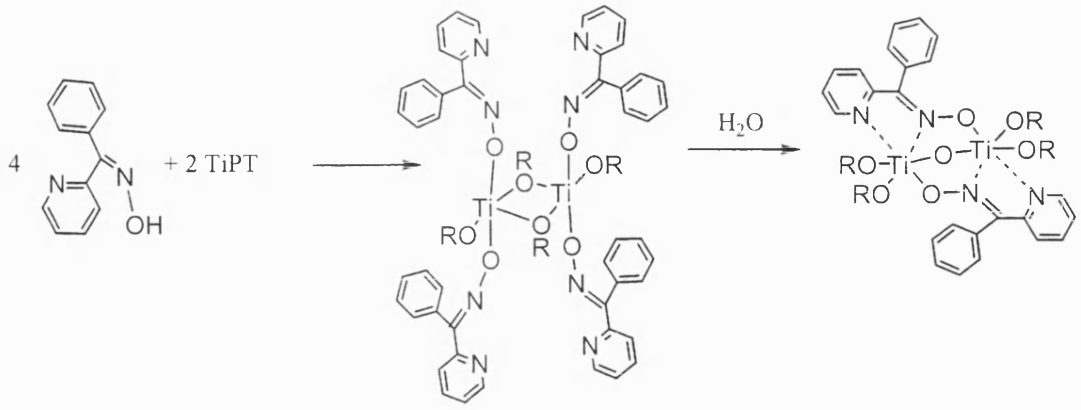

Product A **Product B**

A solution of 0.4g (2mmol) of phenyl-2-pyridine ketoxime, 6.11L, was prepared in dry acetonitrile (5ml) under an inert atmosphere. To this was added 0.6ml (2mmol) of TiPT to give a yellow solution. This solution was vigorously stirred at reflux for one hour to give a yellow solution. On cooling this solution yielded a yellow fibrous product (product A), which was recovered by filtration, and the solution left to stand. On standing for 24 hours this solution yielded a crop of small yellow needles (Product B).

Yield = 0.43g (total yield) (29.0%)
Melting Point = 210-214°C

^{1}H NMR Spectrum: 400MHz, solvent $CDCl_3$ (product A)

δ/ppm	Integral	Multiplicity	Coupling/Hz	Assignment
0.67-1.42	~24H	series of doublets		Isopropyl C**H**$_3$
4.33-5.00	~4H	series of septets		Isopropyl C**H**
6.77-9.40	~36H	complex multiplet		Aromatic region

^{1}H NMR Spectrum: 400MHz, solvent $CDCl_3$ (product B)

δ/ppm	Integral	Multiplicity	Coupling/Hz	Assignment
0.92	6H	doublet	6.0	Isopropyl C**H**$_3$
0.94	6H	doublet	6.0	Isopropyl C**H**$_3$

1.22	6H	doublet	6.0	Isopropyl C**H**$_3$
1.27	6H	doublet	6.2	Isopropyl C**H**$_3$
4.56	2H	septet	6.1	Isopropyl C**H**
5.00	2H	septet	6.1	Isopropyl C**H**
7.02-7.19	12H	multiplet		Aromatic C**H**
7.60	2H	broad triplet		Aromatic C**H**
8.86	2H	multiplet		Aromatic C**H**

$^{13}C\{^{1}H\}$ NMR Spectrum: 75.5MHz, solvent $CDCl_3$ (product B)

δ/ppm	**Assignment**
25.4, 25.6, 26.3, 26.9	Isopropyl **C**H$_3$
75.7, 76.4	Isopropyl **C**H
121.6, 122.7, 128.2, 128.9, 129.8, 130.6, 138.9, 147.7, 151.0, 153.9	Aromatic **C**
No observed signal	Imine **C**

Elemental Analysis: $Ti_2C_{36}H_{48}N_4O_7$

	C	H	N
Calculated %	58.1	6.49	7.52
Observed %	57.8	6.19	7.49

Complex 6.12: Hydrolysis product of the complex of di-2-pyridine-ketoxime and TiPT

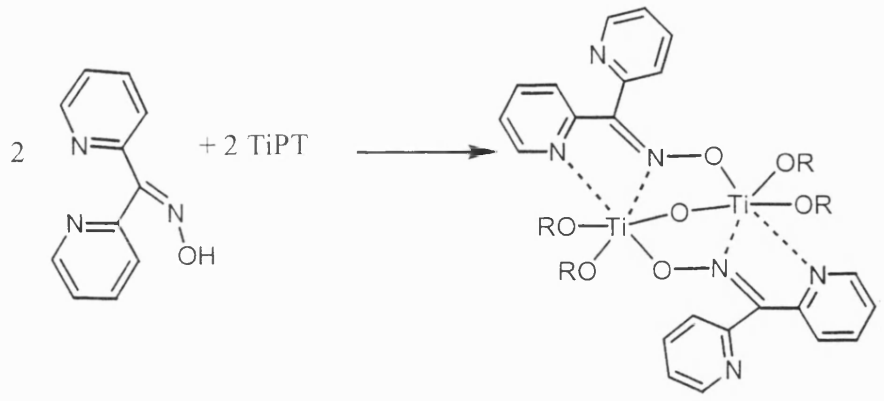

6.12L Complex 6.12

A solution of 0.2g (1mmol) of di-2-pyridine ketoxime, 6.12L, was prepared in dry toluene (15ml) under an inert atmosphere. To this was added 0.3ml (1mmol) of TiPT to give a yellow suspension. This suspension was vigorously stirred at reflux for one hour to give a yellow solution. On cooling this solution yielded a small amount of yellow powder, which was discarded, and the solution left to stand. On standing for 24 hours this solution yielded two large yellow crystals.

Yield = 0.16g (43.1%)
Melting Point = 204-207°C

^{1}H NMR Spectrum: 400MHz, solvent $CDCl_3$

δ/ppm	Integral	Multiplicity	Coupling/Hz	Assignment
0.93	6H	doublet	6.0	Isopropyl C**H**$_3$
0.97	6H	doublet	6.2	Isopropyl C**H**$_3$
1.26	6H	doublet	6.1	Isopropyl C**H**$_3$
1.30	6H	doublet	6.0	Isopropyl C**H**$_3$
4.55	2H	septet	6.0	Isopropyl C**H**
5.02	2H	septet	6.2	Isopropyl C**H**
7.05	2H	multiplet		Aromatic C**H**
7.20	2H	multiplet		Aromatic C**H**

7.30	2H	multiplet		Aromatic C**H**
7.36	2H	multiplet		Aromatic C**H**
7.66	4H	multiplet		Aromatic C**H**
8.50	2H	broad doublet		Aromatic C**H**
8.94	2H	broad doublet		Aromatic C**H**

$^{13}C\{^{1}H\}$ NMR Spectrum: 75.5MHz, solvent $CDCl_3$

δ/ppm	**Assignment**
25.5	Isopropyl **C**H_3
26.4	Isopropyl **C**H_3
75.8	Isopropyl **C**H
76.9	Isopropyl **C**H
122.8, 123.0, 123.6, 127.4, 135.7, 139.0	Aromatic **C**H
146.6	Aromatic **C**
149.1	Aromatic **C**
149.4	Aromatic **C**H
150.6	Aromatic **C**H
153.4	Imine **C**

Elemental Analysis: $C_{34}H_{44}N_6O_7Ti_2$ and toluene C_7H_8

	C	H	N
Calculated %	58.9	6.26	10.05
Observed %	58.2	6.14	9.89

3.4 Experimental data for chapter 7

3.4.1 Ligand syntheses

For all of the reactions detailed in this chapter the ligands used were purchased from Aldrich and used as received. The ligands used in the chapter are detailed in the figure below.

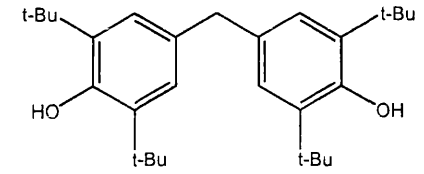

7.1L

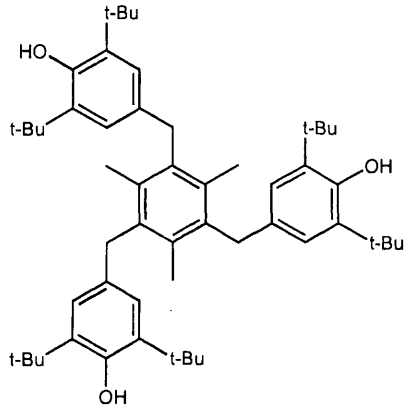

7.3L

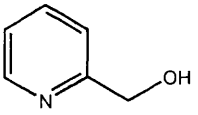

7.4L

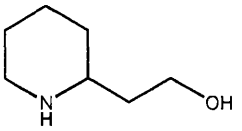

7.5L

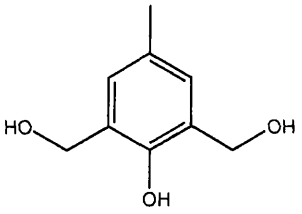

7.6L

Ligands used in chapter 7

3.4.2 Complex synthesis

Complex 7.1: Complex of 4,4'-methylene-bis-(2,6-di-*tert*-butyl-phenol) and one equivalent of TiPT

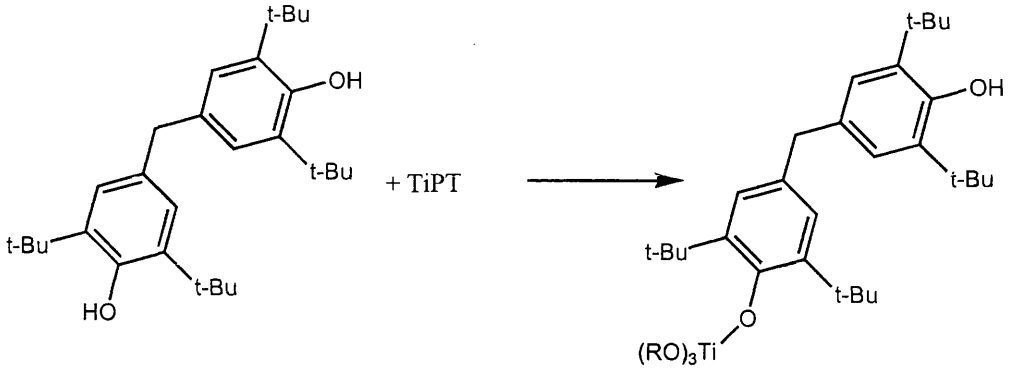

7.1L

Complex 7.1

A suspension of 2.12g (5mmol) of 4,4'-methylene-bis-(2,6-di-*tert*-butyl-phenol), 7.1L, was prepared in dry hexane (10ml) under an inert atmosphere. To this was added 1.5ml (5mmol) of TiPT to give a yellow solution. This solution was vigorously stirred for one hour and heated to reflux. Approximately three quarters of the solvent was removed *in vacuo*. The solution was left to stand at –20°C and yielded a significant amount of yellow fibrous product.

Yield = 2.02g (62.4%)
Melting Point = 48-49 °C

^{1}H NMR Spectrum: 400MHz, solvent $CDCl_3$

δ/ppm	Integral	Multiplicity	Coupling/Hz	Assignment
1.28	18H	doublet	6.4	Isopropyl CH_3
1.44	36H	doublet	5.6	*t*-Butyl CH_3
3.85	2H	singlet		Methylene CH_2
4.66	3H	septet	6.4	Isopropyl CH
5.05	1H	doublet	6.8	Phenolic OH
7.04	4H	singlet		Aromatic CH

$^{13}C\{^{1}H\}$ NMR Spectrum: 75.5MHz, solvent $CDCl_3$

δ/ppm	Assignment
26.5	Isopropyl **C**H_3
30.7, 31.1	*t*-Butyl **C**H_3
35.3	**C**H_2
41.8, 68.38	*t*-Butyl **C**
78.6	Isopropyl **C**H
125.6, 125.9, 131.6, 132.4, 135.9, 139.0	Aromatic
163.0, 152.2	Aromatic ipso to phenol

Complex 7.2: Complex of 4,4'-methylene-bis-(2,6-di-*tert*-butyl-phenol) and two equivalents of TiPT

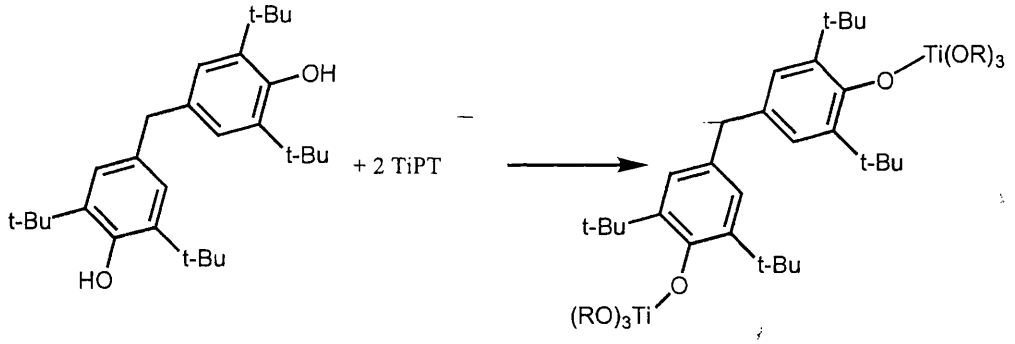

7.1L Complex 7.2

A suspension of 2.12g (5mmol) of 4,4'-methylene-bis-(2,6-di-*tert*-butyl-phenol), 7.1L, was prepared in dry hexane (10ml) under an inert atmosphere. To this was added 3ml (10mmol) of TiPT to give a yellow solution. This solution was vigorously stirred for one hour and heated to reflux. Approximately three quarters of the solvent was removed *in vacuo*. The solution was left to stand at –20°C and yielded a significant amount of yellow fibrous product.

Yield = 3.12g (71.6%)
Melting Point = 75-77°C

^{1}H NMR Spectrum: 400MHz, solvent $CDCl_3$

δ/ppm	Integral	Multiplicity	Coupling/Hz	Assignment
1.27	36H	doublet	5.6	Isopropyl C**H**$_3$
1.44	36H	doublet	5.6	*t*-Butyl C**H**$_3$
3.83	2H	singlet		Methylene C**H**$_2$

4.64	6H	septet	6.4	Isopropyl **CH**
7.03	4H	singlet		Aromatic **CH**

$^{13}C\{^{1}H\}$ NMR Spectrum: 75.5MHz, solvent $CDCl_3$

δ/ppm	**Assignment**
26.7	Isopropyl **C**H_3
31.1	*t*-Butyl **C**H_3
35.3	**C**H_2
41.9	*t*-Butyl **C**
78.5	Isopropyl **C**H
125.6, 131.8, 139.0	Aromatic
163.0	Aromatic ipso to phenol

Elemental Analysis: $C_{47}H_{84}O_8Ti_2$

	C	H	N
Calculated %	64.7	9.70	0
Observed %	63.8	9.38	0

Complex 7.3: Complex of 1,3,5-trimethyl-2-4-6-tris(3,5-di-*tert*-butyl-4-hydroxybenzyl)benzene and TiPT

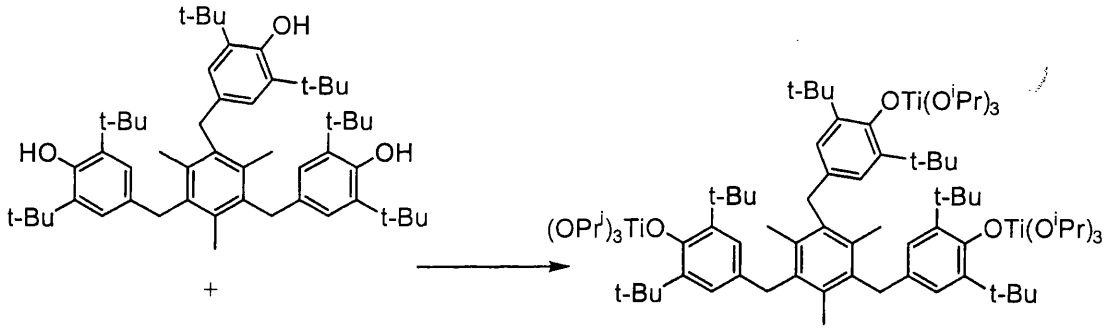

A suspension of 3.88g (5mmol) of 1,3,5-trimethyl-2-4-6-tris(3,5-di-*tert*-butyl-4-hydroxybenzyl)benzene, 7.3L, was prepared in dry hexane (10ml) under an inert atmosphere. To this was added 4.5ml (15mmol) of TiPT to give a pale yellow solution. This solution was vigorously stirred for one hour and heated to reflux. Approximately half of the solvent was removed *in vacuo*. The solution was left to stand at –20°C and yielded a crop of pale yellow blocks.

Yield = 5.4g (74.7%)
Melting Point = 183-185°C

^{1}H NMR Spectrum: 400MHz, solvent $CDCl_3$

δ/ppm	Integral	Multiplicity	Coupling/Hz	Assignment
1.19	54H	doublet	6.0	Isopropyl C**H**$_3$
1.29	54H	singlet		*t*-Butyl C**H**$_3$
2.19	9H	singlet		Aromatic C**H**$_3$
3.94	6H	singlet		Methylene C**H**$_2$
4.56	9H	septet	6.4	Isopropyl C**H**
6.80	6H	singlet		Aromatic C**H**

^{13}C{^{1}H} NMR Spectrum: 75.5MHz, solvent $CDCl_3$

δ/ppm	Assignment
17.7	Aromatic **C**H$_3$
27.0	Isopropyl **C**H$_3$
31.2	*tert*-Butyl **C**H$_3$
36.7	Methylene **C**H$_2$
78.4	Isopropyl **C**H
124.7, 130.8, 134.5, 135.9, 138.9, 162.8	Aromatic

Elemental Analysis: $C_{81}H_{138}O_{12}Ti_3$

	C	H	N
Calculated %	67.2	9.61	0
Observed %	67.5	9.55	0

Complex 7.4: Complex of 2-hydroxymethyl pyridine and TiPT

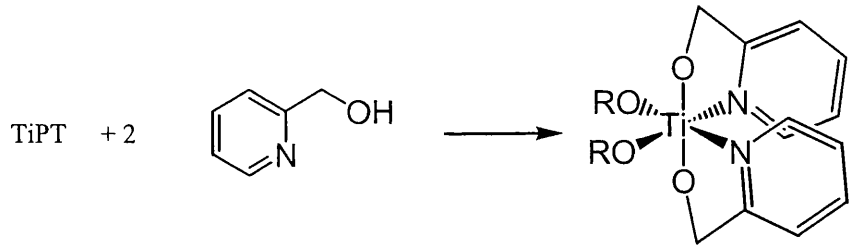

7.4L Complex 7.4

A solution of 0.96ml (10mmol) of 2-hydroxymethyl pyridine, 7.4L, was prepared in dry toluene (10ml) under an inert atmosphere. The resulting solution was added, via cannula, to a solution of 1.5ml (5mmol) of TiPT in 10ml of dry toluene at –78°C. The resulting colourless solution was vigorously stirred for one hour and heated to reflux. The solvent was removed *in vacuo* to give a white solid product. This product was suspended in hexane and toluene added until dissolution occurred on warming. Standing at room temperature yielded a crop of large colourless blocks.

Yield = 1.72 g (90.0%)
Melting Point = 116-117 °C

^{1}H NMR Spectrum: 300MHz, solvent $CDCl_3$

δ/ppm	Integral	Multiplicity	Coupling/Hz	Assignment
0.94	12H	doublet	6.1	Isopropyl **C**H_3
4.55	2H	septet	6.1	Isopropyl **C**H
5.5	4H	singlet		Methylene **C**H_2
7.06-7.09	4H	multiplet		Aromatic **C**H
7.52-7.58	2H	multiplet		Aromatic **C**H
8.53-8.56	2H	multiplet		Aromatic **C**H

$^{13}C\{^{1}H\}$ NMR Spectrum: 75MHz, solvent $CDCl_3$

δ/ppm	Assignment
24.6	Isopropyl **C**H_3
73.3	Methylene **C**H_2
74.2	Isopropyl **C**H
117.9	Aromatic **C**H *meta* to pyridine
120.8	Aromatic **C**H *meta* to pyridine

136.5	Aromatic **C**H *para* to pyridine
146.1	Aromatic **C**H *ortho* to pyridine
165.0	Aromatic **C** *ipso* to hydroxymethyl group

Elemental Analysis: $C_{18}H_{26}N_2O_4Ti$

	C	H	N
Calculated %	56.5	6.81	7.33
Observed %	56.0	6.71	7.33

Complex 7.5: Complex of 2-hydroxyethyl piperidine and TiPT

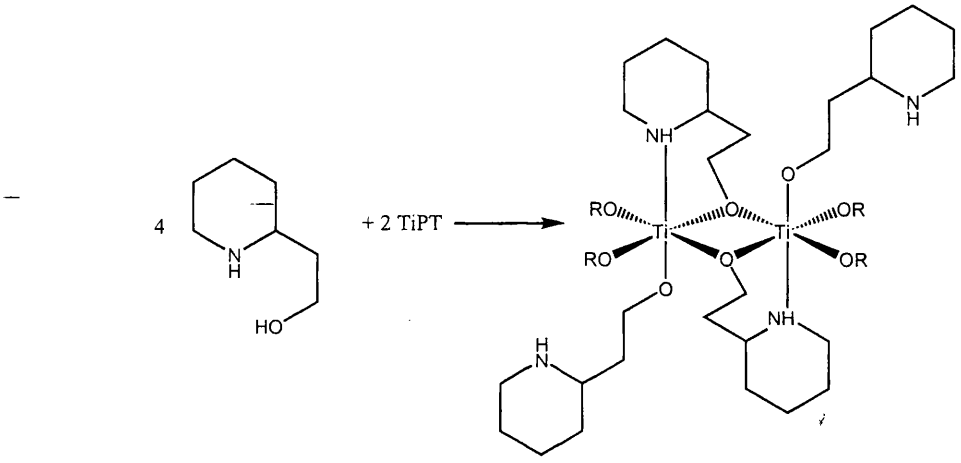

7.5L Complex 7.5

A solution of 1.29g (10mmol) of 2-hydroxyethyl piperidine, 7.5L, was prepared in dry toluene (10ml) under an inert atmosphere. The resulting solution was added, via cannula, to a solution of 1.5ml (5mmol) of TiPT in 10ml of dry toluene at –78°C. The resulting colourless solution was vigorously stirred for one hour and heated to reflux. The solvent was removed *in vacuo* to give a white solid product. This product was suspended in hexane and toluene added until dissolution occurred on warming. Standing at room temperature yielded a crop of small colourless blocks.

Yield = 1.76 g (83.4%)
Melting Point = 98-101 °C

^{1}H NMR Spectrum: 300MHz, solvent $CDCl_3$

δ/ppm	**Integral**	**Multiplicity**	**Coupling/Hz**	**Assignment**
1.14	24H	doublet		Isopropyl **C**H$_3$
1.22-1.69	32H	broad multiplet		Cyclohexyl **C**H$_2$

2.53-2.63	12H	broad multiplet		Methylene CH_2 and Cyclohexyl C**H**
3.08	4H	broad singlet		N**H**
4.27	8H	broad singlet		CH_2CH_2O
4.71-4.73	4H	broad multiplet		Isopropyl C**H**

$^{13}C\{^1H\}$ NMR Spectrum: 75MHz, solvent $CDCl_3$

δ/ppm	**Assignment**
21.6	Isopropyl CH_3
23.7, 25.6, 30.6, 33.2, 46.4, 54.8, 70.5	Ligand
74.8	Isopropyl CH

Elemental Analysis: $C_{40}H_{84}N_4O_8Ti_2$

	C	H	N
Calculated %	56.9	10.02	6.63
Observed %	57.2	10.02	6.30

Complex 7.6: Complex of 2,6-bis-hydroxymethyl-*para*-cresol and TiPT

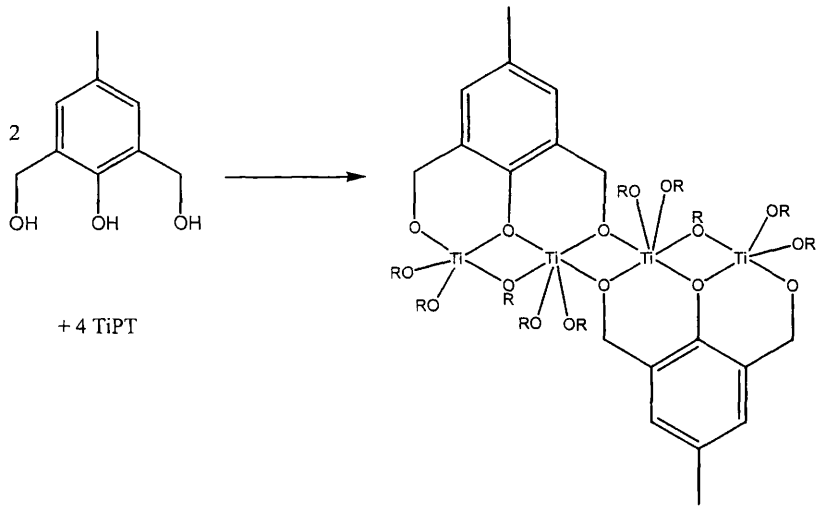

7.6L Complex 7.6

A solution of 1.68g (10 mmol) of ligand 7.6L was prepared in dry hexane (10ml) under an inert atmosphere. To this was added 6ml (20mmol) of TiPT to give an orange/brown suspension. This suspension was heated to reflux and filtered hot. On standing the filtrate yielded a crop of off white crystals.

Yield = 3.80g (34.2%)
Melting Point = 94-97°C

^{1}H NMR Spectrum: 400MHz, solvent $CDCl_3$

δ/ppm	Integral	Multiplicity	Coupling/Hz	Assignment
1.23-1.46	60H	multiplet		Isopropyl C**H**$_3$
2.22	6H	three singlets		Aromatic C**H**$_3$
4.49	5H	broad septet		Isopropyl C**H**
4.80-5.40	5H	several multiplets		Benzylic C**H**$_2$
6.70-6.90	4H	several peaks		Aromatic C**H**

Elemental Analysis: $C_{48}H_{88}O_{16}Ti_4$

	C	H	N
Calculated %	51.8	7.97	0
Observed %	50.8	7.81	0

3.5 Experimental data for chapter 8

3.5.1 Ligands

The acidic reagents used in this section are shown in the figure below, in the case of 8.1L and 8.3L these were purchased from Aldrich and used as received. Ligand 8.2L was purchase from Acros and used as received.

HBF_4 in Et_2O **8.1L**

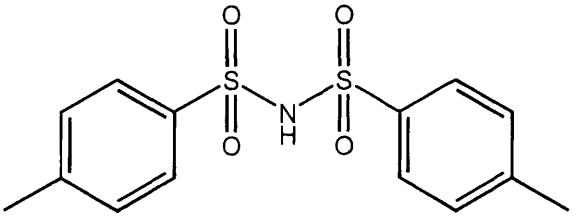

8.2L

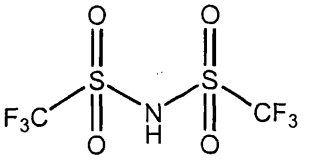

8.3L

Acidic reagents used in chapter 8

3.5.2 Complex synthesis

Complex 8.1: Reaction of titanium bis 8-hydroxyquinolinate bis isopropanolate with HBF_4

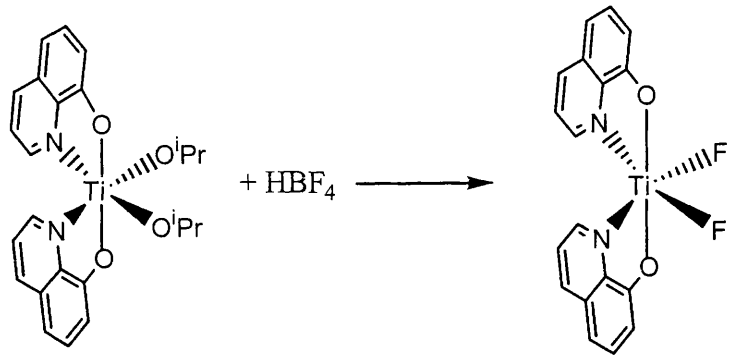

Complex 8.1

A solution of 1.14g (2 mmol) of titanium bis-8-hydroxyquinolinate-bis-isopropanolate was prepared in dry diethyl ether (10ml) under an inert atmosphere and cooled to –78°C. To this was added 0.3ml (2mmol) of HBF_4 in diethyl ether to give an orange suspension. The product was recovered by filtration and dissolved in 10ml dry acetonitrile to give a red solution from which a bright red crystalline product crystallised.

Yield (initial solid) = 1.0g (The structural form of this initial product is unknown so a percentage yield is impossible to calculate.)
Melting point = >350°C

^{1}H NMR Spectrum: 400MHz, solvent CD_3CN (both products)

δ/ppm	Integral	Multiplicity	Coupling/Hz	Assignment
7.04	2H	broad doublet		Aromatic CH
7.44	4H	multiplet		Aromatic CH
7.61	2H	broad triplet		Aromatic CH
8.38	2H	multiplet		Aromatic CH
8.61	2H	broad singlet		Aromatic CH

^{19}F NMR Spectrum: 376 MHz, solvent $CDCl_3$ (initial product)

δ/ppm	Multiplicity	Assignment
-152.01	singlet	BF_4
-151.95	singlet	BF_4
191.59	singlet	Ti-**F**

^{19}F NMR Spectrum: 376 MHz, solvent $CDCl_3$ (recrystallised product)

δ/ppm	Multiplicity	Assignment
191.47	singlet	Ti-**F**

Elemental Analysis: $C_{24}H_{26}F_2O_4Ti$

	C	H	N
Calculated %	57.8	3.23	7.49
Observed %	57.7	3.38	8.34

Complex 8.2: Complex of di-*p*-toluene sulfonamide and TiPT

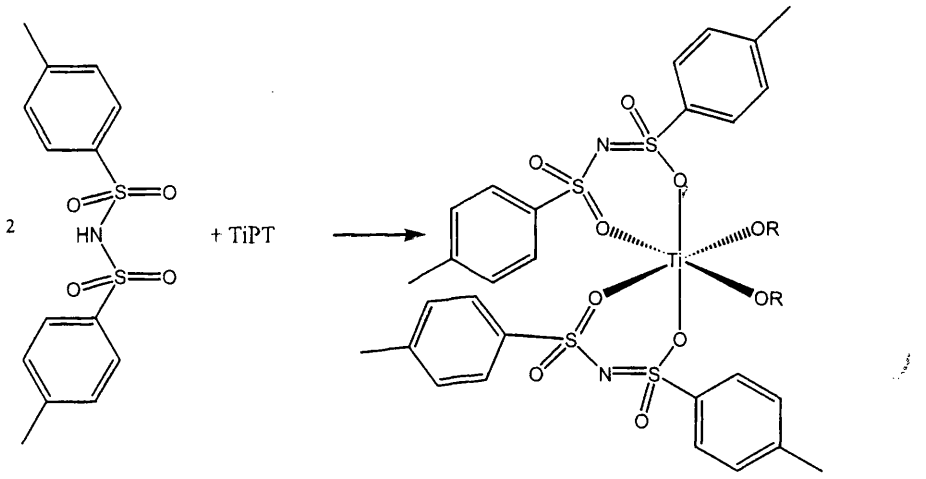

8.2L Complex 8.2

A solution of 0.33g (1 mmol) of di-*p*-tolyl sulfonamide, 8.2L, was prepared in dry toluene (10ml) under an inert atmosphere. To this was added 0.3ml (1mmol) of TiPT to give a clear solution. This solution was vigorously stirred for two hours at reflux. The solvent was removed *in vacuo* to give a white residue. This product was suspended in hexane and toluene added until dissolution occurred on warming. Standing at room temperature yielded a crystalline white product, which was washed with hexane.

Yield = 0.38g (80.9%)
Melting Point = 152-155 °C

^{1}H NMR Spectrum: 300MHz, solvent $CDCl_3$

δ/ppm	Integral	Multiplicity	Coupling/Hz	Assignment
1.29	12H	broad singlet		Isopropyl C**H**$_3$
2.24	12H	broad singlet		*p*-Tolyl C**H**$_3$
5.21	2H	broad singlet		Isopropyl C**H**
6.82-7.83	16H	broad multiplet		Aromatic C**H**

$^{13}C\{^{1}H\}$ NMR Spectrum: 75.5MHz, solvent $CDCl_3$

δ/ppm	Assignment
20.4	*p*-Tolyl **C**H$_3$
23.7	Isopropyl **C**H$_3$
85.9	Isopropyl **C**H
125.7	Aromatic **C**H
128.0	Aromatic **C**H
128.6	Aromatic **C** *ipso* Me
142.1	Aromatic **C** *ipso* SO_2

Elemental Analysis: $C_{34}H_{42}N_2S_4O_{10}Ti$

	C	H	N
Calculated %	50.1	5.16	3.44
Observed %	52.6	5.43	3.69

Complex 8.3: Complex of triflamide and TiPT

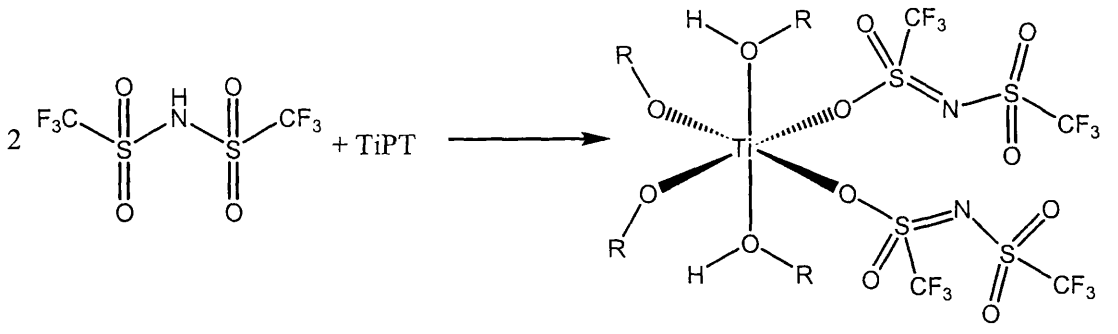

8.3L Complex 8.3

A solution of 0.28g (1 mmol) of ligand 8.3L was prepared in dry toluene (10ml) under an inert atmosphere. To this was added 0.3ml (1mmol) of TiPT to give a clear solution. This solution was vigorously stirred for two hours at reflux. The solvent was removed *in vacuo* to give a white residue. This product was suspended in hexane and toluene added until dissolution occurred on warming. Standing at room temperature yielded a crystalline white product, which was washed with hexane.

Yield = 0.47g (81.0%)
Melting Point = 76-80 °C

^{1}H NMR Spectrum: 300MHz, solvent $CDCl_3$

δ/ppm	Integral	Multiplicity	Coupling/Hz	Assignment
1.19	24H	singlet		Isopropyl CH_3
4.41	2H	singlet		Isopropyl **CH**
4.79	2H	singlet		Isopropyl **CH**
8.13	2H	singlet		Isopropyl **OH**

$^{13}C\{^{1}H\}$ NMR Spectrum: 75.5MHz, solvent $CDCl_3$

δ/ppm	Assignment
23.8	Isopropyl CH_3
24.9	Isopropyl CH_3
78.8	Isopropyl **CH**
91.2	Isopropyl **CH**-OH
119.1 (quartet, J=340Hz)	CF_3

^{19}F NMR Spectrum: 376 MHz, solvent $CDCl_3$

δ/ppm	Multiplicity	Assignment
-78.8	broad singlet	CF_3

Elemental Analysis: $C_{16}H_{30}F_{12}N_2S_4O_{12}Ti$

	C	H	N
Calculated %	22.	3.55	3.31
Observed %	21.5	3.56	3.16

Complex 8.4: Complex of triflamide and 7.3

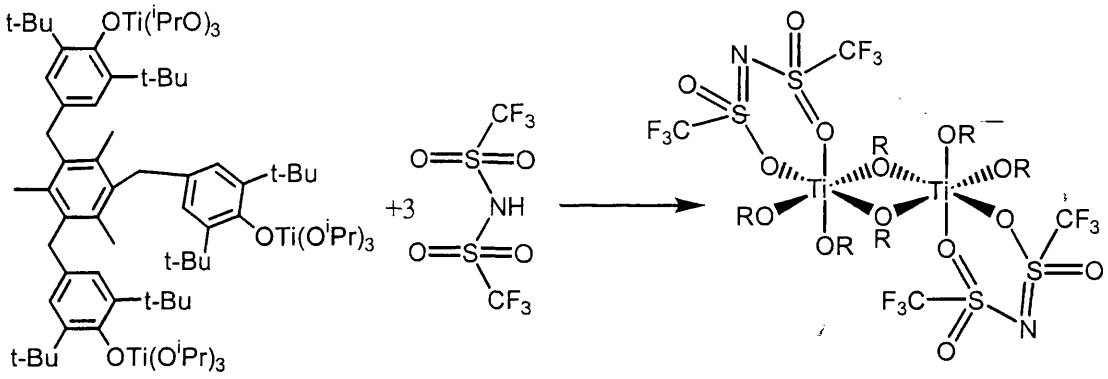

Complex 7.3 8.3L Complex 8.4

A solution of 0.84g (3 mmol) of triflamide, 8.3L, was prepared in dry toluene (10ml) under an inert atmosphere. This was added via cannula to a solution of the titanium species complex 7.3 (1.45g, 1mmol) in toluene (10ml) at –78°C giving a red solution. On warming to room temperature this solution went clear and the resulting solution was vigorously stirred for two hours at reflux. The solvent was removed *in vacuo* to give a white residue. This product was suspended in hexane and toluene added until dissolution occurred on warming. Standing at room temperature yielded a crystalline white product, which was washed with hexane.

Yield = 1.02g (66.4%)
Melting Point = 101-103 °C

^{1}H NMR Spectrum: 300MHz, solvent $CDCl_3$

δ/ppm	Integral	Multiplicity	Coupling/Hz	Assignment
1.38	36H	doublet	9.0	Isopropyl CH_3

4.98	6H	septet	6.0	Isopropyl **CH**

$^{13}C\{^{1}H\}$ NMR Spectrum: 75.5MHz, solvent $CDCl_3$

δ/ppm	**Assignment**
26.2	Isopropyl **C**H_3
84.6	Isopropyl **C**H
119.3 (quartet, J=319Hz)	**C**F_3

^{19}F NMR Spectrum: 376 MHz, solvent $CDCl_3$

δ/ppm	**Multiplicity**	**Assignment**
-78.87	broad singlet	C**F**$_3$

Elemental Analysis: $C_{22}H_{42}F_{12}N_2S_4O_{14}Ti_2$

	C	H	N
Calculated %	26.1	4.16	2.77
Observed %	24.7	5.00	3.03

Complex 8.5: Reaction of triflamide and complex 7.4

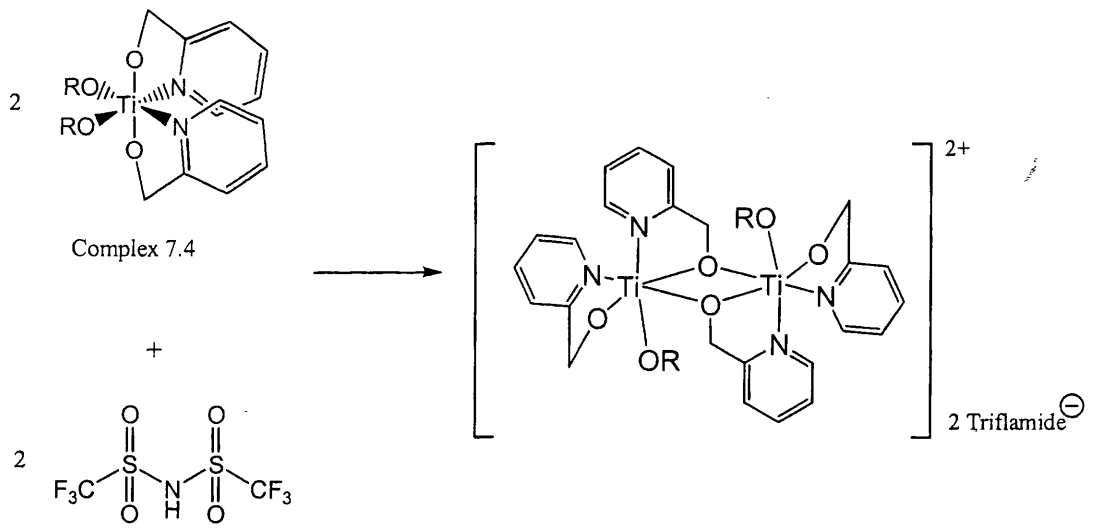

A solution of 0.28g (1 mmol) of triflamide, 8.3L, was prepared in dry toluene (10ml) under an inert atmosphere and cooled to –78°C. To this was added 0.38g (1mmol) of complex 8.5 to give a white suspension. On warming to room temperature an oily product was formed. The solvent was removed *in vacuo* to give a white oily residue.

This product was recrystallised from dry THF to give a crystalline white product, which was washed with hexane.

Yield = 0.43g (35.75%)
Melting Point = 223-229 °C

^{1}H NMR Spectrum: 300MHz, solvent CD_2Cl_2 (Major product; non-aromatic region)

δ/ppm	Integral	Multiplicity	Coupling/Hz	Assignment
2.38	36H	doublet	6.2	Isopropyl C**H**$_3$
4.87	6H	septet	6.2	Isopropyl C**H**
5.76	6H	doublet	19.5	Diastereotopic methylene C**H** (*a* coupled to *b*)
6.00	6H	doublet	16.9	Diastereotopic methylene C**H** (*c* coupled to *d*)
6.17	6H	doublet	16.6	Diastereotopic methylene C**H** (*d* coupled to *c*)
6.28	6H	doublet	19.4	Diastereotopic methylene C**H** (*b* coupled to *a*)

^{1}H NMR Spectrum: 300MHz, solvent CD_2Cl_2 (Minor product; non-aromatic region)

δ/ppm	Integral	Multiplicity	Coupling/Hz	Assignment
0.79	6H	doublet	6.2	Isopropyl C**H**$_3$
1.08	6H	doublet	6.2	Isopropyl C**H**$_3$
4.53	2H	septet	6.2	Isopropyl C**H**
5.56	2H	doublet	16.8	Diastereotopic methylene C**H** (*e* coupled to *f*)
5.90	2H	doublet	19.8	Diastereotopic methylene C**H** (*g* coupled to *h*)
6.05	2H	doublet	17.3	Diastereotopic methylene C**H** (*f* coupled to *e*)
6.22	2H	doublet	18.6	Diastereotopic methylene C**H** (*h*coupled to *g*)

^{1}H NMR Spectrum: 300MHz, solvent CD_2Cl_2 (Both products; aromatic region)

δ/ppm	Integral	Multiplicity	Coupling/Hz	Assignment
6.56	6H	triplet		Aromatic
7.14	6H	doublet		Aromatic

7.26-7.46	16H	multiplet		Aromatic
7.55-7.66	16H	multiplet		Aromatic
7.86-7.99	12H	multiplet		Aromatic
8.16-8.25	8H	multiplet		Aromatic

$^{13}C\{^{1}H\}$ NMR Spectrum: 75.5MHz, solvent $CDCl_3$

δ/ppm	**Assignment**
25.5	Isopropyl **C**H_3
78.6, 81.0	Methylene **C**H_2
86.1	Isopropyl **C**H
122.1, 123.0, 124.5, 126.1, 141.0, 142.8, 146.6, 147.2, 159.0, 165.5	Aromatic **C**

^{19}F NMR Spectrum: 376 MHz, solvent $CDCl_3$

δ/ppm	**Multiplicity**	**Assignment**
-81.4	singlet	**C**F_3

Elemental Analysis: $C_{34}H_{38}F_{12}N_6S_4O_{10}Ti_2$

	C	H	N
Calculated %	35.7	3.33	7.36
Observed %	30.8	2.88	6.48

Chapter 4

The Synthesis, Isolation and Structural Characterisation of a Series of Titanium Isopropoxide Complexes of Bidentate Monoanionic Schiff Bases

The following chapter deals with the synthesis and characterisation of titanium alkoxide complexes of monoanionic bidentate Schiff base ligands of the type shown in figure 4.1 below.

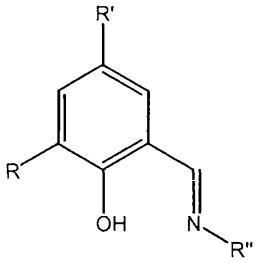

R and R' = alkyl, halide, H, NO_2, NR_2, OR etc.

R" = alkyl, aryl

Figure 4.1: Monoanionic bidentate Schiff base/salicylaldimine

These highly versatile ligands are ubiquitous in coordination chemistry due to the ease of variation of their steric and electronic properties by variation of the substituents R, R' and R'' shown above.

The chapter begins with a review of the extant literature involving these ligands and their complexes with titanium. This is followed by a discussion of the structural aspects of a number of complexes, which we have synthesised from these ligands and titanium tetra-isopropoxide (TiPT).

4.1 Introduction

4.1.1 Historical context of Schiff bases and stereochemical considerations

Schiff bases are compounds containing imine groups, which are formed by the condensation reaction between a carbonyl group and a primary amine resulting in the evolution of water (figure 4.2 below).

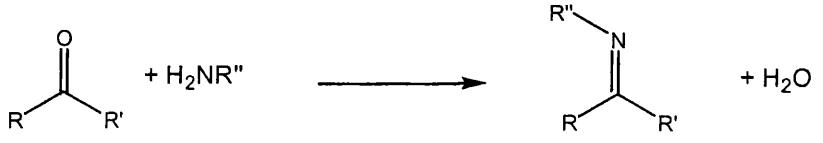

Figure 4.2: Synthesis of a Schiff base

These compounds were first reported in 1864 by Hugo J. Schiff, whose name they take[1], and have been utilised ever since in many different fields. This general reaction has almost unlimited scope and is used to form an immense library of compounds in almost all fields of chemistry. One of the most important groups of Schiff base complexes in respect to coordination chemistry are those based on salicylaldehyde and a monofunctional alkyl or aryl primary amine as shown in figure 4.3 below.

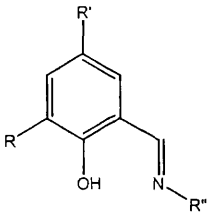

Figure 4.3: Salicylaldimine Schiff base

These compounds allow for formation of chelated aryloxide complexes, which are known for a huge range of metals with diverse uses including as catalysts for ethylene polymerisation and olefin metathesis. A search of the Cambridge Structural Database[2] for the fragment shown in figure 4.4 below generates 2762 hits, a result which highlights the huge amount of work carried out on the coordination chemistry of these ligands.

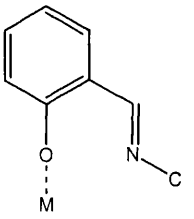

Figure 4.4: Salicylaldimine metal complex CSD search fragment[2]

Before discussing the chemistry of the salicylaldimine ligands with titanium species it is important to note the preferred geometry attained in complexes of the type formed in these reactions. In general homoleptic titanium species such as TiPT and $TiCl_4$ react with bidentate salicylaldimine ligands (SalH) to yield distorted octahedral

[1] H.J. Schiff, *Ann.Chem.*, **131**, 118 (1864)
[2] F.H. Allen and O. Kennard, *Chem. Des. Autom. News*, **8**, 1 (1993)

complexes with the formula $Ti(Sal)_2X_2$. Octahedral complexes of this type can have five isomeric forms as shown in figure 4.5 below.

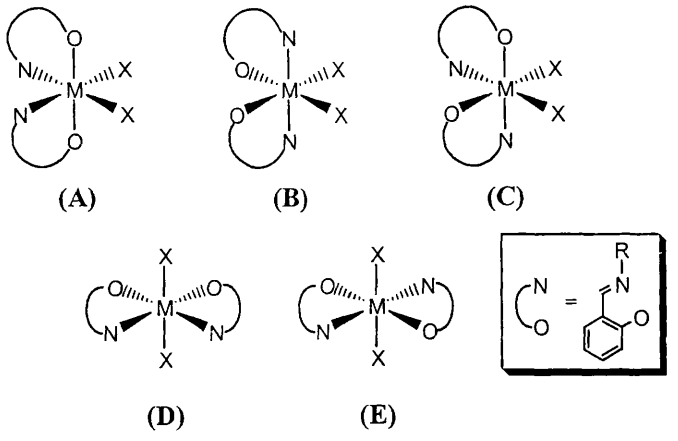

Figure 4.5: Isomeric forms for titanium salicylaldimine complexes

Previous X-ray crystallographic studies such as those which will be described in the following introductory sections have established that of the five possible structures, A-E in figure 4.5 above, the preferential arrangement is A. Structure A has trans-axial phenolic oxygen donors, cis-equatorial imine nitrogen donors and cis-equatorial monodentate X ligands. This favourable arrangement has been rationalised by simple VSEPR concepts[3] and DFT calculations have shown this confirmation to be the most favourable in the gas phase[4]. Analysis of donor atom repulsion in $Ti(Sal)_2X_2$ complexes reveals that cis-X configuration is preferred and that axial donor atom-donor atom repulsions are weaker than those at equatorial positions, predicting that in complexes containing both symmetrical and unsymmetrical bidentate ligands the axial donor forms the shortest bonds to the metal.

[3] D.L. Keppert, In '*Progress In Inorganic Chemistry*' (S.L. Lippard Ed.), John Wiley and Sons Inc., New York, **23**, Chapter 1 (1997)
[4] S. Matsui, M. Mitani, J. Saito, Y. Tohi, H. Makio, N. Matsukawa, Y. Takagi, K. Tsuru, M. Nitabaru, T. Nakano, H. Tanaka, N. Kashiwa and T. Fujita, *J. Am. Chem. Soc.*, **123**, 6847 (2001)

4.1.2 Early structural reports of titanium complexes

The following section details the structure and reactivity of the complexes of bidentate monoanionic salicylaldimines and titanium species. This is not however an exhaustive review due to lack of space and in particular the reactions of salicylaldimines with cyclopentadienyl titanium species will not be covered in detail.

The first reaction of a salicylaldimine, of the type described above, and a titanium species was reported by Bradley et al. in 1969[5]. The product was characterised by single crystal X-ray crystallography and found to have the structure shown in figure 4.6 below.

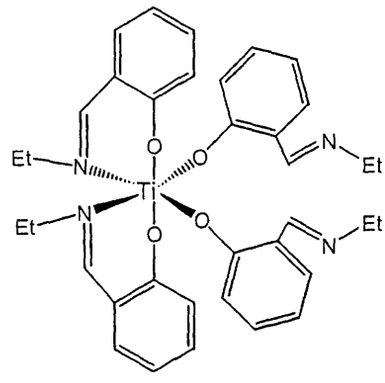

Figure 4.6: The first structurally characterised titanium salicylaldimine complex

The product was formed by the reaction of $Ti(NMe_2)_4$ and the corresponding ligand and has two chelating and two terminal salicylaldimine ligands, which are seen to exchange on the NMR timescale.

In the same year workers in the U.S.S.R. reported reactions of salicylaldimine ligands and titanium tetrachloride giving products with the formula TiL_2Cl_2 whose structures they characterised by infra-red spectroscopy[6].

Gupta et al reported the first use of the ligands with titanium tetra-isopropoxide in 1970[7]. Several simple salicylaldimine ligands were refluxed with titanium tetra-

[5] D.C. Bradley, M.B. Hursthouse and I.F. Rendall, *Chem. Comm.*, 672 (1969)
[6] V.P. Sokolov, V.A. Kogan, O.A. Osipov and L.G. Kolomin, *Zh. Neorg. Khim.*, **14**, 2401 (1969)

isopropoxide in ratios ranging from 1:1 to 1:4 (M:L) in benzene. The resulting products were characterised by infra-red spectroscopy and using ebullioscopic molecular weight determinations.

Kriza et al carried out further reactions of salicylaldimines with $TiCl_4$[8] to form complexes with the empirical formula TiL_2Cl_4. In these complexes the salicylaldimine ligand was postulated to be acting as a simple Lewis base and bonding through the imine nitrogen with the phenol remaining protonated and uncoordinated. The reason for this lack of observed deprotonation is probably the lack of a base in the reaction mixture.

In 1978 Mehrotra et al. synthesised titanium isopropoxide derivatives of the four ligands shown in figure 4.7 below[9].

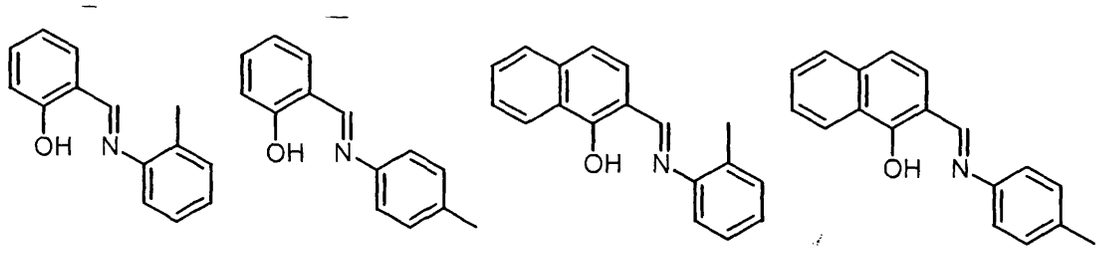

Figure 4.7: Schiff base ligands used by Mehrotra et al.

These reactions were carried out in ratios from 1:1 to 1:3 to form mono, bis and tris derivatives of titanium which were characterised by infra-red spectroscopy, elemental analysis and using ebullioscopic molecular weight determinations.

Further work with titanium tetra-isopropoxide and salicylaldimines was carried out in 1985 by Garnovskii et al. who carried out the synthesis of the product below with the formula $TiL_2(OR)_2$ and assigned its configuration by ^1H NMR spectroscopy[10]. In addition some variable temperature work was carried out and inversion of the

---

[7] S.R. Gupta and J.P. Tandon, *Z. Naturforsch. B*, **25**, 1090 (1970)
[8] D. Nogoiu and A. Kriza, *An. Univ. Bucuresti Chim.*, **20**, 39 (1971)
[9] J. Uttamchandi, S.K. Mehrotra, A.M. Bhandari and R.N. Kapoor, *Synth. React. Inorg. Met.-Org. Chem.*, **8**, 439 (1978)
[10] A.D. Garnovskii, I.S. Vasil'chenko, S.G. Kochin, L.S. Minkina, V.D. Khavryuchenko and L.E. Nivorozhkin, *Koord. Khim*, **11**, 1156 (1985)

complex configuration between the two optical rotamers observed at high temperature.

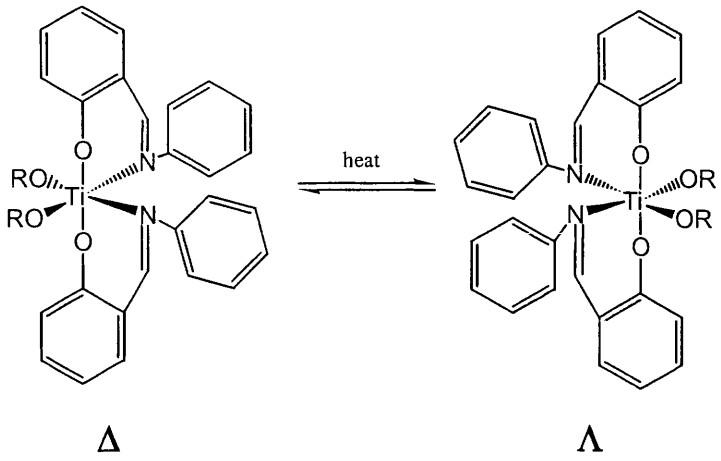

Figure 4.8: Inversion of configuration with heat

4.1.3 Development and use of chiral ligands

The majority of the work described above was carried out either for purely structural information or, more commonly, to produce new precursors for the sol-gel process. During the 1990s, due to the success of metallocene-based polymerisation of olefins, a large amount of work was carried out on synthesising both novel metallocene type complexes and single-site complexes with other ligands as metallocene analogues. Schiff bases are one of the groups of ligands used as metallocene analogues. In addition, following the success of the Sharpless epoxidation, synthesis of novel titanium complexes containing chiral ligands also became a significant area of research for many groups. These complexes could be used both for organic transformations and as stereospecific Ziegler-Natta type catalysts. Some of this work, which relates specifically to the bidentate monoanionic salicylaldimines is described in the following section, the reader is referred to chapter 5 for a review of related work involving multidentate systems.

In 1995, Floriani et al. used the oxazoline ligands in figure 4.9 below as chiral auxiliary ligands for the synthesis of titanium complexes from $TiCl_4$ and $TiCl_3$[11].

[11] P.G. Cozzi, C. Floriani, A. Chiesi-Villa and C. Rizzoli, *Inorg. Chem.*, **34**, 2921 (1995)

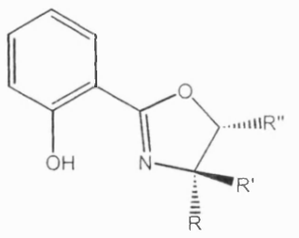

R = Me, R' = Me, R'' = H
R = Bz, R' = H, R'' = H
R = ^{i}Pr, R' H, R'' = H
R = Me, R' = H, R'' = Ph
R = Ph, R' = H, R'' = H

Figure 4.9: Chiral oxazoline ligands used in the synthesis of titanium complexes[11]

The crystal structure of the Ti(IV) complex of one of these ligands is shown in figure 4.10 below.

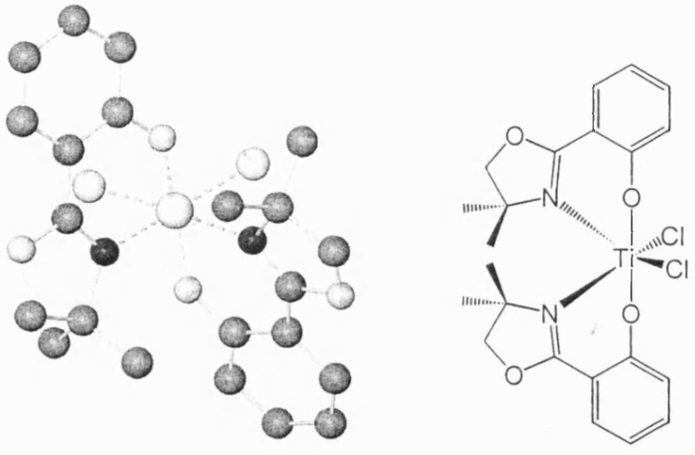

Figure 4.10: Bis-oxazoline titanium dichloride

The Ti(IV) structure shows the typical geometry of a titanium complex of this type with the phenolic ligands having a trans-axial arrangement and the chloro and imine ligands being cis-equatorial (Type A in figure 4.5 above). The bond angle at the phenolic oxygen (C-O-Ti) was found to be approximately 140°. The authors suggested that this could be due to some double bonding character between the metal and oxygen[11].

The Ti(IV) complex was further derivatised by reaction with two equivalents of silver triflate to give the bis-oxazoline, bis-triflate complex[12]. This product $TiL_2(OTf)_2$ was then used as a chiral Lewis acid catalyst for a number of reactions including Mukaiyama reactions, catalytic allylation, Diels-Alder reactions and catalytic hydrocyanation and this will be discussed further in chapter 8.

Hoyveda et al. developed a second use of bidentate salicylaldimine ligands as asymmetric catalysts in 1998 for the synthesis of non-proteinogenic α-amino acids[13]. They discovered that Ti-tripeptide Schiff base complexes with ligands of the type shown in figure 4.11 below catalysed enantioselective hydrocyanation, the products of which can then be converted to amino acids efficiently.

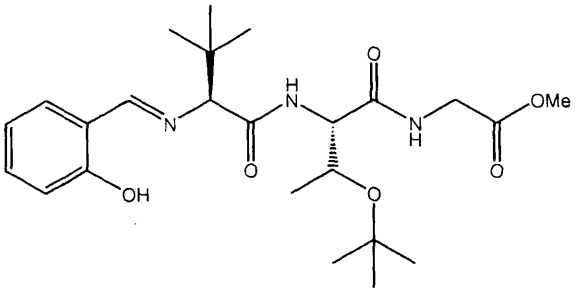

Figure 4.11: Tri-peptide Schiff base ligand

Using high throughput techniques Hoyveda et al. discovered that the ligand shown in figure 4.11, above, was most efficient for the enantioselective hydrocyanation reaction. The complex formed from this ligand and titanium tetra-isopropoxide was formed *in-situ* and gave excellent results with conversions in excess of 90% and ee values of 80-95%.

4.1.4 Polymerisation catalysts

Some of the most exciting work using bidentate monoanionic Schiff base complexes of titanium in recent years has been in the field of polyolefin catalysis. Significant

[12] P.G. Cozzi and C. Floriani, *J. Chem. Soc. Perkin Trans. 1*, 2557 (1995)
[13] K.D. Shimizu, M.L. Snapper and A.H. Hoyveda, *Chem. Eur. J.*, **4**, 1885 (1998); C.A. Kreuger, K.W. Kuntz, C.D. Dzierba, W.G. Wirschun, J.D. Gleason, M.L. Snapper and A.H. Hoyveda, *J. Am. Chem. Soc.*, **121**, 4284 (1999)

recent developments in the use of titanium Schiff base polyolefin catalysts include work in the groups of Fujita, Coates and Erker, which is summarised below.

Erker et al. have synthesised and structurally characterised the three complexes shown in figure 4.12 overleaf[14]. They discovered that use of the salicylaldimine with $TiCl_4$ gave only the coordination product (complex A in figure 4.12) with a protonated imine nitrogen atom. This result is similar to that obtained by Kriza et al. (page 121) who had postulated that the phenolic group would remain protonated. Erker discovered that use of a base such as NEt_3 was required to produce the other complexes shown in figure 4.12 which show a variation in structure, which depends on the steric bulk of the group on the salicylaldimine nitrogen atom. For a sterically undemanding ligand (complex B in figure 4.12) they observed complexes with trans-axial phenolic oxygen atoms and cis-equatorial chloro ancillary ligands (configuration A in figure 4.5). However on increasing the steric demand set by the salicylaldimine substituents (complex C in figure 4.12) he saw a change in configuration resulting in a complex with trans-axial imine nitrogen donors (configuration B in figure 4.5). This change in configuration allowed the sterically demanding groups to be moved away from each other resulting in a loss of steric strain.

[14] J. Strauch, T.H. Warren, G. Erker, R. Frohlich and P. Saarenkento, *Inorg. Chim. Acta*, **300-302**, 810 (2000)

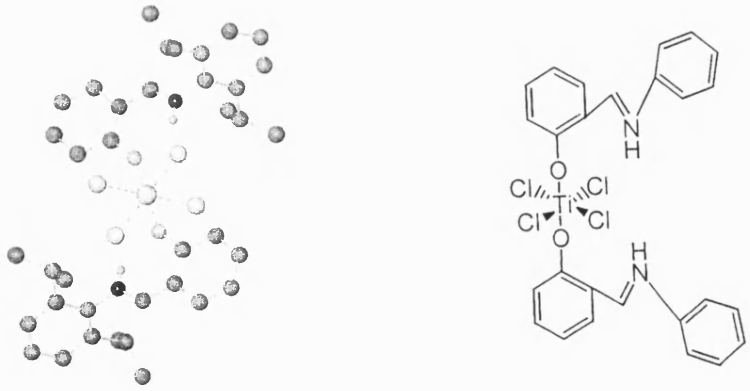

Complex A

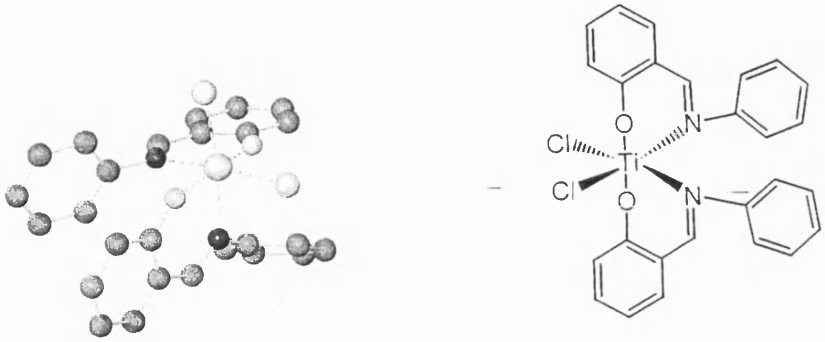

Complex B

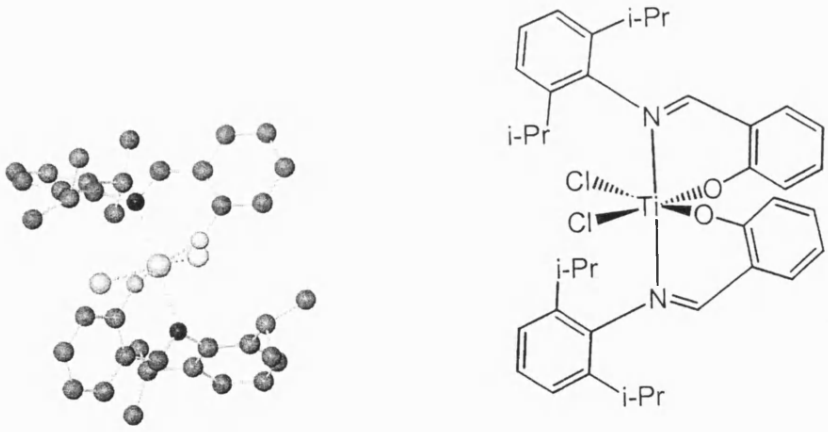

Complex C

Figure 4.12: Salicylaldimine complexes of $TiCl_4$

Although some other groups have also looked at the synthesis of these types of complexes Fujita and co-workers at Mitsui Chemicals Ltd., who have produced a series of highly active polyolefin catalysts[15], and Coates et al. have carried out by far the greatest amount of work in this field.

The initial report by Fujita et al. in 1999 detailed the synthesis of novel salicylaldimine complexes of $TiCl_4$ of the ligands shown in figure 4.13 below[16].

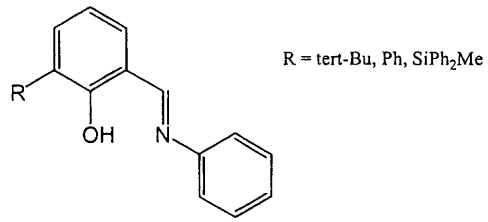

Figure 4.13: Salicylaldimine ligands for polyolefin catalysts

The stereochemistry of the titanium centre was calculated by DFT methods to have trans-axial phenolic oxygen atoms, cis-equatorial chloro ligands and also cis-equatorial imine ligands. This structure was confirmed by single crystal X-ray data for the complex in figure 4.14 below, which proved this as the lowest energy configuration of the complex and corresponds to configuration A in figure 4.5.

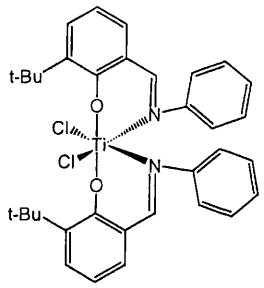

Figure 4.14: Polyolefin catalyst showing trans-phenolic arrangement

[15] Y. Suzuki, T. Matsugi, Y. Takagi, Y. Yoshida, J. Saito, S. Matsui, Y. Inoue and T. Fujita, *PCT Int. appl.*, PIXXD2 WO 0202649 A1 20020110, (2002); Y. Suzuki, T. Matsugi, Y. Takagi, Y. Yoshida, J. Saito, S. Matsui, T. Nakano, Y. Inoue and T. Fujita, *Eur. Pat. Appl.*, EPXXDW EP 1170308 A2 20020109, (2002)

[16] S. Matsui, Y. Tohi, M. Mitani, J. Saito, H. Makio, H. Tanaka, M. Nitabaru, T. Nakano and T. Fujita, *Chem. Lett.*, 1065 (1999)

This configuration was known to be ideal for polyethylene synthesis, which requires a cationic species with two mutually-cis monodentate ligand sites for polymerisation to occur. This cationic species was produced by use of methyl aluminoxane (MAO) as a co-catalyst and the three species in figure 4.13 were all found to be highly active for the polymerisation of ethylene. The most active complex was shown to yield 47.8kg of polyethylene per mmol of titanium under a pressure of ethylene of 0.9Mpa, which is considered to be suitable for industrial production.

Following from this initial report, and the publishing of a patent by Mitsui Chemicals Ltd.[15], several papers were published over the next three years detailing the use of related ligands in ethylene polymerisation with both titanium and zirconium including pyrrole Schiff base complexes and zirconium salicylaldimine complexes[17].

The next advance which Fujita and co-workers discovered was that by careful choice of ligand they could use certain of their catalysts to catalyse the living polymerisation of ethylene at room temperature and higher which is an unprecedented result[18]. They synthesised a range of fluoroaniline containing salicylaldimine catalysts with the ligands shown in figure 4.15 below.

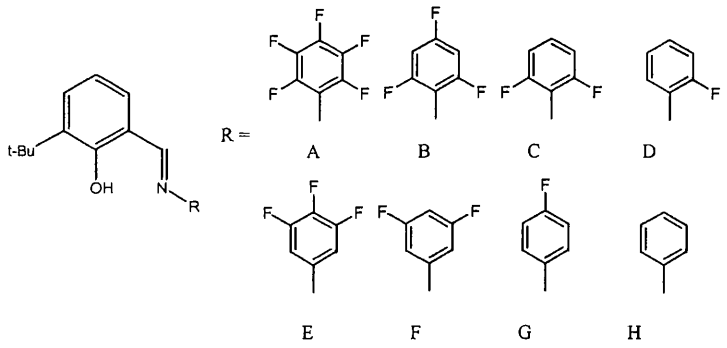

Figure 4.15: Fluorinated salicylaldimine ligands

[17] Y. Yoshida, S. Matsui, Y. Takagi, M. Mitani, T. Nakano, H. Tanaka, N. Kashiwa and T. Fujita, *Organometallics*, **20**, 2791 (2001); T. Matsugi, S. Matsui, S. Kojoh, Y. Takagi, Y. Inoue, T. Fujita and N. Kashiwa, *Chem. Lett.*, **6**, 566 (2001); S. Matsui, M. Mitani, J. Saito, Y. Tohi, H. Makio, H. Tanaka and T. Fujita, *Chem. Lett.*, **12**, 1293 (1999); S. Matsui, M. Mitani, J. Saito, N. Matsukawa, H. Tanaka, T. Nakano and T. Fujita, *Chem. Lett.*, **5**, 554 (2000); Y. Yoshida, S. Matsui, Y. Takagi, M. Mitani, M. Nitabaru, T. Nakano, H. Tanaka and T. Fujita, *Chem. Lett.*, **11**, 1270 (2000)

[18] J. Saito, M. Mitani, J. Mohri, Y. Yoshida, S. Matsui, S. Ishii, S. Kojoh, N. Kashiwa and T. Fujita, *Angew. Chem. Int. Ed. Engl.*, **40**, 2918 (2001); J. Saito, M. Mitani, J. Mohri, Y. Yoshida, S. Matsui, S. Ishii, S. Kojoh, K. Tsuru, T. Nakano, H. Tanaka, T. Matsugi, N. Kashiwa and T. Fujita, *J. Am. Chem. Soc.*, **124**, 3327 (2002)

The complexes were found to have the same overall coordination geometry at titanium as the previous catalysts. Of the fluorinated ligands, shown in figure 4.15 above, only those with ligands with a fluorine atom at the carbon *ortho* to the imine nitrogen (A-D) were found to give living polymerisation. For those catalysts that did not give living polymerisation end group analysis showed that the reason was the termination of the polymerisation by β-hydrogen transfer. The reason for the lack of β-hydrogen transfer in the complexes which gave living polymer was postulated to be the interaction between the *ortho* fluorine and the metal centre in the catalytically active cationic complex. This hypothesis is backed up by both single crystal X-ray data and DFT calculations which both show evidence for this interaction which cannot occur in the catalysts which give non-living polymerisations.

At the same time as the publication of the work by Fujita et al. the first report of similar catalysts by Coates et al. was published[19]. They had utilised combinatorial techniques to synthesise a library of twelve salicylaldimine ligands from the starting materials, which are shown in figure 4.16 below.

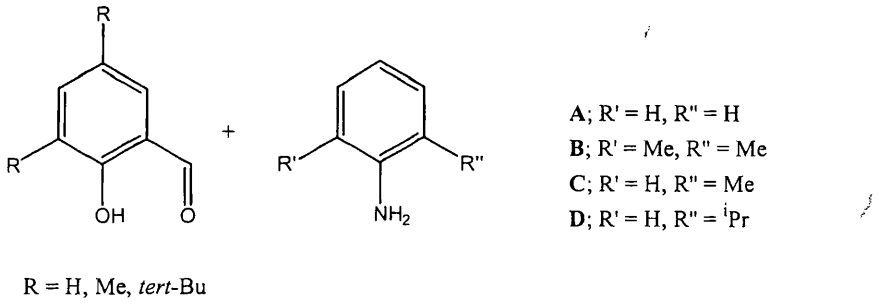

Figure 4.16: Ligand library for combinatorial complex synthesis

These ligands were reacted together in different, defined mixed groups and then reacted with $TiCl_4$ using BuLi to give several pools of complexes. Each of these pools was then used as a catalyst for the synthesis of polypropylene and the resulting polymers analysed for their tacticity and hence their stereospecificity. Using this data it was possible for the workers to single out which catalysts were responsible for production of syndiotactic polypropylene and finally to show that the catalyst shown

[19] J. Tian and G.W. Coates, *Angew. Chem. Int. Ed. Engl.*, **39**, 3626 (2000)

in figure 4.17 below, which is almost identical to the initial complex utilised by Fujita et al., formed 100% syndiotactic polymer.

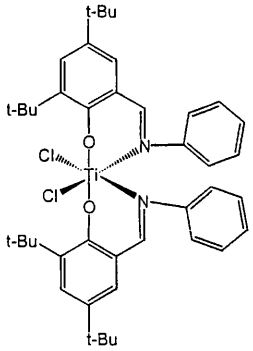

Figure 4.17: Salicylaldimine catalyst for formation of syndiotactic polypropylene

Although this catalyst produced syndiotactic polypropylene it showed very little control over molecular weight. In a similar manner to Fujita et al. the next catalyst reported by Coates et al. was a complex containing perfluoro aniline salicylaldimine shown in figure 4.18 below[20].

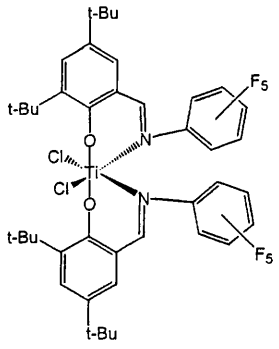

Figure 4.18: Salicylaldimine catalyst for the living polymerisation of syndiotactic polypropylene

They found that not only was this catalyst an order of magnitude more active than the non-fluorinated analogue it also produced polymer with a very narrow polydispersity and no olefinic end groups both of which are indicative of living polymerisation. In addition they also used it to produce high molecular weight

[20] J. Tian, P.D. Hustad and G.W. Coates, *J. Am. Chem. Soc.*, **123**, 5134 (2001)

polypropylene/polyethylene block co-polymers containing syndiotactic polypropylene, the first example of this type of polymer.

Since the publication of this work by Coates and Fujita more publications have appeared in this area including studies of the mechanism of the stereospecific polymerisations[21] and it seems that these salicylaldimine complexes are set to continue as a large area of academic interest in the future.

4.1.5 Relevance to polyurethanes

The success of the complexes of salicylaldimine ligands described above, for polyolefin catalysis, led us to study analogous complexes as catalysts for the synthesis of polyurethanes. For this purpose we synthesised a range of complexes of this general type but with ancillary alkoxide ligands on the metal centre to allow isocyanate insertion. Although, as described above, a great deal of work has been carried out to synthesise complexes of salicylaldimine ligands with chloro ancillary ligands there has been no recent systematic structural study of the complexes of these ligands with titanium alkoxides.

The results in this chapter consist of a systematic structural study of the reactivity of a range of ligands of this type with TiPT. The ligands involved were chosen to give a wide spectrum of steric and electronic environments for the metal centre. This was done in the hope that it would be possible to use the results obtained to provide a basis for the formation of some structure/activity relationships for these complexes in polyurethane synthesis.

The remainder of this chapter discusses the results we have obtained in this area. Firstly the following section describes the ligands used and this is followed by a discussion of the structural aspects of the complexes we have synthesised.

[21] M. Lamberti, D. Pappalardo, A. Zambelli and C. Pellecchia, *Macromolecules*, **35**, 658 (2002)

4.2 Discussion of Results

4.2.1 Ligands

This chapter covers the reactions of a large number of simple salicylaldimine ligands with TiPT. Figure 4.19 below shows the ligands used in this chapter.

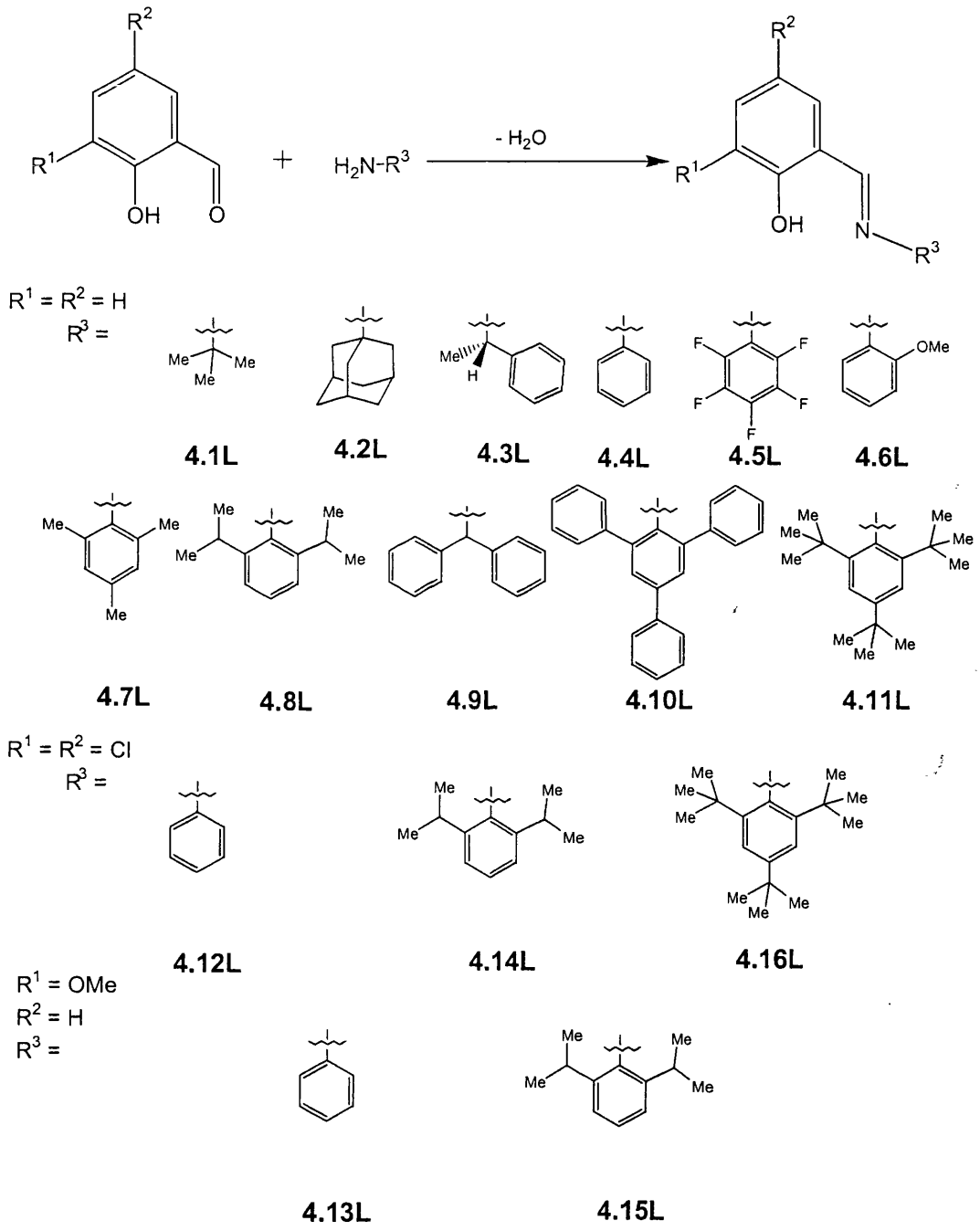

Figure 4.19: The ligands used in chapter 4

4.2.2 Complexes 4.1-4.6: Sterically undemanding ligands

The following section discusses titanium isopropoxide complexes of salicylaldimine ligands, which have sterically undemanding groups on the salicylaldimine nitrogen atom. The discussion begins with those complexes for which single crystal X-ray structures have been obtained followed by those for which this proved unsuccessful.

Complex 4.3

Two equivalents of ligand 4.3L react readily with one equivalent of TiPT to yield a yellow crystalline product that was suitable for single-crystal X-ray diffraction. The asymmetric unit contains two structurally similar molecules of the product complex which has the expected $Ti(4.3L)_2(O^iPr)_2$ form and a distorted octahedral geometry at the metal centre. Overall the complex has the most favourable geometry (A) described in the introduction to this chapter (figure 4.5) with the phenolic oxygen donors in a trans-axial arrangement, the imine donors in a cis-equatorial arrangement and the alkoxide donors also in a cis-equatorial arrangement.

The metal to ligand bond lengths in the complex are all of the expected order with the isopropoxide ligands having bond lengths of 1.777(2)Å [Ti(1)-O(2)], 1.817(2)Å [Ti(1)-O(3)], 1.778(2)Å [Ti(2)-O(9)] and 1.826(2)Å [Ti(2)-O(6)]. The phenolic oxygen donors also have typical bond lengths to the metal centre {1.926(2)Å [Ti(1)-O(1)], 1.931(2)Å [Ti(1)-O(4)], 1.918(2)Å [Ti(2)-O(8)] and 1.942(2)Å [Ti(2)-O(6)]} as do the imine nitrogen atoms {2.299(2)Å [Ti(1)-N(2)], 2.347(2) [Ti(1)-N(1)], 2.300(2)Å [Ti(2)-N(4)] and 2.321(2)Å [Ti(2)-N(3)]} which, as expected, have the longest bond lengths.

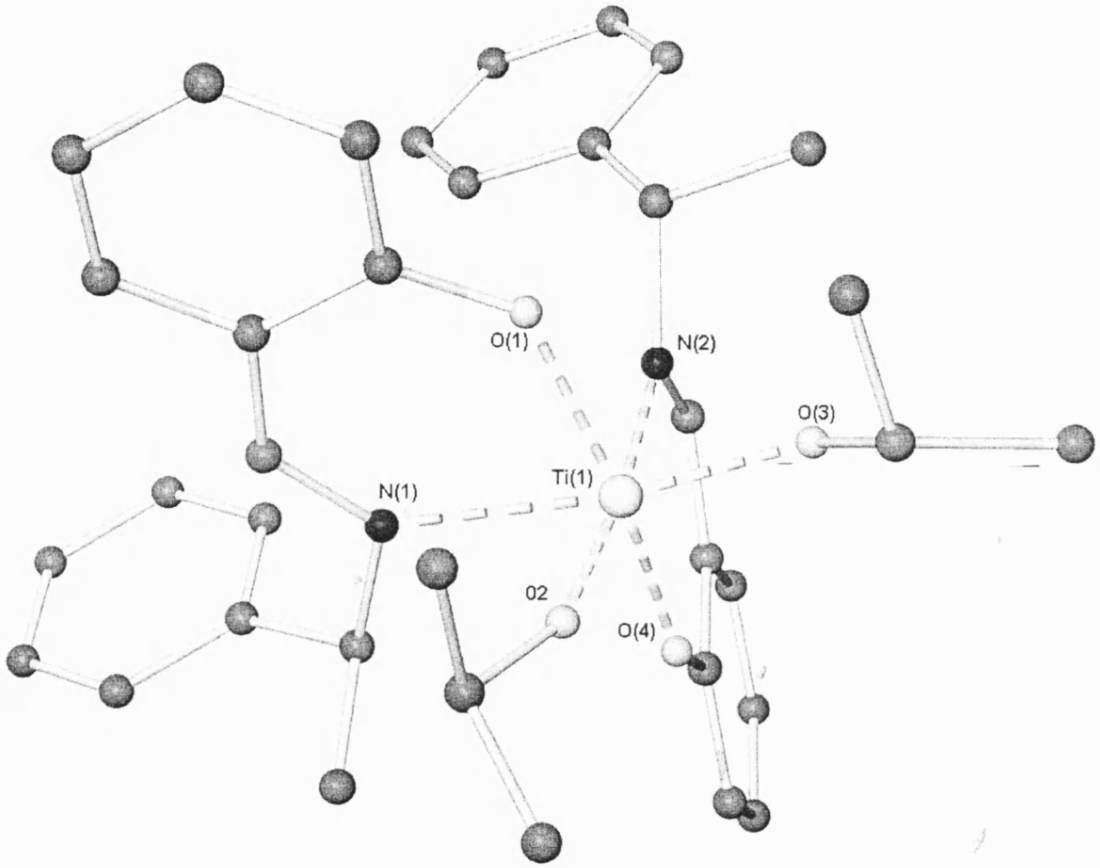

Figure 4.20: Molecular structure of complex 4.3 (only one molecule from the asymmetric unit shown, hydrogen atoms not shown for clarity)

The ^{1}H and ^{13}C NMR spectra for complex 4.3 suggest that the gross solid-state structure is maintained in solution with easily identifiable resonances due to the isopropoxide and imine protons. Signals due to the isopropoxide ligands are observed in the ^{1}H NMR spectrum at 4.67ppm for the C**H** protons and 1.02ppm for the CH_3 protons along with a sharp singlet due to the imine C**H** protons at 7.88ppm. The ^{13}C NMR spectrum has the expected form with signals due to the isopropoxide groups at 25.7ppm (CH_3) and 78.6ppm (**C**H) and a signal at 164.7ppm due to the imine **C**H group.

Complex 4.4

Two equivalents of ligand 4.4L react readily with one equivalent of TiPT to yield a yellow crystalline product that was suitable for single-crystal X-ray diffraction. The asymmetric unit contains one molecule of the product complex which has the expected $Ti(4.4L)_2(O^iPr)_2$ form and a distorted octahedral geometry at the metal centre. One of the salicylaldimine phenol rings in the complex is disordered over two positions in a ratio of 1:1. Overall the complex has the most favourable geometry (A) described in figure 4.5 with the phenolic oxygen donors trans-axial, the imine nitrogen donors cis-equatorial and the alkoxide donors also cis-equatorial.

The metal to ligand bond lengths in the complex are similar to those observed for complex 4.3 and typical for bonds of their type. The isopropoxide ligands have bond lengths to the metal centre of 1.813(1)Å [Ti(1)-O(3)] and 1.819(1)Å [Ti(1)-O(4)] while those to the phenoxides are 1.895(1)Å [Ti(1)-O(1)] and 1.904(1)Å [Ti(1)-O(2)]. As expected the bond lengths from the metal to the imine nitrogen atoms are the longest ligand to metal interactions with bond lengths of 2.328(2)Å [Ti(1)-N(1)] and 2.305(2)Å [Ti(1)-N(2)].

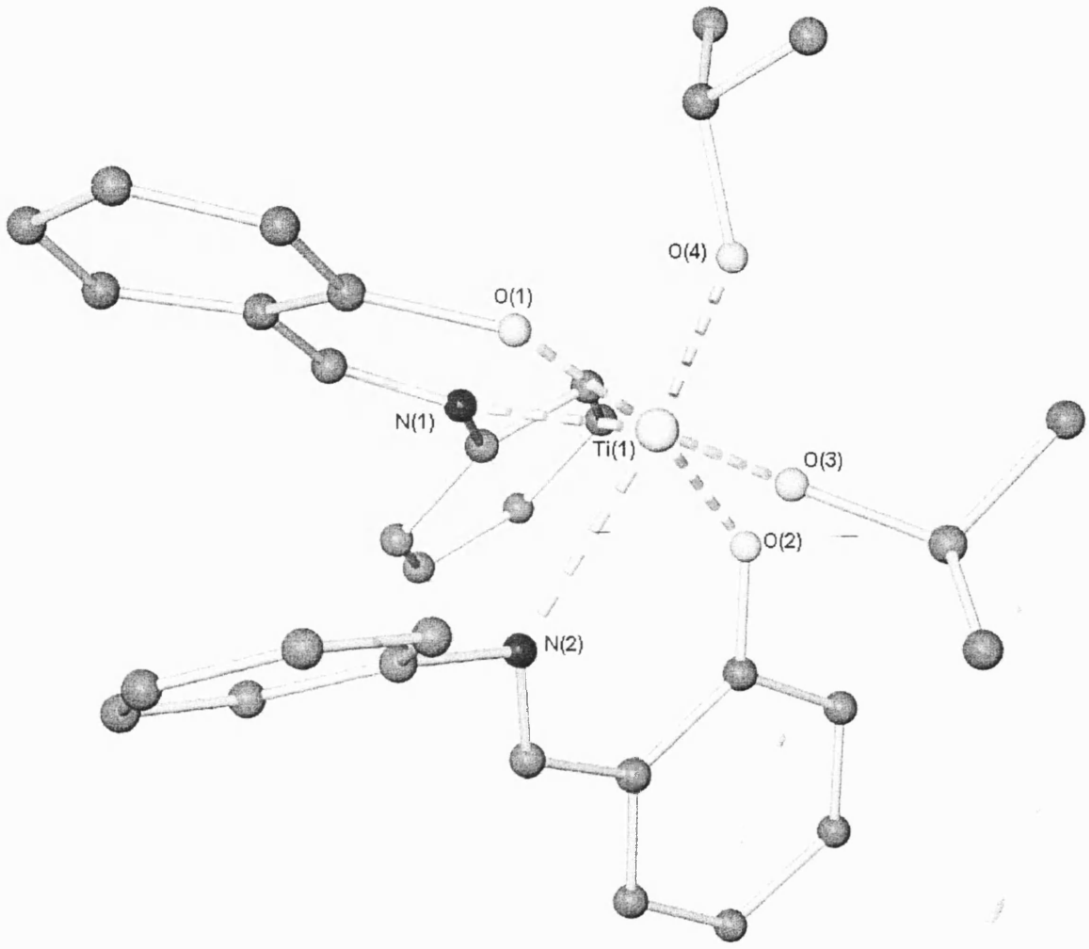

Figure 4.21: Molecular structure of complex 4.4 (hydrogen atoms not shown for clarity)

The ^{1}H and ^{13}C NMR spectra for complex 4.4 suggest that the gross solid-state structure is maintained in solution with similar resonances for the isopropoxide and imine protons to those seen in complex 4.3. Signals due to the isopropoxide ligands are observed in the ^{1}H NMR spectrum at 4.90ppm for the C**H** protons and 1.23ppm for the C**H**$_3$ protons along with a sharp singlet due to the imine C**H** protons at 7.87ppm. The ^{13}C NMR spectrum is also similar to that for complex 4.3 with signals due to the isopropoxide groups at 26.0ppm (**C**H$_3$) and 79.1ppm (**C**H) and a signal at 166.3ppm due to the imine **C**H group.

Complex 4.5

Two equivalents of ligand 4.5L react readily with one equivalent of TiPT to yield a yellow crystalline product that was suitable for single-crystal X-ray diffraction. The asymmetric unit contains one molecule of the product complex which has the expected Ti(4.5L)$_2$($O^{i}Pr$)$_2$ form and a distorted octahedral geometry at the metal centre. As with the previous two crystal structures, the complex has the most favourable geometry (A) described in figure 4.5 with the phenolic oxygen donors trans-axial, the imine donors cis-equatorial and the alkoxide donors cis-equatorial.

The metal to ligand bond lengths in the complex are similar to those observed for complexes 4.3 and 4.4 and typical for bonds of their type. There is a slight asymmetry in the bond lengths from the metal centre to the isopropoxide ligands {1.798(2)Å [Ti(1)-O(3)] and 1.779(2)Å [Ti(1)-O(4)]} and a similar difference is observed between the two titanium-aryloxide bond lengths {1.933(2)Å [Ti(1)-O(1)] and 1.919(2)Å [Ti(1)-O(2)]}. As with the previous crystal structures the longest metal to ligand bonds are found to the imine groups which also show much less asymmetry in bond length than the other two ligand types {2.328(2)Å [Ti(1)-N(1)] and 2.340(2)Å [Ti(1)-N(2)]}.

The ^{1}H and ^{13}C NMR spectra for complex 4.5 suggest that the gross solid-state structure is maintained in solution with similar resonances for the isopropoxide and imine protons to those seen in complexes 4.3 and 4.4. Signals due to the isopropoxide ligands are observed in the ^{1}H NMR spectrum at 4.77ppm for the C**H** protons and

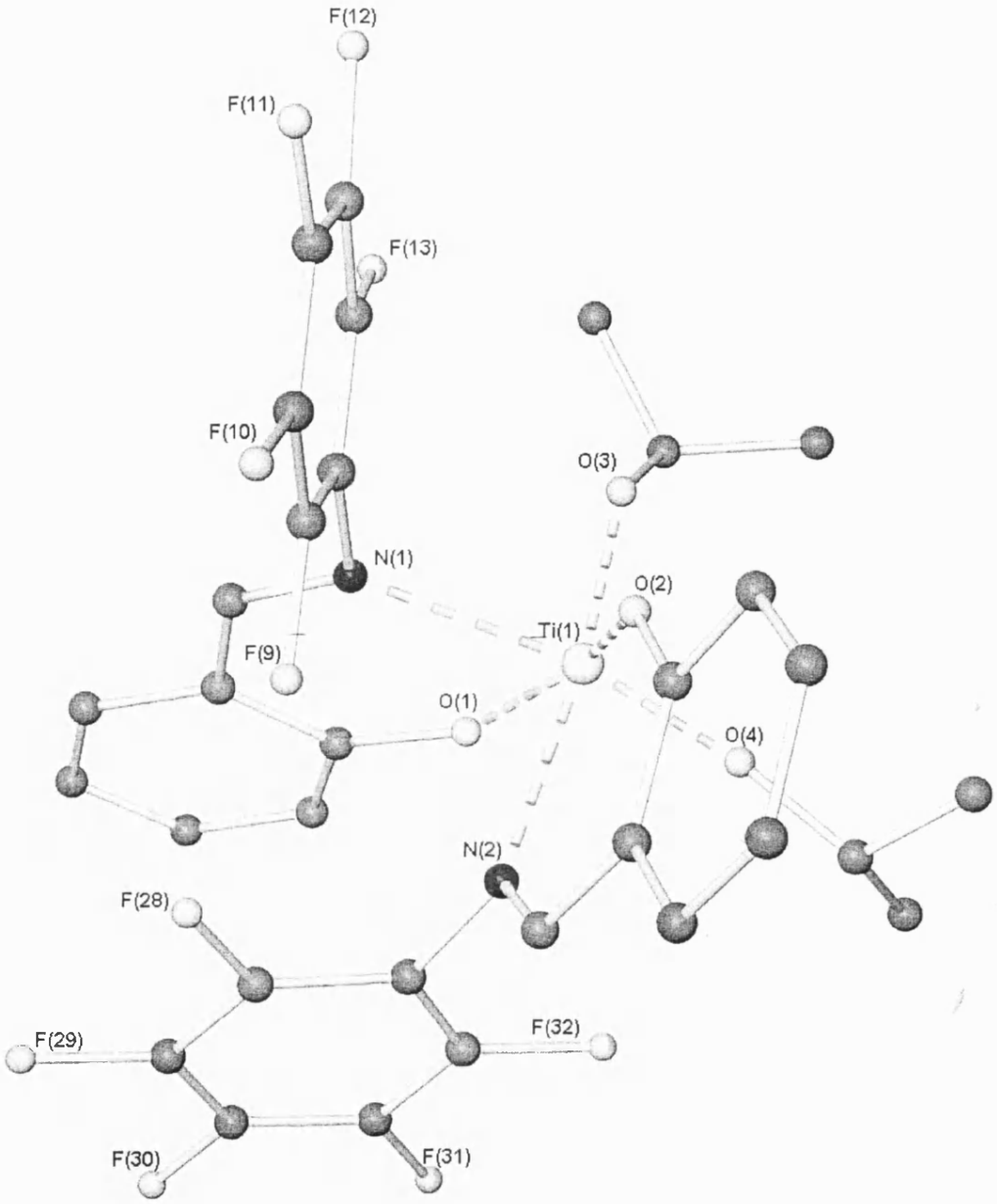

Figure 4.22: Molecular structure of complex 4.5 (hydrogen atoms not shown for clarity)

1.11ppm for the CH_3 protons along with a sharp singlet due to the imine C**H** protons at 8.07ppm. The ^{13}C NMR spectrum is also similar to 4.3 and 4.4 with signals due to the isopropoxide groups at 25.5ppm (CH_3) and 80.7ppm (**C**H) and a signal at 171.8ppm due to the imine **C**H group. In addition the ^{19}F spectrum for complex 4.5 shows the expected signals due to the pentafluorophenyl imine groups.

Complex 4.1

Two equivalents of ligand 4.1L react readily with one equivalent of TiPT to yield a yellow microcrystalline product that was unsuitable for single-crystal X-ray diffraction. The ^1H and ^{13}C NMR spectra of complex 4.1 confirmed that a complex of the formula $Ti(4.1L)_2(O^iPr)_2$ had been formed. The ^1H NMR spectrum showed similar signals to those observed for complexes 4.3-4.5 with one set of sharp resonances due to the isopropoxide groups with a septet at 4.62ppm for the C**H** protons and a signal at 1.17ppm for the CH_3 protons. In addition the spectrum also showed a single sharp resonance for the imine C**H** proton at 8.34ppm. The ^{13}C NMR spectrum also gave similar results to the earlier complexes with signals for the isopropoxide **C**H (77.6ppm) and CH_3 groups (25.8ppm) and also the imine **C**H group (166.5ppm). This correlation of the NMR spectra of complex 4.1 with complexes 4.3-4.5 leads us to suggest that it has the same overall geometry as these earlier complexes with trans-axial phenol donors (A in figure 4.5).

Complex 4.2

Two equivalents of ligand 4.2L react readily with one equivalent of TiPT to yield a yellow powder that was unsuitable for single-crystal X-ray diffraction. The ^1H and ^{13}C NMR spectra of complex 4.2 confirmed that a complex of the formula $Ti(4.2L)_2(O^iPr)_2$ had been formed. The ^1H NMR spectrum was similar to that obtained for 4.1 and 4.3-4.5 and showed one set of sharp resonances due to the isopropoxide groups with a septet at 4.69ppm for the C**H** protons and a signal at 1.22ppm for the CH_3 protons. In addition the spectrum also showed a single sharp resonance for the imine C**H** proton at 8.30ppm. The ^{13}C NMR spectrum also gave similar signals to the previous complexes with signals for the isopropoxide **C**H (78.4ppm) and CH_3 groups (26.0ppm) and also the imine **C**H group (162.9ppm). In addition, in the carbon spectrum it was possible to identify the signals due to the different carbon atoms in the adamantyl cage as shown in the experimental section of this report. The similarity

between the NMR spectra of complex 4.2 and the previous complexes leads us to suggest, as for complex 4.1, that this complex has a similar structure (A in figure 4.5) to that of the crystallographically characterised complexes 4.3-4.5.

Complex 4.6

Two equivalents of ligand 4.6L react readily with one equivalent of TiPT to yield a yellow powder that was unsuitable for single-crystal X-ray diffraction. The ^{1}H and ^{13}C NMR spectra of complex 4.6 confirmed that a complex of the formula $Ti(4.6L)_2(O^iPr)_2$ had been formed. The ^{1}H NMR spectrum showed one set of sharp resonances due to the isopropoxide groups with a septet at 4.88ppm for the C**H** protons and a signal at 1.19ppm for the C**H**$_3$ protons. In addition the spectrum also showed a single sharp resonance for the imine C**H** proton at 7.89ppm. The ^{13}C NMR spectrum confirmed these results {isopropoxide **C**H (79.5ppm), **C**H$_3$ (26.8ppm) and imine **C**H (169.7ppm)}. The similarity between the NMR spectra of complex 4.6 and the previous complexes leads us to suggest, as for complexes 4.1 and 4.2, that this complex has a similar structure (A in figure 4.5) to that of the crystallographically characterised complexes 4.3-4.5.

Summary

The sterically undemanding ligands 4.1L-4.6L all react readily with TiPT and yield easily characterised products. The molecular structures, which have been obtained for compounds 4.3, 4.4 and 4.5, all exhibit the same basic structure with a distorted octahedral metal centre, trans-axial aryloxide ligands, cis-equatorial imine nitrogen atoms and cis-equatorial monodentate alkoxides. As was described in the introduction to this chapter, this structure (configuration A in figure 4.5) is the preferred geometry for complexes of the type $Ti(Sal)_2(X)_2$ and the formation of complexes with this geometry is unsurprising with ligands which have little steric influence over the metal centre.

The metal-ligand bond lengths in all three of the crystallographically characterised complexes are very similar, with ranges from the longest to the shortest bond length for each ligand type of no greater than 0.05Å across all three complexes. This fact seems to suggest that the imine substituent has very little electronic effect on bond length as the change from aniline (complex 4.4) to the much more strongly electron

withdrawing pentafluoroaniline (complex 4.5) shows no significant effect on titanium-imine bond length in the solid-state.

The asymmetry observed, in some of the monodentate alkoxides in the crystal structures, is almost certainly due to crystal packing effects as the ^{1}H NMR spectra invariably show only one signal for the isopropoxide groups and therefore in solution they are equivalent.

The ^{1}H NMR spectra of compounds 4.1 to 4.6 are very similar with the resonances due to the C**H** protons of the isopropoxide groups, which are usually indicative of the structure of the complex, varying very little as the imine substituent is altered (4.62-4.88ppm). This fact suggests that, in solution, the complexes 4.1-4.6 retain the same gross structure as observed in the solid-state, with trans-axial phenolic ligands and the other ligand types being cis-equatorial, and also confirms the conclusion drawn from the X-ray data that the electronics of the imine group have little effect on the electronics of the metal centre.

4.2.3 Complexes 4.7-4.8: Sterically intermediate ligands

The following section discusses titanium isopropoxide complexes of salicylaldimine ligands, which have more sterically demanding groups on the salicylaldimine nitrogen atom than those in complexes 4.1-4.6. The discussion begins with a complex for which a single crystal X-ray structure has been obtained followed by one for which this proved unsuccessful.

Complexes 4.1-4.6 show that variation of the electronic properties of the imine substituents has little effect on the configuration of the ligands in the product complex. However increasing the steric bulk at the imine does have an effect as can be seen in the following complexes.

Complex 4.8

Two equivalents of ligand 4.8L react readily with one equivalent of TiPT to yield yellow crystals, which were suitable for single-crystal X-ray diffraction. The asymmetric unit contains half a molecule of toluene, which is disordered over two

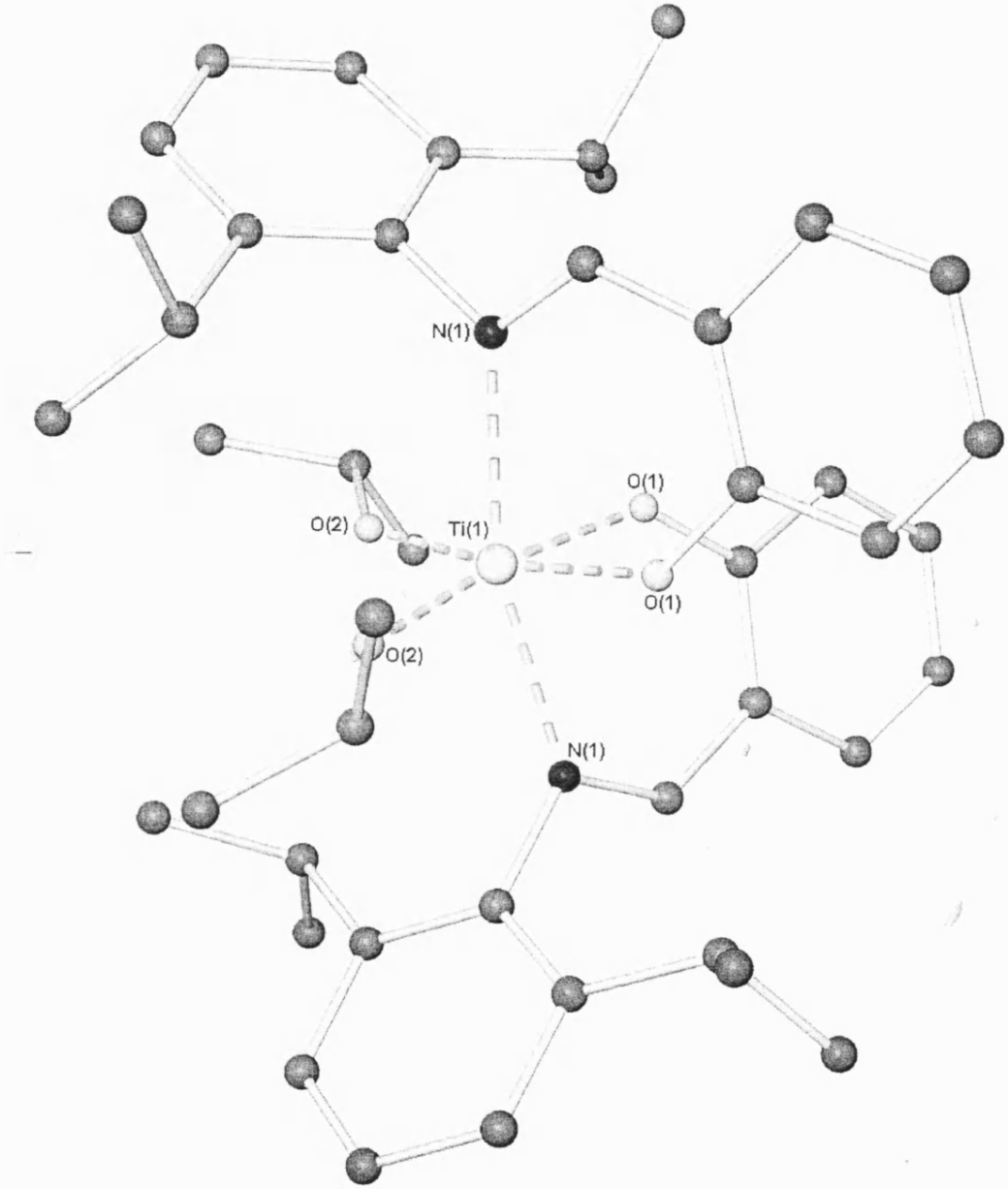

Figure 4.23: Molecular structure of complex 4.8 (hydrogen atoms not shown for clarity)

positions, and half a molecule of the titanium complex. Complex 4.8 has the expected $Ti(4.8L)_2(O^iPr)_2$ stoichiometry and a distorted octahedral geometry at the metal centre, but has a different arrangement of the ligands around the metal centre to the previous complexes (4.1-4.6). Unlike complexes 4.1-4.6 the complex does not have the normal isomeric form at the metal centre due to the increased steric bulk at the imine substituents. The ligands are arranged with the imine nitrogen atoms in the trans-axial positions and the aryloxides and alkoxides in cis-equatorial arrangements (isomer B in figure 4.5). This ligand arrangement has been observed by Erker et al. using the same ligand with $TiCl_4$ (see page 125-126 above)[14]. This change in configuration allows the bulky salicylaldimine substituents to move further away from the sterically crowded metal centre and therefore relieves steric strain around it.

The metal-salicylaldimine ligand bond lengths in complex 4.8 are significantly different to those observed in the complexes with the usual isomeric form, due to the new ligand arrangement at the metal centre. The bond length from titanium to the aryloxide {1.975(1)Å [Ti(1)-O(1)]} is significantly lengthened relative to the earlier structures by around 0.04Å. Concomitant to this the titanium to imine bond length {2.228(2)Å [Ti(1)-N(1)]} exhibits a similar decrease. In contrast the titanium-alkoxide bond lengths appear to be insensitive to the trans ligand with no significant difference when compared to these bonds in 4.3-4.5 {1.806(1)Å [Ti(1)-O(2)]}. The ^1H NMR spectrum of complex 4.8 shows a significant difference to the spectra for 4.1-4.6. Although no difference is seen in the bond lengths at the isopropoxide ligands a significant shift in the signals for the isopropoxide groups is observed compared to complexes 4.1-4.6 and this can probably be attributed to the different trans influence, which these ligands are now subject to. The ^1H NMR spectrum showed one set of sharp resonances due to the isopropoxide groups with a septet at 3.77ppm for the C**H** protons, almost 1ppm lower than that observed for complexes 4.1-4.6 correlating with the change in complex structure. This effect is carried over into the signal for the C$\mathbf{H}_3$ protons of the isopropoxide, which are also much lower than in the previous complexes at 0.51ppm. A similar shift is not observed in the ^{13}C spectrum, which has similar signals to those observed for the complexes with the more favoured configuration. The spectrum has signals for the isopropoxide **C**H (77.8ppm) and **C**H_3 groups (25.3ppm) and also the imine **C**H group (169.5ppm), values that are similar to those observed in 4.1-4.6.

Complex 4.7

Two equivalents of ligand 4.7L react readily with one equivalent of TiPT to yield a yellow powder that was unsuitable for single-crystal X-ray diffraction. The ^{1}H and ^{13}C NMR spectra of complex 4.7 confirmed that a complex of the formula $Ti(4.7L)_2(O^iPr)_2$ had been formed. However, as with complex 4.8, the ^{1}H NMR spectrum showed differences to the complexes with the usual configuration at the metal centre with a similar shift for the isopropoxide signals. The ^{1}H NMR spectrum showed one set of sharp resonances due to the isopropoxide groups with a septet at 3.45ppm for the **CH** protons, almost 1ppm lower than that observed for complexes 4.1-4.6 suggesting a significant change in complex structure as shown for complex 4.8. This effect is carried over into the signal for the CH_3 protons of the isopropoxide, which are also much lower than in the previous complexes at 0.38ppm. No significant change is seen however for the imine C**H** proton that showed a single sharp resonance at 7.88ppm, a value which is very similar to that observed in the earlier complexes. Unlike the ^{1}H NMR spectrum the ^{13}C NMR spectrum showed little difference to the earlier complexes (4.1-4.6 and 4.8) with signals for the isopropoxide **C**H (77.7ppm) and CH_3 groups (24.9ppm) and also the imine **C**H group (169.2ppm), values that are similar to those seen in 4.1-4.6.

The ^{1}H NMR spectrum of 4.7 suggests that a change has occurred in the geometry of the metal centre due to the increase in steric bulk at the salicylaldimine nitrogen atom. This change is probably the same as that observed in 4.8 with the complex having the B configuration from figure 4.5 and trans-axial nitrogen donors, cis-equatorial-aryloxide donors and cis-equatorial alkoxide donors. This change, as with 4.8, allows the sterically bulky salicylaldimine substituents to move away from the sterically congested metal centre.

Summary

Complexes 4.7 and 4.8 show that although the electronics of the imine substituents seem to have little effect on complex structure, variation of the steric properties at this group can force the complex to attain new geometries at the metal centre, an observation that correlates with a similar observation by Erker. The following complexes look at the effect of increasing this steric bulk still further.

4.2.4 Complexes 4.9-4.11: Sterically demanding ligands

Complexes 4.7 and 4.8 showed that increasing the steric bulk at the imine substituents of salicylaldimine groups can cause the formation of unusual ligand configurations at the metal centre. The following three complexes investigate the effects observed on increasing this steric bulk yet further.

Complex 4.10

Two equivalents of ligand 4.10L react readily with one equivalent of TiPT to yield yellow crystals, which were suitable for single-crystal X-ray diffraction. The asymmetric unit contains one molecule of the product complex and a molecule of toluene. The structure does have the expected $Ti(4.10L)_2(O^iPr)_2$ stoichiometry but unlike the earlier structures the titanium centre is only five coordinate. One of the salicylaldimine ligands chelates the metal centre as expected whereas the second is coordinated only through the aryloxide group and no coordination is observed from the imine nitrogen. Thus, the titanium centre is coordinated by one chelating salicylaldimine ligand, one monodentate salicylaldimine ligand and two terminal isopropoxide ligands (one of which is disordered over two positions). The geometry of the metal centre lies between trigonal bipyramidal and square pyramidal: an octahedral arrangement in which one of the equatorial sites is left vacant. The two aryloxide ligands are arranged trans to each other while the terminal isopropoxides are mutually cis. Adoption of this geometry allows the monodentate salicylaldimine ligand to rotate approximately 180° about the C-CNR bond to relieve the steric congestion around the metal centre.

The bond lengths in the complex all fall within the expected ranges for titanium interactions of these types. The aryloxide to titanium bond length in the chelating salicylaldimine {1.942(2)Å [Ti(1)-O(2)]} is similar to the bond lengths to chelating ligands of this type in complexes 4.1-4.6, probably due to the fact that it is trans to a second aryloxide ligand in a similar way to the aryloxides in these earlier complexes. In contrast, as would be expected, the bond length to the monodentate salicylaldimine ligand is much shorter {1.862(2)Å [Ti(1)-O(2)]} with a similar length to other monodentate phenoxides. The titanium-imine bond length {2.215(2)Å [Ti(1)-N(2)]} in the chelating ligand is closer to the shorter interactions of this type observed for

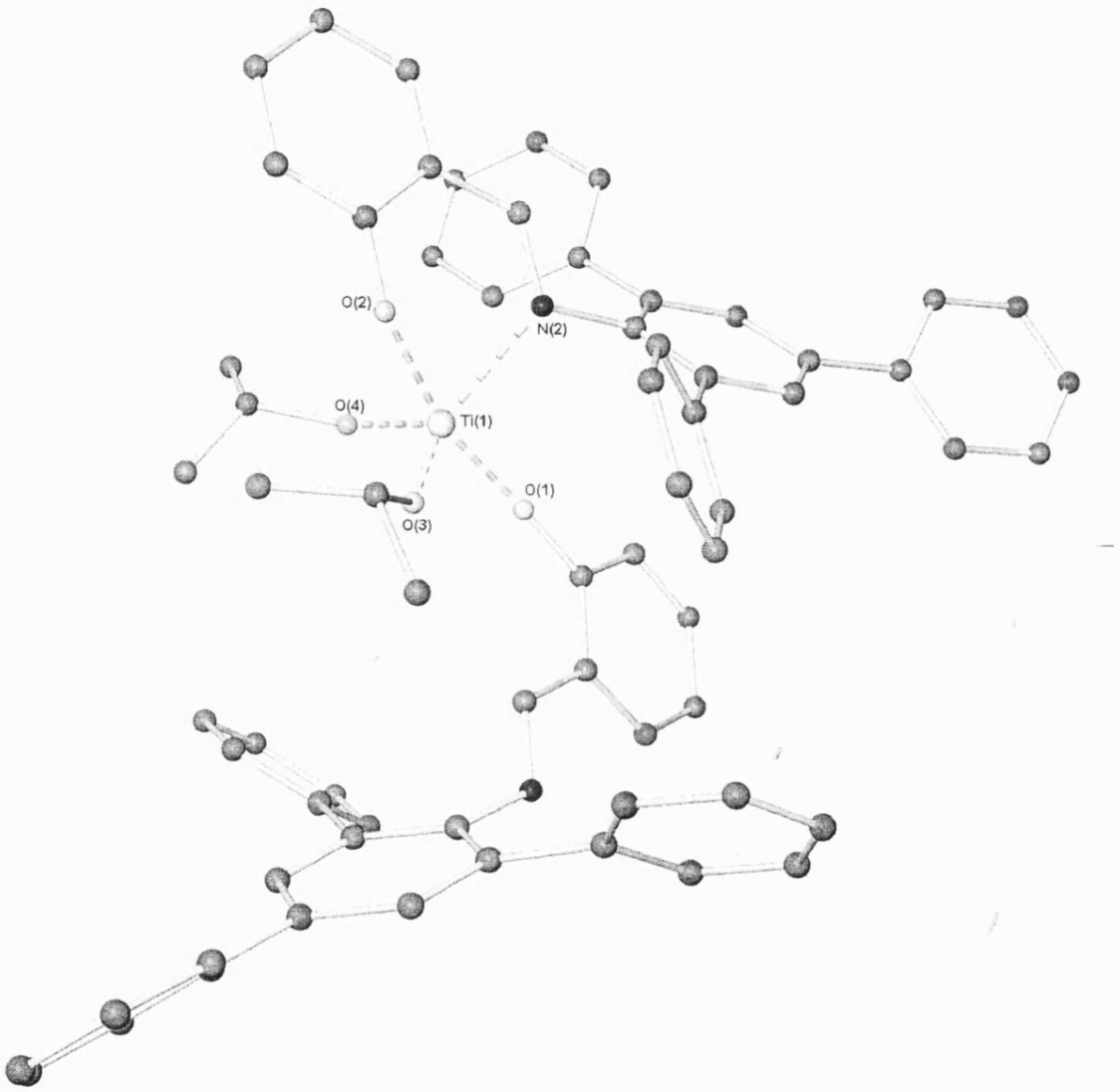

Figure 4.24: Molecular structure of complex 4.10 (hydrogen atoms not shown for clarity)

complexes 4.7 and 4.8 than to the similar bonds in complexes 4.1-4.6. As with the previous structures, the bond lengths to the isopropoxide ligands {1.791(2)Å [Ti(1)-O(3)] and 1.773(2)Å [Ti(1)-O(4)]} seem to be little affected by the change in geometry at the titanium centre and are of a similar length to those observed in all of the crystallographically characterised salicylaldimine complexes discussed previously.

The ^{1}H NMR spectrum shows one set of sharp resonances due to the isopropoxide groups with a septet at 4.14ppm for the C**H** protons of the isopropoxide group, a value which lies between that observed for complexes 4.1-4.6 and the lower value observed for complexes 4.7-4.8 as does the signal for the isopropoxide C**H**$_3$ groups, which is observed at 0.70ppm. The fact that there is only one signal due to the isopropoxide groups indicates that they are equivalent in solution. In addition only one signal is observed for the imine C**H** proton (8.29ppm), indicating that in solution the two salicylaldimine ligands are also equivalent. This equivalence of the ligands could be caused either by both ligands being monodentate in solution or by a rapid exchange process between bi- and monodentate coordination in both ligands. When combined with the ^{1}H NMR evidence from the earlier complexes the spectrum of 4.10 suggests that of these two possibilities the most likely explanation is of a four coordinate species in solution. The chemical shifts of the isopropoxide groups seem to be dependant on the trans ligand and more particularly on the relative positions of the aryloxides to the isopropoxides. In complexes 4.1-4.6 the O_{Ar}-Ti-O_{Alk} angle is approximately 90° and the C**H** signal comes around 4.8ppm. In contrast in complexes 4.7-4.8 the O_{Ar}-Ti-O_{Alk} angle is approximately 180° and the C**H** signal comes around 3.5ppm. If the chemical shift of this group is an indicator of the O_{Ar}-Ti-O_{Alk} angle then its value in 4.10 (4.14ppm) would suggest an angle between 90° and 180° which would be attained in a tetrahedral four coordinate form.

Unlike the ^{1}H NMR spectrum the ^{13}C NMR spectrum showed little difference to the earlier complexes with signals for the isopropoxide **C**H (80.6ppm) and **C**H$_3$ groups (25.6ppm) and also the imine **C**H group (165.9ppm), values which are similar to those seen in 4.1-4.8.

The structure of complex 4.10 can be seen as an analogue of the transition state in the interconversion of the enantiomers found in octahedral complexes (Δ and Λ). Octahedral complexes of the type $M(AB)_2X_2$ can undergo an inversion of configuration between their Δ and Λ forms as shown in figure 4.25 below.

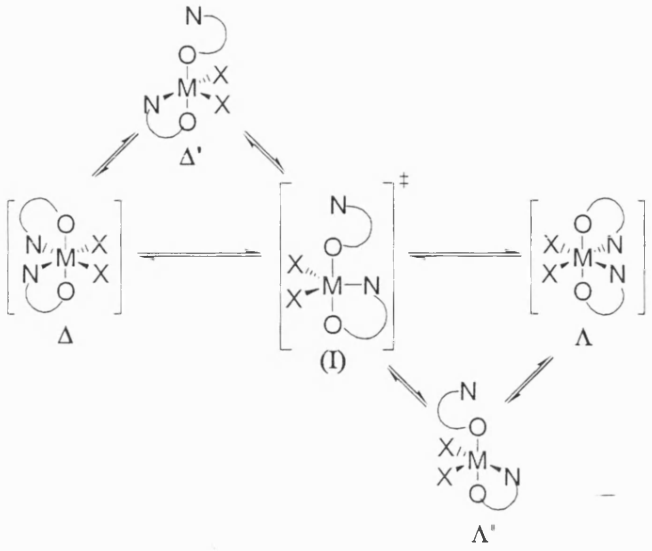

Figure 4.25: Interconversion between enantiomers in an octahedral complex via a five coordinate species (bond rupture). Δ' and Λ' correspond to stable complexes such as 4.10

This inversion of configuration can occur via one of two mechanisms; a twist mechanism in which no bonds are broken and the inversion goes via a sterically encumbered trigonal prismatic transition state or a bond rupture mechanism, shown in figure 4.25 above, which goes via a five coordinate intermediate. The most favourable mechanism for complexes such as ours, with relatively bulky chelating NO ligands, is bond rupture, which avoids the need to pass through a sterically encumbered intermediate[22]. By increasing the steric bulk of the imine substituents we have inhibited the formation of either the Δ or Λ states and instead have formed a complex with a structure of type Δ' or Λ', which must closely resemble the transition state ‡ in the Δ ⇌ Λ process shown in figure 4.25 above.

[22] X. Bei, D.C. Swenson and R.F. Jordan, *Organometallics*, **17**, 3282 (1997); T. Tsukahara, D.C. Swenson and R.F. Jordan, *Organometallics*, **17**, 3303 (1997); I. Kim, Y. Mishihara, R.F. Jordan, R.D. Rogers, A.L. Rheingold and G.P.A. Yap, *Organometallics*, **17**, 3314 (1997)

Complex 4.9

Two equivalents of ligand 4.9L react readily with one equivalent of TiPT to yield a yellow powder that was unsuitable for single-crystal X-ray diffraction. The ^{1}H and ^{13}C NMR spectra of complex 4.7 confirmed that a complex of the formula $Ti(4.7L)_2(O^iPr)_2$ had been formed however, as with complex 4.10, significant differences were seen in the spectra when compared to the spectra of 4.1-4.8. The ^{1}H NMR spectrum showed one set of sharp resonances due to the isopropoxide groups with a septet at 4.50ppm for the C**H** protons of the isopropoxide group, a value which, although slightly higher than the same signal in 4.10, lies between that observed for complexes 4.1-4.6 and the lower value observed for complexes 4.7-4.8. As was stated in the discussion of 4.10 this would suggest a change in configuration at the metal centre. This effect is carried over into the signal for the C**H**$_3$ protons of the isopropoxide, which also lie between the values for complexes 4.1-4.6 and those for 4.7 and 4.8 at 0.92ppm. As with all the previous complexes no significant change is seen however for the imine C**H**=proton, which showed a single sharp resonance at 7.79ppm, a value which is very similar to that observed in the earlier complexes. Unlike the ^{1}H NMR spectrum, the ^{13}C NMR spectrum showed little difference to the earlier complexes with signals for the isopropoxide **C**H (77.8ppm) and **C**H$_3$ groups (24.3ppm) and also the imine **C**H group (166.3ppm), values that are similar to those seen in 4.1-4.8 and 4.10.

The ^{1}H NMR spectrum of complex 4.9 seems to suggest that it has a similar structure in solution to complex 4.10 and therefore would probably form a similar five-coordinate complex in the solid-state.

Complex 4.11

Increasing the steric bulk further from ligand 4.10L to 4.11L causes a further change in structure. Two equivalents of ligand 4.11L react readily with one equivalent of TiPT to yield yellow crystals, which were suitable for single-crystal X-ray diffraction. The asymmetric unit contains one molecule of the product complex and a molecule of toluene that is disordered over two positions. Unlike the previous structures the complex does not have the expected $Ti(4.11L)_2(O^iPr)_2$ stoichiometry and instead a monosubstituted product with a stoichiometry of $Ti(4.11L)(O^iPr)_3$ is formed. The complex is dimeric with two titanium centres bridged by two isopropoxide ligands

with each metal centre having one salicylaldimine bonded to it through the aryloxide group only. In addition, each titanium centre also retains two terminal isopropoxide ligands giving five coordinate metal centres with a distorted trigonal bipyramidal geometry.

The metal-ligand bond lengths in the complex are typical for interactions of this type with similar terminal isopropoxide bond lengths to those observed in the previous complexes {1.762(2)Å [Ti(1)-O(2)], 1.778(2)Å [Ti(1)-O(3)], 1.788(2)Å [Ti(2)-O(6)] and 1.766(2)Å [Ti(2)-O(7)]}. The bridging isopropoxides, as would be expected, have longer Ti-O bonds. As is normal for Ti_2O_2 rings the alkoxides bridge unsymmetrically {2.120(2)Å [Ti(1)-O(4)], 1.929(2)Å [Ti(1)-O(5)], 1.924(2) [Ti(2)-O(4)] and 2.112(2)Å [Ti(2)-O(5)]}. The aryloxides have similar bond lengths to the titanium centres to the monodentate aryloxide ligand in complex 4.10 {1.882(2)Å [Ti(1)-O(1)] and 1.883(2)Å [Ti(2)-O(8)]}. The imine nitrogen atoms play no part in bonding to the metal centre.

The ^{1}H NMR spectrum for complex 4.11 shows only one signal due to the isopropoxide ligands C**H** (4.43ppm) and C**H**$_3$ groups (0.99ppm), which suggests that one of two processes is occurring. Either the dimer, which is observed in the solid state, is not maintained in solution, and a monomer is formed or the isopropoxide ligands are fluxional and undergo rapid exchange between bridging and terminal bonding modes. The ^{1}H spectrum also exhibits a signal for the imine C**H** proton at 8.56ppm. The ^{13}C NMR spectrum is very similar to those observed for previous salicylaldimine complexes with clearly identifiable signals due to the isopropoxide **C**H (77.6ppm) and **C**H$_3$ (26.6ppm) groups and the imine **C**H group (168.2ppm).

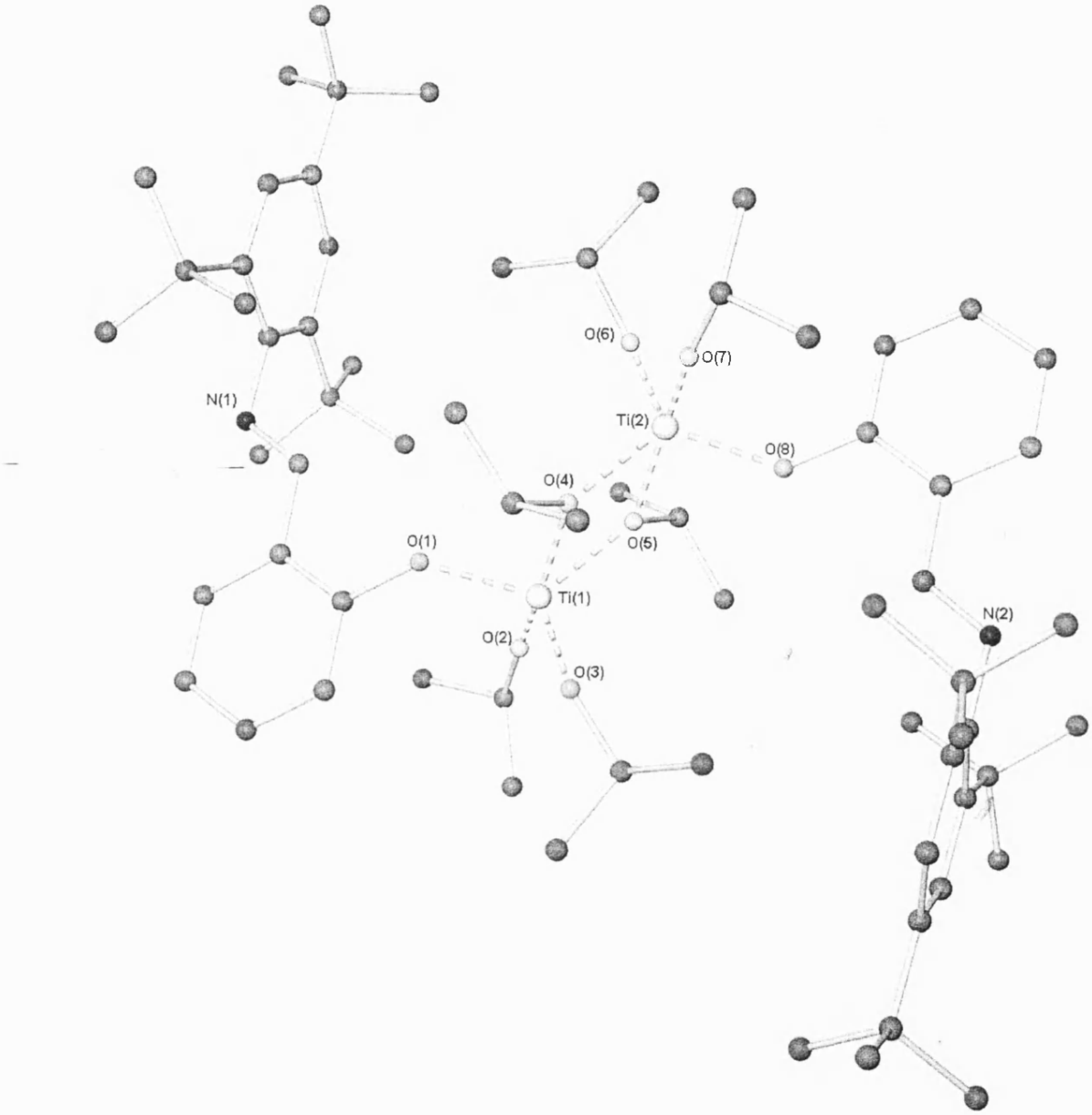

Figure 4.26: Molecular structure of complex 4.11 (hydrogen atoms not shown for clarity)

4.2.5 Complexes 4.12-4.16: Investigating electronic effects on the phenolic group of salicylaldimine ligands

Complexes 4.1-4.11 investigated the effect of varying the substituents on the imine group of the salicylaldimine ligand on the structure of the resulting complex with TiPT. This showed that electron withdrawing and donating groups on the imine group had little, or no, effect on complex structure. Whereas increasing the steric demand of the ligand had a marked effect on complex structure. The following complexes, 4.12-4.16, investigate the effect of adding electron withdrawing and donating groups around the phenyl ring of the aryloxide group of the ligand to see if this is influential on complex structure.

Complex 4.12

Two equivalents of ligand 4.12L react readily with one equivalent of TiPT to yield a yellow crystalline product that was suitable for single-crystal X-ray diffraction. The asymmetric unit contains one molecule of the product complex which has the expected $Ti(4.12L)_2(O^iPr)_2$ form and a distorted octahedral geometry at the metal centre. The complex has the same gross structure as the analogue with no Cl atoms present, complex 4.4.

The metal-ligand bond lengths in the complex are very similar to those observed for complex 4.4 and no significant effect due to the chloro groups is observed. The isopropoxide ligands have bond lengths to the metal centre of 1.803(2)Å [Ti(1)-O(3)] and 1.768(2)Å [Ti(1)-O(2)] while those the phenoxides are 1.940(2)Å [Ti(1)-O(1)] and 1.914(2)Å [Ti(1)-O(4)]. As expected the bond lengths from the metal to the imine nitrogen atoms are the longest ligand to metal interactions with bond lengths of 2.339(2)Å [Ti(1)-N(11)] and 2.287(2)Å [Ti(1)-N(2)].

The ^1H and ^{13}C NMR spectra for complex 4.12 suggest that as with previous complexes the overall solid-state structure is maintained in solution with mostly similar resonances for the isopropoxide and imine protons to those seen in complex 4.4. Signals due to the isopropoxide ligands are observed in the ^1H NMR spectrum at 4.90ppm for the **CH** protons and 1.23ppm for the CH_3 protons, which is lower than the signal seen for the methyl protons in complex 4.4. The ^1H NMR spectrum also has

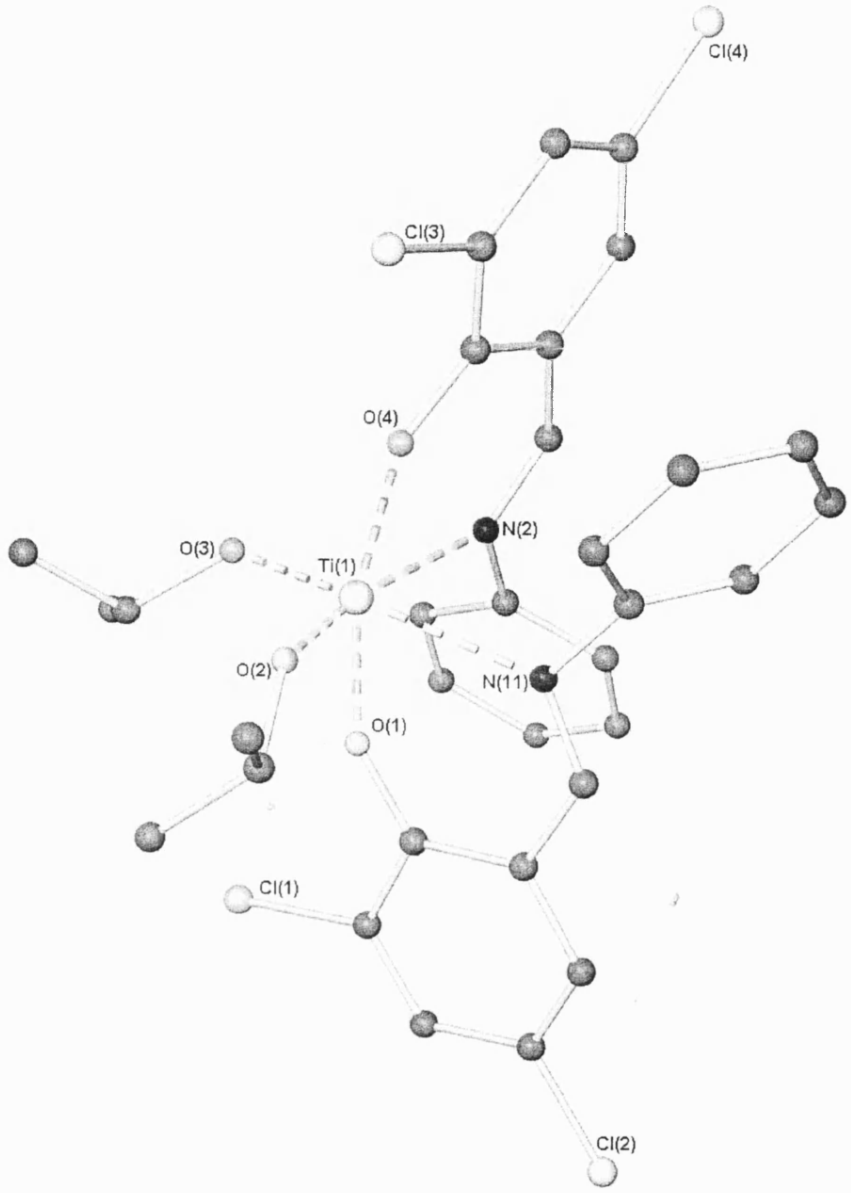

Figure 4.27: Molecular structure of complex 4.12 (hydrogen atoms not shown for clarity)

a sharp singlet due to the imine C**H** protons at 7.75ppm. The ^{13}C NMR spectrum also gives similar results with signals due to the isopropoxide groups at 26.0ppm (**C**H_3) and 80.8ppm (**C**H) and a signal at 164.6ppm due to the imine **C**H group.

Complex 4.13

Two equivalents of ligand 4.13L react readily with one equivalent of TiPT to yield a yellow crystalline product that was suitable for single-crystal X-ray diffraction. The asymmetric unit contains one molecule of the product complex which has the expected $Ti(4.13L)_2(O^iPr)_2$ form and a distorted octahedral geometry at the metal centre. The complex has the same structure as the analogous products with no OMe groups present, complex 4.4, and the chloro derivative 4.12. As with those complexes, 4.13 has the most favourable geometry (A) shown in figure 4.5 in the introduction to this chapter with the phenolic oxygen donors trans-axial, the imine groups cis-equatorial and alkoxide donors also cis-equatorial.

The metal to ligand bond lengths in the complex are very similar to those observed for complexes 4.4 and 4.12 and no significant electronic effect due to the methoxy group is observed. The isopropoxide ligands have bond lengths to the metal centre of 1.821(3)Å [Ti(1)-O(1)] and 1.809(3)Å [Ti(1)-O(2)] while those to the phenoxides are 1.901(3)Å [Ti(1)-O(3)] and 1.895(3)Å [Ti(1)-O(5)]. As expected the bond lengths from the metal to the imine nitrogen atoms are the longest ligand to metal interactions with bond lengths of 2.329(3)Å [Ti(1)-N(1)] and 2.317(3)Å [Ti(1)-N(2)].

The ^1H and ^{13}C NMR spectra for complex 4.13 suggest that the gross solid-state structure is maintained in solution with similar resonances for the isopropoxide and imine protons to those seen in complex 4.4 and 4.12. Signals due to the isopropoxide ligands are observed in the ^1H NMR spectrum at 4.85ppm for the C**H** protons and 1.21ppm for the C**H**$_3$ protons. The ^1H NMR spectrum also has a sharp singlet due to the imine C**H** protons at 7.73ppm. The ^{13}C NMR spectrum confirms these results with signals due to the isopropoxide groups at 26.0ppm (**C**H_3) and 78.7ppm (**C**H) and a signal at 165.5 ppm due to the imine **C**H group.

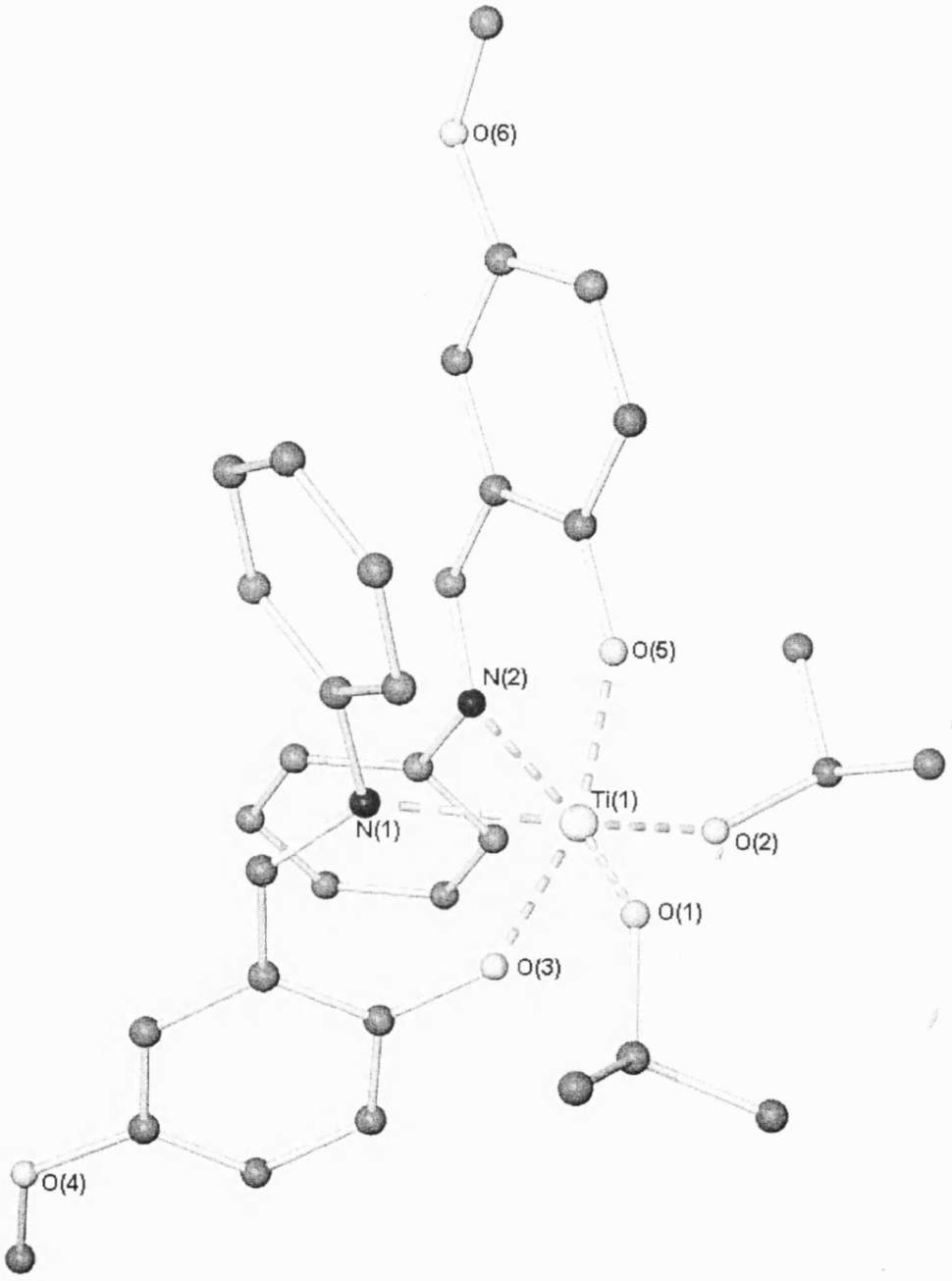

Figure 4.28: Molecular structure of complex 4.13 (hydrogen atoms not shown for clarity)

Complex 4.14

Two equivalents of ligand 4.14L react readily with one equivalent of TiPT to yield a yellow crystalline product that was suitable for single-crystal X-ray diffraction. The asymmetric unit contains one molecule of the product complex which has the expected $Ti(4.14L)_2(O^iPr)_2$ stoichiometry and a distorted octahedral geometry at the metal centre. The complex has a similar structure to complex 4.8. As with the non-chloro analogue the complex does not have the most favoured isomeric form at the metal centre due to the increased steric bulk at the imine substituents. The ligands are arranged with the imine nitrogen atoms in the trans-axial positions and the aryloxides and alkoxides in cis-equatorial arrangements (isomer B in figure 4.5) thereby allowing the sterically demanding groups on the imine substituents to be moved away from the sterically congested metal centre.

The bond lengths to the metal centre are very similar to those observed in complex 4.8 and no significant electronic effect is observed due to the addition of chloro substituents around the salicylaldimine phenyl ring. The bond lengths from titanium to the aryloxides {1.988(2)Å [Ti(1)-O(1)] and 1.991(2)Å [Ti(1)-O(2)]} are similar in length to the same bonds in complex 4.8 and are significantly lengthened compared to structures with the more favourable configuration (4.1-4.6 and 4.12-4.13). Concomitantly the titanium-imine bond lengths {2.235(2)Å [Ti(1)-N(1)] and 2.226(2)Å [Ti(1)-N(2)]} exhibit a similar decrease. This is in contrast to the titanium-alkoxide bond lengths, which appear to be insensitive to the trans ligand {1.785(2)Å [Ti(1)-O(3)] and 1.798(2)Å [Ti(1)-O(4)]}.

The ^1H NMR spectrum of complex 4.14 showed similar features to those observed in complex 4.7 and 4.8. Although no difference is seen in the bond lengths at the isopropoxide ligands, as with the previous complex, a significant shift in the signals for the isopropoxide groups is observed compared to complexes 4.1-4.6 and 4.12-4.13 and this can probably be attributed to the different trans influence, which these ligands are subject to. The ^1H NMR spectrum showed one set of sharp resonances due to the isopropoxide groups with a septet at 4.35ppm for the **CH** protons which is a smaller change in chemical shift than observed in complexes 4.7 and 4.8 and actually more similar to that observed for the five coordinate complexes 4.10 and 4.11. This effect is carried over into the signal for the $\mathbf{CH_3}$ protons of the isopropoxide, which are also

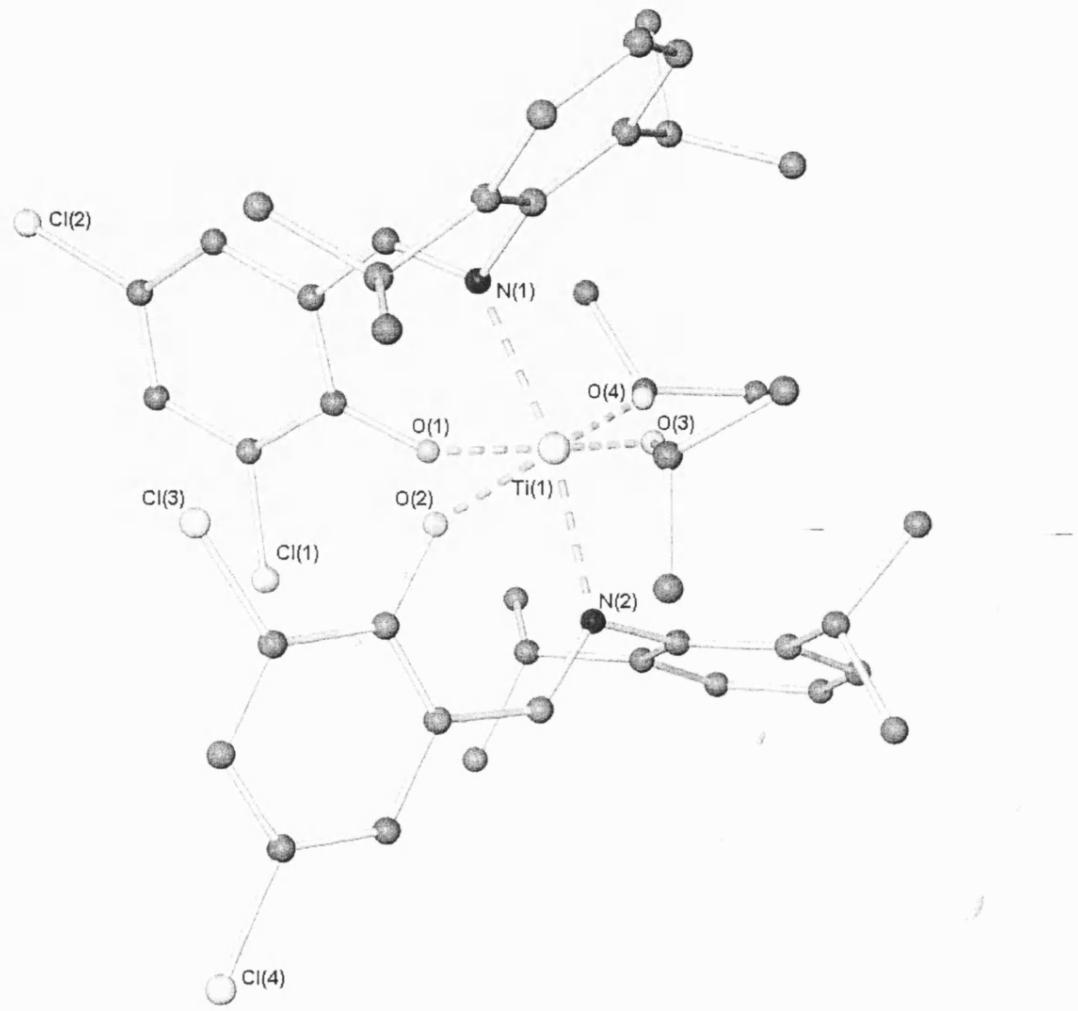

Figure 4.29: Molecular structure of complex 4.14 (hydrogen atoms not shown for clarity)

similar to those observed for complexes 4.10-4.11 at 0.70ppm. As with previous complexes the ^{13}C spectrum appears to be insensitive to the variation in ligand and has similar signals to those observed for all of the previous complexes. The spectrum has signals for the isopropoxide **C**H (78.3 ppm) and **C**H_3 groups (23.2ppm) and also the imine **C**H group (159.3ppm).

Complex 4.15

Two equivalents of ligand 4.15L react readily with one equivalent of TiPT to yield a yellow crystalline product that was suitable for single-crystal X-ray diffraction. The asymmetric unit contains one molecule of the product complex which has the expected Ti(4.15L)$_2$(O^iPr)$_2$ form and a distorted octahedral geometry at the metal centre. The complex has the same structure as the analogous complexes with an unsubstituted (complex 4.8) or dichloro substituted (complex 4.14) salicylaldimine phenyl ring. As with the unsubstituted and dichloro analogues, complex 4.15 possesses a ligand arrangement with the imine nitrogen atoms in the trans-axial positions and the aryloxides and alkoxides in cis-equatorial arrangements (isomer B in figure 4.5).

The bond lengths to the metal centre are very similar to those observed in complexes 4.8 and 4.14 and no significant effect is observed due to the addition of the methoxy substituent on the salicylaldimine phenyl ring.

The bond lengths from titanium to the aryloxides {1.985(2)Å [Ti(1)-O(1)] and 1.970 (2)Å [Ti(1)-O(3)]} are similar in length to the same bonds in complexes 4.8 and 4.14 and are significantly lengthened compared to structures with the usual configuration (4.1-4.6 and 4.12-4.13). Concomitant to this the titanium-imine bond lengths {2.223(2)Å [Ti(1)-N(1)] and 2.233(2)Å [Ti(1)-N(2)]} exhibit a similar decrease. In contrast the titanium-alkoxide bond lengths appear to be insensitive to the trans ligand {1.794(2)Å [Ti(1)-O(5)] and 1.830(2)Å [Ti(1)-O(6)]}.

The ^1H NMR spectrum of complex 4.15 showed similar features to those observed in complex 4.14. Although no difference is seen in the bond lengths at the isopropoxide ligands, as with the previous complex, a significant shift in the signals for the isopropoxide groups is observed compared to complexes 4.1-4.6 and 4.12-4.13 and

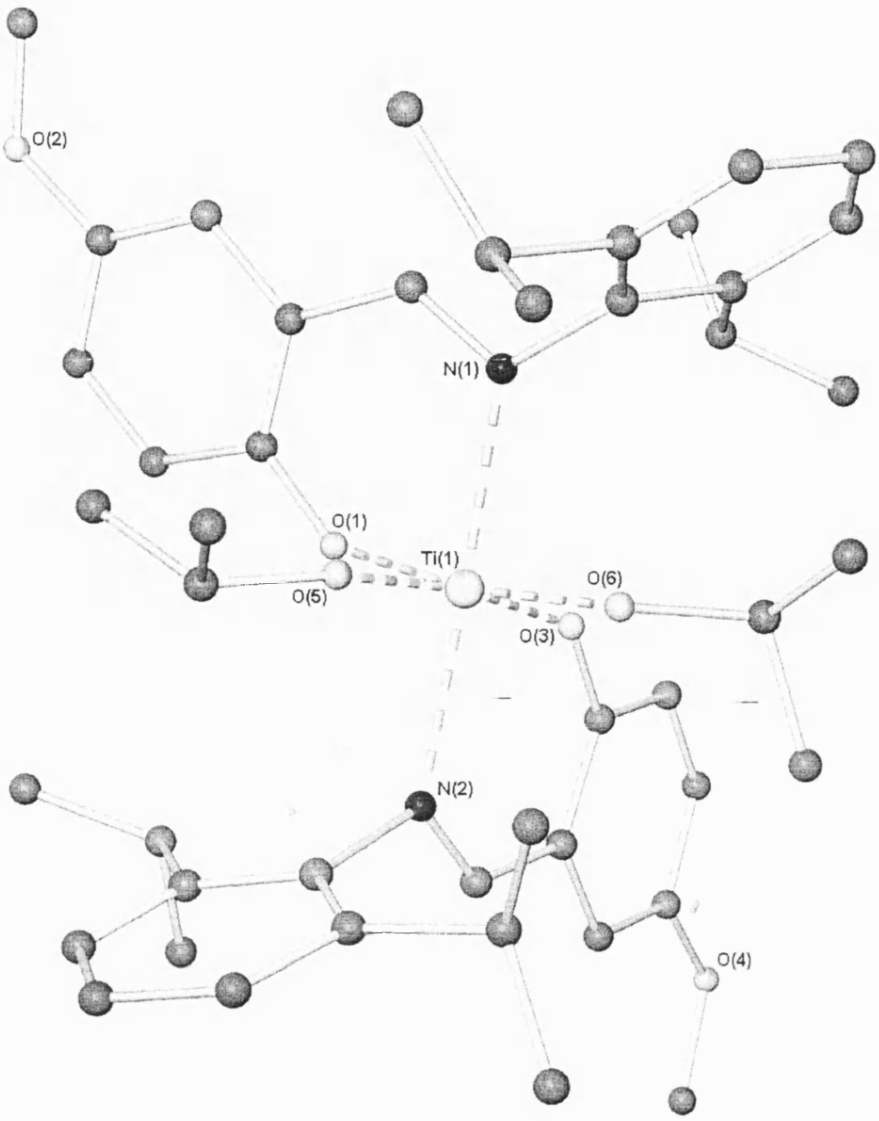

Figure 4.30: Molecular structure of complex 4.15 (hydrogen atoms not shown for clarity)

this can probably be attributed to the different trans influence, which these ligands are subject to. The ^{1}H NMR spectrum showed one set of sharp resonances due to the isopropoxide groups with a septet at 4.40ppm for the C**H** protons with a similar shift to that observed for complex 4.14. This effect is carried over into the signal for the C**H**$_3$ protons of the isopropoxide, which are also similar to those in 4.14 at 0.82ppm.

Complex 4.16

Two equivalents of ligand 4.16L react readily with one equivalent of TiPT to yield yellow crystals, which were suitable for single-crystal X-ray diffraction. The asymmetric unit contains half a molecule of the product complex. As with the earlier complex with a ligand of this type the complex does not have the usual Ti(4.16L)$_2$(O^iPr)$_2$ stoichiometry due to its large steric bulk and instead a monosubstituted product is formed. The complex is dimeric with two titanium centres bridged by two isopropoxide ligands and with each metal centre having one salicylaldimine bonded to it through the aryloxide group only. In addition, each titanium centre also retains two isopropoxide ligands giving five coordinate metal centres with distorted trigonal bipyramidal geometry.

The metal to ligand bond lengths in the complexes are similar to those observed in complex 4.11 with terminal isopropoxide bond lengths close to those observed in the unsubstituted analogue {1.764(2)Å [Ti(1)-O(3)] and 1.765(2)Å [Ti(2)-O(4)]}. The bonds to the bridging isopropoxides, as would be expected, are longer than the terminal ones with each alkoxide having a pair of unsymmetrical bonds to the metal centres {1.975(2)Å [Ti(1)-O(2)] and 2.058(2)Å [Ti(1)-O(2#)]}. The aryloxides have similar bond lengths to the titanium centres to the monodentate aryloxide ligands in complexes 4.10 and 4.11 {1.913(2)Å [Ti(1)-O(1)]}.

As with complex 4.11 the ^{1}H NMR spectrum for complex 4.16 shows only one signal due to the isopropoxide ligands C**H** (4.45ppm) and C**H**$_3$ groups (0.82ppm), which suggests that one of two processes is occurring. Either the dimer, which is observed in the solid state, is not maintained in solution, and a monomer is formed or the isopropoxide ligands are fluxional and undergo rapid exchange between bridging and terminal bonding modes in a similar fashion to complex 4.11. The ^{1}H spectrum also exhibits a signal for the imine C**H** proton at 8.35ppm.

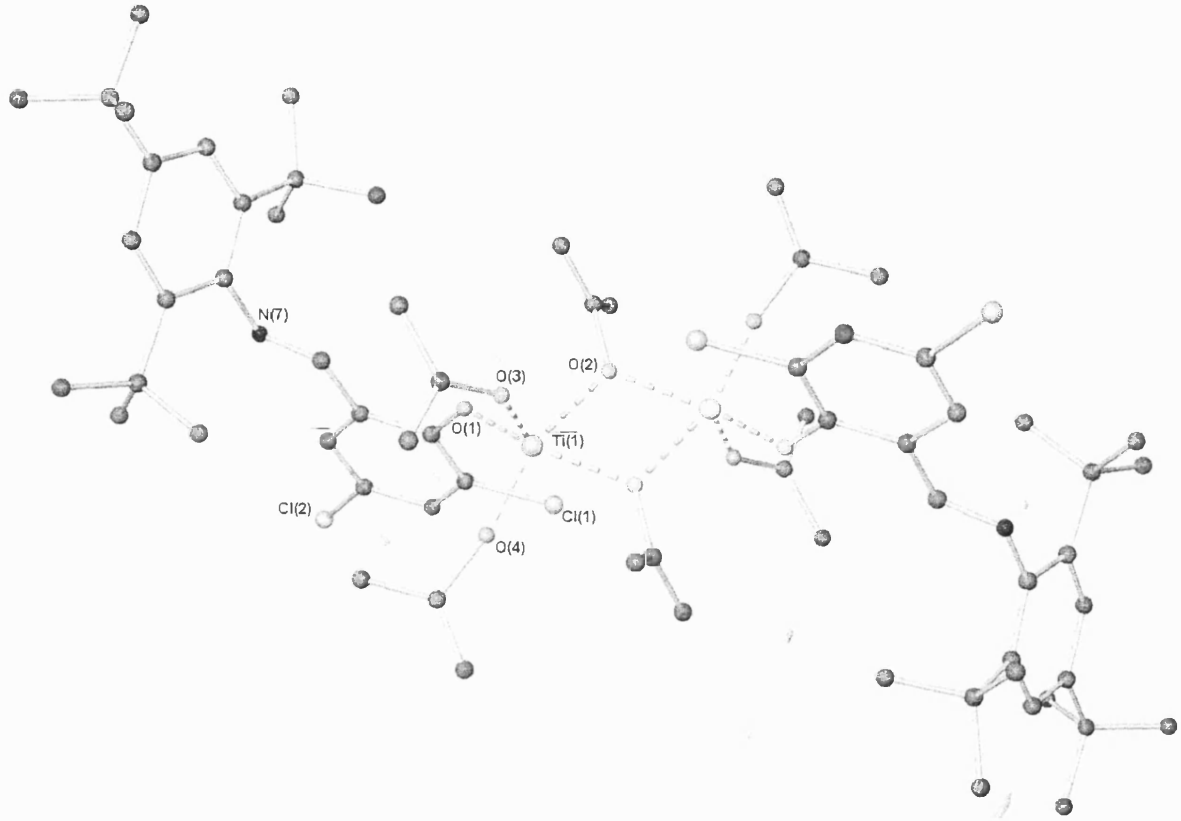

Figure 4.31: Molecular structure of complex 4.16 (hydrogen atoms not shown for clarity)

Summary

Complexes 4.12-4.16 looked at the effect of adding electron withdrawing or donating groups to the aryloxide ring of the salicylaldimine ligands. In all cases very little or no effect is observed in the solid-state structures of these complexes when compared to the analogous complexes where these substituents are not present. In solution it is possible that complexes 4.14 and 4.15 may have a different form from the parent compound 4.8 although this is not entirely clear from the data obtained.

4.2.6 Summary of complexes 4.1-4.16

In complexes 4.1-4.16 we have looked at the effect of varying various properties of the simple salicylaldimine ligands on the structure of the resulting complex with TiPT. This work has shown that variation of the electronic properties of the ligand, either at the imine or aryloxide group, seems to have little effect on the structure of the resulting complex. Comparison of the phenyl (complex 4.4) and pentafluorophenyl (complex 4.5) salicylaldimine complexes shows little difference due to the addition of the highly electron withdrawing fluorine atoms. In addition comparison of any of the compounds 4.12-4.16 with the parent unsubstituted analogues shows that variation of the electronic properties of the salicylaldimine group also has little effect on complex structure in the solid-state. To illustrate this the table below gives selected solution and solid-state data for complexes 4.4, 4.5, 4.12 and 4.13.

Complex	Ti-O^{i}Pr (Å)	Ti-OPh (Å)	Ti-N (Å)	^{i}Pr C**H** (ppm)	^{i}Pr C**H**$_3$ (ppm)	Imine C**H** (ppm)
4.4	1.81-1.82	1.90	2.30-2.33	4.90	1.23	7.87
4.5	1.78-1.80	1.92-1.93	2.33-2.34	4.77	1.11	8.07
4.12	1.77-1.80	1.91-1.94	2.29-2.34	4.90	1.23	7.75
4.13	1.81-1.82	1.90	2.32-2.33	4.85	1.21	7.73

Figure 4.32: Comparison of structural parameters and ^{1}H NMR chemical shifts for a range of complexes

This data shows no significant difference in any of the parameters due to the electron withdrawing and donating groups on the ligand. In contrast variation of the steric bulk at the imine substituents has been shown, throughout the range of complexes, to have a powerful effect on structure and has allowed the isolation of four different forms of titanium complex from the simple trans-phenolic complexes, 4.1-4.6 and 4.12-4.13, through the sterically more hindered trans-imine complexes, 4.7-4.8 and 4.14-4.15, the five-coordinate transition state analogues, 4.9-4.10, and finally to the monosubstituted products, 4.11 and 4.16. Figure 4.33 below shows the four structural types with the ligands from 4.1L-4.11L, which form them.

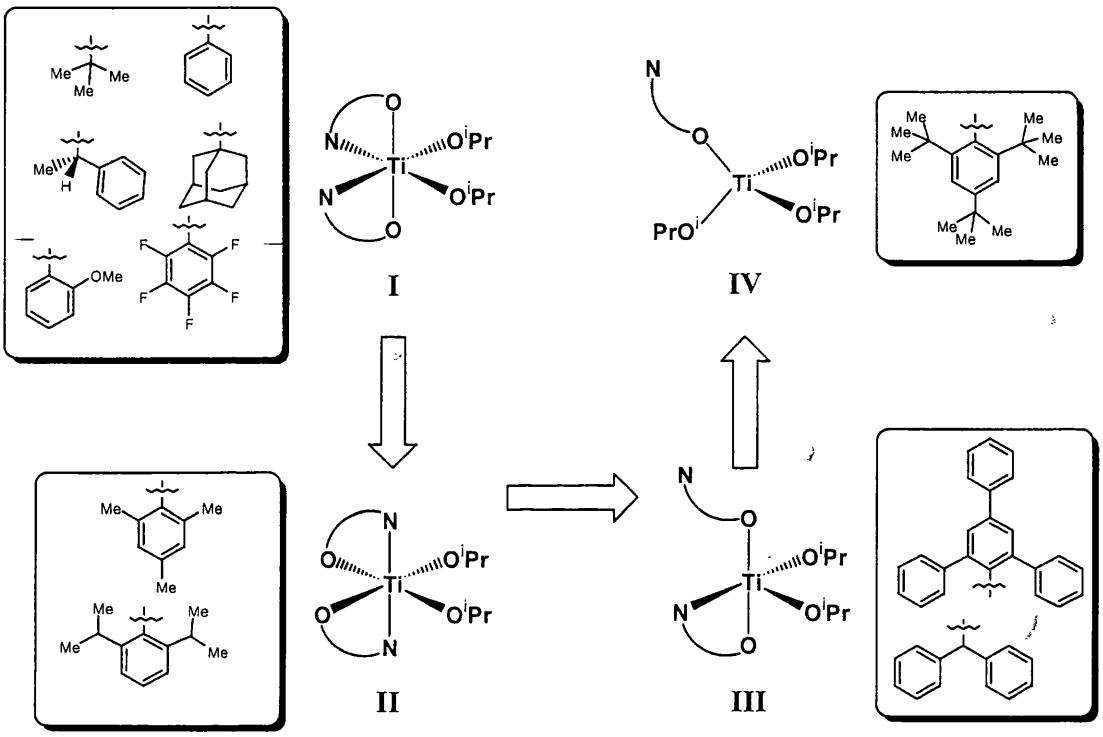

Figure 4.33: The structural forms of titanium salicylaldimine complexes

Two of these forms, the five coordinate (III) and the monosubstituted (IV) are the first examples of titanium complexes of this type with salicylaldimine ligands. With the five coordinate being particularly interesting as it may be an analogue of the transition state in the interconversion of octahedral isomers.

^{1}H NMR studies of the synthesisied complexes have proven to be an effective probe of the complexes in solution. In particular the chemical shift of the signals due to the

isopropoxide groups in solution seem to correlate to the solid-state structure obtained with the approximate ranges for each structural type shown below shown in figure 4.34 below.

Structural Type	^{i}Pr C**H** (ppm)	^{i}Pr C**H**$_3$ (ppm)
Trans OAr groups (A in figure 4.5)	> 4.60	> 1.0
Trans imine groups (B in figure 4.5)	< 4.0	< 0.6
Five coordinate species	4.0-4.6	0.6-1.0

Figure 4.34: Approximate ranges for ^{1}H NMR chemical shifts of isopropoxide groups in salicylaldimine complexes

In contrast no significant change in the ^{13}C NMR spectra is observed throughout the series of sixteen complexes.

The wide variety of structural types observed in complexes 4.1-4.16 both in the solid state and solution will provide the basis to obtain structure/activity relationships for these catalysts in polyurethane synthesis. The work described in this chapter has shown that a large number of titanium complexes can be formed from a simple family of monoanionic ligands. The following chapter describes some complexes, formed with TiPT, which utilise Schiff base ligands, which have increased numbers of anionic donors.

Chapter 5

The Synthesis, Isolation and Structural Characterisation of Titanium Isopropoxide Complexes of Multidentate Polyanionic Schiff Bases

Chapter 4 was concerned with the synthesis and characterisation of titanium alkoxide complexes of monoanionic bidentate Schiff base ligands. In chapter 5 we will discuss selected examples of other types of Schiff bases, which contain more than one anionic donor ligand. These ligands, the most common family of which are the 'salen' family shown in figure 5.1 below, are, if anything used even more widely than their monoanionic counterparts.

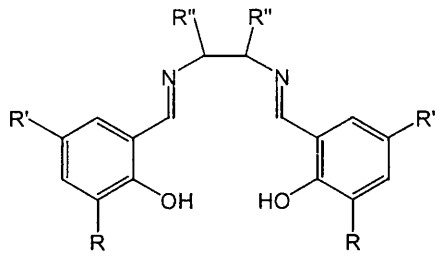

Figure 5.1: The salicylaldimine (salen) family of ligands

The chapter begins with an introduction to the chemistry of a selected range of ligands, which fall into this category. This introduction is followed by a discussion of the solution and solid-state structures of a number of titanium isopropoxide complexes of ligands in this group, which we have synthesised.

5.1 Introduction

The huge number of different ligand families, which can be classed in this group of ligands, is beyond the scope of this thesis. The following discussion will concentrate on two main areas, which are particularly relevant to this thesis and titanium chemistry. These two areas are 'salen' complexes and O-N-O ligands and it is hoped that the following discussion gives a flavour of the variety of roles even two small families from this large group of compounds can participate in.

5.1.1 Salen complexes

'Salen' type ligands are synthesised by the condensation reaction of 1,2 diamino compounds with two equivalents of an aldehyde containing a monoanionic donor as shown in figure 5.2 overleaf.

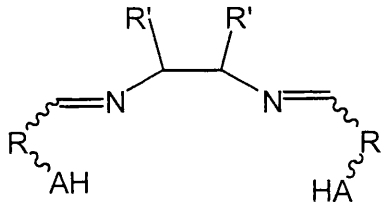

Figure 5.2: Salen ligands

The most common examples are derivatives of (N,N'-bis(salicylaldehyde)ethylenediamine), figure 5.1 above, but the first salen ligand, figure 5.3 below, and its copper complex, were synthesised in 1889 by Combes[1].

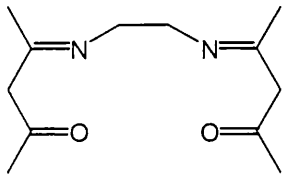

Figure 5.3: The first reported salen ligand

More recently complexes of bis-salicylaldimine salen ligands and their derivatives have become increasingly important in catalysis, particularly in asymmetric reactions. This section briefly reviews the use of these 'salen' type ligands in catalysis and then discusses in more detail the complexes they form with titanium species and the use of the resulting complexes as catalysts.

By far the most common 'salen' complexes to be used in asymmetric catalysis are those of manganese. The most well-known manganese 'salen' catalyst is Jacobsen's catalyst shown in figure 5.4 overleaf[2].

[1] A. Combes, *C. R. Acad. Fr.*, **108**, 1252 (1889)
[2] E.N. Jacobsen, in *Comprehensive Organometallic Chemistry II*, Eds. W. Abel, F.G.A. Stone and E. Willinson, Pergamon, New York, **12**, 1097 (1995)

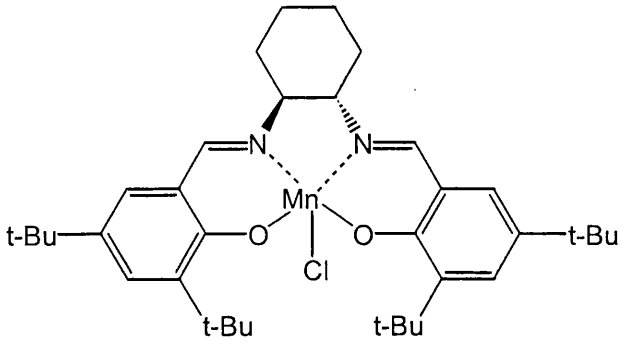

Figure 5.4: Jacobsen's Catalyst

This is currently the most efficient catalyst for the enantioselective epoxidation of unfunctionalised olefins. The reaction gives yields of up to 97% and enantiomeric excesses (e.e) of up to 98%. In the reaction shown below, the oxidant is usually sodium hypochlorite or an organic peracid and the co-oxidant (which avoids the formation of μ-oxo dimers) is an N-oxide.

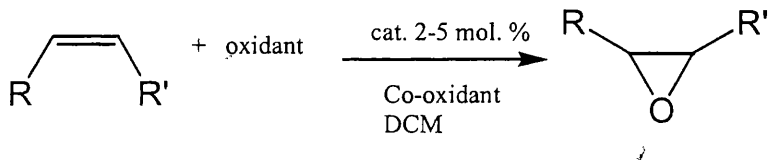

Figure 5.5: Asymmetric epoxidation of an olefin

Slightly before the work on Jacobsen's catalyst was published Katsuki published work using the catalyst shown below for the same reaction[3]. This complex showed less enantioselectivity than Jacobsen's catalyst although Katsuki was the first to show that the donor co-oxidant is necessary for enantioselectivity.

[3] T. Katsuki, *J. Mol. Catal. A: Chemical*, **113**, 87 (1996)

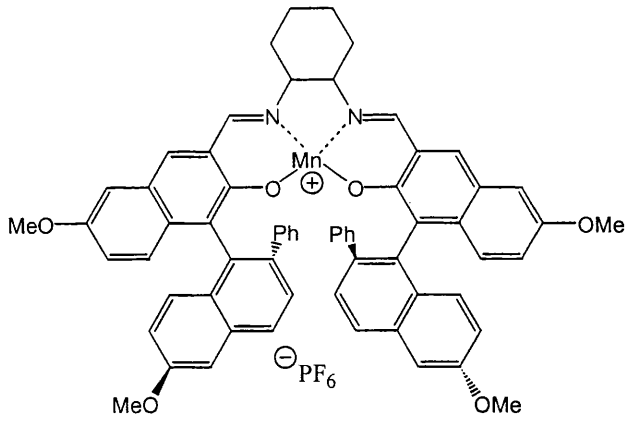

Figure 5.6: Katsuki's catalyst

Since the initial work on epoxidation Jacobsen's catalyst, and related complexes, have been used in a variety of other organic transformations such as the oxidation of sulfides[4], hydroxylation[5], aziridination[6], oxidation of keto-silyl ethers[7] and in the resolution of racemic allenes[8].

Cobalt complexes of 'salen-like' ligands such as the one shown in figure 5.7 below have been used for several organic transformations including hydroxylations[9], cyclopropanation[10], epoxide ring opening[11] and hydrolytic kinetic resolution[12].

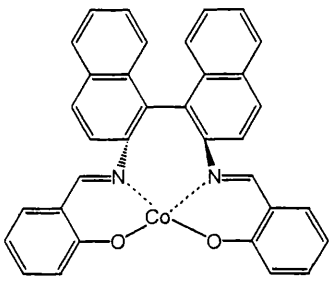

Figure 5.7: A cobalt salen complex

[4] M. Palucki, P. Hanson and E.N. Jacobsen, *Tetrahedron Lett.*, **33**, 13895 (1992)
[5] K. Hamachi, R. Irie and T. Katsuki, *Tetrahedron Lett.*, **37**, 4979 (1996)
[6] K.J. O'Connor, S.J. Wey and C.J. Burrows, *Tetrahedron Lett.*, **33**, 1001 (1992)
[7] D.R Reddy and E.R. Thornon, *Chem. Comm.*, 173 (1992)
[8] Y. Noguchi, H. Takiyama and T. Katsuki, *Synlett*, 543 (1998)
[9] A. Nishinaga, H. Yamato, T. Abe, K. Maruyama and T. Matsuura, *Tetrahedon Lett.*, **29**, 6309 (1988)
[10] T. Fukuda and T. Katsuki, *Synlett*, 825 (1995)
[11] E.N. Jacobsen, F. Kakiuch, R.G. Konsler, J.F. Larrow and M. Tokunaga, *Tetrahedron Lett.*, **38**, 773 (1997)
[12] B.D. Brandes and E.N. Jacobsen, *Tetrahedron: Asymmetry*, **8**, 3927 (1997)

The chromium complex in figure 5.8 below has been shown by Gilheany et al. to epoxidise styrene derivatives with good e.e. and since this report other related ligands have been used to increase the e.e. by utilisation of solvent effects[13].

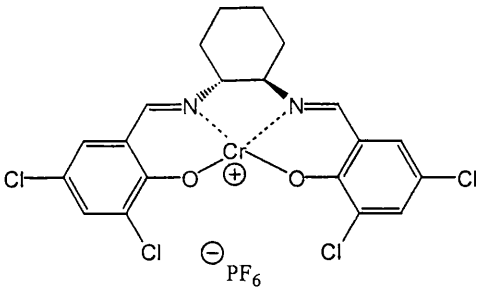

Figure 5.8: A chromium salen complex for epoxidising styrene derivatives

Other related chromium 'salen' complexes have also been used as catalysts for the asymmetric ring opening of epoxides[14], and Jacobsen et al. have used a modified chromium catalyst (figure 5.9) in hetero Diels-Alder reactions with up to 99% e.e. being observed after crystallisation of the product[15].

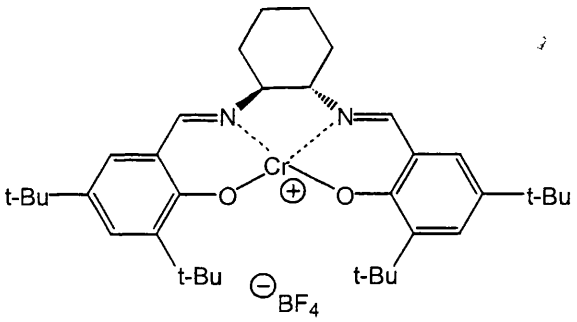

Figure 5.9: A chromium salen Diels-Alder catalyst

The first titanium 'salen' complex to be characterised by single crystal X-Ray diffraction is shown below. It was reported by Beddoes et al. in 1972 and predated the next publication by 15 years[16].

[13] C. Bousquet and D.G. Gilheany, *Tetrahedron Lett.*, **36**, 7739 (1995)
[14] M.H. Wu and E.N. Jacobsen, *Tetrahedron Lett.*, **38**, 1693 (1997)
[15] S.E. Schaus, J. Branalt and E.N. Jacobsen, *J. Org. Chem*, **63**, 403 (1998)
[16] G. Gilli, D.W.J. Cruickshank, R.L. Beddoes and O.S. Mills, *Acta Cryst. Section B*, **28**, 1889 (1972)

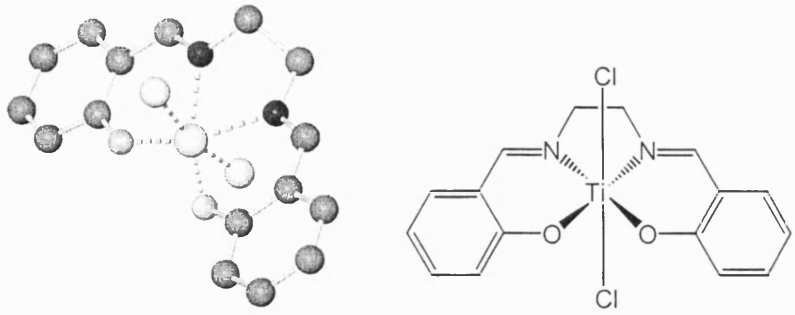

Figure 5.10: Beddoes' titanium salen complex

In 1987 Fujita et al. reported the use of the titanium salen complex below in the asymmetric oxidation of methyl phenyl sulfide[17].

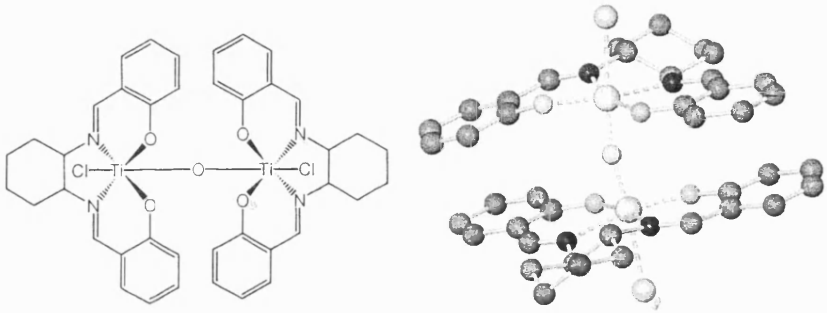

Figure 5.11: Catalyst for asymmetric oxidation of sulfides

The oxo bridge was presumed to be formed by the presence of either a trace of water in the solvent used or by moisture from the air. The isolated complex was used for the oxidation, which was carried out using the oxidant trityl hydroperoxide as shown below giving approximately 90% yield and e.e. values of over 50%.

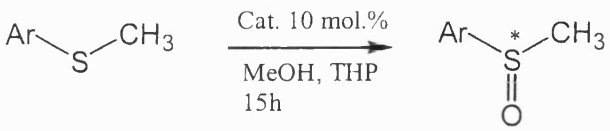

Figure 5.12: Asymmetric oxidation of methyl phenyl sulfide

[17] K. Nakajima, C. Sasaki, M. Kojima, T. Aoyama, S. Ohba, Y. Saito and J. Fujita, *Chem. Lett.*, 2189 (1987)

In 1996 North and Belokon et al. reported the use of the chiral titanium salen ligands, shown below in figure 5.13, to form catalysts with TiPT *in situ* which were then used to catalyse the asymmetric addition of trimethylsilyl cyanide to aldehydes giving yields of around 70% and e.e. values of 75%.[18]

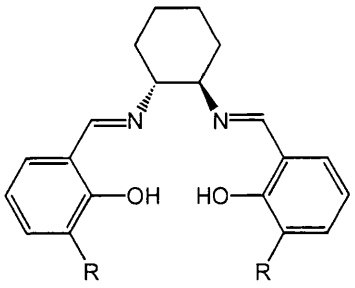

R = H or t-Bu

Figure 5.13: Proligands for catalysis of the addition of TMSCN to aldehydes

In a follow up paper in 1997 they tested a greater range of catalysts to investigate the effects of the R groups on the salicylaldimine components of the ligands and found that the optimum was the one shown below, which gave yields of over 95% and e.e. values of over 75%[19].

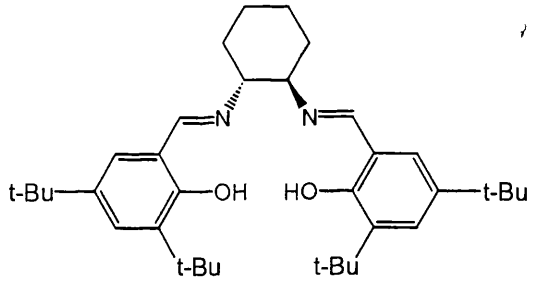

Figure 5.14: Optimum ligand for addition TMSCN to aldehydes

A crystal structure of one of their catalysts is shown in figure 5.15 overleaf[20].

[18] Y. Belokon, N. Ikonnikov, M. Moscalenko, M. North, S. Orlova, V. Tararov and L. Yashkina, *Tetrahedron: Asymmetry*, 7, 851 (1996)
[19] Y. Belokon, N. Ikonnikov, M. Moscalenko, M. North, V. Tararov, M. Flego, C. Orizu and M. Tasinazzo, *J. Chem. Soc. Perkin Trans. 1*, 1293 (1997)
[20] Y. Belokon, N. Ikonnikov, M. North, V. Tararov, C. Orizu, D.E. Hibbs, M.B. Hursthouse and K.M. Abdul Malik, *Chem. Comm.*, 387 (1998)

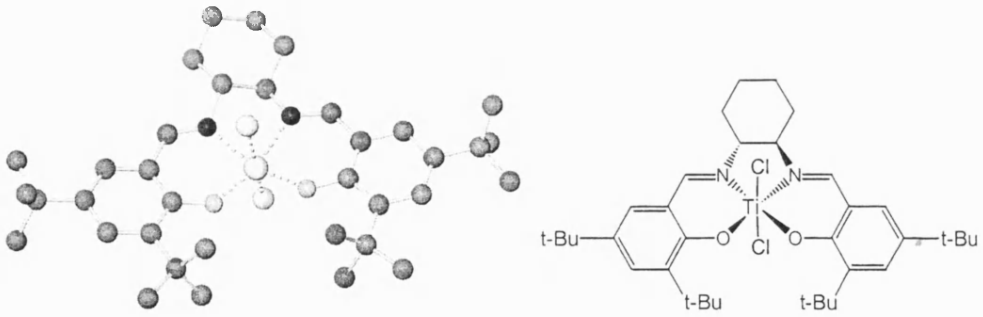

Figure 5.15: Catalyst for addition of TMSCN to aldehydes

More recently North and Belokon et al. have published further work on the addition of trimethylsilyl cyanide to aldehydes in which they have shown that the most active species in the reaction are the μ-oxo bridged structures of the type shown in figure 5.16 below[21] which are similar to those shown to be active in oxidations by Fujita et al. in 1987. These oxo compounds are formed by water in the reaction mixture and use of strictly anhydrous conditions reduces activity of the catalyst.

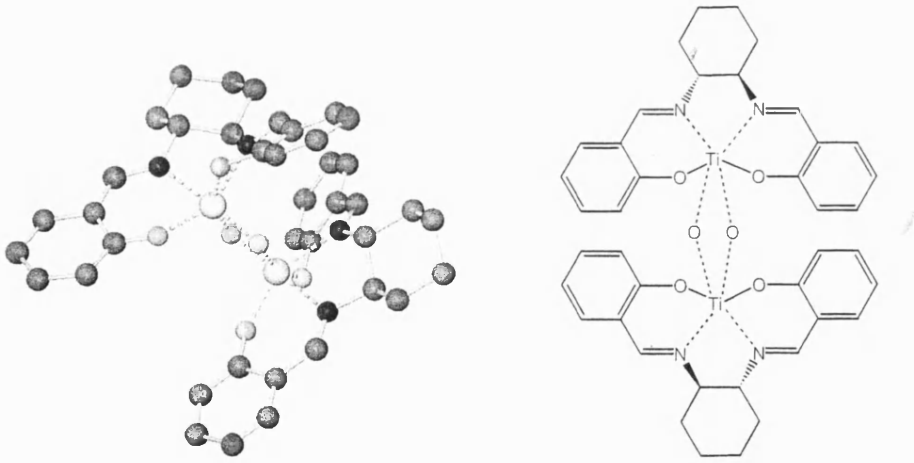

Figure 5.16: Oxo bridged salen catalyst

[21] Y.N. Belokon, S. Caveda-Cepas, B. Green, N.S. Ikonnikov, V.N. Khrustalev, V.S. Larichev, M.A. Moscalenko, M. North, C. Orizu, V. I. Tararov, M. Tasinazzo, G.I. Timofeeva and L.V. Yashkina, *J. Am. Chem. Soc.*, **121**, 3968 (1999)

At around the same time as North and Belokon reported their catalysts, Jiang et al reported a similar family of catalysts for the same reaction using the ligands shown in figure 5.17 below[22].

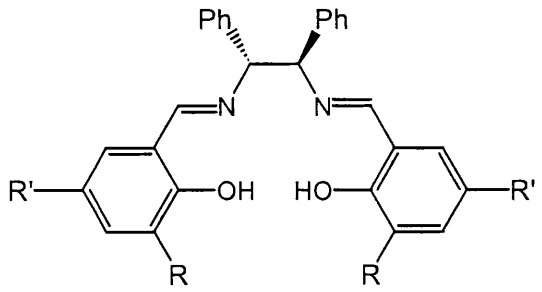

R = R' = t-Bu
R = $CHPh_2$, R' Me
R = OMe, R' = H
R = R' = H
R = H, R' = NO_2
R = H, R' = Br
R = H, R' = Cl
R = H, R' = OMe

Figure 5.17: Ligands used by Jiang et al.

The optimum catalyst for the reaction was found to be the complex shown in figure 5.18 below which under almost identical conditions to those used by North et al., gave yields and e.e. values of approximately 80%. Interestingly the catalysts used by Jiang et al. gave the R enantiomer in excess in contrast to those used by North et al. which gave S.

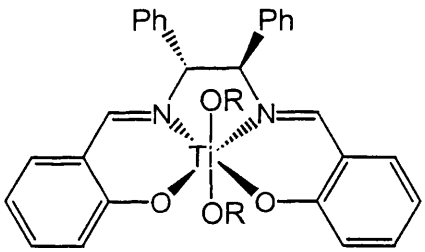

R = ^{i}Pr

Figure 5.18: Optimum catalyst for addition of TMSCN to benzaldehyde

Since this work by the groups of North and Jiang, a number of follow up papers by other groups have been published. Notably Gagne et al. published a study of the structure and reactivity of a number of titanium salen complexes[23]. Focussing particularly on the ease of substitution of the monodentate ancillary ligands by other

[22] Y. Jiang, L. Gong, X. Feng, W. Hu, W. Pan, Z. Li and A. Mi, *Tetrahedron*, **53**, 14327 (1997)
[23] H. Chen, P.S. White and M.R. Gagne, *Organometallics*, **17**, 5358 (1998)

species such as triflate or aryloxide ligands. They concluded that ease of substitution depended on the acidity of the ligand for oxygen donors with isopropoxide being the easiest to replace and triflate being easiest to add but that this trend was not followed for other donors such as N-benzyl-triflamide, which is more acidic than phenol but cannot replace isopropoxide.

Other structural papers have reported titanium salen compounds with other ancillary ligands including imido[24], fluoro and bromo[25]. Moore et al. have synthesised titanium 'salen' complexes such as the one shown in figure 5.19 below which, through careful modification of the 'salen' backbone, have the ancillary ligands in a cis configuration in contrast to the complexes described above in which they are trans[26].

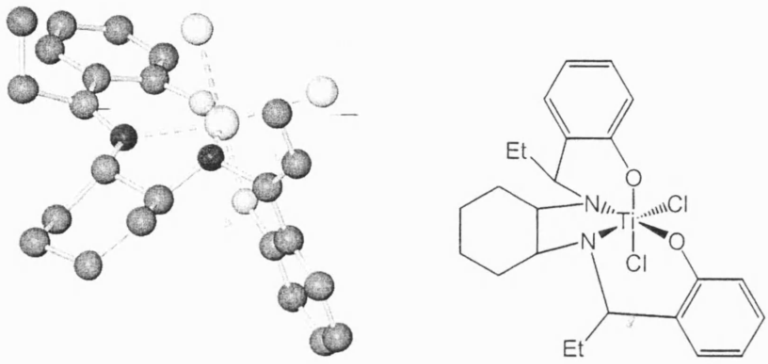

Figure 5.19: Salen complex with cis ancillary ligands

As was described in Chapter 4 this cis configuration is necessary for polyolefin synthesis and Moore et al. went on to react the complex with $AlMe_3$ to mimic the action of MAO during polyolefin synthesis, giving adduct products. In addition the complexes were shown to be active for polyolefin synthesis in the presence of MAO.

[24] J.M. Mcinnes, D. Swallow, A.J. Blake and P. Mountford, *Inorg. Chem.*, **37**, 5970 (1998)
[25] S.J. Coles, M.B. Hursthouse, D.G. Kelly, A.J. Toner and N.M. Walker, *J. Chem. Soc. Dalton Trans.*, 3489 (1998)
[26] J.P. Corden, W. Errington, P. Moore and M.G.H. Wallbridge, *Chem. Comm.*, 323 (1999)

5.1.2 O-N-O Ligands

The second important group of multianionic Schiff base complexes are the O-N-O ligands of the type shown in figure 5.20 below.

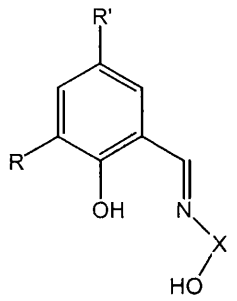

Figure 5.20: An O-N-O ligand

For these complexes the R and R' groups on the salicylaldimine phenyl ring and the X group linking the imine to the second anionic group can vary greatly. The most commonly used ligands of this type have chiral groups in the X linker and are used as ligands for asymmetric catalysis. The following section discusses the use of these ligands with titanium and concentrates on the use of these complexes in asymmetric catalysis.

A number of papers were published in the 1970s reporting the synthesis and spectroscopic characterisation of titanium complexes of O-N-O ligands of the type shown above[27]. However, the first report of their use as catalysts came in 1993 when Oguni et al. reported the use of the ligands in figure 5.21 as catalysts for the trimethylsilylcyanation of aldehydes three years prior to the work described above by North et al. with 'salen' ligands[28].

[27] P. Prashar, J.P. Tandon, *Z. Anorg. Allg. Chem.*, **383**, 81 (1971); N.S. Biradar, V.B. Mahale and V.H. Kulkarni, *Inorg. Chim Acta*, **7**, 267 (1973); R.K. Sharma, R.V. Singh and J.P. Tandon, *J. Indian Chem. Soc. Sect. A*, **18A**, 360 (1974); R.K. Sharma, R.V. Singh and J.P. Tandon, *Synth. React. Met.-Org. Chem.*, **9**, 519 (1979); E.C. Alyea, A. Malek and P.H. Merrell, *Trans. Met. Chem.*, **4**, 172 (1979)
[28] M. Hayashi, Y. Miyamoto, T. Inoue and N. Oguni, *J. Org. Chem.*, **58**, 1515 (1993)

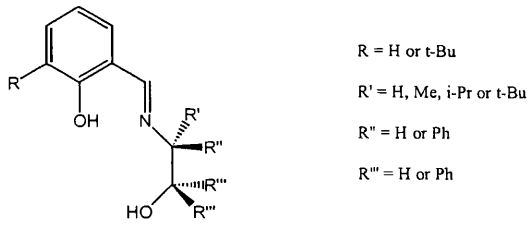

Figure 5.21: Ligands used to form O-N-O catalysts

The most effective catalyst with regards to optical yield (85% e.e.) for the reaction with benzaldehyde was discovered and spectroscopic techniques and mass spectrometry were used to try and confirm the solution structure of the catalyst. ^{1}H NMR spectroscopy of an equimolar mixture of ligand and titanium alkoxide showed resonances for the monosubstituted product alone (complex a in figure 5.22 below), while mass spectrometry showed a mixture of this compound and the di-substituted complex. However, NMR spectroscopy showed that complex b below was the sole product observed from a reaction of two equivalents of the ligand with one equivalent of the titanium alkoxide. Oguni et al. concluded that the disubstituted product was formed under the conditions of mass spectrometry and also showed that the disubstituted species showed no reactivity for the trimethylsilylcyanation concluding that the monosubstituted complex was the active catalyst in solution.

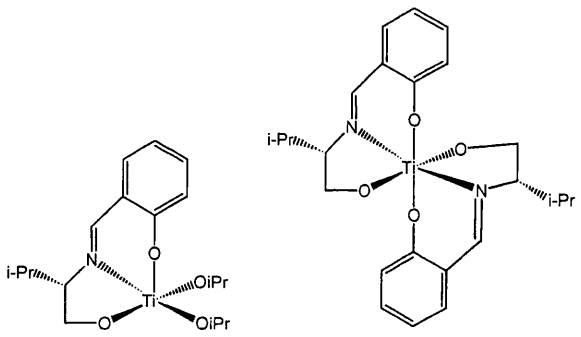

Complex a **Complex b**

Figure 5.22: The two forms of O-N-O catalyst observed

A second paper by Oguni et al., which confirmed the initial results, also reported the use of these catalysts for the enantioselective addition of diketenes to aldehydes as shown in figure 5.23 below to yield 5-hydroxy-3-oxoesters[29].

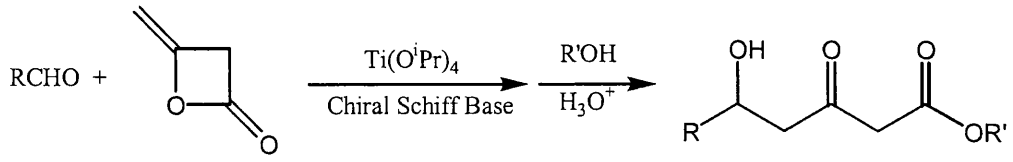

Figure 5.23: Addition of a diketene to an aldehyde

This reaction proceeded with yields and e.e. values of approximately 85% for the most active catalyst, which corresponded to the most active and selective catalyst for the trimethylsilylcyanation reaction described above. Unlike the trimethylsilylcyanation the catalyst for the diketene addition had to be used in stoichiometric amounts as catalytic amounts gave greatly reduced yields, although e.e. was unaffected.

In 1996 Yaozhong et al. reported their findings on the use of O-N-O ligands, similar to those used by Oguni et al. (figure 5.24), for trimethylsilylcyanation of benzaldehyde[30], investigating the effect of ligand to metal ratio on the enantioselectivity of the reaction.

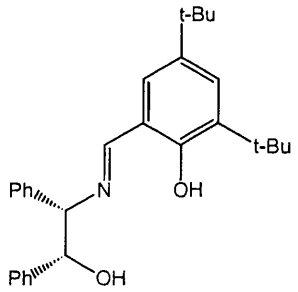

Figure 5.24: Yaozhong O-N-O ligand

[29] M. Hayashi, Y. Miyamoto, T. Inoue and N. Oguni, *Tetrahedron*, **50**, 4385 (1994)
[30] J. Yaozhong, Z. Xiangge, H. Wenhao, L. Zhi and M. Aiqiao, *Tetrahedron: Asymmetry*, **6**, 2915 (1995)

Studies concluded that increasing the relative amount of ligand increased the e.e. of the reaction. The results they obtained (figure 5.25) suggest that unlike the catalyst reported by Oguni the TiL_2 species of this ligand must be catalytically active. However, the reduction of the yield for the 2:1 species relative to the 1.5:1 may be due to the di-substituted species being less active.

Schiff base : Ti	Isolated Yield %	E.E. %
1.1 : 1	85.3	53.2
1.3 : 1	86.5	80.4
1.5 : 1	88.7	89.2
2 : 1	72.0	92.0

Figure 5.25: Effect of mole ratio of ligand on selectivity and yield

Because of the poor understanding of the titanium species involved in the work carried out by Oguni and Yaozhong, Braun et al. reported results in which they determined the solid-state structures of some O-N-O ligand complexes of titanium[31].

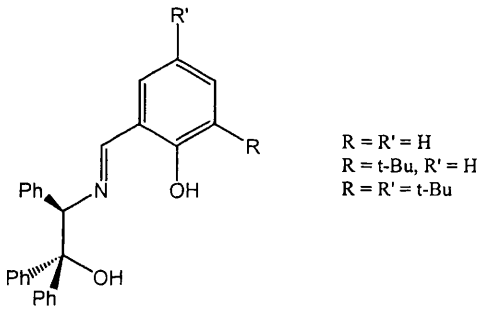

Figure 5.26: Ligands used for the structural study of O-N-O complexes

1:1 reactions of the ligands and the titanium species were carried out in situ and the products found to be the highly unstable monosubstituted products. These monosubstituted products, when isolated, decomposed even under inert conditions. In contrast the 2:1 reactions yielded the disubstituted products as expected and these were isolated and characterised and found to be much more stable. In addition Braun

[31] R. Fleischer, H. Wunderlich and M. Braun, *Eur. J. Org. Chem.*, 1063 (1998)

et al. discovered that these di-substituted products reacted with $Ti(Hal)_4$ (where Hal = F or Cl) by ligand scrambling to give relatively stable complexes with the formula $Ti(Hal)_2(L)$.

Isolation and structural characteristion of titanium complexes containing one O-N-O ligand was achieved by Rao et al. by use of a titanium acetylacetonate complex as a titanium source[32]. They reacted the ligands shown in figure 5.27 below with $Ti(acac)_2(O^iPr)_2$ in a 1:1 ratio to give complexes of the type $Ti(L)(acac)(O^iPr)$.

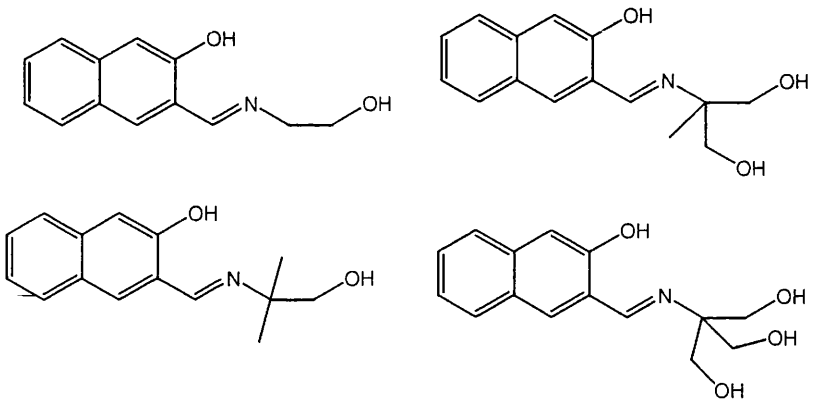

Figure 5.27: Ligands used by Rao et al.

These complexes were isolated and characterised by spectroscopic methods and an X-ray crystal structure obtained for one complex (figure 5.28). This increased stability of the mono-substituted product is probably due to the coordinative saturation of the product in contrast to the complexes described above formed from TiPT. However reactions of two equivalents of ligand with the titanium bis-acetylacetonate compound again formed the di-substituted products seen above.

[32] P.V. Rao, C.P. Rao, E.K. Wegelius, E. Kolehmainen and K. Rissanen, *J. Chem. Soc. Dalton Trans.*, 4469 (1999)

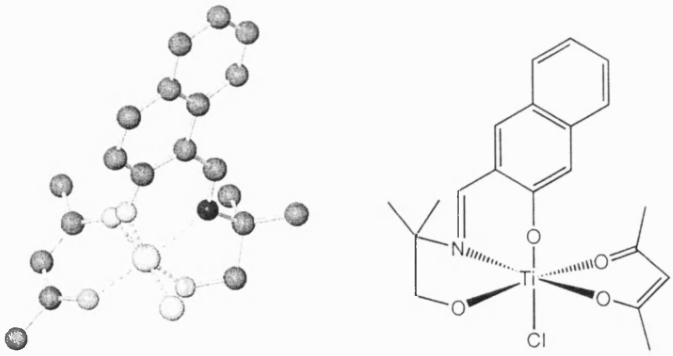

Figure 5.28: Crystallographically characterised mono O-N-O complex

More recently Somanathan et al. have used the ligands below to further improve the enantioselectivity of the trimethylsilylcyanation of benzaldehyde[33]. They showed that bulky substituents in the *ortho* position of the phenol ring (R group in figure 5.29 below) increased yield and e.e. As steric bulk here would inhibit di-substitution this result supports the proposal by Oguni et al. that the TiL_2 di-substituted species is inactive for the reaction

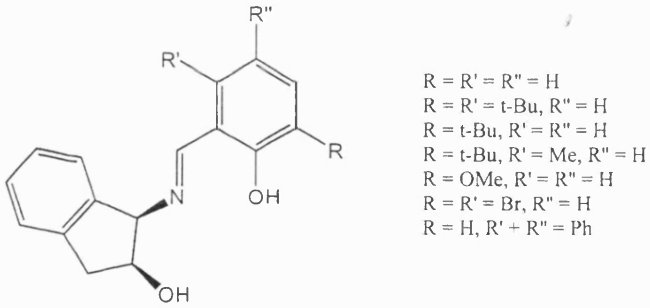

Figure 5.29: Somanathan's indanol based O-N-O ligands

Finally, Riant et al. have shown that chiral O-N-O ligand complexes are also active for the coupling of aldehydes to form pinacol products as shown by the reaction scheme in figure 5.30 overleaf[34].

[33] L.Z. Floria-Lopez, M. Parra-Hake, R. Somanathan and P.J. Walsh, *Organometallics*, **19**, 2153 (2000)
[34] A. Bensari, J.L. Renaud and O. Riant, *Org. Lett.*, **3**, 3863 (2001)

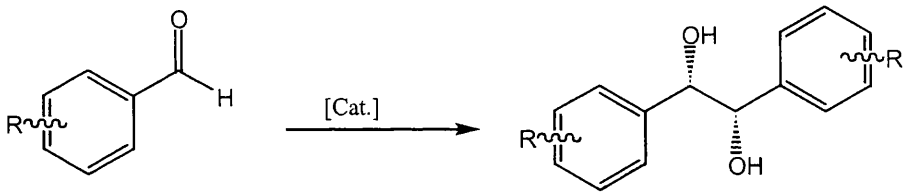

Figure 5.30: Pinacol coupling of aldehydes using a titanium O-N-O catalyst

5.1.3 Relevance to polyurethane synthesis

The introduction section to this chapter discusses the chemistry of just two families of polyanionic Schiff base ligands. These two families form only a small example of the range of products that can be considered part of this category of ligand.

The previous chapter covered an in depth structural study into one particular type of salicylaldimine ligand with the intention of observing the effect that small systematic changes to ligand structure would have on the resulting complex. By contrast the following section discusses a range of complexes from diverse, though related, ligand families with only one or two examples of each. The reason for studying such a broad range of ligands was to look at what effect the variation in functionality would have on the structure of the resulting titanium complexes. By varying the number, nature and orientation of the neutral and anionic donors in the ligands we hoped to be able to investigate the effect on polyurethane catalysis of the new structural types formed. In particular we were interested in varying the number of titanium centres per ligand and the ratio of reactive monodentate alkoxides to metal atoms in each complex.

It is important to note that the eight complexes we have synthesised which are described in this chapter are only a small sample of the vast range of ligands, which could be included in such a study, and in each case a systematic study of the kind described in chapter 4 could be carried out to optimise the properties of the complex.

5.2 Discussion of results

5.2.1 Ligands

This chapter covers the reactions of a wide range of ligands with TiPT. As a guide, the diagram below shows all the ligands discussed in this chapter.

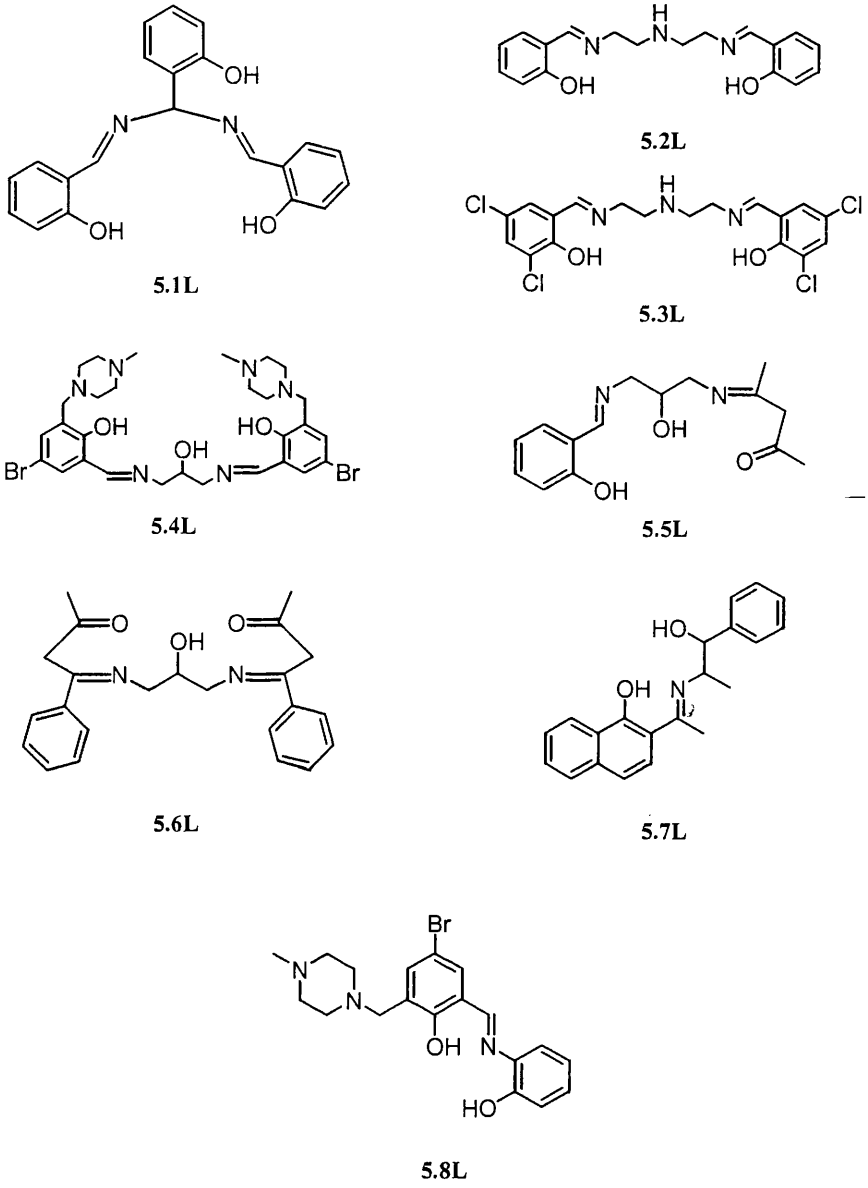

Figure 5.31: Ligands used in chapter 5

5.2.2 Complex 5.1: A monomeric bimetallic Ti complex

Ligand 5.1L reacts readily with two equivalents of TiPT to yield pale orange crystals suitable for single crystal X-ray analysis. The crystal structure contains one molecule of disordered toluene in the lattice and one complex in which the ligand 5.1L is triply deprotonated complexing two titanium centres which are bridged by one isopropoxide ligand and the central aryloxide of the 5.1L ligand. In addition each titanium centre has two terminal isopropoxide ligands and a chelating salicylaldimine ligand. In all six donors around each metal centre are arranged with a distorted octahedral arrangement at each titanium atom. The core of the molecule consists of a four-membered Ti_2O_2 ring and four six-membered rings formed by the salicylaldimine nitrogen, the bridging aryloxide and a titanium atom as shown in figure 5.32 below. The two aryloxide ligands are arranged trans to each other with the terminal isopropoxides arranged cis. If the imine and the isopropoxide trans to it are considered as being axial donors then the remaining four equatorial ligands bend slightly away from the axial isopropoxide ligand, with deviations of between 2 and 10° towards the imine nitrogen.

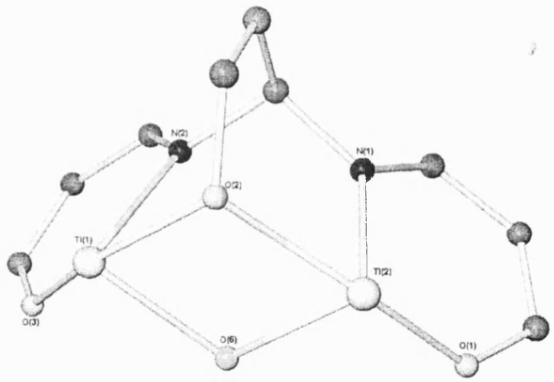

Figure 5.32: Central core of complex 5.1

The salicylaldimine aryloxide ligands have typical bond lengths for interactions of this type {1.907(2)Å [Ti(1)-O(3)] and 1.911(2)Å [Ti(2)-O(1)]} as does the bridging aryloxide {2.068(2)Å [Ti(1)-O(2)] and 2.052(2)Å [Ti(2)-O(2)]}. The bond lengths between the terminal isopropoxides and titanium depend on the trans donor, with the two ligands trans to imine nitrogen atoms having greater bond lengths {1.812(2)Å Ti(1)-O(7) and 1.827(2)Å Ti(2)-O(4)} than those trans to the bridging isopropoxide

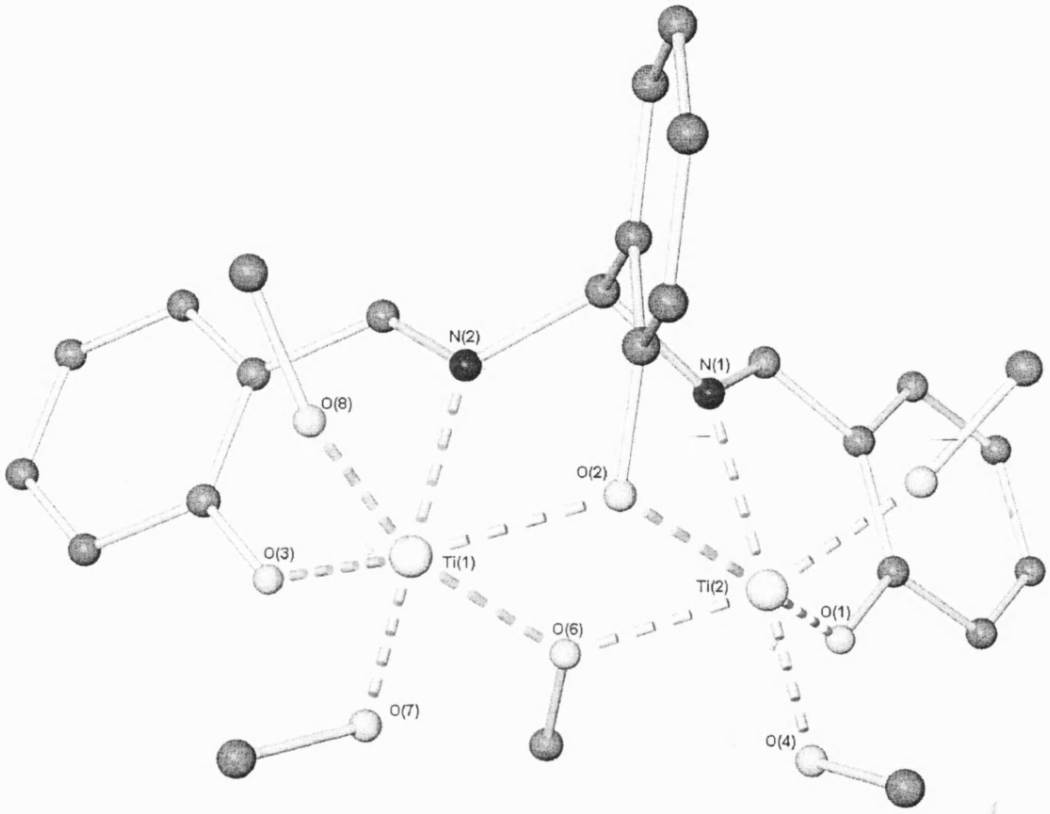

Figure 5.33: Molecular structure of complex 5.1 (hydrogen atoms and isopropoxide methyl groups not shown for clarity)

ligands {1.789(2)Å Ti(1)-O(8) and 1.794(2)Å Ti(2)-O(5)}. The bonds to the imine nitrogen atoms themselves are typical for these interactions {2.296(2)Å [Ti(1)-N(2)] and 2.277(2)Å [Ti(2)-N(1)]}.

The ^{1}H NMR spectrum of the complex suggests that the gross overall structure of 5.1 is maintained in solution with three distinct isopropoxide **CH** septet signals for the groups trans to the imine nitrogen (3.37ppm), bridging (4.76ppm) and trans to the bridging isopropoxide (5.18ppm). The ^{13}C NMR spectrum also confirms the retention of structure in solution with all the expected signals being present.

The bridging of two metals by ligand 5.1L is typical and is also observed in all other crystallographically isolated metal complexes of this ligand including those with iron(II and III)[35], manganese(II and III)[36] and vanadium(III)[37].

5.2.3 Complexes 5.2 and 5.3: Monomeric monometallic complexes involving spontaneous ligand rearrangement

Complex 5.2

Ligand 5.2 reacted readily with TiPT and on purification gave orange needle like crystals, which were suitable for single crystal X-ray diffraction. Examination of the resulting complex showed that on reaction with the metal the ligand had undergone a metal mediated rearrangement. The proposed mechanism for this rearrangement is shown in figure 5.34 overleaf.

The mechanism is proposed to proceed via initial formation of a bis-salicylaldimine complex, formation of which polarises the imine C=N bonds. One of these imine bonds is then subject to nucleophillic attack at carbon by the secondary amine in the ligand backbone to form a ring-closed zwitterionic transition state, followed by a proton transfer to form the product complex with a tertiary amine donor.

[35] B.S. Snyder, G.S. Patterson, A.J. Abrahamson and R.H. Holm, *J. Am. Chem. Soc.*, **111**, 5214 (1989)
[36] S.B. Yu, C.P. Wang, E.P. Day and R.H. Holm, *Inorg. Chem.*, **30**, 4067 (1991)
[37] P. Chaudhuri, M. Hess, T. Weyhermuller, E. Bill, H.J. Haupt and M. Florke, *Inorg. Chem. Commun.*, **1**, 39 (1998)

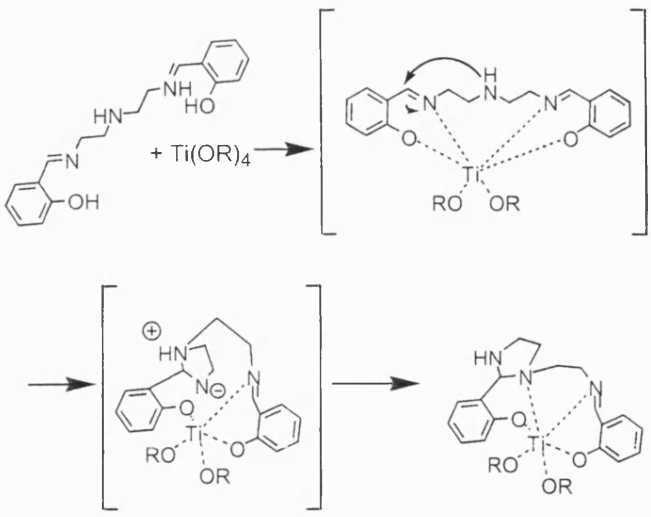

Figure 5.34: Ligand rearrangement of 5.2L

This sort of rearrangement is not unknown and has been previously observed during the reaction of macrocyclic salicylaldimine ligands containing the N-CH_2CH_2-NH-CH_2CH_2-N linker and iron[38] when only one metal centre is complexed. In contrast when these macrocyclic ligands complex two iron centres the ring closure does not occur and it seems likely that complexation to a single metal centre is required. The ring closure results in the formation of a chiral centre at C(7) although the product we have synthesised is racemic.

The titanium centre in the complex is chelated by the new ring closed $5.2L^{rc}$ ligand with two aryloxide donors, one imine donor and a tertiary amino donor. In addition the titanium atom also retains two isopropoxide ligands. The two aryloxide ligands have a mutually cis configuration, as do the two alkoxides and the two nitrogen donors (configuration C in figure 4.5). As described in the previous chapter the most favourable geometry for an octahedral complex has trans-axial phenolic ligands with cis-equatorial nitrogen donors and monodentate alkoxide ligands (configuration A in figure 4.5). The unfavourable geometry around the titanium centre in complex 5.2 is enforced by the constraints of the ligand. The titanium centre has a distorted octahedral configuration and if the imine and the isopropoxide trans to it are

[38] H. Firutachi, A. Ishida, H. Miyasaka, N. Fukita, M. Ohba, H. Okawa and M. Koikawa, *J. Chem. Soc. Dalton Trans.*, 367 (1999)

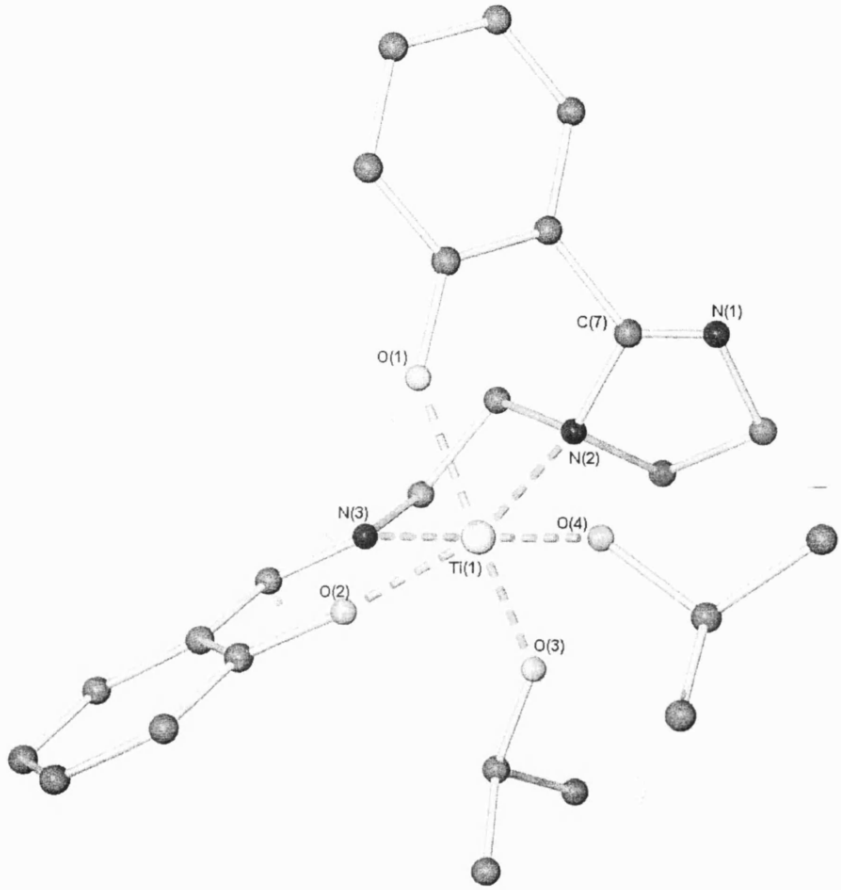

Figure 5.35: Molecular structure of complex 5.2 (hydrogen atoms not shown for clarity)

considered as the axial ligands then the other four, equatorial, ligands can be seen to bend slightly away from the isopropoxide and towards the imine nitrogen (2-5°).

The titanium to aryloxide bond lengths show the effect of the trans ligands with the bond to the ligand trans to the amine {1.900(3)Å [Ti(1)-O(2)]} being shorter than the bond to the ligand trans to the isopropoxide {1.9619(3)Å [Ti(1)-O(1)]}. In contrast no significant trans effect is observed in the bonds between the titanium centre and the two isopropoxide ligands which are identical within error {1.830(4)Å [Ti(1)-O(4)] and 1.835(3)Å [Ti(1)-O(3)]}. The bond lengths to the two nitrogen ligands are also quite similar to that to the amine {2.241(4) [Ti(1)-N(2)]} being slightly longer than that to the imine {2.199(4) [Ti(1)-N(3)]}. All of the ligand-titanium bond lengths in the complex are within the expected ranges when compared to similar interactions in other complexes in this thesis.

The ^{1}H and ^{13}C NMR spectra for the complex suggest that the gross solid-state structure is maintained in solution with two distinct septet signals for the isopropoxide C**H** groups of the ligand trans to the imine and trans to the aryloxide (4.28ppm and 5.00ppm). In addition the potentially chiral C(7)-**H** proton gives a doublet signal (3.99ppm) probably due to coupling to the N(1)-**H** proton although the signal for this proton is not observed.

Although this is the first example of a titanium complex containing a ligand of this type it is somewhat reminiscent of the constrained 'salen' complex synthesised by Moore et al.[26] (Figure 5.19). As with that complex the constraints of the ligand force a cis arrangement of the reactive monodentate ligands, a prerequisite for polyolefin catalysis. In addition, if it is possible to separate the two enantiomers, which are formed during the reaction, then complexes of this type may be useful asymmetric catalysts providing that the ring closing equilibrium is controllable and does not promote racemisation in solution.

Complex 5.3

Ligand 5.3L is a direct analogue of 5.2L but prepared with 2,4-dichloro salicylaldehyde. As with complex 5.2 the ligand undergoes a metal mediated ring closure on reaction with TiPT to give an octahedral titanium centre chelated by one

$5.3L^{rc}$ via its two aryloxide groups, a tertiary amino group and an imine nitrogen atom, in addition the titanium centre retains two isopropoxide ligands.

The geometry around the titanium centre is distorted octahedral with the same mutually cis arrangement of aryloxides, alkoxides and nitrogen donors seen in complex 5.2. As with 5.2 if the imine and the isopropoxide trans to it are considered as the axial ligands then the other four ligands bend away from the isopropoxide towards the imine causing a distortion (0-10°), which is larger in magnitude than that seen in 5.2. The bond lengths around the titanium centre are all within the expected ranges for the interactions seen. The aryloxide to titanium bonds exhibit a trans influence with the bond trans to the isopropoxide {1.967(1)Å [Ti(1)-O(1)]} being longer than that trans to the amine {1.920(1)Å [Ti(1)-O(2)]} as observed in 5.2. As with 5.2 the bond lengths to the isopropoxide ligands show no significant difference due to the effect of the trans ligands, with similar bond lengths for both the ligand trans to the aryloxide {1.818(1)Å [Ti(1)-O(3)]} and the ligand trans to the imine {1.812(1)Å [Ti(1)-O(4)]}. The nitrogen donors have Ti-N bond lengths all within the expected ranges {2.299(2)Å [Ti(1)-N(2)] and 2.226(2)Å [Ti(1)-N(3)]}. When the metal to ligand bond lengths for 5.3 are compared to those of the analogous compound 5.2 some trends can be observed which may be due to the presence of the chloro groups on the aryloxides. The aryloxides have slightly longer bonds to titanium in the chlorinated ligand complex, particularly the salicylaldimine aryloxide, which has a bond length, which is extended by 0.02Å when compared to the equivalent bond in 5.2. In addition both nitrogen donors also have extended bond lengths in the chlorinated ligand complex with the greatest effect being observed in the bond to the tertiary amine group, which is 0.09Å longer than in 5.2. These effects could be due to the chloro groups on the aryloxides, which pull electron density from the donor atoms causing the $5.3L^{rc}$ ligand to be more weakly bound than $5.2L^{rc}$.

The ^{1}H and ^{13}C NMR spectra of the complex suggest that the gross solid-state structure is maintained in solution with distinct septet signals for the C**H** protons of the isopropoxide ligands at 4.38ppm and 4.97ppm and a signal for the potentially chiral C(7) proton at 3.99ppm. The NMR spectra of 5.3 show no significant difference to those of 5.2 with the chemical shifts being almost identical.

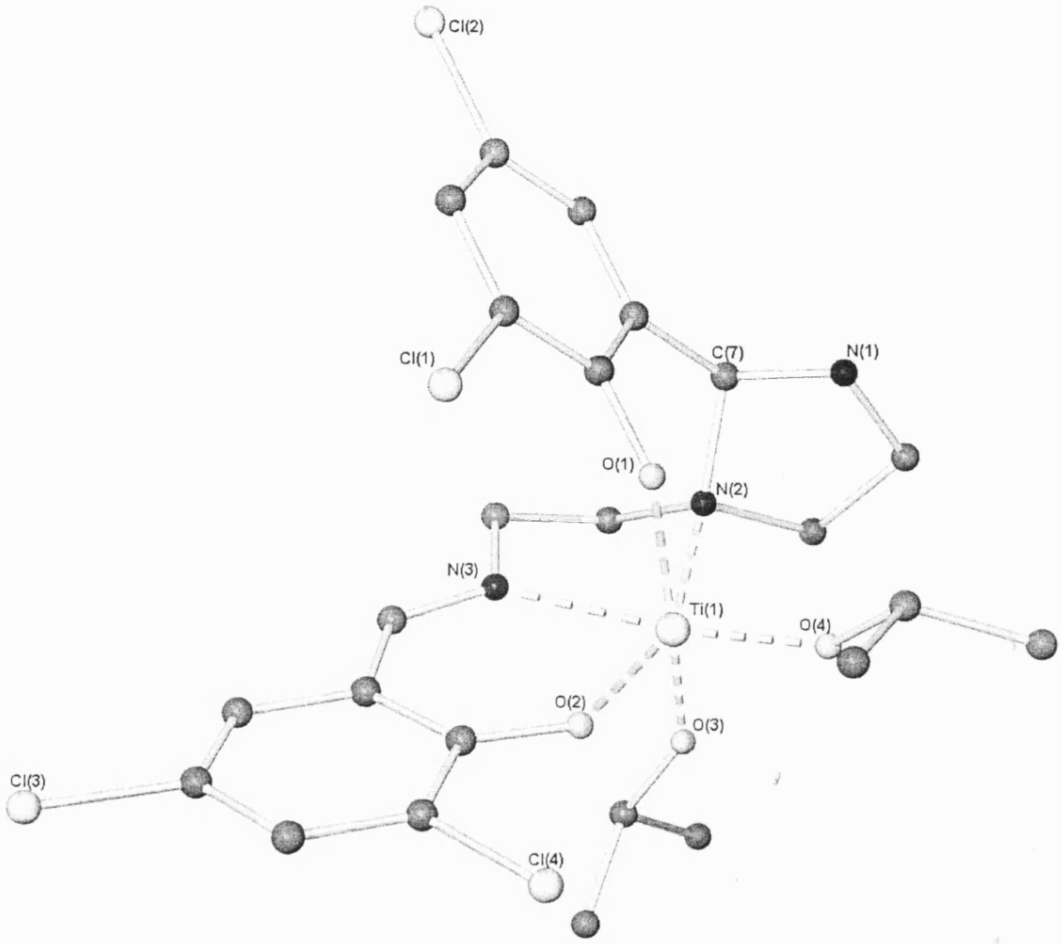

Figure 5.36: Molecular structure of complex 5.3 (hydrogen atoms not shown for clarity)

5.2.4 Complexes 5.4-5.6: Monomeric, monometallic complexes with one reactive alkoxide

Complex 5.4

Ligand 5.4L reacted readily with TiPT to give a crystalline product, the crystals were however extremely thin plates unsuitable for single-crystal X-ray diffraction. However, NMR studies of the product showed that the ligand was triply deprotonated and had an empirical formula of Ti(5.4L)(OR). This empirical formula of the complex can be deduced by the ratio of isopropoxide C**H** protons (4.79ppm) to imine C**H** protons (8.06ppm), which is 1:2 suggesting two possible complex structures as shown in figure 5.37 below.

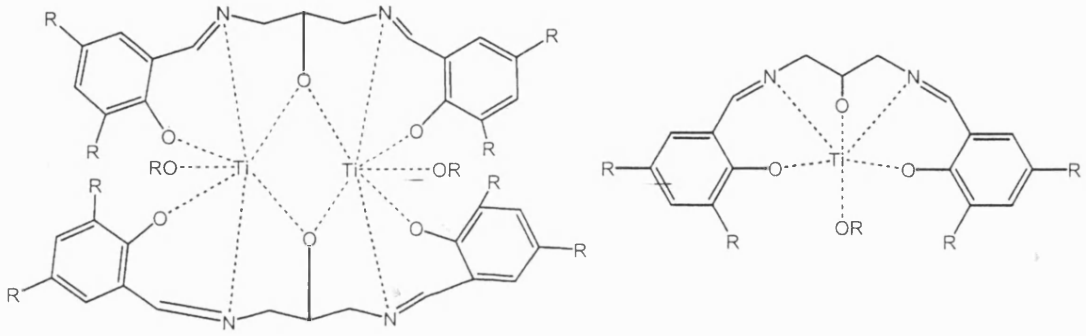

Figure 5.37: Possible structures for complex 5.4

The first structural type is known in the solid-state for other metals such as manganese and iron[39] while the second has only been reported once before as part of a macrocyclic complex of lead[40]. However, a major advantage of the second structure is that it affords the titanium centre its preferred octahedral geometry unlike the first one, which requires a seven coordinate titanium centre.

The ^{1}H NMR spectrum shows that on complexation the signals for the protons on the isopropyl backbone of 5.4L are split and the sharp peaks for each of the sets of protons on this backbone show that the ligand-metal complex is stable in solution

[39] H. Aneetha, K. Panneerselvam, T.F. Liao, T.H. Lu and C.S. Chung, *J. Chem. Soc. Dalton Trans.*, 2689 (1999); A. Gelasco and V.L. Pecorano, *J. Am. Chem. Soc.*, **115**, 7928 (1993); M.L. Kirk, J.W. Kampf, A. Gelasco and V.L. Pecorano, *Inorg. Chem.*, **36**, 1829 (1997); J.A. Bonadies, M.L. Kirk, M.S. Lah, D.P. Kessissoblou, W.E. Hatfield and V.L. Pecorano, *Inorg. Chem.*, **28**, 2037 (1989); M. Mikuriya, Y. Yamato and T. Tokii, *Bull. Chem. Soc. Jpn.*, **65**, 1466 (1992)

[40] S.S. Tandon and V.K. Mckee, *J. Chem. Soc. Dalton Trans.*, 19 (1989)

with the two protons in the methylene groups of this backbone being inequivalent. In addition the methylene protons on the linker to the piperazine group are also split diastereotopically, which is possibly evidence for the complexation of the titanium centre by the piperazine nitrogen atoms although more likely it arises from a restricted rotation around this bond in the complex causing the protons to become inequivalent (see discussion of complex 6.5 p.222).

Complex 5.5

Ligand 5.5L, which is based on the same diamino isopropanol backbone as 5.4L, also reacts readily with TiPT to yield a microcrystalline product which is unsuitable for single crystal X-ray analysis.

As with 5.4 the ^{1}H NMR spectrum suggests a complex with the empirical formula Ti(5.5L)(OR) due to the ratio of isopropyl C**H** protons (4.86ppm) to imine C**H** protons (8.19ppm) being 1:2. On complexation, the protons in the isopropyl backbone are split with a signal for each of the five protons in the unsymmetrical ligand. The suggested structures for the complex are shown in figure 5.38 below and the ^{1}H NMR evidence, particularly the sharp, coupled signals for the isopropyl ligand backbone, suggests that the gross structure is maintained in solution.

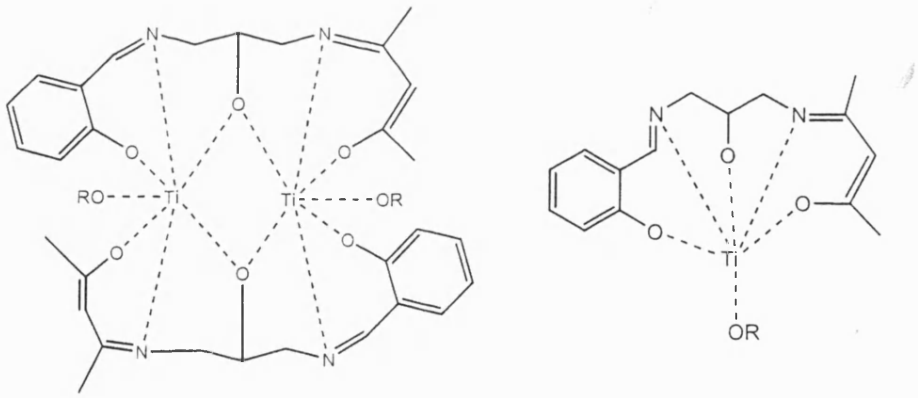

Figure 5.38: Suggested structures for complex 5.5

Complex 5.6

The impure ligand 5.6L reacted readily with TiPT to give a crop of crystals, which were suitable for single crystal X-ray diffraction. The structure shows a complex with

the empirical formula seen for 5.4 and 5.5 consisting of one titanium atom chelated by the triply deprotonated ligand 5.6L and retaining one isopropoxide ligand. During the following discussion the chelating arms formed by the mono imino derivative of an acetylacetonate will be referred to as 'nacac' ligands. The titanium centre has a highly distorted octahedral geometry with the angle between the oxygen atoms on the two 'nacac' chelate arms {O(1) and O(3)} and titanium being very open {112.83(8)°} due to the geometrical constraints of the ligand.

The bond lengths between the ligand groups and titanium are generally typical for these types of interactions. The monodentate isopropoxide bond length to titanium {1.798(2)Å [Ti(1)-O(4)]} is significantly shorter than that from the ligand alkoxide to the titanium centre {1.902(2)Å [Ti(1)-O(2)]} which is actually 0.1Å longer than the upper end of the average range for isopropoxide ligands, probably due to the constraints caused by the chelation of the ligand 5.6L. The bonds between the two oxygen atoms of the chelating 'nacac' arms of the ligands and titanium show slight effects due to the trans ligand with the bond trans to the ligand isopropoxide group {1.953(1)Å [Ti(1)-O(3)]} being slightly longer than that trans to a nitrogen donor. {1.931(1)Å [Ti(1)-O(1)]}. The titanium-nitrogen bonds also show a slight effect with the ligand trans to the monodentate isopropoxide ligand {2.174(2)Å [Ti(1)-N(1)]} having a shorter bond length than that trans to a ligand nacac oxygen {2.195(2)Å [Ti(1)-N(2)]}.

The crystal structure of 5.6 can be seen as evidence that ligands of this type, with two chelating groups linked by the 1,3-diamino-isopropanol unit, can wrap around a single titanium centre. This is valuable evidence in assigning the structures of complexes 5.4 and 5.5 and suggests that they too could have this Ti(L)(OR) structure rather than the bimetallic structures shown in figures 5.37 and 5.38.

Although some titanium complexes containing 'nacac' ligands have been reported in the past[41], 5.6 is the first titanium 'nacac' complex with an ancillary alkoxide to be

[41] A.A. Diamantis, M. Manikas, M.A. Salam, M.R. Snow and E.R.T. Tielnik, *Aust. J. Chem.*, **41**, 453 (1988); S. Doherty, R.J. Errington, N. Housley, J. Ridland, W. Clegg and R.J. Elsegood, *Organometallics*, **18**, 1018 (1999); J.M. Rosset, C. Floriani, M. Mazzanti, A. Chiesi-Villa ad C. Guastini, *Inorg. Chem.*, **29**, 3991 (1990); L. Kakaliou, W.J. Scanlon, B. Qian, S.W. Baek, M.R. Smith

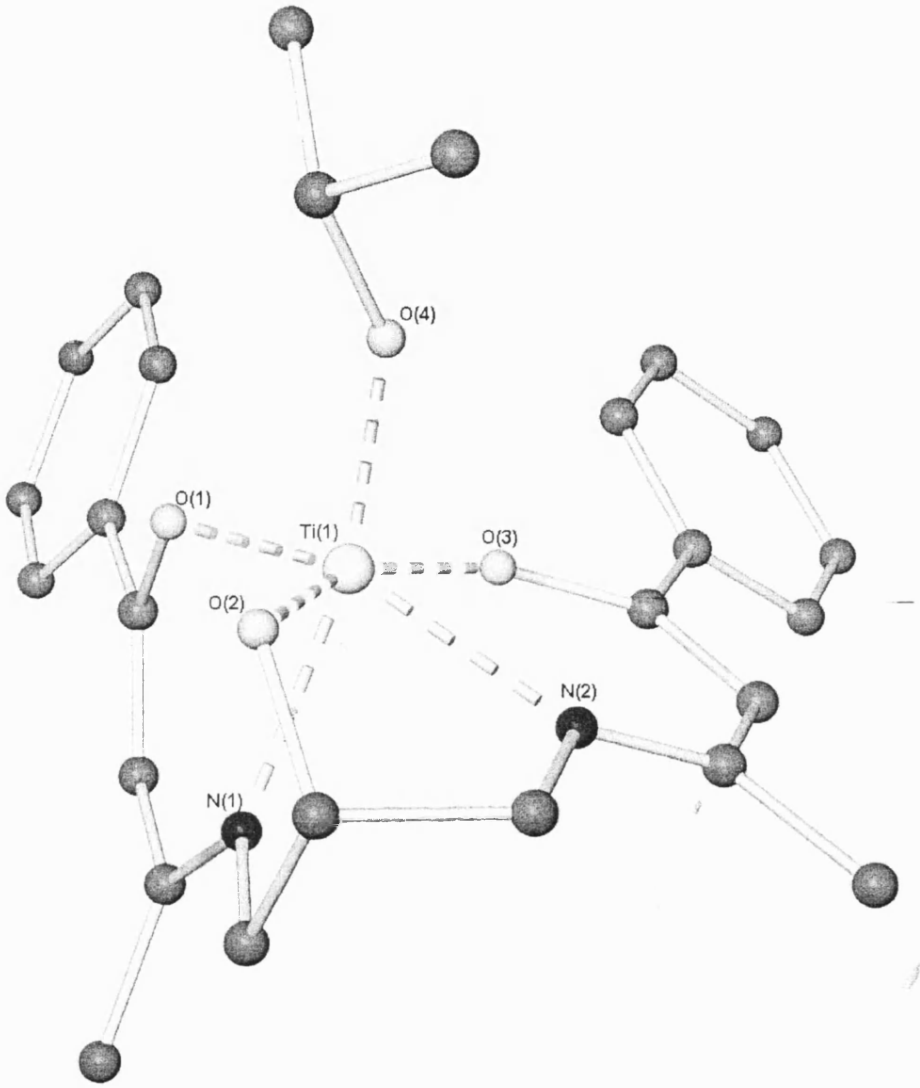

Figure 5.39: Molecular structure of complex 5.6 (hydrogen atoms not shown for clarity)

---

and D.H. Motry, *Inorg. Chem.*, **38**, 5964 (1999); F. Franeschi, E. Gallo, E. Solari, C. Floriani, A. Chiesi-Villa, C. Rizzoli, N. Re and A. Sgammellotti, *Chem.-Eur. J.*, **2**, 1466 (1996).

crystallographically isolated and also the first crystallographically defined metal complex containing the ligand 5.6L or any ligand with two N-O chelate pairs linked by the 1,3-diamino-isopropoxide linker.

The ^{1}H NMR spectrum of complex 5.6 suggests retention of the gross solid-state structure in solution with signals due to both 5.6L and the single isopropoxide ligand (a septet at 4.82ppm for the isopropyl C**H**). As with complexes 5.4 and 5.5 the protons of the isopropyl backbone are split due to complexation of the ligand and coupling is seen between the two pairs of non-equivalent methylene protons. The sharp, distinct, coupled peaks for these protons show that the complex is stable in solution.

5.2.5 Complexes 5.7-5.8: Complexes of O-N-O ligands

Complex 5.7

Ligand 5.7L reacts readily with TiPT to yield a product, which is crystalline below 0°C, but becomes amorphous on warming to room temperature and therefore was not suitable for X-ray diffraction. The ligand is an analogue of the chiral O-N-O ligands described in the introduction to this chapter. As with the known O-N-O ligands on reaction of one equivalent of 5.7L with one equivalent of TiPT the 2L:1Ti complex is the only isolated product in the solid-state as shown by the ^{1}H NMR spectrum of the recovered product which shows no signals for isopropoxide groups. Presumably the 2L:1Ti product is formed in preference to the 1L:1Ti due to the desire of the titanium centre for an octahedral geometry and the absence of steric constraint imposed by the ligand. The steric bulk of the ligand is not sufficient to make the formation of the 2L:1Ti product unfavourable and an increase in steric bulk will be necessary to isolate products with the 1L:1Ti form.

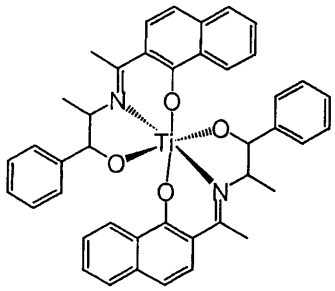

Figure 5.40: The proposed structure of complex 5.7

Complex 5.8

Ligand 5.8L is an achiral analogue of the O-N-O ligands, of which 5.7L is an example, but with a greatly increased steric bulk at the carbon atom *ortho* to the phenol group. The ligand reacts readily with TiPT to give a crop of deep red crystals, which are suitable for single crystal X-ray diffraction.

The crystal structure shows that the ligand has reacted with TiPT in a 1:1 fashion and that two of the resulting $Ti(5.8L)(OR)_2$ fragments come together to form a dimer bridged by two isopropoxide ligands. This dimer formation allows the titanium centre to achieve the favoured octahedral geometry at titanium. The asymmetric unit of the crystal structure consists of half of this dimer.

The two aryloxide groups and the imine nitrogen of one of the 5.8L ligands chelate each of the titanium centres. In addition two bridging and one terminal isopropoxide groups also ligate each titanium centre. The geometry at the titanium centres is distorted octahedral with trans-axial aryloxide ligands, cis-equatorial bridging alkoxides and the remaining two ligands also cis-equatorial. The chelating O-N-O part of ligand 5.8L, consisting of the two phenyl groups and the imine, is almost planar. The piperazine group on 5.8L plays no part in bonding to the metal centre and also no hydrogen bonding interactions can be observed in the crystal lattice.

The bond lengths between the aryloxide ligands and titanium fall in the expected range and are also very similar to each other {1.907(3)Å [Ti(1)-O(1)] and 1.931(3)Å [Ti(1)-O(2)]}. The imine to titanium and terminal isopropoxide to titanium bond lengths are also typical {2.218(3)Å [Ti(1)-N(5)] and 1.766(3)Å [Ti(1)-O(3)]}. The bridging isopropoxide has two inequivalent bond lengths with one being significantly longer than the other {1.922(3) [Ti(1)-O(4)] and 2.123(3) [Ti(1)-O(4#)]} this is typical in bridging ligands of this type although the large difference in this complex may suggest that the dimer is rather weakly bonded together. This observation, that the dimer is only weakly bonded together, is borne out by the ^{1}H and ^{13}C NMR spectra, which show only one signal for the isopropoxide groups on the titanium centre (a broad singlet at 4.62ppm in the ^{1}H NMR and a single signal at 80.3ppm in the ^{13}C).

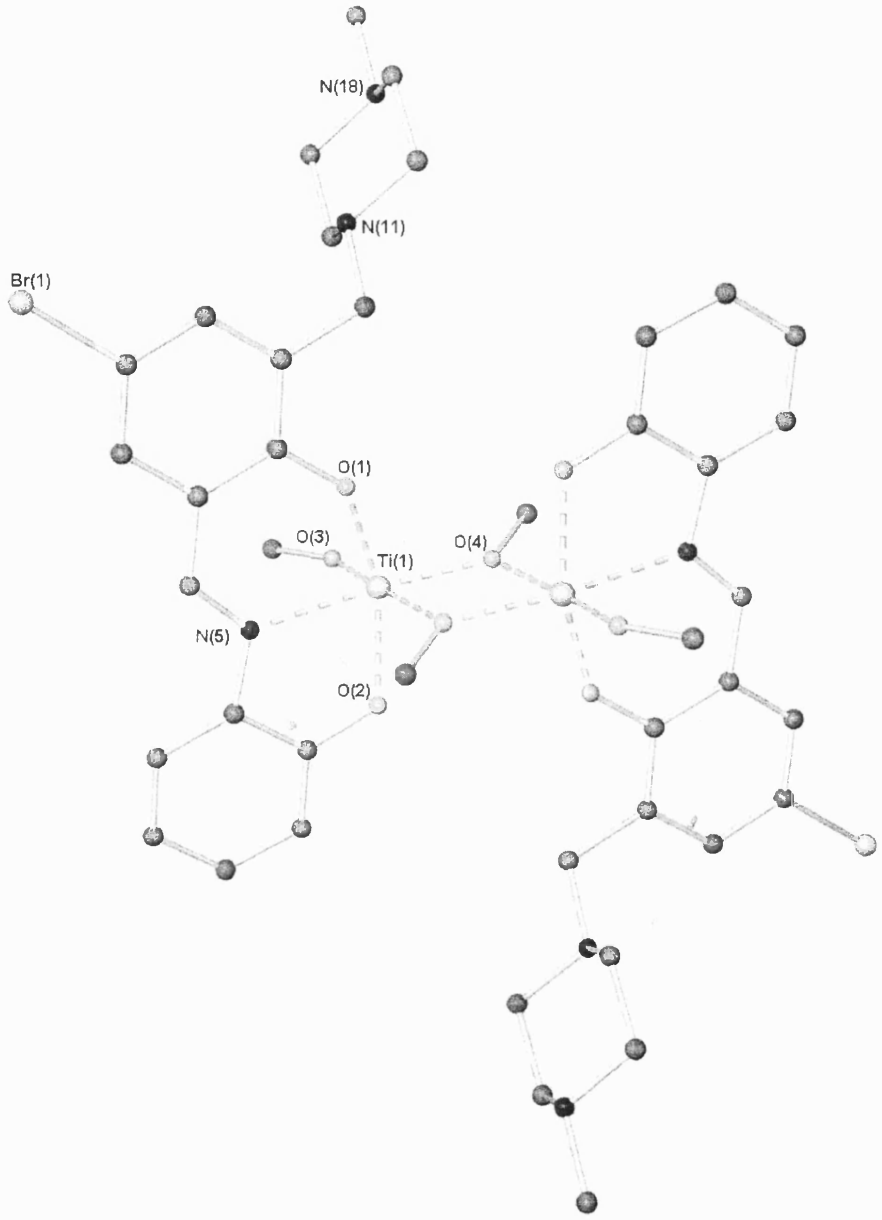

Figure 5.41: Molecular structure of complex 5.8 (hydrogen atoms not shown for clarity)

This means that on the NMR timescale in solution all the isopropoxide groups are equivalent and that one of two processes is occurring. The two possibilities are rapid exchange of bridging and terminal isopropoxide groups with no loss of the overall dimeric structure or a monomer/dimer equilibrium as shown in figure 5.42 below.

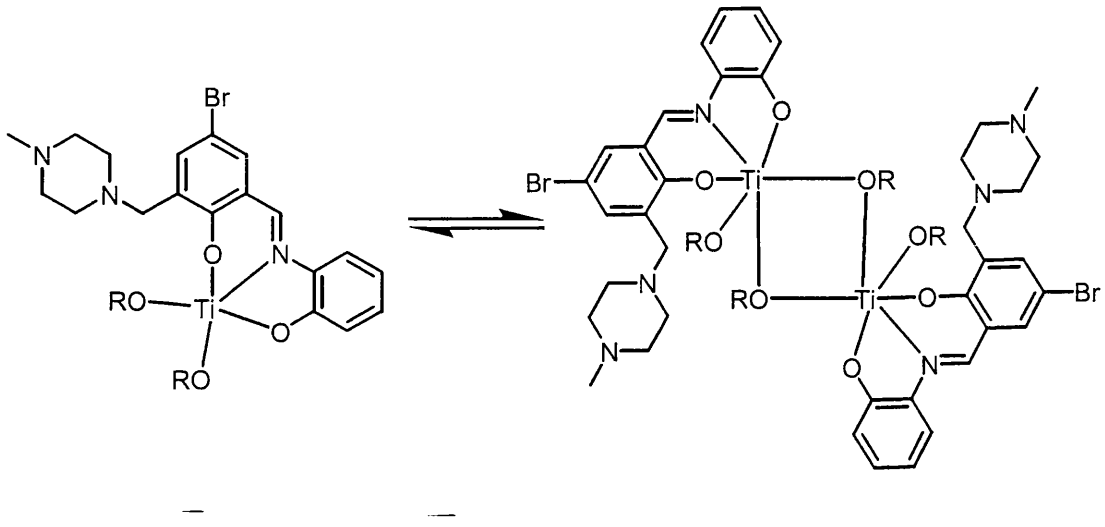

Figure 5.42: Possible solution equilibrium of complex 5.8

Complex 5.8 is the first example of a titanium alkoxide complex of an O-N-O ligand which has been isolated in the 1Ti:1L form and this is believed to be due to the increased steric bulk of the ligand caused by the use of the piperazine groups. These piperazine groups, which play no part in coordination to the metal centre, make the formation of the usual 1Ti:2L complex highly disfavoured and lead to the formation of the weak dimer seen above.

5.2.6 Summary of complexes 5.1-5.8

In complexes 5.1-5.8 we have looked at a wide range of ligand types based on Schiff bases, and, with one exception, on salicylaldimines, which have two or more anionic donor groups. The complexes of these ligands have a range of structural properties and vary in the numbers of titanium atoms and monodentate alkoxides they contain.

In the cases of complexes 5.1-5.6 the complexes discussed are the first examples of titanium complexes with ligands of these types and as such could form the basis for

more detailed study of the structural properties of titanium complexes with these ligands.

We have described the first examples of the metal mediated ligand rearrangement seen in complexes 5.2 and 5.3 with titanium and shown that this reaction occurs for complexes with differing substituents on the salicylaldimine phenyl ring.

In addition we have investigated a new family of ligands based on the 1,3-diamino-isopropanol backbone which yield complexes with only one reactive monodentate alkoxide per titanium centre. These complexes seem to form the same structure independently of the anionic Schiff base donor employed and could be useful in a study of the effect of anionic donor type on polyurethane synthesis.

Finally we have reported the first example of a structurally characterised 1:1 Ti:O-N-O ligand complex through increasing the steric demand of the ligand. If chiral analogues of this complex were isolated they could prove to be effective catalysts for some of the organic transformations described in the introduction to this chapter.

Chapter 6

The Synthesis, Isolation and Structural Characterisation of Titanium Isopropoxide Complexes of Hydrazones, Azines and Oximes

The following chapter discusses the synthesis and structural chemistry of the titanium complexes of three families of ligands closely related to the Schiff bases, the oximes, hydrazones and azines. These ligands are synthesised in a similar way to the Schiff bases in that they are produced by a condensation reaction between an aldehyde and a primary amine.

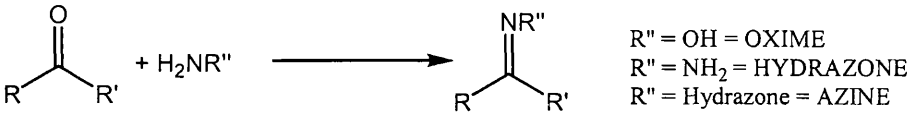

Figure 6.1: Synthesis of oximes, hydrazones and azines

In the case of the oximes and the hydrazones this results in the addition of a second protic group in the ligand, whereas for the azines it results in the linking of two functional groups through a N-N bond as shown in figure 6.2 below.

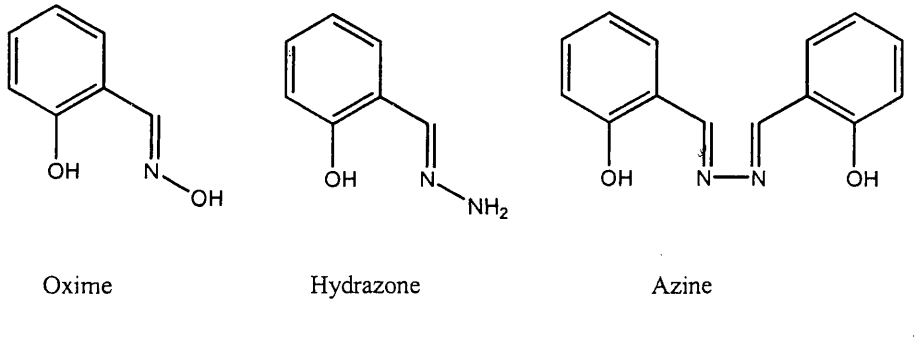

Oxime Hydrazone Azine

Figure 6.2: Examples of an oxime, a hydrazone and an azine

The following chapter begins with a brief description of the chemistry of these classes of compounds with titanium before a discussion of the solution and solid-state structures of a number of compounds of this type, which we have synthesised.

6.1 Introduction

6.1.1 Hydrazones

Hydrazones are formed by the condensation reaction of aldehydes and ketones with hydrazine[1] and for the purposes of this thesis we will only consider those formed from salicylaldehyde derivatives as shown in figure 6.3 below.

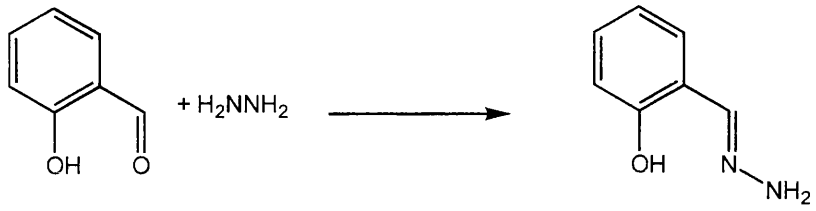

Figure 6.3: Synthesis of a salicylaldehyde hydrazone

Salicylaldehyde hydrazones have been studied very little as ligands and only one crystal structure of a transition metal complex has been reported, with vanadium[2]. Some early work was carried out in the 1970s and the early 1980s on the reactivity of these ligands with titanium species but the products are poorly characterised and few structural conclusions are reached[3].

6.1.2 Azines

Azines are formed by the condensation reaction between a salicylaldehyde hydrazone and a second equivalent of salicylaldehyde[1].

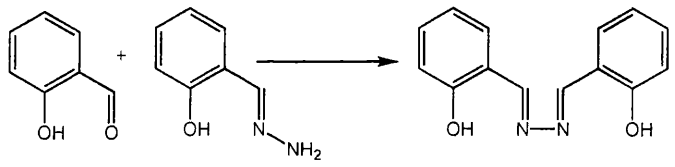

Figure 6.4: Synthesis of an azine

[1] B. Khera, A.K. Sharma and N.K. Kaushik, *Bull. Chem. Soc. Jpn.*, **58**, 793 (1985).
[2] D.L. Hughes, G.J. Leigh and J.R. Sanders, *J. Chem. Soc. Dalton Trans.*, 3235 (1990)
[3] S.A. Pardy, S. Gopinathan and C. Gopinathan, *Synth. React. Inorg. Met.-Org. Chem.*, **13**, 385 (1983);); B. Khera, A.K. Sharma and N.K. Kaushik, *Indian J. Chem. (A)*, **25**, 865 (1986)

As with the hydrazones these ligands have not been very widely studied and only six metal complexes (with Co, Cu, Fe, Rh, Ru and Zn) have been characterised by single crystal X-ray diffraction[4]. In all of these complexes the azine bridged between two metal atoms, with two complexes having a trans configuration for the azine and four having a cis configuration.

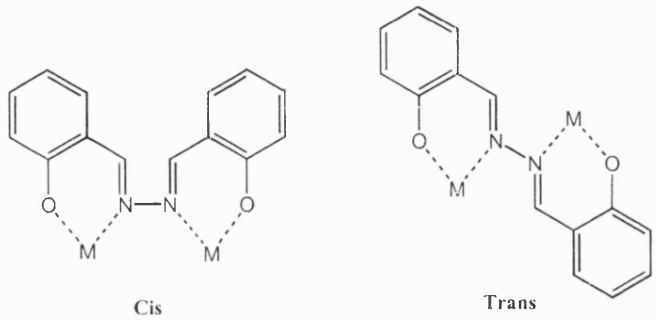

Figure 6.5: Two bonding modes for a metal azine complex

As with both the oximes and the hydrazones some work was carried out on the complexes of these ligands with titanium but this work has few conclusions on the structure of the products[5,1].

6.1.3 Oximes

Oximes are well known compounds synthesised by the reaction of an aldehyde or ketone with hydroxylamine as shown in figure 6.1 above[6]. They have been widely used in coordination chemistry although the reactivity of titanium systems is poorly studied.

---

[4] S. Gopinathan, S.A. Pardhy, C. Gopinathan, V.G. Puranik, S.S. Tavale and T.N.G. Row, *Inorg. Chim. Acta*, **111**, 133 (1986); R.C. Aggarwal, N.K. Singh and R.P. Singh, *J. Ind. Chem. Soc.*, **63**, 466 (1986); J. Saroia, V. Manivannan, P. Chakrabarty and S. Pal, *Inorg. Chem.*, **34**, 3099 (1995); M. Mikiyura and M. Fukuya, *Chem. Lett.*, 421 (1998); S. Pal and S. Pal, *Inorg. Chem.*, **40**, 4807 (2001)

[5] R.K. Sharma and J.P. Tandon, *J. Prakt. Chem.*, **322**, 161 (1980); S. Gopinathan, S.A. Pardhy and C. Gopinathan, *Indian J. Chem. (A)*, **22**, 73 (1983);

[6] S. Dayagi and Y. Degani in '*The Chemistry Of The Carbon Nitrogen Double Bond*', Ed. S. Patai, Interscience, New York, 61 (1970)

Although there were a number of reports of reactions of various oximes with titanium species in the 1970s and early 1980s the products are poorly characterised and few conclusions are reached about the structure of the products[7].

More recently there has been some work reported by Thewalt et al. on the reactivity of di- and monoximes with Cp_2TiCl_2 in water using NaOH which give complexes with each oxime group bonded to a single metal centre through its nitrogen and oxygen donor atoms. In all six titanium oximate single crystal structures were reported in this paper and an example with the formula $[(\eta^5\text{-}C_5H_5)_4Ti_2(H_2O)_2(\text{oximato})]^{2+}X^{2-}$ is shown in figure 6.6 below[8].

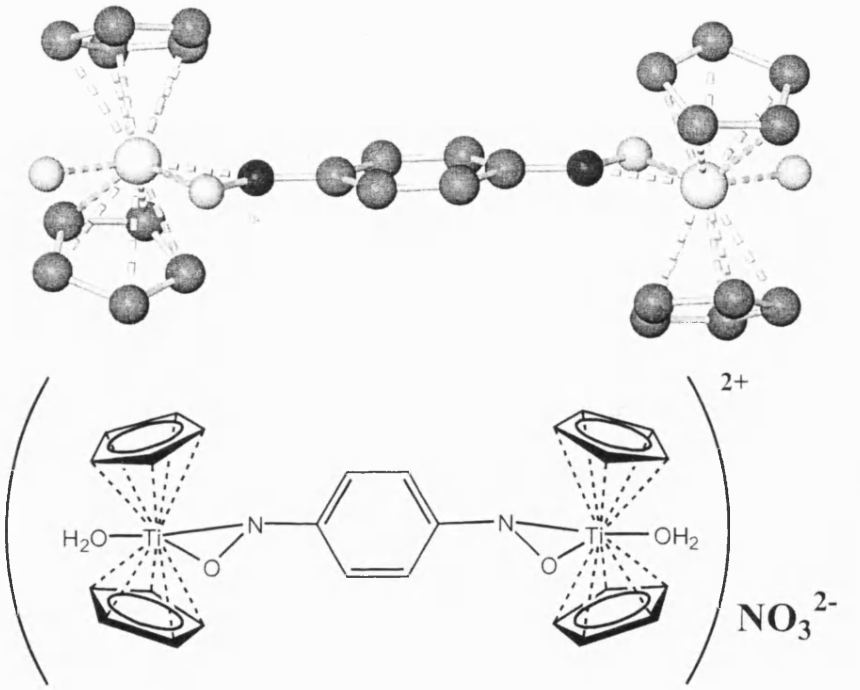

Figure 6.6: Thewalt dioxime complex

Figure 6.6 shows the molecular structure of the complex with a dioxime bridging two cationic titanium centres; the nitrate counterions are not shown for clarity.

---

[7] S. Mandal and A.K. Dey, *J. Inorg. Nucl. Chem.*, **30**, 1221 (1968); J. Charalambous and M.J. Frazer, *J. Chem. Soc. (A)*, 2361 (1968); A. Singh, C.K. Sharma, A.K. Rai, V.D. Gupta and R.C. Mehrotra, *J. Chem. Soc. (A)*, 2440 (1971); A. Singh, A.K. Rai and R.C. Mehrotra, *Indian J. Chem.*, **12**, 512 (1974); L. Nigam, V.D. Gupta and R.C. Mehrotra, *Indian J. Chem. (A)*, **20**, 61 (1981)

[8] U. Thewalt and R. Friedrich, *Z. Naturforsch*, **46b**, 475 (1991)

6.1.4 Relevance to polyurethane synthesis

The low number of reports in the literature describing the coordination chemistry of hydrazones, azines and oximes, discussed above, with titanium led us to feel that they presented an opportunity to synthesise a range of new pre-catalyst species. We felt that the differing functionalities represented in the three ligand types should allow us to synthesise a range of structural types with varied properties, which could then be utilised in catalysis. These opportunities potentially included the formation of titanium cluster complexes, the utilisation of unreacted Lewis acid/base groups to form mixed metal complexes or to complex substrates and the formation of supramolecular arrays through hydrogen bonding and other weak interactions in the solid-state.

The following section describes the synthesis and characterisation of a number of complexes of these ligand types with TiPT. The solution and solid-state properties of the complexes are described followed by a discussion of the conclusions we have reached.

6.2 Ligands

This chapter covers the reactions of a range of ligands, related to the Schiff bases, with additional functionality at the imine nitrogen atom. The ligands used are split into the three families described in the introduction: the hydrazones, azines and oximes. Figure 6.7 below shows all the ligands discussed in this chapter.

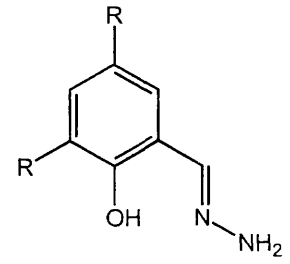

6.1L: R = H
6.2L: R = t-Bu

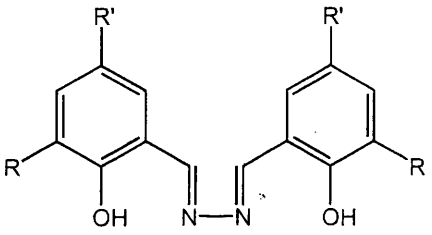

6.3L: R = t-Bu, R' = t-Bu
6.4L: R = OMe, R' = H
6.5L: R = CH_2-(Methylpiperazine), R' = Br

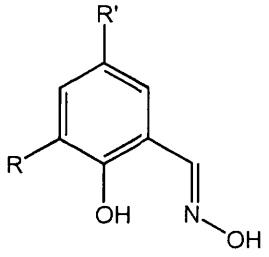

6.6L: R = H, R' = H
6.7L: R = Cl, R' = Cl
6.8L: R = H, R' = NO_2

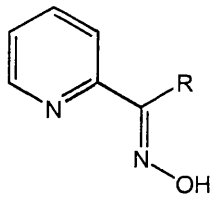

6.9L: R = H
6.11L: R = Ph
6.12L: R = Py

Figure 6.7: Ligands used in chapter 6

6.3 Discussion of the complexes

As with the rest of this chapter the following discussion will be split into three sections discussing in turn the hydrazones, azines and oximes.

6.3.1 Hydrazones

The following two complexes are the first examples of crystallographically characterised titanium salicylaldehyde hydrazone complexes and only the second examples of salicylaldehyde hydrazone complexes of any metal. The following discussion initially describes the solution and solid-state structures of the complexes followed by the formation through intra- and intermolecular hydrogen bonds of supramolecular arrays by these complexes in the solid state.

Complex 6.1

Two equivalents of ligand 6.1L react readily with one equivalent of TiPT to yield yellow crystals, which are suitable for X-ray diffraction. In the crystal structure each 6.1L moiety is deprotonated once, at the phenolic group, and chelates the metal centre through the resulting aryloxide and the imine nitrogen of the hydrazone group. In addition, the metal centre retains two isopropoxide ligands, one of which {C(41), C(42) and C(43)} is disordered over two positions in a 1:1 ratio.

The titanium centre has a distorted octahedral geometry with the two aryloxide ligands in a trans-axial configuration, the imine donors cis-equatorial and the isopropoxide ligands also cis-equatorial. The solid-state structure of 6.1 is very similar to the structure of some of the titanium complexes of monoanionic Schiff bases described in chapter 4 (4.1-4.6 and 4.12-4.13) and the complex has the most favourable geometry as described in the introduction to that chapter (configuration A in figure 4.5 on page 119). The addition of the NH_2 functionality on the ligand seems to have little effect on the gross structure of the metal complex and forms interactions only in the solid-state.

The bond lengths between the titanium centre and its ligands are of the expected order for these types of interaction. The aryloxide to titanium bonds are identical within

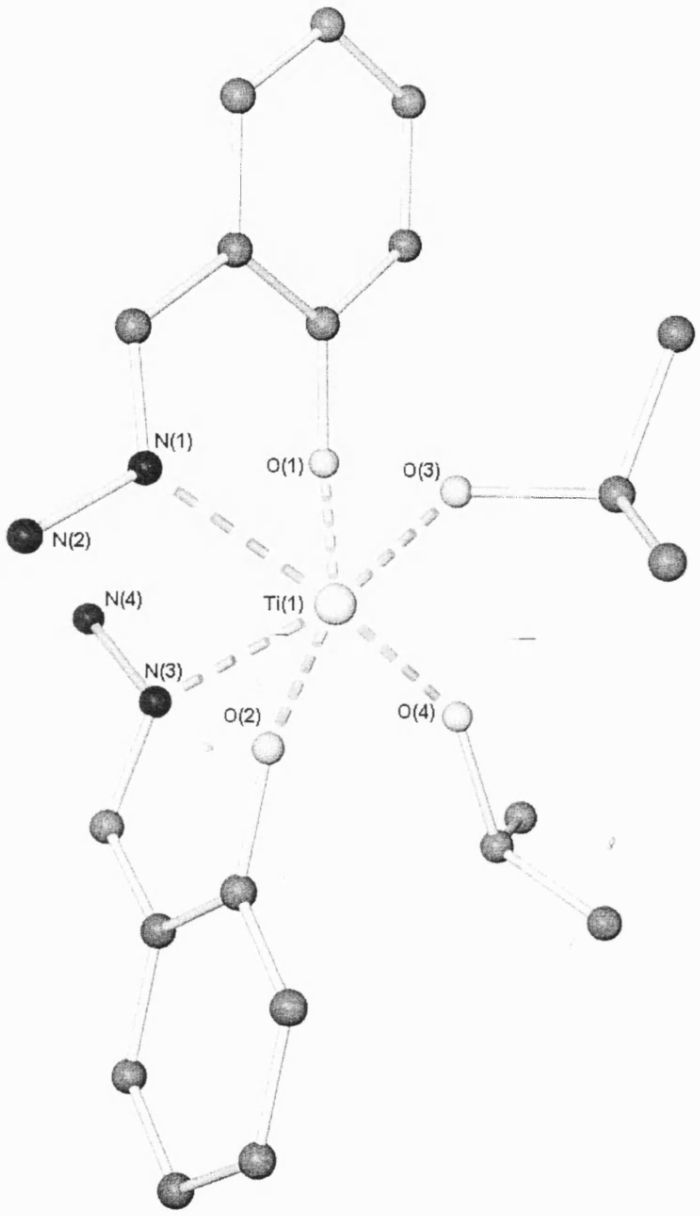

Figure 6.8: Molecular structure of complex 6.1 (hydrogen atoms not shown for clarity)

experimental error {1.943(2)Å [Ti(1)-O(2)] and 1.950(2)Å [Ti(1)-O(1)]} as are the imine to titanium bonds {2.256(3)Å [Ti(1)-N(1)] and 2.264(3)Å [Ti(1)-N(3)]}. In contrast the titanium to isopropoxide bonds are inequivalent with the bond to the disordered isopropoxide being shorter {1.763(3)Å [Ti(1)-O(4)]} than that to the more ordered one {1.846(2)Å [Ti(1)-O(3)]} which is also a hydrogen bond acceptor (see below) which could explain the extended bond length.

The ^{1}H and ^{13}C NMR spectra of the complex suggest that the gross solid-state structure is maintained in solution with well-defined peaks in the ^{1}H NMR for the isopropoxide C**H** protons (4.63ppm), C**H**$_3$ protons (1.04ppm) and the hydrazone N**H**$_2$ protons (5.57ppm).

Complex 6.2

Ligand 6.2L differs only from 6.1L due to increased steric bulk around the phenolic ring due to the presence of *tert*-butyl groups at the 2- and 4- positions. Two equivalents of the ligand react readily with one equivalent of TiPT to give red crystals, which were suitable for X-ray diffraction. The asymmetric unit consists of half a molecule of hexane and one ligand-metal complex; the complex has the same overall structure as 6.1. The titanium centre has a distorted octahedral geometry with the two aryloxide ligands in a trans-axial configuration, the imine donors cis-equatorial and the isopropoxide ligands also cis-equatorial (c.f. 6.1, 4.1-4.6 and 4.12-4.13).

As with complex 6.1 the bond lengths are within the expected range for interactions of this type with the titanium-aryloxide bonds having no significant difference in length {1.912(2)Å [Ti(1)-O(1)] and 1.913(2)Å [Ti(1)-O(2)]}. The imine-titanium bonds also show no significant difference {2.271(2)Å [Ti(1)-N(3)] and 2.282(2)Å [Ti(1)-N(1)]} unlike the titanium-isopropoxide bonds which have non-equivalent lengths {1.777(2)Å [Ti(1)-O(3)] and 1.853(2)Å [Ti(1)-O(4)]} with the longer bond being to the isopropoxide which acts as an intermolecular H-bond acceptor (see below). When the bond lengths to the metal centre in 6.2 are compared to the bond lengths to the titanium centre in 6.1 differences are observed. The bond lengths to the aryloxide ligands in 6.2 are slightly shorter than those observed in the unsubstituted hydrazone

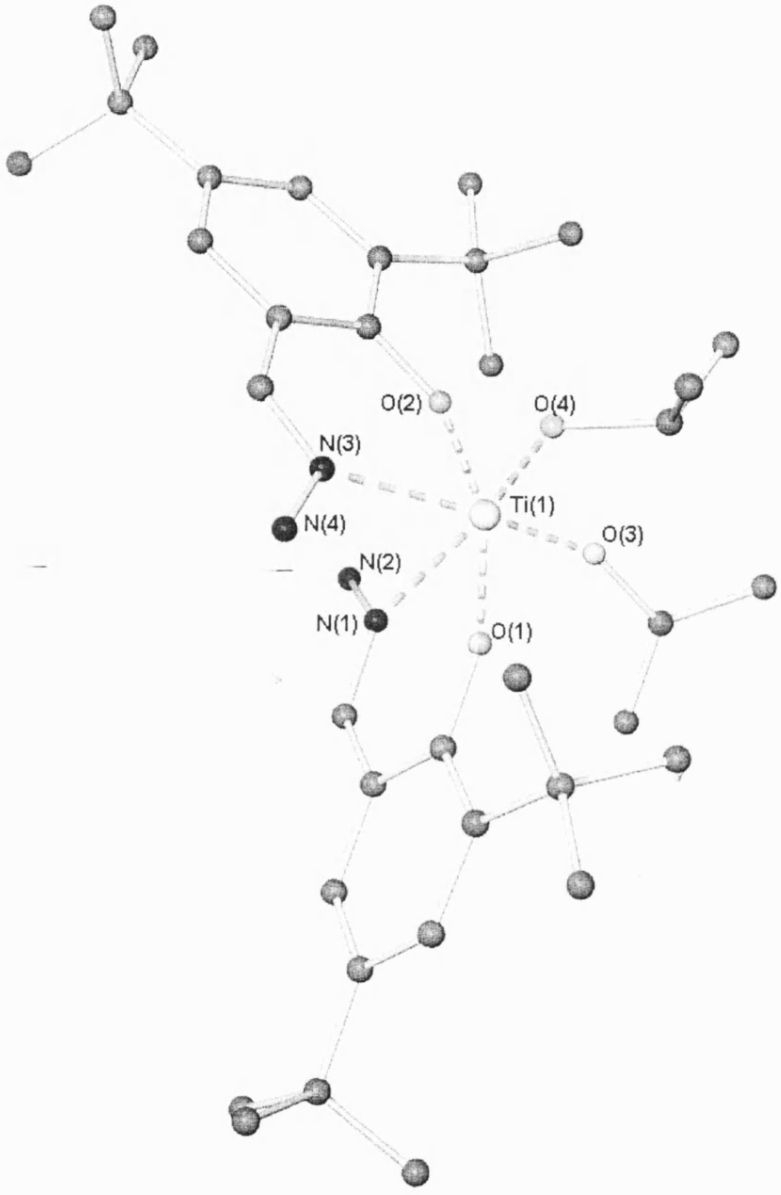

Figure 6.9: Molecular structure of complex 6.2 (hydrogen atoms not shown for clarity)

complex, by around 0.03-0.04Å, while the bond lengths to the monodentate alkoxides are slightly longer, by around 0.01Å.

The ^{1}H and ^{13}C NMR spectra for complex 6.2 suggest that the gross solid-state structure is maintained in solution with well-defined peaks in the ^{1}H NMR spectrum for the isopropoxide C**H** protons (4.55ppm), C**H**$_3$ (0.90ppm) and the hydrazone N**H**$_2$ protons (5.48ppm).

Hydrogen bonding and the formation of supramolecular arrays in 6.1 and 6.2

As was stated in the discussion of crystal structures of complexes 6.1 and 6.2 they closely resemble the Schiff base complexes described in chapter 4 with the salicylaldimine alkyl or aryl group replaced by an NH_2 group. However, unlike the Schiff bases the hydrazone complexes form supramolecular arrays in the solid state due to the presence of the protic hydrazone NH_2 groups. In complexes 6.1 and 6.2 these protic groups form a number of intra- and intermolecular hydrogen bonding interactions in the solid-state. These combine to form supramolecular structures, which vary between the two complexes due to the differing steric demands of the two ligands 6.1L and 6.2L. Recently there has been much interest in the formation of supramolecular structures of this type particularly in the field of crystal engineering[9] and these complexes and analogous ones with other metals are potentially useful supramolecular synthons, which could be utilised in this field.

In the extended packing diagram of complex 6.1 hydrogen bonding can be observed between the hydrogen atoms on the hydrazone NH_2 groups and hydrogen bond acceptor groups on both their own complex and neighbouring complexes (the NH_2 hydrogen atoms are freely refined). Both hydrazone NH_2 groups act as hydrogen bond donors for intramolecular hydrogen bonds to the aryloxide oxygen of the other ligand in the same complex; the bonds are quite short and non-linear {N(2)-H···O(2) [O(2)···H 2.057Å; N(2)-O(2) 2.841Å and N(2)-H-O(2) 131.8°]} and {N(4)-H···O(1) [O(1)···H 2.369Å; N(4)-O(1) 2.826Å and N(4)-H-O(1) 121.42°]}.

[9] D. Braga, F. Grepioni and G.R. Desiraju, *Chem. Rev.*, **98**, 1375 (1998)

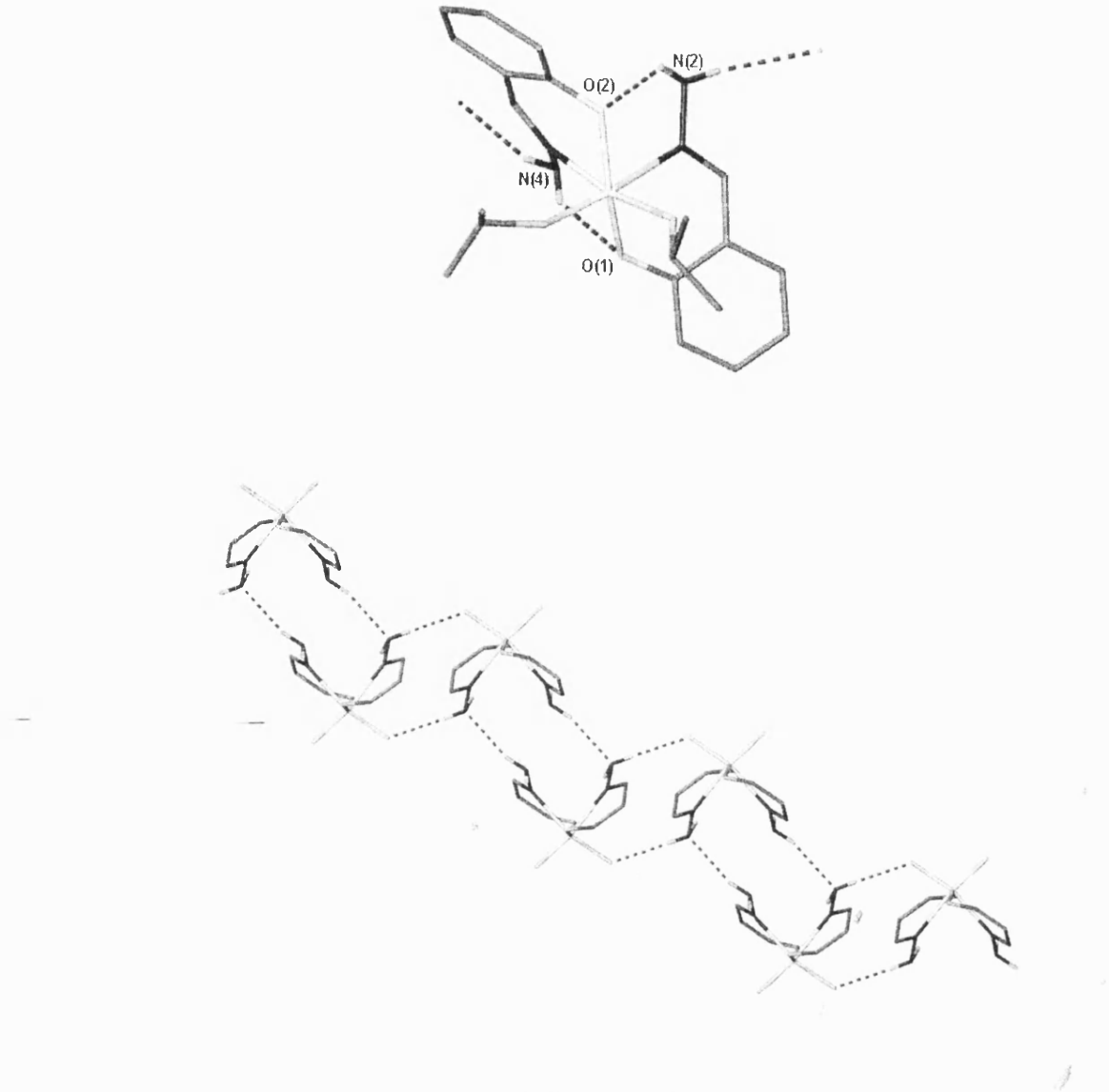

Figure 6.10: H-bonds in complex 6.1

Both hydrazone groups also act as intermolecular hydrogen bond donors. The hydrazone group at N(2) acts as a H-bond donor to an isopropoxide oxygen in a neighbouring molecule {N(2)-H···O(3*) [O(3)···H 2.292Å; N(2)-O(3) 3.059Å and N(2)-H-O(3) 173.2°]} and as a hydrogen bond acceptor in an interaction with the N(4) hydrazone NH_2 group of a third molecule {N(4*)-H···N(2) [N(2)···H 2.390Å; N(2)-N(4) 3.243Å and N(2)-H-N(4) 161.4°]}. These intermolecular hydrogen bonds are longer and more linear than the intramolecular ones and lead to the formation of a ribbon-like structure in the solid state as shown in figure 6.10 above.

In complex 6.2, as with complex 6.1, both intra- and intermolecular hydrogen bonding can be observed but to a lesser extent. Unlike 6.1 only three of the four available hydrazone NH_2 protons are involved in the interactions and only one hydrogen bond is formed to a neighbouring molecule along with two intramolecular interactions (All hydrazone NH_2 hydrogen atoms are freely refined).

Both hydrazone NH_2 groups act as hydrogen bond donors for intramolecular hydrogen bonds to the aryloxide oxygen of the other ligand in the same complex as shown in figure 6.11 below. {N(2)-H···O(2) [O(2)···H 2.223Å; N(2)-O(2) 2.874Å and N(2)-H-O(2) 130.8°]} and {N(4)-H···O(1) [O(1)···H 2.284Å; N(4)-O(1) 2.876Å and N(4)-H-O(2) 133.2°]}.

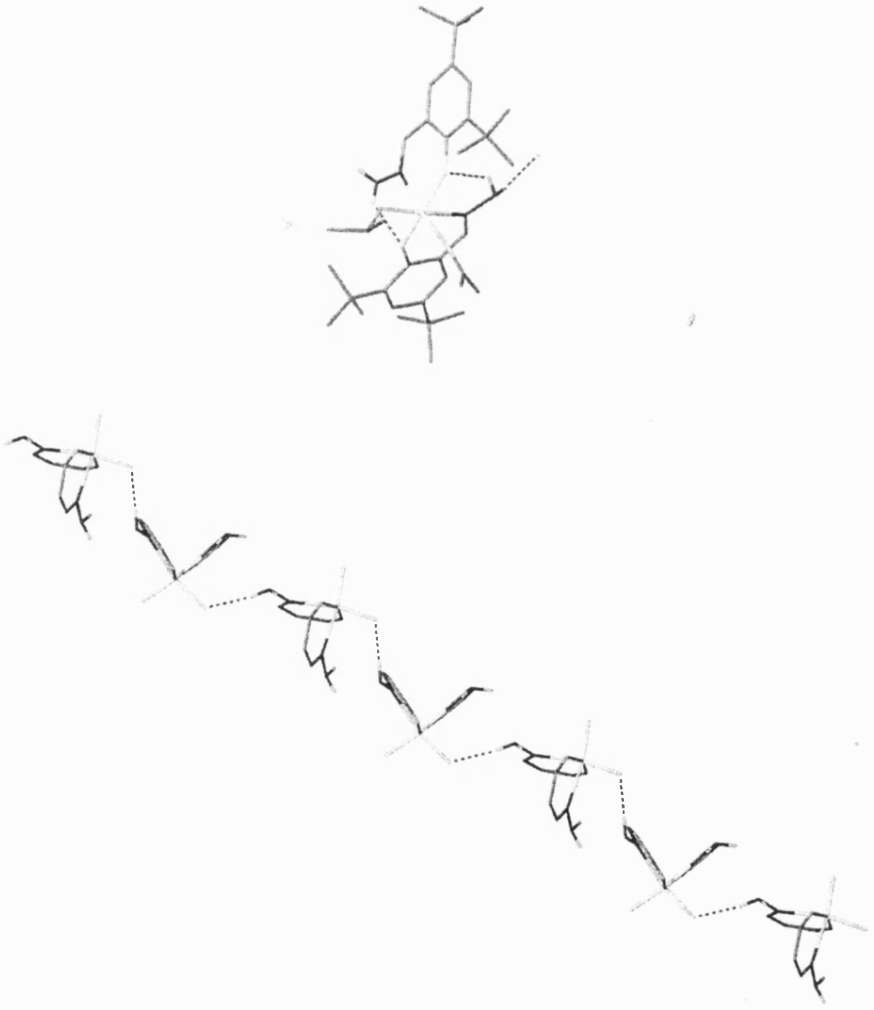

Figure 6.11: H-bonds in complex 6.2

Unlike complex 6.1 only one intermolecular H-bond is observed in 6.2, probably due to the steric bulk of the ligand *t*-butyl groups. The hydrazone group at N(2) acts as a H-bond donor to an isopropoxide oxygen in a neighbouring molecule {N(2)-H···O(4*) [O(4)···H 2.219Å; N(2)-O(4) 3.013Å and N(2)-H-O(4) 156.8°]}. This results in the formation of an extended chain-like structure in the solid state as shown in figure 6.11 above.

Summary

Complexes 6.1 and 6.2 are the first examples of titanium complexes of salicylaldehyde hydrazone derivatives to be structurally characterised and only the second structural report of metal complexes of these ligands.

Superficially these complexes are very similar to the Schiff base complexes described in chapter 4. However, the protic NH_2 groups in the product complex make their structural chemistry more diverse leading to the formation of supramolecular arrays in the solid-state. The change in supramolecular architecture observed between 6.1 and 6.2 shows that it should be possible, through systematic variation of the salicylaldimine R groups in the complexes, to form a range of supramolecular structures.

In addition to this supramolecular chemistry, the potentially reactive protic NH_2 groups, which remain on the complex, may allow further reactions to be carried out at these positions. The most interesting potential reaction at these sites would be to react 6.1 or 6.2 with a reactive metal species to form a mixed metal complex, which could have interesting catalytic properties.

6.3.2 Azines

Very little previous work has been carried out using the azines based on salicylaldehyde with titanium and therefore there is no structural precedent in the literature for comparison for the following complexes. Attempts were made to synthesise a titanium complex of an azine ligand with no substituents on the phenyl ring but these led to formation of an intractable solid product. This product is

probably polymeric with a trans configuration around the azine N-N bond but the nature of the product precluded analysis (see figure 6.5).

Complex 6.3

One equivalent of ligand 6.3L reacts readily with two equivalents of TiPT to yield a crop of yellow crystals, which were suitable for single crystal X-ray diffraction. The asymmetric unit contains one molecule of toluene in the crystal lattice and one molecule of the titanium complex. The titanium complex consists of one 6.3L ligand, which is doubly deprotonated at the phenolic groups. Each of the salicylaldimine N-O chelate pairs in the ligand is complexed to a different titanium centre and in this way the ligand bridges the two centres. In addition the titanium centres are also bridged by two isopropoxide ligands and also retain two monodentate alkoxide ligands each. Each titanium centre has six ligand donors giving the metal atom a distorted octahedral geometry.

The ligand itself is distorted away from a planar arrangement with the salicylaldimine units to either side of the N-N bond. This distortion is manifested in two ways, the carbon atoms of the imine groups are offset to either side of the N-N azine bond with a torsion angle between them of 53.3° {C(7)-N(1)-N(2)-C(27)}.

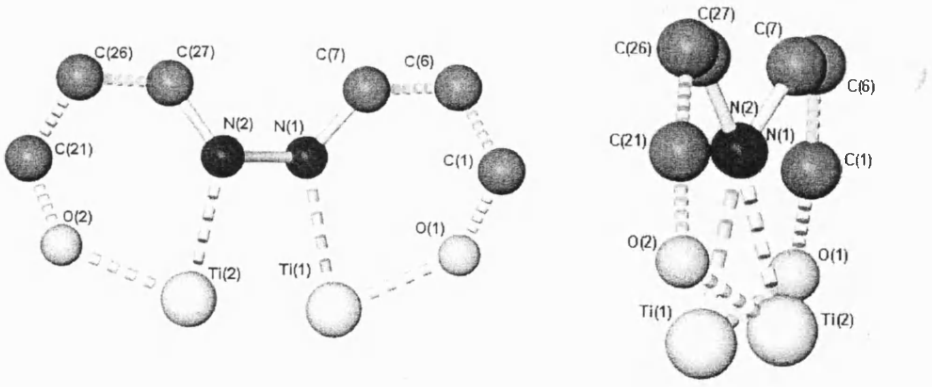

Figure 6.12: Side-on and end-on pictures of the ligand distortion from planarity in complex 6.3

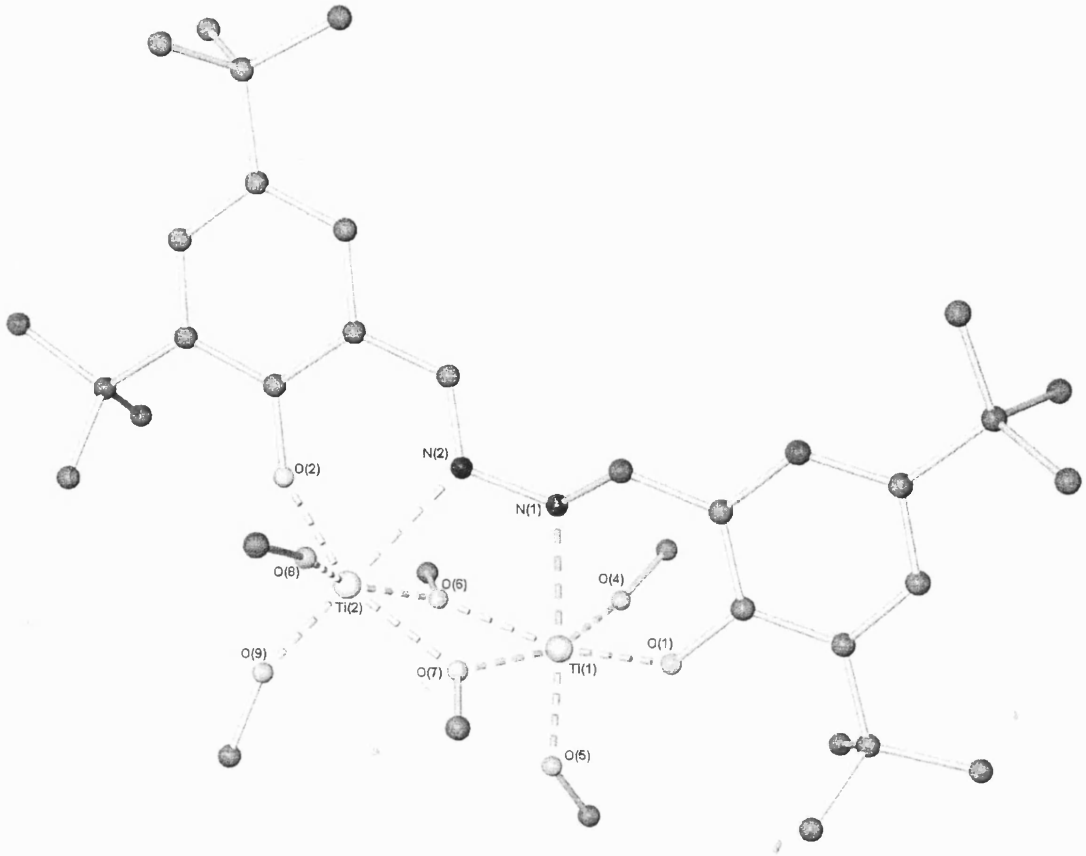

Figure 6.13: Molecular structure of complex 6.3 (hydrogen atoms and isopropoxide methyl groups not shown for clarity).

In addition this distortion is compensated for, slightly, by the phenolic rings, which bend back towards the azine bond reducing the torsion angle between them and the azine N-N bond to 45.4° {O(1)···(N1)-N(2)···O(2)}. The ligand distortion from planarity suggests that there is little conjugation between the two salicylaldimine units of the azine and that the N-N bond has little π-bonding character.

The core of the complex is made up of three rings, one Ti_2O_2 ring made up of the two titanium centres and the two bridging alkoxides, and two five membered rings made up of the two titanium atoms, a bridging alkoxide and the azine N-N bond.

The bond lengths between the various ligands and titanium are within the expected ranges for typical interactions of these types. The aryloxide to titanium bond lengths are very similar for both titanium centres {1.919(2)Å [Ti(1)-O(1)] and 1.935(2)Å [Ti(2)-O(2)]} as are the terminal isopropoxide to titanium bond lengths {1.785(3)Å [Ti(1)-O(4)], 1.800(2)Å [Ti(1)-O(5)], 1.784(3)Å [Ti(2)-O(8)] and 1.782(3)Å [Ti(2)-O(9)]}. The bond lengths to the azine nitrogen atoms from the respective titanium centres show some differences with the bond to Ti(1) {2.320(3)Å [Ti(1)-N(1)]} being longer than that to Ti(2) {2.262(3)Å [Ti(2)-N(2)]}. The bridging isopropoxides are typical for these types of interactions in that each alkoxide has one long bond {2.061(2)Å [Ti(1)-O(7)] and 2.091(2)Å [Ti(2)-O(6)]} and one short bond {2.009(2)Å [Ti(1)-O(6)] and 2.007(2)Å [Ti(2)-O(7)]}.

The ^1H and ^{13}C NMR spectra suggest that the gross solid-state structure is maintained in solution with distinct signals in the ^1H spectrum for the isopropoxide C**H** protons corresponding to two separate pairs of terminal isopropoxides and a pair of bridging isopropoxides (4.37, 4.77ppm and 4.88ppm). One of the isopropoxide groups (at 4.77ppm) is observed in the ^1H NMR spectrum to have restricted rotation. This is clearly indicated by its coupling, in the proton-proton COSY spectrum, to two defined isopropoxide C$\mathbf{H}_3$ signals at 1.02 and 1.20ppm rather than just one. This inequivalence of the isopropoxide methyl groups is probably due to the steric bulk of the azine ligand causing the rotation of this ligand group to be restricted. This is carried on into the ^{13}C spectrum, which also shows three signals for the isopropoxide

CH carbon atoms (72.3, 75.1 and 75.9ppm), and two distinct isopropoxide **C**H_3 signals for one of these isopropoxide groups (22.0 and 23.1ppm).

The structure fits the usual pattern for the few structurally characterised azine metal complexes, as described in the introduction to this chapter, with the azine bridging two metal centres and the salicylaldimine units in a cis orientation around the azine N-N bond.

Complex 6.4

Ligand 6.4L reacts readily with two equivalents of TiPT to yield a crop of yellow crystals, which are suitable for X-ray diffraction. The asymmetric unit contains half of the titanium complex. The overall structure of the complex is very similar to that observed for complex 6.3 and has the same overall features. Each titanium centre has six ligand donors giving the metal atom a distorted octahedral geometry.

As observed in complex 6.3 the ligand in 6.4 is distorted from planarity with the two salicylaldimine groups offset to either side of the N-N azine bond (see figure 6.14 below). The distortion seen in the ligand is similar to that observed for 6.3 with a slightly larger C(8)-N(1)-N(1#)-C(8#) torsion angle of 55.7° and a smaller O(2)···N(1)-N(1#)···O(2#) torsion angle of 41.2°. The change from *t*-butyl groups to an OMe group seems to have had very little effect on the distortion.

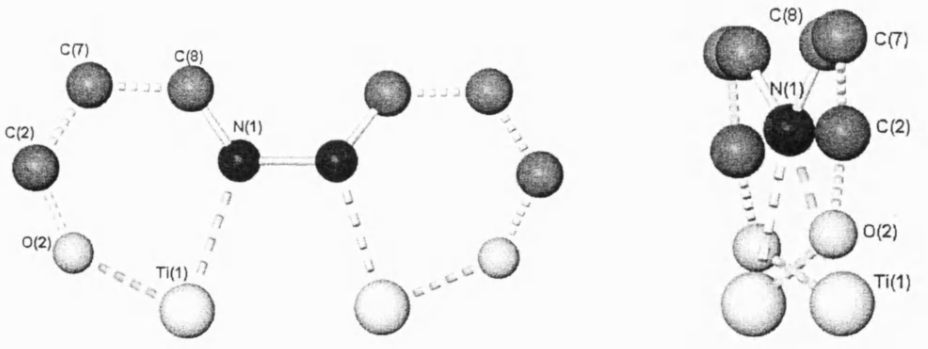

Figure 6.14: Side-on and end-on pictures of the ligand distortion from planarity in complex 6.4

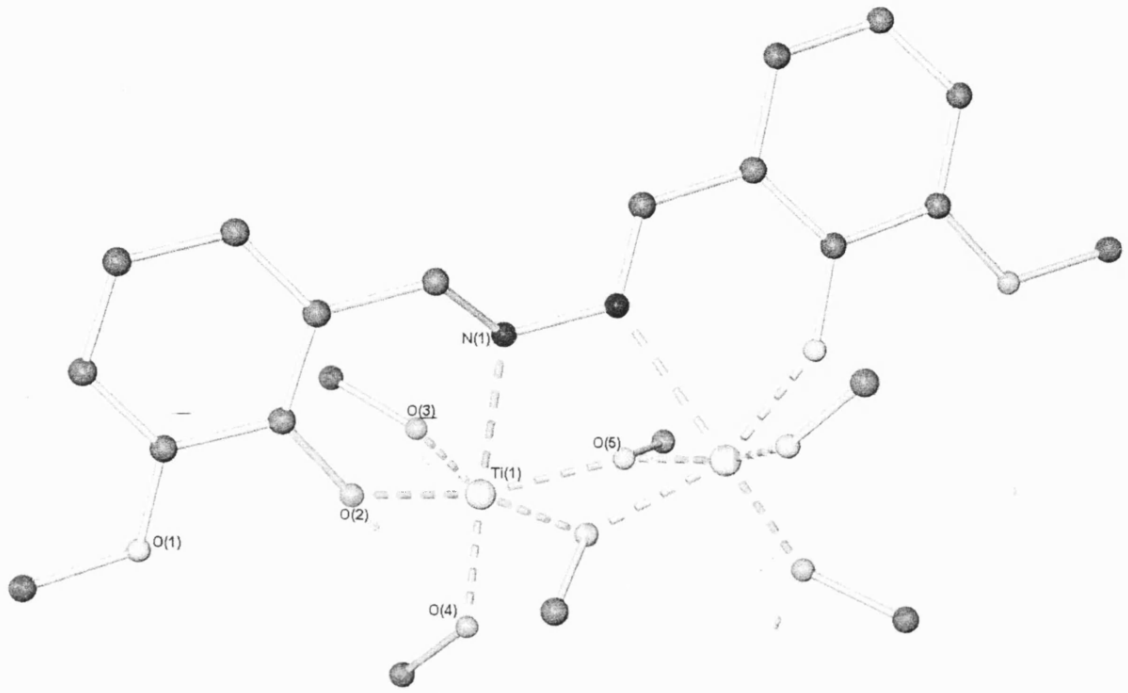

Figure 6.15: Molecular structure of complex 6.4 (hydrogen atoms and isopropyl methyl groups not shown for clarity)

The bond lengths between the different ligands and titanium are within the expected ranges for typical interactions of these types. The titanium-aryloxide {1.930(2)Å [Ti(1)-O(2)]} and titanium to terminal isopropoxide {1.797(2)Å [Ti(1)-O(3)] and 1.798(2)Å [Ti(1)-O(4)]} bond lengths are very similar to those observed in complex 6.3, as is the titanium-imine bond {2.320(2)Å [Ti(1)-N(1)]}. As with complex 6.3 each of the bridging isopropoxides has two inequivalent bond lengths {1.990(2)Å [Ti(1)-O(5)] and 2.074(2)Å [Ti(1)-O(5#)]}.

Although the change in azine substituents from *tert*-butyl to OMe seems to have little effect on the distortion of the ligand and the metal to ligand bond lengths it does allow the formation of intramolecular interactions in the solid-state. These interactions are weak hydrogen bonds between the vanillin OMe group and a C**H** of one of the terminal isopropoxide ligands as shown in figure 6.16 below (the hydrogen atom is not freely refined). {C(41)-H···O(1) [C(41)-O(1) 3.470Å and C(41)-H-O(1) 151.9°]}.

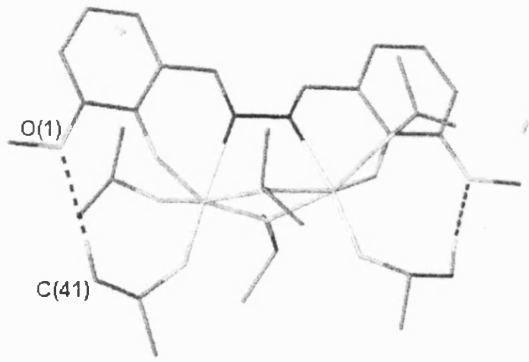

Figure 6.16: Intramolecular hydrogen bonding in 6.4

As with complex 6.3 the ^{1}H and ^{13}C NMR spectra suggest that the gross solid-state structure is maintained in solution with three distinct signals in the ^{1}H NMR spectrum for the three sets of isopropoxide C**H** protons with one showing restricted rotation. However unlike complex 6.3 the signal for the isopropoxide with restricted rotation can be found at a higher chemical shift (4.95ppm) than both of those with equivalent methyl groups (4.39 and 4.71ppm). The signals for the two distinct methyl groups of the isopropoxide ligand with restricted rotation coming at slightly lower chemical

shifts (0.80 and 1.12ppm) than for the previous example. The ^{13}C NMR spectrum also shows signals for the three different isopropoxide environments with resonances at 76.3 and 79.6ppm for the isopropoxide **C**H groups with free rotation and a corresponding signal at 80.7ppm for the same group in the restricted isopropoxide ligand. The differences observed here could be due to the hydrogen bonding described above although this is difficult to prove from the evidence available.

Complex 6.5

One equivalent of ligand 6.5L reacts readily with two equivalents of TiPT to yield a crop of red crystals, which are suitable for X-ray diffraction. The asymmetric unit contains half of the titanium complex. The complex has the same gross structure as complexes 6.3 and 6.4. Each titanium centre has six ligand donors giving the metal atom a distorted octahedral geometry.

The ligand itself shows a distortion away from a planar arrangement in a similar manner to 6.3 and 6.4 with the two salicylaldimine units at either side of the N-N bond, but to an even greater extent. The distortion seen in the ligand is much larger than for 6.3 and 6.4 with a C(7)-N(1)-N(1#)-C(7#) torsion angle of 66.8°. The twist in the phenyl rings back towards the N-N plane is also much greater than observed in the previous two structures and reduces the O(1)···N(1)-N(1#)···O(1#) torsion angle to only 14.3°, which allows the bond lengths from the ligands to the titanium to be maintained at almost exactly the same for complex 6.5 as for the previous two structures. This difference can be seen in figure 6.17, below, which shows the twist and its effect on the central core of the molecule, which differs from that observed for 6.3 and 6.4 (figures 6.12 and 6.14 above).

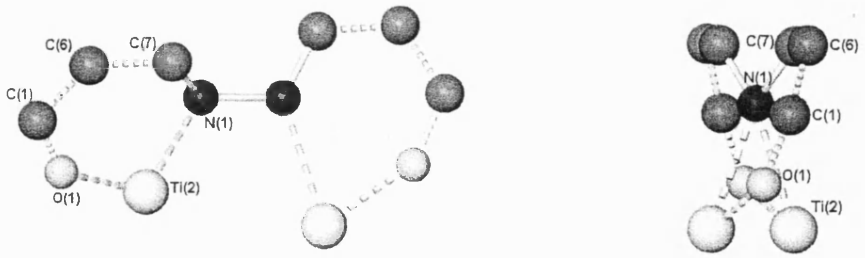

Figure 6.17: Ligand distortion in complex 6.5

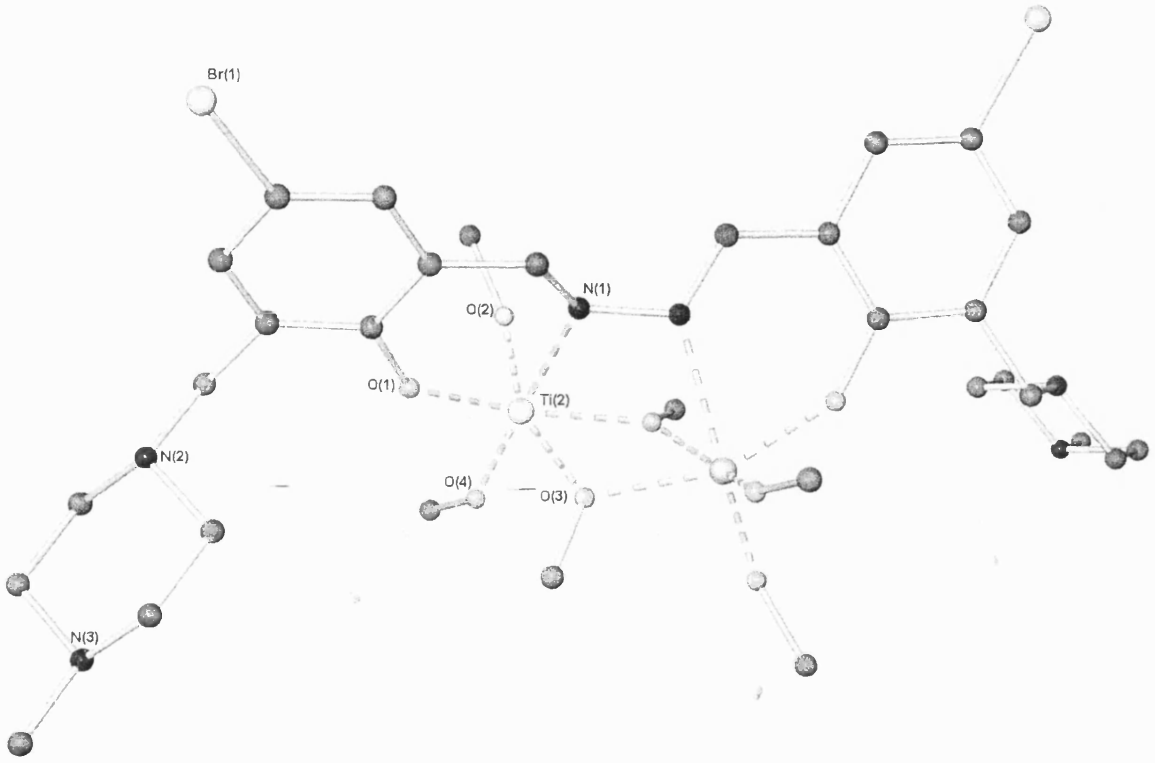

Figure 6.18: Molecular structure of complex 6.5 (hydrogen atoms and isopropoxide methyl groups not shown for clarity)

The core of the complex is made up of three rings, one Ti_2O_2 ring made up of the two titanium centres and the two bridging alkoxides, and two five membered rings made up of the two titanium atoms, a bridging alkoxide and the azine N-N bond.

The bond lengths between the different ligands and titanium are within the expected ranges for typical interactions of these types. The titanium aryloxide {1.935(2)Å [Ti(2)-O(1)]} and titanium to terminal isopropoxide {1.797(2)Å [Ti(2)-O(4)] and 1.800(2)Å [Ti(2)-O(2)]} bond lengths are very similar to those observed in complexes 6.3 and 6.4, as is the titanium to imine bond {2.314(2)Å [Ti(2)-N(1)]}. As with complexes 6.3 and 6.4 each of the bridging isopropoxides has two inequivalent bond lengths {2.004(2)Å [Ti(2)-O(3)] and 2.081(2)Å [Ti(2)-O(3#)]}.

As with complexes 6.3 and 6.4 the ^1H and ^{13}C NMR spectra suggest that the gross solid-state structure is maintained in solution with three distinct signals in the ^1H NMR spectrum for the three sets of isopropoxide C**H** protons. However the pattern of signals for these groups has returned to that observed for complex 6.3 with the signal for the ligand with restricted rotation (4.64ppm) falling between those with no restriction (4.34 and 4.89ppm). Another interesting feature of the ^1H NMR spectrum of complex 6.5 is that the hydrogen atoms on the methylene linker between the piperazine and the phenyl ring are inequivalent and two doublets are observed. This effect is due to a restriction of the rotation around this bond in the complex which fixes each of the hydrogen atoms in this methylene group in either an 'up' or 'down' configuration and leads to their inequivalence. There are two possible explanations for this restriction of rotation at the methylene group; the first possible reason is a clash between one of the terminal isopropoxide ligands and the piperazine group although there is little evidence for this in the solid-state. The second possible reason is an intermolecular bromine-nitrogen interaction; this interaction is observed in the solid state and causes the formation of a ladder like supramolecular array in the crystal as shown in figure 6.19 overleaf. These types of interactions have been reported previously in the literature[10] and if maintained to some extent in solution could

[10] R.B. Walsh, C.W. Padgett, P. Metrangolo, G. Resnati, T.W. Hanks and W.T. Pennington, *Crys. Growth & Des.*, **1**, 165 (2001); P. Pyykko, *Chem. Rev.*, **97**, 597 (1997); D.S. Reddy, D.C. Craig, A.D.

explain the methylene proton inequivalence. The interaction observed results in an ordering of the piperazine amine nitrogen atom such that its lone pair is directed towards the bromine atom of a neighbouring molecule, with a Br(1)-N(3) interaction of 3.034Å and a C(4)-Br(1)-N(3) angle of 172.2°. The Br-N distance is typical for an interaction of this type, which typically vary from ~2.6-3.2Å, and is significantly shorter than the sum of the Van der Waals radii of the two atoms.

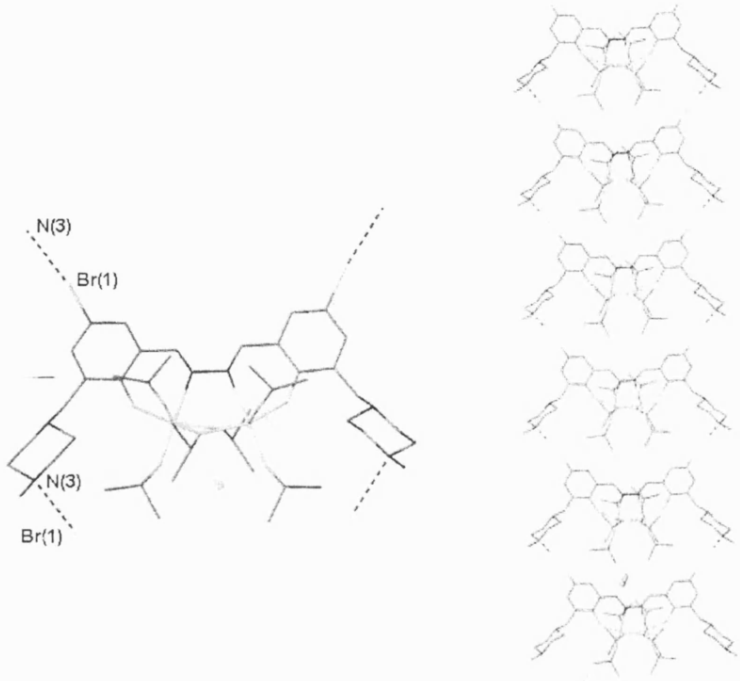

Figure 6.19: Bromine nitrogen interactions in complex 6.5

The ^{13}C NMR spectrum also shows signals for the three different isopropoxide environments with resonances at 77.0 and 78.0ppm for the unrestricted isopropoxide **C**H groups and a corresponding signal at 73.8ppm for the same group in the isopropoxide ligand with restricted rotation.

Summary

When comparing the three complexes with azine ligands, described above, it becomes apparent that although the differing substituents around the phenyl ring of the azine

---

Rae and G.R. Desiraju, *Chem. Comm.*, 1737 (1993); S.C. Blackstock and J.K. Kochi, *J. Am. Chem. Soc.*, **109**, 2484 (1987); S.C. Blackstock, J.P. Lorand and J.K. Kochi, *J. Org. Chem.*, **52**, 1451 (1987).

seem to have very little effect on the ligand to titanium bond lengths in the complexes and their overall gross structures, they do, however, change the properties of the complexes in the solid-state. The addition of Lewis basic groups at the 2-position on the salicylaldimine ring allows the formation of inter- and intramolecular interactions in the crystal lattice. In the future it may be possible to utilise these Lewis base groups to either; complex further metals to form mixed metal species or; to order the substrates in catalytic reactions such as the synthesis of polyurethanes. It may also be possible to exploit the intermolecular interactions seen in both these complexes and the hydrazone complexes, discussed prior to them, to form new supramolecular arrays with interesting properties.

6.3.3 Oximes

The following section discusses the synthesis and characterisation of several titanium oximates. The first group of complexes discussed are salicylaldoximates, which are closely related to the Schiff bases, hydrazones and azines described previously in this thesis. Complexes of some pyridine derivatives, which also contain oxime groups, follow these. We initially studied these ligands as a comparison to the simple Schiff bases described in chapter 4 to look at the effect of introducing a further hydroxyl group on product structure and to attempt to obtain titanium cluster complexes.

As with the hydrazone and azine complexes discussed earlier there is no literature precedent for crystallographically defined titanium complexes of salicylaldoxime ligands and only one previous paper has reported the crystallographic characterisation of titanium oximates of any kind[8]. However, prior to the work described in this thesis the Davidson group had synthesised and structurally characterised, by single crystal X-ray diffraction, a complex of salicylaldoxime (Ligand 6.6L), which is shown in figure 6.20 below. The complex was synthesised by reaction of an excess of ligand 6.6L with TiPT and consists of a cluster of four titanium atoms with a periphery of six salicylaldoxime ligands and one terminal alkoxide on each titanium centre. The salicylaldoxime ligands bridge the metal centres in two distinct ways. For the outer pairs of titanium atoms, Ti(1) and Ti(2), bridging is through the oxime with the nitrogen and oxygen atoms bonding with adjacent titanium centres to form bicyclic $Ti_2N_3O_3$ groups. In comparison oxime oxygen atoms bridge the central two titanium

centres, Ti(2) and Ti(2A) resulting in the formation of a central core consisting of a Ti_2O_2 ring. Unfortunately the extremely low solubility of this product in common solvents has made it impossible for us to repeat this experiment and led to us being

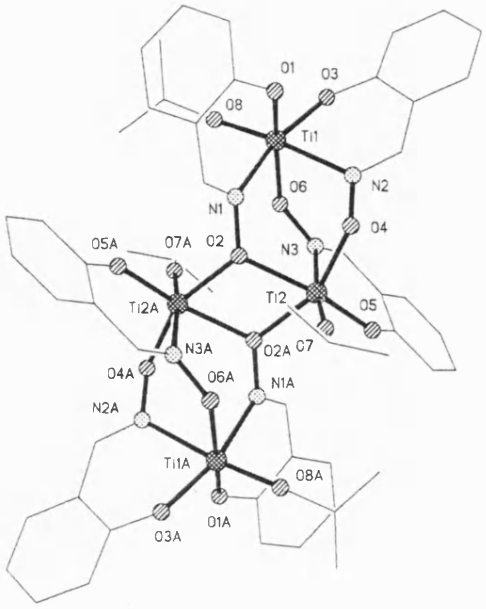

Figure 6.20: Molecular structure of the insoluble salicylaldoxime/TiPT complex

unable to perform NMR experiments on the product. In addition similar problems have accompanied attempts to synthesise analogues of this complex with derivatised salicylaldoxime ligands. Some crystals have been isolated for the vanillin oxime derivative (2-methoxy-salicylaldoxime) and these gave an X-ray crystal structure with the same overall structural features. However, the poor quality data obtained precluded the formation of a definitive model and therefore this work will not be presented here. As with the salicylaldoxime complex extremely low solubility of the derivatised products meant that NMR experiments on the products proved impossible.

Complex 6.6

Due to the problems encountered in trying to reproduce the synthesis of the salicylaldoxime described above a reaction was carried out using an excess of the titanium source to try and isolate a soluble titanium salicylaldoximate. Two equivalents of ligand 6.6L react readily with three equivalents of TiPT to yield a crop

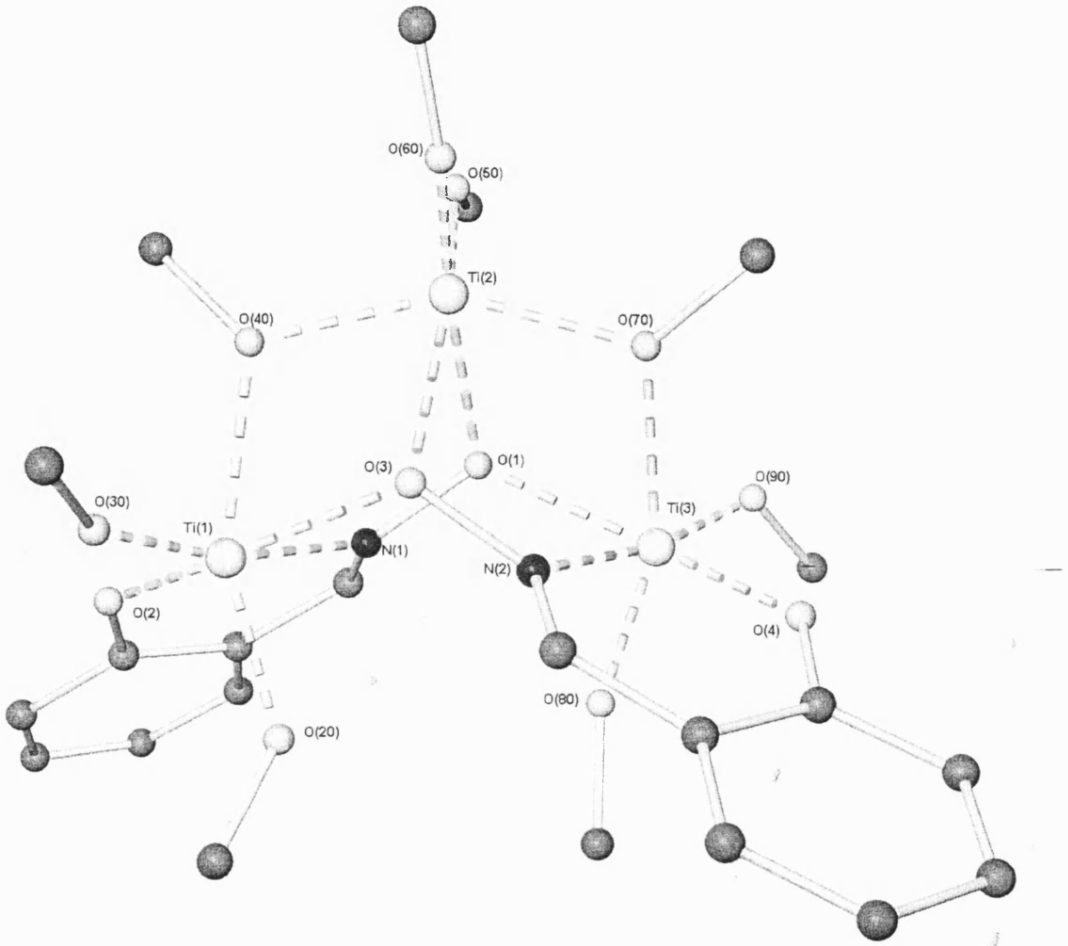

Figure 6.21: Molecular structure of complex 6.6 (hydrogen atoms and isopropoxide methyl groups not shown for clarity)

of orange crystals. Complex 6.6 consists of three titanium centres, linked as a cluster by the two salicylaldoxime ligands. Two of the centres, Ti(1) and Ti(3), are joined in a six membered ring consisting of the two metal centres and the two oximate NO groups. The nitrogen atom of one oximate and the oxygen atom of the second coordinate these centres, which have a distorted octahedral geometry. The coordination spheres of Ti(1) and Ti(3) are completed by the phenolic oxygen atoms of the salicylaldoxime ligands and two terminal isopropoxide ligands. The third titanium, Ti(2), sits above the rest of the molecule and is linked to it by two bridging isopropoxides and the two oximate oxygen atoms which bridge between it and each of the other two metal centres. In total the core made up of the metal centres consists of one six membered ring, two five membered rings and two of the familiar Ti_2O_2 four membered rings as shown in figure 6.22 below.

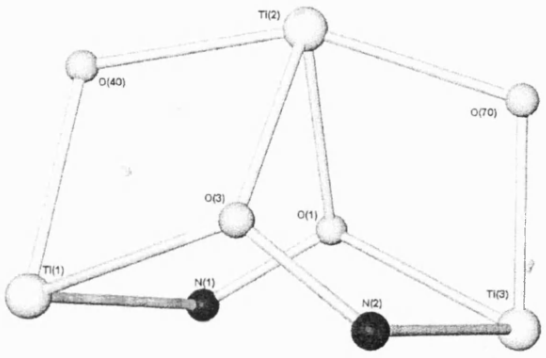

Figure 6.22: Molecular structure of the core of complex 6.6

The terminal isopropoxides have typical bond lengths varying between 1.781(1)Å and 1.820(1)Å. The interactions between the bridging isopropoxides and the two metal centres they bridge are asymmetric in nature and in both cases the bond to Ti(2) which sits above the other two {1.977(1)Å [Ti(2)-O(70)] and 1.989(1)Å [Ti(2)-O(40)]} is noticeably shorter than the bond to the other metal centre {2.131(1)Å [Ti(1)-O(40)] and 2.106(1)Å [Ti(3)-O(70)]} all of these bond lengths are however within the expected range for a bridging isopropoxide. The oximato NO groups are triply bridging with the nitrogen atoms bonding to one titanium centre and the oxygen atoms bridging the other two, for example N(2) is bonded to Ti(3) and its related oxygen O(3) bridges between Ti(1) and Ti(2). This structure, along with the previous structure with the same ligand, is the first known example of this type of NO triply

bridging oxime coordination known for a titanium oximate, although it is common in oximates of other metals including Ag, Cr, Cu, Fe, Hg, La, Mn, Mo, Ni, V, and W[11]. The nitrogen to titanium bond lengths are 2.232(2)Å [Ti(1)-N(1)] and 2.236(2)Å [Ti(3)-N(2)] respectively. The oximate oxygen atoms each bridge two titanium atoms, as has been stated above, and, as for the bridging alkoxides, are asymmetric in nature with in both cases the bond to Ti(2) {2.165(1)Å [Ti(2)-O(1) and 2.161(2)Å [Ti(2)-O(3)]} being longer than to the other metal centre {2.068(1)Å [Ti(3)-O(1)] and 2.067(1)Å [Ti(1)-O(3)]}. The bonds to the oximate oxygen atom are similar in length to those seen in the only previously reported oximates of titanium in which both the oxime nitrogen and oxygen atoms chelate one metal centre, in these the Ti-O bond varies between 2.060 and 2.149Å. By comparison the Ti-N bond lengths described above are longer than the equivalent bonds in these chelating, non-bridging, oximes, which vary between 2.044 and 2.066Å. The salicylaldoxime phenoxy groups have bond lengths to titanium of 1.890(1)Å [Ti(1)-O(2)] and 1.899(1)Å [Ti(3)-O(4)] which are quite typical for Ti-O bond lengths in non-bridging phenoxides.

Solution Dynamics of Complex 6.6

When considering the structure of complex 6.6, Ti(2), which sits above the other two metal centres, can be considered to be part of a 'trapped' $Ti(O^iPr)_4$ molecule, dissociation of which would not lead to any gross structural changes to the remainder of the complex. The bond lengths between this $Ti(O^iPr)_4$ fragment and the rest of the complex are in every case the longest bonds in their respective Ti-O-Ti bridges and this would suggest that the complex does not tightly hold this group and that it perhaps dissociates in solution as seen in figure 6.23 overleaf. However, the proton NMR spectrum of complex 6.6 seems to show that this is not the case and that no dissociation occurs in solution at room temperature. The ^1H NMR spectrum has four isopropyl C**H** septets of equal intensity (4.39, 4.73, 4.80 and 4.93ppm) corresponding to the pairs of protons A, B, C and D in the associated complex in figure 6.23 and not the dissociated pairing of $Ti(O^iPr)_4$ and $Ti_2(6.6L)_2(O^iPr)_4$ which should in theory give

[11] Selected examples include; A.D. Cutland, J.A. Halfen, J.W. Kampf and V.L. Peccarano, *J. Am. Chem. Soc.*, **123**, 6211 (2001) [La/Cu]; V. Zerbib, F. Robert and P. Gouzerk, *Chem. Comm.*, 2179 (1994) [V]; M.S. Ma, R.J. Anjielici, D. Powell and R.A. Jacobson, *Inorg. Chem.*, **19**, 3121 (1980)[Ag]; J.M. Thorpe, R.L. Beddoes, D. Collison, C.D. Garner, M. Helliwell, J.M. Holmes and P.A. Tasker, *Angew. Chem. Int. Ed. Engl.*, **38**, 1119 (1999) [Fe].

three signals in the ratio of 2:1:1 corresponding to the groups of protons represented by A, B and C in the dissociated complex in figure 6.23 below.

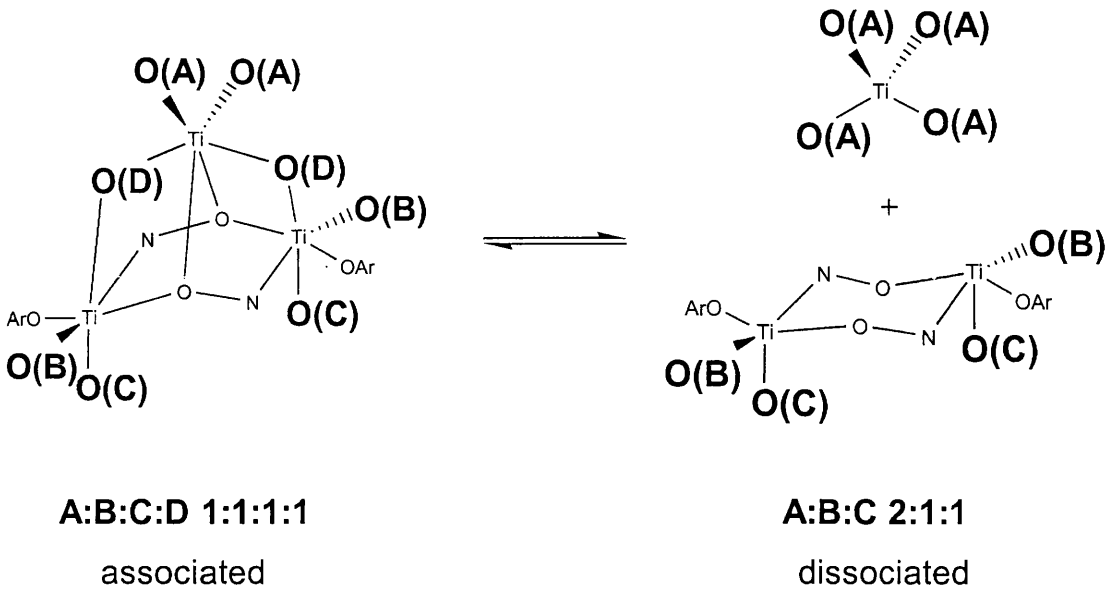

Figure 6.23: Associated and dissociated structures of 6.6

One possible reason for this apparent resistance to dissociation may be that presence of the $Ti(O^iPr)_4$ group allows all the titanium centres in the complex to retain their preferred pseudo-octahedral coordination geometry.

In fact, variable temperature studies (Figure 6.24 on the following page) have shown that even when heated to 80°C in deuterated toluene dissociation is not observed, with the only visible process being exchange between the A and D sets of protons as the temperature is raised (assignment of the A and D proton signals was possible through NOESY experiments).

^{13}C NMR spectroscopy also confirms the structure in solution with distinct peaks for separate isopropoxide **C**H environments (75.6, 77.6, 78.7 and 79.1ppm).

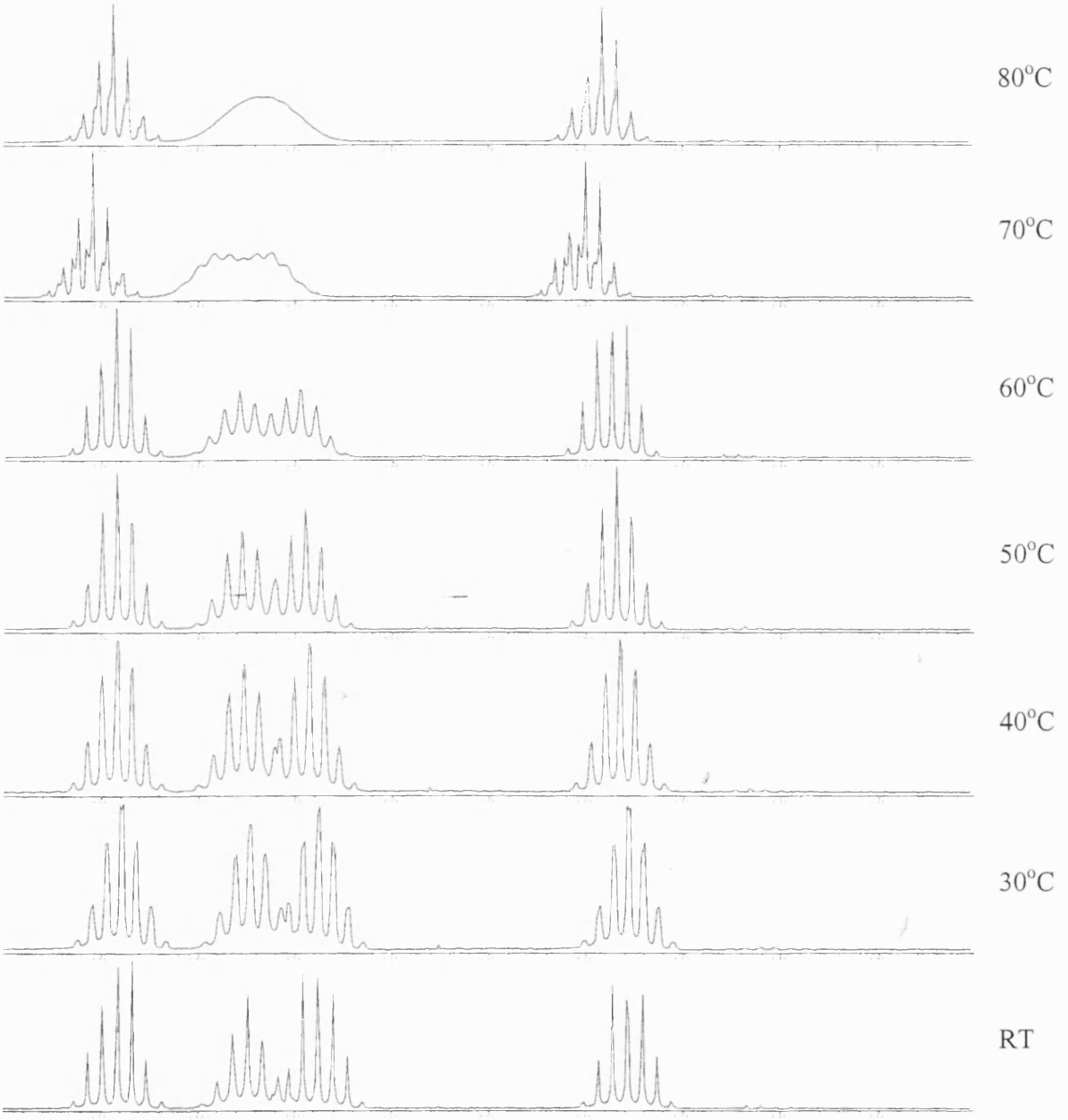

Figure 6.24: VT ^{1}H NMR spectra of the isopropoxide CH region (4-5ppm) of complex 6.6. The spectra shows exchange at high temperature but no dissociation.

Complex 6.7

Two equivalents of ligand 6.7L react readily with three equivalents of TiPT to give an orange crystalline product, which was suitable for single crystal X-ray diffraction. Complex 6.7 consists of three titanium centres, linked as a cluster by the two 6.7L ligands. The complex has the same gross structure as 6.6 with the same central core of two titanium atoms bridged together by the two oxime groups of 6.7L and with a third titanium centre 'trapped' above these two and joined to them by bridging oxime oxygen atoms and isopropoxide ligands. In total the core made up of the metal centres consists of one six membered ring, two five membered rings and two of the familiar Ti_2O_2 four membered rings as observed in complex 6.6. Each of the titanium centres has a distorted octahedral geometry.

The terminal isopropoxide ligands have typical bond lengths varying between 1.770(3)Å and 1.793(2)Å which is slightly shorter than the bond lengths seen in 6.6. As with complex 6.6 the bridging isopropoxides have asymmetric bond lengths with the bond to Ti(2), which sits above the other two metal centres, being shorter {1.966(2)Å [Ti(2)-O(70)] and 1.981(2)Å [Ti(2)-O(40)]} than the bond to the other metal centre {2.073(2)Å [Ti(3)-O(70)] and 2.083(3)Å [Ti(1)-O(40)]}. As with the terminal isopropoxide bonds, the bonds to the bridging isopropoxide are slightly shorter than the equivalent interactions in complex 6.6. Complex 6.7 is a third example of the triply bridging bonding mode for an oximate with titanium and the oximates have typical nitrogen to titanium bond lengths {2.249(3)Å [Ti(1)-N(1)] and 2.249(3)Å [Ti(3)-N(2)]} which are slightly larger than those observed in 6.6. The oxygen atoms on the oximate groups each bridge two titanium centres with the bridging bonds being asymmetric in nature. In both cases the titanium-oxygen bond from the oximate is longer to Ti(2) {2.188(2)Å [Ti(2)-O(1)] and 2.199(3)Å [Ti(2)-O(3)]} than to the other metal centre {2.060(2)Å [Ti(1)-O(3)] and 2.054(2)Å [Ti(3)-O(1)]}. In comparison to the corresponding bond lengths in complex 6.6 these bonds are more asymmetric with the bonds to Ti(2) being longer and the bonds to the other metal centres being slightly shorter. The aryloxide ligands have typical bond lengths {1.924(3)Å [Ti(1)-O(2)] and 1.916(3)Å [Ti(3)-O(4)]} which are again slightly longer than those observed in the complex of the non-derivatised oxime.

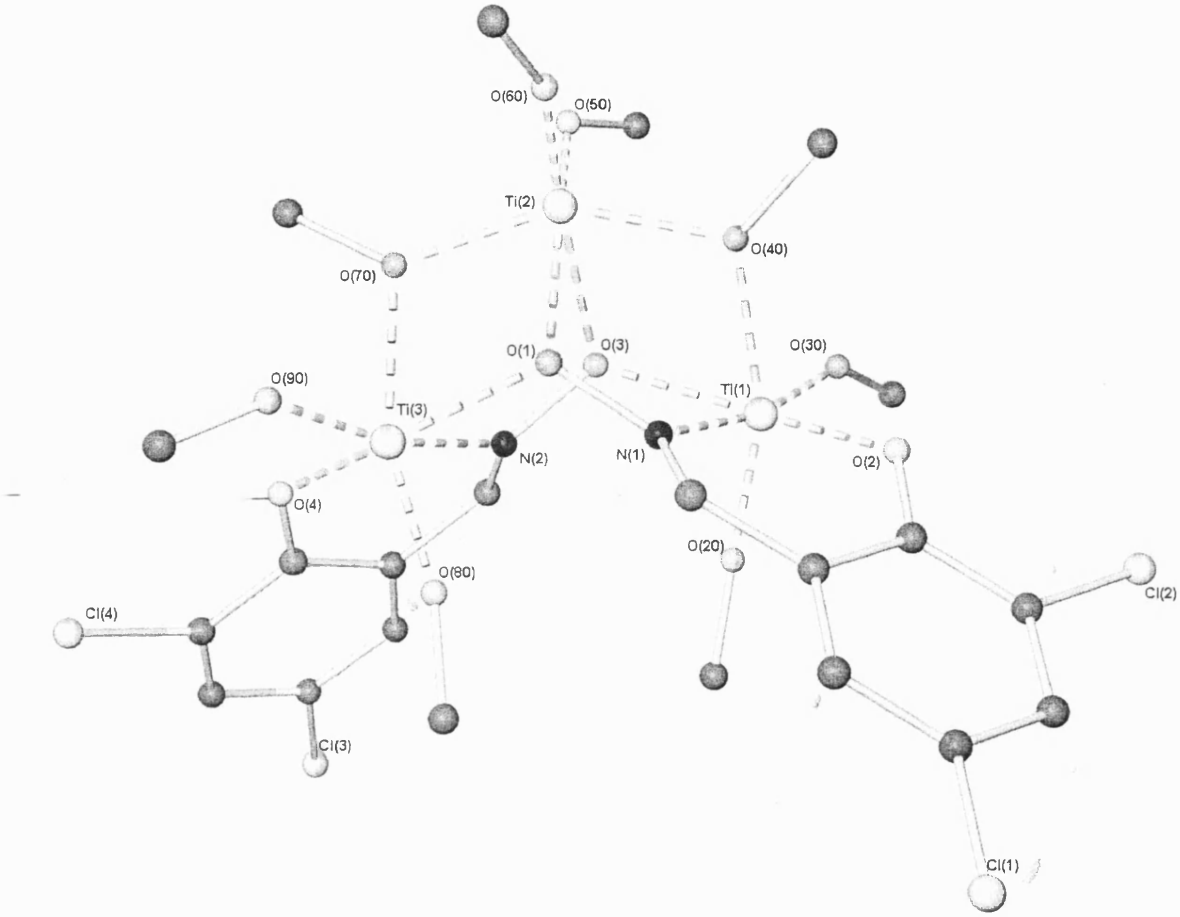

Figure 6.25: Molecular structure of complex 6.7 (hydrogen atoms and isopropoxide methyl groups not shown for clarity)

Solution Dynamics of Complex 6.7

The ^{1}H NMR spectrum of the complex shows the same features as seen in 6.6 with distinct signals for the isopropoxide C**H** protons which are associated with Ti(2) (4.66-4.83ppm) and those which are not (4.39 and 4.94ppm). This distinctive pattern of signals shows that no dissociation of the 'trapped' TiPT molecule occurs in solution at room temperature, as discussed previously for 6.6. ^{13}C NMR data for 6.7 also suggests that the gross solid-state structure is maintained in solution with four signals for the isopropoxide **C**H carbon atoms (74.7, 78.1, 78.4 and 79.0ppm).

Complex 6.8

Two equivalents of ligand 6.8L react readily with three equivalents of TiPT to give a yellow crystalline product, which was suitable for single crystal X-ray diffraction. Complex 6.8 consists of three titanium centres, linked as a cluster by the two 6.8L ligands. The complex has the same gross structure as 6.6 and 6.7 with the same central core of two titanium atoms bridged together by the two oxime groups of 6.8L and with a third titanium centre 'trapped' above these two and joined to them by bridging oxime oxygen atoms and isopropoxide ligands. In total the core made up of the metal centres consists of one six membered ring, two five membered rings and two of the familiar Ti_2O_2 four membered rings.

The terminal isopropoxide ligands have Ti-O bond lengths ranging from 1.763(4)Å to 1.816(3)Å which is much broader than the range observed for the previous two structures and actually covers almost the complete range of bond lengths observed in both these structures. As with the previous two complexes the bridging isopropoxides have asymmetric bond lengths with the bonds to Ti(3), which lies above the other two metal centres {1.970(4)Å [Ti(3)-O(13)] and 1.985(4)Å [Ti(3)-O(16)]} being shorter than those to the other two centres{2.091(3)Å [Ti(1)-O(13)] and 2.093(3)Å [Ti(2)-O(16)]}. The oximate groups bonding mode is identical to that observed in 6.6 and 6.7, with typical nitrogen to titanium bond lengths {2.229(4)Å [Ti(1)-N(2)] and 2.220(4)Å [Ti(2)-N(4)]} and asymmetric bonds to the oximate oxygen atoms with longer bonds to the 'trapped' Ti(3) {2.188(3)Å [Ti(3)-O(8)] and 2.192(3)Å [Ti(3)-O(4)]} than to the other metal centre {2.034(4)Å [Ti(1)-O(8)] and 2.056(3)Å [Ti(2)-O(4)]}. The titanium-aryloxide bond lengths are also typical for these types of

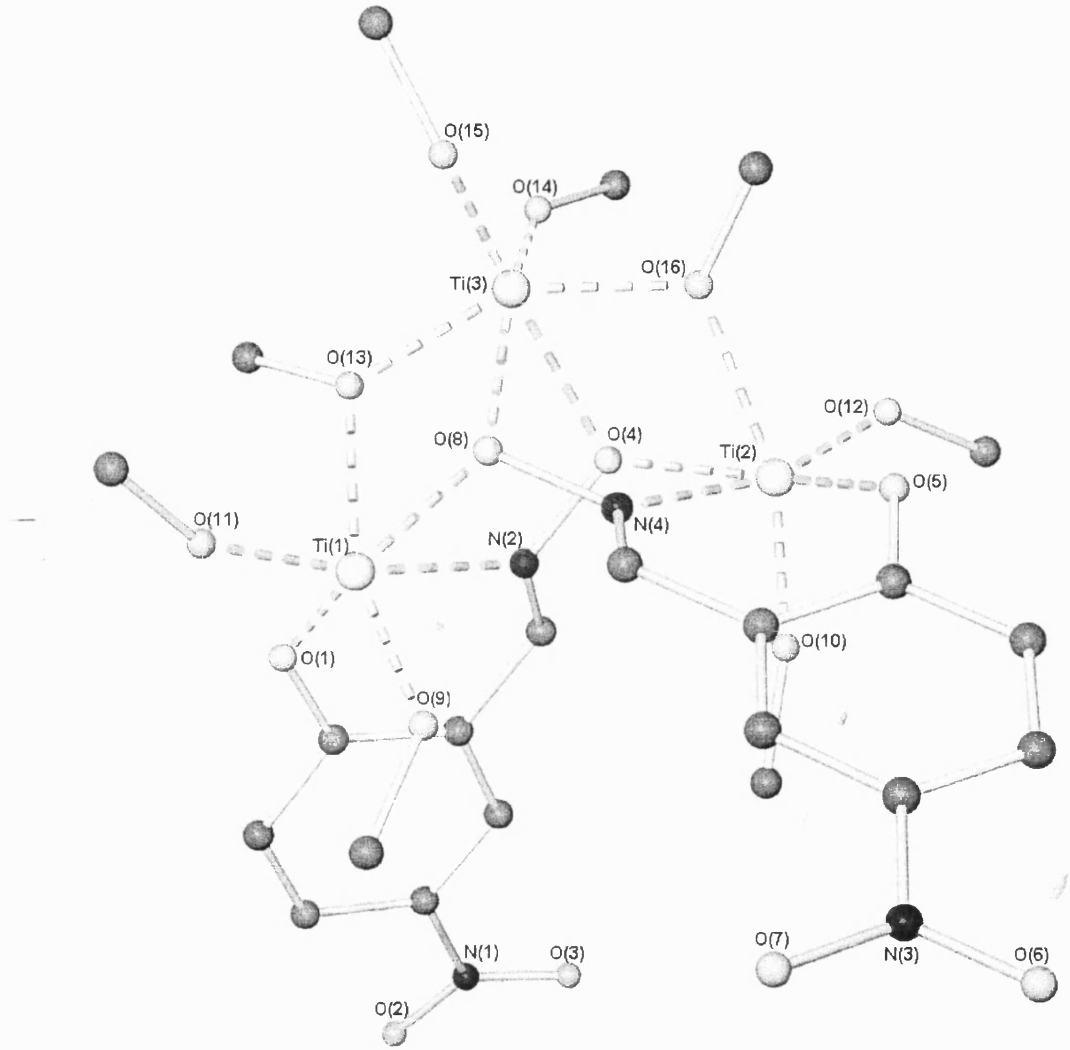

Figure 6.26: Molecular structure of complex 6.8 (hydrogen atoms and isopropoxide methyl groups not shown for clarity)

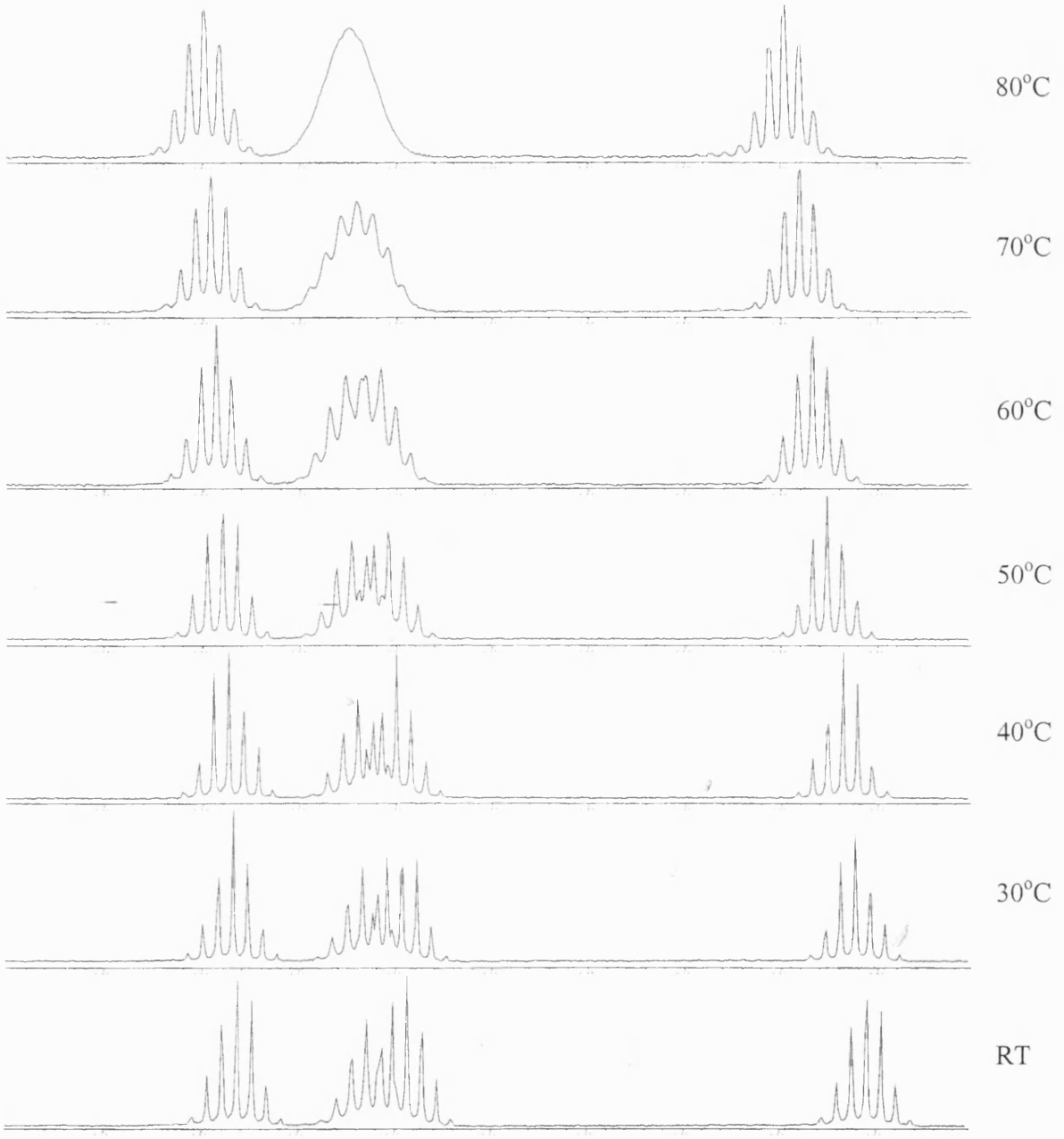

Figure 6.27: VT ^{1}H NMR spectra of the isopropoxide CH region (4-5ppm) of complex 6.6. The spectra shows exchange at high temperature but no dissociation.

interaction {1.923(4)Å [Ti(1)-O(1)] and 1.939(4)Å [Ti(2)-O(5)]} and of similar length to those observed in complex 6.7.

Solution Dynamics of Complex 6.8

The ^{1}H NMR spectrum of the complex shows the same features as seen in complexes 6.6 and 6.7 with distinct signals for the isopropoxide C**H** protons which are associated with Ti(3) (4.70 and 4.77ppm) and those which are not (4.42 and 4.95ppm). This distinctive pattern of signals shows that no dissociation of the 'trapped' TiPT molecule occurs in solution at room temperature, as discussed previously for 6.6. As with complex 6.6 when a variable temperature ^{1}H NMR experiment is carried out on the complex the only process observed is exchange of the isopropoxide groups on the 'trapped TiPT' group (Figure 6.28 on the previous page). ^{13}C NMR data for 6.8 also confirms that the gross solid-state structure is maintained in solution with four signals for the isopropoxide **C**H carbon atoms (76.1, 80.0, 80.3 and 80.6ppm).

Summary of Salicylaldoximates

The three complexes (6.6, 6.7 and 6.8) described above are, with the complex previously synthesised by our group, the first salicylaldoximate complexes of titanium to be crystallographically characterised. Although some small variations in bond lengths are observed in the different complexes, which could be due to the substituents on the phenyl ring, there is very little difference between each of the structures and their gross features are identical. Although we have failed to isolate suitable crystals of the other form of titanium salicylaldoximate the results described above show that ligands of this type form at least two structural forms with TiPT depending on the stoichiometry of the reaction. We have also shown that the different forms synthesised in this way have widely differing properties and that these salicylaldoxime based ligands are highly versatile for the formation of various titanium alkoxide complexes.

Complex 6.9

In addition to studying the chemistry of phenolic oximes with titanium alkoxides we also wished to look at the reactivity of ligands in which an oxime was the only anionic group. To do this we carried out a number of reactions of TiPT with 2-pyridine aldoxime and its derivatives.

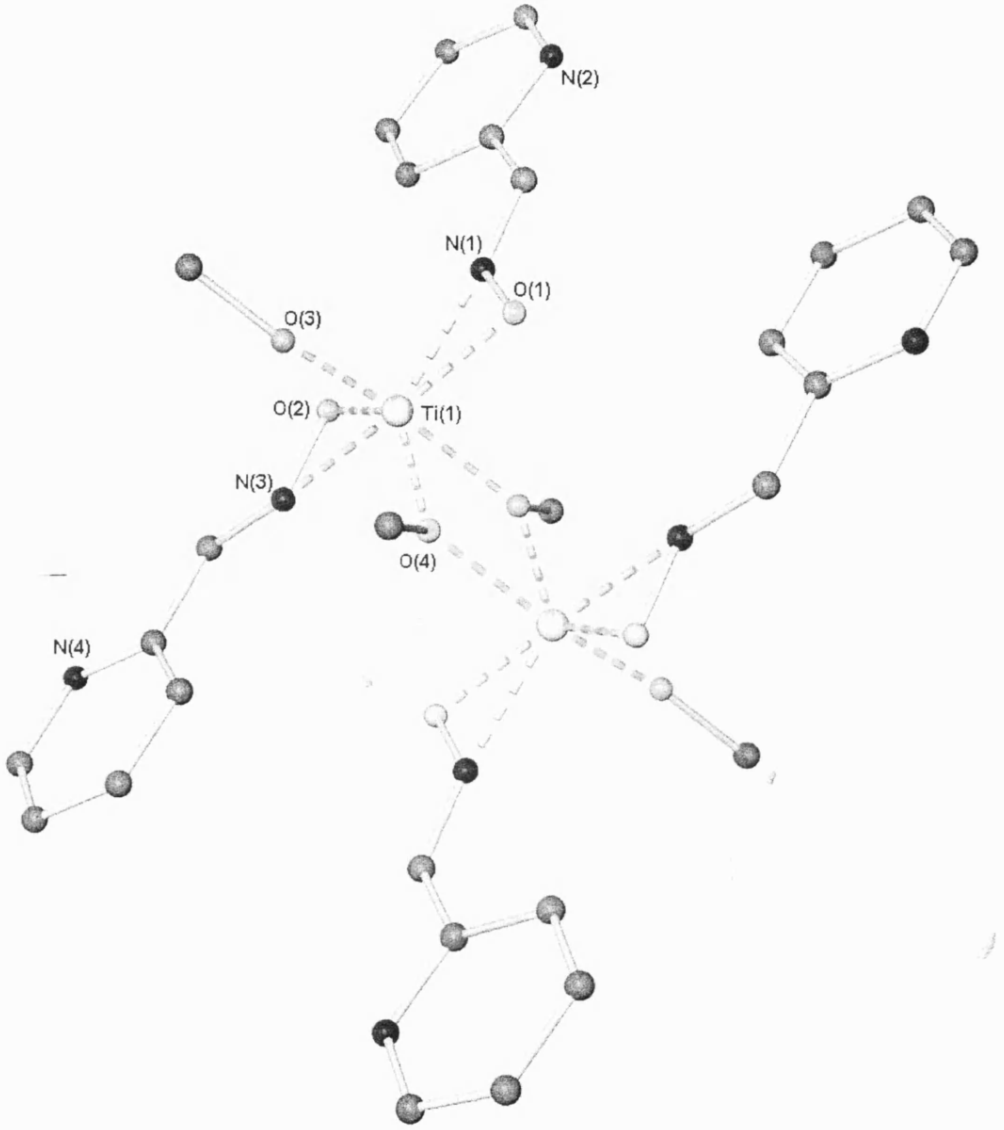

Figure 6.29: Molecular structure of complex 6.9 (hydrogen atoms and isopropoxide methyl groups not shown for clarity)

Two equivalents of Ligand 6.9L react readily with one equivalent of TiPT to yield a crop of colourless crystals, which were suitable for single crystal X-ray diffraction. The asymmetric unit for the complex consists of half of the molecule with all of the isopropoxide ligands disordered over two positions. The resulting complex consists of two titanium centres, which are bridged by two isopropoxide ligands. In addition each of the metal centres is ligated by two oximate groups, which coordinate through both their nitrogen and oxime atoms, and a monodentate isopropoxide ligand. This gives each titanium centre a total coordination number of seven.

The bond lengths from titanium to the ligands are typical for these types of interaction. The terminal alkoxides have normal bond lengths {1.782(3)Å [Ti(1)-O(3)]} and the bridging alkoxides show a familiar asymmetry in their bond lengths {1.988(2)Å [Ti(1)-O(4#)] and 2.082(2)Å [Ti(1)-O(4)]}. The oximes are non-bridging and bond to a single metal centre through the oxygen and nitrogen atoms of the oximate group, the pyridyl nitrogen takes no part in bonding. This bonding mode through nitrogen and oxygen to a single metal centre has been observed by Thewalt et al. in the only previously characterised titanium oximate complexes, as described in the introduction to this chapter[8], but is actually quite rare in metal oximate complexes and is only observed with a few metals including Cu, Mo, Os and Ru[12]. The bond lengths to the oxime oxygen {1.978(3)Å [Ti(1)-O(1)] and 1.969(3)Å [Ti(1)-O(2)]} are significantly shorter than those to the nitrogen atoms {2.047(3)Å [Ti(1)-N(1)] and 2.149(3)Å [Ti(1)-N(2)]}. As would be expected the bond lengths to both oximate atoms are shorter than those observed in compounds 6.6-6.8 due to the non-bridging nature of the oximato group.

As with most of the following complexes with 2-pyridyl aldoxime derived ligands the ^{1}H NMR spectrum of complex 6.9 was very broad and difficult to assign, possibly due to a monomer-dimer equilibrium. Only one broad signal was observed for the isopropoxide C**H** protons (4.52ppm), which suggests that the complex is fluxional in solution.

---

[12] Examples include; R. Ruiz, J. Sanz, F. Lloret, M. Julve, J. Faus, C. Bois and M.C. Munoz, *J. Chem. Soc. Dalton Trans.*, 3035 (1993) [Cu]; G.P. Khare and R.J. Doedens, *Inorg. Chem.*, **16**, 907 (1977) [Mo]; R. Castarlouas, M.A. Esteruelas, E. Gutierrez-Puebla, Y. Jean, A. Lledos, M. Martin and J. Tomas, *Organometallics*, **18**, 4296 (1999) [Os]; H. Werner, T. Daniel, W. Knaup and D. Nurnberg, *J. Organomet. Chem.*, **462**, 309 (1993) [Ru]

Complex 6.10

Complex 6.9 is highly moisture sensitive and after its recovery by filtration the resulting liquid yielded a number of large colourless crystals, which were suitable for single-crystal X-ray diffraction. The X-ray crystal structure obtained from these crystals was found to be the product of partial hydrolysis of complex 6.9 along with two molecules of acetonitrile. The product retains two titanium centres but these are now bridged by a μ-oxo group and the nitrogen and oxygen atoms of two oximate ligands. Each of the two oximate ligands bonds to one titanium through its nitrogen atom and the other through its oxygen atom. In addition each titanium centre is also coordinated to two monodentate alkoxides, one of which, at O(5), is disordered over two positions, and the pyridyl group of one of the oxime ligands. In total each of the metal centres has six ligand donors and this results in a distorted octahedral arrangement at the metal centre. The core of the molecule now consists of two five membered rings made up of the two titanium atoms, the oxo bridge and one of the oxime N-O groups.

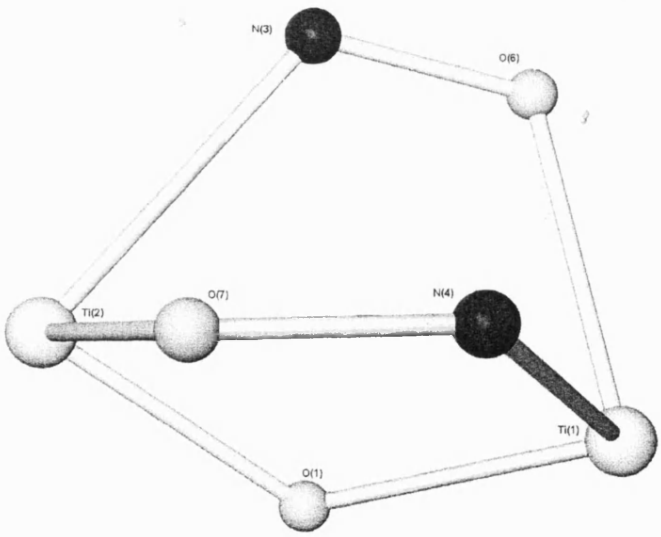

Figure 6.29: Molecular structure of the core of complex 6.10

The bond lengths to the terminal isopropoxide ligands are typical for titanium complexes with little variation {1.815(2)Å [Ti(1)-O(2)], 1.821(2)Å [Ti(1)-O(3)], 1.819(2)Å [Ti(2)-O(4)] and 1.828(2)Å [Ti(2)-O(5)]} although in each case the ligand

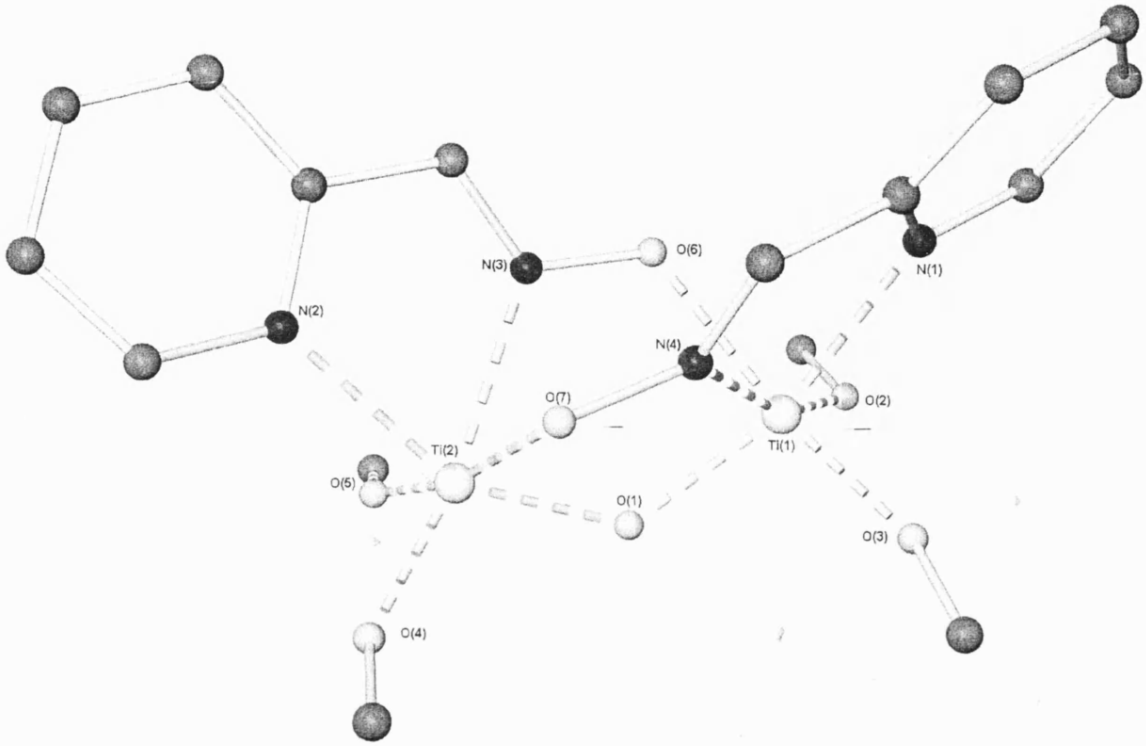

Figure 6.30: Molecular structure of complex 6.10 (hydrogen atoms and isopropoxide methyl groups not shown for clarity)

trans to the oximate oxygen atom has a slightly longer bond than that trans to the oximate nitrogen atom. The bridging oxo-group also has typical bond lengths {1.842(2)Å [Ti(1)-O(1)] and 1.832(2)Å [Ti(2)-O(1)]} as do the pyridyl nitrogen groups {2.248(2)Å [Ti(1)-N(1)] and 2.244(2)Å [Ti(2)-N(2)]}} which take part in the bonding in the hydrolysed product. The bond lengths to the oxime groups from the metal centre are significantly longer in 6.10 than they were in the parent compound and are similar in length to those seen in the bridging oxime groups in compounds 6.6-6.8. The nitrogen atoms of the oximate groups {2.231(2)Å [Ti(1)-N(4)] and 2.223(2)Å [Ti(2)-N(3)]} have similar bond lengths at both Ti centres as do the oxygen atoms {2.088(2)Å [Ti(1)-O(6)] and 2.113(2)Å [Ti(2)-O(7)]}.

The hydrolysis of 6.9 during normal air sensitive manipulations seems to suggest that the complex containing terminally ligated oxime ligands is very moisture sensitive. As of yet we have been unable to prove what the source of hydrolysis is although the most likely explanation is that the glassware was not completely dry and adventitious water is involved. An interesting feature of the hydrolysis is that the ligands which are displaced are terminal oximates rather than isopropoxide ligands suggesting either that these are the most reactive sites in complex 6.9 or that the thermodynamic stability of complex 6.10 drives the reaction.

The ^{1}H NMR spectrum of 6.10 correlates well with the stoichiometry of the crystal structure with all the expected peaks present. The spectrum shows two distinct septets for the isopropyl C**H** groups (4.49 and 4.99ppm), which suggests that the complex is not fluxional in solution. The origin of the two peaks is probably the fact that the two isopropoxide groups are in different environments on the titanium centre with one trans to an oximate nitrogen donor and one trans to an oximate oxygen donor. The fact that these two types of isopropoxide groups give rise to separate signals in the NMR suggests that little or no exchange of these isopropoxides is taking place in solution.

Complex 6.11

The reaction of 6.11L with TiPT was carried out under identical conditions to those used for the synthesis of complex 6.9 and resulted in the formation of a small amount

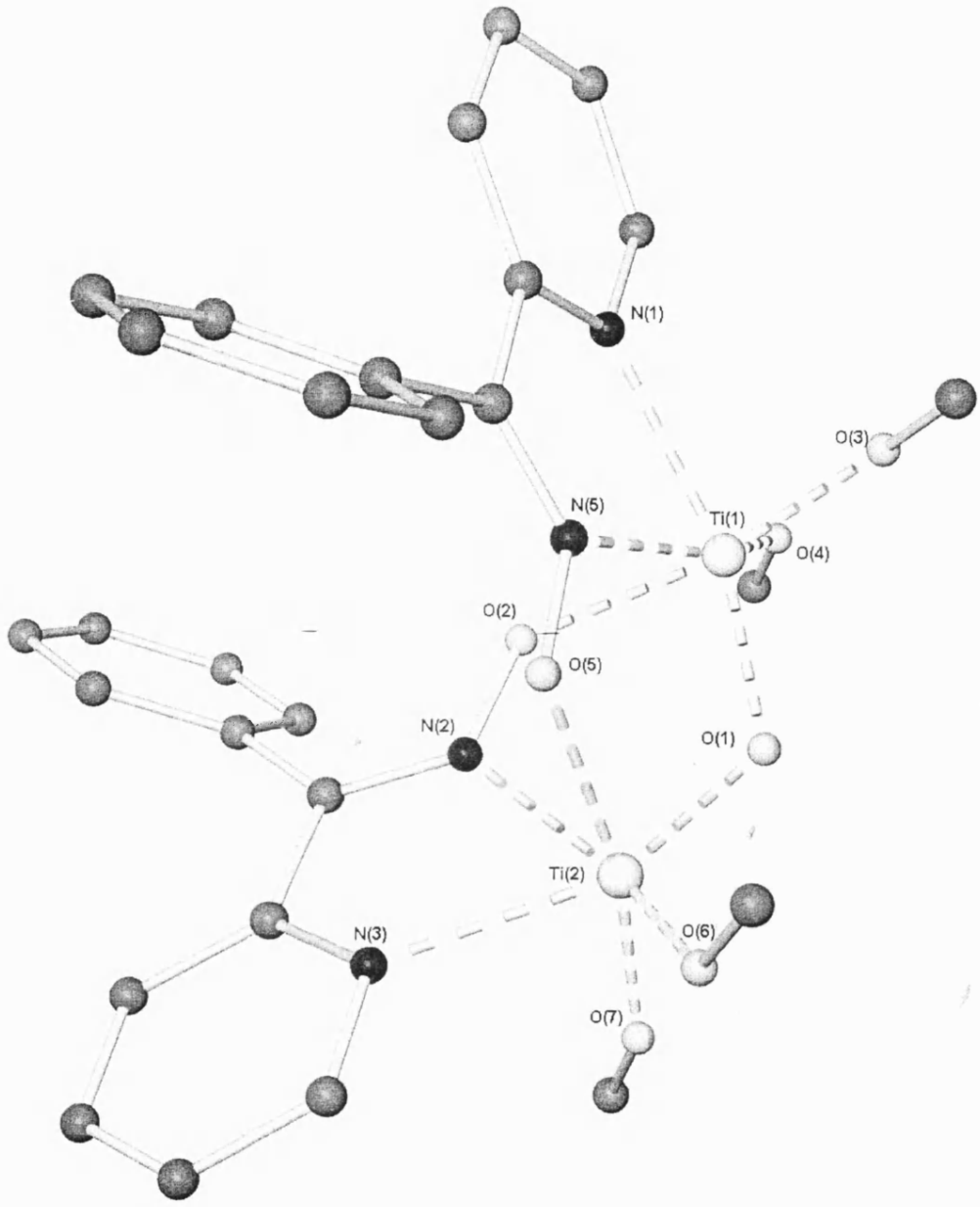

Figure 6.31: Molecular structure of complex 6.11 (hydrogen atoms and isopropoxide methyl groups not shown for clarity)

of a solid product. This product was recovered by filtration and the liquid stored under argon. The ^{1}H NMR spectrum of the first product was very broad and difficult to assign but seems to suggest that the initial product is an analogue of complex 6.9. On standing the filtrate yielded a small number of large crystals of a second product, complex 6.11, which were suitable for single crystal X-ray-diffraction. The crystal structure was found to consist of one molecule of an analogue of the hydrolysis product 6.10 and two molecules of acetonitrile. The product has two titanium centres which are bridged by a μ-oxo group and the nitrogen and oxygen atoms of two oxime ligands. Each of the two oxime ligands bonds to one titanium through its nitrogen atom and the other through its oxygen atom. In addition each titanium centre is also coordinated to two monodentate alkoxides and the pyridyl group of one of the oxime ligands. In total each of the metal centres has six ligand donors and this results in a distorted octahedral arrangement at the metal centre. The core of the molecule consists of two five membered rings made up of the two titanium atoms, the oxo bridge and one of the oximate N-O groups.

The bond lengths at the metal centres are all typical for interactions of their type. No distinction in bond length is seen between each of the terminal isopropoxides which are all of similar length {1.820(3)Å [Ti(1)-O(3)], 1.821(3)Å [Ti(1)-O(4)], 1.831(3)Å [Ti(2)-O(6)] and 1.813(3)Å [Ti(2)-O(7)]}. The bridging oxo-group also has typical bond lengths {1.836(3)Å [Ti(1)-O(1)] and 1.824(3)Å [Ti(2)-O(1)]} as do the pyridyl nitrogen groups {2.240(4)Å [Ti(1)-N(1)] and 2.229(4)Å [Ti(2)-N(3)]}} which take part in the bonding in the hydrolysed product as seen in complex 6.10. The bond lengths to the oximate groups from the metal centre are similar in length to those seen in the bridging oximate groups in compound 6.10. The nitrogen atoms of the oximate groups {2.228(4)Å [Ti(1)-N(5)] and 2.218(4)Å [Ti(2)-N(2)]} have similar bond lengths at both Ti centres as do the oxygen atoms {2.103(3)Å [Ti(1)-O(2)] and 2.091 (3)Å [Ti(2)-O(5)]}.

As with the hydrolysis product 6.10 we still do not know what is the cause of the hydrolysis we have observed to form complex 6.11. However, the reactivity of the initial terminally-bound oxime product to the hydrolysing species must be extremely high as the reactions were carried out under rigorous moisture and oxygen free

conditions under which no other titanium species which we have synthesised have been hydrolysed.

The ^{1}H and ^{13}C NMR spectra of the hydrolysis product 6.11 showed two distinct septets for the isopropoxide C**H** groups (4.56 and 5.00ppm), evidence which suggests that the complex is not fluxional in solution.

Complex 6.12

The reaction of 6.12L with TiPT was carried out under identical conditions to those used for the synthesis of complexes 6.9 and 6.11 and resulted in the formation of a small amount of a solid product. This was recovered by filtration and the liquid stored. The ^{1}H NMR of the first product was very broad and difficult to assign but seems to suggest that the initial product is an analogue of complex 6.9. On standing the filtrate yielded a small number of large crystals of a second product, complex 6.12, which were suitable for single crystal X-ray-diffraction. The crystal structure was found to consist of two molecules of an analogue of the hydrolysis products 6.10 and 6.11 and four molecules of acetonitrile, two of which were disordered over two positions. The product has two titanium centres, which are bridged by a μ-oxo group and the nitrogen and oxygen atoms of two oximate ligands. Each of the two oximate ligands bonds to one titanium through its nitrogen atom and the other through its oxygen atom. In addition each titanium centre is also coordinated to two monodentate alkoxides and the pyridyl group of one of the oximate ligands. In total each of the metal centres has six ligand donors and this results in a distorted octahedral arrangement at the metal centre. The core of the molecule consists of two five membered rings made up of the two titanium atoms, the oxo bridge and one of the oximate N-O groups.

The bond lengths in the two molecules in the asymmetric unit are very similar and therefore this discussion will describe only the bond lengths on the molecule around Ti(1) and Ti(2). The bond lengths to the terminal isopropoxide are typical for interactions of this type {1.800(3)Å [Ti(1)-O(4)], 1.825(3)Å [Ti(1)-O(5)], 1.813(3)Å [Ti(2)-O(6)] and 1.831(3)Å [Ti(2)-O(7)]} as are the bond lengths to the oxo bridge {1.833(2)Å [Ti(1)-O(3)] and 1.827(2)Å [Ti(2)-O(3)]}. In each of the oximate ligands

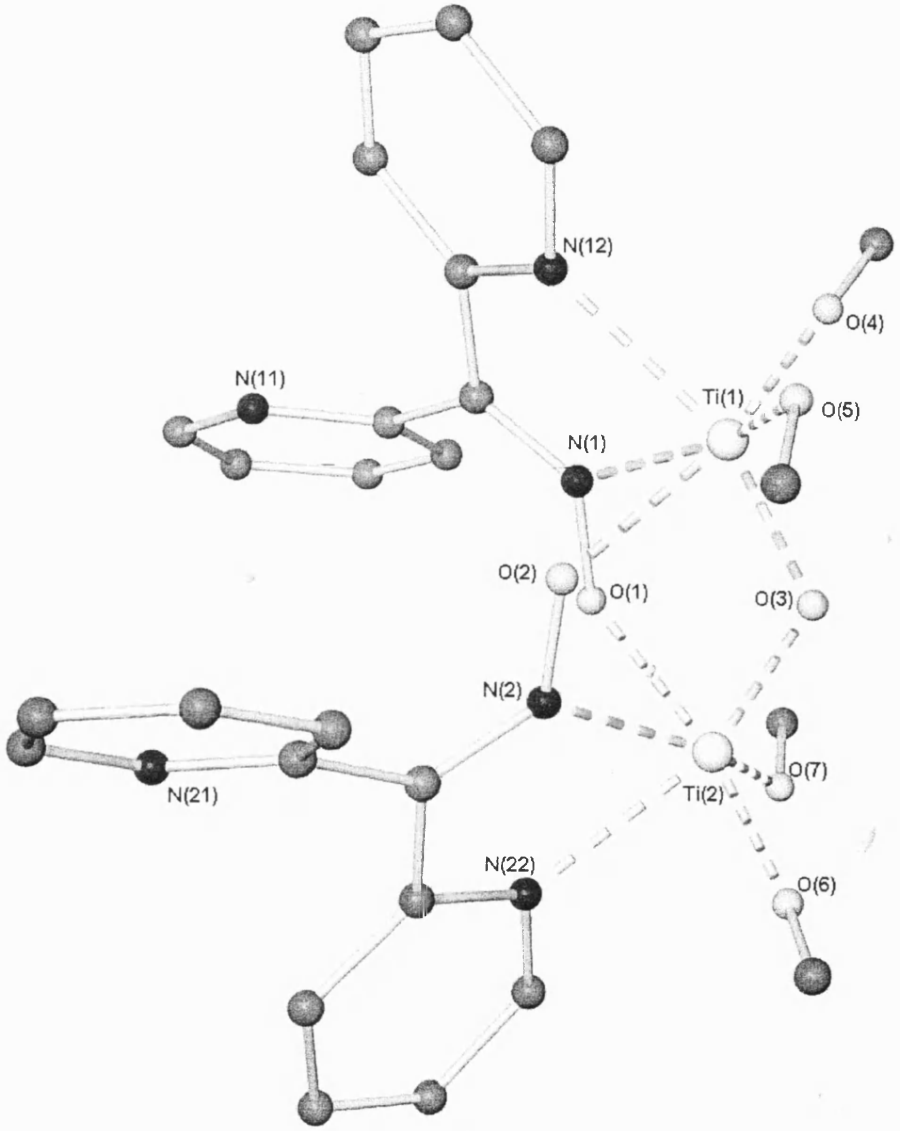

Figure 6.32: Molecular structure of complex 6.12 (hydrogen atoms and isopropoxide methyl groups not shown for clarity)

one of the pyridyl nitrogen atoms is bonded to a titanium atom while the other plays no part in bonding. The bond lengths from the pyridyl nitrogen atoms to the metal centres are of typical lengths {2.232(3)Å [Ti(1)-N(12)] and 2.234(3)Å [Ti(2)-N(22)]}. The bond lengths to the oximate groups from the metal centre are similar in length to those seen in the bridging oximate groups in compounds 6.10 and 6.11. The nitrogen atoms of the oximate groups {2.227(3)Å [Ti(1)-N(1)] and 2.229(3)Å [Ti(2)-N(2)]} have similar bond lengths at both Ti centres as do the oxygen atoms {2.106(2)Å [Ti(1)-O(2)] and 2.099 (2)Å [Ti(2)-O(1)]}.

As with the hydrolysis products discussed previously (6.10 and 6.11) we still do not know what the cause of the hydrolysis we have observed to form complex 6.12 is. However, the reactivity of the initial terminally bound oximate product to the hydrolysing species must be extremely high as the reactions were carried out under rigorous moisture and oxygen free conditions under which no other titanium species which we have synthesised have been hydrolysed.

The ^{1}H and ^{13}C NMR spectra of the hydrolysis product 6.12 show that the solid-state structure is maintained in solution. The ^{1}H NMR spectrum shows two distinct septet signals for the isopropoxide C**H** protons at 4.55ppm and 5.02ppm, which suggests that the isopropoxide ligands undergo no exchange processes on the NMR timescale and that the gross solid-state structure is maintained. In addition the ^{13}C spectrum also shows two signals at 75.8ppm and 76.9ppm for the isopropoxide **C**H atom confirming the above evidence.

Summary

The reactions with the non-phenolic oxime ligands 6.9L, 6.11L and 6.12L follow the same route for all three ligands with initial synthesis of an unstable complex with terminally bound oxime ligands. These compounds are then readily hydrolysed, even under inert atmosphere conditions, to the more stable complexes 6.10, 6.11 and 6.12 in which the oximate ligands bridge two metal centres. In all cases the ligand lost in the hydrolysis process is a terminally bound oximate resulting in dimeric products with two titanium atoms, two bridging oximates and a bridging oxo species.

We still have no evidence for why an oximate ligand is lost rather than an isopropoxide during this hydrolysis and this could be due to either the lability of the ligand or the stability of the resulting complex. These complexes, which are readily hydrolysed to known products, may be useful starting materials for the sol-gel process described in the introduction to this thesis as well as being possible pre-catalysts for the synthesis of polyurethanes.

6.4 Summary of Complexes 6.1-6.12

The complexes described in chapter 6 cover a range of ligands related to the Schiff bases described in the earlier chapters but with new functionalities. In all cases they are the first structurally characterised titanium complexes with these ligands and represent the basis for a large amount of future work. The work described has shown that addition of functionality in this way can allow the formation of novel structural types with widely varying solution and structural properties which were not possible to form with Schiff bases.

Hydrazones

The complexes of the hydrazone ligands (6.1 and 6.2) showed no deprotonation of the hydrazone NH_2 group, probably due to the oxophillicity of Ti. This led to formation of interesting supramolecular architectures the form of which could be altered, and potentially controlled, by the R groups on the salicylaldimine aryloxide ring of the hydrazone ligand. In addition these NH_2 groups may, in the future, allow formation of mixed metal complexes or play an active part in polymerisation catalysis.

Azines

The complexes of the azine ligands (6.3-6.5) had similar structures to previously reported metal complexes of these ligands. At the molecular level the substituents on the salicylaldimine aryloxide groups had little effect on the structures. However, on the supramolecular level introduction of Lewis base groups in the 2-position allowed formation of intramolecular H-bonds and intermolecular N-Br interactions, which caused formation of a supramolecular ladder. In the future it may be possible to exploit these Lewis base groups in the formation of mixed metal complexes or to order substrates during catalytic reactions.

Oximes

Three salicylaldoxime complexes have been fully reported (6.6-6.8) along with a brief description of a second type of titanium salicylaldoximate. These cluster complexes with multiple Ti centres have been shown to be stable even at elevated temperatures and their formation to be stoichiometrically controlled. In addition these complexes exhibit a new triply bridging oximate bonding mode, which has not been previously observed in titanium oximates.

Finally, a number of highly moisture sensitive non-phenolic titanium oximates have been reported along with their hydrolysis products. These show the lability of terminally bound oximate ligands and the relative stability of the same groups when bridging. As well as being potentially effective pre-catalysts these hydrolytically unstable complexes may be useful sol-gel precursors.

In summary, this chapter describes the first investigations into the synthesis of complexes with these ligand types as potential pre-catalysts and shows the large range of structural attributes, which can be observed in the product complexes even with a small range of ligands.

Chapter 7

Synthesis, Isolation and Structural Characterisation of Some Miscellaneous Titanium Alkoxide Complexes

The following chapter discusses the synthesis and characterisation of a number of titanium alkoxide complexes, which do not fit easily into the other sections of this thesis, but are interesting either as pre-catalysts in their own right or as precursors for the activated complexes in the subsequent chapter.

The three main groups discussed in the following chapter are ligands containing the 2,6-di-*tert*-butyl phenol group, amino alcohol ligands and the tris-hydroxy ligand 2,6-bis-hydroxymethyl-*p*-cresol. As an introduction to this chapter the first section will describe the previous work using these ligands with titanium, which has been reported in the literature, followed by a discussion of the solution and solid-state structures of the complexes we have synthesised.

7.1 Introduction

7.1.1 2,6-Di-*tert*-butyl Phenol Ligands

Although the reactivity of titanium alkoxides with monodentate phenols has been extensively studied in the past[1], some papers have alluded to the seemingly anomalous reactivity of ligands containing the 2,6-di-*tert*-butyl phenol group. The following section describes the reports, which have appeared in the literature, of the reactivity of these ligands with titanium species. The main aspect of these papers is that titanium species and particularly titanium tetra-isopropoxide (TiPT) do not react as readily with this phenol as with others. For most titanium (IV) species a maximum of two phenol ligands can be reacted with the starting material unless complex routes are used. For alkoxides higher than ethoxide only one phenol can be reacted and this is thought to be due to the steric demands of the ligands.

The first example of a titanium complex with a ligand of this type to be structurally characterised was reported in 1984 by Jones et al[2].

[1] D.C. Bradley, R.C. Mehrotra, I.P. Rothwell and A.Singh, '*Alkoxo and Aryloxo Derivatives of Metals*', Academic Press, London, Chapter 6, (2001)
[2] R.A. Jones, J.G. Hefner and T.C. Wright, *Polyhedron*, **3**, 1121 (1984)

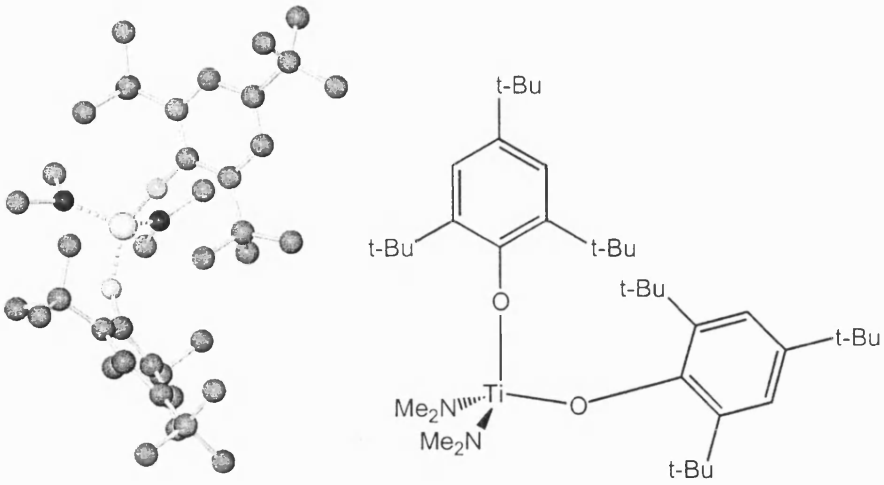

Figure 7.1: Jones' bis-phenolate complex

They discovered that on reaction of a large excess of the ligand with $Ti(NMe_2)_4$ a maximum of two of the amide ligands were replaced due to the steric bulk of the phenol. They also showed that by reaction with Me_3SiCl the corresponding bis-chloro complex could be formed.

In 1985 Rothwell et al. reported the reaction shown in figure 7.2 below, to synthesise compounds with the formula $Ti(OAr)_2(Hal)_2$ but found it impossible to substitute more than two halogen ligands by this route[3].

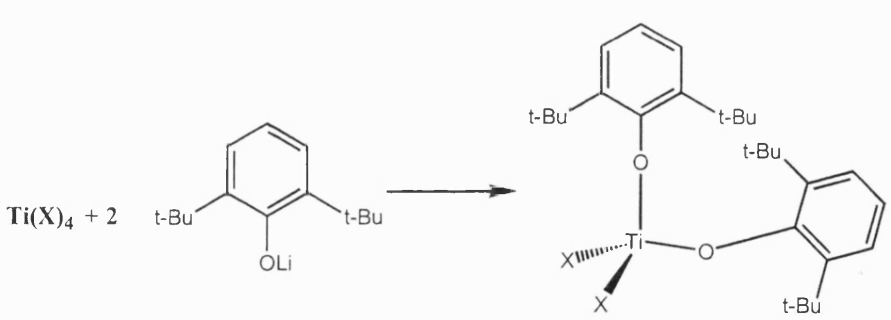

Figure 7.2: Rothwell route to the bis-phenolates

[3] S.L. Latesky, J. Keddington, A.K. Mcmullen, I.P. Rothwell and J.C. Huffman, *Inorg. Chem.*, **24**, 995 (1985)

Rothwell et al. did manage to produce compounds with the formula $Ti(OAr)_3(Hal)$ but only through oxidation of the extremely reactive starting material $Ti(OAr)_3$ which itself could only be synthesised by the reaction shown in figure 7.3 below.

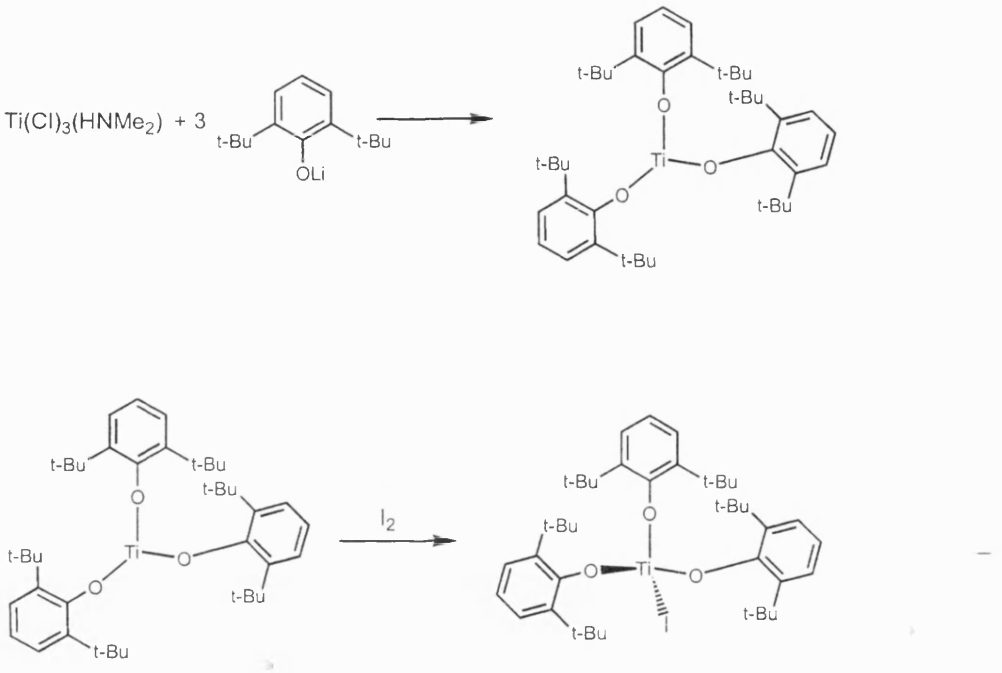

Figure 7.3: Route to a tris-phenolate

The crystal structure of the highly hindered complex $Ti(OAr)_3(I)$ is shown in figure 7.4 below.

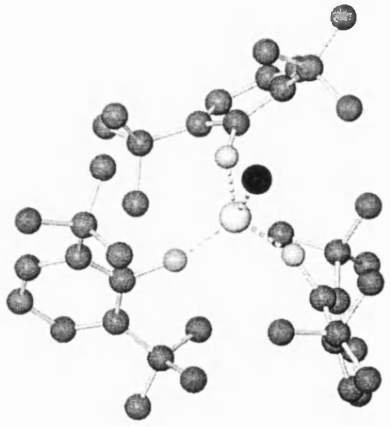

Figure 7.4: Sterically hindered tris-phenolate

In 1986 Lappert et al. reported the synthesis of a series of new compounds with the formula $Ti(OAr)_2(Cl)_2$ in which the OAr ligand was a 2,6-di-*tert*-butyl phenol derivative[4]. They reacted these titanium species with a series of sodium alkoxides including sodium methoxide, ethoxide and *tert*-butoxide and found that only the methoxide could exchange for both chloro ligands with the other alkoxides giving the monosubstituted product.

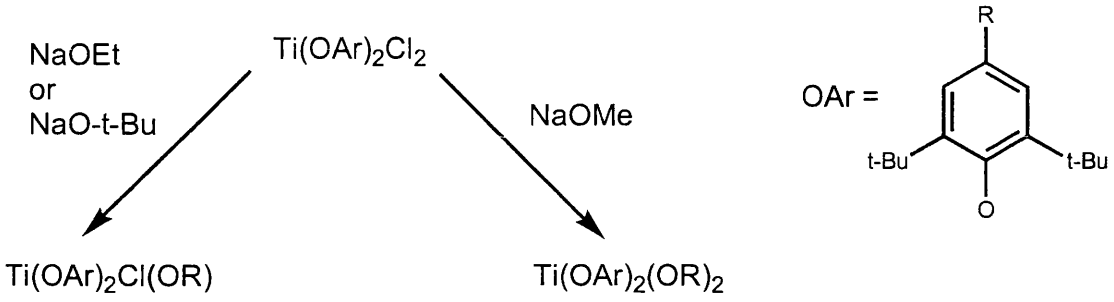

Figure 7.5: Synthesis of mixed alkoxide/aryloxide complexes

In 1994 Heppert et al. reported the first use of ligands with more than one 2,6-di-*tert*-butyl phenol unit when they reacted the ligand below with one and two equivalents of TiPT to give the products shown below[5].

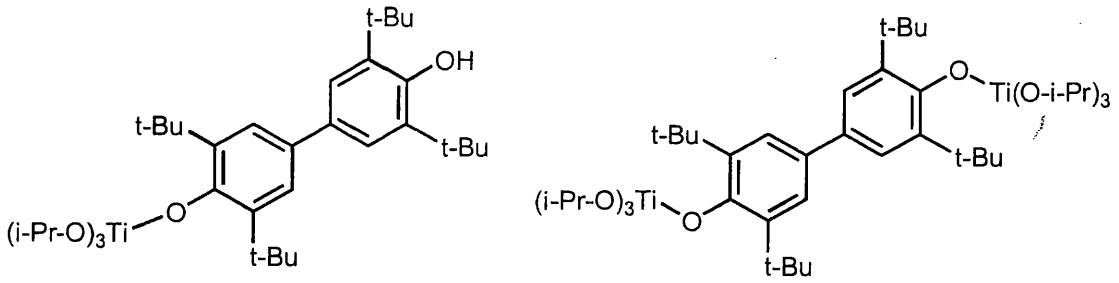

Compound **X** Compound **Y**

Figure 7.6: Mono and di-substituted bis-phenolates

They reported that compound **X** could be observed in solution but when attempts were made to isolate it in the solid-state only compound **Y** was seen. During the report they

[4] A.W. Duff, R.A. Kamarudin, M.F. Lappert and R.J. Norton, *J. Chem. Soc. Dalton Trans.*, 489 (1986)
[5] D.L. Barnes, N.W. Eilerts and J.A. Heppert, *Polyhedron*, **13**, 743 (1994)

also describe the reactions of similar ligands with sterically less demanding groups in the ortho positions on the phenol. These compounds were shown to form complexes with two or more phenols coordinated to each titanium centre, an observation which was not seen for the sterically crowded phenol which only ever substituted one alkoxide on each titanium. This observation is evidence to suggest that the replacement of two isopropoxide ligands by these phenols is disfavoured.

In 1996 Matilainen et al. reported the crystal structure of the complex in figure 7.7 below which was synthesised by the reaction of $TiCl_4$ with the appropriate sodium aryloxide. They reported that the compound was an effective catalyst for polyolefin synthesis although quantitative values were not given[6].

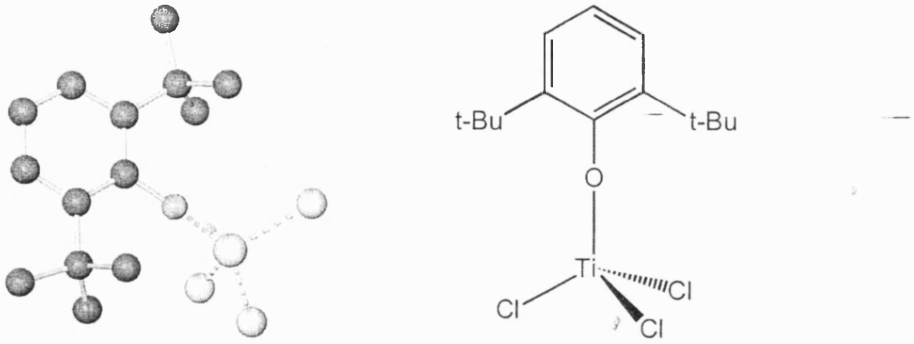

Figure 7.7: Matilainen's mono-phenolate complex

Finally in 2000 Nielson et al. reported the synthesis of a further $Ti(OAr)(Cl)_3$ compound which they showed to be unreactive with neutral donor ligands such as bipy despite the coordinatively unsaturated nature of the titanium centre, a fact which they ascribed to the steric demand of the phenoxide[7].

In summary, the chemistry of the aryloxides of these sterically demanding phenols has been covered in a number of papers but very little work has been done to describe their reactivity with titanium tetra-alkoxides or to utilise their unusual, sterically driven, reactivity.

[6] L. Matilainen, M. Klinga and M. Leskela, *Polyhedron*, **15**, 153 (1996)
[7] A.J. Nielson, P. Schwerdtfeger and J.M. Waters, *J. Chem. Soc. Dalton Trans.*, 529 (2000)

7.1.2 Amino alcohol chelates

The following section describes some of the previous work carried out with ligands containing one non-phenolic hydroxyl group and an amino group and in particular their reactions with titanium species. The reactivity of these ligands with metal alkoxides has been studied for most metals and various bonding modes observed. However complexes of these ligands with titanium alkoxides are not well known and only a few reports have been published in the literature. In almost all of the reports no deprotonation is seen at the amino group in contrast to other metals where it can be quite common.

In 1974 Mehrotra et al. reported some reactions of amino ethanol derivatives with titanium tetra-ethoxide and isopropoxide with formulae ranging from $TiL(OR)_3$ to the homoleptic tetra-amino-alkoxide. These derivatives were almost all oils and were characterised by infra red spectroscopy and elemental analysis[8].

As part of a wider study, Jordan et al., reported the formation of the complexes shown in figure 7.8 below formed by the reaction of the parent ligands with $Ti(NMe_2)_4$.

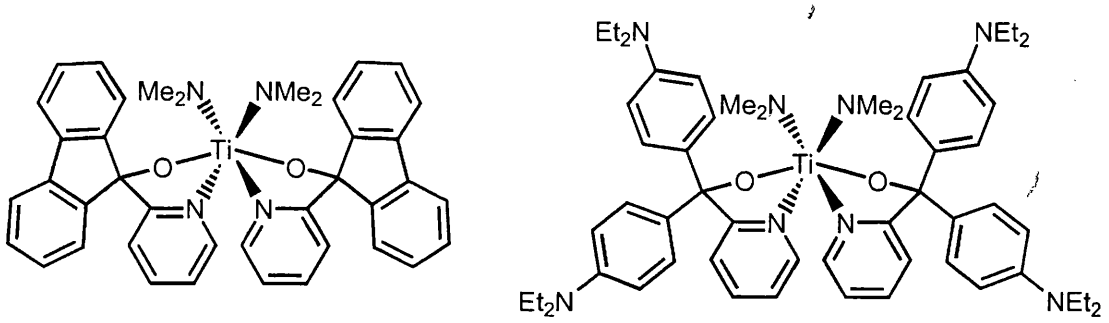

Figure 7.8: Polyolefin catalysts based on amino-alcohol liogands

These complexes were shown to be active for polyethylene synthesis, although in neither case, were they as active as the corresponding zirconium compound[9].

[8] P.C. Bharara, V.D. Gupta and R.C. Mehrotra, *Z. Anorg. Allg. Chem.*, **403**, 337 (1974); P.C. Bharara, V.D. Gupta and R.C. Mehrotra, *J. Indian. Chem. Soc.*, 859 (1974)
[9] I. Kim, Y. Nishihara, R.F. Jordan, R.D. Rogers, A.L. Rheingold and G.P.A. Yap, *Organometallics*, **16**, 3314 (1997)

In 1998 Gagne et al. reported the synthesis of a number of complexes of the chiral amino alcohol shown in figure 7.9 below and other related ones with titanium tetra-amides and tetra-isopropoxide[10].

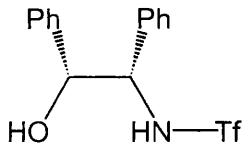

Figure 7.9: A chiral amino alcohol with an activated amine

This work resulted in the synthesis of several complexes, one of which is shown below, in which two titanium centres were bridged by the amino alcohol ligands. These ligands were deprotonated at the amino nitrogen atom due to the strongly electron withdrawing groups which increased the acidity of the NH group.

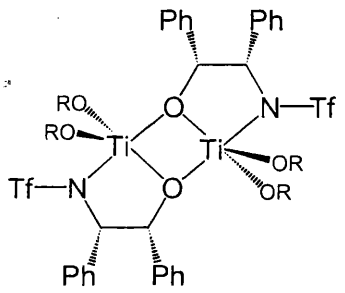

Figure 7.10: Titanium species formed from a chiral amino alcohol

7.1.3 2,6-bis-hydroxymethyl-*p*-cresol

Almost no work has been published on the use of this ligand with titanium species. The only report in the primary literature is by Henry et al. in 2001 in which they reacted the ligand in a 2:1 ratio with titanium tetra-ethoxide in air. The resulting complex which had the formula $Ti_4(O)_2(LH_2)_2(LH)_2(L)_2$ is shown in figure 7.11 overleaf[11].

[10] L.T. Armistead, P.S. White and M.R. Gagne, *Organometallics*, **17**, 4232 (1998)
[11] A. Rammal, F. Brisach and M. Henry, *J. Am. Chem. Soc.*, **123**, 5612 (2001)

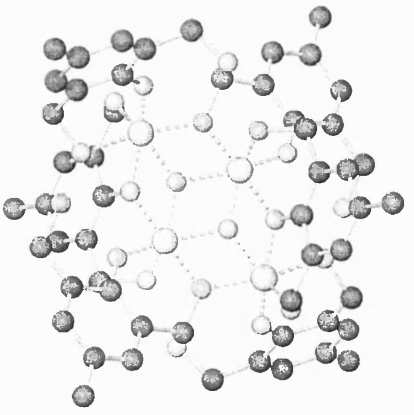

Figure 7.11: Titanium oxo cluster formed with 2,6-bis-hydroxymethyl-*p*-cresol

They used this hydrolysed complex both to observe the hydrolysis of a chelate complex of this kind and to study the inclusion properties of the cavities formed by the ligands.

7.1.4 Relevance to polyurethane synthesis

The work described in the introduction to this chapter covers a diverse range of titanium alkoxide complexes. Of the complexes described, those with amino alcohols and the *p*-cresol derivative should be interesting as pre-catalysts for polyurethane synthesis in their own right. Study of non-phenolic amino alcohol complexes will allow us to assess the effect that the lack of a phenolic group has on the catalytic properties of a titanium alkoxide chelate while complexes of the *p*-cresol derivative should allow us to study the use of cluster complexes of titanium as catalysts. The third type of complex, with 2,4-di-*tert*-butyl phenoxide ligands, will be exploited as an alternative source of $Ti(OR)_x$ fragments in the synthesis of the activated complexes discussed in the following chapter.

7.2 Discussion of the complexes

The ligands used in the chapter are shown in figure 7.12 below.

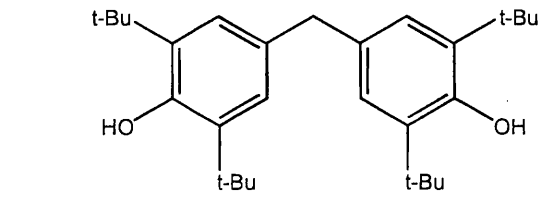

7.1L

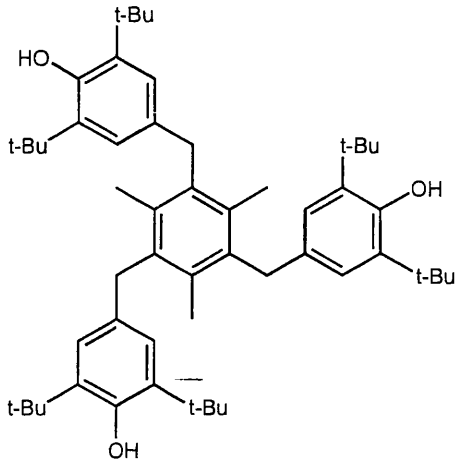

7.3L

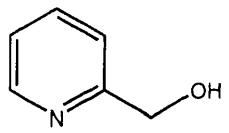

7.4L

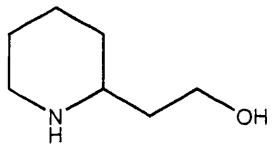

7.5L

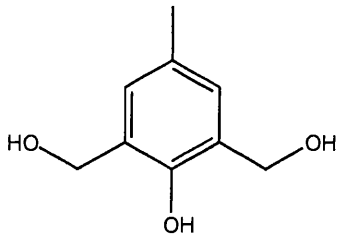

7.6L

Figure 7.12: Ligands used in chapter 7

7.2.1 Complexes with 2,6-di-*tert*-butyl phenol ligands

Complex 7.1

The ligand 4,4'-methylene-bis-(2,6-di-*tert*-butyl phenol) reacted readily with one equivalent of TiPT to yield a yellow fibrous product, which was highly soluble in all common organic solvents and unsuitable for single crystal X-ray diffraction. The ^{1}H NMR spectrum of the product showed that reaction of 7.1L (LH_2) with the metal source had yielded a compound with the formula $Ti(LH)(O^iPr)_3$ with the ligand being deprotonated only once and with the phenol that remains protonated seeming to have no interaction with a metal centre.

The ^{1}H NMR spectrum showed distinct peaks for the isopropoxide groups at 4.66ppm (C**H**) and 1.28ppm (CH_3) and these groups were seen to be in 3:1 ratio to the ligand. In addition to the expected signals for the ligand moiety a signal was observed at 4.96ppm, which correlated to one O**H** group per complex, showing that only one phenol on each ligand was deprotonated. It is also interesting to note that the signal for the phenolic O**H** proton consists of two peaks, which, as no coupling is seen to other groups are probably due to two distinct environments rather than coupling to a second group. Sufficient explanation for the presence of two peaks due to this group has not been reached although it is probably due to the presence of two O**H** isomers in solution, which interconvert slowly on the NMR timescale when the bisphenol is bound to titanium.

It is extremely rare in the chemistry of titanium alkoxides to find a complex with a protonated phenolic group, due to the ease of substitution of a monodentate alkoxide by a phenol. The probable explanation for why further deprotonation of the ligand does not occur is probably the large steric bulk of the phenol. The results agrees with the observations by Heppert et al.[5] using a similar ligand who had seen behaviour of this type in solution but had been unable to isolate the product.

Complex 7.2

One equivalent of the ligand 4,4'-methylene-bis-(2,6-di-*tert*-butyl phenol) reacted readily with two equivalents of TiPT to yield a yellow product, which was soluble in all common organic solvents and unsuitable for single crystal X-ray diffraction. The

^{1}H NMR spectrum of the product showed that reaction of LH_2 with two equivalents of the metal source had yielded a compound with the formula $(O^iPr)_3Ti$-(L)-$Ti(O^iPr)_3$ with the ligand being deprotonated twice and bridging two metal centres. As with the previous complex each titanium centre seems to be ligated by only one 2,6-di-*tert*-butyl phenol group.

The ^{1}H NMR spectrum showed distinct peaks for the isopropoxide groups at 4.64ppm (**CH**) and 1.27ppm (CH_3) and these groups were seen to be in 6:1 ratio to the ligand. Unlike the previous complex no signal is observed for the phenolic **OH** group and all the other expected ligand signals are present. The ^{13}C NMR spectrum also gave the expected signals at 26.7ppm (CH_3) and 78.5ppm (**C**H) for the isopropoxide groups.

Although it proved impossible to isolate suitable crystals for X-ray diffraction for complexes 7.1 and 7.2 we are able to postulate the structures of these complexes from the available data. The predicted structures for the two complexes are shown in figure 7.13 below.

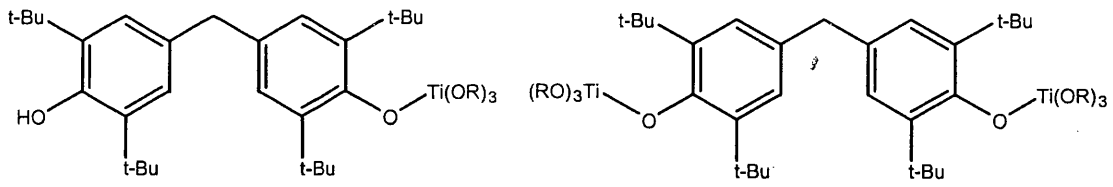

7.1 **7.2**

Figure 7.13: Proposed structures of 7.1 and 7.2

Complex 7.3

To extend our study of the reactivity of 2,6-di-*tert*-butyl phenol containing ligands with TiPT we moved from the bis-phenol ligand used in the previous two complexes to a tris-phenol ligand containing three of the sterically hindered phenol groups. One equivalent of 7.3L reacted readily with three equivalents of TiPT to yield a crop of pale yellow crystals, which were suitable for single crystal X-ray analysis. The asymmetric unit consists of one molecule of the metal complex, which consists of one equivalent of the ligand with each phenolic group bonded to one metal centre and a

ratio of ligand to metal of 1:3. Each titanium centre is four coordinate and has a distorted tetrahedral geometry, the coordination sphere consisting of one phenolic ligand and three isopropoxide groups. Of the nine isopropoxide ligands in the structure seven are disordered over two positions {these are the groups at O(2), O(3), O(12), O(13), O(14), O(22) and O(24)}.

Unexpectedly the three titanium-containing arms of the ligand all point above the plane of the central benzene ring, something which might be expected to be disfavoured by the steric bulk of these arms. However this arrangement of the phenolic arms is also observed in the single crystal X-ray structure of the unreacted ligand (shown in figure 7.14 below), which also has all three arms above the plane of the central ring. Steric clashes are minimised by a twist of the rings, which moves them away from each other.

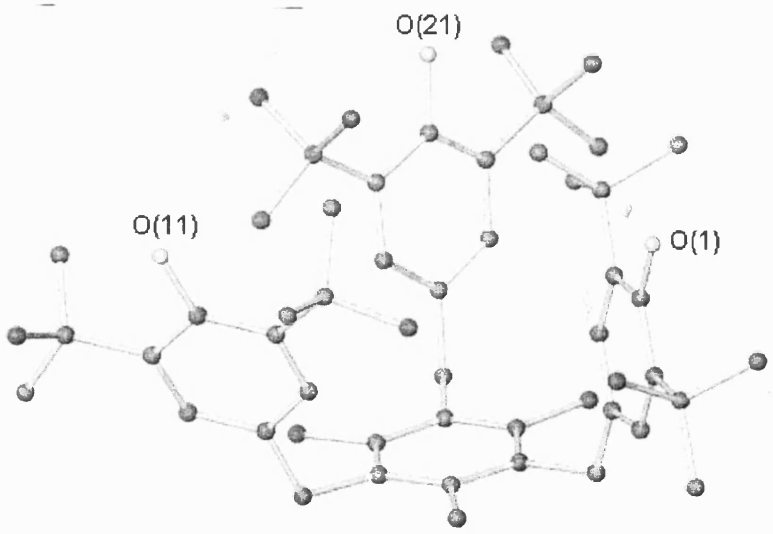

Figure 7.14: Molecular structure of ligand 7.3L (hydrogen atoms not shown for clarity).

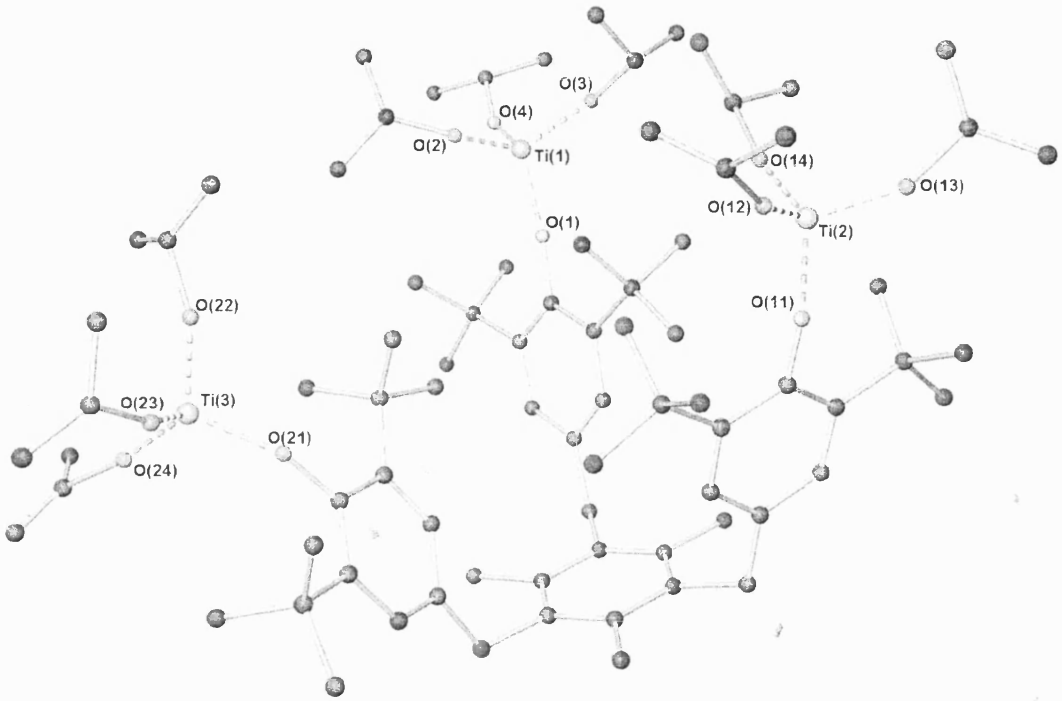

Figure 7.15: Molecular structure of complex 7.3 (hydrogen atoms not shown for clarity)

The bond lengths to the titanium centres are all typical for interactions of these types although the bonds to the aryloxides are quite short {1.807(2)Å [Ti(1)-O(1)], 1.823(2)Å [Ti(2)-O(11)] and 1.817(2)Å [Ti(3)-O(21)]}. The bonds to the terminal isopropoxides range between 1.73 and 1.78Å, values which are similar to these interactions in most titanium isopropoxide complexes.

The short titanium-aryloxide bond lengths in the crystal structure could suggest multiple bonding character in these bonds due to donation of π-electrons from the oxygen lone pairs to the metal centre. This observation is borne out by the C-O-Ti bond angles which are close to linear {170.3(2)° [C(14)-O(1)-Ti(1)], 167.5(2)° [C(44)-O(11)-Ti(2)] and 157.1(2)° [C(74)-O(21)-Ti(3)]} indicating that some double bonding character may be present. These values are similar to the bond angles observed in a product of the 1:1 reaction of TiPT with mesitol which had the same $Ti(OAr)(O^iPr)_3$ stoichiometry but which forms a dimer in the solid state with bridging alkoxides[12]. This mesitol complex had Ar-O-Ti bond angles of 166.2° and bond lengths of 1.812Å. In contrast a third titanium aryloxide, with the same $Ti(OAr)(O^iPr)_3$ stoichiometry and dimeric structure as the mesitol complex, but with 2,6-di-isopropyl phenol[13] has less linear bond angles (138.6°) and consequently a longer Ti-OAr bond length (1.856Å). Although these observations could point to some multiple bonding character in these complexes systematic analysis of titanium-isopropoxide bond lengths and angles in crystallographically defined complexes show little correlation, as has been previously stated in the introduction to this thesis (p. 8-10). The results may, in fact, be due to the highly electropositive and coordinatively unsaturated nature of the titanium centre coupled with the steric demands of the ligand.

If the carbon-oxygen bond lengths in the aryloxide groups of the complex are compared to the same lengths in the ligand they can be seen to be slightly shorter although the effect is not a large one. This effect would be expected as coordination to titanium would make the oxygen atom slightly more positive and shorten the C-O bond length. The values are shown in figure 7.16 overleaf.

[12] S.C. James, N.C. Norman and A.G. Orpen, *Acta Cryst. (Sect. C)*, **54**, 1261 (1998)
[13] D.R. Click, B.L. Scott and J.G. Watkins, *J. Chem. Cryst.*, **29**, 921 (1999)

Bond	Ligand (7.3L)	Complex (7.3)
O(1)-C(14)	1.388(2)Å	1.373(4)Å
O(11)-C(44)	1.386(2)Å	1.367(4)Å
O(21)-C(74)	1.381(2)Å	1.376(4)Å

Figure 7.16: Comparison of bond lengths in ligand 7.3L and complex 7.3

The ^{1}H NMR spectrum of complex 7.3 shows good agreement with the crystal structure with the expected signals for the isopropoxide groups at 1.19ppm (CH_3) and 4.56ppm (**C**H) and the expected ratio of isopropoxide groups to ligands of 9:1. The ^{13}C spectrum also gives the expected signals at 27.0ppm (CH_3) and 78.4ppm (**C**H) for the isopropoxide ligands.

The crystal structure of complex 7.3 is the first reported for a metal complex of this ligand although the ligand has been used to make polymeric products with tri-methyl aluminium, which are then used in separation technology for molecular recognition of ethers[14]. The structure of complex 7.3 seems to confirm the earlier results with ligand 7.1L and only one substitution is seen at each metal centre in contrast to the aluminium example above in which the metal centre is doubly substituted. The most probable reason for each metal only reacting with one phenol is that the steric bulk of the ligand combined with the isopropoxide ligands disfavours further reaction. This also agrees with the work described in the introduction that showed that with other ancillary ligands a second substitution is possible but that this is never observed in alkoxides higher than methoxide.

A further interesting point about complexes 7.1-7.3 is that on reaction with chelating ligands, such as 8-hydroxyquinoline or the Schiff bases described in Chapter 4, the new ligand displaces the aryloxide rather than an isopropoxide as shown in figure 7.17 overleaf.

[14] K. Maruoka, S. Nagahara and H. Yamamoto, *J. Am. Chem. Soc.*, **112**, 6115 (1990)

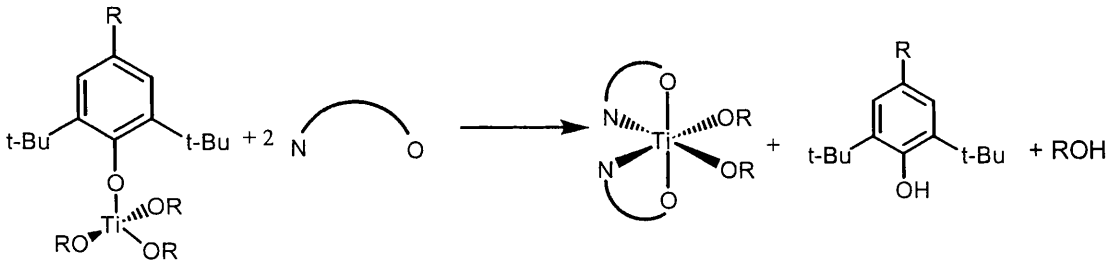

Figure 7.17: Reaction of a titanium-2,6-di-*tert*-butyl phenolate and a chelate ligand

This shows that in these reactions the aryloxide ligand is the most labile group in the complex although whether the driving force for the reaction is the lability of the aryloxide or the stability of the resulting product has not been discovered.

7.2.2 Complexes of amino alcohol ligands

Complex 7.4

Two equivalents of ligand 7.4L react readily with one equivalent of TiPT to yield a crop of large colourless crystals, which were suitable for single crystal X-ray diffraction. In addition both a charge density study and a neutron diffraction experiment were carried out, although these are outside the scope of this thesis.

The asymmetric unit of the single crystal X-ray structure consisted of one molecule of the complex which has a formula of $Ti(7.4L)_2(O^iPr)_2$. The titanium centre is six coordinate with the two ligands deprotonated at the hydroxyl group and chelating the metal centre through its oxygen and nitrogen donors. The geometry at the metal centre is distorted octahedral with the 7.4L oxygen donors in a trans-axial arrangement, the pyridyl donors cis-equatorial and isopropoxide ligands also cis-equatorial. The geometry is the most favourable one for complexes of this type as described in chapter 4 (configuration A, figure 4.5, p. 119).

The bond lengths of the alkoxide ligands to the metal centre are slightly outside the norm for bonds of this type with the terminal isopropoxide ligands having bonds to the metal, which are slightly longer than observed in most titanium isopropoxide structures {1.836(1)Å [Ti(1)-O(3)] and 1.835(1)Å [Ti(1)-O(4)]} but are still shorter than the bonds to the ligand hydroxymethyl alkoxide groups of ligand 7.4L

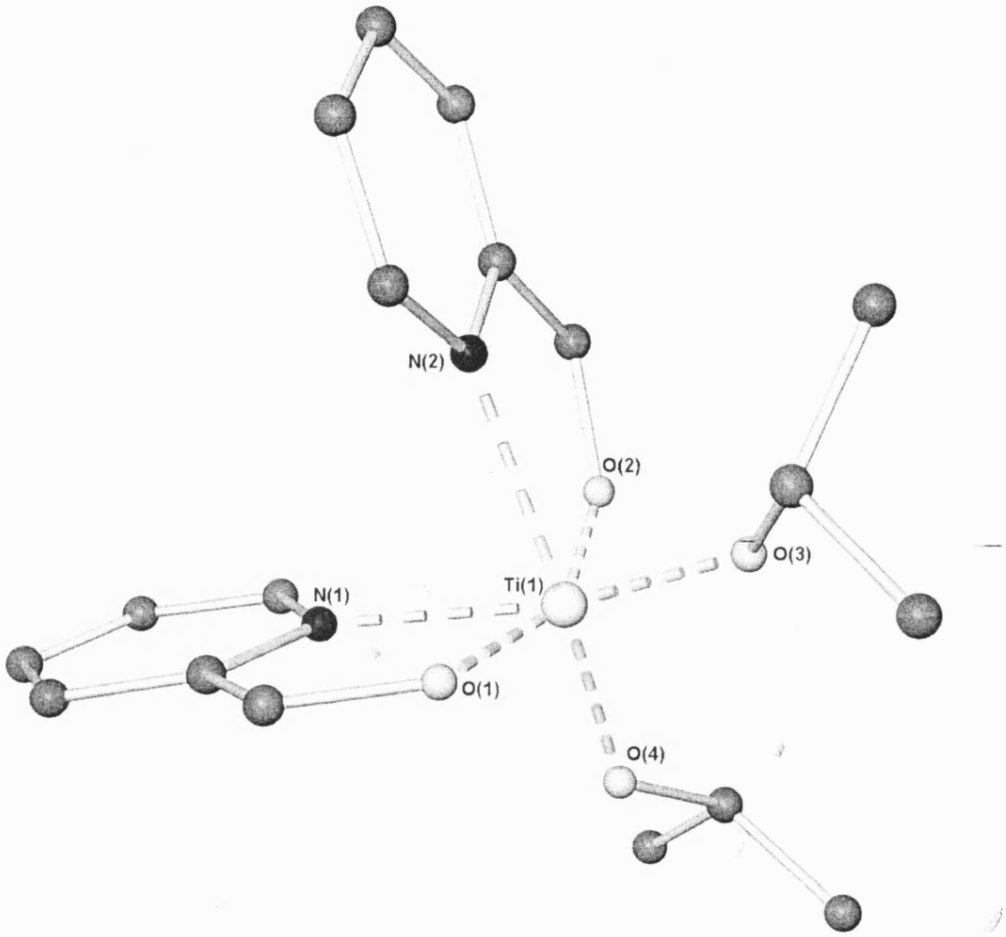

Figure 7.18: Molecular structure of complex 7.4 (hydrogen atoms omitted for clarity)

{1.900(1)Å [Ti(1)-O(1)] and 1.917(1)Å [Ti(1)-O(2)]}. The longer bond lengths to the 7.4L alkoxides could be due either to the constraints caused by chelation of the ligand or to the fact that these ligands are trans to each other while the monodentate isopropoxides are trans to pyridyl nitrogen donors. However, evidence from the structure of complex 7.6 would seem to suggest that the majority of the effect is due to the trans effect they experience. The pyridyl nitrogen donors themselves have typical bond lengths to titanium of 2.260(2)Å [Ti(1)-N(1)] and 2.281(1)Å [Ti(1)-N(2)].

The ^{1}H NMR spectrum of the complex suggests that the gross solid-state structure is maintained in solution with distinct signals for the isopropoxide groups, at 0.94ppm (CH_3) and 4.55ppm (C**H**), and the ligand in the correct ratio. It is important to note however that the signal for the methylene group of the ligand is a singlet (5.50 CH_2), which indicates that the ligand coordination is fluxional in solution making the two hydrogen atoms of this group equivalent. The ^{13}C NMR spectrum also agrees with the solid-state structure with signals for the isopropoxide ligands at 24.6ppm (CH_3) and 74.2ppm (**C**H).

Complex 7.5

Two equivalents of ligand 7.5L react readily with one equivalent of TiPT to yield a crop of colourless crystals, which were suitable for single crystal X-ray diffraction. The asymmetric unit consists of half a molecule of the titanium complex. The complex consists of two titanium centres each of which has one monodentate and one chelating 7.5L ligand, which are only deprotonated at oxygen, the chelating ligand bridges the dimer through its hydroxyethyl group. In addition each titanium centre retains two monodentate isopropoxide groups and has an overall coordination number of six. The titanium centres have a distorted octahedral geometry with the equatorial positions taken up by the cis monodentate isopropoxide ligands and the cis bridging chelate alkoxides. The NH of the chelating 7.5L moiety and the alkoxide of the terminal 7.5L ligand fill the axial positions. Each of the ligands is deprotonated only at the hydroxyethyl groups with the NH groups of the pyrrolidine groups being retained.

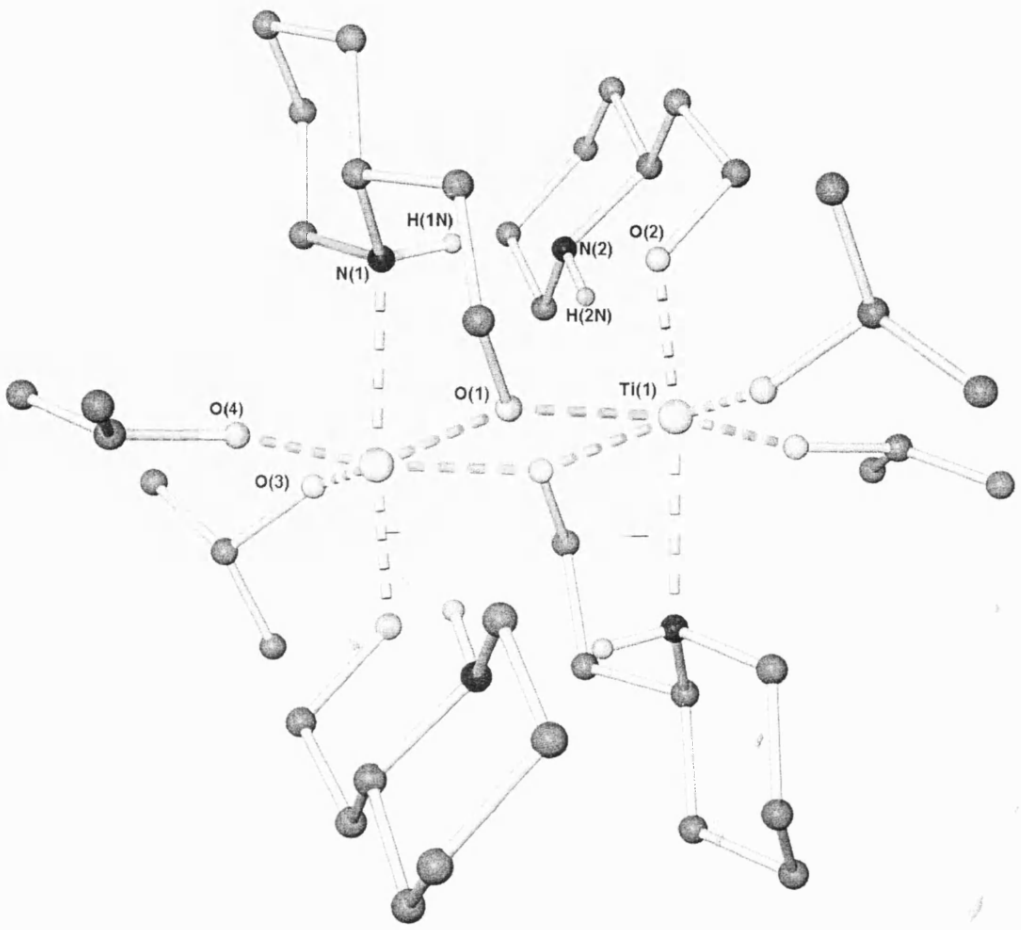

Figure 7.19: Molecular structure of complex 7.5 (non-amino hydrogen atoms omitted for clarity)

The bond lengths to the terminal isopropoxide ligands are non-equivalent with one being 0.03Å longer than the other {1.808(2)Å [Ti(1)-O(4)] and 1.841(2)Å [Ti(1)-O(3)]}. This difference in bond length correlates with a large difference in C-O-Ti bond angle for these two groups with the shorter bond having a bond angle which is much more linear {165.8° [C(40)-O(4)-Ti(1)]} than the longer bond {134.1° [C(30)-O(3)-Ti(1)]} which could be due to increased π-electron donation from the alkoxide at O(4). The bond lengths to the monodentate 7.5L ligands {1.858(2)Å [Ti(1)-O(2)]} are slightly longer than those to either of the monodentate isopropoxide ligands while as would be expected the bonds to the bridging 7.5L alkoxide are the longest and show a slight asymmetry {2.088(2)Å [Ti(1)-O(1)] and 2.038(2)Å [Ti(1)-O(1#)]}. The bond length to the pyrrolidine NH group from the titanium centre {2.348(2) [Ti(1)-N(1#)]} is of a typical length for a R_3N-Ti interaction.

Both the NH groups of the pyrrolidine ligands act as hydrogen bond donors in intramolecular hydrogen-bonding interactions in the solid-state as shown in figure 7.20 below. N(2) acts as a hydrogen bond donor to the hydroxyethyl oxygen atom of its own ligand {N(2)-H···O(2) [O(2)···H 2.237Å; N(2)-O(2) 2.922Å and N(2)-H-O(2) 130.0°]}. N(1) acts as a hydrogen bond donor in an interaction with the hydroxyethyl oxygen atom of the neighbouring terminal 7.5L ligand {N(1)-H···O(2) [O(2)···H 2.359Å; N(1)-O(2) 3.099Å and N(1)-H-O(2) 143.5°]}. The pyrrolidine NH hydrogen atoms are freely refined.

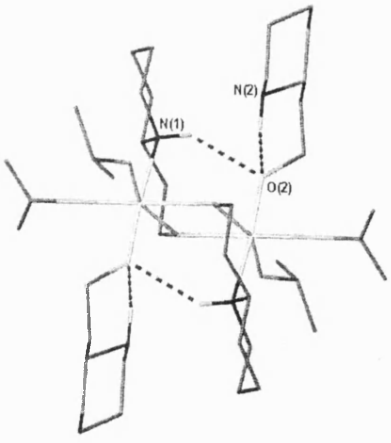

Fig 7.20: Intramolecular hydrogen bonding in complex 7.5

The ^{1}H NMR spectrum of complex 7.5 is quite broad and shows little fine structure. Signals due to the isopropoxide groups can be observed at 1.14ppm (CH_3) and 4.72ppm (CH) and only one signal is seen for the pyrrolidine NH groups (3.08ppm) suggesting that the solid-state structure is not maintained in solution. Two possible structures for the complex in solution are; an octahedral complex with two chelated 7.5L ligands or a four coordinate complex with all the ligands monodentate. The reality is probably a mixture of different compounds, which are rapidly interchanging in solution. The ^{13}C spectrum for the complex agrees with the ^{1}H spectrum in that it shows peaks for only one type of ligand environment and one isopropoxide environment (21.6ppm, CH_3, and 74.8ppm, CH).

7.2.3 Complex of a *p*-cresol derivative

Complex 7.6

Two equivalents of ligand 7.6L react readily with four equivalents of TiPT to yield a crop of colourless crystals, which were suitable for single crystal X-ray diffraction. The asymmetric unit consists of half a molecule of the titanium complex. The complex consists of four titanium centres, which are bridged by two of the 7.6L ligands, and ten isopropoxide ligands, two of which are bridging. The four titanium centres are linked in a chain in the centre of the cluster and can be split into two pairs; the outer two titanium atoms {Ti(2) and Ti(2#)} are five coordinate and have a distorted trigonal bipyramidal geometry, the inner two titanium centres {Ti(1) and Ti(1#)} are six coordinate and have a distorted octahedral geometry. The outer titanium atoms coordination sphere is made up of two terminal and one bridging isopropoxide ligands, a terminal ligand hydroxymethyl group and a bridging phenoxide. The inner titanium atoms coordination sphere is made up of two terminal and one bridging isopropoxides, two bridging ligand hydroxymethyl groups and a bridging phenoxide. The central core of complex 7.6 consists of a series of three corner sharing Ti_2O_2 rings (figure 7.23 p.276) similar to those seen in a number of poly-titanium complexes seen earlier in this thesis.

The bond lengths from the titanium centres to the terminal isopropoxides are all very similar {1.790(2)Å [Ti(1)-O(4)], 1.784(2)Å [Ti(1)-O(5)], 1.799(2)Å [Ti(2)-O(2)] and 1.788(2)Å [Ti(2)-O(3)]} and shorter than the titanium-ligand bond lengths for the

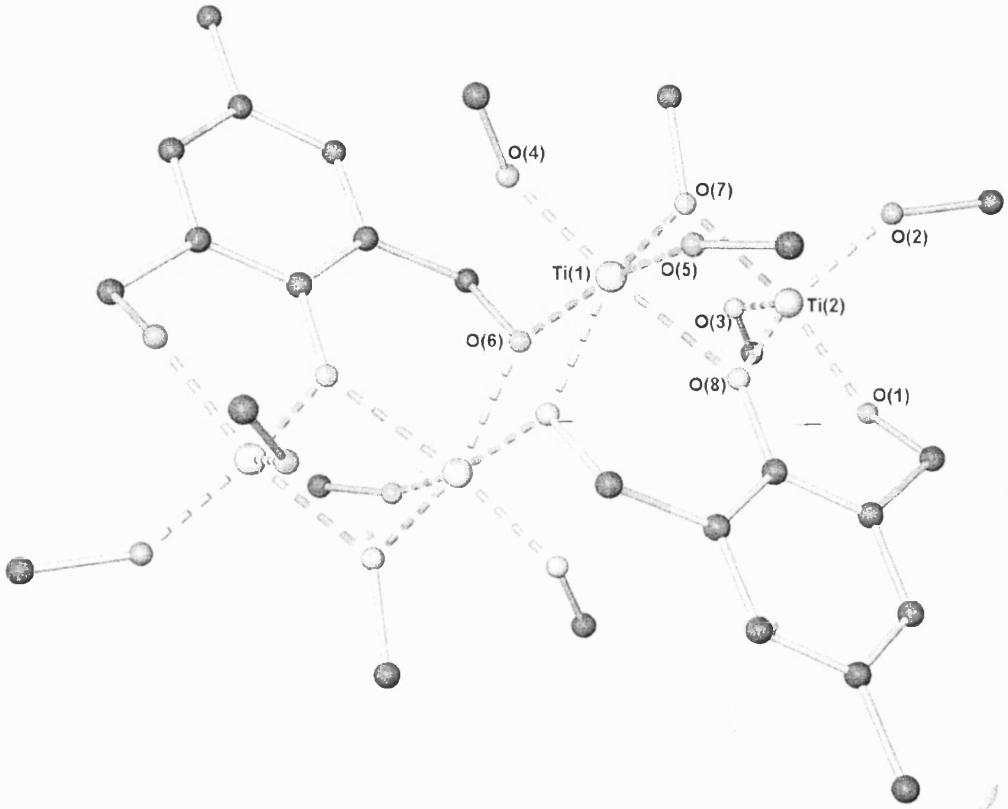

Figure 7.21: Molecular structure of complex 7.6 (hydrogen atoms and isopropyl methyl groups not shown for clarity)

terminal 7.6L hydroxymethyl groups {1.840(2)Å [Ti(2)-O(1)]}. The terminal hydroxymethyl titanium-ligand bond lengths are however substantially shorter than the similar interactions in complex 7.4 (see p.267) suggesting that the formation of a chelate ring is not the major reason for these bonds being so long in 7.4. When compared to the same interaction in the triply chelating ligand in the only previously reported titanium complex of this ligand[11] the bond lengths of these terminal ligand hydroxymethyl groups can be seen to be very similar (1.808 and 1.857Å in the literature complex). As is expected the bridging alkoxide ligands have longer bonds than their terminal counterparts and asymmetry is observed in each pair of bonding interactions. Little difference is observed in the bond lengths to the bridging isopropoxides {1.980(2)Å [Ti(1)-O(7)] and 2.045(2)Å [Ti(2)-O(7)]} and to the bridging hydroxymethyl groups {2.102(2)Å [Ti(1)-O(6)] and 1.961(2)Å [Ti(1)-O(6#)]} although the asymmetry observed in the bond lengths is larger in the bridging ligand hydroxymethyl groups which hold the two 'Ti_2(7.6L)(O^iPr)$_5$' groups together. The bridging phenoxide ligands have typical bond lengths with the expected asymmetry {2.152(2)Å [Ti(1)-O(8)] and 2.003(2)Å [Ti(2)-O(8)]} and are of similar length to the same interactions in the previously reported titanium complex of this ligand[11] (2.085 and 2.047Å).

If the structure of 7.6 is compared to the previously reported titanium complex of ligand 7.6L, described in the introduction[11], we can see it shares a number of features. Both complexes consist of two triply deprotonated 7.6L ligands and four titanium centres but the hydrolysis of the literature compound has moved the central Ti_2O_2 rings into a side on arrangement and formed two extra Ti_2O_2 rings (figure 7.24) and the isopropoxides have been replaced by further 7.6L ligands and oxo groups. We would postulate that hydrolysis of our complex would lead to a similar core to that observed in the previously reported complex as shown in the scheme overleaf. The suggested mechanism shown in figure 7.22 would proceed initially by hydrolysis of the bridging isopropoxide ligands in complex 7.6 and their replacement by hydroxyl moieties. This first hydrolysis step would be followed by the hydrolysis of a second, terminal isopropoxide group by each of the formed hydroxyl groups leading to an intermediate with μ_2-oxo groups. A ligand exchange process with the bridging hydroxymethyl groups of the ligand 7.6L along with a translation would then lead to the formation of a complex with a core analogous to that observed in the literature

complex with μ_3-oxo groups. In our case the remaining ligands not shown in the scheme below would be isopropoxides in contrast to the literature complex in which they are further, partially protonated, 7.6L groups.

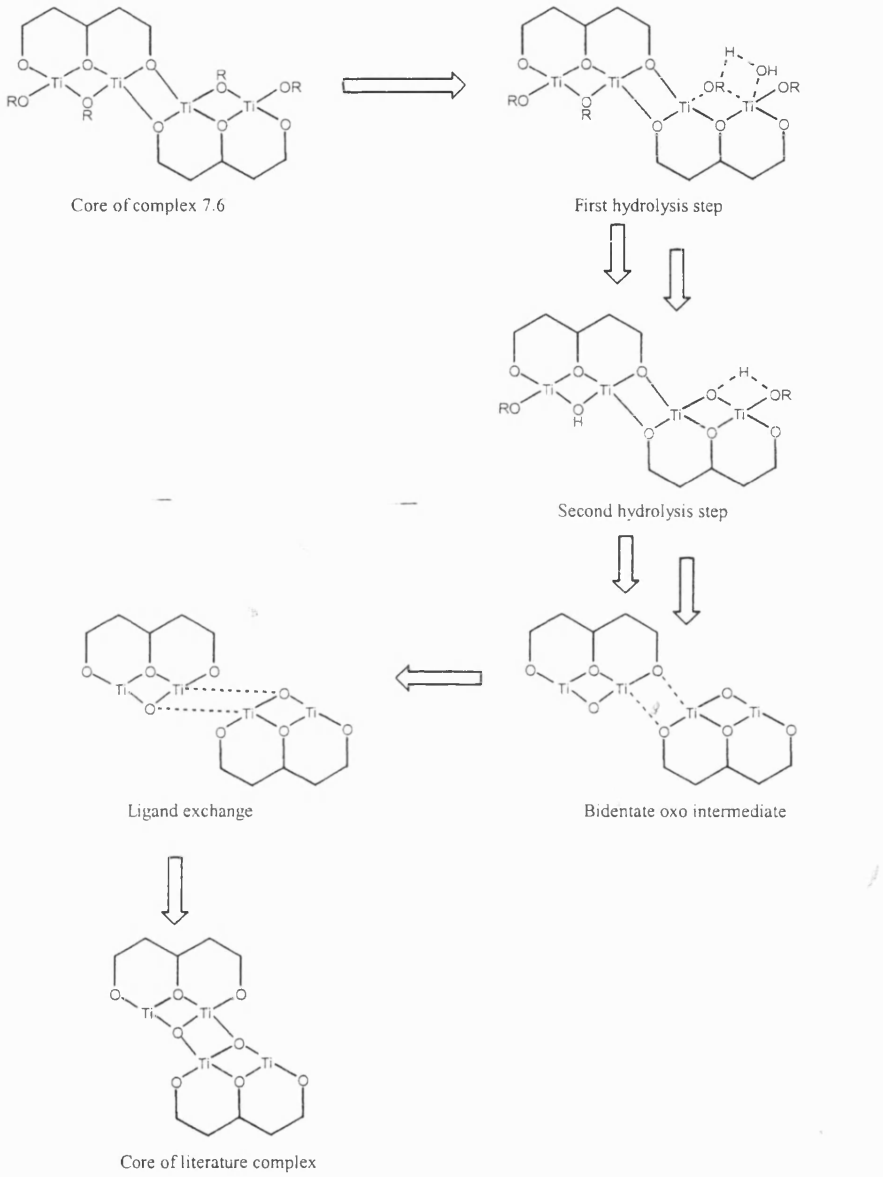

Figure 7.22: Possible hydrolysis route for complex 7.6

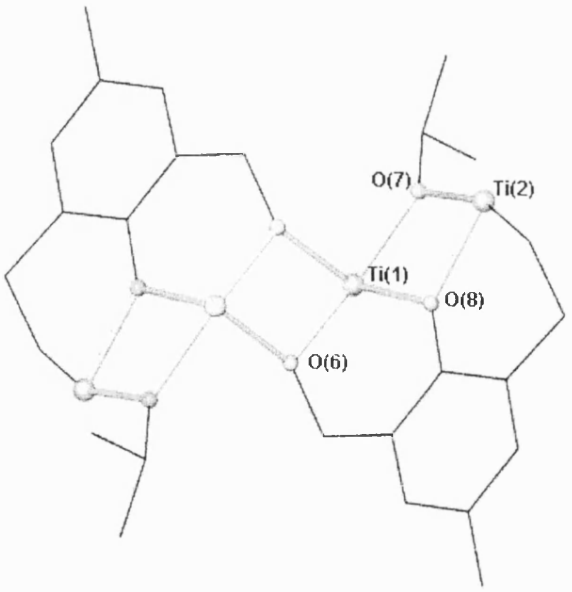

Figure 7.23: Core of complex 7.6

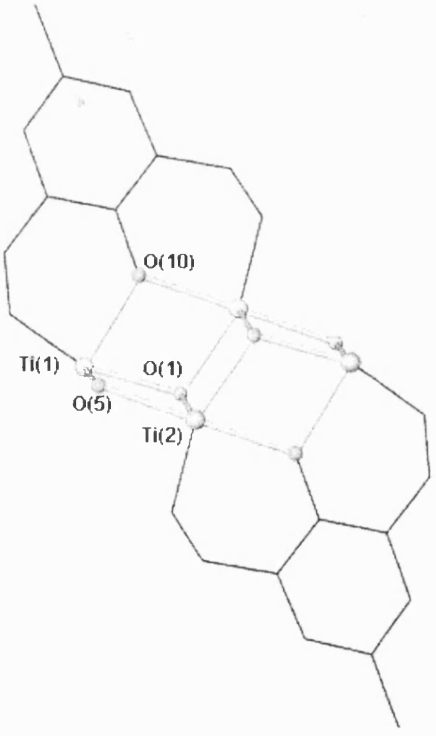

Figure 7.24: Core of previously reported titanium complex of ligand 7.6L (see introduction p.258-259)

The ^{1}H NMR spectrum of 7.6 has the expected ratio of isopropoxide to chelate of 5:1 however there are at least three signals for the ligands toluenic methyl groups and a corresponding number of signals for the aromatic ligand protons. This suggests that in solution there is a complicated dynamic equilibrium possibly between the dimer seen in the crystal structure and the corresponding monomer, $Ti_2(O^iPr)_5$(7.6L), and possibly also some isopropoxide exchange from bridging to terminal. Because of this there are large number of signals for both isopropoxide C**H** groups and the diastereotopic benzyl C**H**$_2$ groups, which both occur in the same region of the spectrum (4.4 to 5.2ppm) making this region particularly difficult to assign. Low temperature ^{1}H NMR studies have shed no further light on this process as reducing the temperature seems to increase the number of signals as they decoalesce.

7.3 Summary of complexes 7.1-7.6

As was stated in the introduction to this chapter the complexes discussed above do not fall easily into the families of ligands described in the other structural chapters in this thesis. Despite this, each of the three groups of complexes described above has interesting properties, which can be utilised in the synthesis of polyurethanes.

The complexes containing 2,6-di-*tert*-butyl phenol ligands (7.1-7.3) help to confirm the observations of earlier workers which outlined the anomalous reactivity of these ligands with TiPT. In each case the titanium centre was substituted only once by these ligands and further reactivity was not observed. Complex 7.3 is the first example of a crystallographically characterised complex of one of these ligands with TiPT and confirms in the solid-state the observations in solution. The titanium complexes obtained with these ligands can be used as starting materials in the synthesis of novel pre-catalysts as will be seen in chapter 8 when they are used in the synthesis of activated species.

The two complexes of amino alcohols include the first titanium alkoxide to be characterised by neutron diffraction and charge density studies (7.4) and a complex with interesting intramolecular interactions that confirms the general inability of TiPT to deprotonate unactivated amino groups. Both of these complexes are potentially

useful pre-catalysts in their own right and 7.4 will be used in chapter 8 as a precursor in the formation of a potentially useful activated species.

Finally the complex with 2,6-bis(hydroxymethyl)-*p*-cresol is the first non-hydrolysed titanium complex of a ligand of this type and should be an interesting pre-catalyst due to its cluster like nature. In addition when considered alongside hydrolysed derivatives of this ligand it may provide some insight into the mechanism of their hydrolysis.

Chapter 8

Activation of Titanium Alkoxide Complexes

The following chapter discusses the synthesis and characterisation of a number of titanium complexes formed by the reaction between acidic reagents and titanium alkoxide species. This work was conducted in order to form activated titanium alkoxide catalysts, and with an aim to form highly reactive cationic titanium alkoxide species as shown in figure 8.1 below.

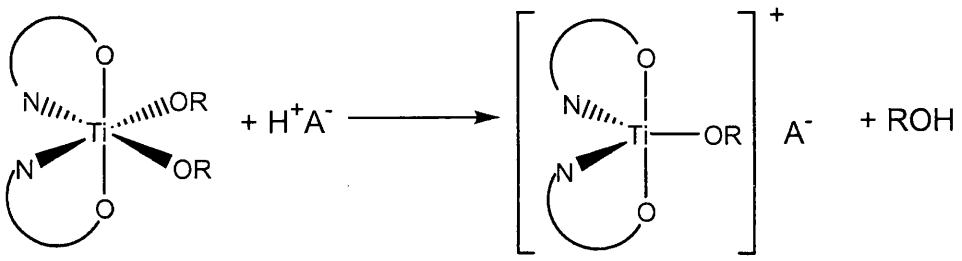

Figure 8.1: Activation of a titanium alkoxide by an acidic reagent

The first section of this chapter introduces the topic by discussing briefly the use of acids to activate titanium alkoxides and also some of the uses of cationic titanium species with non-coordinating anions.

8.1 Introduction

8.1.1 Acid activated titanium alkoxide complexes

Simple titanium compounds, such as TiX_4 where X = halide or alkoxide, are widely used as Lewis acid catalysts for a huge range of organic transformations. In a recently published book[1], which reviews the use of metal species as Lewis acid catalysts, they make up by far the largest section and are shown to be active in many reactions including Diels-Alder reactions, Friedel-Crafts reactions, epoxidations, reductions and aldol reactions.

One way, which has been investigated recently, of increasing the Lewis acidity of these reagents, and thereby increasing their activity, is by reactions with acids and predominantly triflic acid is used. Recent publications have reported use of these

[1] H. Urabe and F. Sato, in '*Lewis Acids in Organic Synthesis*', (Ed. H. Yamamoto), Wiley-VCH, Weinheim, (2000).

titanium triflates as catalysts in addition of allyl stannanes to imines[2], Diels-Alder reactions[3] and esterifications[4].

In 1997 Mikami et al. reported the use of titanium alkoxy/triflates as catalysts for Diels-Alder reactions[5]. They reacted the parent alkoxide with triflic acid, as shown in figure 8.2 below, to generate active catalysts, which were highly moisture sensitive.

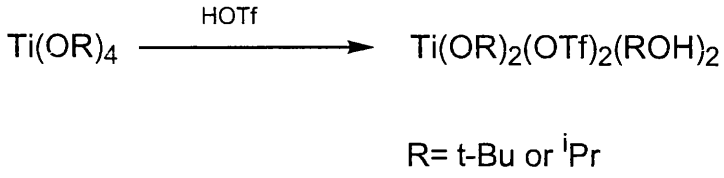

Figure 8.2: Synthesis of a mixed titanium triflate/alkoxide

In the case of the *tert*-butoxide catalyst they isolated crystals, which were suitable for X-ray diffraction, which were shown to contain a μ-oxo bridge and bridging triflate ligands.

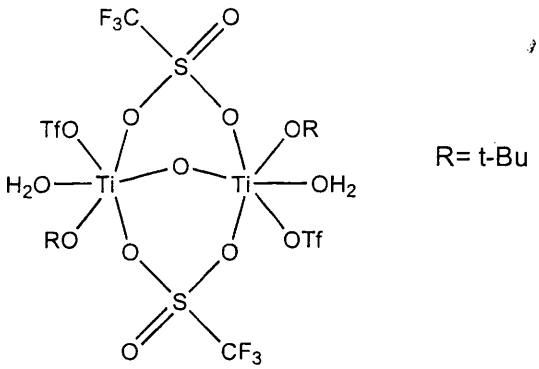

Figure 8.3: Crystallographically defined mixed titanium alkoxide/triflate

Further reacting the isopropoxide compound with 2,2'-bipyridine ligands resulted in the formation of two distinct complexes, shown in figure 8.4 overleaf, which were separated by fractional crystallisation.

---

[2] P. Perlmutter, '*Conjugate Addition Reactions in Organic Synthesis*', Pergamon, Oxford, (1992)
[3] R. Mahrwald, *Chem. Ber.*, **128**, 919 (1995)
[4] K. Schierle, R. Vahle and E. Steckhan, *Eur. J. Org. Chem.*, 509 (1998)
[5] Y. Motoyama, M. Tanaka and K. Mikami, *Inorg. Chim. Acta*, **256**, 161 (1997)

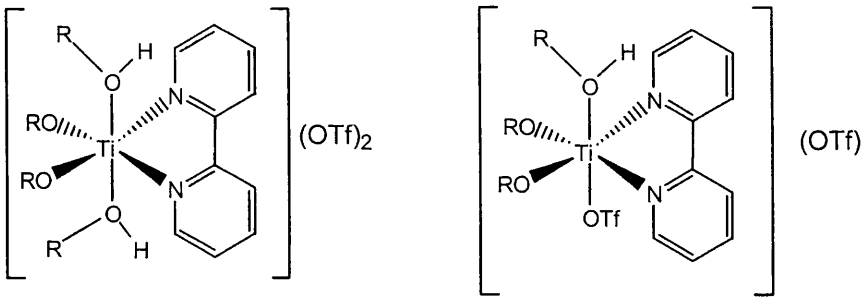

Figure 8.4: 2,2'-bipy stabilised titanium triflate species

Mikami et al. used these catalysts, along with the parent isopropoxide/triflate complex, as catalysts in the Diels-Alder reaction shown in figure 8.5 below.

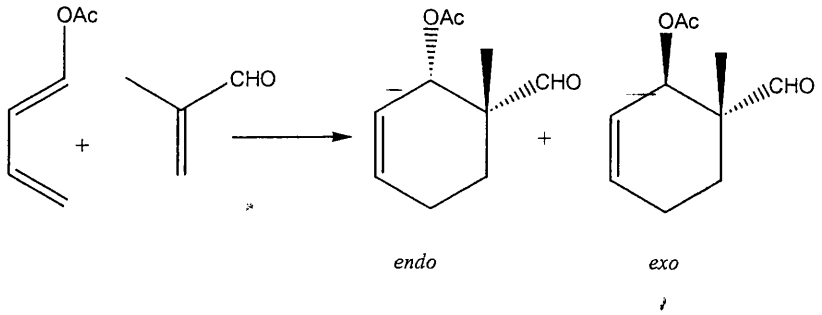

Figure 8.5: Titanium triflate catalysed Diels-Alder reaction

All three were shown to be active, in contrast to use of $Ti(O^iPr)_2Cl_2$ which showed no reaction after 12 hours. The complexes with bipyridyl ligands stabilising the complex (figure 8.4) were found to give better yields (98-99%) compared to the non stabilised complex (50%) which decomposed the diene substrate due to their extremely high Lewis acidity.

In addition to the use of triflate groups to activate heteroleptic titanium species some recent papers have also detailed the activation of titanium chelate species by reaction with triflic acid.

Floriani et al. showed that the catalyst shown in figure 8.6 below was active in a number of reactions including aldol reactions, Mukaiyama-Michael reactions, catalytic allylations using allyl stannanes and Diels-Alder reactions[6].

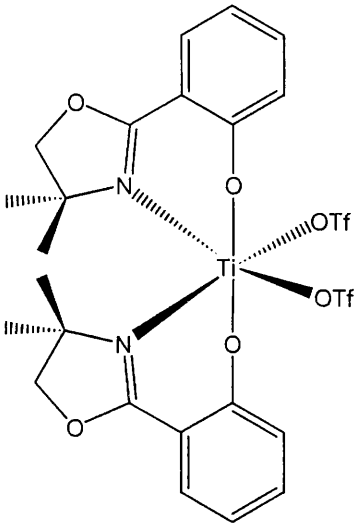

Figure 8.6: Floriani titanium triflate catalyst

More recently Gleason et al. used the asymmetric titanium triflate catalysts shown in figure 8.7 below in the catalysis of homo-aldol reactions[7].

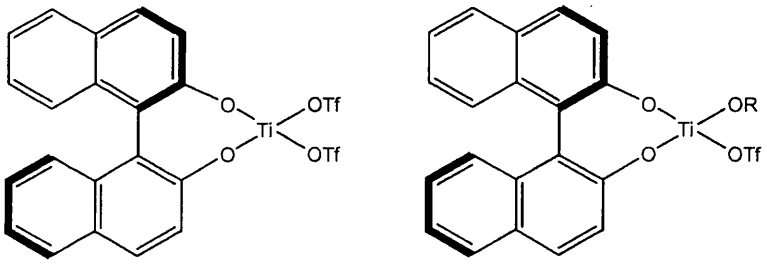

Figure 8.7: Mixed binol/triflate titanium catalysts

The bis-triflate catalyst, formed by the reaction of the parent dichloride and silver triflate, gave only modest yields but the mono-triflate/mono-alkoxide catalyst, formed from the parent bis-alkoxide and triflic acid gave yields of up to 99%.

[6] P.G. Cozzi and C. Floriani, *J. Chem. Soc. Perkin Trans. 1*, 2557 (1995)
[7] E.O. Martins and J.L. Gleason, *Org. Lett.*, **1**, 1643 (1999)

The majority of acidic activation of titanium Lewis acid catalysts has concentrated on the use of triflate as the activating ligand/anion. However in 1996 Mikami et al. showed that use of the related compound triflamide shown in figure 8.8 below gives an even greater enhancement of activity along with increased stability[8].

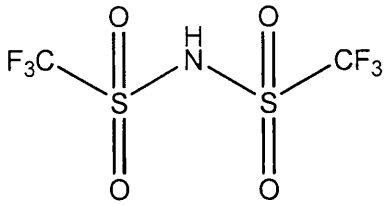

Figure 8.8: Triflamide

The structurally undefined catalyst '$Ti(O^iPr)_2(NTf_2)_2$' has been used in both Friedel-Crafts acylations and the acylation of alcohols with yields in excess of 99% in under 10 minutes and at much faster rates than the corresponding titanium alkoxo/triflate species.

8.1.2 Cationic group IV species with non-coordinating anions as catalysts for polymerisations

The following section is in no way an exhaustive review of this subject and is intended to give a brief background to our work in this area. A large amount of work has been reported in recent years on the use of non-coordinating anions as components of catalyst systems[9]. These anions, as the name suggests, do not, in theory, coordinate to the metal centre and leave an apparently vacant coordination site on the highly Lewis acidic cationic metal centre at which catalysis can occur. In practice however one of the four interactions shown in figure 8.9 overleaf occurs to fill the gap left by the poorly coordinating anion.

The cationic complex with a vacant coordination site, complex (i) in figure 8.9 overleaf, is never observed and instead one of the four products shown is observed. The vacant coordination site may be filled by a molecule of solvent (ii) or the

[8] K. Mikami, O. Kotera, Y. Motoyama, H. Sakaguchi and M. Maruta, *Synlett*, 171 (1996)
[9] S.H. Strauss, *Chem. Rev.*, **93**, 927 (1993); C.A. Reed, *Acc. Chem. Res.*, **31**, 133 (1998); J.N. Pedetour, K. Radhakrishnan, H. Cramail and A. Deffieux, *Macromol. Rapid. Comm.*, **22**, 1095 (2001)

counterion may coordinate weakly to the metal centre (iii). Alternatively the supporting ligand L may change its bonding mode to bidentate to fill the vacant site (iv) or a dimerisation process may occur with the L ligands taking bridging bonding modes (v). Because of the presence of these interactions it has been stated that in practice reference should be made to *virtual* rather than *vacant* coordination sites[9].

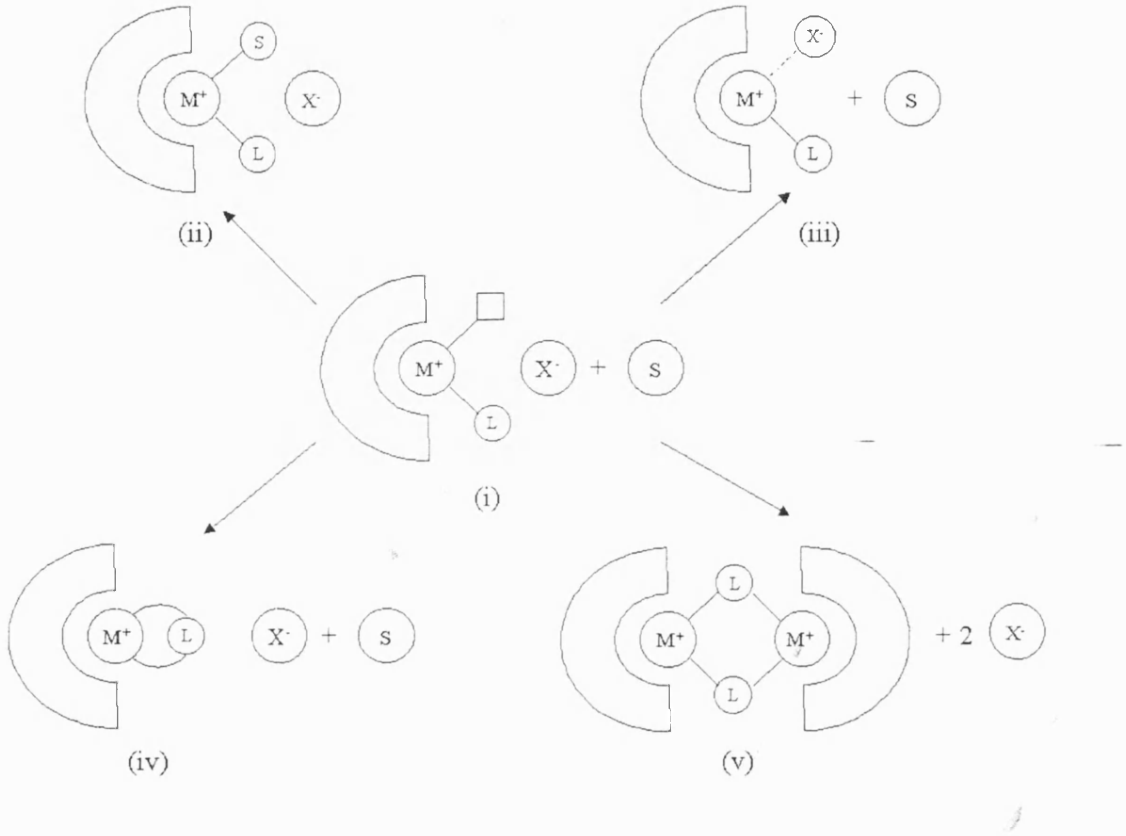

Figure 8.9: Potential ways a 'vacant' coordination site may be filled

Many different anions are utilised in this field; the chemistry of a wide range of these anions such as BPh_4^-, $CB_{11}H_{12}^-$, $OTeF_5^-$, polyoxometallates and methylaluminoxanes has been reviewed by Strauss[9] and therefore for the purpose of this discussion we will briefly discuss one example of a family of co-catalysts used in industrial polymerisations. This family includes, $B(C_6F_5)_4^-$, also called 'BArF', which, with related pentafluorophenyl compounds, is used as a co-catalyst in metallocene polyolefin catalysis.

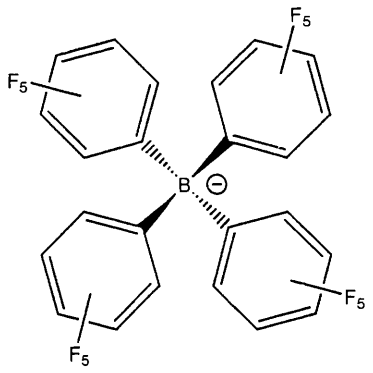

Figure 8.10: BArF anion

In recent years a large amount of work has been published on the use of group IV single-site and metallocene based compounds as polyolefin pre-catalysts[10]. These compounds, which include some of the titanium Schiff base complexes discussed in the introduction to Chapter 4, are used alongside a co-catalyst, which is generally a main-group organometallic species[11]. The co-catalyst has two main roles; firstly it transforms the group IV pre-catalyst into the active catalyst and secondly, as the anionic component of a catalytically active ion pair, it can influence the polymerisation itself and thereby the properties of the resulting polymer. The two most commonly used co-catalysts in metallocene and single site polyolefin synthesis are MAO (an oligomeric mixed alkyl/oxo aluminium species) and pentafluoro aryl boron derivatives, the action of which will be briefly described below.

Although $B(C_6F_5)_3$ (FAB) has been known since 1964[12] it was only shown in the early 1990's that it was an excellent co-catalyst for the synthesis of polyolefins[13]. FAB reacts with zirconocene di-alkyls, as shown in figure 8.11 overleaf, to yield zwitterionic activated catalyst species, which polymerise olefins.

[10] examples include: G.J.P. Britovsek, V.C. Gibson and D.F. Wass, *Angew. Chem. Int. Ed.*, **38**, 428 (1999); R.F. Jordan (Ed.), *J. Mol. Catal.*, **128**, 1-337 (1998); M. Bochmann, *J. Chem. Soc. Dalton Trans.*, 255 (1996)
[11] E.Y. Chen and T.J. Marks, *Chem. Rev.*, **100**, 1391 (2000)
[12] A.G. Massey and A.J. Park, *J. Organomet. Chem.*, **2**, 245 (1964)
[13] X. Yang, C.L. Stern and T.J. Marks, *J. Am. Chem. Soc.*, **113**, 3623 (1991); X. Yang, C.L. Stern and T.J. Marks, *J. Am. Chem. Soc.*, **116**, 10015 (1993)

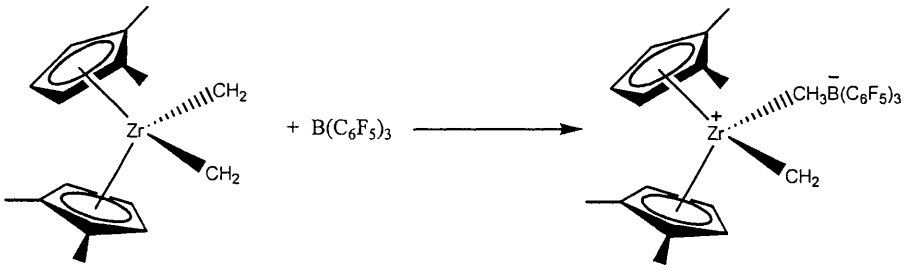

Figure 8.11: Activation of a zirconium alkyl by FAB

In 1991 BArF type reagents were also shown to activate group IV di-alkyl metallocenes by complete removal of one of the alkyl groups to leave an apparently vacant coordination site[14]. The most common BArF type co-catalysts, which are used, are those with trityl counterions, which abstract an alkyl group to leave zwitterionic catalytic species of the type shown in figure 8.12 below.

$$Et(Ind)_2ZrMe_2 + Ph_3C^+B(C_6F_5)_4^- \longrightarrow Et(Ind)_2ZrMe^+B(C_6F_5)_4^- + Ph_3C\text{-}Me$$

Figure 8.12: Zirconium alkyl activation by BArF

A large amount of work has been carried out on the use of these perfluoro aryl boron compounds and this is covered in a review by Marks and Chen and therefore will not be further discussed here[11].

8.1.3 Relevance to polyurethanes

The use of co-catalysts to activate group IV metal polyolefin catalysts has allowed a significant increase in both rate and selectivity for this reaction and stimulated a large amount of academic research in this area. We wished to use a similar activation technique in our studies of polyurethane synthesis. Unfortunately the activating species used in polyolefin synthesis to abstract alkyl groups are ineffective for the abstraction of alkoxides. To look at similar activation in our systems we combined the theory of activation used in polyolefin synthesis with the activation of titanium alkoxides for Lewis acid catalysts used in organic transformations described in 8.1.1

[14] X. Yang, C.L. Stern and T.J. Marks, *Organometallics*, **10**, 840 (1991); J.C.W. Chien, W.M. Tsai and M.D. Rausch, *J. Am. Chem. Soc.*, **113**, 8570 (1991)

above. We hoped that by utilisation of some of the reagents used in the organic transformations we would be able to form activated analogues of both our chelated titanium alkoxide pre-catalysts and homoleptic titanium alkoxides. The activating species we chose to carry out this study were HBF_4 and triflamide derivatives. The following chapter describes some initial investigations in this area including the attempted activation using these species.

8.2 Discussion

The activating reagents used in this section are shown in figure 8.13 below,

HBF_4 in Et_2O **8.1L**

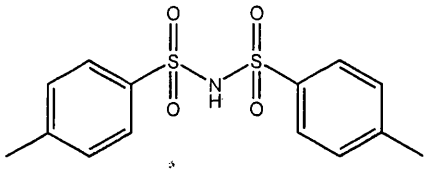

8.2L

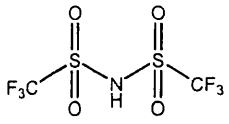

8.3L

Figure 8.13: Acidic reagents used in chapter 8

As described in the introduction to this chapter the concept of using these reagents with titanium species was to activate the metal centre and possibly to form cationic titanium alkoxide species as shown in figure 8.1 on page 280.

Complex 8.1

HBF_4 was reacted with a highly stable titanium alkoxide complex, titanium-bis-8-hydroxyquinolinate-bis-isopropoxide, which was synthesised by standard literature methods[15]. The hope was that the HBF_4 would protonate the isopropoxide ligands to give isopropanol that would be lost on work up to yield a cationic titanium centre with one or two BF_4^- counterions.

[15] R.S.P. Coutts, *Aust. J. Chem.*, **34**, 653 (1981)

The initial reaction yielded an orange product, which was unsuitable for single crystal X-ray diffraction and which was soluble only in acetonitrile. In the ^{1}H NMR spectrum of this product in CD_3CN signals were observed for the 8-hydroxyquinoline ligands but no signals were present for isopropoxide groups. This observation indicated to us that we had achieved our goal of removing the isopropoxides by protonation. However, the ^{19}F NMR spectrum showed that we had a mixture of products, two sets of signals were observed; the first was two singlets at –151.95 and -152.01ppm in a 1:3 ratio which were due to BF_4^- groups. The second signal was a broad singlet at 191.59ppm, which is due to Ti-F groups. We believe this result correlates to more than one product in solution although these products have been difficult to identify definitively.

Recrystallisation of the product mixture from acetonitrile however led to the formation of a crop of bright red crystals, which were suitable for single crystal X-ray diffraction which revealed the complex to have the formula $Ti(8\text{-}HQ)_2F_2$. The crystal structure consists of half a molecule of the product complex which consists of a titanium centre ligated by two chelating 8-hydroxyquinoline groups and two fluorine ligands. The titanium has a distorted octahedral geometry and the overall structure is a direct analogue of the same complex with isopropoxide or chloro ancillary ligands[16] with the fluorine and pyridyl groups in cis-equatorial positions and the phenoxide ligands in a trans-axial arrangement.

The titanium-fluorine bonds are 1.811(1)Å [Ti(1)-F(1)] in length which is typical for bonds of this type[17]. The bond lengths from the chelate ligands to titanium are similar to the same bonds in analogues with other ancillary ligands {1.903(1)Å [Ti(1)-O(1)] and 2.216(1)Å [Ti(1)-N(1)]} although they are some of the shortest observed in complexes of this type probably due to the high electronegativity of fluorine.

[16] B.F. Studd and A.G. Swallow, *J. Chem. Soc. Sect. A*, 1961 (1963); W. F. Zeng, Y. S. Chen, M. Y. Chiang, S. S. Chern and C. P. Cheng, *Polyhedron*, **21**, 1081 (2002)

[17] Examples include; D. Schwarzenbach, *Helv. Chim. Acta*, **55**, 2990 (1972); A. Bodner, P..Jeska, T. Weyhermuller, K. Wieghardt, E. Dubler. H. Schmalle and B. Nuber, *Inorg. Chem.*, **31**, 3737 (1992); P. Yu, T. Pape, I. Uson, M.A. Said, H.W. Roesky, M.L. Montero, H.G. Schmidt and A. Densar, *Inorg. Chem.*, **37**, 5117 (1998); S. J. Coles, M.B. Hursthouse, D.G. Kelly, A.J. Toner and N.M. Walker, *J. Chem. Soc. Dalton Trans.*, 3489 (1998); P. Yu, P. Muller, H.W. Roesky, M. Noltemeyer, A. Demsar and I. Uson, *Angew. Chem. Int. Ed. Engl.*, **38**, 3319 (1999)

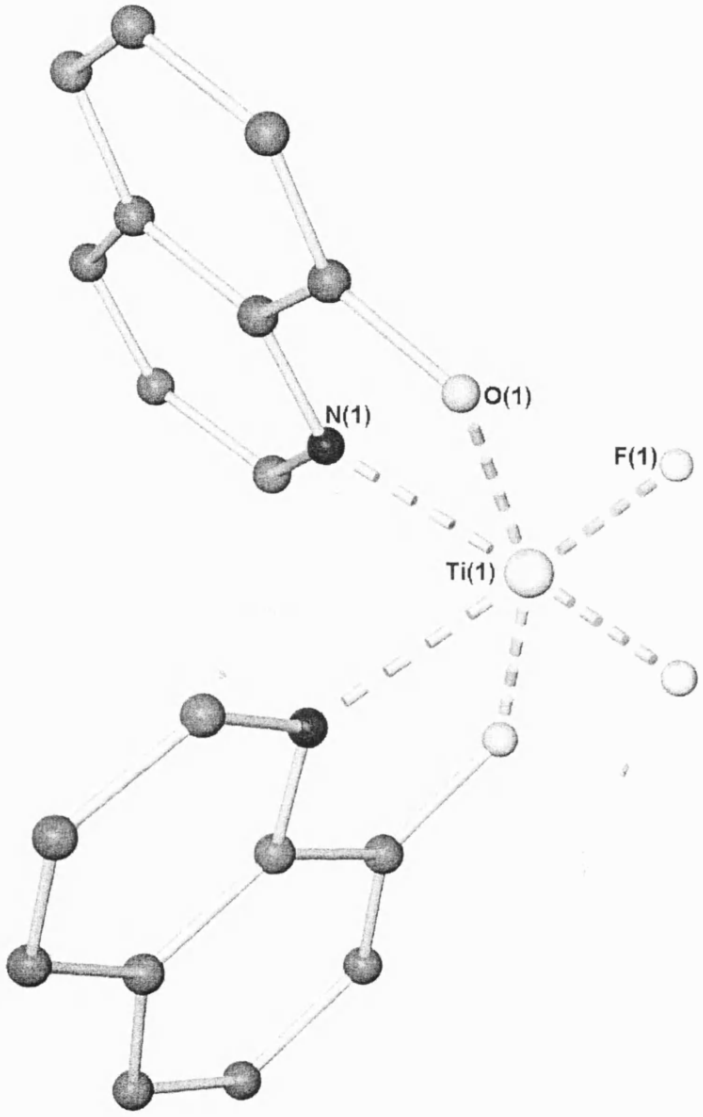

Figure 8.14: Molecular structure of complex 8.1 (hydrogen atoms not shown for clarity)

The ^{1}H NMR spectrum of the isolated di-fluoride complex is identical to that for the mixture of products described above, while the ^{19}F NMR spectrum shows only a sharp signal at 191.47ppm due to Ti-F bonds which seems to suggest that complex 8.1 is at least one component of the mixture isolated initially.

The formation of titanium fluoride complexes using reagents based on the BF_4^- ion has some literature precedent[18] although this is the first example using HBF_4. Earlier work has concentrated on the use of $AgBF_4$ with titanium chlorides and in some cases an initial product has been isolated which seemed to have a cationic titanium centre. In a similar manner to our initial product however these products have decomposed on work up to the difluoride[19].

Only two previous examples exist in the literature for formation of a titanium fluoride directly from an alkoxide. The first example involves the reaction of an in-situ generated titanium alkoxide, $Cp_2Ti(O\text{-}t\text{-}Bu)_2$, with BF_3[20]. The second example comes from the work of Braun et al. using dianionic O-N-O type ligands (p.179)[21], which was described in chapter 5, they reacted a 1:1 mixture of $Ti(O\text{-}N\text{-}O)_2$ with TiF_4 to yield products with the formula $Ti(O\text{-}N\text{-}O)F_2$ as shown in figure 8.15 below.

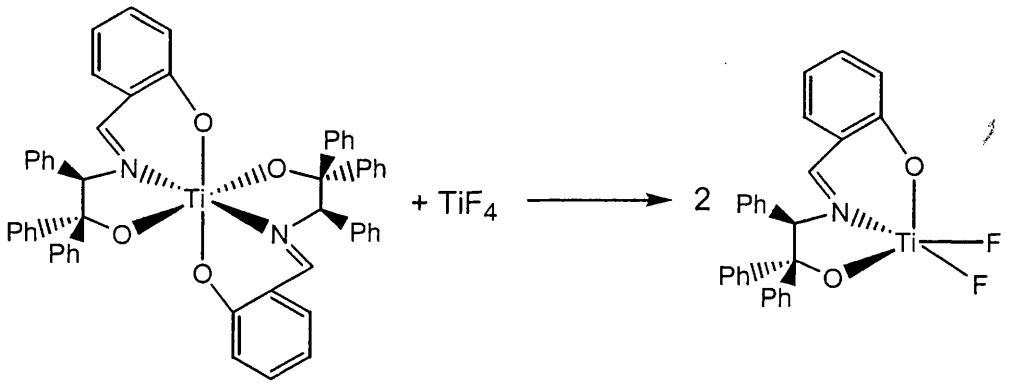

Figure 8.15: Formation of a titanium fluoride by ligand scrambling

[18] M. Bochmann and L.M. Wilson, *Chem. Comm.*, 1610 (1986); A. Seyam, H. Samha and H. Hodali, *Gazz. Chim. Ital.*, **120**, 527 (1990); D. Chakraborty, S. Horchler, H.W. Roesky, M. Noltemeyer and H.G. Schmidt, *Inorg. Chem.*, **39**, 3995 (2000)
[19] C.H. Winter, X. Zhou and M.J. Heeg, *Inorg. Chem.*, **31**, 1808 (1992)
[20] K.C. Ott, E.J.M. deBoer and R.H. Grubbs, *Organometallics*, **3**, 223 (1984)
[21] R. Fleischer, H. Wunderlich and M. Braun, *Eur. J. Org. Chem.*, 1063 (1998)

The results outlined above for the use of HBF_4 show that, although it seems to be unsuitable for synthesis of stable cationic titanium reagents, due to the relative instability of the BF_4^- counterion and stability of Ti-F bonds, we have discovered a simple route for synthesis of titanium fluoro compounds from the parent alkoxides.

Complex 8.2

Due to the problems encountered using the inorganic counterion BF_4^- with our complexes we next investigated the reactions of organic reagents, which could possibly yield weakly coordinating anions. Two equivalents of reagent 8.2L reacted readily with one equivalent of TiPT to yield a crop of crystals, which were suitable for single crystal X-ray diffraction. The resulting complex is the first reported crystal structure of a metal complex of this ligand. The asymmetric unit consists of one molecule of the titanium complex. The complex consists of one Ti centre, which is chelated by two 8.2L ligands, which are deprotonated at the nitrogen atom and bond through two oxygen atoms in a similar manner to an acetylacetonate (acac) ligand. In addition the titanium centre also retains two isopropoxide ligands. The titanium centre has a distorted octahedral geometry with the monodentate alkoxides in cis-equatorial positions.

The two 8.2L ligands are inequivalent in the solid-state; one ligand {around N(1)} has a cis arrangement of *p*-tolyl groups (arrangement A below) while the second {around N(2)} has a trans arrangement (arrangement B below).

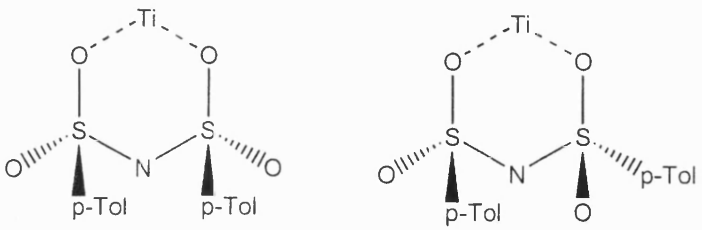

A **B**

Figure 8.16: The two observed ligand configurations in complex 8.2 (all bonds represented as single for clarity)

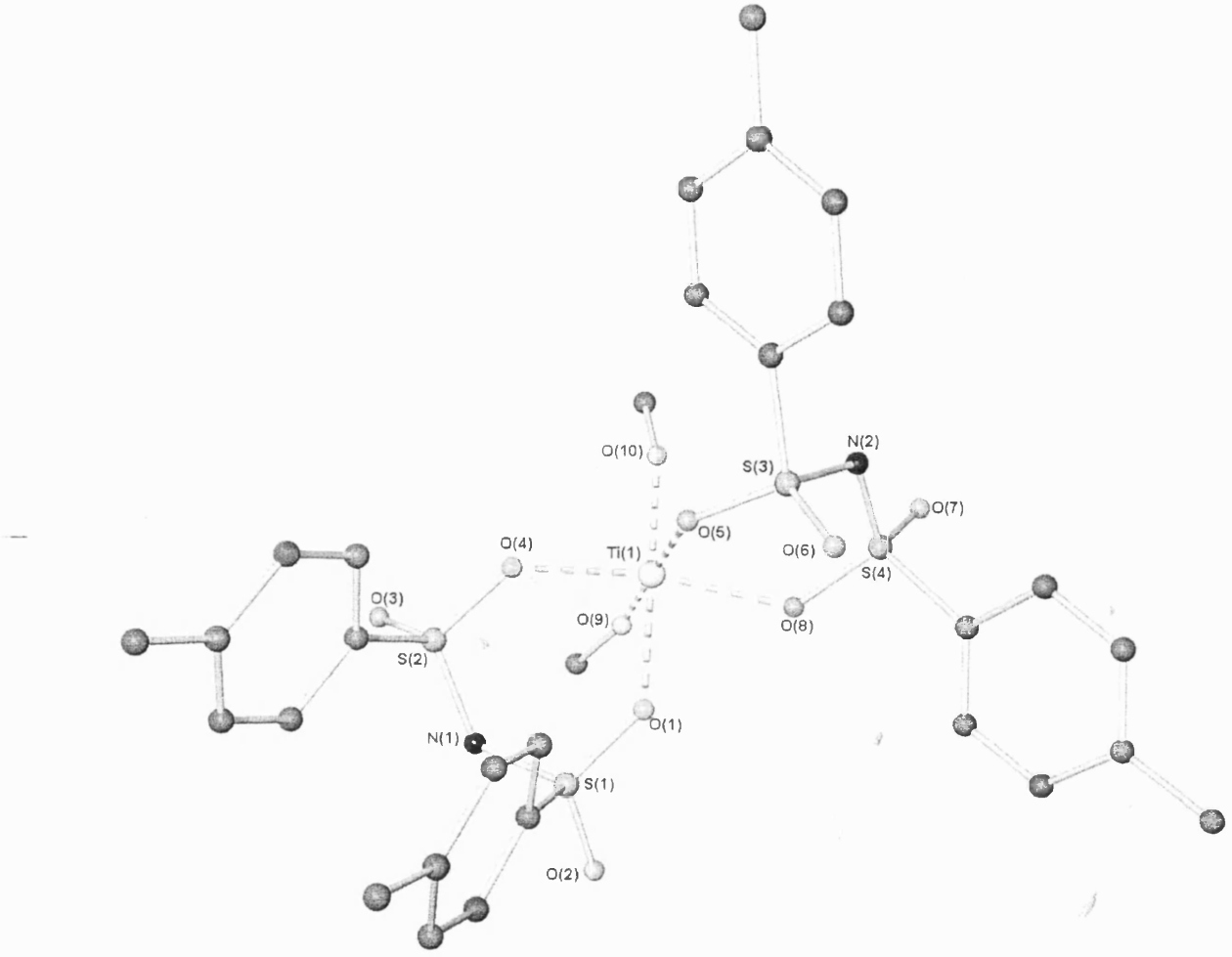

Figure 8.17: Molecular structure of complex 8.2 (hydrogen atoms and isopropoxide methyl groups not shown for clarity)

This difference in ligand geometry has no discernable effect on the bond lengths of the ligands to titanium {2.160(2)Å [Ti(1)-O(1)], 2.048(2)Å [Ti(1)-O(4)], 2.145(2)Å [Ti(1)-O(5)] and 2.048(2)Å [Ti(1)O(8)]} which are similar for both ligands, with each ligand having a longer bond to titanium from the oxygen donor which is trans to an isopropoxide than from its partner. The isopropoxide ligands themselves have typical bond lengths to the titanium centre of 1.734(2)Å [Ti(1)-O(9)] and 1.763(2)Å [Ti(1)-O(10)].

The ^{1}H NMR spectrum of the complex is very broad and shows no evidence for a difference between the two 8.2L ligands on the titanium centre, which are probably exchanging in solution. Because of this, the difference in configuration in the solid-state can probably be ascribed to crystal packing effects.

Complex 8.3

The reaction of ligand 8.2L with TiPT showed that the *p*-tolyl ligand was not sufficiently non-coordinating to form an activated complex of the type we had hoped to synthesise. To try and move to a more non-coordinating analogue we tried some reactions of titanium species with triflamide, 8.3L, which had strongly electron withdrawing groups. As was described in the introduction to this chapter, reagent 8.3L (triflamide), has been used to activate TiPT in organic transformations but, prior to the work described here, the catalyst species had not been structurally characterised.

One equivalent of reagent 8.3L reacted readily with TiPT to yield a crop of white crystals, which were suitable for single crystal X-ray diffraction. The asymmetric unit consisted of half of the complex molecule. The metal complex consists of a titanium centre with two 8.3L ligands which have been deprotonated at the nitrogen atom and which bond terminally through a single oxygen atom. In addition the metal centre is ligated by two isopropoxide ligands and two isopropanol ligands making it six coordinate with a distorted octahedral geometry. The two isopropanol ligands have a trans-axial arrangement with the isopropoxide and triflamide ligands in cis-equatorial configurations. As the ratio of triflamide to ligand in the product is 2:1 it is assumed that the reaction mixture also contains one molecule of TiPT.

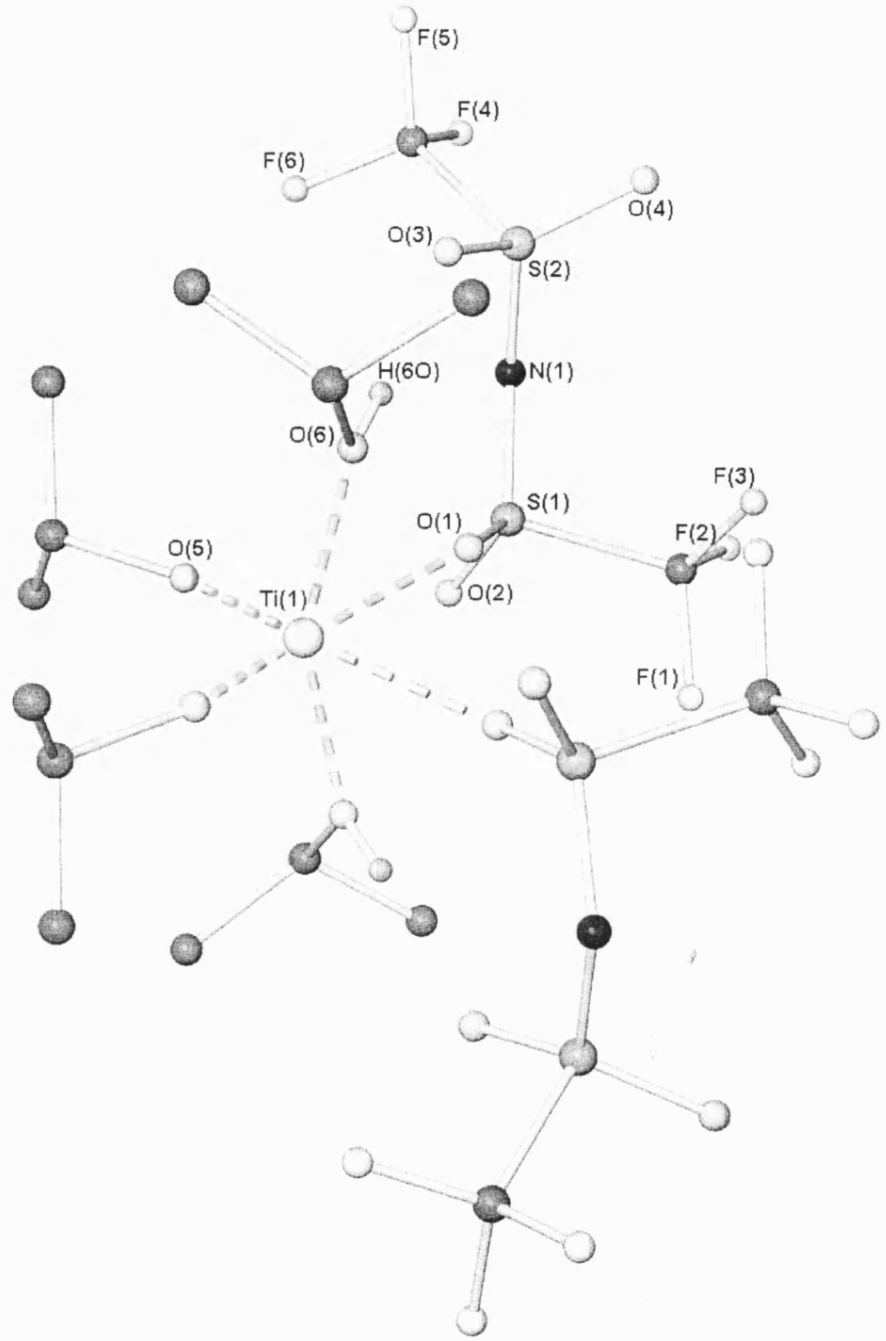

Figure 8.18: Molecular structure of complex 8.3 (all non-hydroxy hydrogen atoms not shown for clarity)

The OH groups of the isopropoxide ligands act as hydrogen bond donors in a pair of intramolecular hydrogen bonds to oxygen atoms on the non-coordinated S=O groups of the two triflamide ligands. The hydrogen bonds are quite short and close to linear {O(6)-H(60)···O(3) [O(60)-H(60) 0.784Å; O(6)···O(3) 2.711Å; O(6)-H(60)-O(3) 174.1°]} and link the isopropanol and triflamide ligands in an eight membered pseudo chelate ring, as shown in figure 8.19 below (ROH hydrogen atoms freely refined).

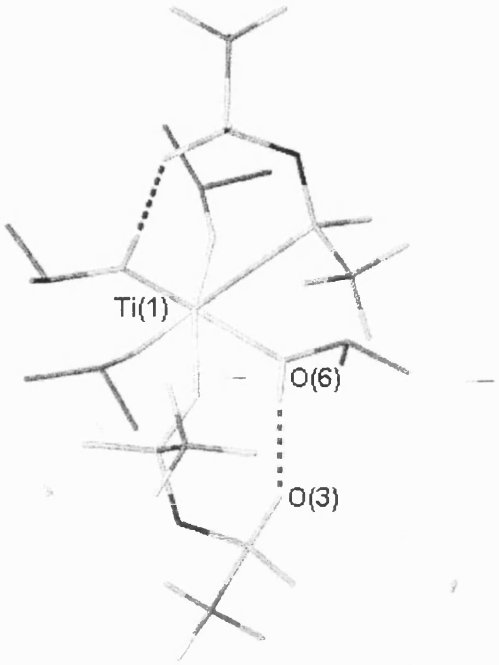

Figure 8.19: Intramolecular hydrogen bonding in complex 8.3

The hydrogen bonding in complex 8.3 seems to suggest that it is an analogue of an intermediate in the formation of complexes of the same type as complex 8.2 with bis-acetylacetonate type ligands. The simplest explanation for the formation of this hydrogen bonded complex rather than a chelated complex analogous to that formed with the *p*-tolyl complex, 8.2, is the strength of the interactions with titanium. The strongly electron withdrawing groups on the triflamide ligand make the formation of a second chelating bond to the titanium centre electronically disfavoured while increasing the strength of the titanium-alcohol bond in the hydrogen bonded complex. Because of this electronic effect of the triflamide CF_3 group the hydrogen-bonded

complex is more stable than a bis-chelate complex and therefore the only isolable product.

The bonds from the triflamide oxygen atoms to the titanium centre are of a similar length to the longer of the two ligand oxygen atom to titanium distances in complex 8.2 {2.198(1)Å [Ti(1)-O(1)]}. The isopropoxide-titanium {1.730(2)Å [Ti(1)-O(5)]} and isopropanol-titanium {2.040(1)Å [Ti(1)-O(1)]} bond lengths are standard for bonds of this type with the isopropanol ligands having the longer interactions, as would be expected.

The ^{1}H, ^{13}C and ^{19}F NMR spectra of the product complex show that the gross features of the solid-state structure are maintained in solution. The ^{1}H NMR spectrum shows the expected resonances for the isopropanol ligands {1.19ppm (CH_3), 4.41ppm (**CH**) and 8.13ppm (**OH**)} and the isopropoxide groups {1.19ppm (CH_3) and 4.79ppm (**CH**)} and the ^{13}C and ^{19}F NMR spectra also show the expected signals.

Complex 8.3 shows the product of the reaction of TiPT with triflamide with this product being the only isolable compound from the reaction of these two reagents in a variety of stoichiometries. The complex has some of the desired features for a highly Lewis acidic catalyst. Two of the isopropoxide ligands have been protonated by the acidic reagent and the triflamide ligand is not sufficiently coordinating to replace these isopropanol groups even with the driving force of the chelate effect. This is probably partly true, in the solid-state at least, to the pseudo-chelate formed due to the intermolecular hydrogen bonding described above, which stabilises the labile isopropanol ligands and the relative strength of the interaction between the activated alcohol and titanium compared to a Ti···O-S bond. Because of this stabilising effect the complex has two *virtual* free coordination sites, which are filled by these isopropanol ligands.

Complex 8.4

We wished to see if by use of an alternative source of $Ti(O^{i}Pr)_x$ we could influence the complex formed in the reaction of triflamide with a titanium alkoxide and to this end we used the titanium mono-aryloxide complex 7.3 as a starting material. At this

point it is important to note that reactions of other TiPT derivatives of 2,6-di-*tert*-butyl phenols with triflamide also yield the same products as described below.

Three equivalents of reagent 8.3L, triflamide, reacted readily with complex 7.3 to yield a crop of colourless crystals, which were suitable for single crystal X-ray diffraction. The asymmetric unit consists of half a molecule of the titanium complex. The complex consists of two titanium centres, which are bridged by two isopropoxide ligands. Each titanium centre also has one chelating 8.3L ligand, which is deprotonated at the nitrogen atom and ligates titanium through two of its oxygen atoms in a similar manner to the ligands in complex 8.2 and acac ligands. The chelate ligands have a trans-arrangement of the CF_3 groups as described for the ligands in complex 8.2, p.292. In addition each titanium centre also has two terminal isopropoxide donors. Each metal centre has a total of six ligand donors and a distorted octahedral geometry.

The titanium to triflamide bond lengths are similar to those observed in the previous structure {2.167(1)Å [Ti(1)-O(1)] and 2.263(1)Å [Ti(1)-O(4)]} with one bond being approximately 0.1Å longer than the other in each ligand. The terminal isopropoxides also have similar bond lengths to titanium as the same ligands in the previous complex with the ligand trans to the longer triflamide bond {1.739(1)Å [Ti(1)-O(6)]} having a shorter bond to titanium than the ligand trans to the short triflamide bond {1.772(1)Å [Ti(1)-O(5)]}. The bridging isopropoxide ligands have the usual asymmetry in its bonding with each titanium centre having one short bond {1.935(1)Å [Ti(1)-O(7)} and one long bond {2.111(1)Å [Ti(1)-O(7#)]} to a bridging alkoxide.

The ^{1}H NMR spectrum of complex 8.4 shows only one set of slightly broadened signals due to the isopropoxide groups {1.38ppm (CH_3) and 4.98ppm (C**H**)}. This suggests that in solution all the isopropoxide ligands are equivalent on the NMR timescale. This equivalence could be due either to the break up of the dimer into two mono-titanium species each with three equivalent monodentate O^{i}Pr ligands or rapid exchange of the ligands in the dimeric species. In reality a combination of these processes is probably occurring. The ^{13}C NMR spectrum also shows only one set of signals for the isopropoxide group {26.2ppm (CH_3) and 84.6ppm (CH)}.

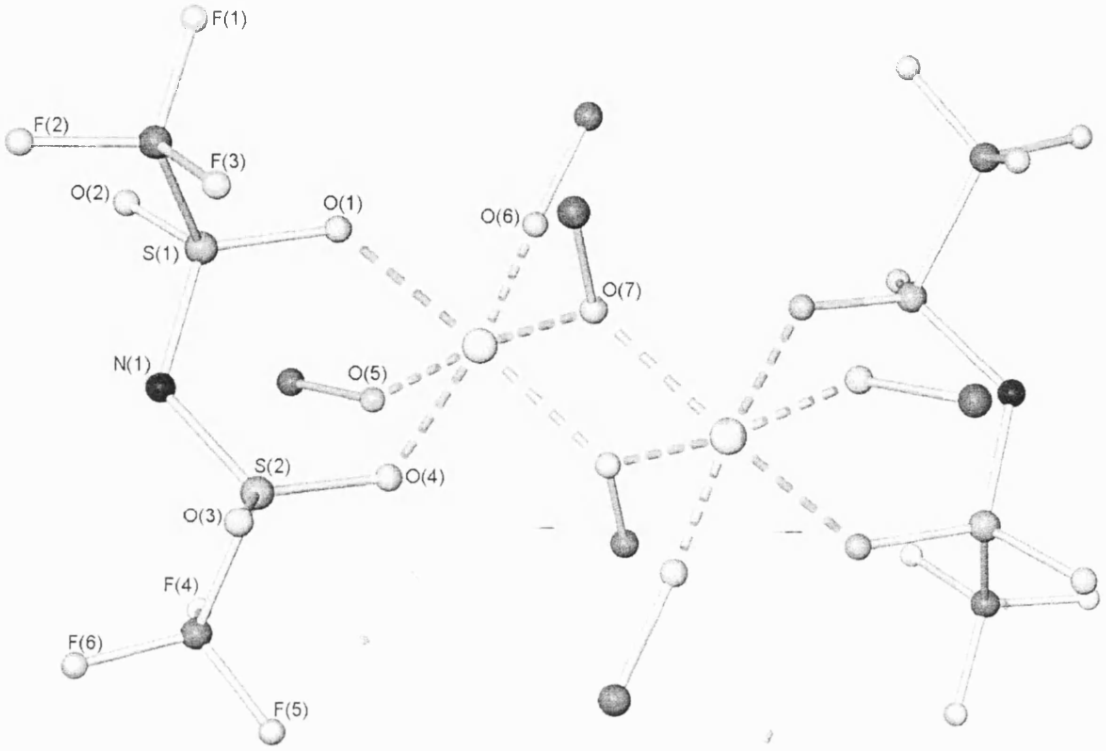

Figure 8.20: Molecular structure of complex 8.4 (hydrogen atoms and iso-propoxide methyl groups not shown for clarity)

Explaining the reactivity observed in 8.3 and 8.4

The most reasonable explanation for the difference in reactivity observed in the formation of complexes 8.3 and 8.4 is due to the steric demand of 2,6-di-*tert*-butyl phenoxide ligands with titanium isopropanolates. When comparing the reactivities we consider three factors to be important:

1) Complex 8.3 has the most favoured structure for a triflamide derivative of a titanium isopropanolate.

2) Complex 8.4 is an intermediate in the formation of complex 8.3, which forms by disproportionation of the dimeric complex 8.4.

3) $Ti(O^iPr)_2(OAr)_2$ with 2,6-di-*tert*-butyl phenoxide ligands is highly disfavoured and has never been isolated.

If these facts are all considered to be true then the synthesis of 8.3 goes via formation of complex 8.4 which disproportionates via reaction with free isopropanol to the stable complex 8.3 and an equivalent of TiPT as shown in figure 8.21 below.

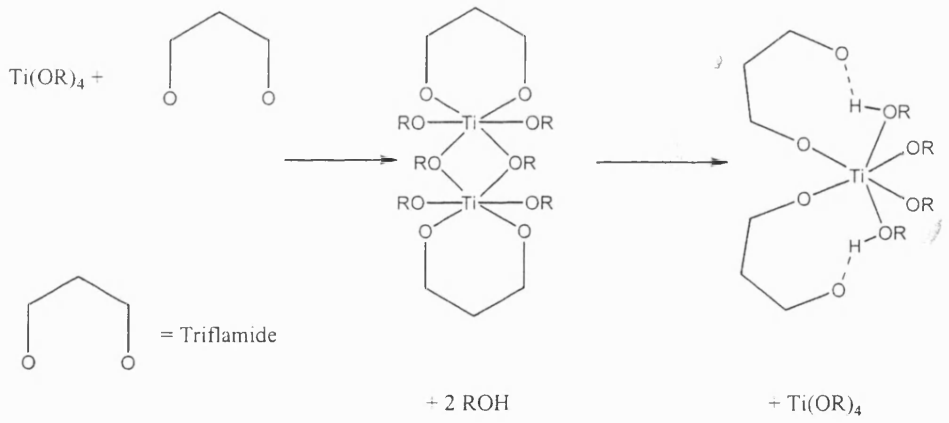

Figure 8.21: Reaction of TiPT with triflamide to form complex 8.3

Analogous reactivity is observed on reaction of triflamide with $Ti(OAr)(O^iPr)_3$ where ArOH is mesitol. In this reaction 8.3 is the exclusive isolated product which means that the previously reported compound $Ti(OAr)_2(O^iPr)_2$ must be formed as a by-product[22] as shown in figure 8.22 overleaf.

[22] A. Shah, A. Singh and R.C. Mehrotra, *Indian J. Chem. Sect. A*, **32**, 632 (1993)

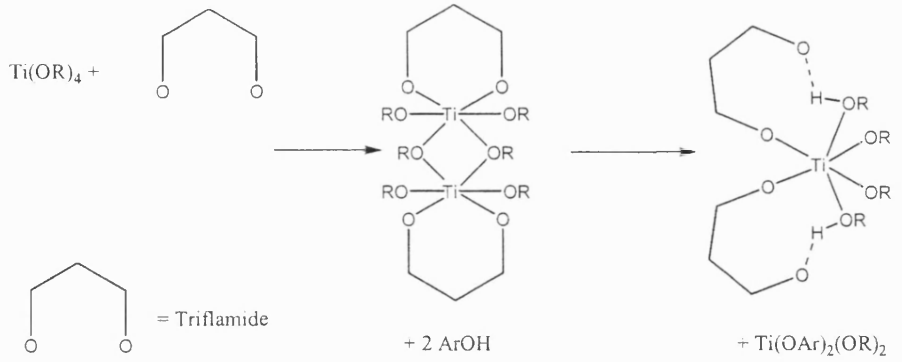

Figure 8.22: Reaction of Ti(OAr)(O^{i}Pr)$_3$ with triflamide to form complex 8.3 (OAr = mesitol)

However, in the reaction with Ti(OAr)(OiPr)$_3$ where OAr is a 2,6-di-*tert*-butyl phenol derivative the reaction stops at the intermediate complex 8.4 (figure 8.23 below). This is because disproportionation to form the more stable triflamide complex 8.3 would, as with mesitol, form the by-product Ti(OAr)$_2$(OiPr)$_2$ which in this case is highly disfavoured due to the high steric demand of this phenoxide ligand (see chapter 7 compounds 7.1 to 7.3).

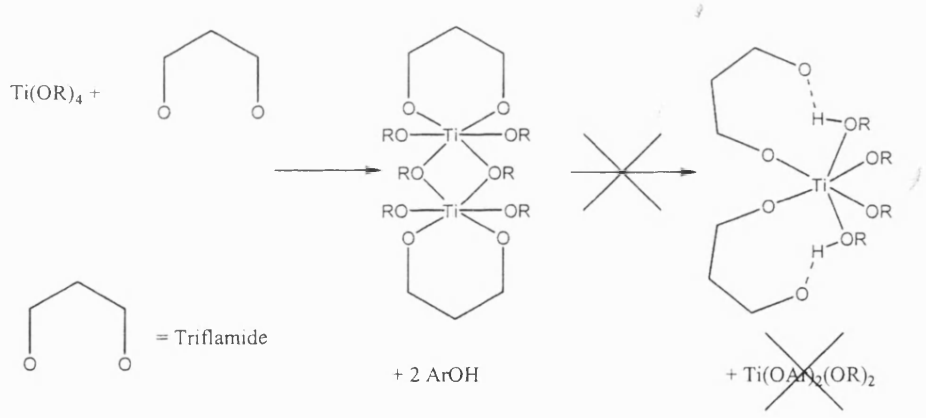

Figure 8.23: Reaction of Ti(OAr)(O^{i}Pr)$_3$ with triflamide to form complex 8.4 (OAr = 2,6-di-*tert*-butyl phenol)

Use of complexes 8.2-8.4 as Lewis acid catalysts

In the introduction to this chapter (p.284) the work of Mikami et al. was discussed. In this work an *in situ* generated titanium-triflamide species was used as a catalyst for the Friedel-Crafts acylation reaction shown in figure 8.24 below.

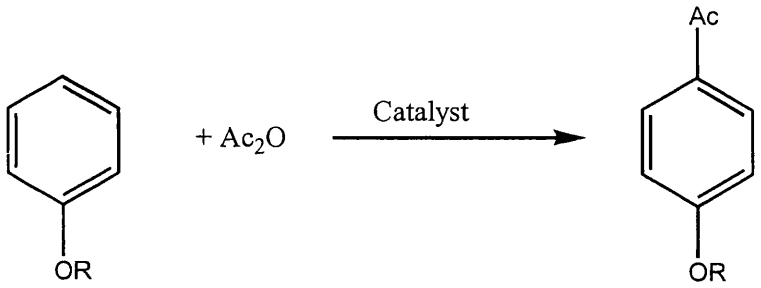

Figure 8.24: Friedel-Crafts acylation using a triflamide catalyst

The catalyst they used was generated by the reaction of two equivalents of triflamide with TiPT and can be assumed to be the complex we isolated from a similar reaction, 8.3. We wished to confirm that the catalyst we had generated gave comparable results to those which Mikami et al. had reported and also whether or not our other two related catalysts, 8.2 and 8.4, were active.

The catalytic reaction was repeated using the method described in the paper with the three catalysts at 5% loading at room temperature and the products analysed after ten minutes. The results for catalysts 8.3 and 8.4 were similar to those observed by Mikami et al. with yields > 90% and a 100% regioselectivity for *para* substitution by ^{1}H NMR. The catalyst containing the more highly coordinating *p*-tolyl ligand, 8.2, showed no reaction after 12 hours and seems to be inactive, a result that is not surprising given the nature of this complex.

Complex 8.5

The previous examples in this chapter have shown that acidic reagents can be used to form activated titanium alkoxide complexes however, none of the complexes have the desired formation of a cationic titanium species with a non-coordinating anion. We tried to produce products of this type using reagent 8.3L by reacting it with a number of titanium complexes which have been described in earlier chapters including the

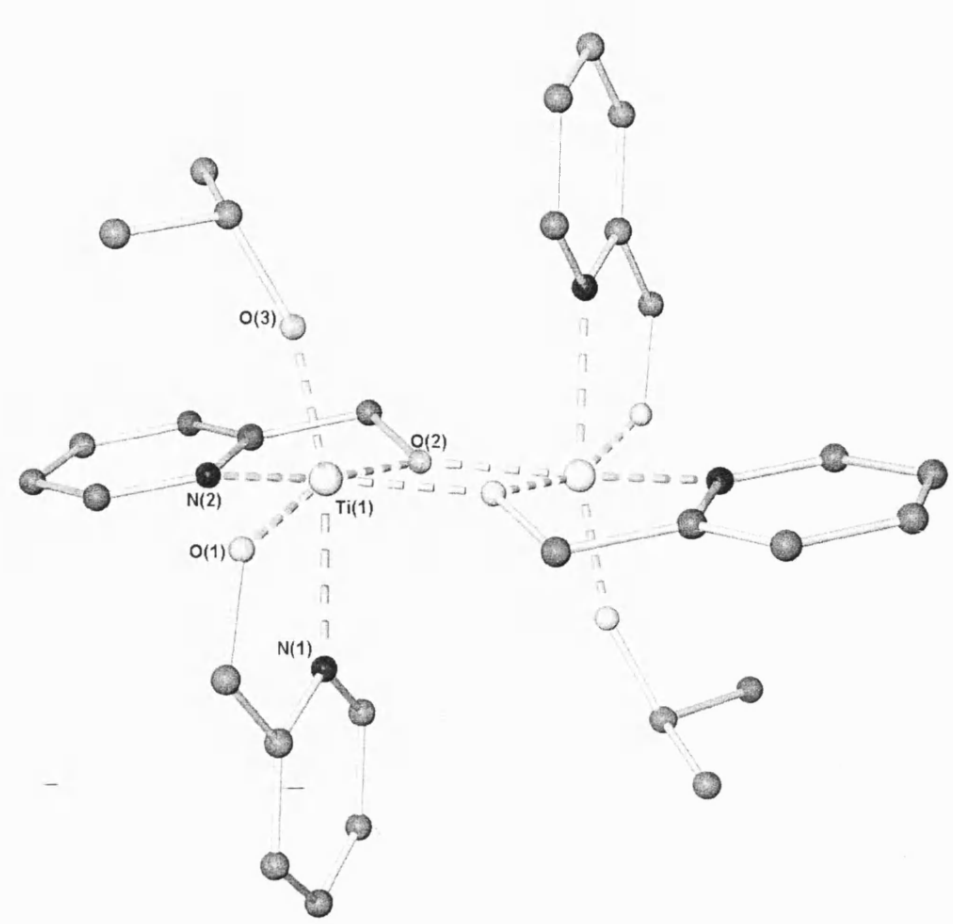

Figure 8.25: Molecular structure of the titanium cation from complex 8.5 (hydrogen atoms omitted for clarity)

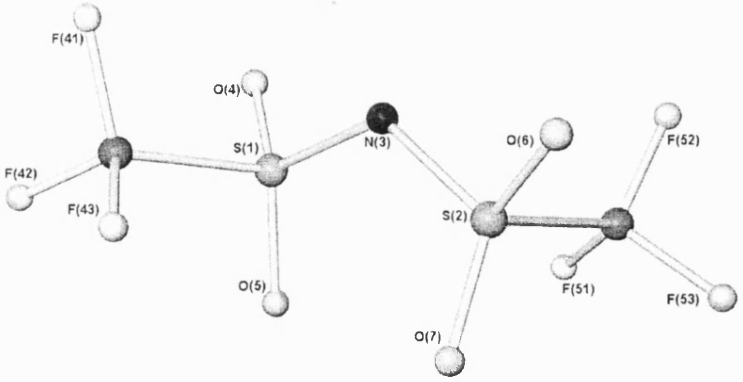

Figure 8.26: Molecular structure of the triflamide anion from complex 8.5

simple Schiff base complexes 4.4 and 4.7, the salicyldoximate 6.6 and the 8-hydroxyquinolinate complex used as a starting material in 8.1. These reactions all resulted in the formation of red oily products, which proved impossible to characterise satisfactorily. After attempting these reactions we looked at the reaction of the non-phenolic titanium complex of hydroxymethyl pyridine, 7.4, with triflamide and reaction of this derivative resulted in the formation of the desired titanium alkoxide based cation.

One equivalent of triflamide (8.3L) reacted readily with one equivalent of complex 7.4 in toluene to yield an oily product, which could be recrystallised from THF, to yield a crop of colourless crystals, which were suitable for single crystal X-ray diffraction. The asymmetric unit of complex 8.5 consisted of half a molecule of the titanium species and a single deprotonated triflamide counterion. The complex consisted of the titanium species and two triflamide counterions, each disordered over two positions, which were not coordinated to the metal centre. The titanium species consists of two metal centres bridged by the hydroxymethyl groups of two 7.4L ligands each of which is also coordinated to the respective Ti atoms through its pyridyl group. In addition each metal centre is also ligated by a second chelating 7.4L ligand and an isopropoxide ligand. The titanium centres are six-coordinate and have a distorted octahedral geometry. The core of the molecule consists of a Ti_2O_2 ring as observed in many of the complexes discussed earlier in this thesis with the two chelate rings formed by the bridging 7.4L ligands on the same plane and the other two chelate rings at ~90° to this plane.

The bond lengths to the metal of the ligands in 8.5 are shorter than the comparable bond lengths in complex 7.4 as would be expected due to the cationic nature of the metal centre. The bond length to the isopropoxide ligand {1.765(3)Å [Ti(1)-O(3)]} is ~0.07Å shorter than the comparable distance in 7.4 which is a similar difference to that seen for the non-bridging hydroxymethyl groups {1.813(3)Å [Ti(1)-O(1)]} which are shorter by ~ 0.09-0.1Å. The bridging hydroxymethyl groups have asymmetric bond lengths to the two metal centres {1.979(3)Å [Ti(1)-O(2)] and 2.043(3)Å [Ti(1)-O(2#)]} and as would be expected are longer than the bonds to the non-bridging equivalent. The bond length to the pyridyl nitrogen atom of the bridging 7.4L ligand from titanium {2.170(3)Å [Ti(1)-N(2#)]} is slightly shorter than the bond to the same

group in the non-bridging ligand {2.236(3)Å [Ti(1)-N(1)]} and both are slightly shorter than the corresponding bonds in 7.4.

The product can be seen to be the result of the protonation of one of the isopropoxide ligands of 7.4 followed by its loss to form an ion pair consisting of a cationic titanium centre with a *vacant* coordination site and a non-coordinated triflamide cation. As was described in the introduction to this chapter (p.284-285) such *vacant* coordination sites do not exist and various interactions can occur to render them into *virtual* coordination sites (fig. 8.9). In the case of complex 8.5 the *vacant* coordination site is converted to a *virtual* one by dimerisation of the metal species in the solid-state (case (v) in figure 8.9).

The ^{1}H NMR spectrum of complex 8.5 shows the formation of two, major and minor, complexes in solution in a 3:1 ratio. Each of these products has a ratio of 7.4L ligands to isopropoxide ligands of 2:1 and therefore the same basic stoichiometry as the solid-state structure obtained from this complex. Each of the complexes also has two distinct 7.4L ligand environments with the methylene CH_2 protons of these groups being split diastereotopically for all four (two in the major and two in the minor). The signals for these protons can be assigned to each of the two products using a simple COSY proton-proton correlation experiment and the relevant region of the spectrum is shown in figure 8.27 below.

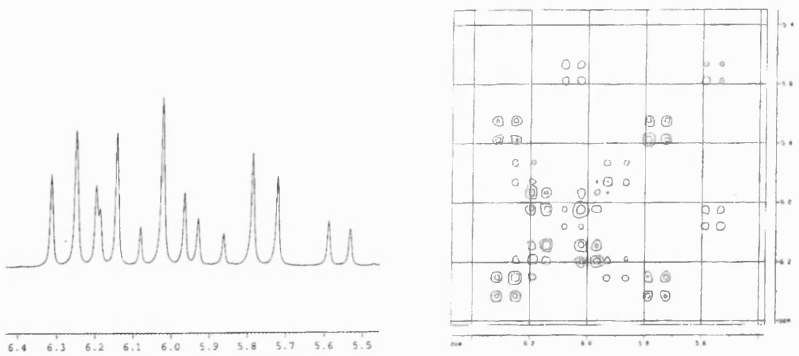

Figure 8.27: Methylene region of ^{1}H NMR spectrum of 8.5 showing major and minor products

Unfortunately it proved more difficult to separate the aromatic region into the two products and for this reason they are quoted together in the experimental section of this thesis.

It is possible to envisage several equilibrium processes taking place in solution to give the two products observed in the NMR and from the evidence which we have been able to obtain spectroscopically it has proved difficult to say which products we have in solution. A number of the possible products, which could be present, are shown in figure 8.28 overleaf and each of these could be formed by a ligand scrambling process similar to the Schlenk equilibrium. Of the complexes shown in figure 8.28, complex **C** is unlikely as it does not fit the NMR data due to the presence of four different 7.4L environments and two isopropoxide environments, complex **B** requires coordination of triflamide which is not observed spectroscopically although this could be due to exchange being fast and the others (**A**, **D** and **E**) could all fit the NMR spectra.

Complex 8.4 is the first reported example of a titanium alkoxide based cationic complex with a non-coordinating anion and fulfils the criteria we set out in the introduction to this chapter with a cationic titanium centre and an anion which seems to play no part in coordination, at least in the solid state.

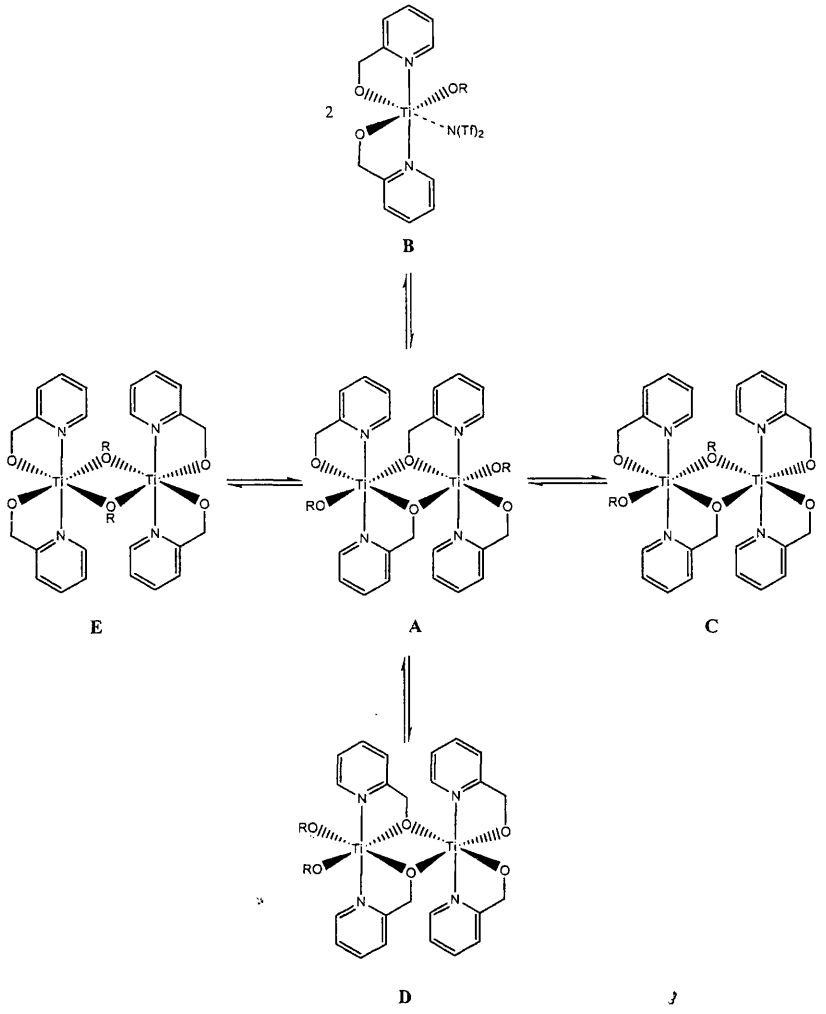

Figure 8.28: Some of the possible structures for the titanium species of 8.4 in solution (solid-state structure, A, shown centrally)

8.3 Summary of Activation of Titanium Alkoxide Complexes

The complexes described in this chapter were synthesised with a view to forming activated catalysts for polyurethane synthesis with, if possible, *virtual* free coordination sites. We wished to synthesise these as analogues of the activated group IV metal catalysts which are currently used in polyolefin catalysis.

Our initial attempt to do this utilised HBF_4 to try and remove an alkoxide from a stable titanium species and form a cationic titanium species with an uncoordinated BF_4^- counterion. This resulted in the formation of a mixture of products, which were unstable and on work up formed exclusively the di-fluoride complex 8.1. We concluded that this was due to the relative stability of Ti-F bonds compared to B-F

bonds and the high Lewis acidity of the cationic titanium complex formed as an intermediate, which induced the cleavage of B-F bonds. Although this was disappointing in that we could not use this method to form a stable cationic titanium complex it is a potentially effective route to form titanium fluoro complexes directly from alkoxide derivatives.

As the inorganic BF_4^- counterion had proved unsuccessful as a tool to form a cationic species we then investigated some sources of organic counterions. Our initial attempt using the *p*-tolyl triflamide derivative 8.2L formed a stable bis-acac type complex with both anionic ligands chelating the metal centre. Although the complex is interesting as a potential pre-catalyst in its own right, and is the first reported metal complex of this ligand we observed no evidence of a *virtual* free coordination site or a non-coordinating anion.

We concluded that to form a cationic centre the species used to form the counterion would need substituents with greater electron withdrawing character than the *p*-tolyl groups in 8.2L. The reagent we chose to do this was triflamide itself and reaction of this compound with TiPT gave us our first evidence of a *virtual* free coordination site. The complex, 8.3, had two coordination sites filled by isopropanol ligands, which had been formed via protonation from the triflamide group. Unfortunately however the anionic triflamide ligands were coordinated terminally and stabilised the isopropanol ligands through hydrogen bonding so we did not have the required non-coordinating anion. Further reaction of the triflamide with $Ti(OiPr)_3(OAr)$ resulted in formation of another form of coordinated triflamide complex, which again showed no evidence for a non-coordinating anion.

We eventually formed a complex of the kind we had been aiming for by reaction of triflamide with the hydroxymethyl pyridine derivative 7.4. The resulting complex had the expected cationic titanium centre whose vacant coordination site was filled by dimerisation of the complex. In addition the complex included two non-coordinated triflamide counterions. It is hoped that use of complexes of this type may prove useful in the future to increase the rate and activity of titanium alkoxide complexes in the formation of polyurethanes.

Chapter 9

Polymerisation studies

The previous chapters have detailed the synthesis and characterisation of a large number of titanium alkoxide based pre-catalysts. As stated in the introduction to this thesis these species have been synthesised with a view to using them as pre-catalysts for the synthesis of polyurethanes. The following chapter details investigations carried out into the use of a cross section of these complexes as catalysts for polyurethane synthesis. The reader is referred to chapter 1 (p.17-25) for a discussion of polyurethanes and the known reaction pathways in these systems.

The chapter is split into two sections: the first (section 9.1) details the use of a model reaction system, which can be observed by ^{1}H NMR spectroscopy, to compare the relative activities of some of our catalysts for formation of a urethane bond; the second (section 9.2) details the use of our catalysts for the synthesis of polyurethane in a similar manner to a simulated commercial process. In the latter instance reactions were followed by infra-red spectrometry.

Each section has a short introduction followed by a description of the experimental procedure used and finally a discussion of the results obtained, which will, where relevant, examine possible correlations between the structural features discussed in chapters 4-8 and the function of the catalysts.

9.1 Kinetic studies of a model polyurethane system

9.1.1 Introduction

As was described in chapter 1, industrially, polyurethanes are synthesised by the formation of urethane linkages in the reaction of di- and polyisocyanates and di- and polyols. These reactions are generally catalysed by tertiary amine and/or tin species and a number of papers have been published looking at the kinetics of these reactions with these and other catalysts[1]. The majority of these papers concentrate on the use of model reactions based on the formation of a urethane linkage from phenyl isocyanate

[1] Examples include; K.K. Majumdar, A. Kundu, I. Das and S. Roy, *App. Organomet. Chem.*, **14**, 79 (2000); R.A. Ligabue, A.L. Monteiro, F.F. de Souza and M.O. de Souza, *J. Molec. Cat. (A)*, **157**, 73 (2000); S.D. Evans and R.P. Houghton, *J. Molec. Cat. (A)*, **164**, 157 (2000); A. Draye and J. Tondeur, *J. Molec. Cat. (A)*, **140**, 31 (2000); A. Draye and J. Tondeur, *J. Molec. Cat. (A)*, **138**, 135 (2000); R.A. Ligabue, A.L. Monteiro, F.F. de Souza and M.O. de Souza, *J. Molec. Cat. (A)*, **130**, 101 (1998); R.P. Houghton and A.W. Mulvaney, *J. Organomet. Chem.*, **518**, 21 (1996); R.P. Houghton and A.W. Mulvaney, *J. Organomet. Chem.*, **517**, 107 (1996); S. Roy and K.K. Majumdar, *Synth. Comm*, **24**, 333 (1994); M. Arangurem and R.J.J. Williams, *Polymer*, **27**, 425 (1986), I. Yilgor and J.E. McGrath, *J. Appl. Pol. Sci.*, **30**, 1733 (1985); S. Sivakamasundari and R. Ganesan, *J. Org. Chem.*, **49**, 720 (1984)

and a mono-alcohol. A search of the literature shows that no work has been published reporting the use of group IV metals in similar reactions. To the best of our knowledge the only report that does mention group IV catalysts describes the gel times of urethanes formed for coating applications, which concludes that titanium and zirconium dionates are active for such reactions but provides no detailed kinetic data[2]. We wished to rectify this lack of information and investigate the activity of some of our catalysts for the simple urethanation reaction using ^{1}H NMR spectroscopy. As a precursor to this work a preliminary study was carried out in our group on one simple catalyst[3].

When studying the kinetics of the urethanation reaction by ^{1}H NMR spectroscopy it is necessary to use a model system, as the industrial reagents would form a polymeric product. The work described in the following section was carried out using the model reagents shown in figure 9.1 below.

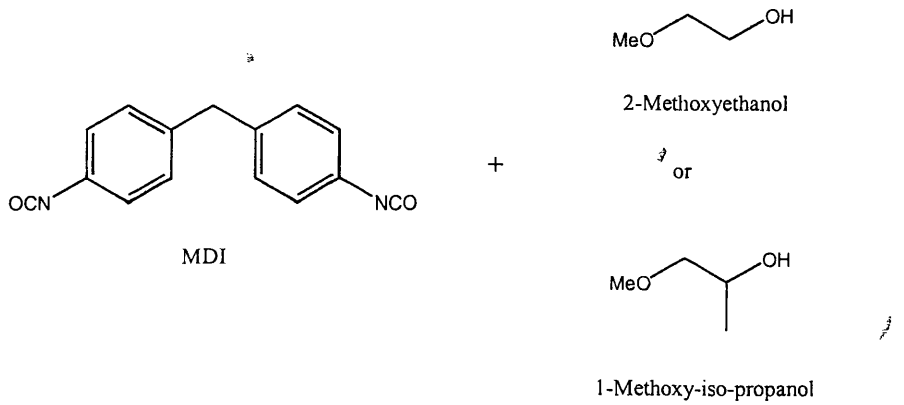

Figure 9.1: Model reagents for urethane kinetics

The di-isocyanate that was used, 4,4'-methylene-bis-phenyl-isocyanate (MDI), is a common starting material in the synthesis of polyurethanes industrially. The two diols which were used are small molecule analogues of the high molecular weight hydroxy terminated polyesters and polyethers used industrially but with one of their reactive hydroxyl groups methylated to stop the reaction after the formation of two urethane linkages per MDI molecule and thereby to stop polymer formation as seen in figure 9.2 below.

[2] W.J. Blank, Z.A. He and E.T. Hessell, *Prog. in Org. Coat.*, **35**, 19 (1999)
[3] M.G. Davidson, P. Taylor and M. Faulhaber, *unpublished results*

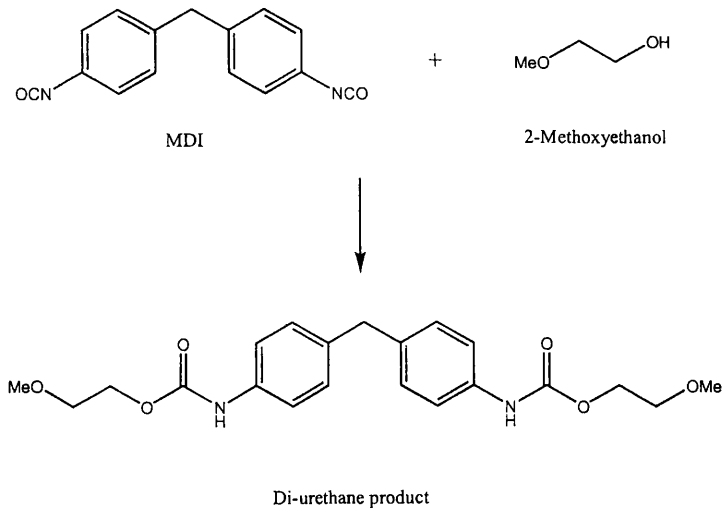

Figure 9.2: The model reaction

The catalysis reactions were carried out in deuterated benzene at various catalyst concentrations with a large excess of the alcoholic component over the MDI and catalyst components to maintain pseudo-first order conditions.

The previous work in our group[3] studied the reactivity of the catalysts shown in figure 9.3 below which were synthesised from the parent tetra methoxy-alkoxides.

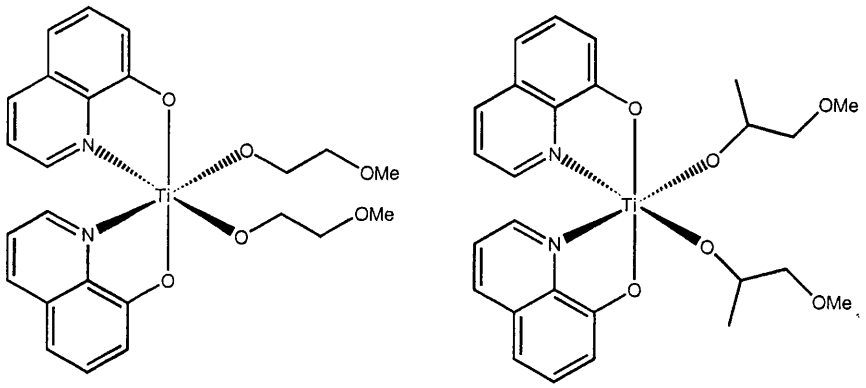

Figure 9.3: Catalysts used in the initial kinetic study

These catalysts were used rather than the isopropoxides as it was felt that this would avoid the effect of ligand exchange on the kinetic data.

The results were analysed by observing the disappearance of the ^{1}H NMR resonances due to the aromatic protons on the isocyanate starting material and the consequent appearance of the resonances due to the same protons on the newly formed urethane product as shown in figure 9.4 below.

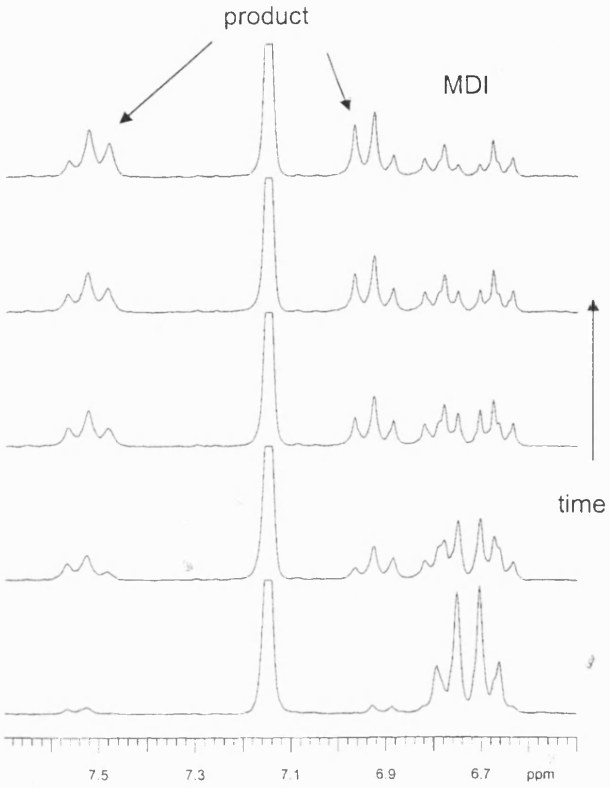

Figure 9.4: ^{1}H NMR spectra from a catalysis run in the initial study

During the work, reactions were carried out in which the concentration of catalyst, isocyanate and alcohol were varied systematically. These resulted in the workers being able to discern the order of the reaction with respect to all of these components. The reaction was found to be first order in all three components, a result which shows that the transition state of the reaction involves all three of the components and that the reaction probably has a concerted mechanism.

The work described above shows that it is possible to assess the activity of catalysts for urethanation using ^{1}H NMR spectroscopy. The following section describes the testing of a number of catalysts using this method. In all cases a series of catalytic

runs were carried out using a range of catalyst concentrations to find a value of k_{obs} for the reaction at that catalyst concentration and therefore the relative rate and rate constant for each catalyst by the method described in the experimental section below. Prior to this a brief overview of the kinetic theory is given.

9.1.2 Theory behind our kinetic method

We carried out our reaction under pseudo first order conditions with a large excess of alcohol:

In the general case the first order rate law for our reaction is defined by the equation:

$$\int_{[MDI]_0}^{[MDI]} d\frac{[MDI]_t}{[MDI]_0} = -\int_0^t k_{obs}\,dt \qquad (1)$$

Leading to the integrated rate equation:

$$\ln\frac{[MDI]_t}{[MDI]_0} = -k_{obs}t \qquad (2)$$

Equation 2 can be rearranged after the removal of the natural log to:

$$[MDI]_t = [MDI]_0 e^{-k_{obs}t} \qquad (3)$$

and:

$$\ln[MDI]_t = -k_{obs}t + \ln[MDI]_0 \qquad (4)$$

It follows from equation 4 that a plot of $\ln[MDI]_t$ against time yields a straight line of gradient $-k_{obs}$ and y intercept of $\ln[MDI]_0$. A straight line in this graph confirms that the reaction is first order in MDI.

In our case, of a pseudo first order reaction, k_{obs} is related to the rate constant k by equation 5:

$$k_{obs} = k[Cat.][ROH] \qquad (5)$$

Thus:

$$k = \frac{k_{obs}}{[Cat.][ROH]} \qquad (6)$$

In theory each of the values of k obtained (for each different catalyst concentration) should be identical. However in practise errors occur during each of the runs and so to get an average value for the rate constant, k, we plot a graph of k_{obs} against catalyst concentration for the catalyst.

The gradient of the straight line obtained in this graph can now be defined as k' where:

$$k = \frac{k'}{[ROH]} \qquad (7)$$

9.1.3 Experimental details for the kinetic investigations

Following on directly from the above theory, in all the runs discussed below the alcohol concentration can be considered to be 6.566 mol l^{-1}, allowing for errors, as the reaction is pseudo first order.

Therefore:

$$k = \frac{k'}{6.566} \qquad (8)$$

This gives us an average value for the rate constant k, which can be compared for each of the catalysts.

Preparation of starting materials and standard solutions

Standard MDI solution

MDI supplied by ICI was dissolved in toluene and any insoluble material removed by filtration. The remaining solution had all solvent removed *in vacuo* at room temperature. The MDI produced was found to be analytically pure by ^1H NMR spectroscopy and was stored at –80°C to avoid dimerisation. A standard 0.75M solution of MDI was prepared by dissolving 4.689g of purified MDI in dry degassed C_6D_6 in a 25 ml volumetric flask. The resulting clear solution was stored under argon over molecular sieves at -20°C.

2-Methoxyethanol

Supplied by Aldrich in sure-seal bottles, degassed and stored under argon over molecular sieves.

C_6D_6

Supplied by Goss Scientific and dried over molecular sieves, degassed and stored under argon.

Standard catalyst solutions

Catalysts were prepared, isolated as analytically pure solids and stored in a glove box. Using inert atmosphere techniques two standard catalyst solutions were prepared. The first solution was prepared in 5ml of C_6D_6 to give an approximate molarity of $5x10^{-2}$ mol l^{-1}. The accurate actual molarity was recorded based on the mass of catalyst added recorded on a three figure balance.

The second solution was prepared by dilution of 0.25ml of solution 1 to 10ml in C_6D_6 to give an approximate molarity of $1.25x10^{-3}$ mol l^{-1}. As before, an accurate molarity was recorded and is given in the discussion section below for each of the catalysts. This second solution was used for all kinetic runs.

Both catalyst solutions were stored under argon at –20°C between runs.

Method for catalytic runs

The reactions were carried out under an atmosphere of argon. A Schlenk tube was charged with 3.5ml of 2-methoxyethanol (0.0476 moles). To this was added x ml of catalyst solution 2 and 1.25-x ml of C_6D_6 to keep the overall reaction volume constant. At t = 0, 2.5ml of standard MDI solution (1.875×10^{-3} moles) was added and the stopwatch started. A sample of the solution was removed under argon and transferred to a rigorously washed and dried NMR tube, which was filled with argon. The tube was sealed under an argon atmosphere and taken to the NMR spectrometer where spectra were taken at regular intervals until approximately 80% of the MDI starting material could be seen to have disappeared. To ensure pseudo first order kinetics the ratio of catalyst to alcohol was maintained at a minimum of 1:25000.

Analysis of Data

The kinetic data was produced by careful analysis of spectra obtained throughout a kinetic run. The chosen indicator of rate for our catalysts was the disappearance of the signals due to the aromatic protons of the starting MDI (6.6-6.85ppm) and the consequent appearance of the signals for the aromatic protons of the new urethane product (6.85-6.96 and 7.35-7.55ppm).

The percentage of MDI remaining was obtained by calculating the ratio of the integral of the peaks due to the starting materials in the aromatic region of the spectrum to the total integral due to the aromatic hydrogen atoms of both starting materials and products.

This percentage was then used to find the concentration of MDI starting material in the reaction mixture at the time at which each spectrum was taken. The natural log of these concentrations was plotted against time for each of the spectra taken to give in all cases a straight line whose gradient was equal to $-k_{obs}$. A plot of k_{obs} versus catalyst concentration was then produced which gave a straight line.

Comparison of the gradients of the lines obtained from these final plots of k_{obs} vs. [Cat.] for each catalyst allowed the relative rates of each catalyst for these reactions to be assessed. More importantly as was stated above when this gradient was divided by

the alcohol concentration (6.566 mol l^{-1}) we could obtain a value of the rate constant for the reaction (k).

9.1.4 Results of the ^{1}H NMR kinetics

Blank runs

The first experiments to be carried out were blanks with no catalyst present, which could then be used as a comparison to the catalysed reactions. Two experiments were carried out with two different methylated diols as the alcohol.

1) The first experiment was carried out using 2-methoxyethanol as the alcohol and with no catalyst present. The reaction proceeded slowly and the formation of the mono and bis urethane products could easily be observed. The reaction had reached 75% conversion by 95 minutes and at this point the experiment was stopped. The k_{obs} for this uncatalysed reaction was found to be 2.452×10^{-4} l mol^{-1} s^{-1}.

2) The second experiment was carried out using 1-methoxyisopropanol as the alcohol and with no catalyst present. The reaction proceeded more slowly than the reaction using 2-methoxyethanol and only 40% conversion had been reached after two hours. k_{obs} for this uncatalysed reaction was found to be 7.520×10^{-5} l mol^{-1} s^{-1}. This lower value for k_{obs} is not unexpected, as secondary alcohols are known to be less reactive than primary ones in the urethanation reaction.

Due to these results the model system employed for the following work utilised 2-methoxyethanol as the methylated alcohol.

8-Hydroxyquinolinate catalysts (8HQa and 8HQb)

Following from the blank runs we wished to carry out kinetic runs using the catalyst shown in figure 9.5 overleaf. This catalyst had been used for the preliminary work described above[3].

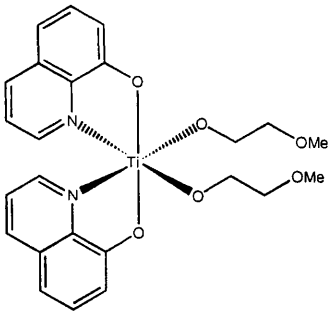

Figure 9.5: Initial catalyst used for test runs (8HQa)

The second, more dilute, catalyst solution (see method page 316), had a molarity of $1.25x10^{-3}$ mol l^{-1} and three runs using various amounts of this solution were carried out.

[Cat] mol l^{-1}	k_{obs}	r
$1.7241x10^{-4}$	$7.173x10^{-4}$ –	0.996
$8.6207x10^{-5}$	$5.900x10^{-4}$	0.997
$4.3103x10^{-5}$	$3.995x10^{-4}$	0.997

When these results were plotted along with the value obtained for the appropriate blank reaction described above a straight-line plot was obtained with a gradient (k') of **2.738 l mol^{-1} s^{-1}** and a standard error in the slope of ± 0.492. As was defined in the theoretical section, 9.1.2 above, this corresponds to a k value of **0.4170 mol^{-2} l^2 s^{-1}** with a standard error in the slope of ± 0.0749. As expected, the catalysed reaction was faster than the uncatalysed reaction by a significant factor with a rate constant that was four orders of magnitude larger than that of the uncatalysed reaction. We felt that this observation allowed us to justifiably ignore the uncatalysed reaction in any comparison of catalytic systems.

Due to the fact that the non-trivial synthesis of the titanium tetra-2-methoxyethanolate rendered the catalyst synthesis time consuming our next experimental series was carried out using the catalyst shown in figure 9.6 overleaf to see if the change in ancillary ligands affected the reaction rate significantly.

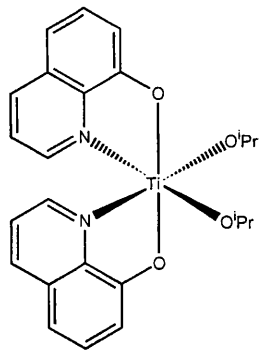

Figure 9.6: Catalyst tested with isopropoxide ancillary ligands (8HQb)

The second, more dilute, catalyst solution (see method, page 316) had a molarity of $1.32x10^{-3}$ mol l^{-1} and four runs using various amounts of this solution were carried out. The following section describes step by step the process used to generate catalytic data for this catalyst to act as an example of how the kinetic data for each of the catalysts described in this section is prepared.

Step by step discussion of the kinetic data obtained for 8-HQb

An initial catalytic run was carried out using a catalyst concentration of $2.278x10^{-4}$ mol l^{-1} and ^1H NMR spectra taken at various time intervals until the reaction approached completion. From these spectra the [MDI] in the reaction mixture could be obtained and these are shown below for this [Cat.] along with the ln [MDI] values calculated from them.

Time (s)	[MDI] mol l^{-1}	ln [MDI]
0	0.2590	-1.3510
300	0.2245	-1.4937
480	0.1904	-1.6584
660	0.1574	-1.8488
900	0.1386	-1.9759
1200	0.1059	-2.2452
1500	0.0653	-2.7282
2100	0.0438	-3.1271
2700	0.0283	-3.5661

The ln [MDI] values for this [Cat.] were then plotted against time to give the graph shown below.

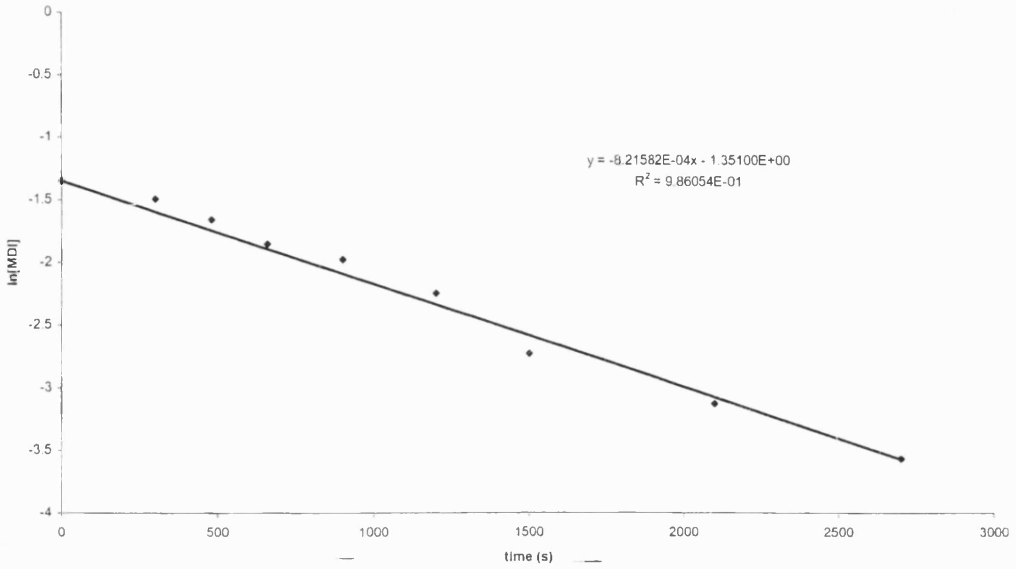

Figure 9.7: Plot of ln[MDI] vs time for [8-HQb] of $2.278x10^{-4}$ mol l^{-1}

As can be seen the graph gave a k_{obs} for this catalyst concentration of $8.216x10^{-4}$ and a correlation coefficient (r) for this graph of 0.986. This process was repeated at three more catalyst concentrations the results of which are shown in the table below.

[Cat] mol l^{-1}	k_{obs}	r
$2.278x10^{-4}$	$8.216x10^{-4}$	0.986
$1.822x10^{-4}$	$6.518x10^{-4}$	0.994
$1.367x10^{-4}$	$7.215x10^{-4}$	0.995
$9.110x10^{-5}$	$4.897x10^{-4}$	0.986

The k_{obs} values obtained were then plotted against catalyst concentration along with the data for the blank run with 2-methoxyethanol described above (p.318). This yielded the graph shown below which has a gradient which is equal to k' as discussed in the theoretical section above.

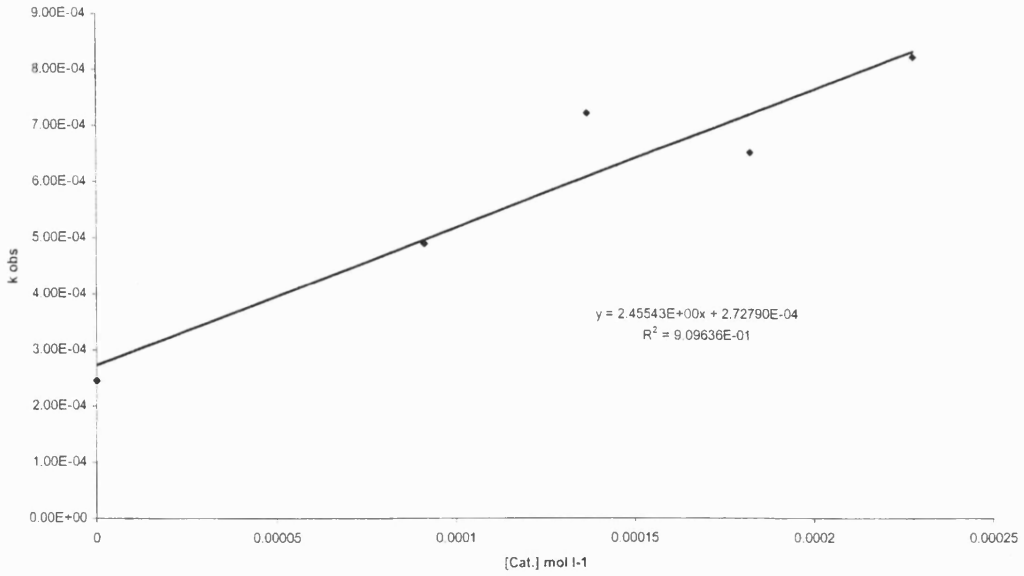

Figure 9.8: Plot of k_{obs} vs [Cat.] for catalyst 8-HQb

From the gradient of this graph a value of k' was obtained of **2.455 l mol^{-1} s^{-1}** with a standard error in the slope of ± 0.447. From this value it is possible to calculate a value of k for the reaction of **0.3739 mol^{-2} l^{2} s^{-1}** with a standard error in the slope of ± 0.0681.

Within error, the value of k obtained shows that ligand exchange has little effect on the observed rate constant allowing us to use isopropanolates for future reactions.

From the above reactions two important conclusions were reached: firstly that the uncatalysed reaction can be ignored in comparison of catalysts; secondly that ligand exchange from pre-catalyst to catalyst species, as shown in figure 9.9 below, is very fast and has little effect on rate which allows us to use titanium isopropanolate pre-catalysts for our kinetic comparisons.

$$L_2Ti(O^iPr)_2 + \text{xs MeO-Et-OH} \rightleftharpoons L_2Ti(\text{O-Et-OMe})_2 + 2\ {}^iPrOH + \text{xs MeO-Et-OH}$$

Figure 9.9: Pre-catalyst alcohol exchange in urethane catalysis

2,2' Methylene bridged bisphenol catalyst

The first new catalyst to be tested was the bisphenolate shown in figure 9.10 below, which is a member of a family of compounds which are known to be active for polyolefin synthesis[4].

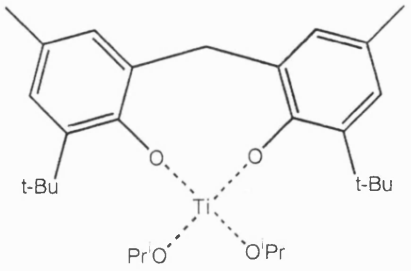

Figure 9.10: Bisphenol catalyst

The second, more dilute, catalyst solution (see method, page 316) had a molarity of 1.33×10^{-3} mol l^{-1} and two runs were carried out at differing titanium concentrations (2.330 mol l^{-1} and 1.864 mol l^{-1}). In both cases on addition of the catalyst to the reaction mixture the bright red colour from the metal species immediately disappeared. When the sample was analysed by ^1H NMR spectroscopy the reactions were found to have reached completion by the time the first sample was taken (<10 minutes).

The reason for this reactivity is thought to be due to the coordinatively unsaturated nature of the titanium centre in the catalytic species. We believe that on dissolution in 2-methoxyethanol a ligand exchange process occurs to form the titanium tetra-2-methoxyethanolate as shown in figure 9.11 overleaf.

[4] C. Floriani, F. Corazza, W. Lesceur, A. Chiesi-Villa and C. Guastini, *Angew. Chem. Int. Ed. Engl.*, **28**, 66 (1989)

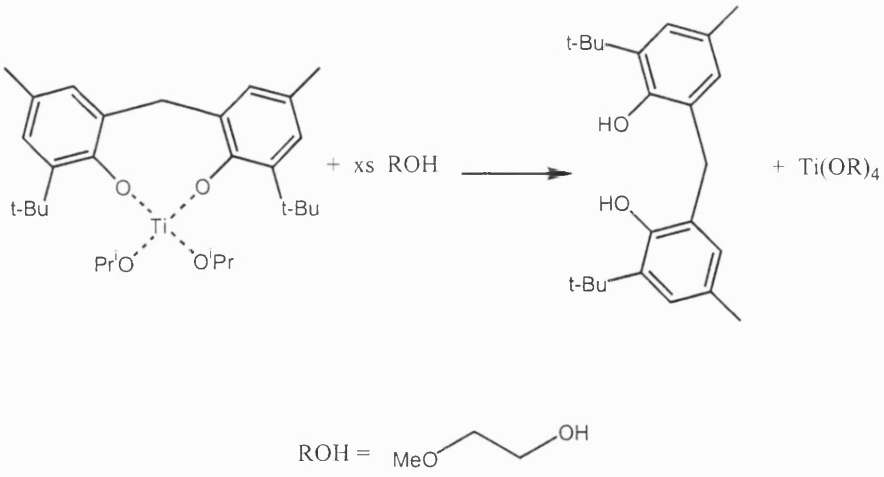

Figure 9.11: Ligand exchange under catalytic conditions

This tetra-product is known, from earlier work in our group[3], to be colourless and highly active for the urethanation reaction but is thought to be of no effective use as a polyurethane catalyst due to its poor selectivity in the non-model reaction. Because of this unexpected reactivity we have not studied this catalyst and others of this type further as potential catalysts for this process and have concentrated on coordinatively saturated titanium alkoxide complexes.

Catalyst 6.6

The catalyst shown in figure 9.12 below which is described in chapter 6, was chosen to be studied next and a catalyst solution with a molarity of 4.15×10^{-4} mol l^{-1} with respect to catalyst was prepared (see method, page 316).

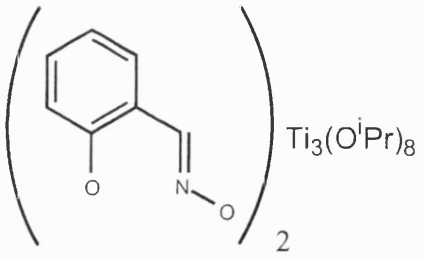

Figure 9.12: Catalyst 6.6

Five catalytic reactions were carried out at various catalyst concentrations and the usual plots drawn. As with the 8-hydroxyquinoline catalysts the reaction was found to be first order in catalyst and MDI.

[Cat] mol l^{-1}	k_{obs}	r
$9.69x10^{-5}$	$2.474x10^{-3}$	0.992
$7.75x10^{-5}$	$2.219x10^{-3}$	0.993
$5.81x10^{-5}$	$1.659x10^{-3}$	0.996
$3.87x10^{-5}$	$7.812x10^{-4}$	0.998
$1.94x10^{-5}$	$6.659x10^{-4}$	0.987

When these results were plotted along with the value obtained for the appropriate blank reaction described above a straight-line plot was obtained with a gradient (k') of **25.48 l mol^{-1} s^{-1}** and a standard error in the slope of ± 2.352. As was defined in the theoretical section, 9.1.2 above, this corresponds to a k value of **3.88 mol^{-2} l^2 s^{-1}** and a standard error in the slope of ± 0.3582.

Catalyst 7.4

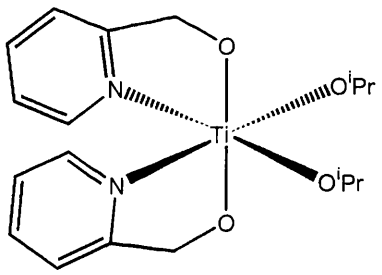

Figure 9.13: Catalyst 7.4

A solution of the catalyst shown in figure 9.13 above with a concentration of $1.399x10^{-3}$ mol l^{-1} with respect to titanium (see method, page 316) was prepared and five catalytic runs carried out at various catalyst concentrations.

[Cat] mol l^{-1}	k_{obs}	r
$2.413x10^{-4}$	$2.429x10^{-3}$	0.985
$1.930x10^{-4}$	$1.980x10^{-3}$	0.988
$1.448x10^{-4}$	$1.121x10^{-3}$	0.999
$9.651x10^{-5}$	$8.687x10^{-4}$	0.9996
$4.826x10^{-5}$	$5.266x10^{-4}$	0.994

When these results were plotted, along with the value obtained for the appropriate blank reaction described above, a straight-line plot was obtained with a gradient (k') of **9.20 lmol^{-1}s^{-1}** and a standard error in the slope of ± 0.972. As was defined in the theoretical section, 9.1.2 above, this corresponds to a k value of **1.401 mol^{-2}l^{2}s^{-1}** and a standard error in the slope of ± 0.148.

Catalyst 4.4

The following catalyst, figure 9.14 below, was the first of a series of salicylaldimine catalysts we tested to try and elucidate some basic structure/activity relationships.

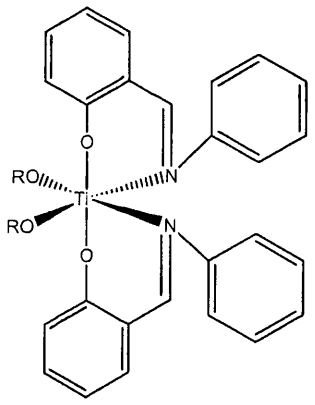

Figure 9.14: Catalyst 4.4

A catalyst solution with a concentration of $1.289x10^{-3}$ mol l^{-1} with respect to titanium was prepared (see method, page 316) and five catalytic runs carried out at various catalyst concentrations.

[Cat] mol l^{-1}	k_{obs}	r
$2.223x10^{-4}$	$3.191x10^{-3}$	0.963
$1.778x10^{-4}$	$2.923x10^{-3}$	0.983
$1.333x10^{-4}$	$2.183x10^{-3}$	0.984
$8.890x10^{-5}$	$1.149x10^{-3}$	0.998
$4.445x10^{-5}$	$7.683x10^{-4}$	0.997

When these results were plotted along with the value obtained for the appropriate blank reaction described above a straight-line plot was obtained with a gradient (*k'*) of **14.28 $lmol^{-1}s^{-1}$** and a standard error in the slope of ± 1.113. As was defined in the theoretical section, 9.1.2 above, this corresponds to a *k* value of **2.176 $mol^{-2}l^2s^{-1}$** and a standard error in the slope of ± 0.1695.

Complex 4.8

The catalyst shown in figure 9.15 below was assessed for activity to see whether the differing steric bulk and configuration at the metal centre would have a significant effect on the catalytic properties of the complex.

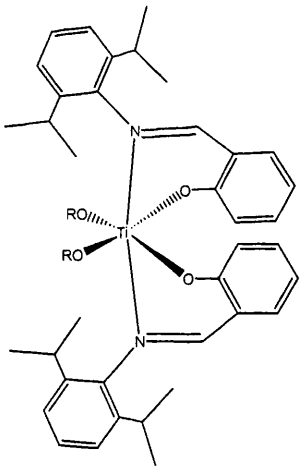

Figure 9.15: Catalyst 4.8

A catalyst solution was prepared and five catalytic runs carried out at various catalyst concentrations. However, the catalyst was found to be unstable on storage as a solution in deuterated benzene and problems were encountered with reproducibility.

Eventually use of a freshly prepared catalyst solution with a concentration of 9.2869 $x10^{-4}$ mol l^{-1} with respect to titanium (see method, page 316) allowed for a series of experiments to be carried out consecutively on the same day giving results which lay on a straight line.

[Cat] mol l^{-1}	k_{obs}	r
$1.601x10^{-4}$	$2.094x10^{-3}$	0.9998
$1.281x10^{-4}$	$1.395x10^{-3}$	0.991
$9.607x10^{-5}$	$9.897x10^{-4}$	0.996
$6.405x10^{-5}$	$7.428x10^{-4}$	0.995
$3.202x10^{-5}$	$6.104x10^{-4}$	0.995

When these results were plotted along with the value obtained for the appropriate blank reaction described above a straight-line plot was obtained with a gradient (k') of **10.57 $lmol^{-1}s^{-1}$** and a standard error in the slope of ± 1.374. As was defined in the theoretical section, 9.1.2 above, this corresponds to a k value of **1.61 $mol^{-2}l^{2}s^{-1}$** and a standard error in the slope of ± 0.209.

Catalyst 4.5

Having assessed the effect of the steric bulk of a Schiff base ligand on the catalytic properties of the titanium complex we now wished to assess the effect of varying the electronics on the imine substituents and to this end the catalyst shown in figure 9.16 below was assessed.

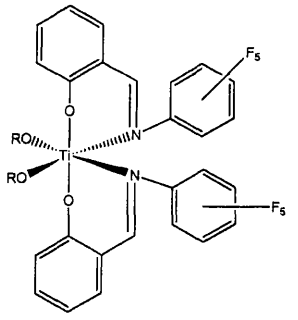

Figure 9.16: Catalyst 4.5

A catalyst solution with a concentration of 9.548 $x10^{-4}$ mol l^{-1} with respect to titanium was prepared (see method, page 316) and four catalytic runs carried out at various catalyst concentrations.

[Cat] mol l^{-1}	k_{obs}	r
$1.317x10^{-4}$	$2.207x10^{-3}$	0.983
$9.877x10^{-5}$	$1.442x10^{-3}$	0.991
$6.585x10^{-5}$	$1.243x10^{-3}$	0.9996
$3.292x10^{-5}$	$8.171x10^{-4}$	0.977

When these results were plotted along with the value obtained for the appropriate blank reaction described above a straight-line plot was obtained with a gradient (k') of **13.81 l $mol^{-1}s^{-1}$** and a standard error in the slope of ± 1.394. As was defined in the theoretical section, 9.1.2 above, this corresponds to a k value of **2.10 $mol^{-2}l^{2}s^{-1}$** and a standard error in the slope of ± 0.212.

Catalyst 4.13

To further assess the effect of the electronic properties of a Schiff base ligand on the activity of the catalyst the species shown in figure 9.17 below was used as a catalyst in the urethanation reaction.

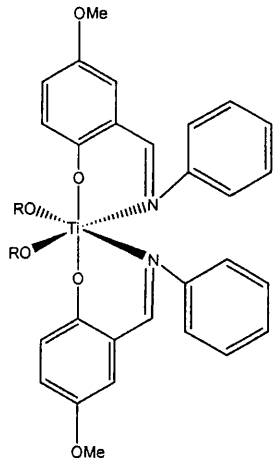

Figure 9.17: Catalyst 4.13

A catalyst solution with a concentration of 1.342 $x10^{-3}$ mol l^{-1} with respect to titanium was prepared (see method, page 316) and four catalytic runs carried out at various catalyst concentrations.

[Cat] mol l^{-1}	k_{obs}	r
$1.851x10^{-4}$	$2.555x10^{-3}$	0.957
$1.388x10^{-4}$	$1.981x10^{-3}$	0.996
$9.255x10^{-5}$	$1.417x10^{-3}$	0.995
$4.628x10^{-5}$	$7.470x10^{-4}$	0.944

When these results were plotted along with the value obtained for the appropriate blank reaction described above a straight-line plot was obtained with a gradient (k') of **12.65 l $mol^{-1}s^{-1}$** and a standard error in the slope of ± 0.272. As was defined in the theoretical section, 9.1.2 above, this corresponds to a k value of **1.93 $mol^{-2}l^{2}s^{-1}$** and a standard error in the slope of ± 0.0414.

Di-butyl-tin-di-laurate

This catalyst (shown in figure 9.18 below) was tested to see how our catalysts compared to a commercial tin catalyst in the urethanation reaction. The catalyst was supplied by Synetix and used as received.

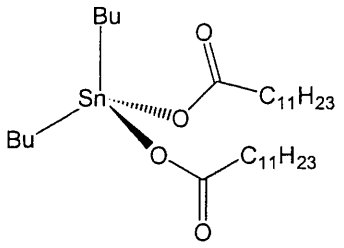

Figure 9.18: Di-butyl-tin-di-laurate

A catalyst solution with a concentration of $1.322x10^{-3}$ mol l^{-1} with respect to tin was prepared (see method, page 316) and catalytic runs carried out at various catalyst concentrations. However, other than the weakest of these initial runs, the catalysis was too quick for us to obtain suitable kinetic data and a third catalyst solution was

prepared with a concentration of $1.322x10^{-4}$ mol l^{-1}. This new catalyst solution was used to carry out catalytic runs at various catalyst concentrations.

[Cat] ML^{-1}	k_{obs}	r
$9.118x10^{-5}$	$3.292x10^{-3}$	0.998
$4.559x10^{-5}$	$2.496x10^{-3}$	0.9994
$2.280x10^{-5}$	$1.610x10^{-3}$	0.991
$1.824x10^{-5}$	$1.323x10^{-3}$	0.992
$1.368x10^{-5}$	$1.002x10^{-3}$	0.965

When these results were plotted along with the value obtained for the appropriate blank reaction described above a straight-line plot was obtained with a gradient (k') of **32.02** $\mathbf{LM^{-1}s^{-1}}$ and a standard error in the slope of ± 3.717. As was defined in the theoretical section, 9.1.2 above, this corresponds to a k value of **7.49** $\mathbf{M^{-2}L^{2}s^{-1}}$ and a standard error in the slope of ± 0.566.

9.1.5 Discussion of the NMR model study results

The results obtained in the catalytic runs described above are shown in the two graphs on the following pages. The first, figure 9.19, shows the straight line graphs of [Cat.] vs k_{obs} which were obtained for each of the catalysts described. These graphs, which were used to obtain the rate constants for the reaction with each catalyst, show the variation in activity of the catalysts. The second, figure 9.19, shows the relative values of k, the rate constant found for each of the catalysts.

Although only a small selection of our pre-catalysts was tested in this way certain trends can be observed throughout the range. All the species that we tested were active for the formation of urethane bonds with widely varying activities. However, none of the titanium complexes for which we could obtain kinetic data were as fast as the commercially available tin catalyst di-butyl tin di-laurate. We believe the main reason for this is the difference in nature of the tin and titanium species studied rather than an inherent faster rate for tin catalysts over titanium. The titanium catalysts tested have been designed to contain one, or more, stable, control ligands, which play no active part in polymerisation. In contrast, the tin species does not have stable ligands

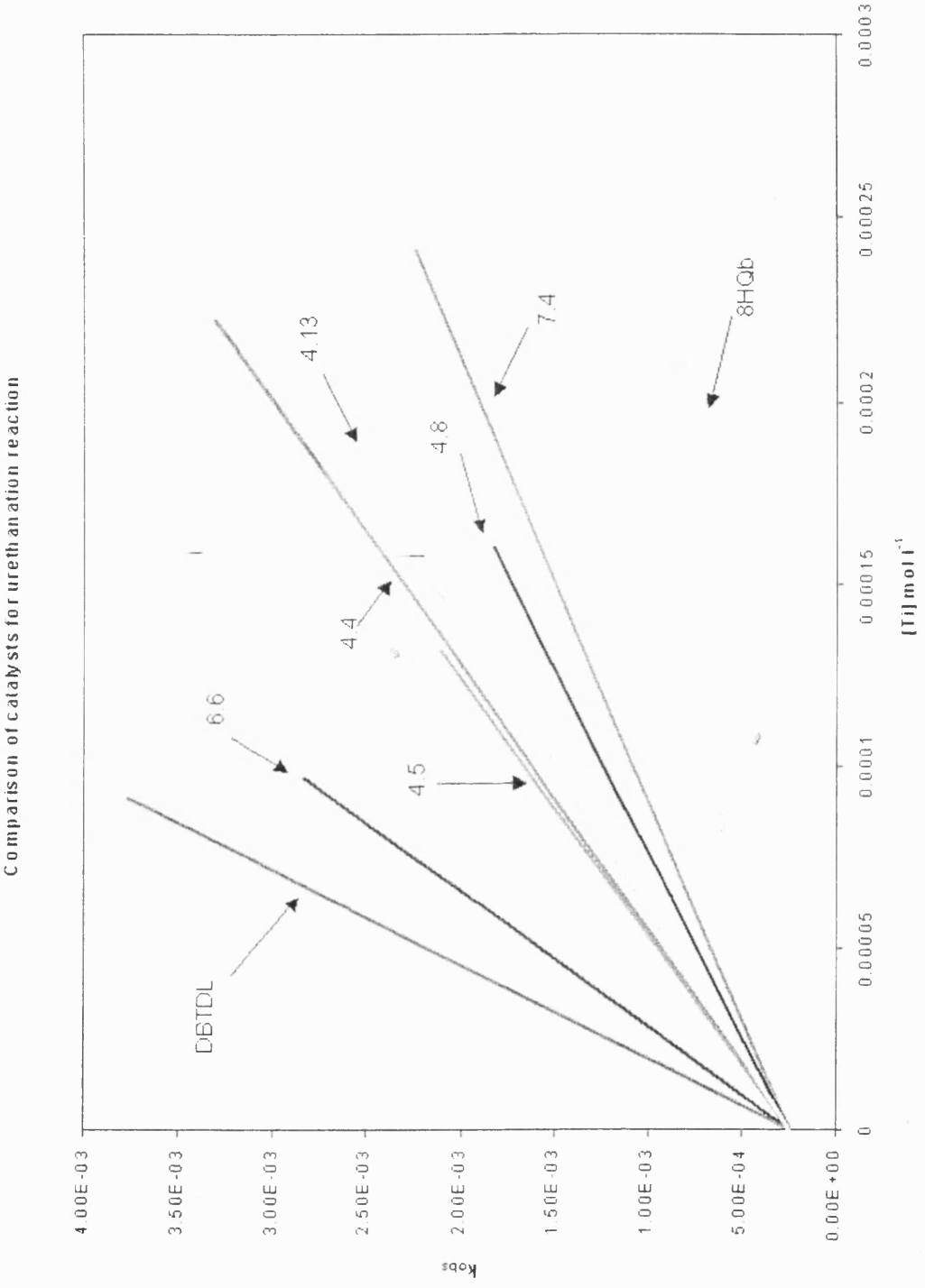

Figure 9.19: Comparison of [Cat.] vs k_{obs} lines for all catalysts

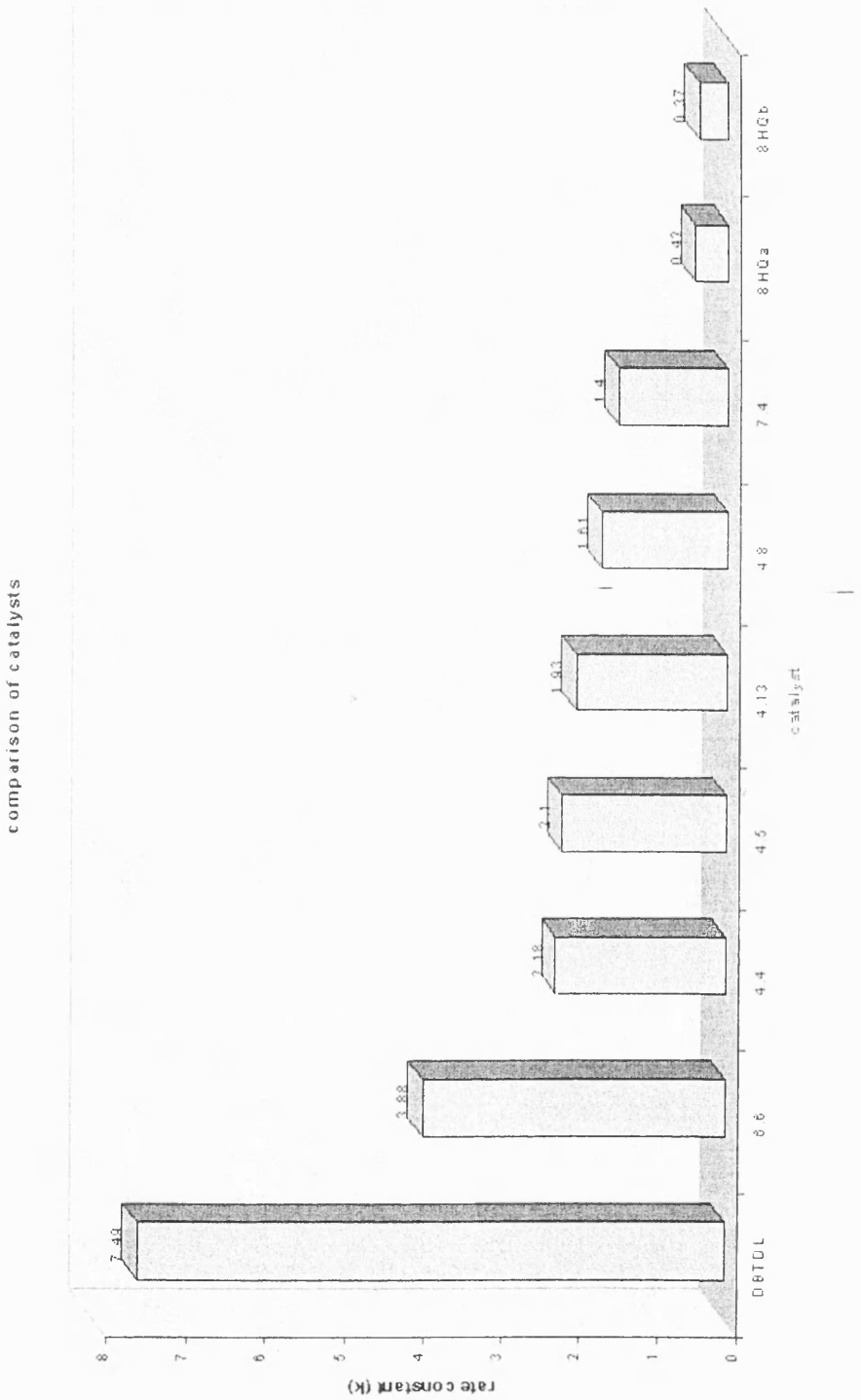

Figure 9.20: Comparison of *k* for all catalysts

of this type and has four active sites for polymerisation. A fairer comparison would be to test tin compounds with similar 'control' ligands or homoleptic titanium alkoxides, which have been tested by our group previously but proved too fast to study effectively by ^{1}H NMR spectroscopy.

The lower rates observed for our catalysts compared to DBTDL are not necessarily a stumbling block in the use of our catalysts commercially. As has been stated earlier in this thesis an increase in rate is not the main driving force behind our study of titanium species for polyurethane catalysis, much more important are selectivity and environmental concerns. The following section will discuss each of the catalysts in turn and try to draw some conclusions from the results obtained.

The titanium catalyst containing the 4,4'-methylene bridged bis-phenol was found to be unstable under the reaction conditions we were using for our study. On dissolution of the titanium species a ligand exchange occurred to form the parent tetra-alkoxide which although highly active is known to have poor selectivity in commercial systems[5]. This ligand exchange by a four-coordinate complex is important to note as it seems to suggest that highly coordinatively unsaturated titanium species such as this will be unstable under reaction conditions employed in polyurethane synthesis, a factor which will be important in future ligand design. Although for our study this meant that we could not study this catalyst effectively, and that we could discount it, it could be useful in another way. The parent bis-phenol ligand, which is released by the exchange process, is a well-known antioxidant used in polymer manufacture. It may be possible using the process described here to use this titanium species as a method of delivering this and other antioxidants directly into the structure of the polymer being synthesised.

The catalyst, which had been used for the more detailed kinetic study, prior to this work, 8-HQ, was found to be by far the slowest of the catalysts studied. This fact, which greatly aided the earlier study, is not unexpected as the complex itself is extremely stable both in the solid-state and solution. This stability along with the very

[5] B. Stengel and M. Partridge, *private communication*

rigid ligand environment formed by the fused aromatic ligand is probably the reason behind its low rate.

When the analogous complex with hydroxymethyl pyridine ligands, 7.4, was used as a catalyst the rate increased by three and a half times. The hydroxymethyl pyridine ligand is a direct analogue of the 8-hydroxyquinoline, with the same N,O donor set and forming the same sized chelate rings. However the ligand in 7.4 has a weaker bonded alkoxide as compared to the 8-HQ ligands aryloxide and has much more freedom in how it can orient itself with respect to the metal. We would suggest that the combination of these two factors contributes to the increase in rate of 7.4 relative to 8-HQ.

The fastest of the titanium species, by far, was the salicylaldoxime-based catalyst, 6.6, which gave a rate constant which was almost double that of the nearest titanium complex and only around half that of the tin catalyst. The most likely explanation for this is the increased number of metal centres per catalyst molecule in this complex compared to the other species studied. It is however interesting to note that although there is more than one metal centre in the molecule the reaction is still first order with respect to catalyst suggesting that the transition state in the urethane formation still involves only one metal centre. A further reason for its increased rate compared to the other Ti species may be the increased number of reactive alkoxides present per metal centre in 6.6 (2.7 per metal atom as compared to 2 for the other catalysts).

The group of catalysts, which we have studied in most detail using the model reaction, are the monoanionic salicylaldimines described in chapter 4. In our structural study of these compounds we showed that the main factor in determining the structure of the titanium complexes of these ligands was the steric demand of the ligand and particularly of the salicylaldimine substituents. In addition we showed that variation of the electronic properties of the ligand had little effect on the structural form observed. We wished to see if this observation carried over into the catalytic properties of the complexes and chose four complexes to assess this.

As a basis for a comparison we chose the aniline salicylaldimine complex 4.4 shown in figure 9.21.

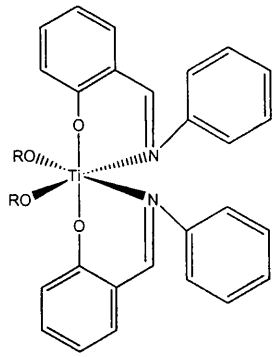

Figure 9.21: Catalyst 4.4

This complex catalysed the reaction and gave the fastest rate, which we had observed so far for a monometallic titanium complex with a rate five times that of 8-HQ.

To look at the effect of electron withdrawing and donating groups on the activity of this catalyst we then looked at the kinetics of the pentafluoroaniline derivative of this ligand (4.5) and an analogue with a methoxy group in the 4-position of the phenolic ring. Both catalysts were active for the model reaction and gave results with a similar rate constant to the parent compound. Although differences were observed between the rate constants for the three reactions they are not large and show no discernable pattern due to the new electronic environment. Because of this we attribute these small differences to experimental error and conclude that introduction of electron withdrawing and donating groups on the two phenyl rings of these ligands seems to have little effect on the rate of this reaction.

In contrast when the steric bulk of the salicylaldimine group on the catalyst was increased a significant difference was observed both in rate and stability of the catalyst. The di-isopropyl aniline derivative (4.8) was chosen as a test for the effect of ligand sterics as it is an example of a complex with a differing configuration at the metal centre due to the steric demand of the ligand. It was discovered that on storage as a benzene solution, unlike the other salicylaldimine compounds, the activity of the catalyst decreased and that to obtain good kinetics it was necessary to use a fresh catalyst solution. Although a reason for this loss of activity was not discovered it points to a lower stability of this catalyst. Once a fresh catalyst solution was employed

the catalyst was found to have a lower activity than the three previously described salicylaldimine catalysts, although still faster than the other monometallic titanium species. The reason for this lower activity and stability is unclear although it is almost certainly due to the differing structure of this complex when compared to 4.4, 4.5 and 4.13.

This result along with those for the other salicylaldimine complexes seems to suggest that in a similar manner to structure, catalytic activity is unaffected by the electronic properties of the ligand while the steric properties have a profound effect. This observation that the electronic properties of the ancillary ligands have little effect on rate has also been observed in salicylaldimine complexes of nickel used for polyolefin synthesis. Ziegler et al. studied the effects of steric bulk and electron withdrawing and donating groups on these systems using DFT calculations and concluded that, while variation of the electronic properties should have little effect on polymerisation, changes in steric demand had a significant effect and in contrast to our results that bulky substituents should increase activity[6].

The results obtained from the ^{1}H NMR studies of the model reaction have shown that a wide range of our titanium catalysts are active for the formation of urethane bonds. They have also shown that the structure of the titanium complex has an effect on the rate at which this urethane formation takes place with a range of rates, which vary tenfold depending on the control ligands employed. In addition they have shown that, although our complexes are not as active as a commercial tin catalyst they do, even in their unoptimised state, give rate constants that have a similar value.

What the results using this model system do not give us, however, is any insight into the selectivity of our catalysts for the various products formed during the synthesis of polyurethanes. To look at this we need to use real systems and produce polyurethane, a reaction which cannot easily be followed by NMR spectroscopy. To do this we have employed in situ infra red spectrometry and this will be described in the following section.

[6] M.S.W. Chan, L. Deng and T. Ziegler, *Organometallics*, **19**, 2741 (2000)

9.2 Testing of real systems using an in-situ infra red probe

9.2.1 Background

As has been described in the previous section the study of a model reaction using ^1H NMR spectroscopy is a very useful tool for comparison of the relative rates of reaction of each of our catalysts during the formation of a urethane linkage. However, this reaction tells us very little about the selectivity of our catalysts. During the synthesis of polyurethane products from a polyol and a di-isocyanate there are a number of side reactions that can occur and each of these will affect drastically the physical properties of the final polymer. These reactions, which are shown in figure 9.21 below, can result in increased cross linking between polymer chains (reactions a, b and c), decreased flexibility and the introduction of crystallinity (reaction d) and the formation of foams through the evolution of gas (reaction e).

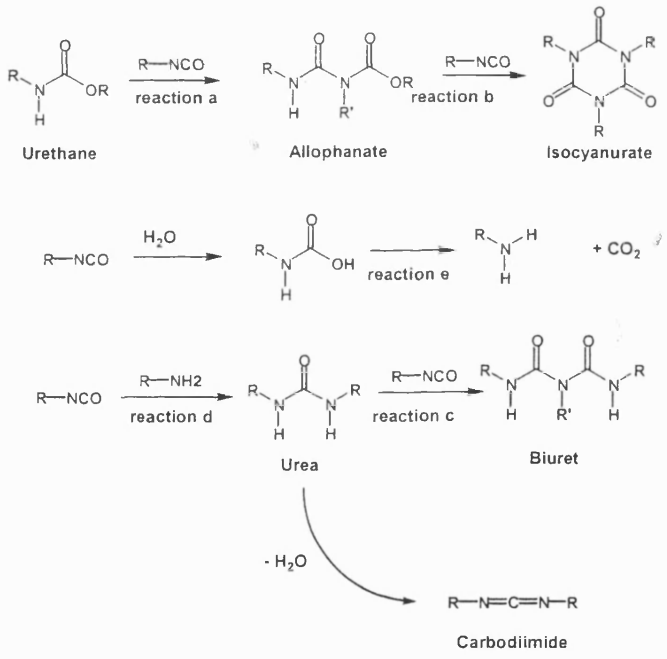

Figure 9.22: By-product formation reactions in polyurethane synthesis

All of these effects will change the structure and therefore the physical properties of the final polymer. We wished to investigate the selectivity of a number of our catalysts, along with some of the standard catalysts produced by Synetix and a commercial tin based catalyst, for their selectivity for each of the expected products. We chose to study a commercially important pre-polymer system consisting of the

high molecular weight polyether, polypropylene glycol (Mw = 4000), and the di-isocyanate, MDI, which we had used in our model NMR reactions.

Unfortunately there is no literature precedent for studying polyurethane synthesis using in situ infra-red spectrometry and the signals due to the various products which can be formed are poorly understood. Our assignment of the peaks was carried out using information supplied by our co-workers at Synetix and the small amount of information available in the literature[7].

The reactions were followed using an ASI Systems React IR 1000 equipped with a DiComp Probe, which can take infra red spectra of the reaction mixture at pre-set time intervals during a reaction. These spectra can then be analysed to try and assign the peaks that are present during the reaction and thereby show which side reactions occur with each catalyst and at what time during the reaction.

9.2.2 Experimental

The catalyst solutions were prepared in a glove box under an inert atmosphere. The polypropylene glycol was used as received from Aldrich. MDI was purified by the standard procedure described for the NMR reactions in section 9.13 (p.316) above and then stored at -4°C. All reactions were carried out under an inert atmosphere using N_2 as a purge gas.

Prior to the addition of any reactants to the reaction flask a background spectrum of the atmosphere in the flask was taken which would then be automatically deducted from the spectra of the products. Following this 100g (0.025 moles) of polypropylene glycol (4000 Mw) were added to the flask along with 35g (0.14 moles) of purified MDI and the temperature gradually raised to 80°C with constant stirring. At this point a spectra was taken and the program started. Following this the catalyst was added either neat or as a toluene solution. After five minutes a spectra was recorded and then a further spectra was recorded every minute for 30 minutes. After this period of time had elapsed a further spectrum was taken every 5 minutes until either no further

[7] V.V. Zharkov, M.Y. Ysarfin, S.V. Vdovina, L.I. Kopusov and A.K. Zhitikina, *Z. Anal. Chim.*, **42**, 1359 (1987); G. Socrates, *'Infra-red Characteristic Group Frequencies'*, 2nd Ed., Wiley, New York (1994)

reaction was observed, the product became too viscous for the spectra to be valid (i.e. stirring stopped) or because the time limit of three hours was reached.

9.2.3 Results

The following section briefly discusses the results for each of the catalysts which were tested and blank runs, which were also carried out. All of the runs are shown in the following table, which details the amount of each catalyst used, the physical state of the polymer product and the identified products; the codes in the catalyst column correspond to the catalysts shown in figure 9.23 overleaf.

On the pages following the table are the in situ infra red spectra of two of the catalytic runs, which will be described in this section. These are given as an example of the data obtained and are for a blank run (figure 9.25) with no catalyst present († in the table in figure 9.24) and a run (figure 9.26) using TiPT in toluene as the catalyst (‡ in the table in figure 9.24).

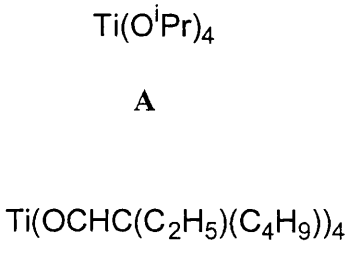

A

B

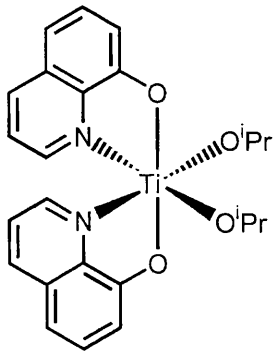

C

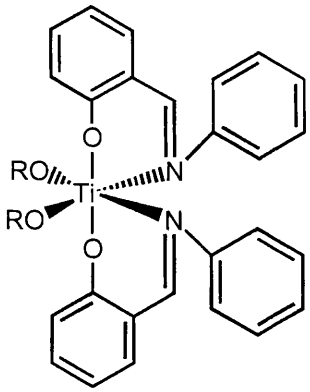

D

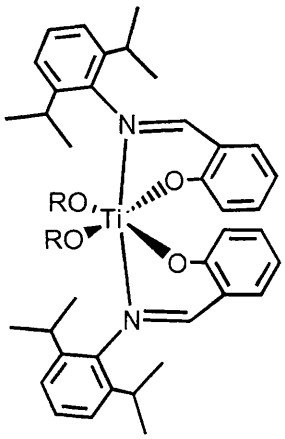

E

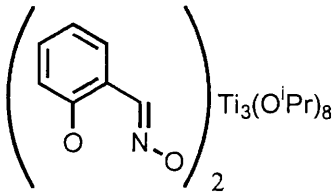

F

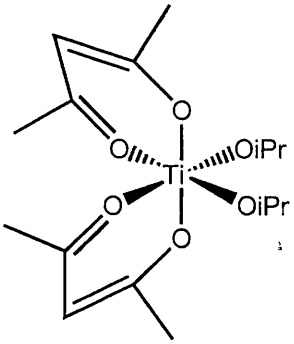

G

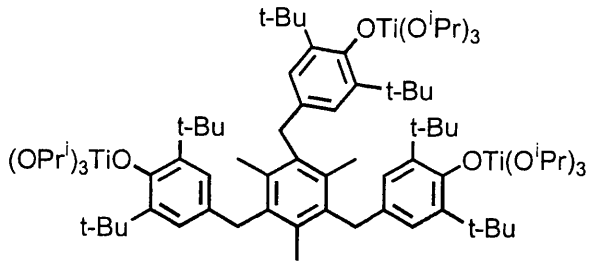

H

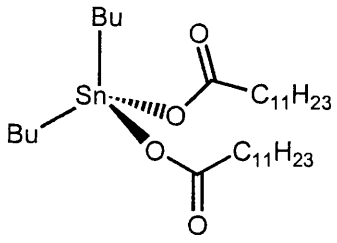

I

Figure 9.23: Catalysts used in in situ infra red study

Catalyst	Solvent?	Time	Moles added	Product	Urethane	Isocyanurate	Allophanate
Blank †	N/A	180	0	Clear, Colourless Liquid	✓		
A ‡	Tol(1ml)	100	$2.5x10^{-4}$	Red Gel	✓	✓	
A	Tol(1ml)	180	$2.5x10^{-7}$	Pale Orange Liquid	✓	✓	
B	N/A	180	$2.5x10^{-4}$	Amber Liquid/Gel	✓	✓	
C	Tol(1ml)	180	$2.5x10^{-4}$	Pale Yellow Liquid	✓		
C	Tol(1ml)	180	$2.5x10^{-7}$	Pale Yellow Liquid	✓	✓	
C	Tol(1ml)	60	$1.25x10^{-3}$	Orange gel	✓	✓	
D	Tol(1ml)	180	$2.5x10^{-4}$	Brown Liquid	✓	✓	
D	Tol(1ml)	30	$2.5x10^{-7}$	Red Gel	✓	✓	✓
E	Tol(1ml)	90	$2.5x10^{-4}$	Red Gel	✓	✓	
E	Tol(1ml)	180	$2.5x10^{-7}$	Orange Gel	✓	✓	
F	Tol(1ml)	180	$2.5x10^{-4}$	Red Liquid	✓		
F	Tol(1ml)	60	$2.5x10^{-7}$	Brown Gel	✓	✓	✓
G	Tol(1ml)	180	$2.5x10^{-4}$	Orange Liquid	✓		
G	Tol(1ml)	180	$2.5x10^{-7}$	Orange Gel	✓	✓	✓
H	Tol(1ml)	180	$2.5x10^{-4}$	Orange Liquid	✓	✓	
H	Tol(1ml)	90	$2.5x10^{-7}$	Orange Gel	✓	✓	
I	N/A	90	$2.5x10^{-4}$	Yellow Gel	✓	✓	✓
I	N/A	180	$2.5x10^{-7}$	Yellow Liquid	✓	✓	✓

Figure 9.24: Table of in situ infra red catalytic runs

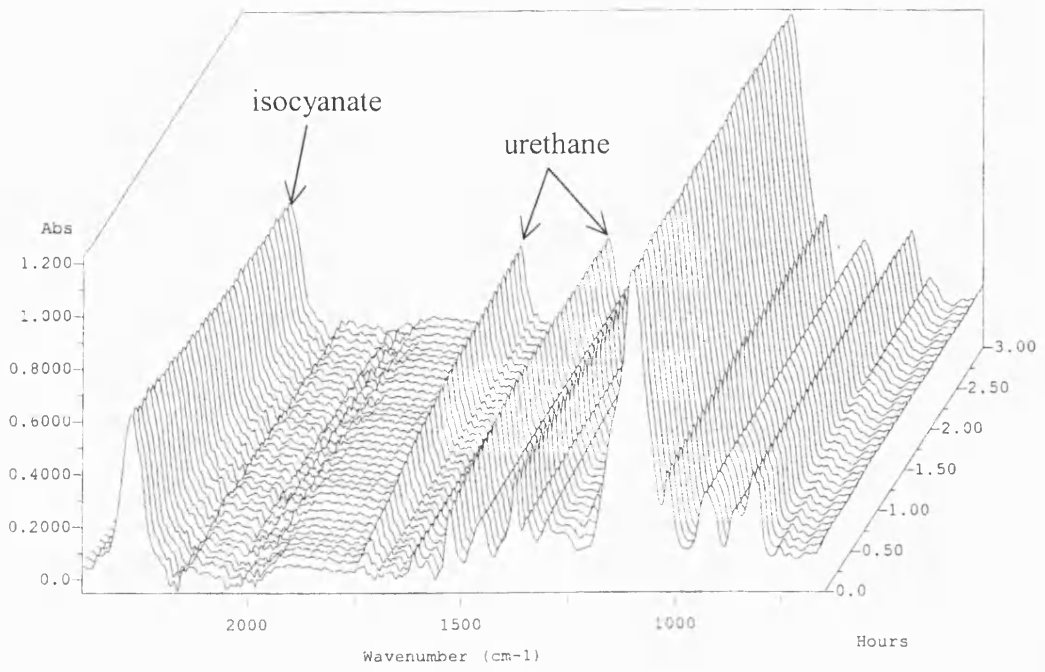

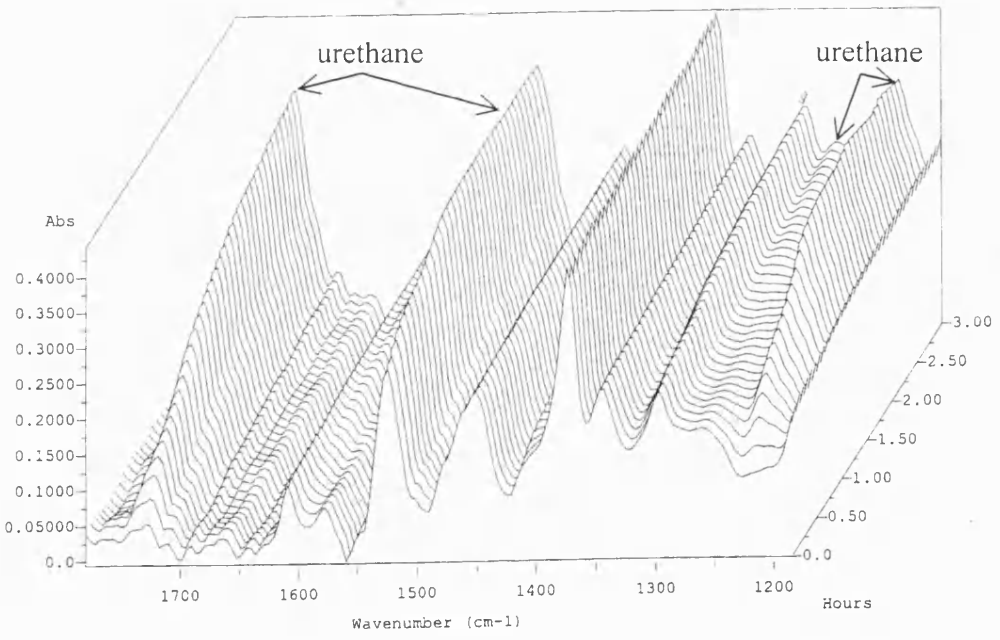

Figure 9.25: Infra red spectra from polyurethane synthesis with no catalyst present (†)

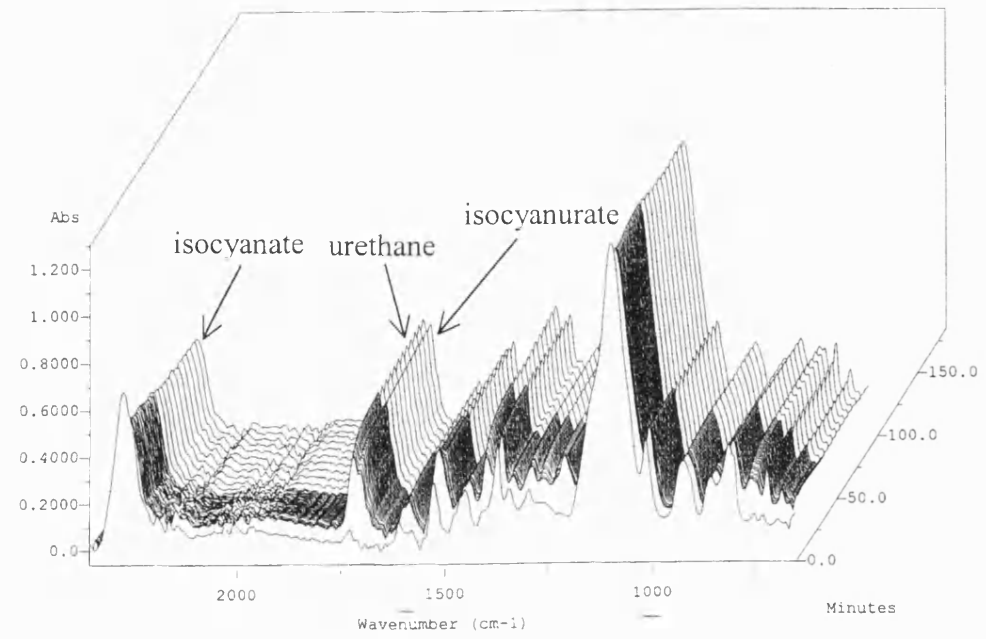

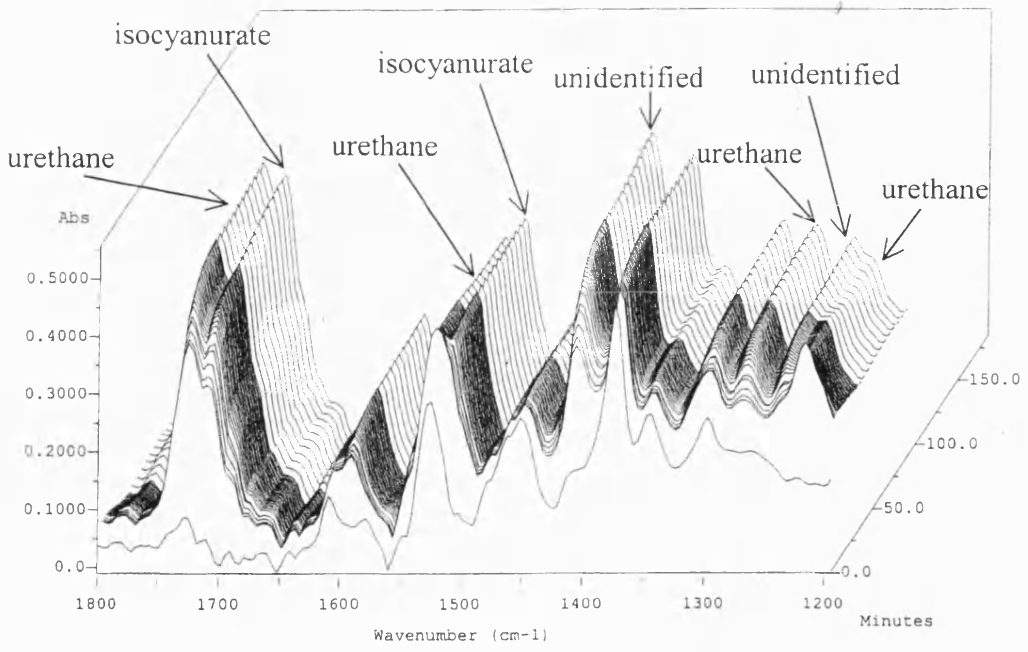

Figure 9.26: Infra red spectra from polyurethane synthesis with TiPT in toluene as a catalyst ($2.5x10^{-4}$ moles added) (‡)

The details of the reactions for each of our catalysts are given below along with assignment of as many of the peaks formed as possible. The individual spectra for each of the reactions are not given in each section but the overall features are shown in the two examples on the previous page (figures 9.25 and 9.26).

Blank

The blank run shows a very slow reaction with peaks appearing very slowly over the course of the run. The identifiable peaks which appear are related only to urethane linkages and no signals are observed for either allophanate, isocyanurate, carbodiimide, dimer, urea or biuret groups. The signals observed for the urethane were 1729cm^{-1} for the carbonyl stretch, 1525cm^{-1} for the NH deformation and C-N stretching vibrations, 1274 cm^{-1} for Ar-N stretching and 1220 cm^{-1} for the amide.The final product of the reaction was clear, colourless liquid after three hours although the reaction had not reached completion.

Catalyst A: Ti(O^{i}Pr)$_4$

Two runs were carried out using TiPT; the first run was carried with the TiPT added in a carrier solvent (toluene) to avoid hydrolysis and with a catalyst loading of 2.5x10^{-4} moles. The reaction mixture quickly went red and began to gel appreciably early in the reaction. By 90-100 minutes the reaction mixture was too viscous to carry on stirring and the run was abandoned. The peaks in the IR spectra show immediate formation of urethane linkages (1729, 1529, 1270 and 1223 cm^{-1}) followed very quickly by signals of almost equal intensity due to the formation of isocyanurate rings at 1710 cm^{-1} for the carbonyl stretch and a further related signal at 1513cm^{-1}. No identifiable signals were observed for other by-products although some unidentified bands grew during the reaction at 1409 and 1239 cm^{-1}.

In the second run with TiPT the concentration of catalyst added was reduced 100 times and it was added in toluene as for the previous reaction. The reaction was significantly slower than that observed for the higher concentration catalyst and after three hours the product was still mobile. Initially a pale orange solution was formed on addition of the catalyst and the viscosity of this increased gradually over time as the reaction continued. Initially only peaks due to the formation of urethane linkages

were observed (1729, 1528, 1270 and 1224 cm^{-1}) but after approximately an hour a peak associated with isocyanurate groups could be observed (1513cm^{-1}) although no peak for the isocyanurate carbonyl stretch appeared. As with the earlier reactions unidentified bands grew during the reaction at 1409 and 1239 cm^{-1}.

Catalyst B: $Ti(OCHC(C_2H_4)(C_4H_9))_4$

One run was carried out using this high molecular weight homoleptic alkoxide added without a carrier solvent. On addition of the catalyst there was a yellow colouration of the product and an exotherm of approximately 20°C. The reaction proceeded at a similar rate to the equivalent reaction with titanium tetra-isopropoxide and resulted in the formation of a viscous amber liquid, which was still mobile after 3 hours. On standing this amber liquid set to a non-mobile gel.

The infra red spectra for the first 135 minutes showed only the peaks for the urethane linkages (1729, 1529, 1270 and 1220 cm^{-1}) but in the last 45 minutes a peak due to the formation of isocyanurate could be seen (1513cm^{-1}) although as for the low concentration tetra-isopropoxide example the carbonyl stretch could not be observed. As with earlier catalysts two further unidentified bands grew during the reaction (1413 and 1243 cm^{-1}).

Catalyst C: Titanium bis-8-hydroxyquinoline bis-isopropoxide, $Ti(8\text{-}HQ)_2(O^iPr)_2$

Three runs were carried out with the titanium bis-8-hydroxyquinolinate bis-isopropoxide at different catalyst concentrations.

The first run was carried out with a catalyst loading of $2.5x10^{-4}$ moles and proceeded gradually over the three hours. By the end of the reaction the product was a clear, pale-yellow viscous liquid which on standing slowly set to form a gel. The infra red spectra showed signals for the formation of urethane linkages only (1733, 1525, 1270 and 1220 cm^{-1}) and no signals for other by-products although as with earlier catalysts unidentified bands were observed at 1409 and 1243 cm^{-1}.

The second run was carried out using 1% of the amount of catalyst used in the first and went slower with a final product that was pale yellow and very mobile in comparison to the previous experiments. The infra red spectra show the expected

peaks for urethane formation (1729, 1529, 1270 and 1224 cm^{-1}) and one of the peaks seen for the isocyanurate groups (1513 cm^{-1}) which appeared after about an hour although as for previous catalysts the expected isocyanurate carbonyl stretch was not observed. As with earlier catalysts unidentified bands were observed at 1413 and 1239 cm^{-1}.

The third run was carried out using five times the concentration of catalyst used in the first run. The reaction went extremely fast and formed a viscous amber liquid which, after an hour, became a golden yellow non-mobile gel at which point the reaction was stopped. In the infra-red spectra peaks are observed which correspond to urethane formation (1728, 1529, 1270 and 1220 cm^{-1}) although these are quickly overtaken by those associated with isocyanurate (1710 and 1509 cm^{-1}) and the unidentified bands at 1409 and 1235 cm^{-1}.

Catalyst D: Complex 4.4, $Ti(4.4L)_2(O^iPr)_2$

Two runs were carried out using the aniline Schiff base catalyst; the first using a titanium addition of $2.5x10^{-4}$ moles and the second at 1% of this loading.

The initial reaction using the higher concentration of catalyst formed a yellow solution which, during the course of the reaction, slowly darkened until after three hours it was a brown colour. The viscosity of the reaction mixture also increased over time, but by the end of the run the product was still a mobile liquid (although highly viscous). The infra red spectrum shows an initial increase both in urethane (1729, 1529, 1270 and 1220 cm^{-1}) and isocyanurate (1710 and 1513 cm^{-1}) before steadying off. Then after approximately an hour there is a second increase in activity and the intensity of the carbonyl stretch due to the urethane increases dramatically while the signal at 1529cm^{-1} splits into two and decreases in intensity. As with many of the other reactions the unidentified signals at 1409 and 1243cm^{-1} are present in the spectra particularly later on in the run.

For the second reaction, using a lower loading of catalyst, the reaction proceeded slightly more slowly but with a much greater increase in viscosity. After less than 30 minutes the reaction mixture was too viscous to stir and the run was abandoned. The final product was a clear red gel, which set solid in the reaction flask. The infra red

showed a slow initial reaction with signals present for urethane (1725, 1529, 1270 and 1220 cm^{-1}), isocyanurate (1710 and 1513 cm^{-1}) and a small amount of allophanate (1690cm^{-1}). Initially the main product seems to be the urethane and as time goes on more of the by-products seem to be produced. The peaks at 1409 and 1239cm^{-1} for this sample were especially large and grew a great deal during the second part of the run when the gellation occurred.

Catalyst E: Complex 4.8, $Ti(4.8L)_2(O^iPr)_2$

Two runs were carried out using the di-isopropyl aniline Schiff base catalyst; the first using a catalyst loading of $2.5x10^{-4}$ moles and the second at 1% of this value.

The initial reaction with the higher catalyst loading resulted in the formation of a red solution, which became more viscous as the reaction proceeded. After approximately 90 minutes the reaction had to be abandoned as the product had gelled and could no longer be stirred efficiently. The infra-red spectra initially showed a large increase in the amount of urethane over the first ten minutes (1729, 1529, 1270 and 1220cm^{-1}). This was followed by an increase in the amount of isocyanurate (1710 and 1510cm^{-1}) and also an increase in the intensity of the unidentified peaks at 1409 and 1239 cm^{-1}.

The reaction with a lower catalyst loading was expectedly slower than the one described above and had a much slower increase in viscosity. By the end of the run (180 minutes) the product was a gel but up until this time it was a highly viscous mobile orange liquid. The infra red spectra showed two phases to the reaction. Initially there was a steady increase in the amount of urethane (1729, 1529, 1270 and 1224cm^{-1}) up until around 15 minutes had passed when this increase begins to plateau off. In the second stage, after approximately 40 minutes, there is a second large increase in the size of the carbonyl stretching peak due to urethane at 1729cm^{-1} along with an increase in the peak due to isocyanurate at 1710cm^{-1}. At the same time as this increase the urethane peaks at 1529 and 1224cm^{-1} both split in two to show the expected isocyanurate peaks alongside the urethane signals. As with all the other catalysts which have at some point during the reaction gelled, the two peaks at 1409 and 1239 cm^{-1} are present.

Catalyst F: Complex 6.6, $Ti_3(6.6L)_2(O^iPr)_8$

Two runs were carried out using the salicylaldoxime catalyst; the first using a catalyst loading of $2.5x10^{-4}$ moles and the second at 1% of this value.

For the first run the catalyst was quite fast and produced a red viscous liquid almost immediately. However no further reaction was observed to form a gel even on standing and after the initial reaction the viscosity did not seem to change appreciably. In the infra red spectra immediate formation of urethane linkages is observed which can be seen by the usual signals (1729, 1598 and 1220 cm^{-1}) although the signal at $\approx$1270cm^{-1} which generally appears later in the reaction is not observed. Although there are slight shoulders on the peaks at 1729 and 1529cm^{-1} there is only a very small amount of isocyanurate formed during the reaction and no other side products are observed.

The second run using this catalyst is in stark contrast to the first. The initial rate of the reaction is slower than the first run, as would be expected. As the reaction proceeds further the mixture quickly increases in viscosity and within an hour is too viscous to continue the reaction. The product at this time is a non-mobile brown gel. The infra red spectrum shows initially (10 minutes) only production of urethane (1729, 1529, 1270 and 1224cm^{-1}) but this is quickly joined by appearance of peaks due to isocyanurate (1710 and 1513 cm^{-1}) and a small amount of allophanate (carbonyl stretch at 1695cm^{-1}). As with previous reactions a large unidentified peak was seen to grow at 1409 cm^{-1} at the same time as isocyanurate peaks increased.

Catalyst G: Titanium bis-acetylacetonate bis-isopropoxide, $Ti(acac)_2(O^iPr)_2$

Two runs were carried out using the bis acetylacetonate titanium catalyst TAA; the first using a catalyst loading of $2.5x10^{-4}$ moles and the second at 1% of this value.

The reaction using the higher catalyst loading proceeded smoothly over course of the reaction and was terminated after three hours. The viscosity did not increase as much as was observed in previous runs with other catalysts and the product after three hours was a highly mobile red liquid. Throughout the reaction the infra red spectra showed

almost exclusively peaks due to the formation of urethane (1729, 1594 and 1220 cm^{-1}) and the only other peak observed was a small increase at 1409cm^{-1}.

At the lower catalyst loading the reaction also went smoothly over the reaction period with a slightly greater increase in apparent viscosity and a final product, which was a yellow liquid. The infra red spectra showed that the reaction went more slowly than for the higher catalyst loading as expected. As with the high catalyst loading the principal product was urethane (1729, 1529, 1270 and 1224cm^{-1}). However, unlike the previous run significant peaks were observed for both isocyanurate (1710 and 1513 cm^{-1}) and allophanate linkages (1695cm^{-1}). In addition the peaks at 1409 and 1239 cm^{-1} were observed.

Catalyst H: Complex 7.3, $Ti_3(7.3L)(O^iPr)_9$

Two runs were carried out using this 2,6-di-*tert*-butyl phenol derivative as a catalyst; the first using a catalyst loading of $2.5x10^{-4}$ moles and the second at 1% of this value.

The first reaction proceeded slowly to give an orange liquid product which gradually became viscous over time to yield a thick but mobile product which was orange in colour. The infra red spectra showed a fast initial reaction followed by a slow increase in products which was still continuing slowly when the reaction was terminated after 3 hours. The main product throughout the reaction seems to be urethane and the signals for these linkages dominate the spectra (1729, 1529, 1270 and 1224cm^{-1}). Later in the run the signal at 1529 cm^{-1} splits in two to give the band at 1513 cm^{-1}, which corresponds to isocyanurate, although the carbonyl stretching signal for this group is not observed. As with other products which remain liquid at the end of the run, the two unassigned bands at 1413 and 1239 cm^{-1} are present but not very large.

The reaction using a lower catalyst loading gave an orange gel within 90 minutes and after this time the run was abandoned. The infra red spectra showed that the reaction was quite slow and that the products appeared slowly over the first 20 minutes. During this initial period the spectra are dominated by peaks due to the formation of urethane linkages (1729, 1529, 1270 and 1224 cm^{-1}). However later in the reaction as the viscosity of the product increases peaks due to isocyanurate formation appear and begin to dominate the spectra by the end of the run (1709 and 1513 cm^{-1}). In addition

unlike the higher catalyst loading the unassigned peaks at 1409 and 1239 cm^{-1} are very large particularly near the end of the run when gellation occurs.

Catalyst I: Di-butyl-tin-di-laurate

Two runs were carried out using the commercial tin catalyst di-butyl tin di-laurate; the first using a catalyst loading of $2.5x10^{-4}$ moles and the second at 1% of this value.

The first reaction using a higher catalyst loading proceeded smoothly with only a very small exotherm and only a slight colour change. The viscosity of the reaction mixture increased rapidly after about half an hour and the reaction was abandoned after 90 minutes due to the formation of a gel. The infra red spectra show that unlike the titanium catalysts there was no significant reaction at the start of the run and an induction period of 30 minutes passed before the reaction began. At this point peaks begin to be seen gradually appearing for urethane (1729, 1529, 1270 and 1220cm^{-1}), isocyanurate (1710 and 1513cm^{-1}) and allophanate (1695cm^{-1}) linkages. In addition the peaks at 1409 and 1243 cm^{-1} are significant and grow to be very large by the point of gellation.

The second reaction at a lower catalyst loading went more quickly with none of the induction period seen in the higher concentration reaction. The viscosity increased throughout the reaction and after three hours had formed a highly viscous yellow liquid. The infra red spectra show that the induction period seen above is not observed and peaks due to products are seen immediately. The peaks grow quite slowly and in addition to urethane (1725, 1529, 1270 and 1220cm^{-1}), which is the main product, significant peaks can be seen for isocyanurate (1710 and 1513cm^{-1}) and a small amount for allophanate (1695cm^{-1}). In addition significant peaks are seen at 1405 and 1239 cm^{-1}.

9.2.4 Discussion of results from in-situ infra red work

Probably the most striking observation to be found from the results described above for the *in situ* infra red study we have carried out is the range of selectivity and reactivity observed for even the small range of catalysts that have been tested. The following section will attempt to draw some conclusions from the data obtained and

discuss the further use of this technique for the testing of potential polyurethane catalysts. To aid in the discussion the potential by-products which may be produced during polyurethane synthesis are reproduced in figure 9.27 below.

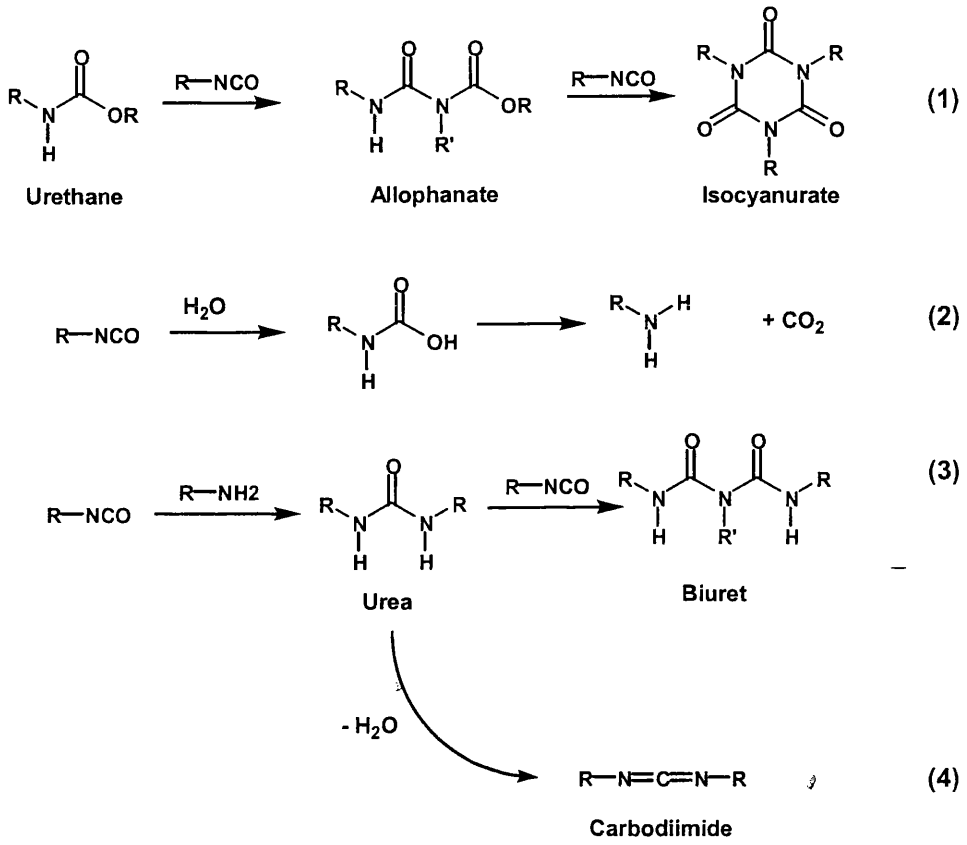

Figure 9.27: Side reactions during polyurethane synthesis

The most important observation to be made from the results described above is that all of the catalysts we tested were effective in the formation of polyurethane under a simulation of industrial conditions. In almost all cases the most prominent signal in the infra red spectrum was that for the carbonyl stretch of a urethane product. This proves that these complexes are potentially useful catalysts for this process.

An additional observation, which holds true for all of the catalysts tested, is that under our standard conditions none of the catalysts used were observed to produce the biuret, urea or carbodiimide products, shown above. This seems to suggest that, for the catalysts we tested, reactions 2-4 in figure 9.27 above are suppressed relative to both urethane synthesis and, in some cases, reaction 1 to allophanate and

isocyanurate. Due to this limited selectivity for our catalysts we can say that in our systems only the reactions shown in figure 9.28 below are observed and are in competition.

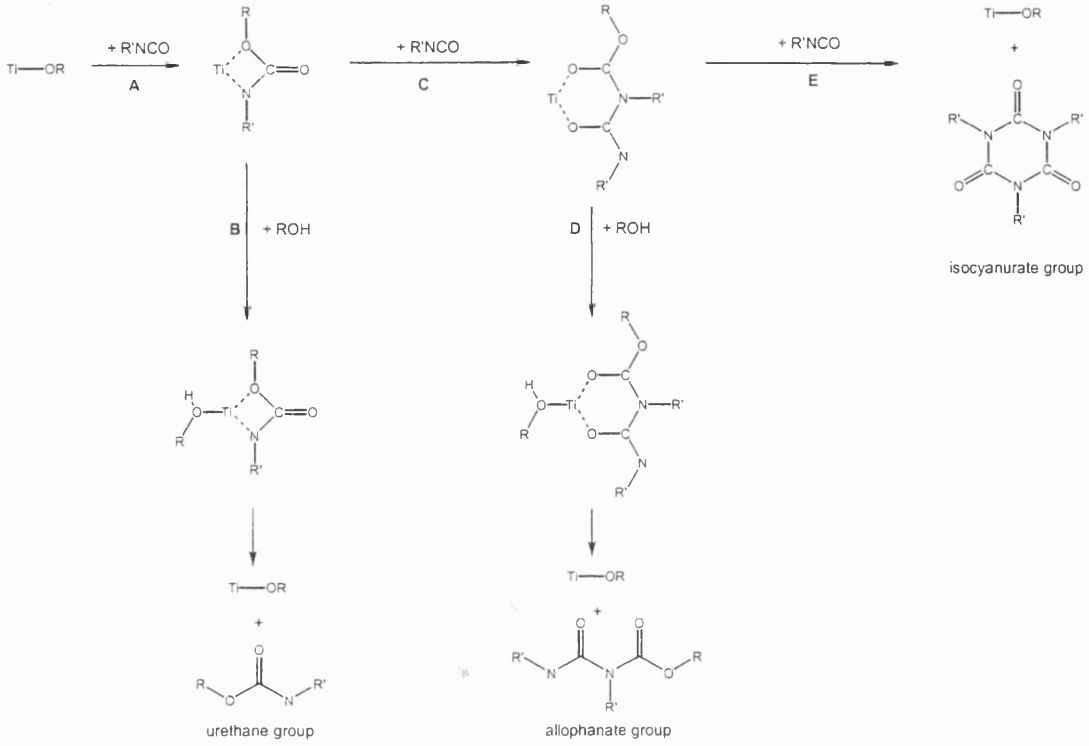

Figure 9.28: Competing reactions during synthesis of polyurethanes in our system

Initially reaction **A** occurs via insertion of an isocyanate group into a titanium alkoxide bond to form a titanium urethanato complex. Following this initial step two competing reactions can occur: either the complex can undergo an exchange reaction (**B**) to liberate a urethane group; or it can undergo a second isocyanate insertion (**C**) to yield a titanium allophanato complex. In the second case the allophanato product can itself be involved in one of two competing pathways: as with the urethanato complex it can either undergo exchange to yield an allophanate group (**D**) or further isocyanate insertion to yield a cyclic isocyanurate group (**E**). We believe that the differing selectivities we have observed in our infra red work are due to the competing nature of these reactions with differing processes being favoured by specific catalysts at specific concentrations. We are still far from understanding the reasons behind the selectivity differences but some initial observations and patterns are discussed below.

Other than urethane groups themselves the most common product we have observed is the isocyanurate trimer. This is observed, to a greater or lesser amount, in all but three of the catalysed reactions described above. The three catalysts for which isocyanurate formation is not observed all yielded liquid products and were synthesised using the higher catalyst loading ($2.5x10^{-4}$ moles). In correlation to this the other liquid products, where isocyanurate formation was observed, showed much weaker signals assigned to this by-product than those that formed gels. These other reactions with liquid products and low isocyanurate formation also tended to be synthesised using the higher catalyst concentration.

The second by-product observed in the catalysed reactions which we have tested using the in-situ infra-red technique is the allophanate. This by-product is only observed in reactions which also produce isocyanurate, and then only approximately one third of these reactions also produce the allophanate. For titanium-based catalysts this allophanate formation is only observed in catalytic runs which are carried out using the lower catalyst loading ($2.5x10^{-7}$ moles). In all cases the catalysts that produce allophanate at low concentrations correspond to those which at high concentrations form liquid products and that, in two cases, show no isocyanurate formation. As allophanate is a proposed intermediate in the synthesis of isocyanurate (figure 9.27 and 9.28 above) it is unsurprising that it is only formed alongside the cyclic product. In addition the fact that allophanate is only observed in reactions with catalysts which, at higher concentrations, show little or no synthesis of isocyanurate is also unsurprising as we would only expect to observe allophanate in reactions for which the catalyst disfavours isocyanurate formation (reaction **E** in figure 9.28).

It seems likely that high rates of isocyanurate formation, both preclude the observation of the allophanate intermediate and promote the formation of gels. This gel formation is sensible in light of the fact that the production of isocyanurate groups during polymer formation would induce cross-linking between polymer chains as, to a lesser extent, would allophanate production.

When considering the titanium catalysts tested we can see a possible pattern in reactivity. The homoleptic alkoxides seem to promote relatively high rates of

isocyanurate formation at all catalyst concentrations and show no signals due to the allophanate intermediate (reaction **E** is much faster than reaction **D** in figure 9.28). This high rate of isocyanurate formation with homoleptic alkoxides agrees with earlier studies both in our group and at Synetix where this was also observed. In addition catalyst H (complex 7.3) exhibits similar selectivity as could be expected due to the high reactivity of its 2,6-di-*tert*-butyl phenoxide ligands which would probably cause generation of a homoleptic alkoxide under the reaction conditions. In contrast, the majority of the titanium complexes that have stable, chelating 'control' ligands which will not be displaced during reaction (catalysts C, D, F and G) show differing reactivity. These catalysts seem to reduce the rate of isocyanurate formation (reaction **E** in figure 9.28) with little or no trimer observed at low catalyst concentration and a significant amount of allophanate observed at higher catalyst concentrations in most cases (reaction **D** competes with reaction **E**). In contrast catalyst E, which does have control ligands but with a differing configuration at titanium, shows anomalous selectivity with a high amount of isocyanurate formation and no allophanate observed. This is not unexpected as this catalyst also exhibited anomalous behaviour in the NMR study described earlier in this chapter. When looked at together these results seem to suggest that a combination of choice of control ligand and variation of catalyst concentration could, in the future, allow control of selectivity in polyurethane synthesis.

In summary we have shown that a varied range of titanium alkoxide based catalysts can produce polyurethane products from industrially relevant pre-polymer systems. We have also shown that through control of the catalyst type and concentration we can vary the properties of the polyurethane products which are synthesised. In addition on comparison with the industrial catalyst di-butyl-tin-di-laurate our catalysts have similar selectivity with no observed formation of urea, biuret or carbodiimide products in detectable amounts. Finally we have concluded that the in situ infra red technique is a potentially powerful tool in the process of catalyst optimisation although a large amount of further work, both in our group and by our industrial partners, will be necessary in the future to explain the observed reactivities. This will allow use of this technique to eventually correlate the structural work described in the earlier chapters of this thesis with selectivity and activity data obtained by this technique.

9.4 Summary of polymerisation studies

1. We have shown a number of our catalysts to be active in the synthesis of urethanes and polyurethanes.
2. We have described two techniques for assessing our catalysts for these reactions, ^{1}H NMR and infra red, and shown that combination of these techniques can give activity and selectivity data for our catalysts.
3. Using both techniques our pre-catalysts have been shown to have comparable activity and selectivity to a commercial tin based catalyst system. Importantly this includes the suppression of reactions to form urea, biuret and carbodiimide groups.
4. We have shown that variation of catalyst concentration and control ligand structure can have large effects on selectivity and reactivity and through this made some initial correlations between structure and activity.
5. The work described here has provided a basis from which more detailed studies into the use of titanium alkoxide based pre-catalysts for polyurethane synthesis can be begun.

Appendix

Crystal structure data

The following section includes brief crystal structure data for each of the crystallographically characterised complexes discussed in this thesis. Full crystallographic data tables and .cif files for the structures can be found on the CD which accompanies this thesis.

Crystal data and structure refinement for complex 4.3

Identification code	4.3	
Empirical formula	C36 H42 N2 O4 Ti	
Formula weight	614.62	
Temperature	150(2) K	
Wavelength	0.71073 Å	
Crystal system	Monoclinic	
Space group	$P2_1$	
Unit cell dimensions	a = 18.1430(3) Å	α= 90°.
	b = 10.1730(2) Å	β= 106.6350(10)°.
	c = 18.3320(4) Å	γ = 90°.
Volume	3241.91(11) Å^3	
Z	4	
Density (calculated)	1.259 Mg/m^3	
Absorption coefficient	0.305 mm^{-1}	
F(000)	1304	
Crystal size	0.28 x 0.08 x 0.08 mm^3	
Theta range for data collection	3.52 to 26.38°.	
Index ranges	-22<=h<=22, -12<=k<=12, -22<=l<=22	
Reflections collected	57745	
Independent reflections	13136 [R(int) = 0.0516]	
Completeness to theta = 26.38°	98.5 %	
Max. and min. transmission	0.9760 and 0.9195	
Refinement method	Full-matrix least-squares on F^2	
Data / restraints / parameters	13136 / 1 / 788	
Goodness-of-fit on F^2	1.008	
Final R indices [I>2sigma(I)]	R1 = 0.0423, wR2 = 0.0990	
R indices (all data)	R1 = 0.0670, wR2 = 0.1119	
Absolute structure parameter	-0.018(16)	
Extinction coefficient	0.0054(6)	
Largest diff. peak and hole	0.521 and -0.304 e.Å^{-3}	

Crystal data and structure refinement for complex 4.4

Identification code	4.4	
Empirical formula	C32 H34 N2 O4 Ti	
Formula weight	558.51	
Temperature	150(2) K	
Wavelength	0.71070 Å	
Crystal system	Monoclinic	
Space group	$P2_1/a$	
Unit cell dimensions	a = 16.77700(10) Å	α= 89.9790(10)°.
	b = 9.9880(2) Å	β= 90.1430(10)°.
	c = 17.2620(3) Å	γ = 89.9930(10)°.
Volume	2892.56(8) $Å^3$	
Z	4	
Density (calculated)	1.283 Mg/m^3	
Absorption coefficient	0.334 mm^{-1}	
F(000)	1176	
Crystal size	0.22 x 0.15 x 0.10 mm^3	
Theta range for data collection	3.54 to 27.48°.	
Index ranges	0<=h<=21, -12<=k<=12, -22<=l<=22	
Reflections collected	41742	
Independent reflections	6582 [R(int) = 0.0380]	
Completeness to theta = 27.48°	99.3 %	
Max. and min. transmission	0.9673 and 0.9301	
Refinement method	Full-matrix least-squares on F^2	
Data / restraints / parameters	6582 / 24 / 411	
Goodness-of-fit on F^2	1.024	
Final R indices [I>2sigma(I)]	R1 = 0.0470, wR2 = 0.1202	
R indices (all data)	R1 = 0.0614, wR2 = 0.1292	
Largest diff. peak and hole	1.235 and -0.754 $e.Å^{-3}$	

Crystal data and structure refinement for complex 4.5.

Identification code	4.5	
Empirical formula	C32 H24 F10 N2 O4 Ti	
Formula weight	738.43	
Temperature	396(2) K	
Wavelength	0.71070 Å	
Crystal system	Monoclinic	
Space group	$P2_1/c$	
Unit cell dimensions	a = 14.3970(2) Å	α= 90°.
	b = 20.1450(4) Å	β= 149.4770(10)°.
	c = 21.5010(4) Å	γ = 90°.
Volume	3167.10(10) Å^3	
Z	4	
Density (calculated)	1.549 Mg/m^3	
Absorption coefficient	0.370 mm^{-1}	
F(000)	1496	
Crystal size	0.25 x 0.17 x 0.15 mm^3	
Theta range for data collection	3.60 to 27.49°.	
Index ranges	0<=h<=18, -26<=k<=26, -27<=l<=13	
Reflections collected	10943	
Independent reflections	6613 [R(int) = 0.0326]	
Completeness to theta = 27.49°	91.0 %	
Max. and min. transmission	0.9466 and 0.9132	
Refinement method	Full-matrix least-squares on F^2	
Data / restraints / parameters	6613 / 0 / 446	
Goodness-of-fit on F^2	1.011	
Final R indices [I>2sigma(I)]	R1 = 0.0466, wR2 = 0.1121	
R indices (all data)	R1 = 0.0814, wR2 = 0.1304	
Largest diff. peak and hole	0.602 and -0.525 e.Å^{-3}	

Crystal data and structure refinement for complex 4.8.

Identification code	4.8	
Empirical formula	C51 H65 N2 O4 Ti	
Formula weight	817.95	
Temperature	150(2) K	
Wavelength	0.71070 Å	
Crystal system	Monoclinic	
Space group	*C2/c*	
Unit cell dimensions	a = 23.1450(4) Å	α= 90°.
	b = 17.0660(4) Å	β= 126.6170(10)°.
	c = 14.5820(4) Å	γ = 90°.
Volume	4623.03(18) Å^3	
Z	4	
Density (calculated)	1.175 Mg/m^3	
Absorption coefficient	0.230 mm^{-1}	
F(000)	1756	
Crystal size	0.25 x 0.17 x 0.15 mm^3	
Theta range for data collection	3.63 to 27.46°.	
Index ranges	0<=h<=30, -22<=k<=22, -18<=l<=15	
Reflections collected	39356	
Independent reflections	5270 [R(int) = 0.1181]	
Completeness to theta = 27.46°	99.5 %	
Max. and min. transmission	0.9663 and 0.9448	
Refinement method	Full-matrix least-squares on F^2	
Data / restraints / parameters	5270 / 0 / 275	
Goodness-of-fit on F^2	1.027	
Final R indices [I>2sigma(I)]	R1 = 0.0511, wR2 = 0.1131	
R indices (all data)	R1 = 0.1035, wR2 = 0.1332	
Extinction coefficient	0.0026(4)	
Largest diff. peak and hole	0.346 and -0.356 e.Å^{-3}	

Crystal data and structure refinement for complex 4.10

Identification code	4.10	
Empirical formula	C75 H66 N2 O4 Ti	
Formula weight	1107.20	
Temperature	150(2) K	
Wavelength	0.71070 Å	
Crystal system	Orthorombic	
Space group	*Pbca*	
Unit cell dimensions	a = 18.2330(2) Å	α= 90°.
	b = 24.8400(2) Å	β= 90°.
	c = 26.3420(3) Å	γ = 90°.
Volume	11930.5(2) $Å^3$	
Z	8	
Density (calculated)	1.233 Mg/m^3	
Absorption coefficient	0.197 mm^{-1}	
F(000)	4672	
Crystal size	0.25 x 0.15 x 0.08 mm^3	
Theta range for data collection	3.54 to 27.49°.	
Index ranges	0<=h<=23, 0<=k<=32, 0<=l<=34	
Reflections collected	26279	
Independent reflections	13649 [R(int) = 0.0620]	
Completeness to theta = 27.49°	99.7 %	
Max. and min. transmission	0.9844 and 0.9525	
Refinement method	Full-matrix least-squares on F^2	
Data / restraints / parameters	13649 / 0 / 758	
Goodness-of-fit on F^2	1.012	
Final R indices [I>2sigma(I)]	R1 = 0.0582, wR2 = 0.1431	
R indices (all data)	R1 = 0.1241, wR2 = 0.1724	
Largest diff. peak and hole	0.637 and -0.611 $e.Å^{-3}$	

Crystal data and structure refinement for complex 4.11.

Identification code	4.11	
Empirical formula	C75 H118 N2 O8 Ti2	
Formula weight	1271.51	
Temperature	150(2) K	
Wavelength	0.71073 Å	
Crystal system	Triclinic	
Space group	P-1	
Unit cell dimensions	a = 15.3200(3) Å	α= 75.5690(10)°.
	b = 15.6480(3) Å	β= 65.0550(10)°.
	c = 18.1500(4) Å	γ = 85.1190(10)°.
Volume	3819.69(13) Å^3	
Z	2	
Density (calculated)	1.106 Mg/m^3	
Absorption coefficient	0.259 mm^{-1}	
F(000)	1380	
Crystal size	0.17 x 0.17 x 0.08 mm^3	
Theta range for data collection	3.91 to 24.98°.	
Index ranges	-18<=h<=18, -18<=k<=18, -21<=l<=19	
Reflections collected	37007	
Independent reflections	13339 [R(int) = 0.0752]	
Completeness to theta = 24.98°	99.3 %	
Max. and min. transmission	0.9808 and 0.9560	
Refinement method	Full-matrix least-squares on F^2	
Data / restraints / parameters	13339 / 24 / 868	
Goodness-of-fit on F^2	0.996	
Final R indices [I>2sigma(I)]	R1 = 0.0556, wR2 = 0.1355	
R indices (all data)	R1 = 0.1004, wR2 = 0.1637	
Extinction coefficient	0.0041(8)	
Largest diff. peak and hole	0.746 and -0.373 e.Å^{-3}	

Crystal data and structure refinement for complex 4.12

Identification code	4.12	
Empirical formula	C32 H30 Cl4 N2 O4 Ti	
Formula weight	696.28	
Temperature	200(2) K	
Wavelength	0.71073 Å	
Crystal system	Monoclinic	
Space group	$P2_1/n$	
Unit cell dimensions	a = 12.04600(10) Å	α= 90°.
	b = 22.1560(2) Å	β= 101.1050(10)°.
	c = 12.4620(2) Å	γ = 90°.
Volume	3263.72(7) $Å^3$	
Z	4	
Density (calculated)	1.417 Mg/m^3	
Absorption coefficient	0.628 mm^{-1}	
F(000)	1432	
Crystal size	0.38 x 0.25 x 0.13 mm^3	
Theta range for data collection	3.65 to 27.51°.	
Index ranges	-15<=h<=15, -28<=k<=28, -14<=l<=16	
Reflections collected	43878	
Independent reflections	7473 [R(int) = 0.0834]	
Completeness to theta = 27.51°	99.5 %	
Absorption correction	None	
Max. and min. transmission	0.9256 and 0.7985	
Refinement method	Full-matrix least-squares on F^2	
Data / restraints / parameters	7473 / 0 / 393	
Goodness-of-fit on F^2	1.030	
Final R indices [I>2sigma(I)]	R1 = 0.0510, wR2 = 0.1198	
R indices (all data)	R1 = 0.1090, wR2 = 0.1535	
Extinction coefficient	0.0041(8)	
Largest diff. peak and hole	0.529 and -0.752 $e.Å^{-3}$	

Crystal data and structure refinement for complex 4.13.

Identification code	4.13	
Empirical formula	C34 H38 N2 O6 Ti	
Formula weight	618.56	
Temperature	150(2) K	
Wavelength	0.71073 Å	
Crystal system	Triclinic	
Space group	P-1	
Unit cell dimensions	a = 9.0980(2) Å	α= 76.6900(10)°.
	b = 11.5910(3) Å	β= 87.5920(10)°.
	c = 15.5540(4) Å	γ = 85.4850(10)°.
Volume	1590.75(7) Å^3	
Z	2	
Density (calculated)	1.291 Mg/m^3	
Absorption coefficient	0.315 mm^{-1}	
F(000)	652	
Crystal size	0.32 x 0.28 x 0.25 mm^3	
Theta range for data collection	3.77 to 30.08°.	
Index ranges	-12<=h<=12, -15<=k<=16, -18<=l<=21	
Reflections collected	25314	
Independent reflections	8191 [R(int) = 0.0752]	
Completeness to theta = 30.08°	87.8 %	
Absorption correction	None	
Max. and min. transmission	0.9253 and 0.9058	
Refinement method	Full-matrix least-squares on F^2	
Data / restraints / parameters	8191 / 0 / 395	
Goodness-of-fit on F^2	1.032	
Final R indices [I>2sigma(I)]	R1 = 0.0854, wR2 = 0.2319	
R indices (all data)	R1 = 0.1142, wR2 = 0.2511	
Extinction coefficient	0.027(5)	
Largest diff. peak and hole	1.908 and -0.527 e.Å^{-3}	

Crystal data and structure refinement for complex 4.14.

Identification code	4.14	
Empirical formula	C44 H52 Cl4 N2 O4 Ti	
Formula weight	862.58	
Temperature	150(2) K	
Wavelength	0.71073 Å	
Crystal system	monoclinic	
Space group	$P2_1/n$	
Unit cell dimensions	a = 13.0410(2) Å	α= 90°.
	b = 18.7880(3) Å	β= 93.9770(10)°.
	c = 18.2710(3) Å	γ = 90°.
Volume	4465.88(12) Å^3	
Z	4	
Density (calculated)	1.283 Mg/m^3	
Absorption coefficient	0.473 mm^{-1}	
F(000)	1808	
Crystal size	0.20 x 0.20 x 0.10 mm^3	
Theta range for data collection	1.99 to 27.49°.	
Index ranges	-15<=h<=16, -24<=k<=24, -23<=l<=23	
Reflections collected	80820	
Independent reflections	10232 [R(int) = 0.1188]	
Completeness to theta = 27.49°	99.9 %	
Max. and min. transmission	0.9542 and 0.9114	
Refinement method	Full-matrix least-squares on F^2	
Data / restraints / parameters	10232 / 0 / 508	
Goodness-of-fit on F^2	0.994	
Final R indices [I>2sigma(I)]	R1 = 0.0470, wR2 = 0.1020	
R indices (all data)	R1 = 0.1109, wR2 = 0.1224	
Largest diff. peak and hole	0.698 and -0.397 e.Å^{-3}	

Crystal data and structure refinement for complex 4.15.

Identification code	4.15	
Empirical formula	C46 H62 N2 O6 Ti	
Formula weight	786.88	
Temperature	150(2) K	
Wavelength	0.71073 Å	
Crystal system	Monoclinic	
Space group	$P2_1$	
Unit cell dimensions	a = 12.1710(3) Å	α= 90°.
	b = 14.3060(3) Å	β= 110.1110(10)°.
	c = 13.1930(3) Å	γ = 90°.
Volume	2157.08(9) Å^3	
Z	2	
Density (calculated)	1.211 Mg/m^3	
Absorption coefficient	0.247 mm^{-1}	
F(000)	844	
Crystal size	0.2 x 0.2 x 0.1 mm^3	
Theta range for data collection	3.66 to 27.48°.	
Index ranges	-15<=h<=15, -18<=k<=18, -17<=l<=17	
Reflections collected	33180	
Independent reflections	9713 [R(int) = 0.0745]	
Completeness to theta = 27.48°	99.5 %	
Absorption correction	None	
Refinement method	Full-matrix least-squares on F^2	
Data / restraints / parameters	9713 / 1 / 511	
Goodness-of-fit on F^2	1.025	
Final R indices [I>2sigma(I)]	R1 = 0.0429, wR2 = 0.0893	
R indices (all data)	R1 = 0.0686, wR2 = 0.1093	
Absolute structure parameter	-0.01(2)	
Extinction coefficient	0.0118(12)	
Largest diff. peak and hole	0.306 and -0.398 e.Å^{-3}	

Crystal data and structure refinement for 4.16

Identification code	4.16	
Empirical formula	C68 H112 Cl4 N2 O8 Ti2	
Formula weight	1323.20	
Temperature	150(2) K	
Wavelength	0.71073 Å	
Crystal system	Monoclinic	
Space group	$P2_1/a$	
Unit cell dimensions	a = 18.6220(2) Å	α= 90°.
	b = 8.98100(10) Å	β= 101.9550(10)°.
	c = 22.2300(3) Å	γ = 90°.
Volume	3637.20(7) $Å^3$	
Z	2	
Density (calculated)	1.208 Mg/m^3	
Absorption coefficient	0.417 mm^{-1}	
F(000)	1420	
Crystal size	0.1 x 0.125 x .075 mm^3	
Theta range for data collection	3.75 to 27.49°.	
Index ranges	-24<=h<=24, -11<=k<=11, -28<=l<=25	
Reflections collected	49105	
Independent reflections	8330 [R(int) = 0.0556]	
Completeness to theta = 27.49°	99.7 %	
Absorption correction	None	
Refinement method	Full-matrix least-squares on F^2	
Data / restraints / parameters	8330 / 0 / 402	
Goodness-of-fit on F^2	1.026	
Final R indices [I>2sigma(I)]	R1 = 0.0515, wR2 = 0.1301	
R indices (all data)	R1 = 0.0691, wR2 = 0.1434	
Extinction coefficient	0.0026(8)	
Largest diff. peak and hole	1.150 and -1.172 $e.Å^{-3}$	

Crystal data and structure refinement for complex 5.1

Identification code	5.1	
Empirical formula	C36 H50 N2 O8 Ti2	
Formula weight	734.58	
Temperature	150(2) K	
Wavelength	0.71073 Å	
Crystal system	Monoclinic	
Space group	*C2/c*	
Unit cell dimensions	a = 33.3480(3) Å	α= 90°.
	b = 14.08600(10) Å	β= 118.86°.
	c = 21.0000(2) Å	γ = 90°.
Volume	8639.13(13) Å^3	
Z	8	
Density (calculated)	1.130 Mg/m^3	
Absorption coefficient	0.413 mm^{-1}	
F(000)	3104	
Crystal size	0.50 x 0.20 x 0.13 mm^3	
Theta range for data collection	3.61 to 26.40°.	
Index ranges	-41<=h<=41, -17<=k<=17, -26<=l<=26	
Reflections collected	72986	
Independent reflections	8810 [R(int) = 0.0567]	
Completeness to theta = 26.40°	99.5 %	
Absorption correction	None	
Max. and min. transmission	0.9501 and 0.8200	
Refinement method	Full-matrix least-squares on F^2	
Data / restraints / parameters	8810 / 0 / 471	
Goodness-of-fit on F^2	1.037	
Final R indices [I>2sigma(I)]	R1 = 0.0525, wR2 = 0.1347	
R indices (all data)	R1 = 0.0670, wR2 = 0.1489	
Largest diff. peak and hole	1.376 and -0.480 e.Å^{-3}	

Crystal data and structure refinement for complex 5.2

Identification code	5.2	
Empirical formula	C24 H31 N3 O4 Ti	
Formula weight	473.42	
Temperature	150(2) K	
Wavelength	0.71073 Å	
Crystal system	Monoclinic	
Space group	$P2_1/n$	
Unit cell dimensions	a = 10.287(2) Å	α= 90°.
	b = 22.435(5) Å	β= 98.59(3)°.
	c = 10.422(2) Å	γ = 90°.
Volume	2378.3(8) Å^3	
Z	4	
Density (calculated)	1.322 Mg/m^3	
Absorption coefficient	0.394 mm^{-1}	
F(000)	1000	
Crystal size	0.17 x 0.10 x 0.05 mm^3	
Theta range for data collection	3.76 to 24.40°.	
Index ranges	-11<=h<=11, -26<=k<=26, -11<=l<=12	
Reflections collected	20251	
Independent reflections	3898 [R(int) = 0.1695]	
Completeness to theta = 24.40°	99.6 %	
Absorption correction	None	
Max. and min. transmission	0.9806 and 0.9342	
Refinement method	Full-matrix least-squares on F^2	
Data / restraints / parameters	3898 / 0 / 294	
Goodness-of-fit on F^2	1.166	
Final R indices [I>2sigma(I)]	R1 = 0.0725, wR2 = 0.1522	
R indices (all data)	R1 = 0.1404, wR2 = 0.1797	
Extinction coefficient	0.0046(15)	
Largest diff. peak and hole	0.959 and -0.533 e.Å^{-3}	

Crystal data and structure refinement for complex 5.3.

Identification code	5.3	
Empirical formula	C24 H28 Cl4 N3 O4 Ti	
Formula weight	612.19	
Temperature	396(2) K	
Wavelength	0.71073 Å	
Crystal system	Orthorhombic	
Space group	$Pn2_1a$	
Unit cell dimensions	a = 9.74400(10) Å	α= 90°.
	b = 13.10600(10) Å	β= 90°.
	c = 22.0140(2) Å	γ = 90°.
Volume	2811.29(4) Å^3	
Z	4	
Density (calculated)	1.446 Mg/m^3	
Absorption coefficient	0.719 mm^{-1}	
F(000)	1260	
Crystal size	0.38 x 0.17 x 0.13 mm^3	
Theta range for data collection	3.48 to 27.47°.	
Index ranges	-12<=h<=12, -17<=k<=16, -28<=l<=28	
Reflections collected	42777	
Independent reflections	6266 [R(int) = 0.0466]	
Completeness to theta = 27.47°	99.7 %	
Absorption correction	None	
Max. and min. transmission	0.9123 and 0.7717	
Refinement method	Full-matrix least-squares on F^2	
Data / restraints / parameters	6266 / 1 / 333	
Goodness-of-fit on F^2	1.044	
Final R indices [I>2sigma(I)]	R1 = 0.0271, wR2 = 0.0635	
R indices (all data)	R1 = 0.0315, wR2 = 0.0661	
Absolute structure parameter	-0.020(17)	
Largest diff. peak and hole	0.170 and -0.294 e.Å^{-3}	

Crystal data and structure refinement for complex 5.6

Identification code	5.6	
Empirical formula	C52 H60 N4 O8 Ti2	
Formula weight	964.84	
Temperature	150(2) K	
Wavelength	0.71073 Å	
Crystal system	Monoclinic	
Space group	$P2_1/n$	
Unit cell dimensions	a = 14.8050(2) Å	α= 90°.
	b = 10.3160(2) Å	β= 101.0700(10)°.
	c = 15.7420(3) Å	γ = 90°.
Volume	2359.51(7) Å^3	
Z	2	
Density (calculated)	1.358 Mg/m^3	
Absorption coefficient	0.398 mm^{-1}	
F(000)	1016	
Crystal size	0.38 x 0.25 x 0.20 mm^3	
Theta range for data collection	3.77 to 27.51°.	
Index ranges	-19<=h<=19, -13<=k<=13, -20<=l<=20	
Reflections collected	45426	
Independent reflections	5408 [R(int) = 0.0686]	
Completeness to theta = 27.51°	99.5 %	
Absorption correction	None	
Max. and min. transmission	0.9247 and 0.8651	
Refinement method	Full-matrix least-squares on F^2	
Data / restraints / parameters	5408 / 0 / 303	
Goodness-of-fit on F^2	1.323	
Final R indices [I>2sigma(I)]	R1 = 0.0503, wR2 = 0.1654	
R indices (all data)	R1 = 0.0666, wR2 = 0.1763	
Extinction coefficient	0.001(3)	
Largest diff. peak and hole	0.533 and -0.550 e.Å^{-3}	

Crystal data and structure refinement for complex 5.8

Identification code	5.8	
Empirical formula	C25 H35 Br N3 O4 Ti	
Formula weight	569.37	
Temperature	293(2) K	
Wavelength	0.71073 Å	
Crystal system	Monoclinic	
Space group	$P2_1/c$	
Unit cell dimensions	a = 12.0890(2) Å	α= 90°.
	b = 9.3120(2) Å	β= 94.1290(10)°.
	c = 23.2360(5) Å	γ = 90°.
Volume	2608.95(9) Å^3	
Z	4	
Density (calculated)	1.450 Mg/m^3	
Absorption coefficient	1.895 mm^{-1}	
F(000)	1180	
Crystal size	0.15 x 0.1 x 0.03 mm^3	
Theta range for data collection	3.70 to 27.08°.	
Index ranges	-15<=h<=15, -11<=k<=11, -29<=l<=29	
Reflections collected	39464	
Independent reflections	5720 [R(int) = 0.1198]	
Completeness to theta = 27.08°	99.5 %	
Absorption correction	None	
Refinement method	Full-matrix least-squares on F^2	
Data / restraints / parameters	5720 / 0 / 312	
Goodness-of-fit on F^2	1.095	
Final R indices [I>2sigma(I)]	R1 = 0.0567, wR2 = 0.1511	
R indices (all data)	R1 = 0.0938, wR2 = 0.1741	
Largest diff. peak and hole	0.731 and -0.741 e.Å^{-3}	

Crystal data and structure refinement for complex 6.1

Identification code	6.1	
Empirical formula	C20 H28 N4 O4 Ti	
Formula weight	436.36	
Temperature	150(2) K	
Wavelength	0.71070 Å	
Crystal system	Triclinic	
Space group	*P*-1	
Unit cell dimensions	a = 9.6440(2) Å	α= 97.4370(10)°.
	b = 10.1880(3) Å	β= 92.9130(10)°.
	c = 11.1420(3) Å	γ = 94.5710(10)°.
Volume	1080.00(5) $Å^3$	
Z	2	
Density (calculated)	1.342 Mg/m^3	
Absorption coefficient	0.429 mm^{-1}	
F(000)	460	
Crystal size	0.16 x 0.20 x .075 mm^3	
Theta range for data collection	1.85 to 27.50°.	
Index ranges	0<=h<=12, -13<=k<=13, -14<=l<=14	
Reflections collected	12241	
Independent reflections	4933 [R(int) = 0.0354]	
Completeness to theta = 27.50°	99.0 %	
Absorption correction	None	
Refinement method	Full-matrix least-squares on F^2	
Data / restraints / parameters	4933 / 3 / 282	
Goodness-of-fit on F^2	1.168	
Final R indices [I>2sigma(I)]	R1 = 0.0578, wR2 = 0.1473	
R indices (all data)	R1 = 0.0768, wR2 = 0.1817	
Extinction coefficient	0.21(2)	
Largest diff. peak and hole	0.876 and -0.824 $e.Å^{-3}$	

Crystal data and structure refinement for complex 6.2

Identification code	6.2	
Empirical formula	C39 H67 N4 O4 Ti	
Formula weight	703.87	
Temperature	150(2) K	
Wavelength	0.71070 Å	
Crystal system	Monoclinic	
Space group	$P2_1/c$	
Unit cell dimensions	a = 17.1180(3) Å	α= 90°.
	b = 13.1600(2) Å	β= 98.2370(10)°.
	c = 18.4250(3) Å	γ = 90°.
Volume	4107.83(12) Å^3	
Z	4	
Density (calculated)	1.138 Mg/m^3	
Absorption coefficient	0.249 mm^{-1}	
F(000)	1532	
Crystal size	0.125 x 0.15 x 0.15 mm^3	
Theta range for data collection	3.56 to 27.49°.	
Index ranges	0<=h<=22, -17<=k<=17, -23<=l<=23	
Reflections collected	52217	
Independent reflections	9335 [R(int) = 0.0794]	
Completeness to theta = 27.49°	99.1 %	
Absorption correction	None	
Refinement method	Full-matrix least-squares on F^2	
Data / restraints / parameters	9335 / 0 / 451	
Goodness-of-fit on F^2	1.036	
Final R indices [I>2sigma(I)]	R1 = 0.0596, wR2 = 0.1616	
R indices (all data)	R1 = 0.0920, wR2 = 0.1844	
Largest diff. peak and hole	0.769 and -0.842 e.Å^{-3}	

Crystal data and structure refinement for complex 6.3

Identification code	6.3	
Empirical formula	C55 H92 N2 O8 Ti2	
Formula weight	1005.11	
Temperature	150(2) K	
Wavelength	0.71070 Å	
Crystal system	Triclinic	
Space group	*P*-1	
Unit cell dimensions	a = 13.4330(3) Å	α= 77.5950(10)°.
	b = 14.2760(3) Å	β= 72.1740(10)°.
	c = 17.6230(4) Å	γ = 64.6450(10)°.
Volume	2893.58(11) $Å^3$	
Z	2	
Density (calculated)	1.154 Mg/m^3	
Absorption coefficient	0.325 mm^{-1}	
F(000)	1088	
Crystal size	1.5 x 1.4 x 0.8 mm^3	
Theta range for data collection	3.54 to 27.46°.	
Index ranges	0<=h<=17, -16<=k<=18, -21<=l<=22	
Reflections collected	42206	
Independent reflections	13131 [R(int) = 0.1268]	
Completeness to theta = 27.46°	99.2 %	
Absorption correction	None	
Refinement method	Full-matrix least-squares on F^2	
Data / restraints / parameters	13131 / 0 / 617	
Goodness-of-fit on F^2	1.032	
Final R indices [I>2sigma(I)]	R1 = 0.0702, wR2 = 0.1626	
R indices (all data)	R1 = 0.1469, wR2 = 0.1976	
Largest diff. peak and hole	1.423 and -0.899 $e.Å^{-3}$	

Crystal data and structure refinement for 6.4		
Identification code	6.4	
Empirical formula	C34 H56 N2 O10 Ti2	
Formula weight	748.61	
Temperature	150(2) K	
Wavelength	0.71073 Å	
Crystal system	Monoclinic	
Space group	*C2/c*	
Unit cell dimensions	a = 11.17200(10) Å	α= 90.0000(10)°.
	b = 15.3760(2) Å	β= 95.4510(10)°.
	c = 22.9730(4) Å	γ = 90.0000(10)°.
Volume	3928.47(9) $Å^3$	
Z	4	
Density (calculated)	1.266 Mg/m^3	
Absorption coefficient	0.459 mm^{-1}	
F(000)	1592	
Crystal size	0.38 x 0.25 x 0.17 mm^3	
Theta range for data collection	3.56 to 27.22°.	
Index ranges	-13<=h<=13, -19<=k<=19, -28<=l<=27	
Reflections collected	18380	
Independent reflections	3952 [R(int) = 0.1257]	
Completeness to theta = 27.22°	89.8 %	
Absorption correction	None	
Max. and min. transmission	0.9260 and 0.8448	
Refinement method	Full-matrix least-squares on F^2	
Data / restraints / parameters	3952 / 0 / 224	
Goodness-of-fit on F^2	1.021	
Final R indices [I>2sigma(I)]	R1 = 0.0497, wR2 = 0.1156	
R indices (all data)	R1 = 0.0804, wR2 = 0.1316	
Largest diff. peak and hole	0.577 and -0.640 $e.Å^{-3}$	

Crystal data and structure refinement for complex 6.5

Identification code	6.5	
Empirical formula	C44 H74 Br2 N6 O8 Ti2	
Formula weight	1070.71	
Temperature	150(2) K	
Wavelength	0.71073 Å	
Crystal system	Monoclinic	
Space group	*C2/c*	
Unit cell dimensions	a = 30.1930(4) Å	α= 90°.
	b = 9.86200(10) Å	β= 95.2140(10)°.
	c = 17.6670(3) Å	γ = 90°.
Volume	5238.82(12) Å^3	
Z	4	
Density (calculated)	1.358 Mg/m^3	
Absorption coefficient	1.882 mm^{-1}	
F(000)	2232	
Crystal size	0.30 x 0.28 x 0.25 mm^3	
Theta range for data collection	3.82 to 27.51°.	
Index ranges	-39<=h<=39, -12<=k<=12, -22<=l<=22	
Reflections collected	33197	
Independent reflections	5985 [R(int) = 0.0440]	
Completeness to theta = 27.51°	99.3 %	
Absorption correction	None	
Max. and min. transmission	0.6505 and 0.6021	
Refinement method	Full-matrix least-squares on F^2	
Data / restraints / parameters	5985 / 0 / 288	
Goodness-of-fit on F^2	1.111	
Final R indices [I>2sigma(I)]	R1 = 0.0358, wR2 = 0.1222	
R indices (all data)	R1 = 0.0424, wR2 = 0.1333	
Extinction coefficient	0.0005(3)	
Largest diff. peak and hole	0.918 and -0.913 e.Å^{-3}	

Crystal data and structure refinement for complex 6.6

Identification code	6.6	
Empirical formula	C25.33 H44 N1.33 O8 Ti2	
Formula weight	591.09	
Temperature	170(2) K	
Wavelength	0.71073 Å	
Crystal system	Triclinic	
Space group	*P*-1	
Unit cell dimensions	a = 11.614(2) Å	α= 75.39(3)°.
	b = 11.744(2) Å	β= 80.94(3)°.
	c = 19.366(4) Å	γ = 61.12(3)°.
Volume	2236.0(8) Å^3	
Z	3	
Density (calculated)	1.317 Mg/m^3	
Absorption coefficient	0.580 mm^{-1}	
F(000)	940	
Crystal size	0.30 x 0.30 x 0.10 mm^3	
Theta range for data collection	3.55 to 27.49°.	
Index ranges	-14<=h<=15, -15<=k<=15, -24<=l<=25	
Reflections collected	35566	
Independent reflections	10224 [R(int) = 0.0440]	
Completeness to theta = 27.49°	99.6 %	
Max. and min. transmission	0.9443 and 0.8452	
Refinement method	Full-matrix least-squares on F^2	
Data / restraints / parameters	10224 / 18 / 573	
Goodness-of-fit on F^2	1.032	
Final R indices [I>2sigma(I)]	R1 = 0.0363, wR2 = 0.0871	
R indices (all data)	R1 = 0.0507, wR2 = 0.0946	
Extinction coefficient	0.0052(7)	
Largest diff. peak and hole	0.655 and -0.367 e.Å^{-3}	

Crystal data and structure refinement for complex 6.7

Identification code	6.7	
Empirical formula	C38 H62 Cl4 N2 O12 Ti3	
Formula weight	1024.40	
Temperature	150(2) K	
Wavelength	0.71070 Å	
Crystal system	Monoclinic	
Space group	$P2_1/n$	
Unit cell dimensions	a = 12.5000(2) Å	α= 90°.
	b = 30.7700(4) Å	β= 101.1330(10)°.
	c = 13.3140(2) Å	γ = 90°.
Volume	5024.53(13) Å^3	
Z	4	
Density (calculated)	1.354 Mg/m^3	
Absorption coefficient	0.732 mm^{-1}	
F(000)	2136	
Crystal size	0.15 x 0.20 x 0.20 mm^3	
Theta range for data collection	3.64 to 25.03°.	
Index ranges	0<=h<=14, -36<=k<=36, -15<=l<=15	
Reflections collected	51616	
Independent reflections	8829 [R(int) = 0.0910]	
Completeness to theta = 25.03°	99.5 %	
Absorption correction	None	
Refinement method	Full-matrix least-squares on F^2	
Data / restraints / parameters	8829 / 0 / 548	
Goodness-of-fit on F^2	1.032	
Final R indices [I>2sigma(I)]	R1 = 0.0527, wR2 = 0.1272	
R indices (all data)	R1 = 0.1007, wR2 = 0.1475	
Largest diff. peak and hole	0.971 and -0.816 e.Å^{-3}	

Crystal data and structure refinement for complex 6.8

Identification code	6.8	
Empirical formula	C38 H64 N4 O16 Ti3	
Formula weight	976.63	
Temperature	150(2) K	
Wavelength	0.71073 Å	
Crystal system	Monoclinic	
Space group	$P2_1/n$	
Unit cell dimensions	a = 12.2750(5) Å	α= 90°.
	b = 21.1760(9) Å	β= 93.2200(10)°.
	c = 19.0670(9) Å	γ = 90°.
Volume	4948.4(4) Å^3	
Z	4	
Density (calculated)	1.311 Mg/m^3	
Absorption coefficient	0.538 mm^{-1}	
F(000)	2056	
Crystal size	0.38 x 0.30 x 0.25 mm^3	
Theta range for data collection	3.53 to 27.45°.	
Index ranges	-15<=h<=15, -27<=k<=27, -24<=l<=24	
Reflections collected	44684	
Independent reflections	10632 [R(int) = 0.1459]	
Completeness to theta = 27.45°	94.0 %	
Absorption correction	None	
Max. and min. transmission	0.8772 and 0.8217	
Refinement method	Full-matrix least-squares on F^2	
Data / restraints / parameters	10632 / 0 / 551	
Goodness-of-fit on F^2	1.118	
Final R indices [I>2sigma(I)]	R1 = 0.0833, wR2 = 0.1697	
R indices (all data)	R1 = 0.1592, wR2 = 0.2095	
Extinction coefficient	0.0012(4)	
Largest diff. peak and hole	0.498 and -0.524 e.Å^{-3}	

Crystal data and structure refinement for complex 6.9

Identification code	6.9	
Empirical formula	C18 H24 N4 O4 Ti	
Formula weight	408.31	
Temperature	170(2) K	
Wavelength	0.71073 Å	
Crystal system	Monoclinic	
Space group	*C2/c*	
Unit cell dimensions	a = 22.047(4) Å	α= 90°.
	b = 9.5800(19) Å	β= 114.13(3)°.
	c = 21.545(4) Å	γ = 90°.
Volume	4152.7(14) $Å^3$	
Z	8	
Density (calculated)	1.306 Mg/m^3	
Absorption coefficient	0.441 mm^{-1}	
F(000)	1712	
Crystal size	0.25 x 0.3 x 0.15 mm^3	
Theta range for data collection	3.59 to 25.00°.	
Index ranges	-26<=h<=23, -11<=k<=11, -19<=l<=25	
Reflections collected	21778	
Independent reflections	3651 [R(int) = 0.0506]	
Completeness to theta = 25.00°	99.6 %	
Refinement method	Full-matrix least-squares on F^2	
Data / restraints / parameters	3651 / 0 / 249	
Goodness-of-fit on F^2	1.055	
Final R indices [I>2sigma(I)]	R1 = 0.0659, wR2 = 0.1695	
R indices (all data)	R1 = 0.0749, wR2 = 0.1760	
Extinction coefficient	0.0014(6)	
Largest diff. peak and hole	1.147 and -1.120 $e.Å^{-3}$	

Crystal data and structure refinement for complex 6.10

Identification code	6.10	
Empirical formula	C27.20 H42.80 N5.60 O7 Ti2	
Formula weight	656.07	
Temperature	170(2) K	
Wavelength	0.71070 Å	
Crystal system	Monoclinic	
Space group	$P2_1/n$	
Unit cell dimensions	a = 14.8370(4) Å	α= 90°.
	b = 14.2520(3) Å	β= 109.3130(10)°.
	c = 17.1160(4) Å	γ = 90°.
Volume	3415.62(14) Å^3	
Z	4	
Density (calculated)	1.276 Mg/m^3	
Absorption coefficient	0.515 mm^{-1}	
F(000)	1381	
Crystal size	0.225 x 0.2 x 0.325 mm^3	
Theta range for data collection	3.60 to 27.51°.	
Index ranges	0<=h<=19, 0<=k<=18, -22<=l<=20	
Reflections collected	14627	
Independent reflections	7815 [R(int) = 0.0225]	
Completeness to theta = 27.51°	99.4 %	
Refinement method	Full-matrix least-squares on F^2	
Data / restraints / parameters	7815 / 9 / 414	
Goodness-of-fit on F^2	1.028	
Final R indices [I>2sigma(I)]	R1 = 0.0468, wR2 = 0.1244	
R indices (all data)	R1 = 0.0625, wR2 = 0.1348	
Extinction coefficient	0.0026(7)	
Largest diff. peak and hole	0.827 and -0.388 e.Å^{-3}	

Crystal data and structure refinement for complex 6.11.

Identification code	6.11	
Empirical formula	C80 H104 N12 O14 Ti4	
Formula weight	549.78	
Temperature	170(2) K	
Wavelength	0.71073 Å	
Crystal system	Orthorhombic	
Space group	*Pbca*	
Unit cell dimensions	a = 15.3639(5) Å	α= 90°.
	b = 20.7898(6) Å	β= 90°.
	c = 27.6641(6) Å	γ = 90°.
Volume	8836.3(4) $Å^3$	
Z	4	
Density (calculated)	1.240 Mg/m^3	
Absorption coefficient	0.413 mm^{-1}	
F(000)	3472	
Crystal size	0.33 x 0.05 x 0.05 mm^3	
Theta range for data collection	3.54 to 22.69°.	
Index ranges	-16<=h<=16, -21<=k<=22, -30<=l<=30	
Reflections collected	59704	
Independent reflections	5899 [R(int) = 0.1565]	
Completeness to theta = 22.69°	99.5 %	
Max. and min. transmission	0.9797 and 0.8776	
Refinement method	Full-matrix least-squares on F^2	
Data / restraints / parameters	5899 / 0 / 507	
Goodness-of-fit on F^2	1.074	
Final R indices [I>2sigma(I)]	R1 = 0.0630, wR2 = 0.1575	
R indices (all data)	R1 = 0.0934, wR2 = 0.1727	
Extinction coefficient	0.0014(3)	
Largest diff. peak and hole	0.582 and -0.399 $e.Å^{-3}$	

Crystal data and structure refinement for complex 6.12

Identification code	6.12	
Empirical formula	C75.80 H95.20 N15.90 O14 Ti4	
Formula weight	1644.68	
Temperature	293(2) K	
Wavelength	0.71073 Å	
Crystal system	Orthorhombic	
Space group	$Pn2_1/a$	
Unit cell dimensions	a = 14.941(3) Å	α= 90°.
	b = 20.291(4) Å	β= 90°.
	c = 28.684(6) Å	γ = 90°.
Volume	8696(3) $Å^3$	
Z	4	
Density (calculated)	1.256 Mg/m^3	
Absorption coefficient	0.420 mm^{-1}	
F(000)	3445	
Crystal size	0.2 x 0.075 x 0.15 mm^3	
Theta range for data collection	3.60 to 25.00°.	
Index ranges	0<=h<=17, -24<=k<=24, -34<=l<=34	
Reflections collected	108413	
Independent reflections	14915 [R(int) = 0.0574]	
Completeness to theta = 25.00°	99.5 %	
Refinement method	Full-matrix least-squares on F^2	
Data / restraints / parameters	14915 / 1 / 1048	
Goodness-of-fit on F^2	1.040	
Final R indices [I>2sigma(I)]	R1 = 0.0450, wR2 = 0.1140	
R indices (all data)	R1 = 0.0569, wR2 = 0.1221	
Absolute structure parameter	0.471(19)	
Extinction coefficient	0.00016(12)	
Largest diff. peak and hole	0.423 and -0.330 $e.Å^{-3}$	

Table 1. Crystal data and structure refinement for 7.3L

Identification code	7.3L	
Empirical formula	C54 H78 O3	
Formula weight	1033.55	
Temperature	150(2) K	
Wavelength	0.71070 Å	
Crystal system	Orthorhombic	
Space group	$P2_12_12_1$	
Unit cell dimensions	a = 10.0480(2) Å	α= 90°.
	b = 17.0850(3) Å	β= 90°.
	c = 27.6130(5) Å	γ = 90°.
Volume	4740.33(15) Å^3	
Z	4	
Density (calculated)	1.086 Mg/m^3	
Absorption coefficient	0.065 mm^{-1}	
F(000)	1704	
Crystal size	0.30 x 0.25 x 0.17 mm^3	
Theta range for data collection	3.65 to 27.48°.	
Index ranges	0<=h<=13, -22<=k<=22, -35<=l<=35	
Reflections collected	68638	
Independent reflections	10834 [R(int) = 0.0664]	
Completeness to theta = 27.48°	99.7 %	
Absorption correction	None	
Max. and min. transmission	0.9888 and 0.9808	
Refinement method	Full-matrix least-squares on F^2	
Data / restraints / parameters	10834 / 0 / 539	
Goodness-of-fit on F^2	1.006	
Final R indices [I>2sigma(I)]	R1 = 0.0410, wR2 = 0.0943	
R indices (all data)	R1 = 0.0520, wR2 = 0.1002	
Absolute structure parameter	0.9(9)	
Extinction coefficient	0.0094(7)	
Largest diff. peak and hole	0.205 and -0.193 e.Å^{-3}	

Crystal data and structure refinement for complex 7.3

Identification code	7.3	
Empirical formula	C78 H117 O18 Ti4.50	
Formula weight	1558.27	
Temperature	170(2) K	
Wavelength	0.71070 Å	
Crystal system	Monoclinic	
Space group	$P2_1/n$	
Unit cell dimensions	a = 22.6370(4) Å	α= 90°.
	b = 14.9130(3) Å	β= 110.0300(9)°.
	c = 27.2290(4) Å	γ = 90°.
Volume	8636.1(3) Å^3	
Z	4	
Density (calculated)	1.198 Mg/m^3	
Absorption coefficient	0.460 mm^{-1}	
F(000)	3312	
Crystal size	0.40 x 0.30 x 0.17 mm^3	
Theta range for data collection	3.54 to 25.00°.	
Index ranges	-26<=h<=26, -17<=k<=17, -32<=l<=32	
Reflections collected	85189	
Independent reflections	15156 [R(int) = 0.0629]	
Completeness to theta = 25.00°	99.7 %	
Absorption correction	None	
Max. and min. transmission	0.9239 and 0.8375	
Refinement method	Full-matrix least-squares on F^2	
Data / restraints / parameters	15156 / 360 / 1089	
Goodness-of-fit on F^2	1.014	
Final R indices [I>2sigma(I)]	R1 = 0.0624, wR2 = 0.1619	
R indices (all data)	R1 = 0.1006, wR2 = 0.1840	
Extinction coefficient	0.0003(2)	
Largest diff. peak and hole	0.355 and -0.719 e.Å^{-3}	

Crystal data and structure refinement for complex 7.4

Identification code	7.4	
Empirical formula	C18 H26 N2 O4 Ti	
Formula weight	382.31	
Temperature	293(2) K	
Wavelength	0.71070 Å	
Crystal system	Monoclinic	
Space group	$P2_1/c$	
Unit cell dimensions	a = 9.0870(2) Å	α= 90°.
	b = 12.1130(2) Å	β= 97.9810(10)°.
	c = 18.0960(4) Å	γ = 90°.
Volume	1972.55(7) Å^3	
Z	4	
Density (calculated)	1.287 Mg/m^3	
Absorption coefficient	0.457 mm^{-1}	
F(000)	808	
Crystal size	0.50 x 0.20 x 0.17 mm^3	
Theta range for data collection	3.42 to 27.49°.	
Index ranges	0<=h<=11, 0<=k<=15, -23<=l<=23	
Reflections collected	8710	
Independent reflections	4515 [R(int) = 0.0286]	
Completeness to theta = 27.49°	99.6 %	
Absorption correction	None	
Max. and min. transmission	0.9243 and 0.8038	
Refinement method	Full-matrix least-squares on F^2	
Data / restraints / parameters	4515 / 0 / 231	
Goodness-of-fit on F^2	1.020	
Final R indices [I>2sigma(I)]	R1 = 0.0374, wR2 = 0.0906	
R indices (all data)	R1 = 0.0548, wR2 = 0.0980	
Extinction coefficient	0.0077(10)	
Largest diff. peak and hole	0.413 and -0.402 e.Å^{-3}	

Crystal data and structure refinement for complex 7.5

Identification code	7.5	
Empirical formula	C20 H42 N2 O4 Ti	
Formula weight	422.46	
Temperature	150(2) K	
Wavelength	0.71073 Å	
Crystal system	Triclinic	
Space group	*P*-1	
Unit cell dimensions	a = 10.3260(6) Å	α= 102.494(2)°.
	b = 10.4830(6) Å	β= 108.024(2)°.
	c = 11.8580(7) Å	γ = 102.411(2)°.
Volume	1135.45(11) $Å^3$	
Z	2	
Density (calculated)	1.236 Mg/m^3	
Absorption coefficient	0.403 mm^{-1}	
F(000)	460	
Crystal size	0.25 x 0.17 x 0.13 mm^3	
Theta range for data collection	3.45 to 27.53°.	
Index ranges	-13<=h<=13, -13<=k<=13, -15<=l<=12	
Reflections collected	13339	
Independent reflections	5181 [R(int) = 0.0710]	
Completeness to theta = 27.53°	98.8 %	
Absorption correction	None	
Max. and min. transmission	0.9514 and 0.9061	
Refinement method	Full-matrix least-squares on F^2	
Data / restraints / parameters	5181 / 0 / 257	
Goodness-of-fit on F^2	1.024	
Final R indices [I>2sigma(I)]	R1 = 0.0539, wR2 = 0.1293	
R indices (all data)	R1 = 0.0763, wR2 = 0.1451	
Extinction coefficient	0.010(3)	
Largest diff. peak and hole	0.669 and -0.594 $e.Å^{-3}$	

Crystal data and structure refinement for complex 7.6

Identification code	7.6	
Empirical formula	C30 H30 O16 Ti	
Formula weight	694.44	
Temperature	150(2) K	
Wavelength	0.71069 Å	
Crystal system	Monoclinic	
Space group	$P2_1/n$	
Unit cell dimensions	a = 12.995(5) Å	α= 90°.
	b = 15.651(4) Å	β= 108.12(3)°.
	c = 14.760(4) Å	γ = 90°.
Volume	2853.1(15) Å^3	
Z	4	
Density (calculated)	1.617 Mg/m^3	
Absorption coefficient	0.385 mm^{-1}	
F(000)	1440	
Crystal size	0.4 x 0.25 x 0.15 mm^3	
Theta range for data collection	2.10 to 26.97°.	
Index ranges	0<=h<=16, 0<=k<=19, -18<=l<=17	
Reflections collected	6642	
Independent reflections	6205 [R(int) = 0.0122]	
Completeness to theta = 26.97°	99.9 %	
Absorption correction	None	
Refinement method	Full-matrix least-squares on F^2	
Data / restraints / parameters	6205 / 0 / 318	
Goodness-of-fit on F^2	1.058	
Final R indices [I>2sigma(I)]	R1 = 0.0466, wR2 = 0.1352	
R indices (all data)	R1 = 0.0561, wR2 = 0.1417	
Largest diff. peak and hole	1.083 and -0.728 e.Å^{-3}	

Crystal data and structure refinement for complex 8.1

Identification code	8.1	
Empirical formula	C9 H6 F N O Ti0.50	
Formula weight	187.10	
Temperature	293(2) K	
Wavelength	0.71070 Å	
Crystal system	Monoclinic	
Space group	*C*2/*c*	
Unit cell dimensions	a = 13.3540(5) Å	α= 90°.
	b = 9.4310(3) Å	β= 110.353(2)°.
	c = 13.2870(5) Å	γ = 90°.
Volume	1568.91(10) Å^3	
Z	8	
Density (calculated)	1.584 Mg/m^3	
Absorption coefficient	0.582 mm^{-1}	
F(000)	760	
Crystal size	0.15 x 0.2 x 0.3 mm^3	
Theta range for data collection	2.70 to 28.72°.	
Index ranges	-18<=h<=17, -11<=k<=12, -17<=l<=17	
Reflections collected	10461	
Independent reflections	2026 [R(int) = 0.0413]	
Absorption correction	None	
Refinement method	Full-matrix least-squares on F^2	
Data / restraints / parameters	2021 / 0 / 138	
Goodness-of-fit on F^2	1.031	
Final R indices [I>2sigma(I)]	R1 = 0.0354, wR2 = 0.0915	
R indices (all data)	R1 = 0.0555, wR2 = 0.1513	
Largest diff. peak and hole	0.312 and -0.399 e.Å^{-3}	

Crystal data and structure refinement for complex 8.2

Identification code	8.2	
Empirical formula	C34 H42 N2 O10 S4 Ti	
Formula weight	814.84	
Temperature	150(2) K	
Wavelength	0.71073 Å	
Crystal system	Triclinic	
Space group	*P*-1	
Unit cell dimensions	a = 11.2960(2) Å	α= 80.6620(10)°.
	b = 11.3390(2) Å	β= 78.0970(10)°.
	c = 15.1870(3) Å	γ = 82.9460(10)°.
Volume	1870.13(6) $Å^3$	
Z	2	
Density (calculated)	1.447 Mg/m^3	
Absorption coefficient	0.510 mm^{-1}	
F(000)	852	
Crystal size	0.25 x 0.17 x 0.13 mm^3	
Theta range for data collection	3.53 to 27.51°.	
Index ranges	-14<=h<=14, -14<=k<=14, -19<=l<=19	
Reflections collected	35400	
Independent reflections	8552 [R(int) = 0.0695]	
Completeness to theta = 27.51°	99.4 %	
Absorption correction	None	
Max. and min. transmission	0.9390 and 0.8831	
Refinement method	Full-matrix least-squares on F^2	
Data / restraints / parameters	8552 / 0 / 469	
Goodness-of-fit on F^2	0.996	
Final R indices [I>2sigma(I)]	R1 = 0.0432, wR2 = 0.0903	
R indices (all data)	R1 = 0.0861, wR2 = 0.1034	
Extinction coefficient	0.0066(7)	
Largest diff. peak and hole	0.426 and -0.403 $e.Å^{-3}$	

Crystal data and structure refinement for complex 8.3

Identification code	8.3	
Empirical formula	C16 H32 F12 N2 O12 S4 Ti	
Formula weight	848.58	
Temperature	170(2) K	
Wavelength	0.71070 Å	
Crystal system	Monoclinic	
Space group	*C2/c*	
Unit cell dimensions	a = 12.5170(2) Å	α= 90°.
	b = 15.8470(3) Å	β= 92.2550(10)°.
	c = 17.8390(4) Å	γ = 90°.
Volume	3535.75(12) $Å^3$	
Z	4	
Density (calculated)	1.594 Mg/m^3	
Absorption coefficient	0.593 mm^{-1}	
F(000)	1728	
Crystal size	0.20 x 0.15 x 0.12 mm^3	
Theta range for data collection	4.29 to 27.47°.	
Index ranges	-16<=h<=16, -20<=k<=20, -22<=l<=23	
Reflections collected	21929	
Independent reflections	4013 [R(int) = 0.0443]	
Completeness to theta = 27.47°	99.0 %	
Absorption correction	Multiscan	
Max. and min. transmission	1.024 and 0.982	
Refinement method	Full-matrix least-squares on F^2	
Data / restraints / parameters	4013 / 0 / 230	
Goodness-of-fit on F^2	1.055	
Final R indices [I>2sigma(I)]	R1 = 0.0395, wR2 = 0.0980	
R indices (all data)	R1 = 0.0544, wR2 = 0.1073	
Extinction coefficient	0.0026(4)	
Largest diff. peak and hole	0.401 and -0.394 $e.Å^{-3}$	

Crystal data and structure refinement for complex 8.4

Identification code	8.4	
Empirical formula	C22 H42 F12 N2 O14 S4 Ti2	
Formula weight	1010.62	
Temperature	150(2) K	
Wavelength	0.71073 Å	
Crystal system	Monoclinic	
Space group	$P2_1/n$	
Unit cell dimensions	a = 12.3950(2) Å	α= 90°.
	b = 10.5830(2) Å	β= 103.9520(10)°.
	c = 16.0020(2) Å	γ = 90°.
Volume	2037.16(6) Å^3	
Z	2	
Density (calculated)	1.648 Mg/m^3	
Absorption coefficient	0.711 mm^{-1}	
F(000)	1032	
Crystal size	0.36 x 0.16 x 0.16 mm^3	
Theta range for data collection	3.84 to 30.01°.	
Index ranges	-17<=h<=17, -14<=k<=14, -22<=l<=22	
Reflections collected	41491	
Independent reflections	5917 [R(int) = 0.0639]	
Completeness to theta = 30.01°	99.7 %	
Absorption correction	Semi-empirical from equivalents	
Max. and min. transmission	0.897 and 0.711	
Refinement method	Full-matrix least-squares on F^2	
Data / restraints / parameters	5917 / 0 / 260	
Goodness-of-fit on F^2	1.018	
Final R indices [I>2sigma(I)]	R1 = 0.0299, wR2 = 0.0755	
R indices (all data)	R1 = 0.0383, wR2 = 0.0808	
Extinction coefficient	0.0092(9)	
Largest diff. peak and hole	0.362 and -0.423 e.Å^{-3}	

Crystal data and structure refinement for complex 8.5

Identification code	8.5	
Empirical formula	C17 H18 F6 N3 O7 S2 Ti	
Formula weight	602.36	
Temperature	150(2) K	
Wavelength	0.71073 Å	
Crystal system	Monoclinic	
Space group	$P2_1/c$	
Unit cell dimensions	a = 10.8330(3) Å	α= 90°.
	b = 14.8850(4) Å	β= 102.0840(10)°.
	c = 15.5460(4) Å	γ = 90°.
Volume	2451.23(11) Å^3	
Z	4	
Density (calculated)	1.632 Mg/m^3	
Absorption coefficient	0.608 mm^{-1}	
F(000)	1220	
Crystal size	0.25 x 0.18 x 0.14 mm^3	
Theta range for data collection	3.75 to 27.57°.	
Index ranges	-14<=h<=14, -19<=k<=19, -20<=l<=20	
Reflections collected	36759	
Independent reflections	5590 [R(int) = 0.0834]	
Completeness to theta = 27.57°	98.8 %	
Absorption correction	None	
Refinement method	Full-matrix least-squares on F^2	
Data / restraints / parameters	5590 / 0 / 337	
Goodness-of-fit on F^2	1.362	
Final R indices [I>2sigma(I)]	R1 = 0.0857, wR2 = 0.2909	
R indices (all data)	R1 = 0.1059, wR2 = 0.3227	
Extinction coefficient	0.000(4)	
Largest diff. peak and hole	1.588 and -0.613 e.Å^{-3}	